TP 2704

PROTECTION OF PROPELLERS IN ICE

Volume 1

Assessment of Protection Schemes

[illegible]

REPORT DOCUMENTATION FORM

1. Transport Canada Report No.
TP 2704

2. TDC Project No.
8951

3. Recipient's Catalogue No.

4. Title and Subtitle
PROTECTION OF PROPELLERS IN ICE (3 Vol.)
Vol. I

5. Report Date
AUGUST 1980

6. Performing Organization Report No.
C-323

7. Author(s)
F.R. Livingstone, M.F. George, T.C. Currie

8. Transport Canada File No.
D500-566-1

9. Performing Organization Name and Address
Davis Engineering
1481 Cyrville Road
Ottawa, Ontario
K1B 3L7

10. DSS File No.
18ST.T8200-8-8557

11. DSS or Transport Canada Contract No.
0ST79-00047

12. Sponsoring Agency Name and Address
Transportation Development Centre (TDC)
1000 Sherbrooke St. West., P.O. Box 549
Montreal, Quebec
H3A 2R3

13. Type of Report and Period Covered
Technical Nov.79-Aug.1980

14. Sponsoring Agency Code
TDC 8951

15. Supplementary Notes

16. TDC Project Officer
R.H.F. Dillon

17. Abstract

This report presents a theoretical appraisal of published and unpublished protection systems. The major concepts identified and investigated include; nozzles, ring propellers, deflecting fins, bilge keels, propeller cages, open partial tunnels and in-hull propulsion systems.

Various devices within each concept are developed and critically reviewed.

Conclusions are drawn with regard to the most suitable and effective devices for use in heavy ice.

Library and Information Centre/
Centre de Documentation (CSLA)
RECEIVED - REÇU LE
DEC 2 1980
Transport Canada / Transports Canada

18. Key Words
Ship, icebreaker, propeller, blade, protection, guard, ice

19. Distribution Statement
Limited number of copies available from Sponsoring Agency

20. Security Classification (of this report)
Unclassified

21. Security Classification (of this page)
Unclassified

22. No. of Pages
200

23. Price
--

TDC/CDT 79-005

FORMULE DE DOCUMENTATION POUR RAPPORT

1. N° du rapport Transports Canada TP 2704	2. N° de l'étude — CDT 8951	3. N° de catalogue du destinataire

4. Titre et sous-titre

PROTECTION OF PROPELLERS IN ICE (3 Vol.)
Vol. I

5. Date du rapport

Août 1980

6. N° du rapport de l'organisme exécutant

C-323

7. Auteur(s)

F.R. Livingstone, M.F. George, T.C. Currie

8. N° de dossier Transports Canada

D500-566-1

9. Nom et adresse de l'organisme exécutant

Davis Engineering
1481 Cyrville Road
Ottawa, Ontario
K1B 3L7

10. N° de dossier — ASC

18ST.T8200-8-8557

11. N° de contrat — ASC ou Transports Canada

0ST79-00047

12. Nom et adresse de l'organisme parrain

Centre de développement des Transports
1000 O., rue Sherbrooke, C.P. 549
Montréal, Québec
H3A 2R3

13. Genre de rapport et période visée

technique nov.79-août 1980

14. Code de l'organisme parrain

CDT 8951

15. Remarques additionnelles

16. Agent de projet — CDT

R.H.F. Dillon

17. Résumé

Ce rapport présente une évaluation théorique des rapports sur les systèmes de protection, publiés et non publiés. Les principaux concepts identifiés et enquêtés sont la buse, l'anneau d'hélice, le dérive déviateur, la stabilité de la quille, la cage de l'hélice, l'ouverture partielle des tunnels et l'intérieur de la coque du système de propulsion.

Plusieurs mécanismes de chaque concept y sont développés et revisés sévèrement.

Les conclusions sont tirées d'après les mécanismes les plus efficaces et les plus appropriés pour fins d'usage en glace épaisse.

18. Mots-clés

navire, brise-glace, hélice, pale, protection, protéger, glace

19. Diffusion

Nombre limité d'exemplaires disponibles au prés de l'organisme parrain

20. Classification de sécurité (de ce rapport) aucune	21. Classification de sécurité (de cette page) aucune	22. Nombre de pages 200	23. Prix --

CDT/TDC 79-005

PROTECTION OF PROPELLERS IN ICE

VOLUME I
ASSESSMENT OF PROTECTION SCHEMES

Prepared For:

TRANSPORT CANADA RESEARCH
AND DEVELOPMENT CENTRE

Prepared By:

DAVIS ENGINEERING LIMITED
CONSULTING ENGINEERS
OTTAWA, CANADA

Authors: Mr. F.R. Livingstone,
Dr. M.F. George,
Mr. T.C. Currie

AUGUST, 1980

TABLE OF CONTENTS

PAGE:

EXECUTIVE SUMMARY i

1.0 INTRODUCTION 1

2.0 DUCTS 3

- 2.1 Accelerating Ducts (Kort-Nozzles) 3
- 2.2 Slotted Nozzles 6
- 2.3 Non-Axisymmetric Ducts 8
- 2.4 Decelerating Ducts 11
- 2.5 Unguarded Ducts as Propeller Protective Devices 14
- 2.6 Ducts with Guards 16
- 2.7 Legal Restrictions on Use of Nozzle Concepts 22

3.0 RING PROPELLER 23

- 3.1 Description 23
- 3.2 Ring Propeller in Ice 27
- 3.3 Partial Ring (Schnitger Propeller) 27

4.0 DEFLECTING FINS 30

- 4.1 Bossing Fins 30
- 4.2 Fins on Skeg 30
- 4.3 Legal Restrictions on the Use of Skeg and Bossing Mounted Deflecting Fins 32

5.0 BILGE KEELS 34

6.0 PROPELLER CAGE 36

TABLE OF CONTENTS (CONTINUED)

PAGE:

7.0 OPEN (PARTIAL) TUNNELS 40

7.1 Description 40
7.2 Suitability of Partial Tunnels for Icebreakers 43

8.0 IN-HULL PROPULSION SYSTEMS 48

8.1 Description 48
8.2 Closed Tunnels 48
8.3 YPASS Propulsion Systems 54
8.4 Countersunk Kort-Nozzles 57

9.0 RUDDERS 61

10.0 GENERAL EVALUATION OF PROPELLER PROTECTIVE DEVICES 66

11.0 TIP CLEARANCE 69

12.0 CONCLUSIONS AND RECOMMENDATIONS 75

12.1 General 75
12.2 Multiple-Screw In-Hull Arrangement 76
12.3 Single-Screw Nozzle Arrangement 76

13.0 REFERENCES 79

APPENDICES

Appendix A - One-Dimensional Flow Analysis of In-Hull Propulsion System

Appendix B - Classified Canadian Patents Related To Protective Devices for Propellers

LIST OF FIGURES

TITLE: PAGE:

Fig. 1 - Accelerating Duct (Kort-Nozzle) 4

Fig. 2 - Open-water Test Results of K_a 4-70 Screw Series in Nozzle No. 19A 5

Fig. 3 - Profile of Slotted Nozzles 7

Fig. 4 - Different Versions of Monnich's Nozzle 9

Fig. 4a - View of Stern of Tanker fitted with Non-Axisymmetrical Ducted Propeller 10

Fig. 4b - Section Profiles of Duct 19B 12

Fig. 5 - Decelerating Ducted Propeller (Pump-Jet) 13

Fig. 6 - Nozzle with Guards 17

Fig. 7 - Guards for Ducted Propeller on Single-Screw Ship with Compound Rudder 19

Fig. 8a - Ice Block held in place by Nozzle Leading Edge, Deflecting Fins and Propeller Inflow 21

Fig. 8b - Modified Deflecting Fin 21

Fig. 9 - Ring Propeller 24

Fig. 10 - Results of Open-Water Tests with Ring Propeller Series R 4-55 25

Fig. 10a - Optimum Diameter at Given Intake Velocity Power and Rotational Speed 26

Fig. 11 - Schnitger Propeller 29

Fig. 12 - Bossing Fins 31

Fig. 13 - Deflecting Fins on Skeg 33

Fig. 14 - Bilge Keel 35

Fig. 15 - Bird Cages on USCG POLAR STAR 37

Fig. 16 - Bird Cage with Upper Openings Sealed Off 38

Fig. 17 - Elevation and Profile Views of Stern with Partial Tunnel (Arch Stern) 41

Fig. 18 - B & W Stern with Semi-Duct 44

Fig. 19 - Tunnel Stern 45

Fig. 20 - Tunnel with Yarrow Flap Abaft Propeller 45

LIST OF FIGURES (CONT'D)

TITLE: PAGE:

Fig. 21 - Overlapping Screws in Partial Tunnels on Triple-Screw Vessel 47

Fig. 22 - Stern with Short Tunnel 50

Fig. 23 - Stern with Long Tunnel 50

Fig. 24 - In-Hull Propulsion System with Bottom Intake 53

Fig. 24a - YPASS Ducted Propulsion System 55

Fig. 24b - Comparison of Optimum Efficiency Values for Different Types of Propulsors 55

Fig. 25 - Tested Ducted Propeller Configurations with Nozzle Ring over 90 or 180 Degrees Countersunk in Tunnel 58

Fig. 26 - Open-Water Test Results with Ducted Propeller Configurations with Nozzle Rings Partly Countersunk in Tunnel 59

Fig. 27 - Open-Water Test Results with Ducted Propeller Configurations with Nozzle Rings Partly Countersunk in Tunnel 59

Fig. 28 - Twin Rudders Behind Propeller Developing Reverse Thrust 62

Fig. 29 - Schematic Flow and Operating Diagrams for a Kitchen Rudder 63

Fig. 30 - Control Volume Assumed in Ducted Propeller Analysis 70

Fig. 31 - In-Hull Protection Device

Fig. 32 - Triple Tunnel Protection Device

Fig. 33 - Modified POLAR 7 with Moulded Stern Guard

Fig. 34 - Squared-off Transom Stern

Fig. 35 - Strong Double-flared Nozzle 77

EXECUTIVE SUMMARY

The objective of this study is to develop a method of protecting the propellers of ice class vessel such that they do not come in contact with large fragments of ice.

The initial task in this study was the investigation and evaluation of propeller protection schemes applicable to single and multi-screw ships.

This interim report presents the results of this investigation. The major concepts identified and investigated are:

1) Ducts (Nozzles)
2) Ring Propellers
3) Deflecting Fins
4) Bilge Keels
5) Propeller Cages
6) Open (Partial) Tunnels
7) In-Hull Propulsion Systems

Various devices within each concept are developed and each device is critically reviewed.

Finally, conclusions are drawn with respect to the most suitable and effective devices to be recommended for Arctic class vessels.

For triple-screw vessels, an in-hull propulsion scheme is proposed in which the three propellers are totally enclosed in separate tunnels with guarded bottom intakes. Three different designs are suggested for the same concept. In the first design, a typical triple-screw hull form is used. In the second design, the aft body shape is altered in order to accommodate the tunnels with all propellers in one plane. The aft end of the tunnels are flush with the ship's hull to improve the performance in astern operation. For the third design, a squared-off transom stern is used together with a wall-sided hull form for simplicity. The exits are also protected with guards.

For twin-screw vessels, an in-hull propulsion scheme is also recommended, with each propeller enclosed in a separate tunnel with guarded bottom intake. The aft end of the tunnels are fitted with removable guards.

For single-screw vessels, a strong double flared duct with deflecting fins on the bossing and skeg is recommended. The trailing edge of the duct is fitted with a removable guard.

Having established the most promising protection schemes, these concepts will be developed using as a basis the hull forms of POLAR 7 (3-screw), PIERRE RADISSON (2-screw), and MV ARCTIC (1-screw). Propeller design and means of maneuvering will be addressed for each case. These designs will be detailed in the Volume II Report.

1.0 INTRODUCTION

Traditionally designed incebreakers, which now tend to work extended seasons, have suffered increasingly from damage to propellers, shafts, and rudders. Such damage may be of decisive consequences to the reliability of service of the vessel. Among recent casualties have been the modern Canadian icebreaker, FRANKLIN, and the U.S. Coast Guard's POLAR STAR.

Therefore the development of a protective device(s) for ice class vessels has become an urgent need. Several protection schemes are reviewed in this report. A description of each concept is provided, followed by an assessment of its worth as a propeller protective device. Many of the schemes described are already used, to some extent, on existing icebreakers, although their primary function may not be one of propeller protection. Rudders and nozzles are examples of such devices. The ability of these devices to protect propellers from ice damage can, in some cases, be improved by simply modifying their design and/or fitting appropriate guards. Such improvements are noted where appropriate.

Each propeller protection concept is assessed on the basis of its anticipated or, when possible, demonstrated capabilities for protecting a propeller from ice damage and, in addition, for its effect on propulsive efficiency. The former assessment is largely qualitative in nature since little information, either experimental or derived from actual operating experience, is available for judging the protective capabilities of most of the concepts. Since the desired product of this investigation is a device capable of providing essentially complete protection against propeller damage, schemes which do not protect the propeller during both forward and astern operation are discarded immediately. Schemes which appear to reduce ice milling and ice ingestion during both forward and astern operation are examined further to see if they have weaknesses or liabilities in other areas. Adequate structural strength, ready applicability to single, twin, or triple-screw vessels, and good hydrodynamic performance (e.g., low thrust deduction) are the remaining requirements of principal importance. In most instances the first and last requirements are conflicting, since the drag of an ice deflecting appendage (e.g., fin) increases as its size and robustness increases. Comments about these considerations will, again, be largely qualitative and general in nature since quantitative results would be applicable only to a specific design.

2.0 DUCTS

The use of nozzles for either increasing bollard thrust, or for extending the cavitation-limited operating range of a propeller, is well established. Several types of nozzle are reviewed in subsequent sections. Different types of nozzles are expected to be similar with respect to their ability to protect propellers in ice, so the performance of nozzles in general, as propeller protective devices, will be discussed in Section 2.5.

2.1 Accelerating Ducts (Kort-Nozzles)

An increase in bollard thrust is obtained with a nozzle which accelerates the propeller inflow in front of the nozzle, thereby lowering the static pressure in that region. The reduced pressure acting on the forward-facing surfaces of the nozzle, combined with the normal hydrostatic pressure acting on rearward-facing surfaces produces a net forward thrust on the nozzle which, at bollard conditions, may constitute a substantial part of the total thrust of the nozzle/propeller combination. An accelerating duct (Kort nozzle) is shown in Figure 1, and typical performance data for a propeller/nozzle combination are shown in Figure 2.

The performance curves shown apply to an NSMB K_a4-70 series propeller in the NSMB standard nozzle, which has a chord/diameter (L/D) ratio of 0.5 and (D_{out}/D) = 1.21, where (D_{out}) and D are the outer diameter of the nozzle and the propeller diameter respectively. The variables in FIG. 2 are defined below:

J = advance coefficient = $\frac{V_A}{nD}$

K_Q = torque coefficient = $\frac{Q}{\rho n^2 D^5}$

K_T = total thrust coefficient = $\frac{T}{\rho n^2 D^4}$

K_{Tn} = thrust coefficient for nozzle = $\frac{T_n}{\rho n^2 D^4}$

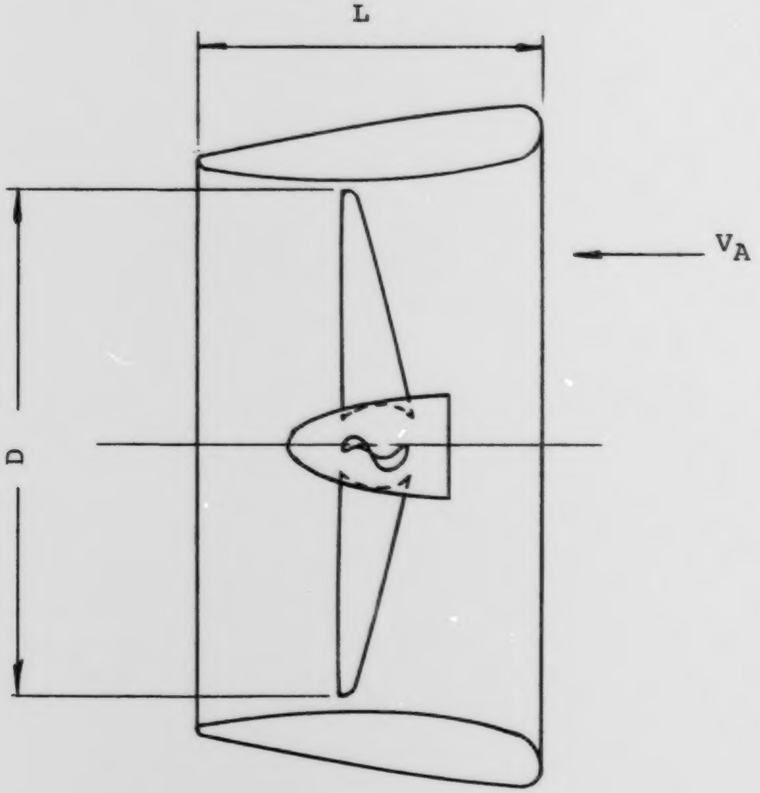

Fig. 1: Accelerating Duct (Kort-Nozzle)

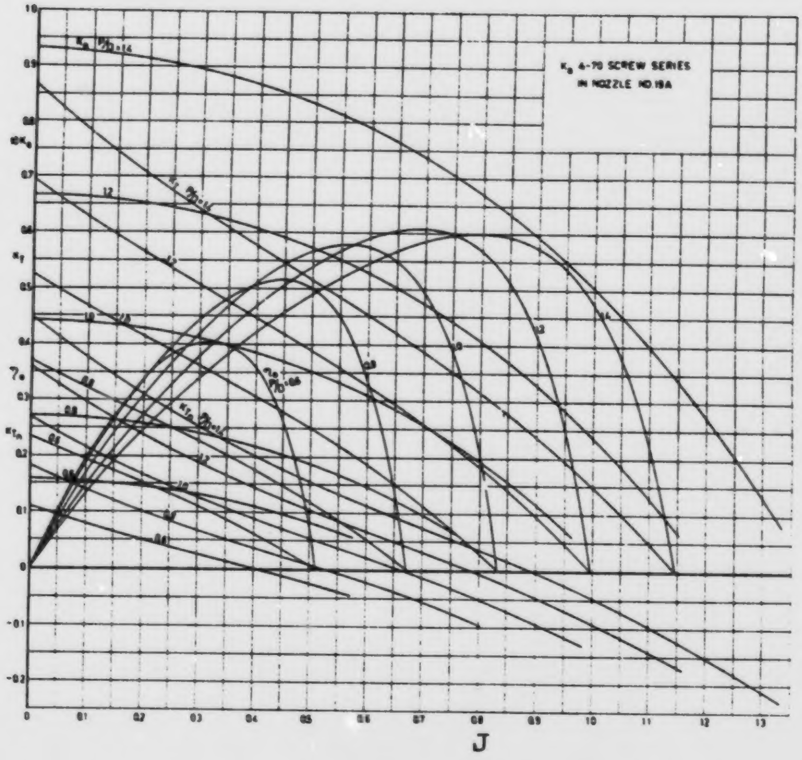

Fig. 2: Open-water test results of Ka 4-70 screw series in nozzle no. 19A.

P/D = propeller pitch/diameter ratio

η_o = efficiency of nozzle/propeller combination (open water)

= thrust power/shaft power

$$= \frac{TV_a}{2\pi nQ} = \frac{JK_T}{2\pi K_Q}$$

where D, P, Q, n = propeller diameter, pitch, torque and speed, respectively.

T = thrust of propeller/nozzle combination

T_n = thrust of nozzle

Va = speed of advance of propeller

The performance curves shown in FIG. 2 illustrate how significant the thrust on the nozzle can be relative to the total thrust of the nozzle/propeller combination. Generally speaking, the thrust on the nozzle at bollard conditions (J=0) is approximately equal to the propeller thrust in this instance.

If the astern thrust of a ducted propeller is important (which is definitely the case with icebreakers), the backing characteristics of the nozzle can be improved by using a well-rounded and relatively thick trailing edge (2) since this prevents flow separation in the nozzle during reverse operation.

2.2 Slotted Nozzles

While a Kort nozzle can substantially increase bollard thrust, the drag (both viscous and induced) of the nozzle is a liability at high ship speeds. As seen in Figure 2, the thrust on the nozzle becomes negative (i.e., opposes forward motion of the ship) at higher values of the advance coefficient. With P/D = 1.4, for example, the thrust acting on the nozzle becomes negative at an advance coefficient of 0.9. An accelerating nozzle at high advance coefficients (i.e., low thrust loadings) can be improved by using a slotted nozzle (see Figure 3) as described by Van Gunsteren in (1). The nozzle shown in Figure 3 diverges after the propeller and hence has a relatively small

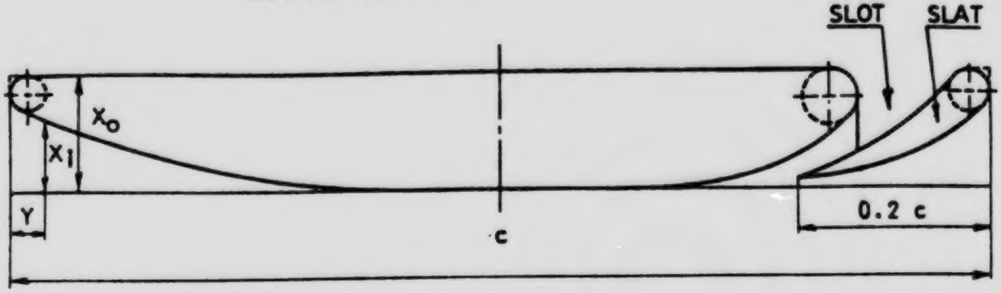
SLOTTED NOZZLE I
SLOT
SLAT
Xo
X1
Y
c
0.2 c

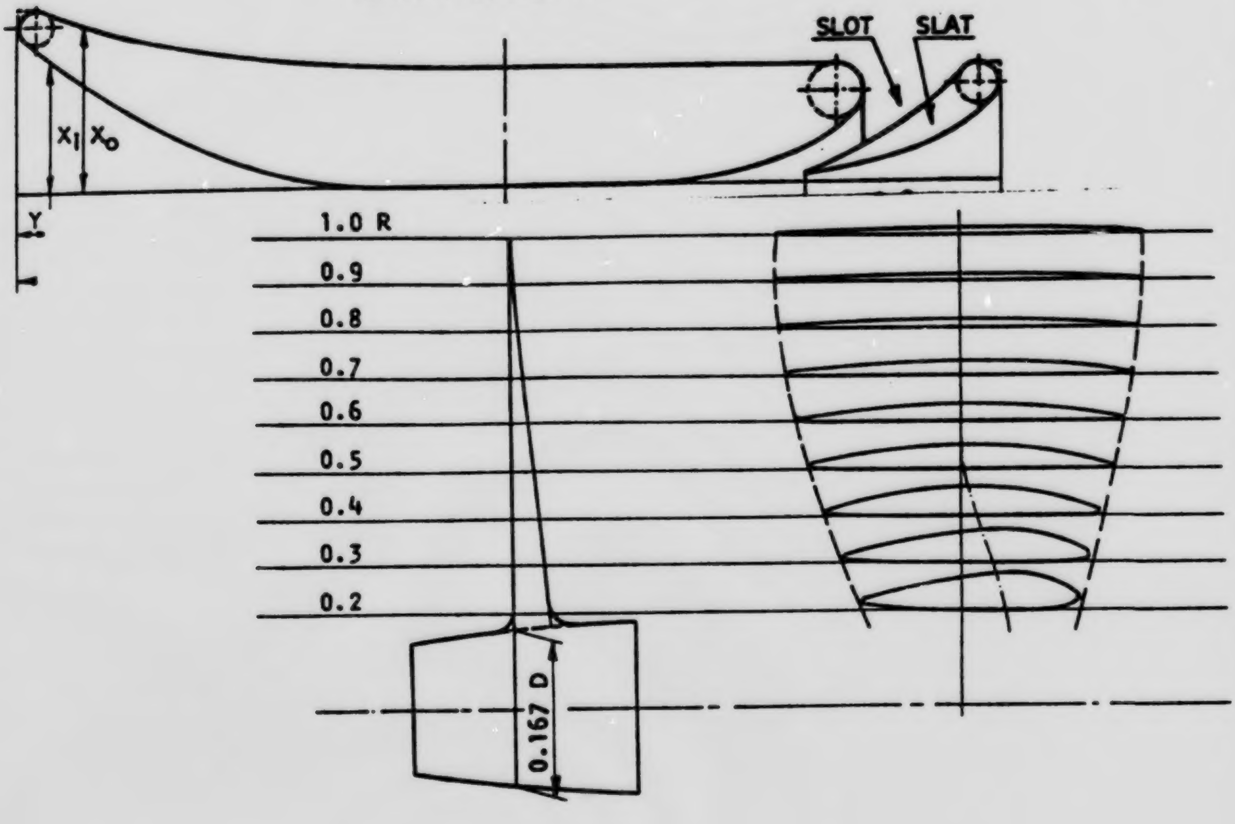
SLOTTED NOZZLE II
SLOT
SLAT
X1
Xo
Y
1.0 R
0.9
0.8
0.7
0.6
0.5
0.4
0.3
0.2
0.167 D

Fig. 3: Profile of Slotted Nozzles

impeller disc area/nozzle exit area ratio. This characteristic enhances the efficiency of the nozzle/propeller combination, as described by Oosterveld (2), but also increases the risk of flow separation on the interior surface of the nozzle. Flow through the slot energizes the boundary layer before the diffusing section, thereby reducing the likelihood of separation. The slot in the nozzle is, therefore, used primarily for boundary layer control.

An unusual variant of the accelerating nozzle has been proposed by Monnich (3). Monnich's nozzle, different versions of which are shown in Figure 4, has pipes or an annular duct extending from the propeller to the rear of the nozzle. It is claimed by the inventor that this feature increases the pressure rise across the propeller and hence the thrust of the propeller/nozzle combination. It is not obvious, however, how the pressure rise across the propeller is increased by the use of this invention. Experimental evidence supporting the inventor's claims is, apparently, available.

2.3 Non-Axisymmetric Ducts

It has been shown by tests that the extent to which a nozzle is accelerating depends mainly on the ratio between propeller disk area and the exit area of the nozzle. In order to make the flow over the propeller disk more constant (circumferentially at a given radius) the aft part of the duct may be replaced by a non-symmetric one. This type of duct has the ability to improve the working conditions of a propeller in a shear flow, similar to that behind a ship, and increases the efficiency. Three types of non-axisymmetric ducts are available.

1) cylindrical at the inside from the L.E. of the nozzle to the impeller, only the aft part is non-axisymmetric but still cylindrical with circular cross sections, (Fig. 4a), (Oosterveld)(2),

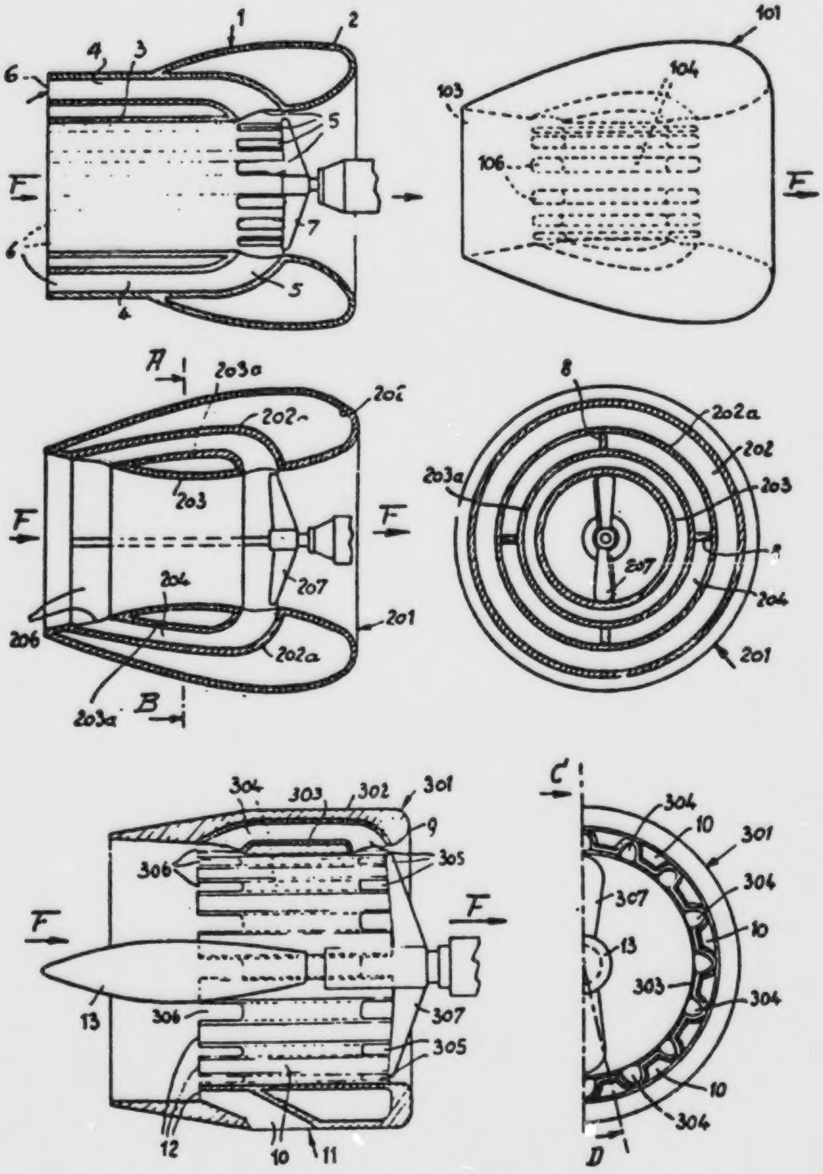
Version 1

Version 2

Version 3

1
2
4
3
6
5
F
7
6
5
4
101
104
103
106
F
A
203a
202
202a
203a
203
F
F
207
204
206
201
202a
203a
B
8
202a
202
203a
203
207
204
201
304
303
302
301
9
306
305
F
F
13
306
307
305
12
10
11
C
304
10
301
307
304
13
10
303
304
10
304
D

Fig. 4: Different Versions of Mönnich's Nozzle

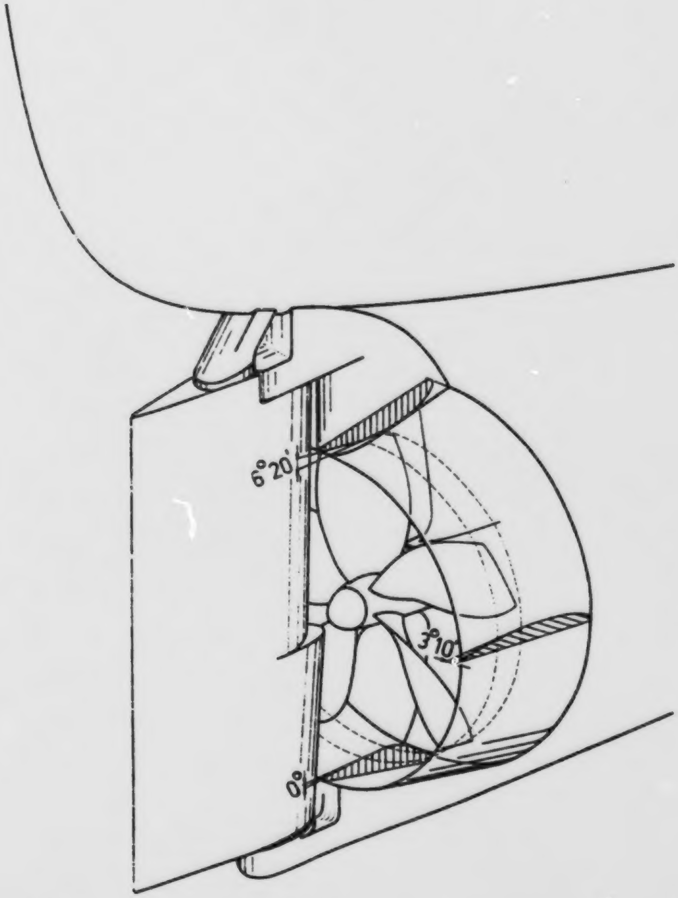

Fig. 4a: View of stern of tanker fitted with non-axisymmetrical ducted propeller.

2) cylindrical from the L.E. of the nozzle to the propeller, only the aft part is non-axisymmetric and non-cylindrical, with elliptical cross sections, (Fig. 4b), (GEORGE, duct 19B) (13), (15), and

3) controlled effective exit area by means of jet-flap mechanism by which a favourable performance could be obtained over a wide range of operating conditions (Oosterveld, and LIPS n.v.)(2). This particular design is not suitable for icebreakers due to the impracticability of such a mechanism to operate in ice conditions.

2.4 Decelerating Ducts

The cavitation-limited operating range of a propeller can be increased by using a nozzle which decelerates the propeller inflow in front of the propeller. Such a nozzle is shown in Figure 5. The static pressure of the propeller inflow increases as it decelerates, thus the static pressure at the propeller disc is higher than the normal hydrostatic pressure. The margin against cavitation is increased in this case. The diffusing duct (pump jet) offers, therefore, the possibility of increasing the cavitation-limited speed of a propeller. Diffusion also allows operation at a lower advance coefficient (J) for the same cavitation - limited forward speed, a factor which can be significant in the design of the propulsion machinery since it allows the propeller rotational speed to be increased.

While the margin against cavitation is increased by diffusing the propeller inflow, drag forces on a decelerating nozzle reduce the propeller thrust instead of augmenting it. Thus a decelerating nozzle has an adverse effect on a vessel's propulsive efficiency. Decelerating nozzle/propeller combinations operate relatively quietly compared to most other propulsor types, and this characteristic, combined with favourable cavitation-reducing properties makes the decelerating nozzle of more interest for naval vessels than for ice class ships.

Ordinates For Nozzle Profile 19A

X/L	0	1.25	2.50	5.0	7.5	10	15	20	25	30	40	50	60	70	80	90	95	100
X_i/L	18.25	14.66	12.80	10.87	8.00	6.34	3.87	2.17	1.10	0.48	circular cylinder			0.29	0.82	1.45	1.86	2.36
X_u/L	-	20.72	21.07	20.80	straight line													±6.36

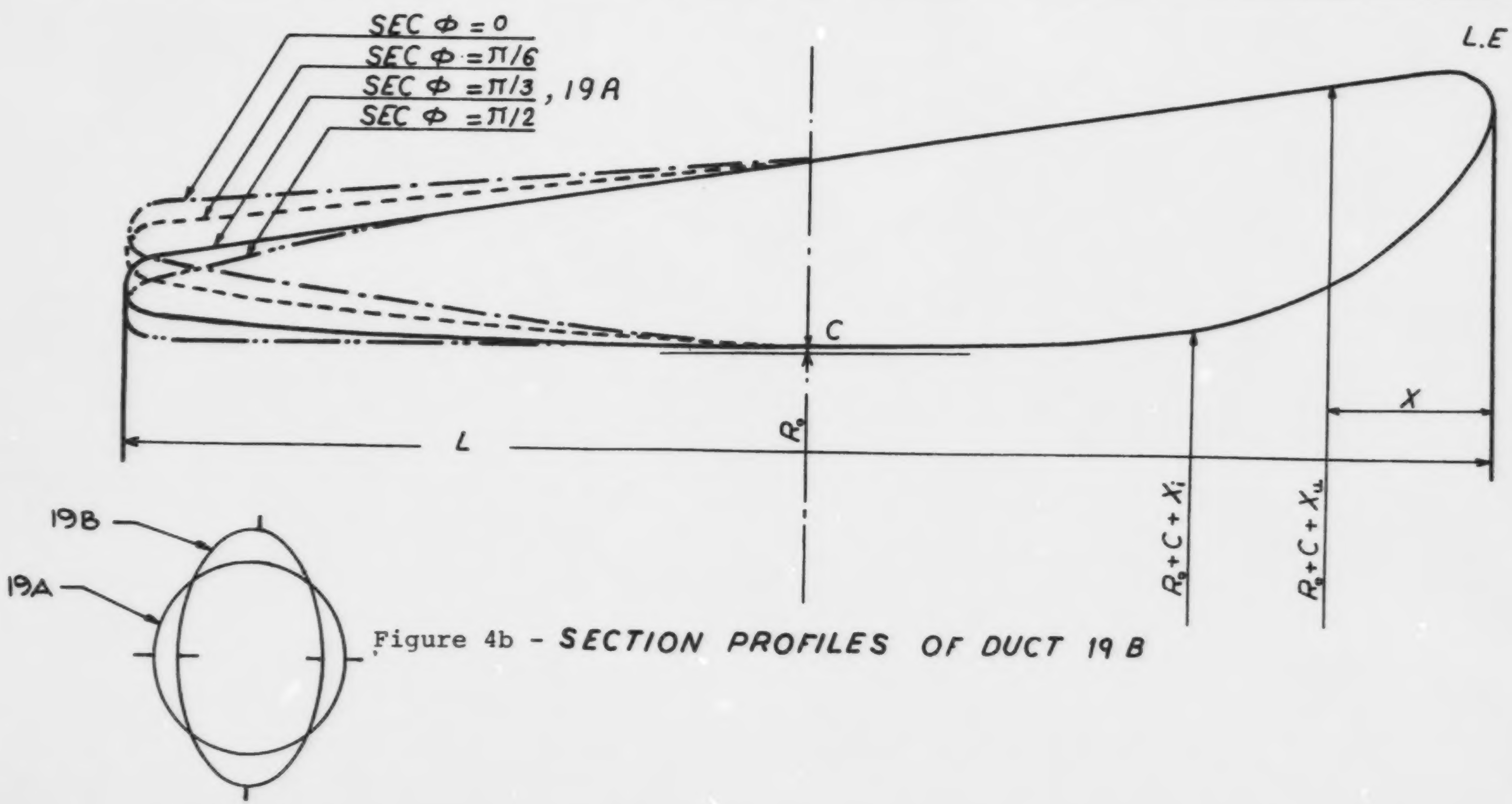
SEC Φ = 0
SEC Φ = π/6
SEC Φ = π/3 , 19A
SEC Φ = π/2
L.E
C
X
L
R_0
$R_0 + C + X_i$
$R_0 + C + X_u$
19B
19A

Figure 4b - SECTION PROFILES OF DUCT 19 B

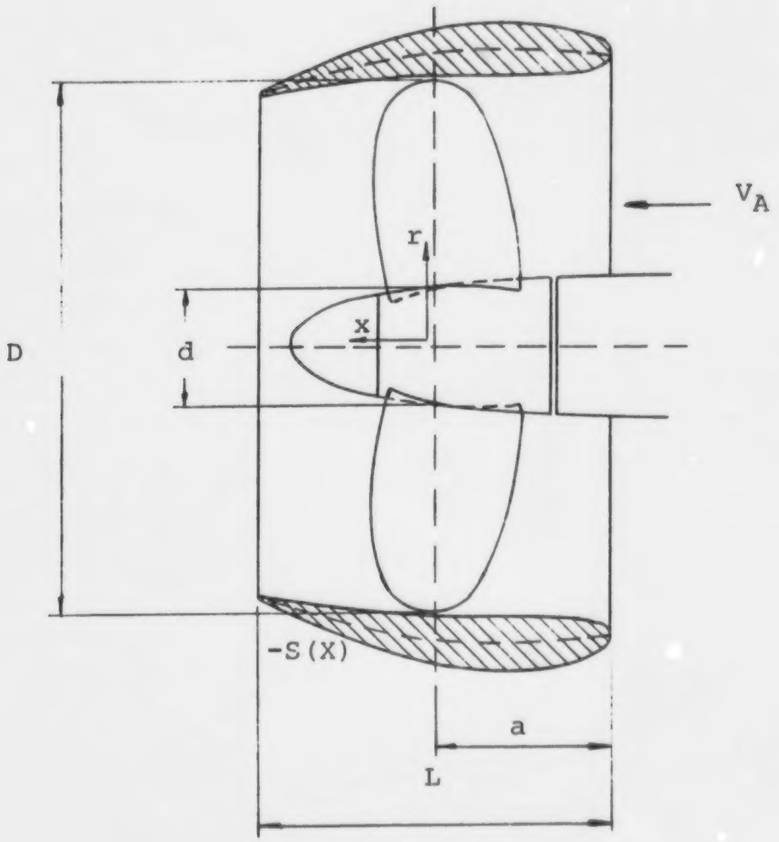
V_A
r
x
D
d
-S(X)
a
L

Fig. 5: Decelerating Ducted Propeller (Pump-jet)

2.5 Unguarded Ducts As Propeller Protection Devices

A nozzle will obviously protect a propeller, to a certain extent, from ice damage. Ice milling, for instance, is reduced when a propeller is surrounded by a nozzle. The size of ice pieces that can collide with a propeller enclosed in a nozzle is circumscribed, in most cases, by the diameter of the nozzle. Ice pieces entering the nozzle must pass through the propeller disc since they cannot be "kicked away" (i.e., pushed radially outwards) by the propeller. Thus impacts between the propeller and ice pieces of small and medium size may be more severe with a "standard" ducted propeller (a combination of an annular aerofoil and an impeller) than with a free propeller. Impacts of this nature may be severe enough to cause damage to the propeller blades and/or nozzle.

Little information is available on the adequacy of nozzles for use in heavy ice. The ice-strengthened class cargo ship, M.V. Arctic, is equipped with a Kort nozzle and a controllable reversible pitch (CRP) propeller. It is reported that large blocks of ice occasionally block the entrance to the nozzle, but that they can be removed by momentarily reversing the pitch on the propeller. The M.V. Arctic is equipped with a thrust-meter, so nozzle blockages causing significant reductions in thrust can be detected as soon as they occur.

Another example is the M.V. "Canmar Kigoriak", Arctic Class 3 icebreaker. It is equipped with a single C.P. propeller with a double flared nozzle. Model tests and the performance of Kigoriak have supported the idea that for a low Arctic Class vessel, a single propeller housed on the centerline behind a skeg and shrouded by a strong nozzle would be at less danger of damage by ice than an open propeller.

Since the flow entering an accelerating ducted propeller is accelerated in front of the nozzle, the suction in front of the nozzle is very high, particularly when high thrust is required at low ship speeds. These conditions, which will tend to promote nozzle clogging, arise when a ship is proceeding through heavy ice, so the worst flow conditions in front of the nozzle, from an ice clogging point of view, occur at a time when broken pieces of ice are in plentiful supply both beside and underneath the hull. Momentary thrust reversals, will be most damaging, for if the ship stops, it may be difficult to start again without backing up since ice/hull and snow/hull (if snow cover is present) friction forces will rise to their static values.

An unguarded nozzle fitted on a high Arctic class vessel would be vulnerable to damage by collisions with large ice blocks or, worse still, with intact ice sheet during astern operation. Damage is also likely to occur when a ship is turning in ice, since the ice will impact the nozzle from the side. The probability of nozzle damage will increase with increasing yaw rate. Since the tip clearance between a propeller and its nozzle is very small, the nozzle would not be able to sustain much damage before contact with the propeller would occur.

From the foregoing observations unguarded nozzles are considered less than adequate for use in high Arctic class vessels due to the possibility of:

a) nozzle clogging while proceeding ahead or astern; and,

b) nozzle damage causing contact between the nozzle and propeller.

Some of the problems expected to arise with nozzles in heavy ice may be avoided by using nozzle guards, as described in the next section.

2.6 Ducts with Guards

Guards can be used to prevent large blocks of ice from entering a nozzle when the ship is going ahead or astern. A suitable guard proposed by Liaaen (4), for preventing the ingestion of large ice pieces during forward operation is shown in FIG. 6. The guard shown uses three fins (items 9, 10, 11) on each side of the centerline skeg to deflect ice pieces. The fins connect the nozzle ring to the skeg and hence provide additional support for the nozzle. The guard, as shown, is only applicable to single screw ships with a large centerline skeg. It would have to be modified to be applicable to the wing propellers on a triple-screw vessel or to either propeller on a twin-screw vessel.

This guard, however, does not prevent ice pieces from entering the nozzle during astern operation. The rudder (which is also very vulnerable to ice damage) obviously shields the rear of the nozzle to a certain extent, but the possibility of nozzle blockage developing due to ice pieces becoming wedged between the rudder and the nozzle makes some sort of ice deflecting grillage at the rear of the nozzle desirable. The grillage would also limit the size of ice pieces that could be ingested by the ducted propeller while astern thrust was applied. It is fairly evident, however, that a suitable protective cage would be difficult to design since the cage would interfere with the rudder. If a compound rudder was used, however, the rearward ends of deflecting fins could be attached to the butt (i.e., the fixed part of the rudder behind which the movable part is located) while the forward ends would be attached to the nozzle

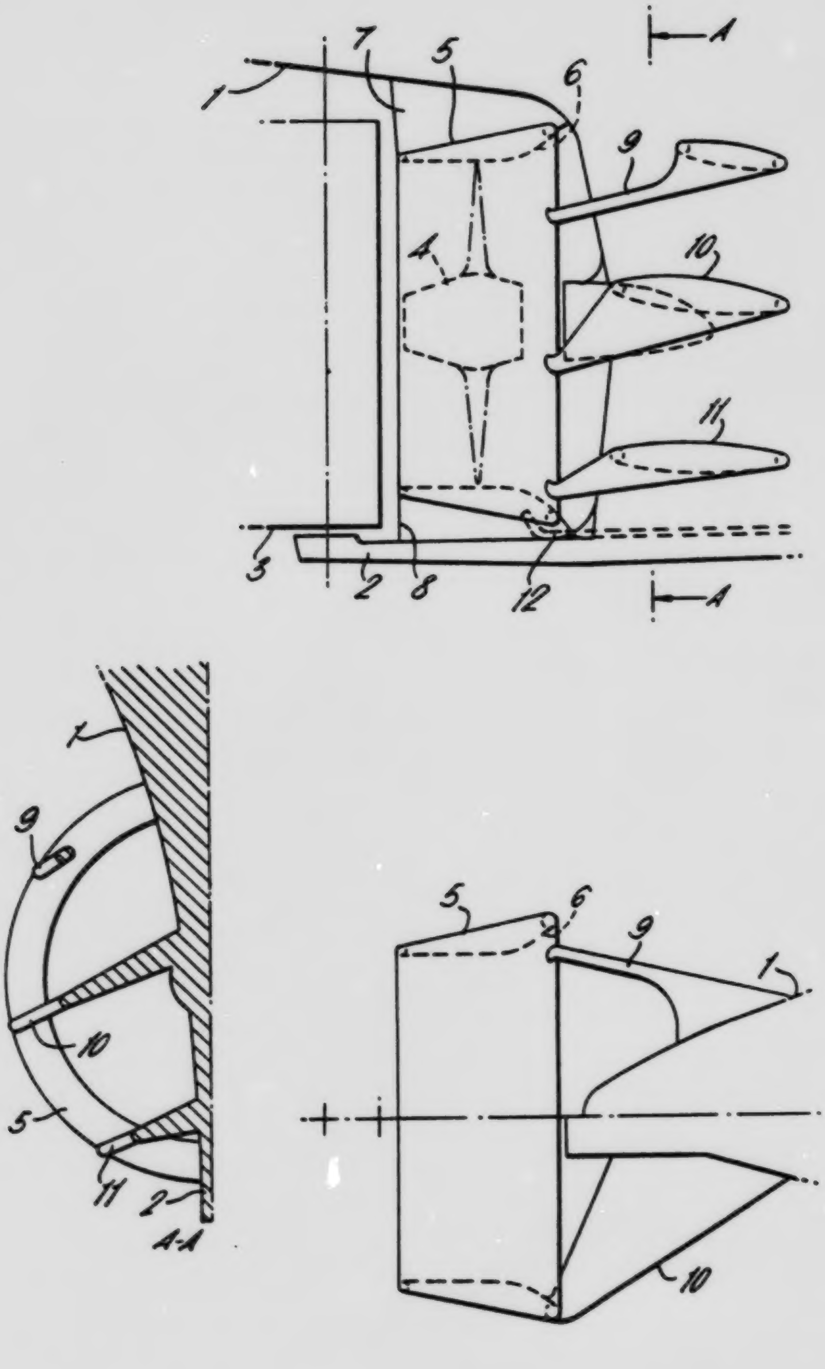
A
1
7
5
6
9
4
10
11
3
2
8
12
A
7
9
10
5
11
2
A-A
5
6
9
1
10

Fig. 6: Nozzle with Guards

ring. Such an arrangement is shown in Figure 7. The deflecting fins at the front of the nozzle are shown with a downward slope in the forward direction (i.e., the attachment points on the skeg are lower than the attachment points on the nozzle). The slope of the fins in cutting plane A-A would also have to be slightly downward, as shown in Figure 6, in order to have the fin surfaces conform to the streamlines (or, more correctly, stream surfaces) of the flow entering the nozzle. The deflecting fins would have to be designed fairly carefully in order to minimize losses, although any design would be a compromise in that optimum fin shapes and orientations are functions of ship speed and thrust since these two variables govern the flow pattern near the nozzle. The influence of ship speed may not be that important since the flow pattern directly in front of the nozzle (and also directly behind the nozzle) is governed, primarily, by the mass flow rate through the nozzle. The mass flow rate through a nozzle is, in turn, far less sensitive to variations in ship speed than is the case with a conventional screw propeller. Thus, it is expected that deflecting fins could be designed which would perform satisfactorily, from a hydrodynamic point of view, over a wide range of operating conditions. The fixed butt abaft the nozzle, and perhaps also the front and rear deflecting fins, could be designed to remove some of the swirl from the propeller outflow, thereby providing a further thrust increase and an improvement in propulsive efficiency.

Guarding the wing nozzles on a multi-screw vessel would be difficult to accomplish neatly, since these nozzles do not fit into apertures in the ship's hull, but rather project outwards from the hull. The deflecting fins for these nozzles would, of necessity, be longer and probably less strong than their single-screw counterparts. When one considers that the wing propellers and nozzles on a multi-screw vessel are particularly vulnerable to ice damage, the prospects of being able to protect them by the use of deflecting fins, (and in addition achieve satisfactory hydrodynamic performance) are not very good.

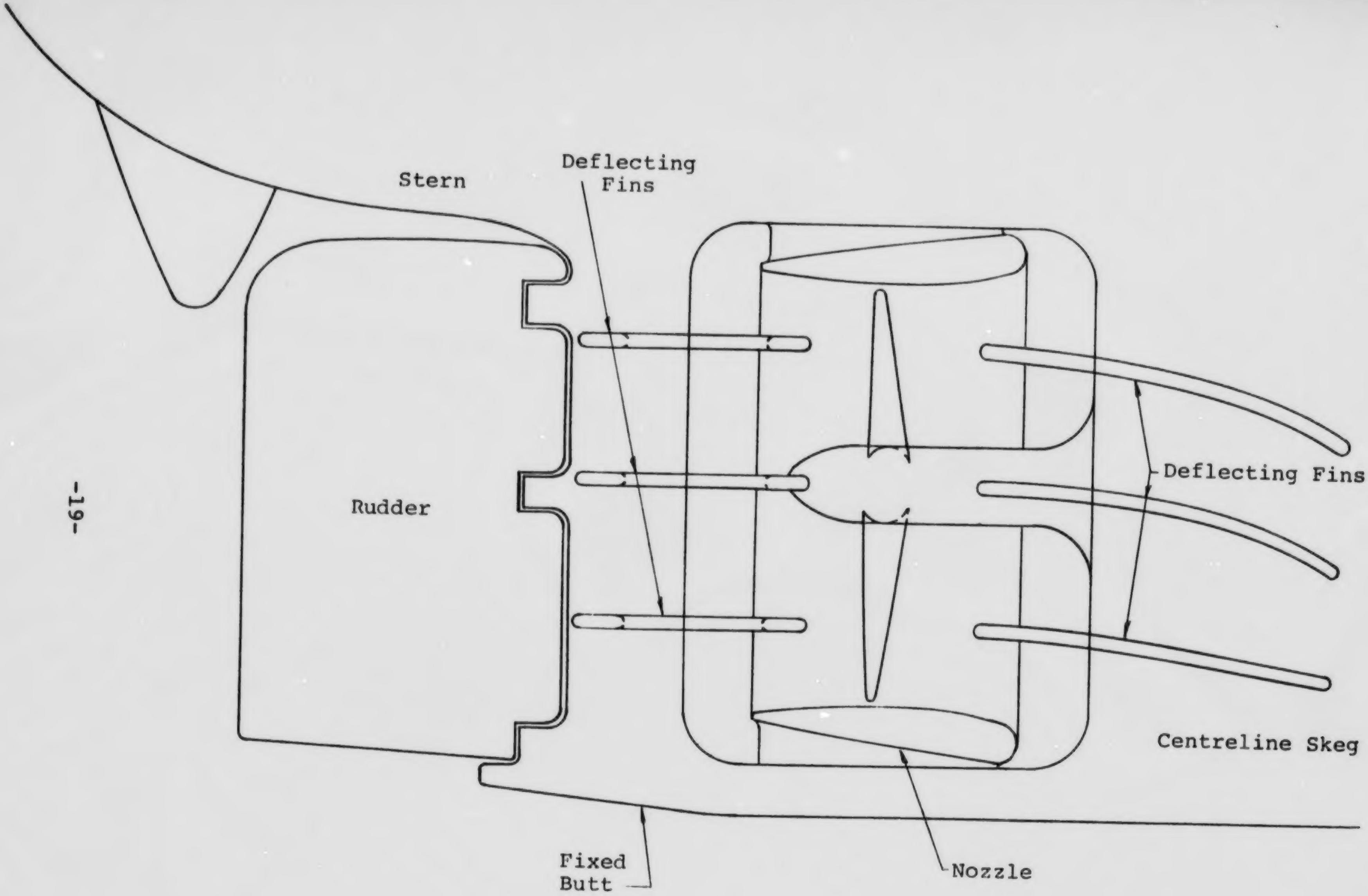
Stern
Deflecting Fins
Rudder
Deflecting Fins
Centreline Skeg
Fixed Butt
Nozzle

Fig. 7: Guards for Ducted Propeller on Single Screw Ship with Compound Rudder

In addition to the problems associated with fitting guards to wing screw nozzles, guarded nozzles are also susceptible to ice clogging. Ice pieces could be held against the deflecting fins of a guarded nozzle by the suction effect of the propeller, with a consequent loss in thrust. If these ice pieces became wedged between adjacent deflecting fins, they could be difficult to remove, particularly if the fins were at all barb-shaped in cross-section. If the edges of the deflecting fins were flush with the outside of the nozzle, as shown in FIG. 6, an ice block sliding along the fins could easily butt up against the leading edge of the nozzle as shown in Figure 8a. The nozzle leading edge, deflecting fins, and hydrodynamic forces created by the propeller inflow would prevent the ice block from moving backwards (for forward thrust), inwards and outwards respectively, so the block would assume a stable position. Other ice pieces would then butt up against the first piece, eventually blocking off most of the nozzle's inlet flow area. This problem could be alleviated to some extent by extending the fin edges past the outside of the nozzle, as shown in FIG 8b.

The suction forces in front of a ducted propeller can be reduced by making the nozzle outer diameter to propeller diameter ratio (D_{out}/D) as large as possible (ie, by using a thick duct), a practice which would also strengthen the duct. Some deterioration in the performance of the ducted propeller at low thrust loading (ie, high ship speeds) would be unavoidable, however. The likelihood of nozzle clogging can be further reduced by making the deflecting fins as long as possible (ie, by increasing the longitudinal distances between the fin attachment points on the nozzle and the attachment points on

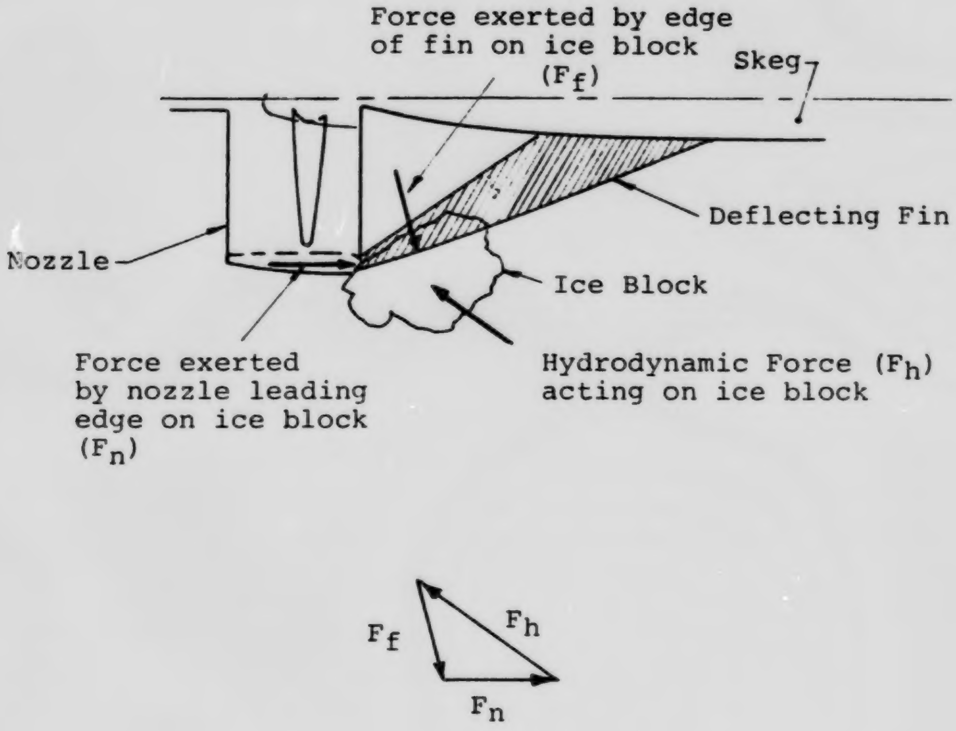
Force exerted by edge of fin on ice block (F_f)
Skeg
Deflecting Fin
Nozzle
Ice Block
Force exerted by nozzle leading edge on ice block (F_n)
Hydrodynamic Force (F_h) acting on ice block
F_f
F_h
F_n

Closed Force Polygon

Fig. 8a: Ice block held in place by nozzle leading edge, deflecting fins and propeller inflow.

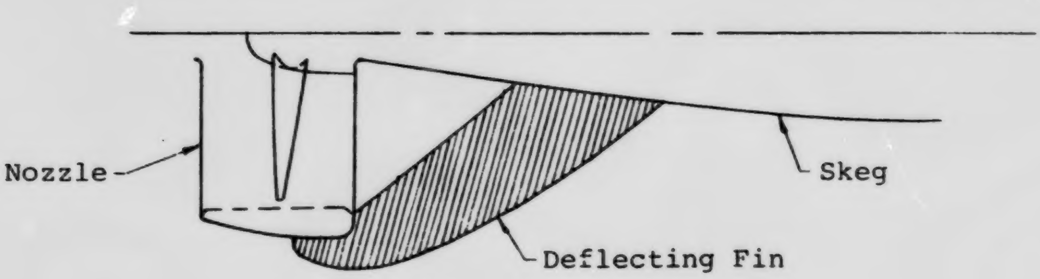
Nozzle
Skeg
Deflecting Fin

Fig. 8b: Modified deflecting Fin

the hull) since the fins will be more closely aligned with the flow entering the nozzle in this case. The allowable lengths of the fins at the rear of a nozzle are limited, however, by the requirement that the rudder butt (to which the fins are attached) be located directly behind the nozzle for maximum rudder effectiveness. It would be more difficult, therefore, to design deflecting fins with favourable anti-clogging characteristics for use at the rear of the nozzle.

2.7 Legal Restrictions on Use of Nozzle Concepts

Canadian patents are held on several nozzle-related devices. A summary of these patents is given in Table 1. All of the devices listed have been described previously.

TABLE 1

CANADIAN PATENTS ON NOZZLE - RELATED DEVICES

DEVICE	PATENT HELD BY	CANADIAN PATENT NO.
Kort nozzle	Ludwig Kort	396724
Nozzle with duct(s) extending from propeller to rear of nozzle	Herbert Monnich	735.219
Deflecting fins in front of Kort nozzle, as shown in Figures 6 and 7	Nils J. Liaaen	981.118

See Appendix B for more details about these classified patents.

3.0 RING PROPELLER

3.1 Description

A ring propeller has a rotating shroud attached to the blade tips, as shown in Figure 9. The shroud is aerofoil-shaped in cross-section and hence is similar to a rotating Kort nozzle. A ring propeller differs from a propeller contained within a Kort nozzle, however, in that leakage past the blade tips, and hence tip vortices, is completely eliminated. Also, the power required to rotate a ring propeller is increased by viscous drag on the ring. The latter factor causes the optimum diameter of the ring propeller for a given application to be lower than that of a propeller in a Kort nozzle. Performance curves for a ring propeller produced by LIPS B.V. (7) are shown in Figure 10. Figure 10a shows a comparison with the Wageningen B4-55 series and the K_a 4-55 series in nozzle 19A. It may be concluded that at given power, rotational speed and intake velocity, the optimim diameter of a ring propeller is about 30% less than that of a conventional one, and the open water efficiency is considerably lower than both the conventional and the ducted propeller. The reason for lower optimum diameter of the ring propeller is the substantial additional drag acting on the rotating nozzle. According to axle momentum theory the propulsion device with a lower diameter may be expected to have inferior efficiency. However, it is claimed in the same reference (7) that fitting of the ring propeller to a ship has resulted in better propulsion performance. The overall propulsive efficiency was approximately 5% higher than with the original conventional propeller despite the model tests which showed lower open water efficiency. Apparently there must have been favourable effects on the wake distribution and on the hull efficiency.

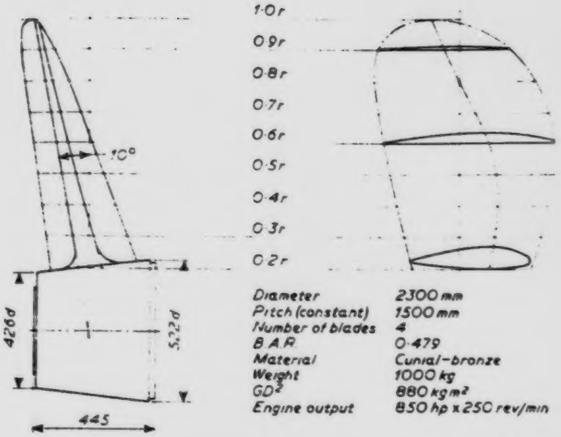
1·0r
0·9r
0·8r
0·7r
0·6r
0·5r
0·4r
0·3r
0·2r
10°
426d
522d
445

Diameter	2300 mm
Pitch (constant)	1500 mm
Number of blades	4
B.A.R.	0·479
Material	Cunial-bronze
Weight	1000 kg
GD^2	880 kgm²
Engine output	850 hp x 250 rev/min

Conventional Propeller of 850 HP coaster

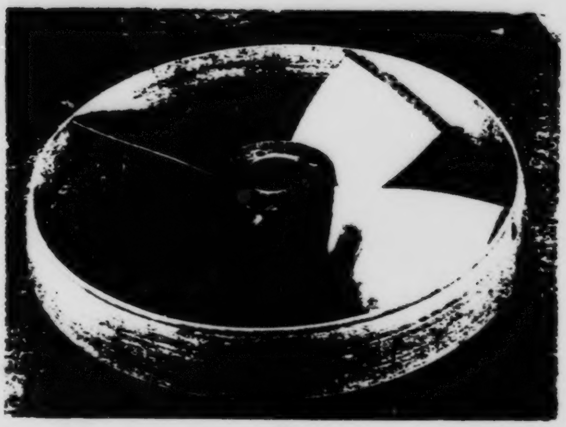

Ring Propeller
after manufacturing

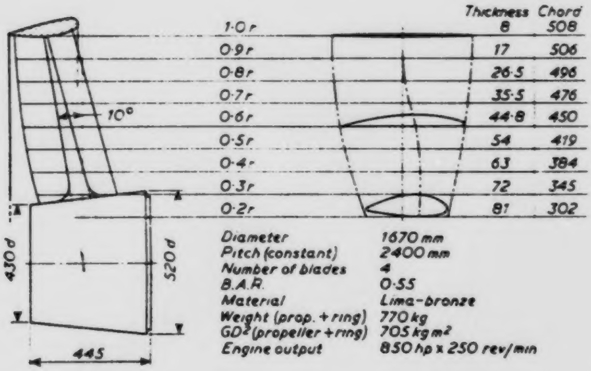
10°
430d
520d
445

	Thickness	Chord
1·0r	8	508
0·9r	17	506
0·8r	26·5	496
0·7r	35·5	476
0·6r	44·8	450
0·5r	54	419
0·4r	63	384
0·3r	72	345
0·2r	81	302

Diameter	1670 mm
Pitch (constant)	2400 mm
Number of blades	4
B.A.R.	0·55
Material	Lima-bronze
Weight (prop. + ring)	770 kg
GD^2 (propeller + ring)	705 kgm²
Engine output	850 hp x 250 rev/min

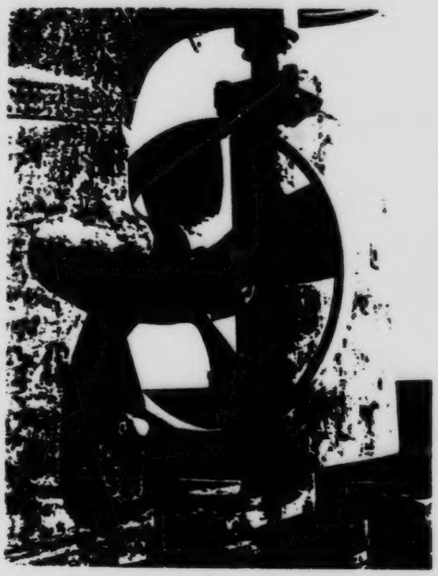

Ring Propeller of 850 coaster

Fig. 9: Ring Propeller

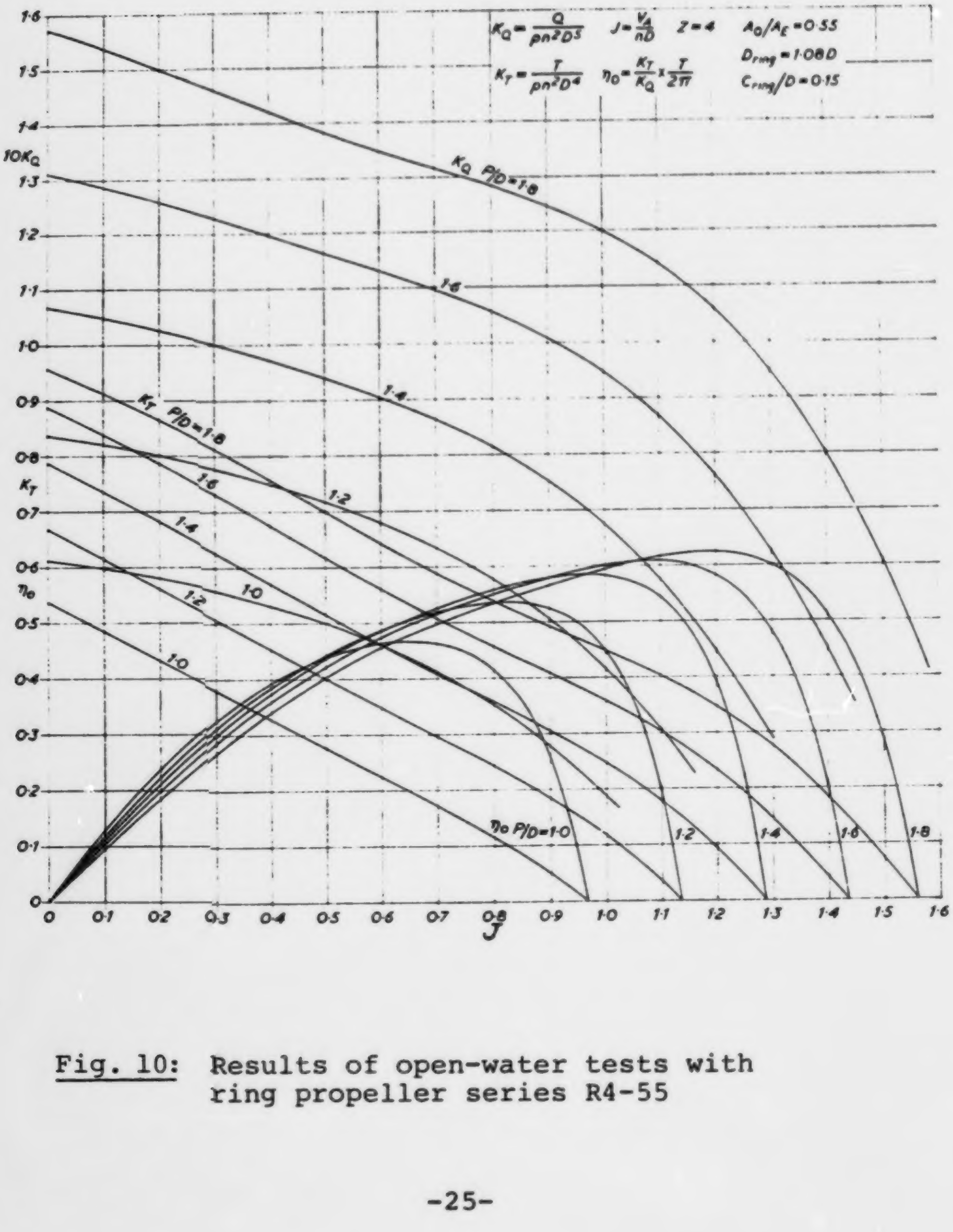

Fig. 10: Results of open-water tests with ring propeller series R4-55

Ring Propellers

Comparison of the B4-55 series without nozzle and the Ka4-55 series in nozzle 19A with the ring propeller series R4-55

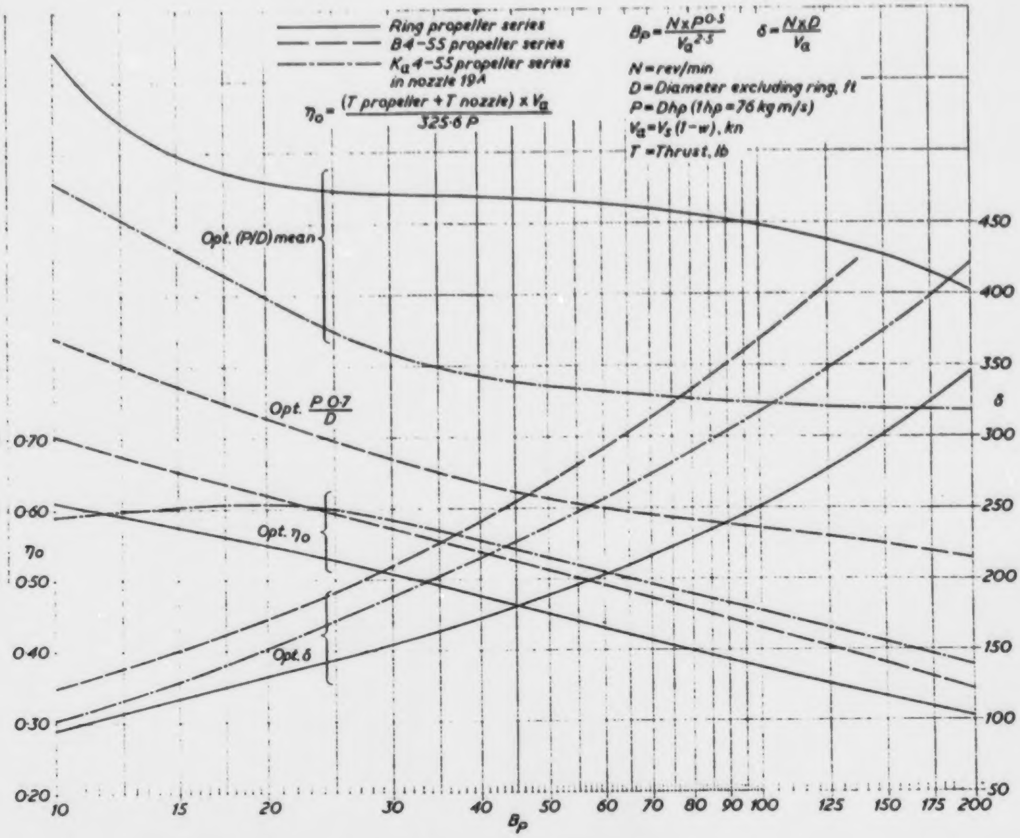

Figure 10a —*Optimum diameter at given intake velocity— power and rotational speed*

3.2 Ring Propeller In Ice

In order to keep the weight and polar moment of inertia of a ring propeller close to the corresponding values for a conventional propeller, the ring itself must be made as light as possible. For this reason, LIPS has developed a ring which consists of foamed plastic encased in a steel sheath. Earlier rings were fabricated entirely from reinforced plastic. It is unlikely that even the steel-encased ring would survive impacts with large ice floes or the intact ice sheet. Failures would probably occur at the ring/propeller attachment points, since these are particularly weak areas (7). The chord/diameter ratio of a ring is typically made much smaller than the chord/diameter ratio of a nozzle in order to reduce viscous losses caused by the ring's rotation. The cross-sectional area, and hence strength, of the ring are proportionately reduced.

From the foregoing, it is evident that a ring propeller is more vulnerable to ice damage than is a propeller in a stationary nozzle. Guards are easily attached to the front and rear of a stationary nozzle to prevent the ingestion of ice pieces, so a nozzle is superior to a rotating ring in this respect also. In addition, use of a ring propeller makes a reversible propulsion system mandatory. In view of the disadvantages of a ring propeller compared to a propeller in a stationery nozzle, ring propellers will not be considered further.

3.3 Partial Ring (Schnitger) Propeller

A partial ring propeller, such as the German Schnitger shown in Fig. 11, has a ring (shroud) attached to the propeller at mid-radius. According to van Gunsteren (7), a partial ring has very little control over the flow entering or leaving a propeller and therefore is of little use for modifying the propeller's performance characteristics. A partial ring strengthens a propeller, however, so it might be a worthwhile addition to an icebreaker's screw for this reason. The ring would also reduce ice milling loads under certain circumstances. A disadvantage of the partial ring propeller is that large ice pieces could become jammed between the ring and the propeller hub, thereby reducing thrust. These blockages could occur under forward or reverse thrust conditions. A further disadvantage of this type of propeller is that its use makes a reversible propulsion system mandatory.

It is apparent therefore that a partial-ring propeller offers few, if any, advantages over the conventional ice-strengthened screw for icebreaking service. The risk of ice blockages developing due to the presence of the ring makes this type of propeller particularly unattractive.

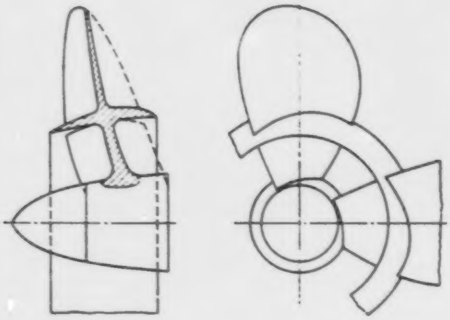

Fig. 11: Schnitger Propeller

4.0 DEFLECTING FINS

4.1 Bossing Fins

Bossing fins are, as the name implies, simply deflecting fins affixed to a shaft bossing for the purpose of deflecting objects (ice pieces) away from the propeller. Bossing fins are shown in Fig. 12. These fins do not provide any protection for the propeller during astern operation and could become clogged with ice during applications of reverse thrust. Ice pieces could conceivably become wedged between the rearward ends of the fins and the propeller, causing damage to the propeller. According to Enkvist et al.(5), bossing fins can reduce ice milling loads by limiting the depth of cut. They do not, of course, prevent ice milling. If designed to conform with the streamlines of the flow approaching the propeller, bossing fins should have negligible drag.

A model of the USCG Polar Star was tested with bossing fins in order to evaluate the effectiveness with which they could remove ice from the propeller inflow during foward operation. The bossing fins proved to be almost totally ineffective as propeller protective devices in those tests (6). The frequency of ice impacts with the center screw was, in fact, higher with the bossing fins fitted than without them.

4.2 Fins On Skeg

Deflecting fins fitted to the centerline skeg of a single-screw vessel, as shown in Fig. 13, are expected to have advantages and disadvantages similar to those described previously for bossing fins. Since a centerline skeg extends the full depth of a propeller, deflecting fins on a skeg provide more protection against ice damage than fins on a bossing. Skeg-mounted deflecting fins are widely used on vessels of Norwegian design.

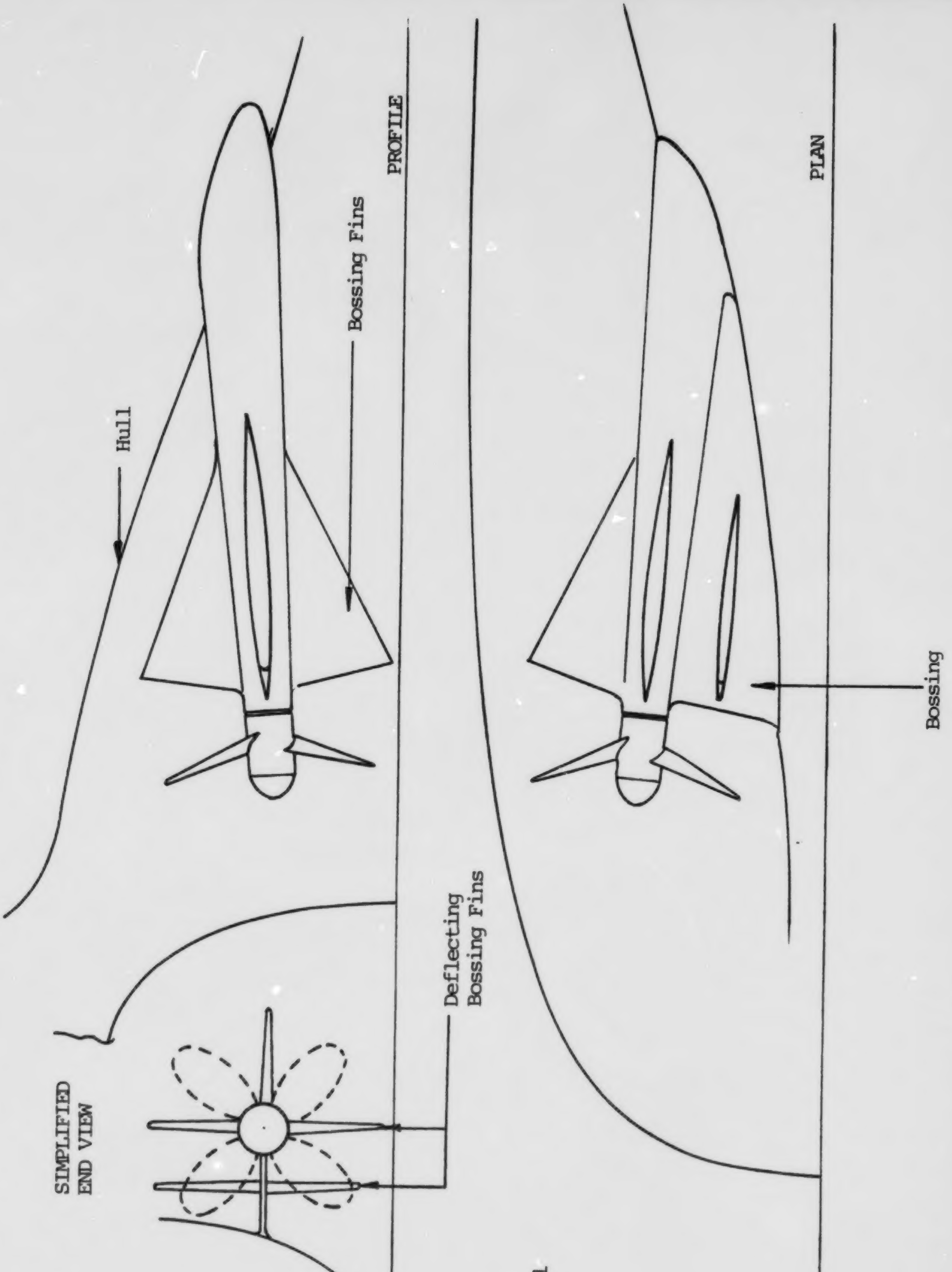
PROFILE
PLAN
Bossing Fins
Hull
Bossing
SIMPLIFIED END VIEW
Deflecting Bossing Fins
Shell

Fig. 12 - Bossing Fins

As discussed in Section 2.6, a combination of deflecting fins and, say, a strong double flared nozzle could provide propeller protection for single and multi-screw ice class vessels. In general, however, deflecting fins, as a propeller protective device, have a limited usefulness.

4.3 Legal Restrictions on the Use of Skeg and Bossing-Mounted Deflecting Fins

A patent for skeg-mounted deflecting fins is held by Nils Liaaen. The patent does not actually stipulate that the fins are attached to a skeg but, instead, describes the fins as being attached to the hull. Thus the patent may also apply to bossing fins. The appropriate Canadian patent number is 509.171.

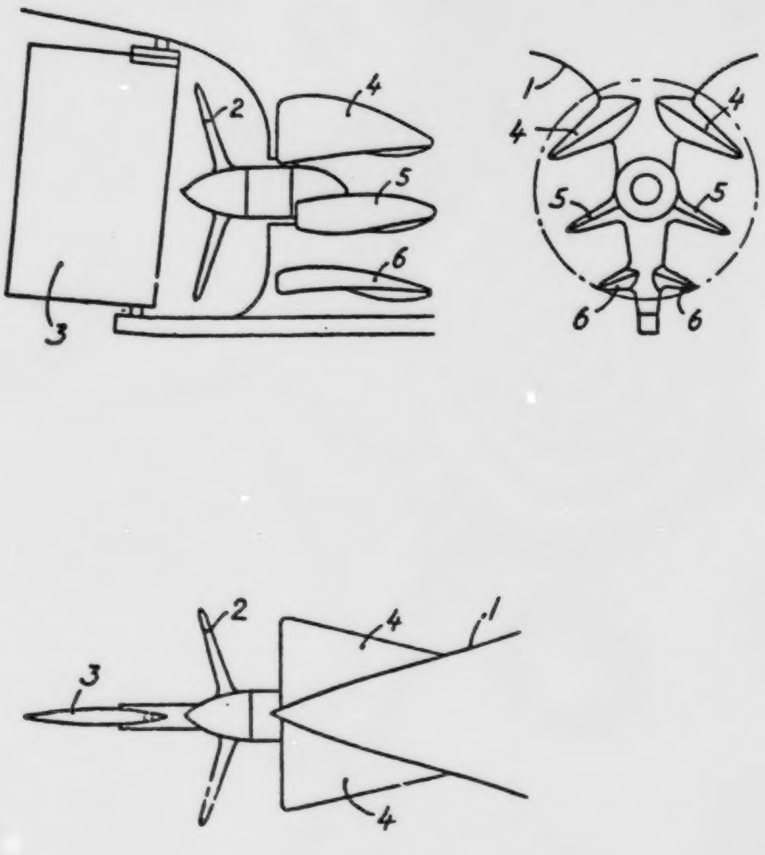
4
2
5
6
3
1
4
4
5
5
6
6
2
4
1
3
4

Fig. 13: Deflecting Fins on Skeg

5.0 BILGE KEELS

Bilge keels, as shown in Fig. 14, shield propellers to a certain extent by preventing ice from sliding along the sides of a hull toward the propellers. They do not, of course, prevent ice milling or protect the propellers while backing up. Nevertheless, tests of the USCG Polar Star, fitted with bilge keels, showed that the keels markedly reduced the frequency of propeller/ice collisions during forward operation. Small bilge keels (10 inches wide) appeared to be more effective than large bilge keels (40 inches wide). It is possible that bilge keels could increase the icebreaking resistance of an icebreaker substantially under certain conditions (eg., while ramming through thick ridges) so they would not appear to be desireable additions to an icebreaker hull. This observation requires experimental verification. In any event, bilge keels, in isolation, do not provide the degree of propeller protection required in this study and hence will not be considered further.

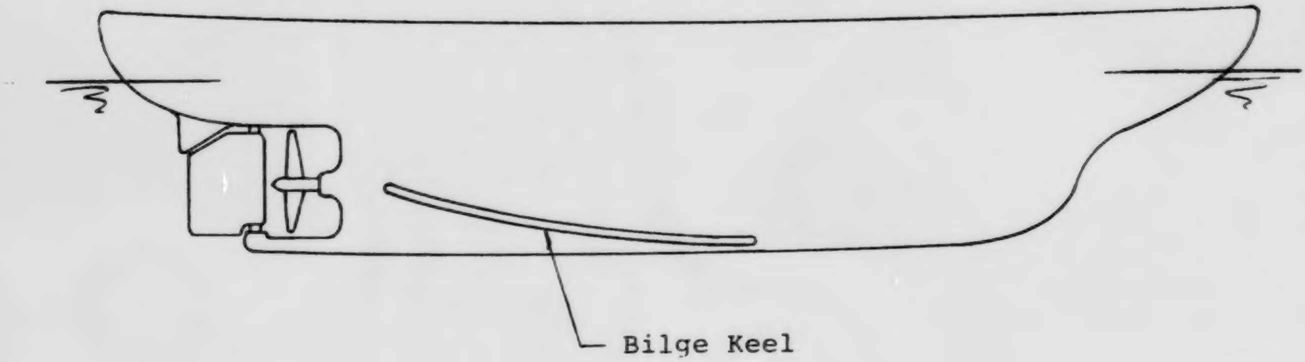

Fig. 14: Bilge Keel

6.0 PROPELLER CAGE

A propeller cage (or bird cage) is simply a cage surrounding a propeller for the purpose of preventing the ingestion of objects (ice pieces) by the propeller. Bird cages were fitted to the wing propellers of a model of the USCG Polar Star, as shown in Fig. 15 and tested in the CRREL ice tank (6). The cages were tested with the model advancing through the ice and hence were left open at their aft ends. The apertures in the cages measured approximately 0.2D in the transverse direction and 1.5→2D in the longitudinal direction (D is the diameter of a wing propeller). In order for an ice piece to pass through the cage, it would have to be smaller than this aperture size in two dimensions. The results of the tests indicated that the cages reduced the frequency of propeller ice impacts slightly, although not enough data was recorded to prove this beyond doubt. It is worth mentioning that a slight reduction of propeller ice impacts should not be considered as a promising result since one or two successive impacts might be enough to result in propeller damage.

It is not likely that a well-designed, large cage would clog with ice over enough of its area to significantly reduce thrust. A small cage, on the other hand, with grillage located in regions where the suction effect of the propeller is large, would be susceptible to clogging. The number of transverse members in a cage should be kept to an absolute minimum since these members would interfere with the passage of ice pieces past the cage.

It is felt that the drag of a bird cage would probably be unacceptably high if the cage was designed with sufficient structural strength to withstand collisions with large ice floes, or worse still, with the intact ice sheet. The requirement of robustness conflicts with the desired characteristic of low drag. If some of the apertures in the cage, particularly those near the hull/ cage attachment points, were sealed off as shown in Fig. 16 with steel plate in order to increase the strength of the cage, the "cage" would, in fact, become a partial tunnel. Since these apertures, which are nearest the waterline, are the ones most

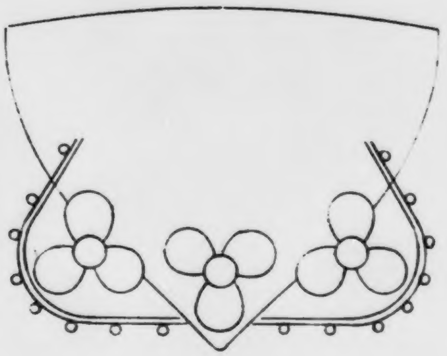

a. Stern view

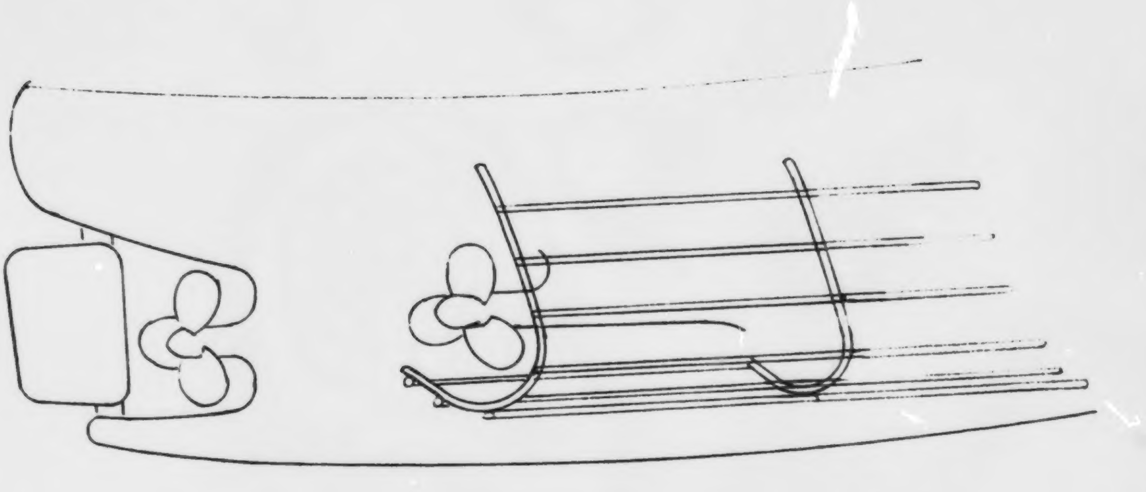

b. Starboard quarter view

Fig. 15: Bird cages on USCG POLAR STAR

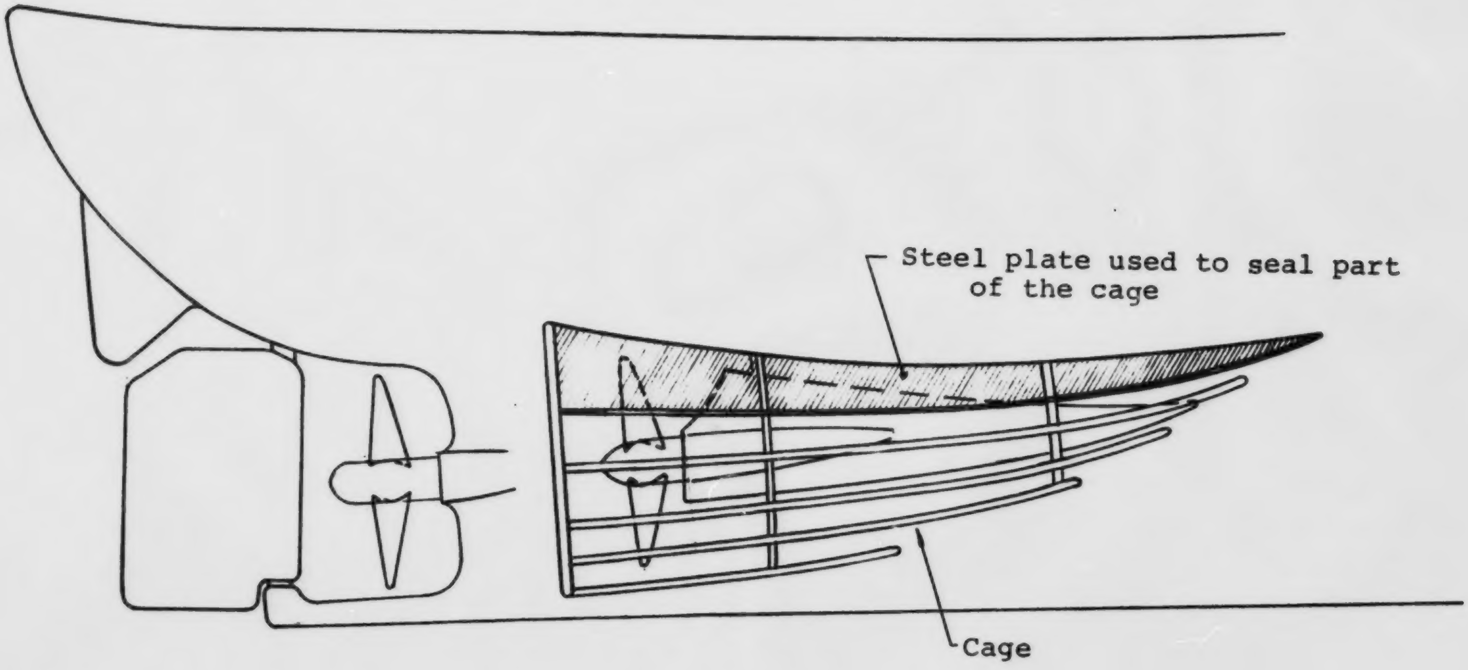
Steel plate used to seal part of the cage
Cage

Fig. 16: Bird Cage with upper openings sealed off

likely to admit ice or become clogged, closing them off would be advisable. This would increase the thrust deduction slightly even though the added plate would have a very small projected area in the transverse direction. A cage can, therefore, be regarded, loosely, as the framework for a tunnel. Partial tunnels and closed tunnels (ducts) are discussed in Sections 7.0 and 8.0 respectively.

7.0 OPEN (PARTIAL) TUNNELS

7.1 Description

As mentioned in Section 6.0, bird cages can be transformed into partial tunnels by closing off the uppermost apertures in the cages with steel plates, as shown in Figure 16. The loss of inlet flow area would cause the flow velocity, and hence the pressure reduction (i.e., suction effect) over the hull surface in front of the propeller(s) to increase slightly. Any attempt to build up the hull in front of the propeller(s) in order to form a more complete tunnel would reduce the fineness of the hull in that region, causing an increase in thrust deduction.

Most of the preceding remarks could be directed toward the partial tunnel design usually referred to as an arch-stern. Since the arch-stern configuration does not require that the hull have fine lines in front of the propeller, it is a design that is readily adapted to multi-screw vessels. Probably the most significant advantage of the arch-stern, that of being able to use a large propeller, is one which would probably be difficult to exploit fully on a multi-screw vessel, however. This point is discussed further in the next section.

The hull in front of a propeller can be hollowed out to form a more complete tunnel, as shown in Figure 17 (taken from (8)). If the tunnel area in front of a propeller is made as large as possible, preferably greater than the propeller disc area, thrust deduction will be minimized. It is difficult, however, to obtain values of thrust deduction that are as low as the values obtainable with open screw on single-screw vessels (8). This disadvantage is offset, to some extent, by the fact that the submergence of a propeller in a tunnel (partial or closed)

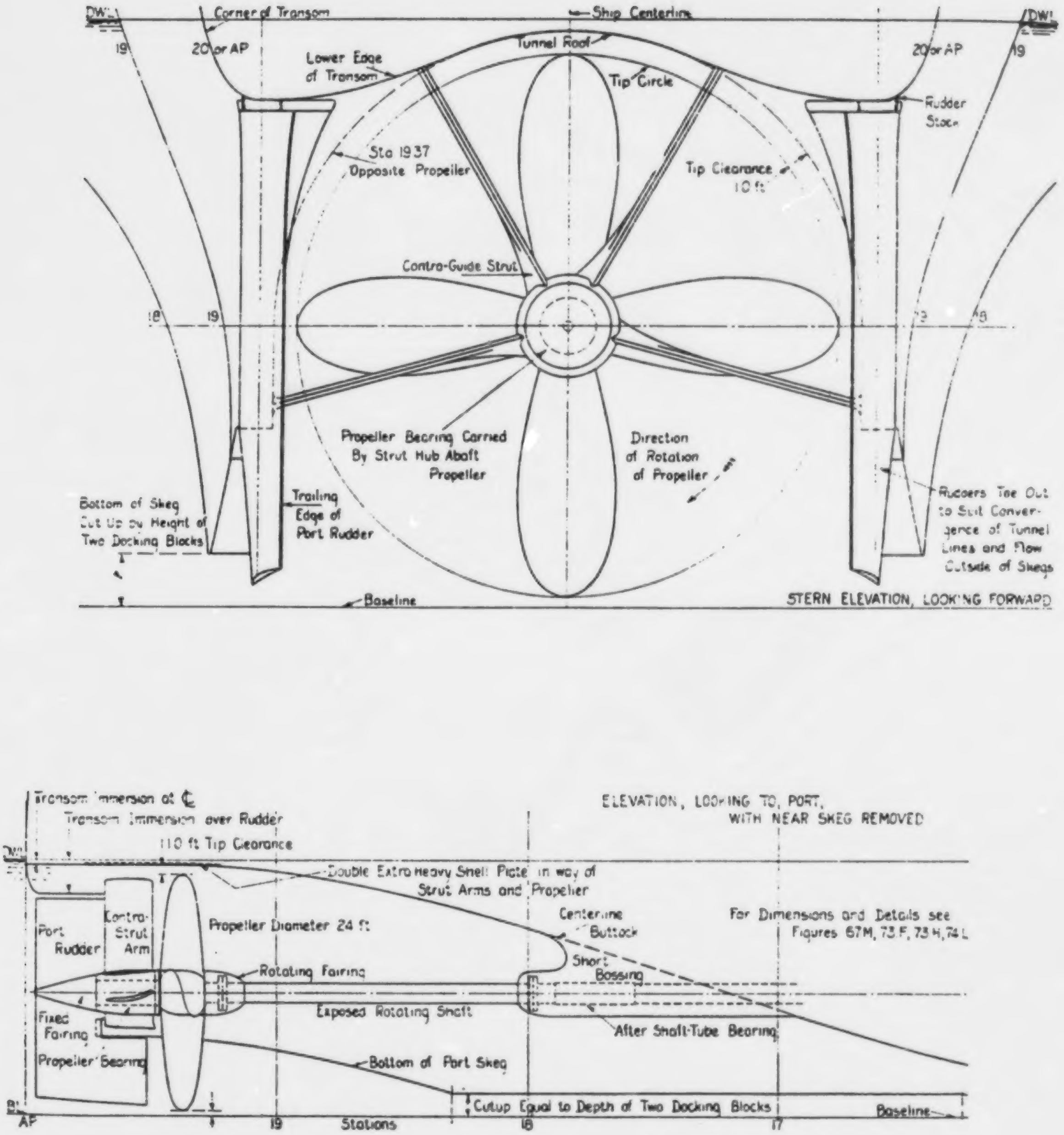
DWL
Corner of Transom
Ship Centerline
DWL
19
20 or AP
Tunnel Roof
20 or AP
19
Lower Edge of Transom
Tip Circle
Rudder Stock
Sta 19.37 Opposite Propeller
Tip Clearance 1.0 ft
Contra-Guide Strut
18
19
19
18
Propeller Bearing Carried By Strut Hub Abaft Propeller
Direction of Rotation of Propeller
Bottom of Skeg Cut Up by Height of Two Docking Blocks
Trailing Edge of Port Rudder
Rudders Toe Out to Suit Convergence of Tunnel Lines and Flow Outside of Skegs
Baseline
STERN ELEVATION, LOOKING FORWARD
Transom Immersion at ℄
Transom Immersion over Rudder
1.0 ft Tip Clearance
ELEVATION, LOOKING TO PORT, WITH NEAR SKEG REMOVED
DWL
Double Extra Heavy Shell Plate in way of Strut Arms and Propeller
Port Rudder
Contra-Strut Arm
Propeller Diameter 24 ft
Centerline Buttock
For Dimensions and Details see Figures 67M, 73F, 73H, 74L
Short Bossing
Rotating Fairing
Exposed Rotating Shaft
Fixed Fairing
After Shaft-Tube Bearing
Propeller Bearing
Bottom of Port Skeg
BL
AP
19
Stations
Cutup Equal to Depth of Two Docking Blocks
18
17
Baseline

Fig. 17: Elevation and profile views of stern with partial tunnel (arch stern)

does not need to be as great as that of an open propeller since the tunnel, which starts well below the waterline, will be full of water even if the top of the propeller extends above the waterline (for forward operation anyway). This permits a large propeller to be used, with its high ideal efficiency, and/or allows the propeller to be located closer to the waterline, where the wake fraction is higher, thus increasing its efficiency.

Since the hull encloses the propeller, the propeller bearing can easily be located aft of the propeller. The bearing support struts, for the arrangement shown in Figure 17, are designed to remove some of the swirl from the propeller outflow, thereby increasing the propeller efficiency.

In addition to being able to operate a propeller in a region of higher wake, a tunnel offers an additional advantage in that the wake distribution at the propeller is more uniform than the distribution behind a skeg, for example. Also, since a propeller in a tunnel is surrounded by the hull over an appreciable part of its circumference, the tip clearance between the propeller and the hull can be made fairly small, causing the propeller to induct most of the boundary layer on the tunnel wall. This causes the average wake fraction at the propeller disc, and hence the propeller efficiency, to be further increased. On the other hand, such a design could involve consequential problems such as cavitation erosion, vibration and noise radiation as a result of using a large propeller with a small tip clearance.

A partial-tunnel stern developed by Burmeister and Wain (B & W)(14) is shown in Figure 18. As can be seen it has fairings on either side of a propeller mounted behind a centerline skeg. The fairings enclose the upper half of the propeller and allow a small tip submergence, and hence a large propeller, to be used without risk of air suction. The propeller efficiency is increased so much by the use of a large propeller that a high propulsive efficiency is obtained even though the hull efficiency suffers somwhat with the partial tunnel. It should be mentioned that the performance, and hence success, of a partial tunnel is a strong function of how it is implemented (i.e., of the details of the design). Experience with these designs is lacking, so any new design must undergo considerable development. B & W, for example, conducted a large number of windtunnel and towing tank tests on their partial tunnel before they finalized the design.

A disadvantage of partial tunnel designs is their poor backing performance, which stems from the fact that the small, or even negative, propeller submergence typical of these designs causes air to be sucked into the propeller during astern operation. This problem can be eliminated by designing the tunnel such that its roof slopes downward aft of the propeller and terminates below the waterline. Such a design is shown in Figure 19. The downward slope of the tunnel roof aft of the propeller reduces the available thrust and the propulsive efficiency during forward operation. Flaps which allow the slope of the tunnel roof aft of the propeller to be varied, have frequently been applied to vessels with tunnel sterns in order to overcome these difficulties. A tunnel with a flap is shown in Figure 20 and it is best suited for clear water operations in shallow waters.

7.3 Suitability of Open Tunnel Sterns for Icebreakers

A propeller in a partial tunnel would have to be surrounded by a cage in order to prevent the ingestion of ice pieces. If the tunnel walls extended below the bottom of the propeller, ice milling would be virtually eliminated even without a cage.

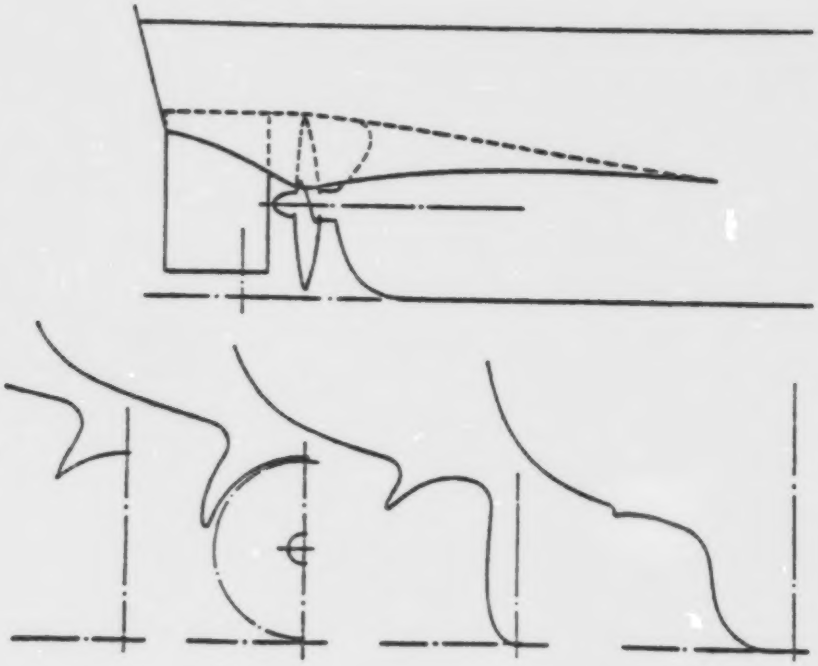

Fig. 18: B & W Stern with semi-duct

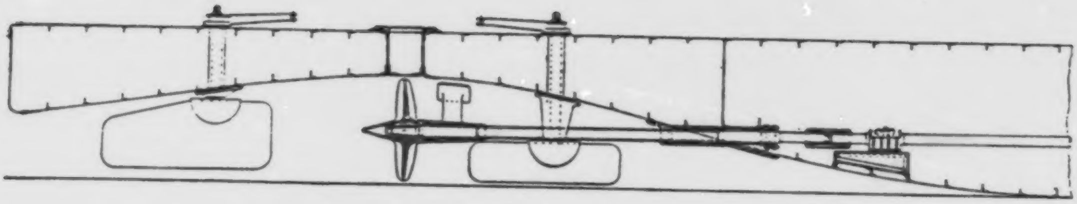

Fig. 19: Tunnel Stern

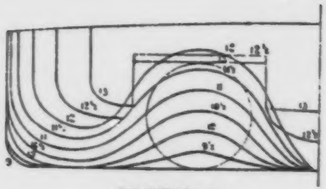

SECTIONS.

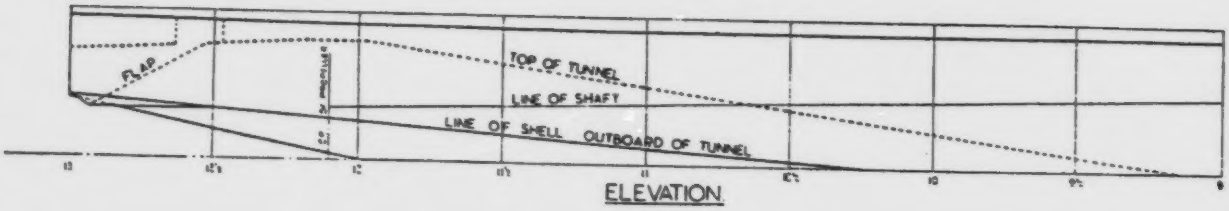
FLAP
TOP OF TUNNEL
LINE OF SHAFT
LINE OF SHELL OUTBOARD OF TUNNEL

ELEVATION.

Fig. 20: Tunnel with Yarrow flap abaft propeller

Collisions between the propeller and the intact ice sheet would also be eliminated. If the tunnel's intake flow area, and hence the area covered by the cage, was large, ice blockages would probably not occur. This observation requires experimental verification, however.

The most serious drawback of a tunnel stern relates to its poor backing characteristics. If a large propeller with small tip submergence is used in order to achieve a high propeller efficiency, the astern thrust will be less than the forward thrust for the reasons given in the previous section. A flap behind the propeller (see Fig. 20) does not appear attractive for an icebreaker since it could be damaged, or at least jammed, by ice. Probably the only practical solution for the problem of poor backing performance would be to maintain an adequate tip submergence and tolerate the associated reduction in propulsive efficiency. Since icebreakers are deep draught vessels, the requirement that an adequate propeller submergence be maintained may not be unduly restrictive. On triple-screw vessels the beam available for accomodating three propellers will probably limit the allowable propeller sizes in any event, particularly if the screws are not overlapped. Overlapping is probably best accomplished by locating the wing screws ahead of, and above, the center screw, as shown in Fig. 21. The outboard sides of the wing screws shown in that figure are covered by fairings, both to prevent air suction and also to shield the propellers, to a certain extent, from ice. The center screw is also partially enclosed by fairings to keep it from ingesting the wakes of the wing screws and, in addition, to provide protection against ice. Cages would have to be installed to provide complete protection for the propellers.

In conclusion, partial tunnels appear to offer a reasonable level of protection for propellers along with the possibility of high propulsive efficiency. Several basic designs are possible, particularly for a triple-screw vessel, but the succes of any one design will be a strong function of the details of that design, as mentioned previously.

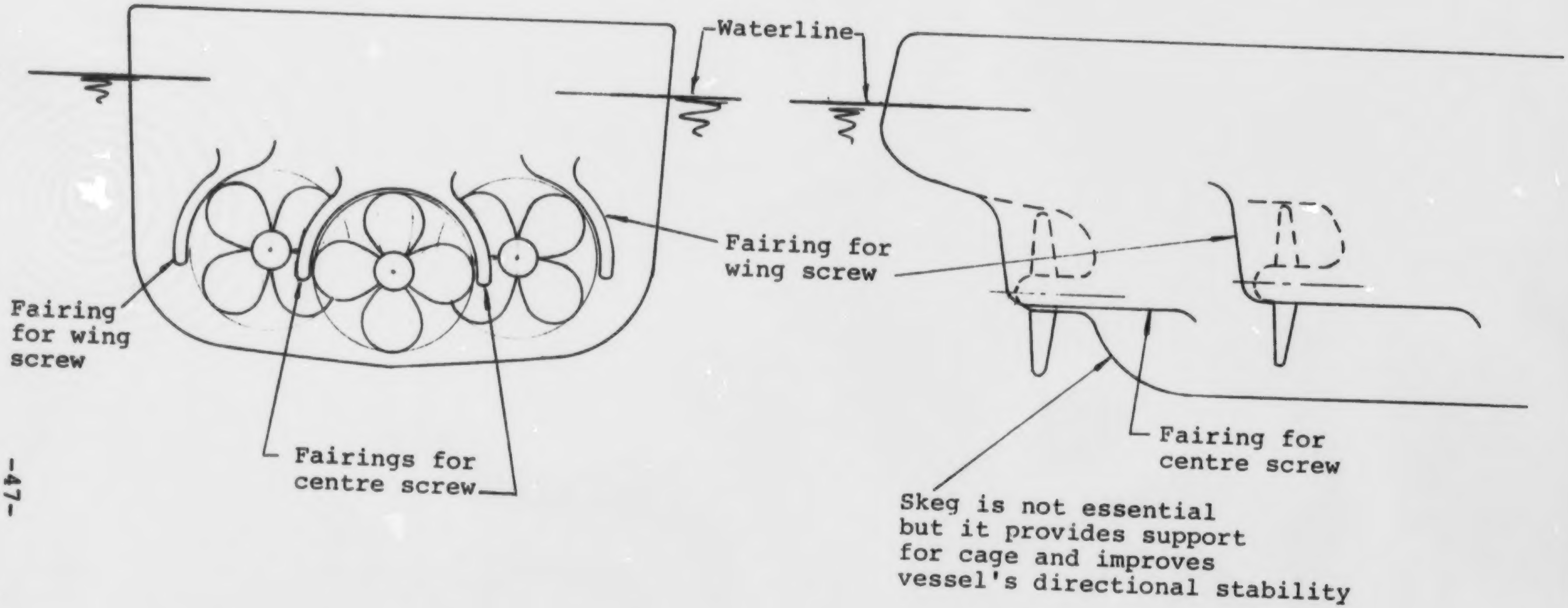
Waterline
Fairing for wing screw
Fairing for wing screw
Fairings for centre screw
Fairing for centre screw
Skeg is not essential but it provides support for cage and improves vessel's directional stability

Fig. 21: Overlapping screws in partial tunnels on triple screw vessel

8.0 IN-HULL PROPULSION SYSTEMS

8.1 Description

In-hull propulsion systems, where the duct is located inside the ship's hull, range from Kort-Nozzles countersunk into partial tunnels to water jet propulsion devices of the types used on some hydrofoils, life boats and high speed crafts.

8.2 Closed Tunnels

These can be created by closing-in the bottom of a partial tunnel (Fig. 17) or a semi-duct (Fig. 18) at the propeller position with an aerofoil-shaped section (i.e., a segment of a Kort nozzle). If this is done, the propeller/hull tip clearance can be made as small as is practical from a fabrication viewpoint in order to reduce induced drag on the propeller blades. A disadvantage stems from using a small tip clearance in this instance, however, in that the loading of the blade tips will vary substantially as they travel from the top of the tunnel, where they presumably pass through a relatively thick boundary layer, to the bottom of the tunnel where the flow is accelerated by the shroud segment and the boundary layer is of smaller thickness. The circumferential variation in blade tip loading may be greater under these conditions than it would be without the shroud at the bottom of the tunnel, and objectionable vibrations may be increased. This effect could perhaps be mitigated by extending the leading edge of the bottom of the tunnel (i.e., the shroud) segment several propeller diameters in front of the propeller in the hope that the circumferential velocity variation at the propeller disc would be reduced further as a result of a thicker boundary layer being developed on the inside surface of the tunnel bottom. The regular arch-stern with a short shroud segment covering the bottom of the propeller is shown in Figure 22 and the modified stern with a much longer tunnel but the same intake area and intake length is shown in Fig. 23. The only additional losses arising from the use of the longer tunnel are frictional losses due to the increased wetted wall area. It is also apparent that the longer the fully enclosed part of the tunnel is made, the smaller will be the circumferential variation in axial velocity at the propeller position. Unfortunately, the tunnel arrangements shown in Figures 22, and 23, for single-screw vessels have some obvious disadvantages. Firstly, it requires a prohibitively long exposed rotating shaft. Secondly, the tunnel occupies a great deal of space in the ship's hull and reduces the displacement volume at the rear of the ship. The latter disadvantage, and its effect on vessel trim, would be offset to some extent by the fact that the propulsion machinery would be located further forward in the hull than it would normally be. If the tunnel was split in front of the propeller to make room for the propulsion machinery, an arrangement similar to the YPASS system tested by Edwards and Allan (9) would be obtained (this system will be discussed later in detail in Section 8.3). The tunnel arrangement shown in Figure 22 seems to be quite adaptable for the wing propellers in a twin-screw vessel.

If three tunnels similar to the one shown in Figure 23 were placed side-by-side and separated by thin skirts to obtain a triple-screw configuration, the wake variation at the wing propellers may be greater than that found at the propeller of a single-screw design. The flow through a wing intake would be asymmetrical about its longitudinal centerline since the flowrate through the side of the wing intake bordering on the intake for the center screw would be higher than that through the other side. If the intake areas were made sufficiently large, however, the flow asymmetry would probably have an inconsequential effect on the wake variations at the wing propellers.

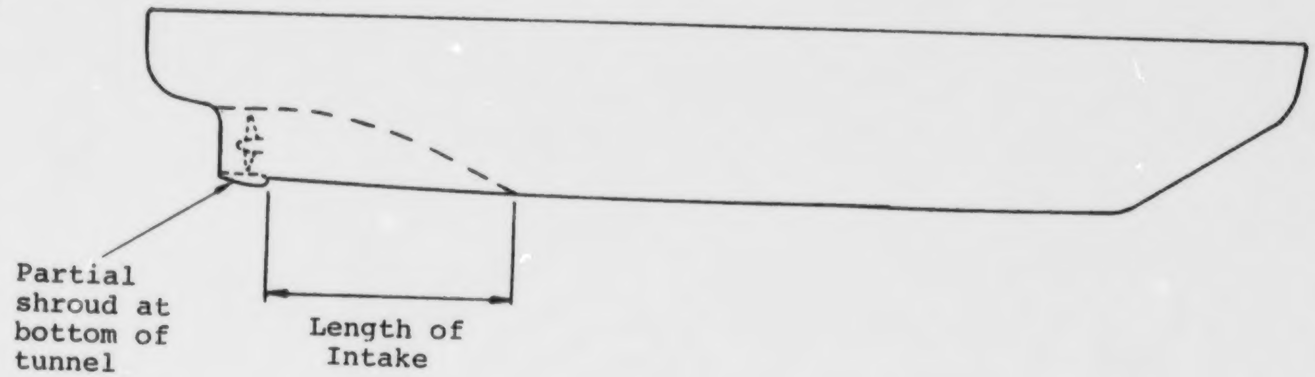
Partial shroud at bottom of tunnel
Length of Intake

Fig. 22: Stern with short tunnel

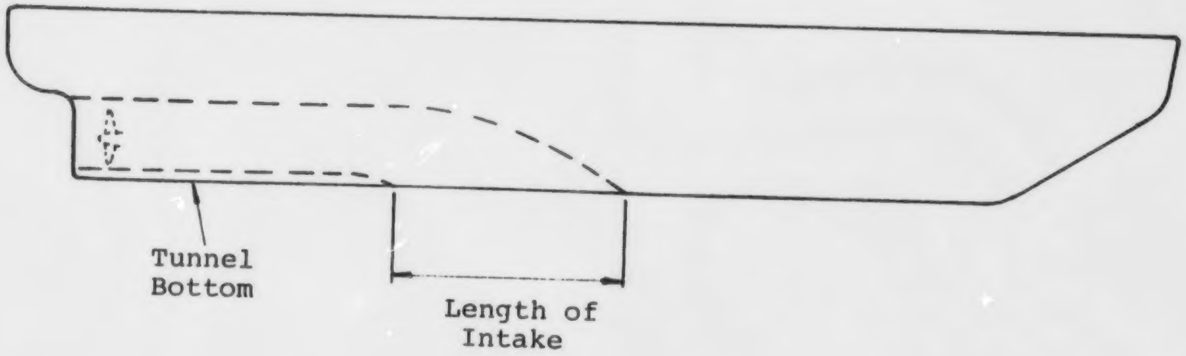
Tunnel Bottom
Length of Intake

Fig. 23: Stern with long tunnel

If an enclosed tunnel, such as that shown in Fig. 22 or Fig. 23, is designed to accelerate the propeller inflow in front of the propeller and prevent contraction of the jet abaft the propeller, the ideal characteristics (as obtained from momentum theory) of the resulting propulsion system will be similar to those of an accelerating ducted propeller (i.e., Kort-Nozzle). In particular, part of the total thrust of the system will be produced by the tunnel, so the propeller loading will be reduced accordingly. From energy and momentum considerations, it can be shown that the thrust on the hull will, ideally, equal the propeller thrust at bollard (i.e., one half of the total thrust will be produced by the hull). The actual thrust on the hull is, in fact, lower than the ideal value because of wall friction forces and inlet and exit losses. The inlet and friction losses are greater for an in-hull propulsion system with an intake that is flush with the bottom or side of the hull than they are for a Kort nozzle, so the performance characteristics of the latter should probably not be used to estimate the characteristics of the in-hull system, even if that system operates at the same diffusion coefficient (K_d)*, (a measure for the propulsive efficiency). The torque coefficient (K_Q) for the Kort nozzle should definitely not be used to calculate the torque coefficient for an in-hull propulsion system with a bottom or side intake since, while the ideal thrusts for the propeller/nozzle combination (T_k) and the in-hull system (T_H) are the same for the same mass flow rate (m) (i.e., $T_k = T_H = m(V_d - V_o)$), the hydraulic powers required to produce these thrusts are not the same. In the case of the Kort nozzle, the hydraulic power (P_{H_K}) added to the fluid is:

$$P_{H_K} = \frac{m}{2} (V_d^2 - V_o^2)$$

---

* $K_d = 1 - (\frac{V_d}{V_o})^2$, where V_d is the velocity far behind the propeller and V_o is the free stream velocity

while in the case of the in-hull system shown in Fig. 24, the hydraulic power (P_{H_H}) is:

$$P_{H_H} = \frac{m}{2} (V_d^{\,2} - (V_o \cos \theta)^2)$$

Thus if $\theta = 30^o$, then $P_{H_H} - P_{H_K} = \frac{m}{8} V_o^{\,2}$. Hence, an in-hull propulsion system with $\theta = 30^o$ would require $mV_o^{\,2}/8$ more power (ideally) than a Kort nozzle to produce the same thrust. The worst case obviously occurs when $\theta = 90^o$, in which case $P_{H_H} - P_{H_K} = \frac{m}{2} V_o^{\,2}$. A Kort nozzle and an in-hull propulsion system require the same power (ideally) to produce the same thrust at bollard condition, i.e., $V_o = 0$.

Entrance and exit separation losses are strong functions of inlet and discharge aperture designs. A low-loss discharge nozzle should have parallel walls to reduce separation losses, while a low-loss intake should be bellmouth-shaped (as found on a Kort nozzle). Departing from these ideal designs increases entrance and exit losses sharply unless measures, such as those used with the slotted nozzle (see. Section 2.2) are taken to prevent flow separation. Entrance and exit losses for a well-designed bow-thruster, for instance, reduce the thrust of the unit by approximately 20% (2). These losses are particularly high in the case of a bow-thruster, however, since this manoeuvring device must be capable of developing a side-thrust in either direction. For this reason, an intake must function equally well as a discharge and vice-versa. In other words, the intake and discharge apertures must be compromise designs. This would also be the case for an icebreaker propulsion system, which must be capable of developing high astern thrust.

The astern thrust of an in-hull propulsion system with an intake such as that shown in Fig. 22 or Fig. 23 would probably be significantly less than the forward thrust, partly because of separation losses in the tunnel and at the discharge aperture (i.e., the bottom intake) and partly because the discharge jet is directed downwards instead of horizontally. The latter loss would amount to about 13% of the total thrust if the angle between the discharge jet and the horizontal was 30°.

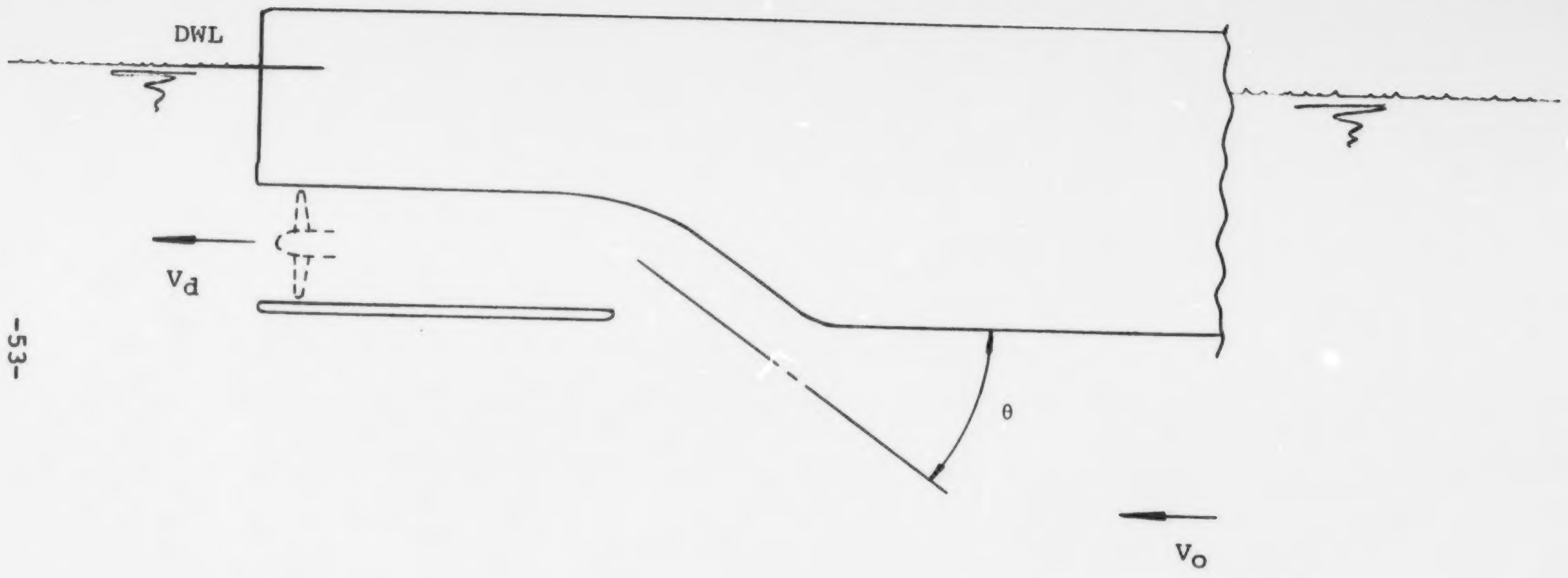

θ = average angle through which fluid
is deflected to enter bottom intake

Fig. 24: In-hull propulsion system with bottom intake

8.3 YPASS Ducted Propulsion System

The essential features of the system are shown in Figure 24a. It has been developed and designed by a Montreal-based firm to offer both protection and maneuverability. The inventor (Dr. David Doust, Canadian Patent No. 910732) claims that this arrangement limits the size of ice which can enter the system, thereby reducing ice-impaction stresses. Model tests* are claimed to have shown that considerably more propulsive force can be obtained with YPASS compared with conventional twin propellers owing to the high flow velocity in the impeller section. Maneuverability in ice was markedly improved compared with conventional means when going astern. For the same thrust capability, substantial reductions in installed horsepower and torque were recorded*. The impellers used in the model test were about two-thirds the diameter of conventional exposed propellers. From Figure 24a we notice the enclosure of two rudders within the internal duct. This arrangement would protect the rudders from damage by ice when going astern. Furthermore, it is claimed by the inventor that an emergency stop could be performed within four ship's lengths from 15 knots by reversing the shaft rotation of the fixed blade impellers. When maneuvering astern, either of the two butterfly valves in the intake ducts may be throttled or closed thus deflecting the exhaust flow more to one side than the other.

In bollard condition, the YPASS system is claimed to give a thrust of about 1.65 times conventional open propeller.

From the foregoing observations and claims, it seems that the YPASS system is quite an impressive device; protecting the propellers of twin and also single-screw vessels from damage by ice, provided that the same claims can be substantiated in full scale.

---

* Journal of the Royal Institution of Naval Architects, March, 1980.

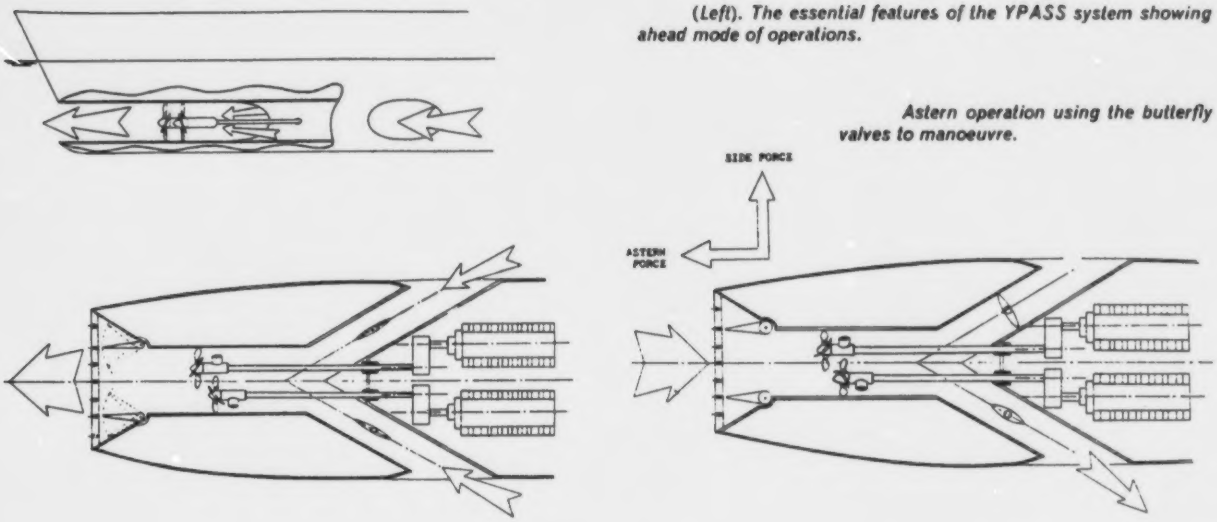

(Left). The essential features of the YPASS system showing ahead mode of operations.

Astern operation using the butterfly valves to manoeuvre.

Figure 24a

YPASS Ducted Propulsion System

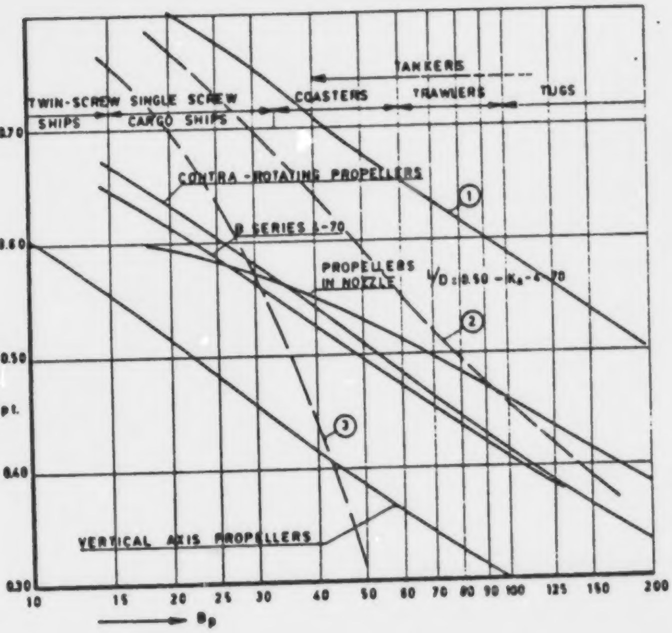

① $\eta_i = \frac{2}{1 + \sqrt{1 + C_{T_i}}}$

② $\eta_i = \frac{1}{1 + 1/4\, C_{T_i}}$

③ $\eta_i = 1 - 1/4\, C_{T_i}$

Figure 24b

Comparison of Optimum Efficiency Values for Different Types of Propulsors

On the other hand, the suitability of the device to operate in severe or medium ice conditions is questionable indeed. It is not quite clear what tip clearance was used in the propeller tunnel arrangement. Increasing the tip clearance would result in excessively bigger tunnel to accommodate the overlapping twin-screw propellers. Reducing the tip clearance would result in vibration being transmitted to the hull. The overlapping twin-screw arrangement was shown by NSMB to have a performance of the same order as obtained by contra-rotating propellers (2) (see Figure 24b). There are some indications in the same reference about the unfavourable cavitation pattern and the interference of the tip vortices observed during model tests on the overlapping arrangement. The enclosure of an overlapping twin-screw in a tunnel, which is the case of the YPASS system, will not make the condition at the propellers any better.

Owing to the eccentricity of each propeller with regard to the tunnel axis, the water reaches the propeller at different speeds in different parts of the propeller circles, with the result that the moving propeller blades pass alternately through fast and slow moving water. This circumferential variation of the axial (and possibly the tangential) velocities is the origin of the periodically fluctuating pressure distributions along the blade chords and on the tunnel walls which is transmitted to the ship's hull. More seriously, the enclosure of overlapping propellers, whether twin or triple-screw, in one duct would be an additional risk due to the fact that any damage is likely to destroy the entire propulsion unit. Another drawback of the YPASS device is the high probability of ice clogging for two reasons: firstly, using the side intakes where the broken ice is in plentiful supply due to the low pressure area near the aft body of the ship and also due to the suction action of the propellers; secondly, the accumulation of deposited ice in the side ducts especially at very low speeds or ramming. The two butterfly valves in the intake ducts are vulnerable to damage by ice, and they are also likely to get jammed and lose their main function of deflecting the outflow when maneuvering astern. As mentioned before, and provided that the inventor's claims can be substantiaged in full scale, the YPASS system seems to be adequate to protect the propellers of twin and single-screw vessels from damage in light ice conditions. The hydrodynamic characteristics of the device are likely to be affected by the propeller/tunnel arrangement whether it is for a single or an overlapping twin-screw.

8.4 Countersunk Kort Nozzles

It is possible, as mentioned previously, to obtain an in-hull propulsion system by simply countersinking a Kort nozzle into the hull, or the roof of a partial tunnel. If the partial tunnel is shallow, entrance losses can be quite low and excellent performance can be obtained even if a substantial part of the nozzle ring is covered by the hull. This was demonstrated by open-water model tests of a push-boat equipped with a partial nozzle (2), in which the nozzle ring was countersunk into the roof of a shallow tunnel over 90° and then 180° of its periphery (see Figure 25). The results of those tests, shown in Figs. 26 and 27, indicated that the open-water efficiency η_o (where $\eta_o = JK_T/2\pi K_Q$), the ratio of the nozzle thrust to total thrust (i.e., $1-\tau$), and the total thrust itself, increased as the fraction of the nozzle periphery covered by the hull increased. It can also be shown from the results presented in Fig. 27 that the thrust/power ratio of the ducted propulsion system at bollard increased as Ψ increased (Ψ is the angle over which the hull covers the nozzle ring). These results emphasize the observation made earlier that the performance (in particular, thrust) characteristics of an in-hull propulsion system designed to prevent the contraction of the propeller outflow abaft the propeller should be similar to those of a Kort nozzle regardless of whether the system bears much resemblance to a Kort nozzle.

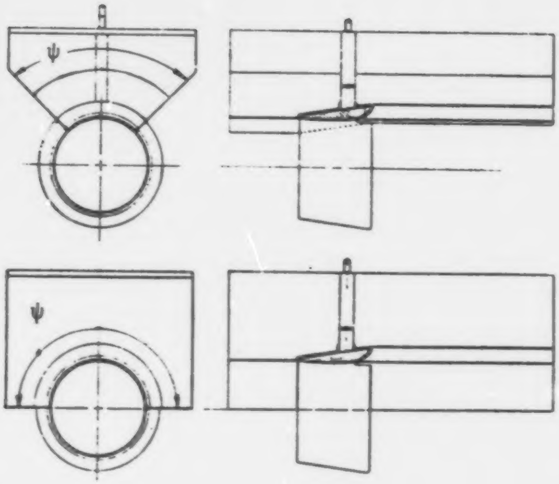

Fig. 25: Tested ducted propeller configurations with nozzle ring over 90 or 180 degrees countersunk in tunnel.

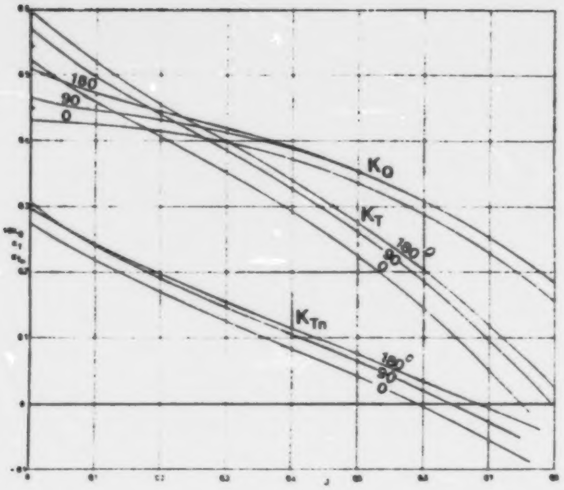

Fig. 26: Open-water test results with ducted propeller configurations with nozzle rings partly countersunk in tunnel.

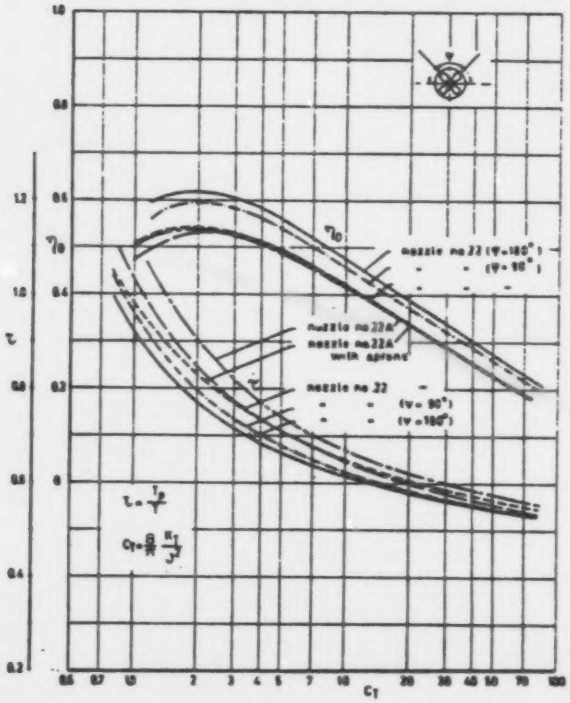

Prop. K_a4-70, P/D 1.0
T_p = Prop. Thrust
T = Total Thrust
ψ = Countersunk Angle

Fig. 27: Open-water test results with ducted propeller configurations with nozzle rings partly countersunk in tunnel.

In conclusion, in-hull propulsion systems appear promising from a hydrodynamic viewpoint, although it is doubtful that the performance of such a system could ever equal that of a propeller in a Kort nozzle. Particular attention should be paid to the design and location of the intake for an in-hull propulsion system, since the intake should:

a) ingest as much of the required fluid as possible from the boundary layer on the bottom or side of the ship.

b) be designed to minimize thrust deduction

c) be designed to minimize losses (due to flow separation) during forward and astern operation,

d) produce a relatively uniform circumferential wake distribution at the propeller disc.

An intake designed and located to satisfy these requirements will obviously be a highly compromised design which may not perform any of the tasks mentioned particularly well.

9.0 RUDDERS

Rudders shield propellers to a certain extent from collisions with ice floes. Different types of rudders provide differing degrees of protection, but only those rudders which are located within the boundaries of the propeller inflow (during ahead or astern operation) or, better still, within the projected area of the propeller discs, are expected to be of much benefit. Two rudders located in the inflow as shown in Figure 28, of a propeller developing reverse thrust, may be able to divert ice more effectively since they will exclude ice pieces above a certain size. Flanking rudders, located in front of the propeller will perform similarly during forward operation. Any device intended to deflect ice away from an open screw must be wedge or cone-shaped, and the propeller must be located at the base of the wedge or cone. A rudder obviously does not fit this description.

When a vessel is going astern a rudder can provide some protection for a propeller during collisions with very large ice floes, which it can help to push aside, or during collisions with intact ice sheet. It cannot prevent ice milling, but it can, in some cases, limit the depth of cut. Since rudders themselves are very vulnerable to ice damage they cannot be relied upon for propeller protection schemes.

From the foregoing observations, it is apparent that fin-type rudders have little to offer as propeller protective devices. Other types of rudders, in particular tubular rudders, might be more useful. One form of tubular rudder, the Kitchen type, is shown in Fig. 29. The two halves of the Kitchen rudder, which surround the propeller, can be used to direct the jet from the propeller and hence the thrust. The Kitchen rudder is similar to a steerable Kort nozzle in this respect. The two halves of

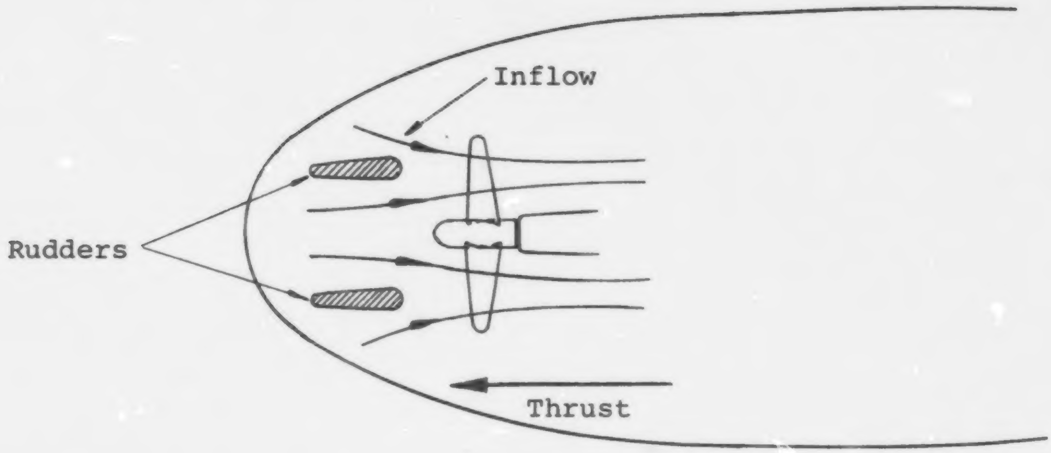
Inflow
Rudders
Thrust

Fig. 28: Twin rudders behind propeller developing reverse thrust

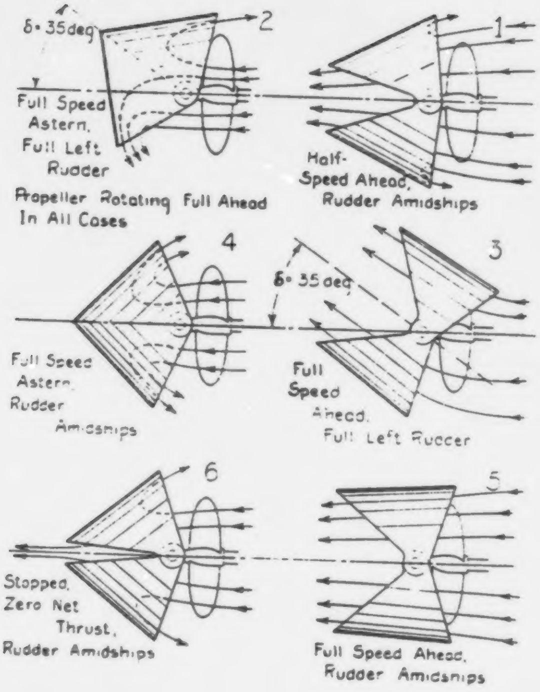
δ = 35deg
2
1
Full Speed Astern, Full Left Rudder
Half-Speed Ahead, Rudder Amidships
Propeller Rotating Full Ahead In All Cases
4
3
δ = 35 deg
Full Speed Astern, Rudder Amidships
Full Speed Ahead, Full Left Rudder
6
5
Stopped, Zero Net Thrust, Rudder Amidships
Full Speed Ahead, Rudder Amidships

Fig. 29: Schematic flow and operating diagrams for a Kitchen Rudder

the Kitchen rudder can also be swung toward each other so that their after ends close. The rudder functions as a thrust reverser in this case, permitting a vessel to proceed astern without reversing shaft rotation (fixed pitch propeller) or reversing propeller pitch (CRP). The rudder shown in Fig. 29 is quite crude and would probably not operate very efficiently as a thrust reverser (ie, the astern thrust would be much lower than the forward thrust). The design could, however, be improved to provide more efficient operation.

A Kitchen rudder would largely eliminate ice milling, particularly if it was designed to enclose the propeller to a greater extent than shown in Figure 29. The propeller would also be protected while proceeding astern, although the rudder might be difficult to maintain in the proper position while backing up in heavy ice. The possibility of ice being sucked into the propeller from the front would exist at all times, and some type of guard would be necessary to prevent this.

Since the Kitchen rudder is not a thrust producing device like a Kort nozzle, its section thickness would have to be kept as small as possible in order to minimize its drag. In order to withstand impacts with ice pieces, however, the section thickness would have to be kept relatively large.

Thus the requirements of adequate structural strength and low drag oppose each other in this instance. Since a Kitchen rudder does not appear to be as useful as a steerable Kort nozzle in most respects, and since its one exceptional capability, specifically that of reversing thrust, is one which is accomplished rather inefficiently, the Kitchen rudder is not worthy of further consideration.

9.1 Legal Restrictions on the Use of Rudders

A patent for several types of tubular rudders, similar to the Kitchen rudder, is held by Edmund Rees. The appropriate Canadian patent number is 227.280.

10.0 GENERAL EVALUATION OF PROPELLER PROTECTIVE DEVICES

In addition to the foregoing discussion and observations some hydrodynamic features which will affect the performance of each device will now be presented.

If the ship resistance is R_s and ship speed is V_s then output from the ship motion (the effective power) is $P_e = R_s \cdot V_s$, the propeller input power is $P_p = 2\pi nQ$, and the propeller thrust is T_p.

Therefore, $$\frac{P_e}{P_p} = \frac{R_s V_s}{2\pi nQ} = \frac{T_p(1 - t)}{2\pi nQ} \left(\frac{V_A}{1-w}\right)$$

with $R_s = T_p(1 - t)$, t = thrust deduction factor

If the ship resistance in this case is considered as made up of the hull resistance R_H and an additional resistance R_a due to the protective device such as ducts, struts, cages, pipe guards, bossing fins, bilge keels, etc., then,

$$\frac{P_e}{P_p} = \frac{(R_H + R_a)V_s}{2\pi nQ}$$

So to maintain the same ship speed, the propeller input power has to be increased.

On the other hand, if the protective device produces a net ahead thrust (in excess to its resistance), as in the case of a Kort nozzle, then

$$\frac{P_e}{P_p} = \frac{[T_p(1 - t) + T_a]}{2\pi nQ} \left(\frac{V_A}{1-w}\right),$$ (where T_a = thrust developed by device)

which applies equally to any other thrust-producing device, separate from the propulsion device.

So to maintain the same ship speed it is possible in this case to reduce the propeller thrust $T_p(1 - t)$ by an amount equivalent to that "gain" in the ahead thrust T_a.

The overall efficiency of propulsion is defined as

$$\eta_p = \begin{bmatrix}\text{Hull Efficiency}\\ \eta_H\end{bmatrix}\begin{bmatrix}\text{Relative Rotative}\\ \text{Eff.}\\ \eta_R\end{bmatrix}\begin{bmatrix}\text{Open Water Eff.}\\ \eta_o\end{bmatrix}$$

If all the efficiency factors for each design (i.e., model or ship plus protective device) are included, which is by no means certain in the present state-of-the-art, then the propulsion efficiency may be considered as a measure for the evaluation of the different devices with respect to hydrodynamics.

Information on all the components of propulsive efficiency can only be derived from model experiments, since only in this way can all the necessary measurements be made and the performance of the propeller in behind condition be determined.

Some of the protective devices suggested in this report will have the effect of converting some of the rotary motion in the propeller slipstream into motion aft and consequently reduces the energy lost in the wake. Others will have the effect of breaking up the propeller trailing vortex sheets with the result of preventing the development of large scale vortices and thus recovering some of the kinetic energy left behind in the outflow jet.

Again, some of the protective devices could have the capability of regulating the inflow jet to the propeller both radially and circumferentially (at a given radius) and this would contribute towards an improved overall propulsion efficiency. Some others might have an adverse effect on the propulsive efficiency due to wake buffeting, or an excessive thrust deduction, or even possible flow separation on the ship's boundary layer flow with the result of disadvantageous flow conditions at the propeller disc.

11.0 TIP CLEARANCE

For shrouded propellers, e. g., propeller in tunnel or ducted propellers, the phenomenon in the gap between the blade tips and the inner surface of the tunnel should not be overlooked. To protect the blade tips from damage by large pieces of ice squeezed in the gap, a reasonable tip clearance is required. On the other hand, the effect of surrounding the propeller by a tunnel (or duct) on both the circulation and the thrust increase, becomes important when the tip clearance approaches a very small value. For a good performance characteristic from a ducted propeller, the tip clearance should be kept as small as possible. Any substantial increase in the tip clearance would result in reducing both the thrust and the efficiency and would increase the risk of cavitation associated with the tip flow. This fact has been substantiated experimentally by Van Manen (11) and theoretically by English (12).

Using the notation of Figure 30, the propeller thrust is given by:

$$T_p = A_2(p_3 - p_2) \qquad (1)$$

and applying Bernoulli's equation between sections 0 and 2, and 3 and 5, we obtain:

$$\Delta p = (p_3 - p_2) = 1/2\rho(V_5^2 - V_o^2) \qquad (2)$$

therefore $T_p = 1/2\rho A_2(V_5^2 - V_o^2)$ (3)

The propeller thrust coefficient $(C_T)_p$ is:

$$(C_T)_p = \frac{T_p}{1/2\rho A_4 V_o^2} = \left[\left(\frac{V_5}{V_o}\right)^2 - 1\right]\frac{A_2}{A_4} = K\frac{A_2}{A_4} \qquad (4)$$

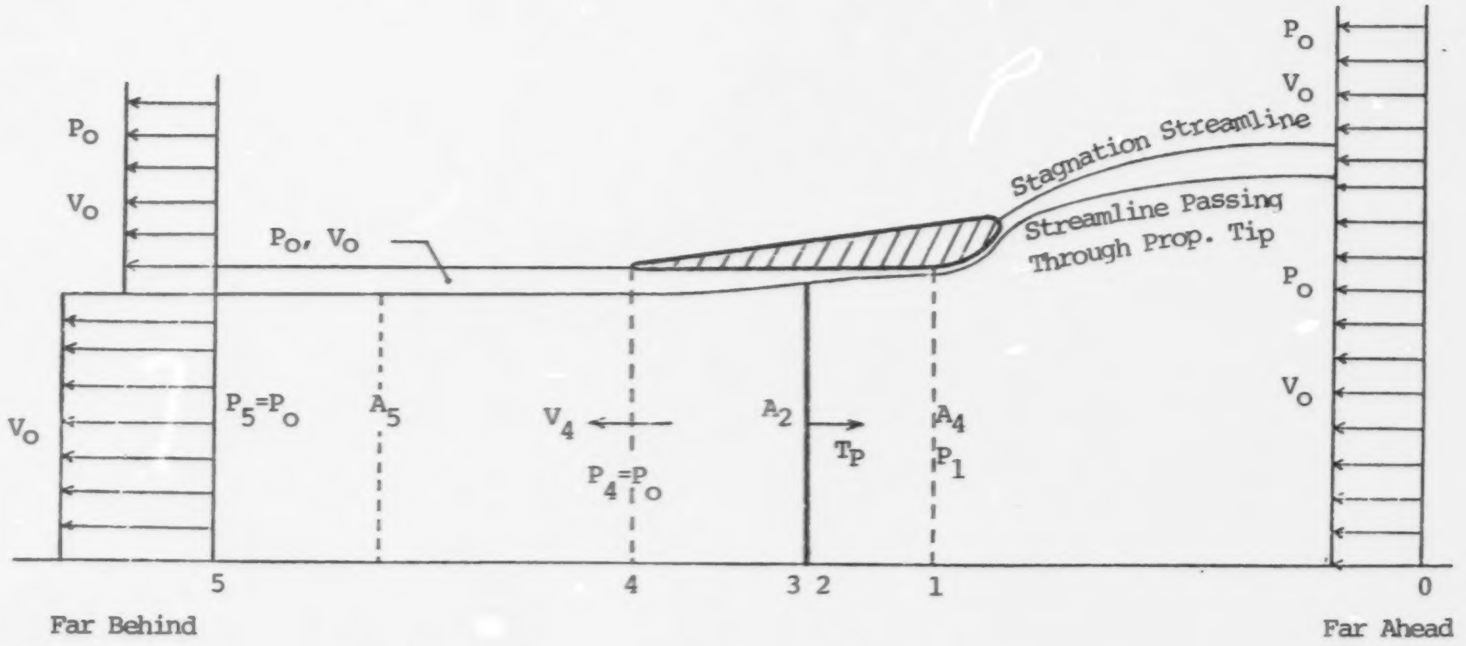
P_o
V_o
Stagnation Streamline
Streamline Passing Through Prop. Tip
P_o
V_o
P_o
V_o
P_o, V_o
V_o
$P_5=P_o$
A_5
V_4
$P_4=P_o$
A_2
T_P
A_4
P_1
5
4
3 2
1
0
Far Behind
Far Ahead

FIGURE 30

CONTROL VOLUME ASSUMED IN DUCTED PROP. ANALYSIS

The total thrust on the system is given by:

$$T_T = \rho A_5 V_5 (V_5 - V_o) \qquad (5)$$

$$= \rho A_5 V_5 V_\infty$$

and in non-dimensional form:

$$(C_T)_T = \frac{T_T}{1/2\ \rho A_4 V_o^2} = 2\ \frac{A_5}{A_4}\ \frac{V_5}{V_o}\ (\frac{V_5}{V_o} - 1) \qquad (6)$$

Applying the continuity equation and momentum theory between sections 1 and 4, and using the long shroud approximation*, thus:

$$\frac{V_1}{V_o} = 1 + \sqrt{1 + K} - \sqrt{1 + K\ (1-A_2/A_4)} \qquad (7)$$

and

$$(C_T)_T = 2\left[\sqrt{1+K} - \sqrt{1+ K\ (1- \frac{A_2}{A_4})}\right]\sqrt{1+K} \qquad (8)$$

The shroud thrust $(C_T)_D$ is given by:

$$(C_T)_D = (C_T)_T - (C_T)_P$$

The ideal power input to the shrouded propeller is given by the change in kinetic energy of the fluid in passing through the unit, or

$$P = 1/2 \rho A_5 V_5 (V_5^2 - V_o^2) \qquad (10)$$

then $$C_P = \frac{P}{1/2 \rho A_4 V_o^3} = \frac{A_5}{A_4}\ \frac{V_5}{V_o}\ \left[(\frac{V_5}{V_o})^2 - 1\right] \qquad (11)$$

---

* For a duct chord to diameter ratio of L/D > 0.4, then $p_4 = p_5 = p_o$ and $V_4 = V_5$

and finally reads:

$$C_P = \left[\sqrt{1+K} - \sqrt{1+K\left(1-\frac{A_2}{A_4}\right)}\right] \sqrt{1+K} \left(\sqrt{1+K}+1\right) \quad (12)$$

The propulsive efficiency is given by (Froude efficiency):

$$\eta_F = \frac{(C_T)T}{P} = \frac{2}{1+\sqrt{1+K}} \qquad (13)$$

which shows that Froude efficiency depends only on the loading of the propeller itself and not on the total thrust.

Now if we define the clearance ratio as $\varepsilon = \frac{D_4 - D_2}{2D_4}$, then

$$\frac{A_2}{A_4} \cong 1 - 4\varepsilon$$

and the efficiency becomes:

$$\eta_i \doteq \frac{2}{1+\sqrt{1+\frac{(C_T)P}{1-4\varepsilon}}} \qquad (14)$$

For a long duct with almost zero tip clearance, the streamline passing through the propeller tip is coincident with the stagnation streamline and the efficiency reads:

$$\eta_i = \frac{4}{3+\sqrt{1+2(C_T)_T}} \qquad (15)$$

From expression (14), it is clear that the efficiency falls as the tip clearance ratio increases or the propeller loading increases.

The flow in the tip clearance region is more complex than that assumed in the above one-dimensional flow analysis. In the actual case one has to deal with a rotor having a finite number of blades and the effect of the blade bound vortices shed at the tip, in addition to the bound vortices due to the annular aerofoil section of the duct itself. Again, for a good duct this tip clearance must be as small as possible, and certainly the system with zero tip clearance is a case of zero induced drag, which occurs with a ring-propeller. The latter device must be regarded as being over-simplified by neglecting the viscous effect of the rotating duct in a real working condition. On the other hand, putting the tip clearance equal to zero to establish a mathematical model (10) does not mean that the shroud is either physically connected to the propeller or rotates with it.

From the practical point of view, it is not possible to have a zero clearance, plus the boundary layer in the gap prevents the equalization of pressure to take place if the tip clearance is too small. The determination of how small is sufficiently small requires an analysis using boundary layer theories. For ducted propellers, a tip clearance of 0.5 - 1% of the propeller diameter is considered a common practice and used by most designers and experimental tanks.

For the tip clearance for in-hull propulsion systems, one must be aware of the differences between the ducted propeller concept and the concept of in-hull propulsion or propellers in tunnels. The two concepts are essentially different. While in the former scheme (ducted propellers) the wall of the nozzle ring is of aerofoil sections (annular aerofoil) the latter scheme is not, or may consist of just a segment of an annular aerofoil. The bound circulation developed on each meridional section of the annular aerofoil produces lift force on that section (Magnus effect), the circumferential integration of its axial component determines the duct thrust in the direction of motion. For an in-hull propulsion system (e.g., propeller in-tunnel with bottom intake) the duct thrust is produced by the segment of the duct where there is a pressure difference between the inner and outer surfaces, i.e., by the segment in-line with the intake opening. Furthermore, as shown in Appendix A, for an in-hull propulsion system there is an additional net forward thrust created by the system and is simply equal to the difference between the total thrust, as the change of momentum, and the propeller thrust, as the change of kinetic energy. This additional forward thrust may be considered as if produced either by the hull or by the segment of the duct, or, generally speaking, by both.

Since the main objective is to develop a device which provides essentially complete protection for propellers in ice, one must consider the tip clearance as a key parameter in designing an effective and efficient in-hull propulsion system. The investigation of the tip clearance effect on the overall performance of the device is certainly outside the scope of the present study, since it requires some complex mathematical modelling (based on boundary layer theories) and systemmatic series of experiments to verify the results. However, bearing in mind the nature of the device and the environment surrounding it, one would recommend a "reasonable" tip clearance between the blade tips and the inner surface of the tunnel.

A tip clearance of about five times as much as commonly used for ducted propellers seems to be adequate, i.e., about 5% of the propeller diameter.

12.0 CONCLUSIONS AND RECOMMENDATIONS

12.1 General

A critical review of the various devices discussed in the foregoing sections of this report indicates clearly that for multiple-screw ships, an in-hull protection scheme is required.

For a single screw ship a nozzle with protecting fins appears to be the most practical arrangement.

In-hull propellers are well-protected from ice damage. Ice milling and ice impact loads are mitigated and ice ingestion can be reduced by fitting guards (grills) to the intake and discharge apertures. These grills, if made sufficiently large, are no more likely to clog with ice than are bird cages or cages fitted to partial tunnels. Model tests will be required to obtain a proper indication of the probability of ice clogging, however.

Grills fitted to the intake and discharge apertures of an in-hull propulsion system will be less complex than their counterparts on an open screw or partial tunnel. Also the grill fitted to the bottom intake, need not be as robust as the grill used aft of the propeller, since impact between ice pieces and the bottom grill will be less severe.

An additional benefit occurring from the use of an in-hull propulsion system is that it allows a CP propeller to be used without risk of costly damage. Transmission components may also be reduced in size from those normally used in icebreaking.

In summary, in-hull propulsion systems appear to offer the best concept for providing virtually complete protection for the propellers. The possibility of developing ice blockages in these systems exists and should be investigated experimentally. It is felt that ice clogging will not be a serious problem if these systems, and their protective grills, are carefully designed. Moreover, in-hull propulsion systems may provide reasonably high hull efficiencies without excessive circumferential wake variation and without objectionable separation or eddying.

12.2 Multiple-Screw In-Hull Arrangement

Four different arrangements for an in-hull scheme for a triple-screw ship are shown in Figures 31 to 34 inclusive. The three propellers are totally enclosed in separate tunnels with guarded bottom intakes. In the first attangement a typical triple-screw hull form is used. In the second arrangement, the aft body shape is altered in order to accommodate the tunnels with propellers in one plane. The aft end of the tunnels are flush with the ship's hull to improve the performance in astern operation. For the third arrangement, a squared-off transom stern is used together with a wall-sided hull form for simplicity.

Arrangements for a twin-screw ship with an in-hull propulsion scheme would be similar to those mentioned above. Each propeller is enclosed in a separate tunnel with guarded bottom intake. The discharge end of the tunnels are fitted with removable guards to facilitate removal and maintenance of propeller, shafts, bearings, etc.

12.3 Single-Screw Nozzle Arrangement

For a single-screw ship a strong double flared nozzle with deflecting fins on the bossing and skeg is recommended, as shown in Figure 35 . The trailing part of the nozzle is fitted with removable guards.

It is proposed therefore to proceed with the design of the twin and triple-screw concepts on the basis of an in-hull design and to develop the nozzle arrangement for the single-screw ship.

Thruster units, instead of rudders, are suggested for use with the above schemes.

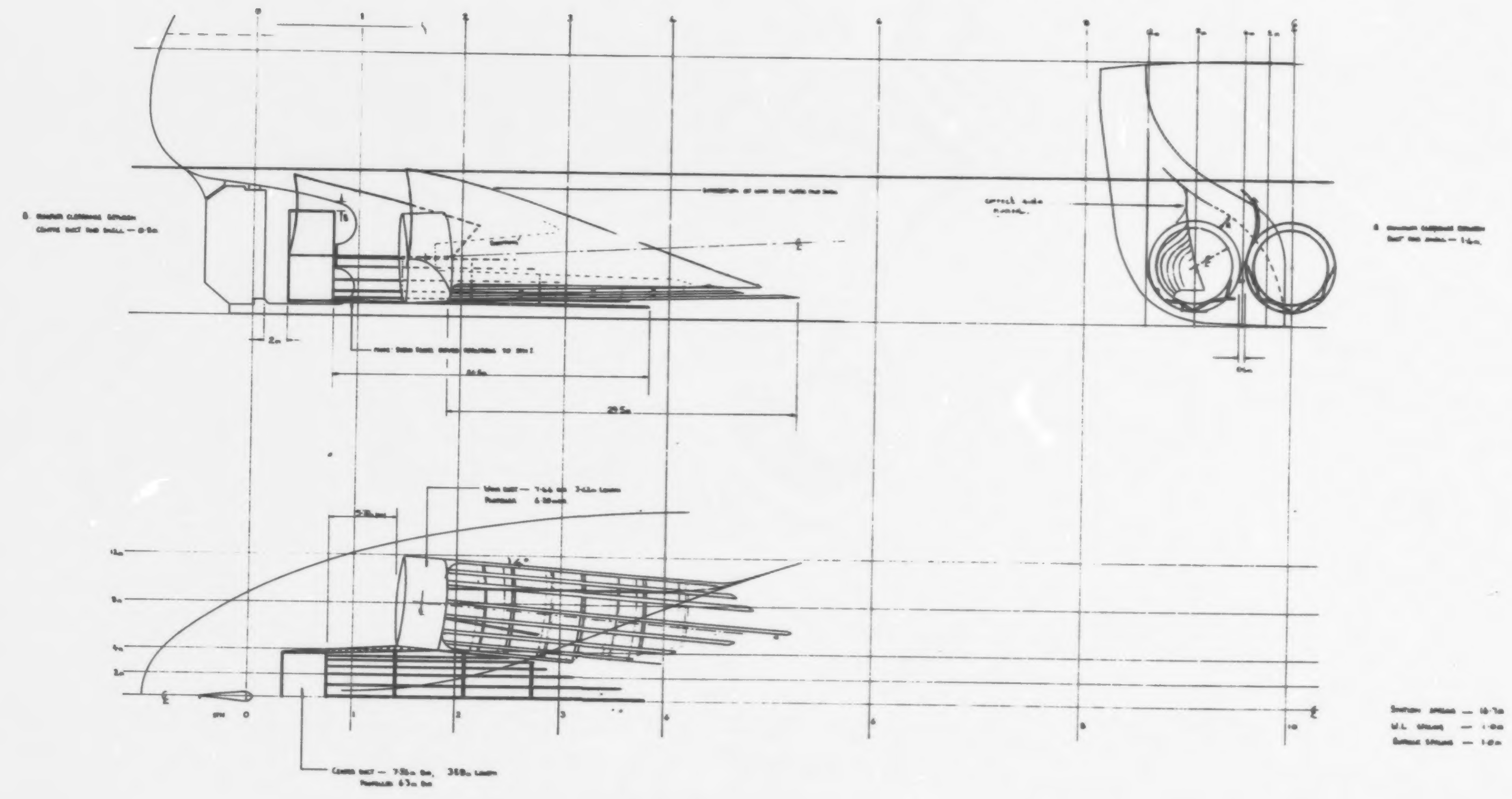
2m
29.5m
12m
8m
4m
2m
0
1
2
3
4
6
8
10

Fig. 31

Davis Engineering

1:200

DE 1478

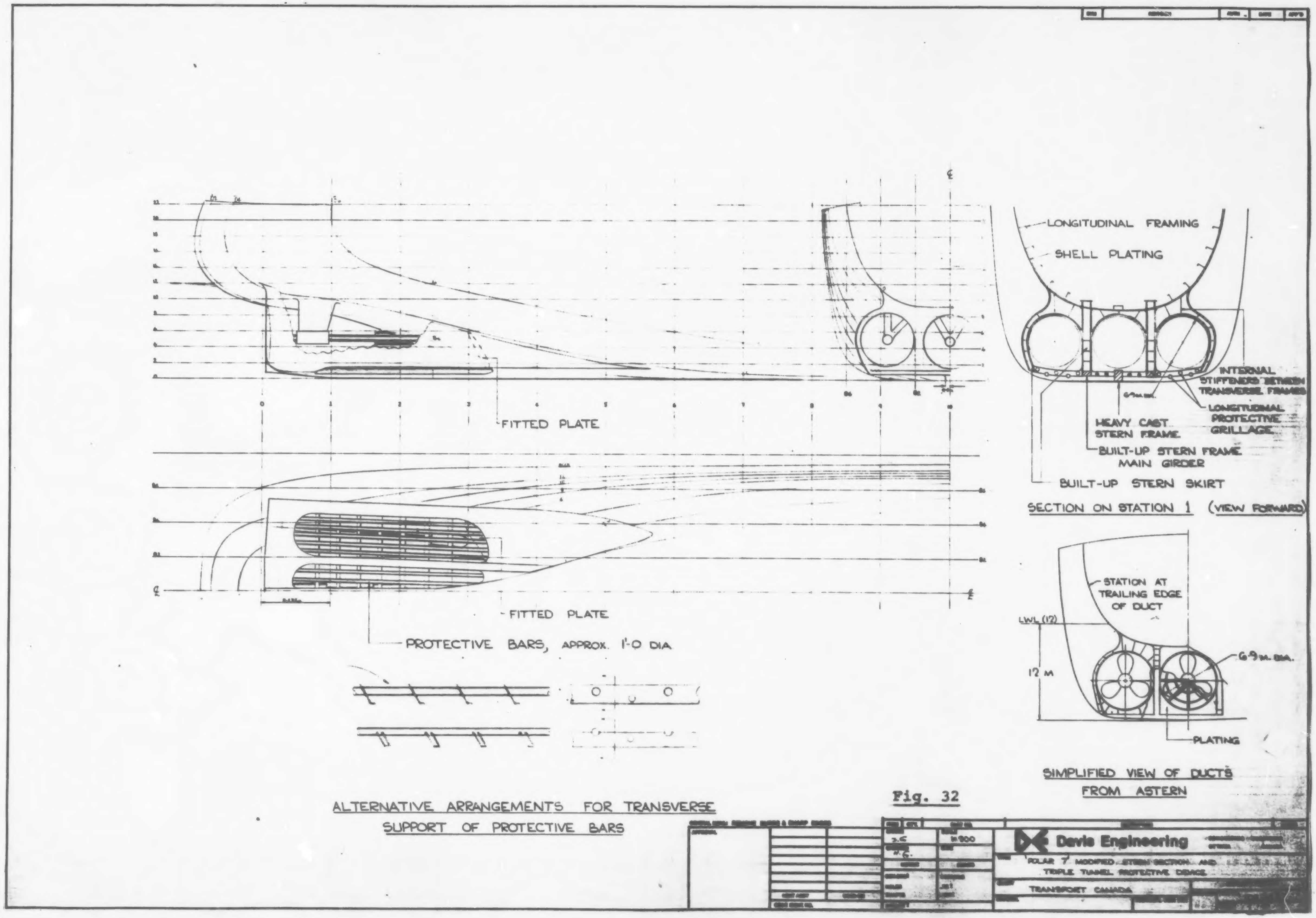
FITTED PLATE
FITTED PLATE
PROTECTIVE BARS, APPROX. 1'-0 DIA
ALTERNATIVE ARRANGEMENTS FOR TRANSVERSE SUPPORT OF PROTECTIVE BARS
LONGITUDINAL FRAMING
SHELL PLATING
INTERNAL STIFFENERS BETWEEN TRANSVERSE FRAMES
6.9 M. DIA
LONGITUDINAL PROTECTIVE GRILLAGE
HEAVY CAST STERN FRAME
BUILT-UP STERN FRAME MAIN GIRDER
BUILT-UP STERN SKIRT
SECTION ON STATION 1 (VIEW FORWARD)
STATION AT TRAILING EDGE OF DUCT
LWL (12)
12 M
6.9 M. DIA.
PLATING
SIMPLIFIED VIEW OF DUCTS FROM ASTERN
Davis Engineering
POLAR 7 MODIFIED STERN SECTION AND TRIPLE TUNNEL PROTECTIVE DEVICE
TRANSPORT CANADA
1:200

Fig. 32

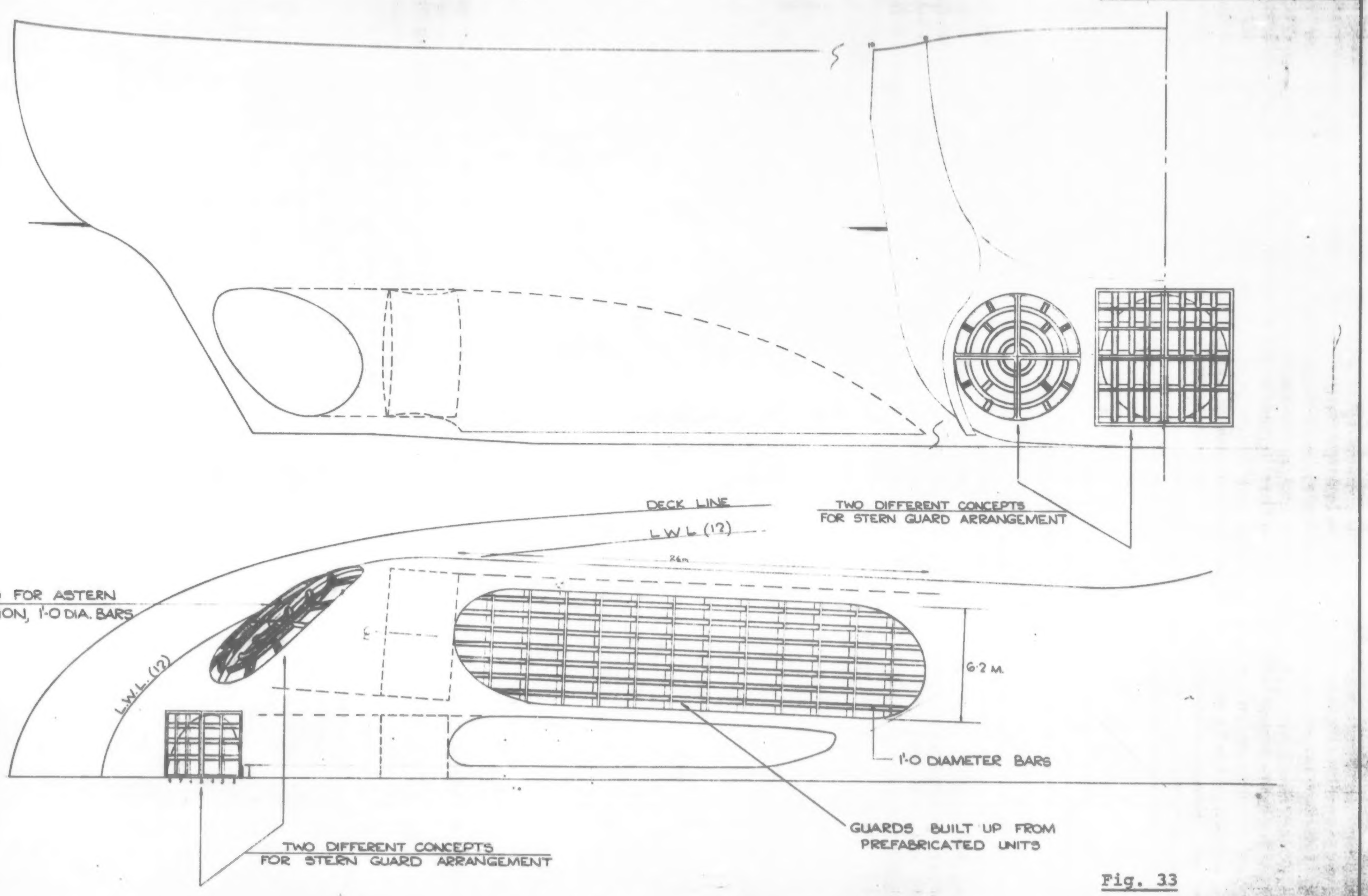
DECK LINE
L.W.L. (12)
TWO DIFFERENT CONCEPTS FOR STERN GUARD ARRANGEMENT
GUARD FOR ASTERN OPERATION, 1'-0 DIA. BARS
L.W.L. (12)
26m
6·2 M.
1'-0 DIAMETER BARS
GUARDS BUILT UP FROM PREFABRICATED UNITS
TWO DIFFERENT CONCEPTS FOR STERN GUARD ARRANGEMENT

Fig. 33

PRELIMINARY DRAWING
Davis Engineering
'POLAR 7' MODIFIED COUNT
WITH MOULDED STERN

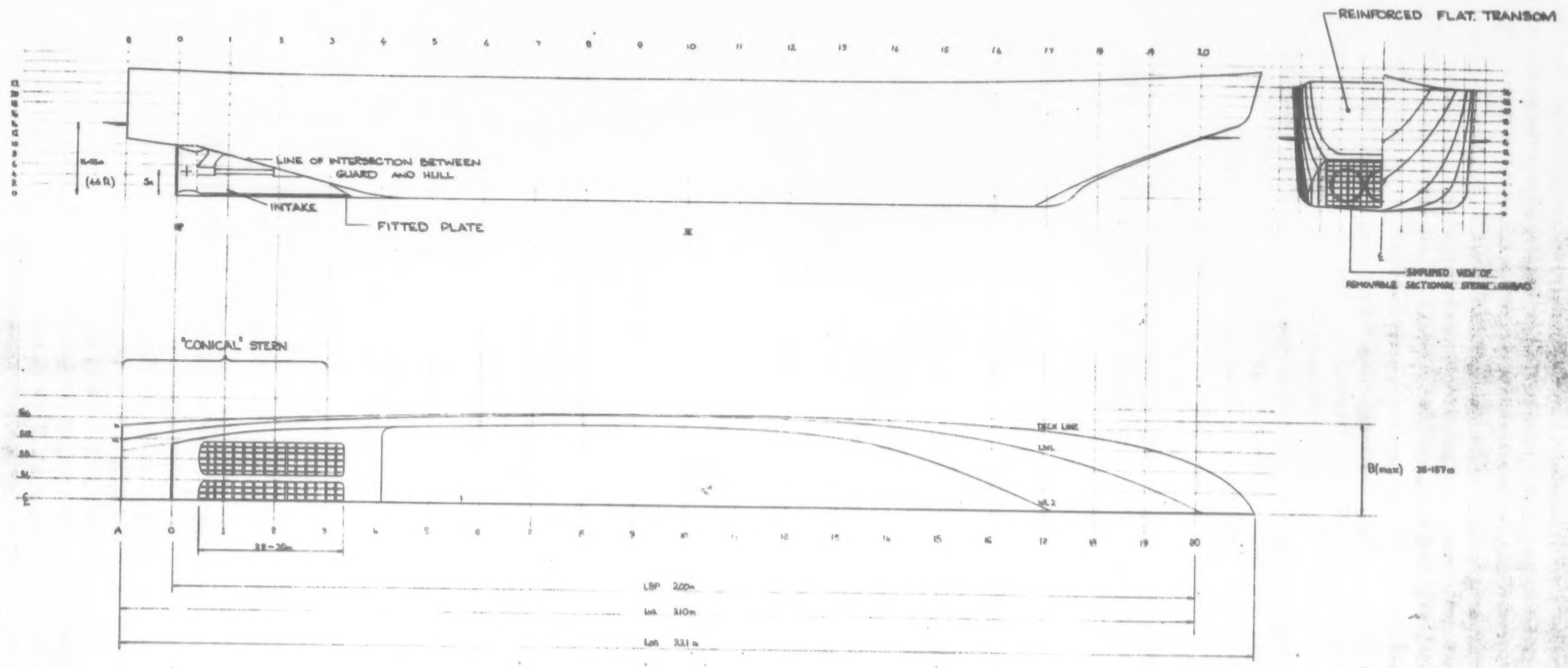
REINFORCED FLAT. TRANSOM
LINE OF INTERSECTION BETWEEN GUARD AND HULL
INTAKE
FITTED PLATE
(46 ft)
3m
SIMPLIFIED VIEW OF REMOVABLE SECTIONAL STERN GUARD
'CONICAL' STERN
DECK LINE
LWL
WL 2
B(max) 35·157m
A
0
1
2
3
4
5
6
7
8
9
10
11
12
13
14
15
16
17
18
19
20
LBP 200m
LWL 210m
LOA 221 m
1:400
Davis Engineering
SIMPLIFIED LINES PLAN

Fig. 34

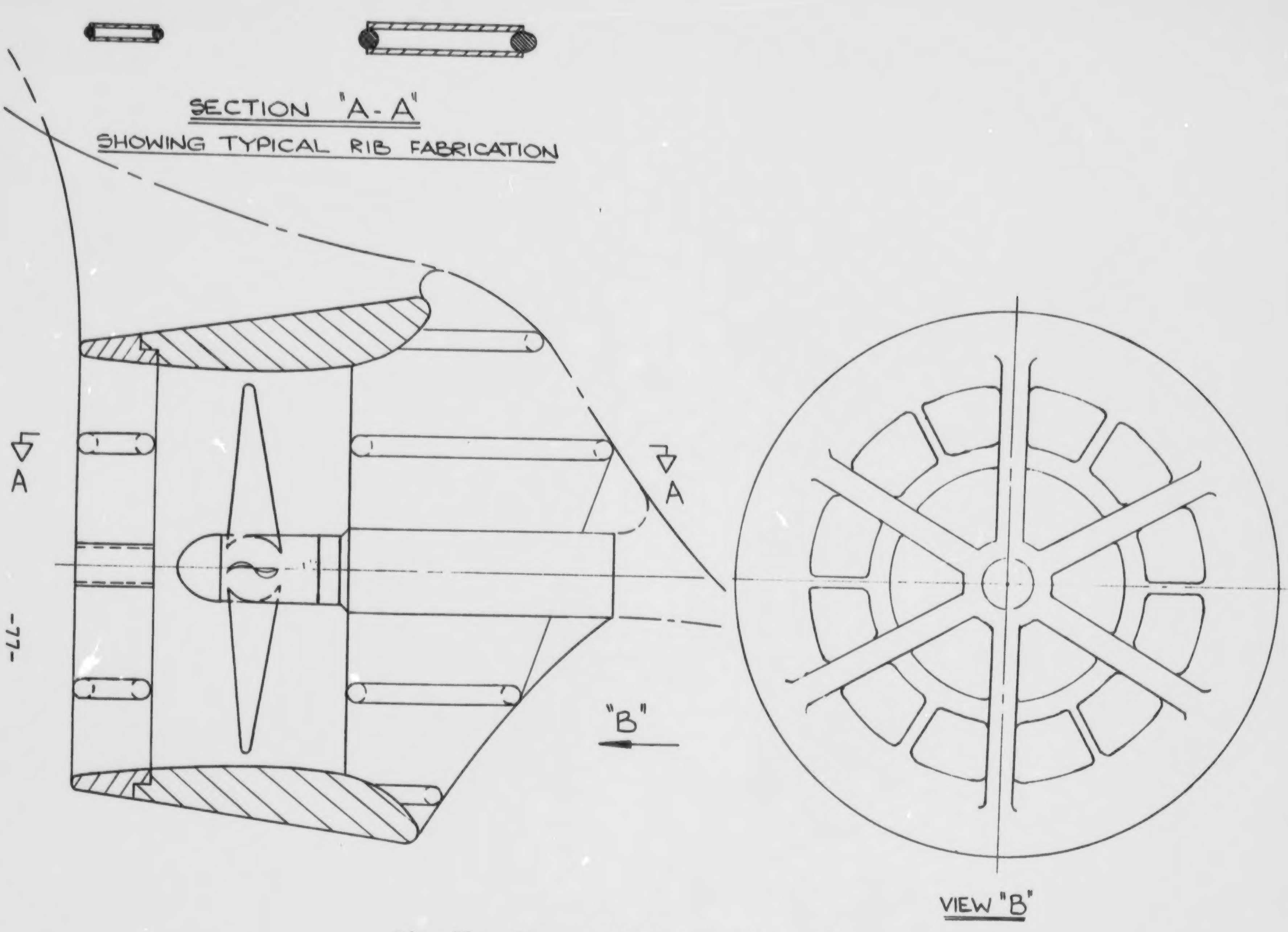
SECTION "A-A"
SHOWING TYPICAL RIB FABRICATION
A
A
"B"
VIEW "B"

Fig. 35: Strong Double-flared Nozzle

Finally, open water model tests (resistance and self-propulsion) in ice-covered water will shed more light on the hydrodynamic characteristics of the ship with the protective device in place. Underwater photographs will illustrate the flow patern of the broken ice, near the stern and close to the slipstream of each propeller.

Finally, structural analysis is required to ensure that the device can withstand stresses imposed by ice impact in ahead and astern operations.

13.0 REFERENCES

(1) Van Gunsteren, L.A.
"Slotted Nozzles",
Proceedings North America Tug Convention, 1973

(2) Oosterveld, M.W.C.,
"Ducted Propeller Systems Suitable for Tugs and Pushboats",
International Shipbuilding Progress, Vol. 19, No. 219, November, 1972.

(3) Monnich, H.
"Screw Propelled Propulsion Devices",
Canadian Patent No. 735.219,
May 31, 1966

(4) Liaaen, Nils J.
"Propeller Guard",
Canadian Patent No. 981118,
January 6, 1976

(5) Enkvist, E., Johanson, B.M.,
"On Icebreaker Screw Design",
European Shipbuilding, 1968, 17(2), pp. 2-14.

(6) Vance, G.P.
"Evaluation of Ice Deflectors On The USCG Icebreaker Polar Star"
Cold Regions Research & Engineering Laboratory,
Hanover, USA, Special Report 80-4, January, 1980

(7) Van Gunsteren, L.A.
"Ring Propellers",
Transactions, The Institute of Marine Engineers,
Vol. 83, 1971, Part 2.

(8) Saunders, H.E.
"Hydrodynamics in Ship Design",
Volume 1

(9) Edwards, R.Y., Allan, R.J.
"YPASS Propulsion System Evaluation",
Transport Canada Report #TP1575,
December, 1978

(10) George, M.F.
"A Model of an Axisymmetrical Ducted Propeller
with Zero Tip Clearance",
J.S.R., Volume 23, pp. 253-259,
December, 1979

(11) Van Manen, J.D.
"Effect of Radial Load Distribution on the
Performance of Shrouded Propellers",
RINA,
1963.

(12) English, J.W.
"One-Dimensional Ducted Propeller Theory",
NPL, R. 94,
1967.

(13) George, M.F.
"Surface Vorticity Technique Applied to Non-Axisymmetric Ducted Propellers",
Awaiting Publication.

(14) Hee, J.M.
"Economic Hull Form for Great Lakes Self-Unloaders",
Canadian Shipbuilding and Ship Repairing Association
Technical Sec. Annual Meeting,
February 5th, 1980

(15) George, M.F.,
"The Aerodynamic Performance of a Propeller in a Non-Axisymmetric Duct",
Ph.D. thesis, Department of Aeronautics,
University of Glasgow,
1976.

APPENDIX A

One-Dimensional Flow Analysis Of In-Hull Propulsion System

APPENDIX A

ONE-DIMENSIONAL FLOW ANALYSIS OF IN-HULL PROPULSION SYSTEM

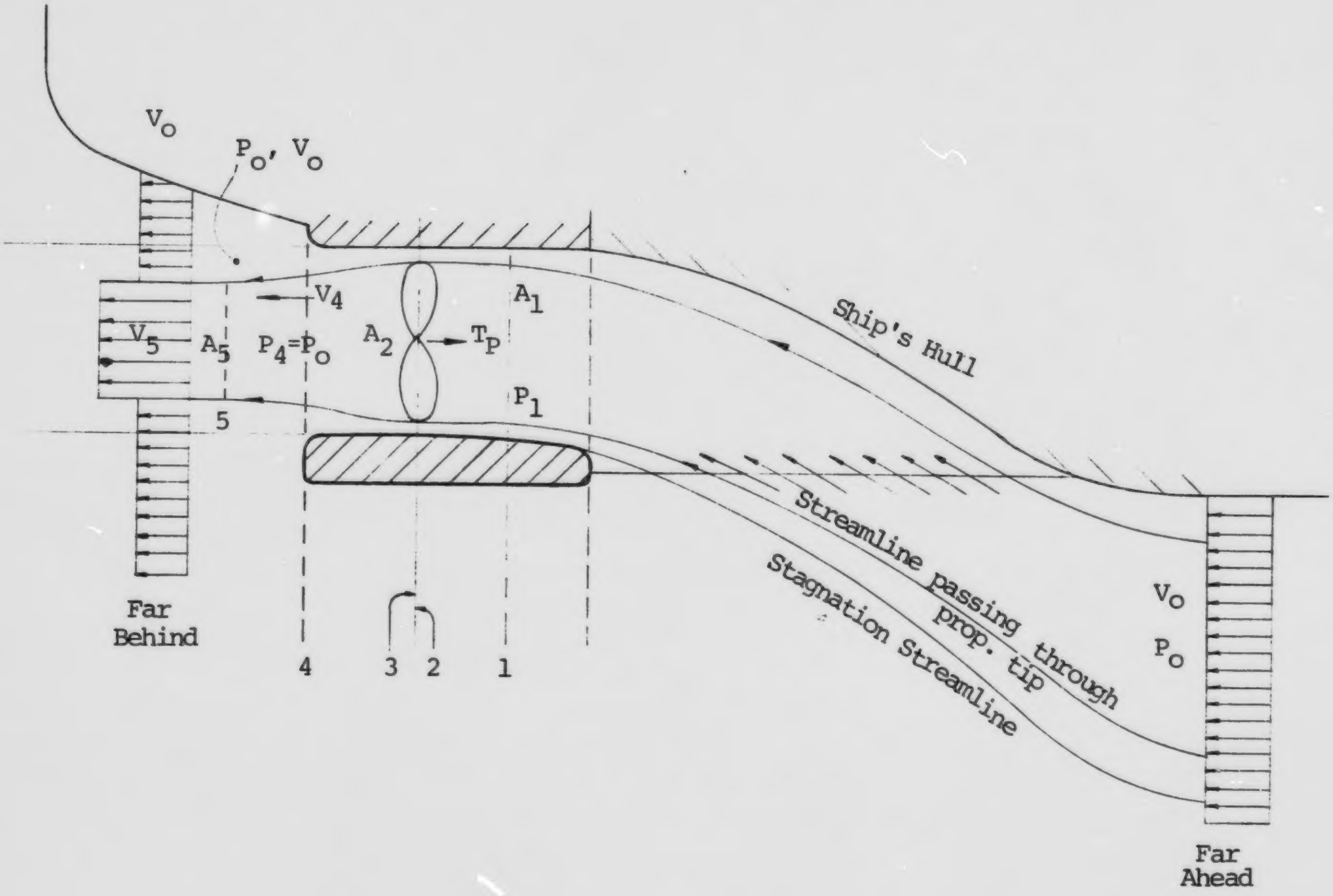
V_o
P_o, V_o
V_4
A_1
Ship's Hull
V_5
A_5
$P_4=P_o$
A_2
T_P
P_1
5
Streamline passing through prop. tip
Stagnation Streamline
V_o
P_o
Far Behind
4
3
2
1
Far Ahead

Control Volume Assumed
in In-Hull Propulsion Analysis

A_2 = propeller disc area

A_4 = tunnel exit area

Assumptions:

1) sufficiently long shroud
$P_5 = P_4 = P_o, \; V_5 = V_4$

2) cylindrical duct from inside (there is no pressure force contribution from the inside duct surface)

3) the fluid at section 4 is assumed parallel with the axis as it is at section 5

Applying Bernoulli's equation to the flow at sections 0, 2, 3, and 5 gives

$$\Delta p = (p_3 - p_2) = \tfrac{1}{2}\rho(V_5^2 - V_o^2) \quad \bullet \quad K = \frac{\Delta p}{\tfrac{1}{2}\rho V_o^2} = \left[\left(\frac{V_5}{V_o}\right)^2 - 1\right]$$

$$\text{Therefore: } V_5 = V_o\sqrt{1+K} \tag{1}$$

$$T_p = \tfrac{1}{2}\rho A_2(V_5^2 - V_o^2)$$

and propeller thrust coefficient

$$C_{T_P} = \frac{T_P}{\tfrac{1}{2}\rho A_4 V_o^2} = \frac{A_2}{A_4}\left[\left(\frac{V_5}{V_o}\right)^2 - 1\right] = K\frac{A_2}{A_4} \tag{2}$$

The total thrust is obtained by applying the momentum theory to the control volume. Hence, the total thrust is given by the rate of change of momentum of the fluid passing through the duct, therefore:

$$T_T = \rho A_5 V_5 (V_5 - V_o) \tag{3}$$

and the total thrust coefficient

$$C_{T_T} = \frac{T_T}{\tfrac{1}{2}\rho A_4 V_o^2} = 2\frac{A_5}{A_4} \cdot \frac{V_5}{V_o}\left(\frac{V_5}{V_o} - 1\right) \tag{4}$$

[For open propeller, i.e. unshrouded or with very large tip clearance, the axial momentum theory indicates that half of the velocity increase takes place at the propeller disk. Therefore:

$$V_2 = V_o + \frac{V_5 - V_o}{2} = \frac{V_5 + V_o}{2} \tag{5}$$

and since $A_5V_5 = A_2V_2$

then,

$$C_{T_P} / C_{T_T} = 1$$

In other words there is no thrust produced by the duct in this case.]

The continuity equation applied between sections 1 and 4 within the duct gives:

$$V_1A_4 = V_4A_5 + V_o(A_4 - A_5) \tag{6}$$

Therfore:

$$A_5 = A_4\left(\frac{V_1 - V_o}{V_4 - V_o}\right) \tag{7}$$

Applying the momentum theorem to the fluid between sections 1 and 4 within the duct we obtain:

$$T_P + p_1A_4 - p_oA_4 = \rho A_5V_5(V_5 - V_1) + \rho(A_4 - A_5)V_o(V_o - V_1) \tag{8}$$

Substituting T_P from equation (1) and using the long duct assumption (8), then:

$$K\frac{A_2}{A_4} = \left(\frac{V_1}{V_o} - 1\right)\left(1 - \frac{V_1}{V_o} + 2\frac{V_4}{V_o}\right) \tag{9}$$

Therefore:

$$\frac{V_1}{V_o} = 1 + \sqrt{1+K} - \sqrt{1+K\left(1 - \frac{A_2}{A_4}\right)} \qquad (10)$$

and finally,

$$C_{T_T} = 2\left[\sqrt{1+K} - \sqrt{1+K\left(1 - \frac{A_2}{A_4}\right)}\right] \sqrt{1+K} \qquad (11)$$

The difference between C_{T_T} and C_{T_P} is the thrust produced by the in-hull tunnel, C_{T_H}

$$C_{T_H} = 2\left[\sqrt{1+K} - \sqrt{1+K\left(1 - \frac{A_2}{A_4}\right)}\right] \sqrt{1+K} - K\frac{A_2}{A_4} \qquad (12)$$

$$= \frac{T_H}{\frac{1}{2}\rho A_4 V_o^2}$$

At bollard, from equations 1 and 3, then

$$\frac{T_P}{T_T} = \frac{\frac{1}{2}\rho A_2 (V_5^2 - V_o^2)}{\rho A_5 V_5 (V_5 - V_o)} \qquad (13)$$

$$= \frac{A_2}{2A_5}$$

and neglecting the slipstream contraction (i.e., $A_5 = A_2$), then

$$\frac{T_P}{T_T} \cong 0.5$$

In other words, the thrust on the hull and the propeller thrust are equal (ideally) at bollard condition.

The ideal power input to the device is given by the change in kinetic energy of the fluid in passing through the unit, or

$$P = \frac{1}{2}\rho A_5 V_5 (V_5^2 - V_o^2) \qquad (14)$$

The power coefficient is given by:

$$C_P = \frac{P}{\frac{1}{2}\rho A_4 V_o{}^3}$$

$$C_P = \frac{A_5}{A_4} \frac{V_4}{V_o} \left[\left(\frac{V_4}{V_o}\right)^2 - 1 \right]$$

$$= \left[\sqrt{1+K} - \sqrt{1+K\left(1 - \frac{A_2}{A_4}\right)} \right] \sqrt{1+K} \left(\sqrt{1+K} + 1 \right) \qquad (15)$$

The efficiency of the propulsion is given by $\eta = \frac{C_{T_T}}{C_P}$,

or $\eta = \frac{2}{1 + \sqrt{1+K}}$ (which is the ideal efficiency based on momentum consideration in a potential flow) (16)

and from equation 1,

therefore $\eta = \frac{2}{1 + \frac{V_5}{V_o}}$

The propulsion efficiency can also be obtained as follows:

$\eta = \frac{T_T \cdot V_o}{P}$, and from equations (3), (14),

therefore $\eta = \frac{2}{1 + \frac{V_5}{V_o}}$

The analysis so far has assumed that the intake area is forward of the propeller and in a plane normal to the propeller axis (e.g., the case of a ducted propeller).

In the case of an in-hull propulsion system with a bottom intake and no scoop to guide the flow into the intake, the only part of the flow's energy that is recoverable is that part associated with the flow velocity component forming an angle θ with the bottom of the hull.

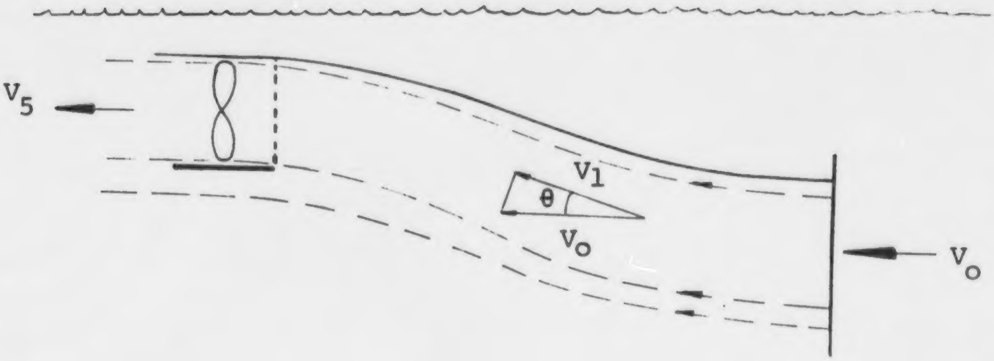

The velocity component at the intake plane in the control volume is

$$V_1 = V_o \cos\theta$$

Consequently, the minimum hydraulic power (change in the kinetic energy) becomes

$$P = \tfrac{1}{2}\rho A_5 V_5 (V_5^2 - V_o^2 \cos^2\theta), \tag{17}$$

and the propeller thrust reads

$$T_P = \tfrac{1}{2}\rho A_2 (V_5^2 - V_o^2 \cos^2\theta), \tag{18}$$

where the total thrust remains unchanged.

Comparing equations (17) and (14) we realize that the minimum power required to produce the same thrust is in fact increased by a factor of $(1 + \frac{\sin^2\theta}{K})$ as a result of having a bottom intake. It must be noted that the hydraulic power, equation (17), is the minimum power required to produce a total thrust $\rho A_5 V_5 (V_5 - V_o)$. Undoubtedly bottom intake losses, frictional losses in the tunnel inlet, and exit losses will increase the required power further to produce the same thrust.

It is usually preferable to study the change in the thrust produced at constant power then the change in the required power at constant thrust.

So for the same input power and the same propulsive efficiency the total thrust is reduced by a factor of $(1 + \frac{\sin^2\theta}{K})$ due to a bottom intake. In other words, the pressure loss in this case is:

$$\Delta P_1 = \frac{\rho A_5}{A_4} V_5 (V_5 - V_o) \cdot (\frac{\sin^2\theta}{K}),$$

$$\Delta P_1 = \frac{m}{A_4} (V_5 - V_o)(\frac{\sin^2\theta}{K}) \quad \text{(where m is the rate of flow)} \quad (19)$$

and non-dimensionally:

$$C(\Delta P_1) = \frac{\Delta P_1}{\frac{1}{2} V_o^2} = C_{T_T} \cdot \frac{\sin^2\theta}{K} \quad (19)A$$

To estimate the thrust loss due to a bottom intake with appropriate guards (grill), for example, one may follow, again, the principles of fluid mechanics.

A grill on the intake would exert a drag force 'D' on the inflow where $D = \sum_i D_i$, D_i = drag of ith member in grill.

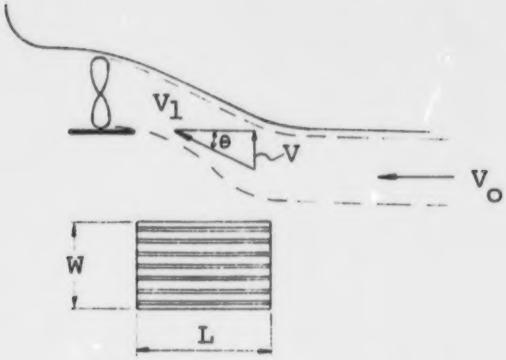

The drag D_i for each grill member may be estimated using quasi-one-dimensional flow.

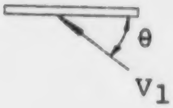

$D_i = C_{Di}\frac{1}{2}\rho SV^2$, where S = projected area of the guard
= $L * d$, if the guards are cylindrical rods

V is the velocity normal to the grill member axis
= $V_o \cos\theta \sin\theta$

and C_{Di} is the drag coefficient for the grill member. The drag coefficient C_{Di} is generally a function of Reynolds number, (based on the diameter and on the velocity component normal to the axis), the cross section, and the surface roughness.

For example, if the grill consists of smooth cylindrical rods (and quite apart from each other) then at subcritical Reynolds number (i.e., $R_e < 2 \times 10^5$), the value of C_{Di} is about 1.2, and at supercritical Reynolds number ($R_e > 5 \times 10^6$), the C_{Di} value is about 0.6.

Having calculated the drag force D due to the grill, then the pressure loss ΔP across the grill can be calculated as:
$\Delta P = D/Wh$

The pressure loss ΔP may be added to the unavoidable intake pressure loss ΔP_1 described previously.

Now, let us consider the case where we have a vessel with a prime mover of fixed power P and with an unguarded bottom intake. Then from expression (17), neglecting all other losses, the minimum power is

$P = \frac{\rho A_5 V_5}{2} (V_5{}^2 - V_o{}^2 \cos^2\theta)$ to produce a total thrust of

$$T = \rho A_5 V_5 (V_5 - V_o)$$

When the grill is fitted there will be an additional head loss, ΔP, as described previously, and assuming the power remains the same then the discharge velocity V_5 decreases by an amount ΔV_5. Therefore:

$$P = \frac{\rho A_5 (V_5 - \Delta V_5)}{2} \left[(V_5 - \Delta V_5)^2 - V_o{}^2 \cos^2\theta - g \frac{\Delta P}{\rho} \right] \qquad (20)$$

So, what we are looking for is in fact the relation between ΔV_5 and ΔP.

$$\therefore \frac{\rho A_5 V_5}{2} \left[V_5{}^2 - V_o{}^2 \cos^2\theta \right] = \frac{\rho A_5 (V_5 - \Delta V_5)}{2} \left[(V_5 - \Delta V_5{}^2) - V_o{}^2 \cos^2\theta - \frac{g\Delta P}{\rho} \right] \qquad (21)$$

$$\therefore V_5{}^3 - V_5 V_o{}^2 \cos^2\theta = (V_5 - \Delta V_5) \left[V_5{}^2 - 2\Delta V_5 V_5 - V_o{}^2 \cos^2\theta - \frac{g\Delta P}{\rho} \right]$$

$$\therefore -3\Delta V_5 \cdot V_5{}^2 - V_5 \frac{\Delta P}{\rho} + \Delta V_5 \cdot V_o{}^2 \cos^2\theta = 0$$

$$\boxed{\therefore \Delta V_5 = \frac{V_5}{\rho \left[3V_5{}^2 - V_o{}^2 \cos^2\theta \right]} \cdot g\Delta P} \qquad (22)$$

The corresponding total thrust is:

$$T - \Delta T = \rho A_5 (V_5 - \Delta V_5) \left[V_5 - \Delta V_5 - V_o \right]$$

$$\therefore \rho A_5 V_5 (V_5 - V_o) - \Delta T = \rho A_5 (V_5 - \Delta V_5) \left[V_5 - \Delta V_5 - V_o \right]$$

$$\therefore \Delta T = 2\rho A_5 V_5 \Delta V_5 - \rho A_5 V_o \Delta V_5$$

$$\boxed{\Delta T = \rho A_5 \left[2V_5 - V_o \right] \Delta V_5} \qquad (23)$$

which is the loss in the total thrust due to a guarded bottom intake.

For bollard condition:

$$\Delta T = \rho A_5 \cdot 2V_5 \cdot \Delta V_5 \text{, and from expression (22)}$$

$$= \rho A_5 V_5 \cdot \frac{2V_5}{\rho \cdot 3V_5^2} \cdot \Delta P$$

$$\Delta T = \frac{2}{3} A_5 \cdot \Delta P \qquad (24)$$

Thus the thrust loss caused by fitting a grill to a bottom intake is roughly $\frac{2}{3} A_5 \Delta P$, at bollard. If the tip clearance is too small, then $A_5 \cong A_2 \cong A_4$

$$\therefore \Delta T = \frac{2}{3} A_2 \cdot \Delta P \qquad (25)$$

Numerical Example:

Assume the propeller thrust coefficient is about 2.

Ducted Propeller $C_{T_P} = 2$, and the tip clearance ratio is say 5%

$$\therefore \frac{A_2}{A_4} \cong 1 - 0.2 = 0.8$$

From expression (2):

$$\therefore K = \frac{2}{0.8} = 2.5$$

and from expression (11):

$$\therefore C_{T_T} = 2\left[\sqrt{1+2.5} - \sqrt{1+2.5(1-0.8)}\right]\sqrt{1+2.5}$$

$$= 2\left[1.8708-1.2247\right] 1.8708$$

$$= 2.4176$$

$$\therefore C_{T_H} = 2.4176 - 2. = 0.4176$$

The power coefficient from expression (15);

$$C_P = \left[\sqrt{1+2.5} - \sqrt{1+2.5(1-0.8)}\right]\cdot\sqrt{1+2.5}\ \ (\sqrt{1+2.5} + 1)$$

$$= \left[\sqrt{3.5} - \sqrt{1.5}\right]\sqrt{3.5}\ \ (\sqrt{3.5} + 1)$$

$$= 3.47$$

and from expression (16):

$$\therefore \eta = \frac{C_{T_T}}{C_P} = \frac{2.4176}{3.47} = 0.697$$

For in-hull propulsion system: with unguarded bottom intake

ε = 5%, tip clearance ratio

$\frac{A_2}{A_4}$ = 0.8 assuming the intake angle $\theta = 30^\circ$, $C_{T_T} = 2.4176$

The propeller thrust is reduced by a factor of:

$$\left(1 + \frac{\sin^2 30}{2.5}\right) = 1.1$$

and the input power is increased by the same factor, i.e., $C_P = 1.1 * 3.47 = 3.817$ to produce the same total thrust. Then the propulsive efficiency becomes:

$$\therefore \eta = \frac{2.4176}{3.817} = 0.633$$

which means that there is a loss of about 6.5% of the propulsive efficiency as a result of a bottom intake with the assumed 30° flow deflection.

Or alternatively, if the change in the total thrust is considered for the same input power and the same propulsive efficiency, i.e.,

$C_P = 3.47$,

then the total thrust is reduced by a factor of 1.1 as a result of the bottom intake. The pressure loss coefficient in this case is obtained from expression (19)A:

$$\begin{aligned} C(\Delta P_1) &= 2.4176 * 0.1 \\ &= 0.24 \end{aligned}$$

To estimate the additional pressure loss as a result of using longitudinal guards in the intake one may proceed are follows:

$$\eta = \frac{2}{1 + \frac{V_5}{V_o}}$$, and with V_o, say, equal to 8 m/sec., then,

$$\therefore 0.697 = \frac{2}{1 + \frac{V_5}{8}} \qquad \therefore V_5 \cong 15 \text{ m/sec.(discharge velocity)}$$

$\therefore$ The rate of flow = $A_5 * V_5$, $A_5 \cong A_4$ for long ducts

$\therefore A_5 = A_2/0.8 = 1.25\ A_2$

For a 6 m propeller then: $A_5 = A_4 = 1.25 * \pi/4 * 36$

$= 33.75\ m^2$

$\therefore$ The rate of flow = 15 * 33.75 = 506.25 m^3/sec.

It is advisable to make the area of the section of the tunnel no greater than is necessary for the admission of 506.25 m^3/sec. which is accelerated to the rear by the propeller.

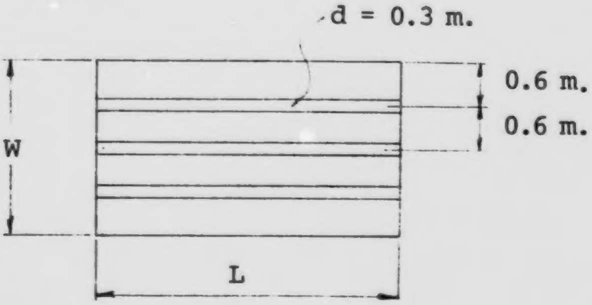

If the intake is a rectangle W * L, and W = D,
= 6 m,

and having openings of 2d, between the guards, then one requires 6 guards.

The velocity normal to the intake area is $V_o\cos\theta\sin\theta$

$$V = 8 * 0.866 \times 0.5 = 3.45 \text{ m/sec.}$$

and the required area of intake = $\frac{506.25}{3.45}$

= 146.74 m^2 (four times the propeller area)

$$\therefore L = \frac{146.74}{6.0 - 6 * 0.3} = 34.9 \text{ m}$$

Reynolds' number for the cylindrical guards = $\frac{Vd}{\nu}$

$$= \frac{3.45 * 0.3}{1.168 \times 10^{-6}} = 8.86 \times 10^5 \quad \text{(critical regieme)}$$

So the drag coefficient C_D is in the range of 1.0.

∴ Then the drag force of the guards is = no. of guards * $\frac{1}{2}\rho$ * S * V^2,
S = L x d

The pressure drop as a result of the intake guards

$$\Delta P = 6 * \tfrac{1}{2}\rho * L * d * V^2/A_4$$

(remember that A_4 is used in calculating all the coefficients), or in a non-dimentional form:

$$C(\Delta P) = \frac{6 * \frac{1}{2}\rho * L * d * V_o^2\cos^2\theta\sin^2\theta}{\frac{1}{2}\rho V_o^2 \qquad A_4}$$

$$= \frac{6 * 44.47 * 0.3 * \cos^2 30\sin^2 30}{33.75}$$

$$= 0.445$$

Then the new pressure difference coefficient across the propeller becomes:

$$\begin{aligned} K_1 &= K - C(\Delta P_1) - C(\Delta P) \\ &= K - 0.1K - 0.445 \\ &= 2.4176 - 0.24176 - 0.445 \\ &= 1.731 \end{aligned}$$

The discharge velocity V_5 decreases by an amount ΔV_5 due to the pressure loss ΔP and from expression (22) then:

$$\Delta V_5 = \frac{V_5}{\rho\left[3V_5{}^2 - V_o{}^2\cos^2\theta\right]}\, g\,\Delta P$$

$$= \frac{15}{\rho\left[3 \times 15^2 - 8^2\cos^2 30\right]} \times 9.81\cdot\frac{6}{2}\; \frac{\rho * 44.47 * 0.3 * 8^2\cos^2 30\, \sin^2 30}{33.75\,\rho\left[3 \times 15^2 - 8^2\cos^2 30\right]}$$

$$= 0.26 \text{ m/sec.}$$

The reduction in the total thrust is obtained from expression (23) as:

$$\Delta T = A_5\left[2V_5 - V_o\right]\,\Delta V_5$$

and in non-dimensional form:

$$C(\Delta T) = \frac{A_5\left[2V_5 - V_o\right]\,\Delta V_5}{\frac{1}{2}\rho A_4 V_o{}^2}$$

$$= \frac{2\left[2 * 15 - 8\right] * 0.26}{8^2}$$

$$= 0.179$$

The total thrust coefficient becomes:

$$C_{T_T} = 2.4176 - 0.179$$

$$= 2.2386$$

Then the propulsive efficiency:

$$\frac{C_{T_T}}{C_P} = \frac{2.2386}{3.47} = 0.645$$

which indicates that there is about 5% reduction in the ideal efficiency of the device due to this particular configuration of in-hull propulsion systems with guarded bottom intake. In practice, one would expect a lower efficiency due to:

1) rotational losses in the fluid;
2) the flow curvature over and between a finite number of propeller blades;
3) the circumferential variation in velocity at propeller location as a result of the development of bound circulation over a limited segment of the duct;
4) profile drag of the propeller blades;
5) frictional losses of the tunnel structure with additional inlet losses as a result of using transverse members to support the longitudinal guards;
6) increased thrust deduction as a result of the tunnel arrangement; and,
7) differences from the optimum design conditions.

If one considers the real efficiency to be, say 0.8 of the upper bound efficiency, then:

$$\begin{aligned} \eta_{real} &= 0.8 * 0.645 \\ &= 0.52 \end{aligned}$$

APPENDIX B

Classified Canadian Patents Related To Protective Devices for Propellers

(The expiry date is 17 years from the date of issue)

Kort Nozzle	Patent No. 396724
Slotted Nozzle (Mönnich)	Patent No. 735219
Deflecting Fins	Patent No. 509171
Propeller Guard	Patent No. 981118
YPASS Propulsion Device	Patent No. 910732

PATENT

No. 396724

DATE MAY 20 [illegible]

FEES RECEIVED

FILING FEE $ 15.00
ADDITIONAL CLAIMS $
REINSTATEMENT FEE $
RESTORATION FEE $
FINAL FEE $ 20.00

ASSIGNMENT FEES	ASSIGNMENTS RECORDED
(1) $	
(2) $	
(3) $	

CARDBOARD DRAWINGS [illegible]

PATENT OFFICE

APPLICATION FOR PATENT

15 No. 459082 [illegible]

FILED Dec. 30, 1938.

APPLICANT Ludwig Kort

ATTORNEY Fetherstonhaugh & Co.
C.P.R. Bldg.
Winnipeg, Man.

INVENTION Screw Propulsion of Ships

ACTION Let & reqs. Dec. 29/31/38.

Acknowledged by Circular I, and receipt mailed Jan. 10 1939
Let. Jan. 14/16/39

new oath called for Cir 2 - Jan. 18/39 Let. [illegible] Oct. 7/21/39 Ack'd.
Nov. 24/39. Let & oath Jan. 16/18/40. Ack'd. & affidavit re delay called for
Feb. 13/40 Let & oath Feb. 17/21/40 Ack'd & oath ret'd. for transl. [illegible] Feb. 29/40
Let & affdts. [illegible] May 27/June 1/40 Ack'd & affts. ret'd June 21/40 Let, [illegible] affidavits
translation of jurat of oath & encl. Aug. 1/3/40 Returned (EB) Sep. 11/40. Let —
$20.00 March 17/19/41 Ack'd. Mar. 24/41. Let March 31/Apr. 2/41
Rec. Med. Apr. 4/41

CITIZEN [illegible]
DECLARED
German.

READY FOR ISSUE

[illegible]

NOTICE OF ALLOWANCE

NOV 12 1940

NOTIFICATION MAILED MAY 30 1941

COST OF COPIES

B-1

This invention relates to screw-propelled ships and has for its principal object the improvement of the efficiency of such ship propulsion.

It is known to surround the screw propeller of a ship by a ring attached to the hull and it is also known to make this ring of nozzle shape closely surrounding the propeller, the cross-sectional area of the ring being a minimum in the neighbourhood of the plane of the propeller and, while not changing materially aft of the said plane, increasing relatively rapidly forwardly thereof to the forward opening of the ring, the cross-sectional area of which is thus substantially larger than that of the rear opening.

The object of these proposals has been to increase the propulsive efficiency and driving thrust for a given engine power and speed of the ship. There are, however, a number of factors which were not considered in the design of these nozzle rings and it is an object of this invention, which is based on the discovery of and a consideration of these factors, to provide an arrangement by means of which results are obtained which are an improvement on those obtained by the known arrangements. The value of these factors and the improved results achieved by taking them into consideration have been verified by numerous tests.

While these factors will be discussed in detail hereinafter, it may be stated here that it is necessary, according to one feature of the invention, to form the walls of the nozzle ring, for at least the greater part of the circumference of the latter, of aerofoil section corresponding to the section of an aeroplane wing, the said walls having their pressure surfaces at the outside of the nozzle and their forward edges of rounded section, and the smallest distance between the plane of the propeller and that of the forward opening of the nozzle being less than one third of the diameter of the propeller.

Preferably the maximum thickness of the wall of the nozzle does not exceed this distance between the propeller and the forward opening of the nozzle, while the hull of the ship forward of the propeller is advantageously so shaped that its surfaces in section form longitudinal curves which at their after ends approach a direction substantially parallel to the propeller shaft before reaching the plane of the mouth of the nozzle.

It is, furthermore, advisable to make the area of the mouth of the nozzle no greater than is necessary for the admission, without it being accelerated in front of the nozzle, of the quantity of water which is accelerated to the rear by the propeller at any given speed and power output.

On many ships owing to the shape of the stern the water reaches the propeller at different speeds in different parts of the propeller circle, with the result that the moving propeller blades pass alternately through fast and slow moving water with the result that the reaction forces acting on the blades vary continually. With a view to avoiding this and improving the efficiency of the propeller whilst reducing vibration, guiding means are, according to a further feature of the invention, provided in front of the propeller in the zones where the speed of the water is below the average to deflect the flow of the water towards the direction of movement of the propeller blades as they pass behind the guiding means.

According to a modification of this arrangement the

4

guiding means may be provided in the zones where the speed of the water is above the average to deflect the flow of water against the direction of movement of the propeller blades. If desired guiding means may be provided both in the zones of the slow moving and fast moving water.

It is also possible, according to yet another feature of the invention, to combine the nozzle with the tunnel or "Thornycroft" stern of a shallow draft ship, while, again, the nozzle according to the invention may be arranged to serve the purpose of a rudder to give not only an increased propulsive efficiency but also improved steering.

Various embodiments of the invention will now be more fully described, by way of example, with reference to the accompanying drawings in which:-

Figure 1 is a part stern view of a ship provided with a nozzle ring according to the invention, the propeller and rudder being omitted but the direction of rotation of the propeller when the ship is going ahead being shown by arrows;

Figure 2 is a side view of the stern of the ship shown in Figure 1;

Figure 3 is a plan view showing various horizontal sections through the nozzle ring, the rudder and the stern of the ship shown in Figures 1 and 2, the sections being taken parallel to and at different levels relatively to the propeller shaft, the section through the nozzle and rudder being taken at the level of the propeller shaft, and the stem of the ship indicated by the lines 14 and the parts within the circle A-B being shown at the level of the line A-B of Figure 2. The line 18 in this Figure represents a waterline just above the top of the rudder 21 (the angles of movement of which are indicated by α) and the line 19 represents the outline of the deck.

Figure 4 is a horizontal section taken on the line C-D of Figure 2 showing the stern post and part of the ship's hull;

Figure 5 is a stern view of a shallow draft ship provided with a combined tunnel stern and nozzle according to the invention;

Figure 6 is a side view of the stern of ship shown in Figure 5;

Figure 7 is a horizontal cross-section taken through the rudder, nozzle tunnel and the stern part of the hull of the ship shown in Figures 5 and 6, the outline of the hull and tunnel at the height of an assumed water line and the outline of the deck being shown in broken lines;

Figure 8 is a stern view of a ship provided with a combined nozzle-rudder according to the invention;

Figure 9 is a side view of Figure 8, and

Figure 10 is a view in horizontal cross-section showing the nozzle-rudder of Figures 8 and 9.

The operation of the arrangement of the improved nozzle ring with the propeller operating within it may be explained from a consideration of the fact that the water is accelerated by the action of the propeller 13 between the forward opening or mouth of the nozzle 4, which has a cross-sectional area E (see Figure 3), and the plane of the propeller where the nozzle has the smaller cross-sectional area F. As a result of this acceleration the hydrodynamic pressure of the water in front of the propeller and nozzle is reduced, while the normal hydrostatic pressure resulting from the head of water and the superposed atmospheric pressure is maintained on the outer surfaces of the nozzle, acting from the side and from the rear. Bearing this fact in mind and considering the projected area E-H which is shown shaded in Figure 1, it will be seen that there is a smaller pressure in front and a larger pressure at the rear of this projected area, the pressure difference acting in the direction of travel of the ship; Since the nozzle ring is rigidly attached to the hull this pressure difference represents a thrust additional to the normal thrust of the propeller.

It follows from this consideration that it is desirable to make the shaded area E-H as large as possible, since the additional thrust will be the product of the mean pressure difference Δ p multiplied by the area E-H. In no case, however, should the area E be larger than is necessary for the admission, without it being accelerated in front of the mouth of the nozzle, of the quantity of water which is accelerated to the rear by the propeller at any given speed and power output. If the area E of the mouth is made too large the nozzle ring will act partly as a brake with the result that there will be a loss of speed and the total propulsive effect of the nozzle may even be a negative one.

The reduced pressure and the resultant suction produced by the action of the propeller and nozzle will act not only on the front surfaces of the nozzle ring, thus adding to the propulsive thrust, but may be felt at the same time on the stern surfaces 14 (Figure 3) of the ship, acting as a brake, and this increased resistance may counteract the increase of the propulsive thrust. In order to avoid this danger it is necessary that the hull of the ship in front of the propeller and nozzle should have fine lines/or that the propeller and nozzle should be placed sufficiently far away from the hull inorder that the water may enter the mouth of the nozzle from forward in a direction practically parallel to the axis of the propeller shaft.

On many ships the stern forward of the propeller shows rather blunt lines above the propeller shaft and much finer lines below the propeller shaft. In consequence of this, especially when the ship is travelling at a fairly high speed, the water passing along the sides of the ship towards the propeller has to fill up the large void rather rapidly and loses much of its speed in front of the upper part of the propeller circle, while the loss of speed in front of the lower part of the circle is a good deal less. Each propeller blade, therefore, passes alternately through fast and slow moving water. The blades pass easily through the fast moving water but they encounter a greater resistance and absorb more torque from the shaft when they pass through the slow moving water.

This difficulty is overcome, according to a further feature of the invention, by providing guiding means between the hull and the mouth of the nozzle in front of the propeller, by means of which the water in the slow moving zones is deflected from its straight fore-and-aft course towards the direction of movement of the passing propeller blades so as to meet the plane of the propeller at an acute angle. Such guiding means are shown in Figures 1, 2 and 3 of the drawings.

In Figure 1 the direction of rotation of a right-handed propeller is shown by arrows. A guide fin 5 having a leading edge F and a trailing edge G is arranged radially to the axis of the propeller shaft. Figures 2 and 3 show how this fin 5 is arranged longitudinally with regard to the ship's stern and to the propeller 13.

In addition, the stern post 15 of the ship is not placed vertically in front of the propeller, as is usual and is indicated by the line between the points 1 and 2 in Figure

2, but is arranged with its upper part raked forward as indicated by the line between the points 2 and 3. Furthermore, the upper part of the stern post is given a shape, as shown in Figure 3, which likewise deflects the water towards the direction of movement of the passing blades. The combined action of the guide fin 5 and of the raked stern post 15 is especially well illustrated by the section within the circle A-B in Figure 3 (see also Figure 2). By this deflecting arrangement, the shape of which may of course be modified so long as it gives the desired result, the angle of impact between the slow moving water and the faces of the fast moving propeller blades is decreased, thereby decreasing at the same time the propeller shaft torque required to turn the propeller blades through the zone of the slow moving water.

This arrangement, the value of which has been proved by careful tests, may be further improved by giving to the stern post below the propeller shaft a cross-section as shown in Figure 4 which is a cross-section taken on the line C-D of Figure 2. The combined guiding means above and below the propeller shaft then decreases the load on the moving blades in the zone of the slow moving water and increases it in the zone of the fast moving water. Both actions combined tend to increase the efficiency of the propeller for a given engine power.

It is, of course, possible to provide guiding means in the zone of the fast moving water only.

It has already been stated that the area E of the mouth of the nozzle, as compared with the area P at the propeller, should be as large as possible, but that it is, on the other hand, limited by the speed and power of the ship. It should be born in mind that the resistance of the ship may vary between wide limits as the ship may have to tow loads of various sizes, or she may be held up by wind and sea. It is, therefore, impossible to give the mouth of the nozzle just the exact area to suit all these various conditions. For these reasons it is very advantageous to make the walls of the nozzle of aerofoil section corresponding to the section of an aeroplane wing, the walls having well-rounded leading edges and their pressure surfaces forming the outside of the nozzle. By this arrangement the resistance of the nozzle passing through the water is kept low and at the same time the mouth of the nozzle is well adapted for dealing with varying quantities and speeds of water.

The effective length L of the forward part of the nozzle between the planes E and P should not be greater than one third part of the diameter of the propeller to ensure that the water entering the mouth of the nozzle at low ship speeds and high loads on the propeller does not separate from the inside walls of the nozzle, which would give a very great loss of propulsive effect. It is found that, as a practical limit, the thickness [illegible] of the walls between the planes E and P should nowhere be greater than the distance L.

Furthermore, it has been found possible to combine the nozzle arrangement described above with the known tunnel or "Thornycroft" stern of a shallow draught ship. Figures 5, 6 and 7 show such an arrangement by way of example.

Figure 6 shows the tunnel stern of the ship seen from the side, 6 being the normal waterline. The top of the tunnel is shown at 7 and it will be seen that the propeller reaches above the waterline. The effect of this known arrangement is that the propeller, when working, lifts the water into the tunnel and thereby operates in solid water over its whole area.

When combining such a tunnel arrangement with a nozzle as shown in Figures 5, 6 and 7, the general requirements of the nozzle must be met, but in addition care must be taken that the cross-sectional areas of the tunnel immediately in front of the mouth A of the nozzle should be made as great as possible. This is indicated in Figure 5, which shows at 5 a section on the line 5-5 of Figure 7, and in Figure 7 by the shape of the lines of intersection of the waterline 6 with the inside of the tunnel.

On shallow draught ships especially, but also on some deep-draft ships with large diameter propellers, it is often necessary to make the bottom part of the nozzle ring of rather thin section. Such a thin section is not of much value for the nozzle effect and is detrimental to the action of the remaining parts of the nozzle. However, by extending the thin section parts well forward beyond the plane A of the mouth of the nozzle proper i.e. beyond the plane where the walls of the nozzle are for the first time continuous round the circumference of the nozzle, the parts of thin section are removed from the zone of the suctional effect of the propeller as the water is then taken into the nozzle chiefly from the sides, thereby making the parts of the nozzle at these sides all the more effective. Such an arrangement is shown in Figures 5, 6 and 7 and also in Figures 9 and 10, but of course it may be applied to any other embodiment of the invention. The effective area E-H of the nozzle of the tunnel stern ship, taking into account the restriction of the tunnel and the thin section 16 of the bottom, is shown shaded in Figure 5.

Figures 8, 9 and 10, which are also given only by way of example, show how a nozzle arrangement according to the invention may be arranged to act as a new and improved type of steering device without losing its propulsive effect. For this purpose the nozzle ring is not rigidly fixed to the ship but is supported in its proper position around the propeller 13 by means of a pivotal connection between the ship and nozzle, the nozzle being connected to the normal rudder post 17 and steering gear. The centre line of the rudder post should be so arranged that it intersects the centre line of the propeller shaft at approximately a right angle and also so that it is in line or nearly in line with the plane of the propeller.

The rudder post 17 is operated from the steering gear of the ship in the same way as the rudder post of an ordinary rudder, as is indicated by the quadrant 8 in Figure 9.

If such a nozzle rudder is in its central position, i.e. with the centre line of the nozzle in alignment with the centre line of the propeller shaft (see Figure 10) there is no other action but the normal effect of nozzle propulsion due to the forward inner parts of the nozzle on each side being located in zones of reduced pressure, as indicated by the curved arrows 9 and 10, in Figure 10. The side forces due to the difference of pressure between the inside and the outside of the walls of the nozzle on the port and starboard sides counteract and balance each other so that there are no unbalanced side forces acting on the stern of the ship.

As soon, however, as the nozzle rudder is turned to one side or the other, as indicated by the angle α between the centre lines of the nozzle 4 and of the dotted new position of the nozzle (see Figure 10), the zone 9 of the reduced pressure on the port side extends to the zone 11, while the zone 10 on the starboard side practically disappears. In other words a powerful force is exerted on the port side of the nozzle tending to swing the stern of the ship to starboard. At the same time the inner part of the starboard side of the nozzle is met by the full force of the race from the propeller. By deflecting this race to port a reaction force is produced which also tends to swing the stern to starboard.

Thus by the combined action of these two forces, both acting in the same direction, a new and very effective method of steering the ship is obtained. These side forces are so great that at small angles of helm they represent many times the sideforces which would be produced by any ordinary rudder arrangement behind the propeller. The arrangement has the further advantage of giving a substantial and absolutely reliable steering effect when going astern, which also is a great advantage over the ordinary rudder arrangement.

The nozzle rudder may be shaped as a ring of uniform wall section for its full circumference, or it may be shaped as shown in Figures 8, 9 and 10 with the outside of the nozzle and the outside of the ship's hull above, or at the side of, the nozzle having a mutually corresponding shape with a relatively small clearance between the adjacent surfaces of the nozzle and hull, so that the outside of the nozzle merges with the hull of the ship. The object of this arrangement is to avoid the losses due to the formation of eddies between the ship's stern and the nozzle.

The action of the nozzle rudder will be still further improved by providing horizontal and/or vertical streamlined vanes 20 in the outlet opening of the nozzle as shown in Figures 8 and 9. The effect of this is to reduce the helical movement of the water resulting from the action of the propeller, thereby increasing the reactional forces of the race from the propeller.

HAVING regard to the foregoing disclosure, the patent of which this specification forms part confers, subject to the conditions prescribed in the Patent Act, 1935, the exclusive right, privilege and liberty of making, constructing, using and vending to others to be used, the invention as defined in claims submitted by the patentee as follows:-

1. A screw-propelled ship having a nozzle ring connected with the hull of the ship and closely surrounding the propeller, wherein the inner cross-sectional area of the nozzle is a minimum in the neighbourhood of the plane of the propeller and while not changing materially aft of the said plane increases relatively rapidly forwardly thereof to the forward opening of the nozzle the cross-sectional area of which is thus substantially larger than that of the rear opening, wherein the walls of the nozzle are, for at least the greater part of the circumference of the latter, formed of aerofoil section corresponding to the section of an aeroplane wing, the said walls having their pressure surfaces at the outside of the nozzle and having their forward edges of rounded section, and wherein the smallest distance between the plane of the propeller and that of the forward opening of the nozzle is less than one third of the diameter of the propeller.

2. A ship as claimed in claim 1, wherein the

[illegible]

15

maximum thickness of the walls of the nozzle does not exceed the said smallest distance between the plane of the propeller and that of the forward opening of the nozzle.

3. A ship as claimed in claim 1, wherein the hull of the ship forward of the propeller is so shaped that its surfaces in section form longitudinal curves which at their after ends approach a direction substantially parallel to the propeller shaft before reaching the plane of the mouth of the nozzle.

4. A ship as claimed in claim 1, wherein parts of the walls of the forward section of the nozzle are thinner in section and are outwardly flared to a lesser extent than are the other parts of the walls of the corresponding section of the nozzle and wherein the thinner parts of the walls extend to a greater distance in front of the plane of the propeller than do the thicker parts.

5. A screw-propelled ship having a propeller so located relatively to the ship that when the ship is moving ahead the water reaches different zones of the propeller circle with different speeds, wherein guiding means are provided in front of the propeller in the zones where the speed of the water is below the average to deflect the flow of the water towards the direction of movement of the propeller blades as they pass behind the guiding means so as to meet the plane of the propeller at an acute angle.

6. A screw-propelled ship having a propeller so located relatively to the ship that when the ship

is moving ahead the water reaches different zones of the propeller circle with different speeds, wherein guiding means are provided in front of the propeller in the zones where the speed of the water is above the average to deflect the flow of the water against the direction of movement of the propeller blades as they pass behind the guiding means.

7. A ship as claimed in claim 1, wherein guiding means are provided in front of the propeller in the zones where the speed of the water is below the average to deflect the flow of the water towards the direction of movement of the propeller blades as they pass behind the guiding means so as to meet the plane of the propeller at an acute angle.

8. A ship as claimed in claim 1, wherein guiding means are provided in front of the propeller in the zones where the speed of the water is above the average to deflect the flow of the water against the direction of movement of the propeller blades as they pass behind the guiding means.

2

9. A screw propelled ship having a nozzle ring connected with the hull of the ship and closely surrounding the propeller wherein the inner cross-sectional area of the nozzle is a minimum in the neighbourhood of the plane of the propeller and while not changing materially aft of the said plane increases relatively rapidly forwardly thereof to the forward opening of the nozzle the area of which is thus substantially larger than that of the rear opening, wherein the walls of the nozzle are, for at least the greater part of the circumference of the latter, formed of aerofoil section corresponding to the section of an aeroplane wing, the said walls having their pressure surfaces at the outside of the nozzle and having their forward edges of rounded section, and wherein guiding means are provided in front of the propeller in the zones where the speed of the water is below the average to deflect the flow of the water towards the direction of movement of the propeller blades as they pass behind the guiding means so as to meet the plane of the propeller at an acute angle.

10. A screw propelled ship having a nozzle ring connected with the hull of the ship and closely surrounding the propeller, wherein the inner cross-sectional area of the nozzle is a minimum in the neighbourhood of the plane of the propeller and while not changing materially aft of the said plane increases relatively rapidly forwardly thereof to the forward opening of the nozzle the cross-sectional area of which is thus substantially larger than that of the rear opening, wherein the walls of the nozzle are, for at least the greater part of the circumference of the latter, formed of aerofoil section corresponding to the section of an aeroplane wing, the said walls having their pressure surfaces at the outside of the nozzle and having their forward edges of

rounded section, and wherein guiding means are provided in front of the propeller in the zones where the speed of the water is above the average to deflect the flow of the water against the direction of movement of the propeller blades as they pass behind the guiding means.

11. A ship as claimed in claim 1, having a tunnel stern, wherein the upper part of the inner surface of the nozzle constitutes part of the upper surface of the tunnel.

12. A ship as claimed in claim 11, wherein the cross-sectional area of the tunnel immediately in front of the mouth of the nozzle is substantially greater than the cross-sectional area at the propeller.

13. A screw-propelled ship having a nozzle ring connected with the hull of the ship closely surrounding the propeller, wherein the inner cross-sectional area of the nozzle is a minimum in the neighbourhood of the plane of the propeller and while not changing materially aft of the said plane increases relatively rapidly forwardly thereof to the forward opening of the nozzle the cross sectional area of which is thus substantially larger than that of the rear opening, wherein the walls of the nozzle are, for at least the greater part of the circumference of the latter, formed of aerofoil section corresponding to the section of an aeroplane wing, the said walls having their pressure surface at the outside of the nozzle and having their forward edges of rounded section, and wherein the nozzle is adapted to be pivoted after the manner of a rudder about an axis which intersects the axis of the propeller shaft substantially at right angles and in the plane of the propeller, and wherein also the smallest distance between the plane of the propeller and that of the forward opening of the nozzle is less than one third of the diameter of the propeller.

FIG. 1.

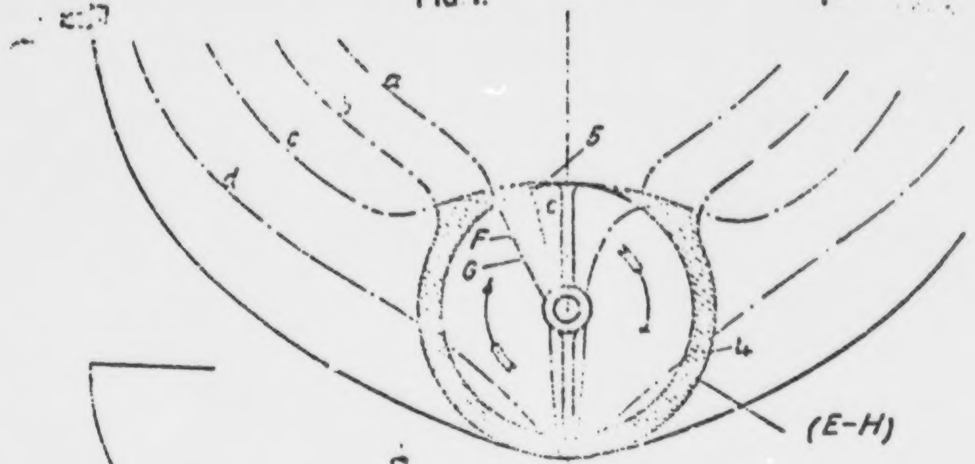
a
b
c
d
5
C
F
G
4
(E-H)

FIG. 2. FIG. 4.

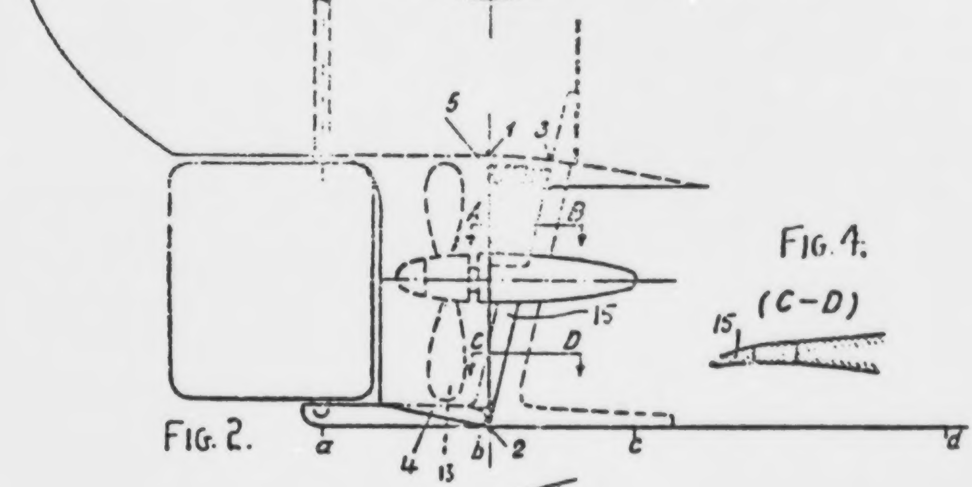
5
1
3
A
B
15
C
D
4
13
a
b
2
c
d
(C-D)
15

FIG. 3.

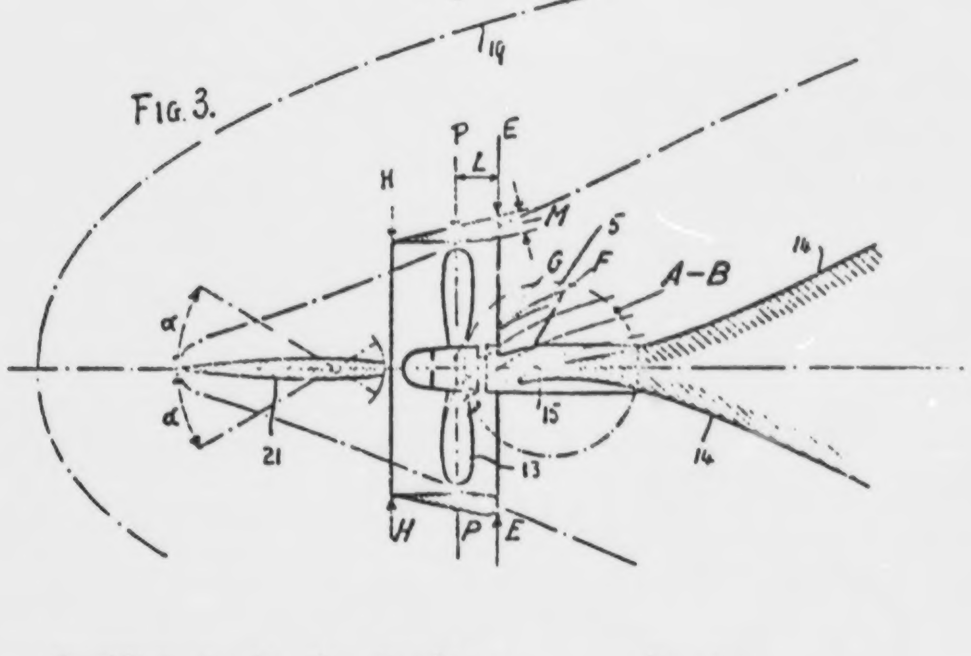
14
P
E
L
H
M
S
G
F
A-B
14
α
α
21
15
13
14
H
P
E

Certified to be the drawings referred to in the specification hereunto annexed.
Hannover, Nov. 26, 1938.

Inventor
Ludwig Kort
by [illegible] atty's.

FIG 5.

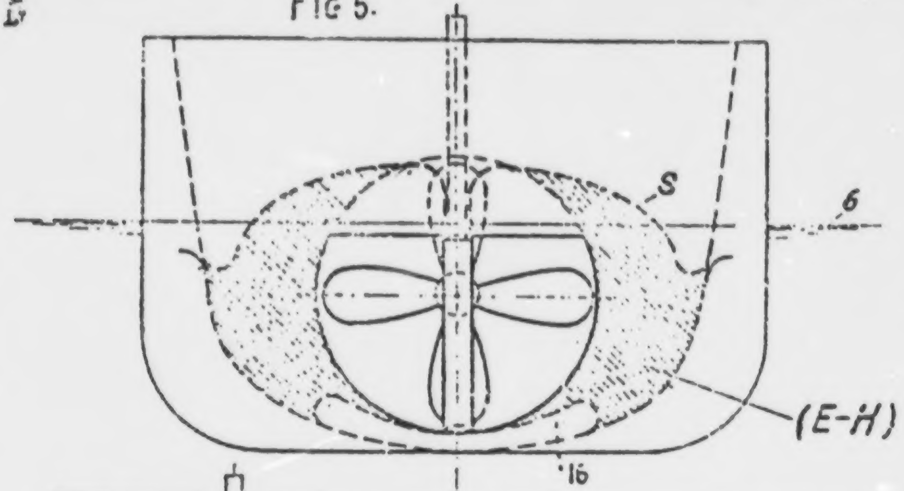

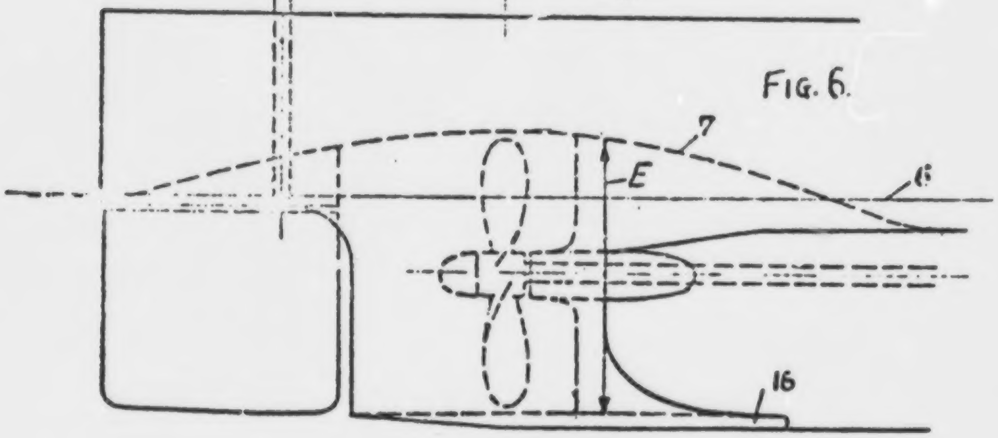

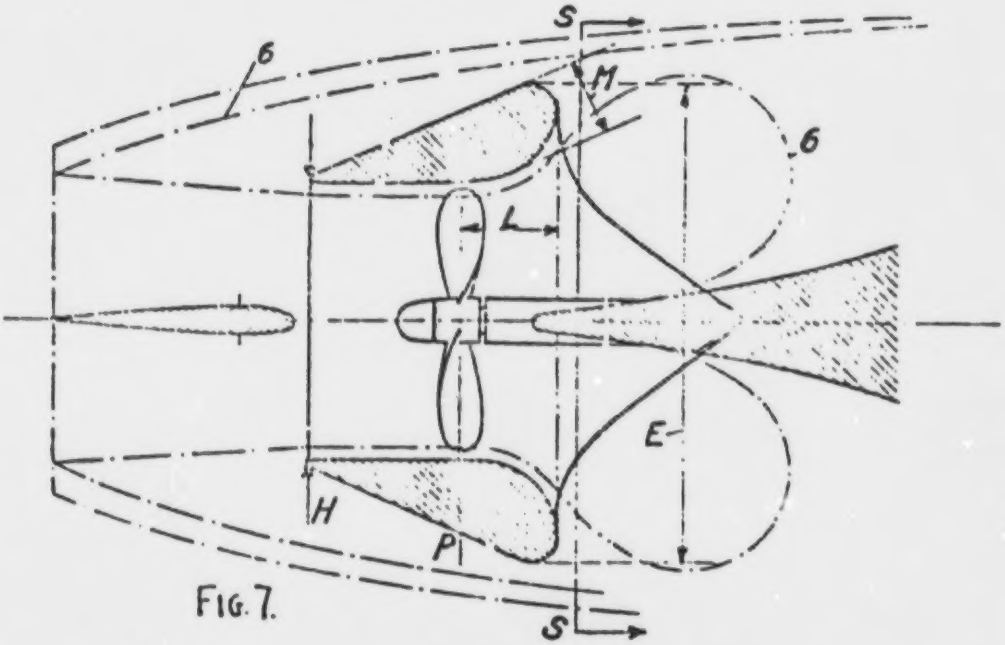

FIG. 7.

Certified to be the drawings referred to in the specification hereunto annexed.
Hannover, Nov. 26, 1938.

Inventor
Ludwig Kort
by [illegible] & Co. Attys.

FIG. 8.

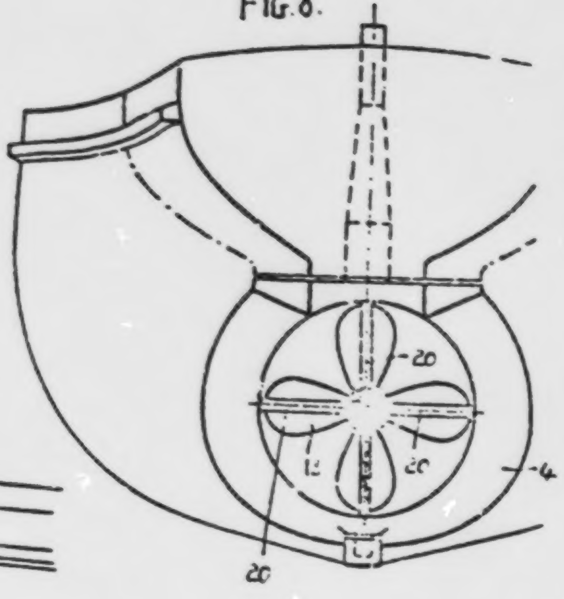

FIG. 9.

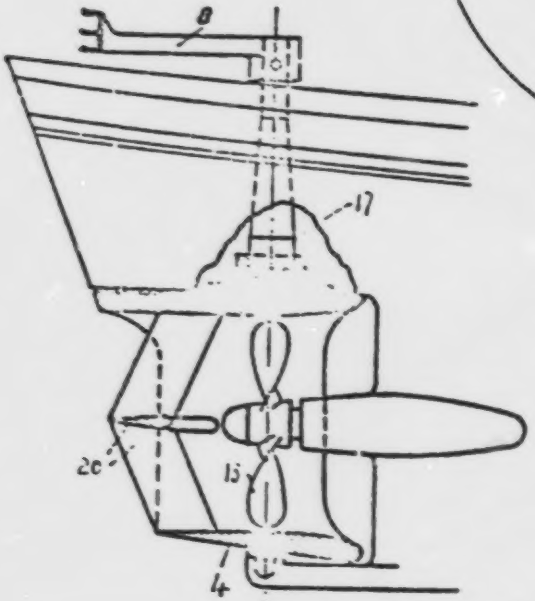

FIG 10.

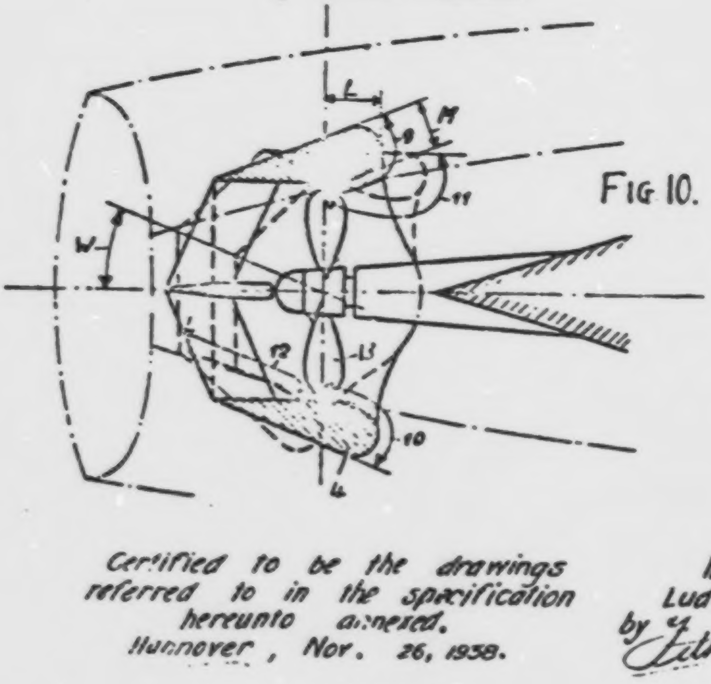

L
M
9
11
W
12
13
10
4

Certified to be the drawings
referred to in the specification
hereunto annexed.
Hannover, Nov. 26, 1938.

Inventor
Ludwig Kort
by Fetherstonhaugh & Co.
attys.

No. 735,219

ISSUED	May 31, 1966
CLASS	115-6

CANADIAN PATENT

SCREW PROPELLED PROPULSION DEVICES

Herbert Mönnich, Bremen-St. Magnus, Germany

APPLICATION No.	880,316
FILED	July 17, 1963
PRIORITY DATE	Nov. 19, 1962 (M 54,866 XI/65f^3-13) Germany
No. OF CLAIMS	9

This invention relates to improvements in screw propeller propulsion devices and is directed particularly to a double walled guide ring for ship propellers, aircraft propellers, or the like. This guide ring has an inlet cross section for a fluid medium which is enlarged in front of the plane of the screw propeller in the form of a flared nozzle in which the screw propeller operates in the manner of an axial pump. With such guide rings there is obtained a local pressure reduction which begins at the front edge of the nozzle and changes gradually to the normal pressure in the plane of the screw propeller. Thus, no increase in pressure is obtained in or behind the plane of the screw propeller as it occurs with a freely operating propeller, even though in limited form.

Since the effective thrust to be obtained by a screw propeller for a given diameter of the propeller is dependent upon the pressure difference in front of and behind the plane of the propeller, there is obtained with a ship's screw propeller with a nozzle-like guide ring an increase in thrust if there is obtained behind the plane of the screw propeller the greatest possible increase in pressure.

This problem forms the basis of the present invention and is attained when the inner wall of the guide ring is provided with inlet openings arranged substantially at the tips of the screw propeller. These inlet openings are connected to outlet openings by means of a common annular duct formed between the two concentrically arranged circular walls of the guide ring or passing through the outer circular wall of the guide ring, or by individual ducts arranged in the same manner as the annular duct. The outlet openings are arranged in the rear third part of the inner circular wall or at the end of the outer wall of the guide ring.

According to one construction of the invention the individual inlet and outlet openings are distributed as uniformly as possible along the periphery in the form of elongated slots which extend in the direction of the guide ring axis or may be of a rounded section or may consist of a continuous annular slot.

Experiments have shown that the thrust of the screw propeller is increased by the employment of the present invention. According to the invention an additional pressure difference is obtained in the plane of the screw propeller so that the thrust action of the nozzle is substantially improved.

The invention is furthermore directed to the problem of overcoming the factors interfering with free travel, namely the piling up of pressure against the nozzle which necessarily occurs in the inlet part of the nozzle which is of progressively smaller dimensions, without thereby affecting the basic effect of the invention, namely an unhindered drop in pressure in the plane of the screw propeller.

The particular difficulty of this problem lies in a considerably reduced effect on the water or other medium with a considerably reduced inlet section or in the absence of such an inlet. With such a guide ring the screw propeller will on the one hand simply receive no more water or other fluid than if it were not surrounded by a casing, and on the other hand its jet must fill out the guide ring in such a manner that no cavitation can appear at its walls since otherwise the overall thrust effect would be still worse than with a free screw propeller not surrounded by a casing.

These difficulties are overcome according to the invention with a considerably reduced inlet section or in the absence of such a section by a cylindrical enlargement of the inner wall of the guide ring, which enlargement is provided at a definite distance behind the screw propeller commencing in stages or steps, wherein the outlet openings of the individual ducts lie partially in the step and, intermediately, the outlet openings of a second duct system for additional medium are provided, the inlet openings of which are arranged at the maximum periphery of the outer wall or where, in the case of a ring duct guide, the outlet openings can in some cases occupy the whole step of widening out, the additional medium system may also consist of a ring duct which overlies the former in such a manner that its outlet opening lies wholly or partially directly behind the step in the widening part and where in addition a guide body is provided lying coaxially to the screw propeller and commencing against the flattened hub end portion thereof.

A pear-shaped guide body offering the minimum resistance and which represents to some extent an extension of the screw hub, has proved a suitable means in association with the other features of the invention in order to obtain even with a reduced screw propeller action the necessary filling out of the jet into the guide ring according to the invention. The correctly proportioned slope of such a guide body guides the jet not only against the inner wall of the guide ring so that it adheres thereto, but also in such a manner as to exert suction on the outlet openings disposed therein. Thereby the jet from the screw is amplified by the amount of the water passing through these openings.

Moreover, the screw jet often receives a necessary further amplification which is obtained by the additional water or fluid referred to which is drawn off from the openings behind the greatest diameter of the outer wall of the guide ring from the surrounding zone and draws it or feeds it between the individual ducts into the inner wall of the guide ring.

A particularly favorable arrangement is obtained if the end of the enlarged part of the inner wall of the guide ring which in the normal case, i.e. with the usual nozzles, conically shaped, has the form of a cylinder commencing with a stepped formation and in the steps of which are disposed both the outlet openings of the duct system according to the invention and also, intermediately, the outlet openings of the additional water or medium system, in which always sufficient water is available for the jet and wherein also a generally favorable and actually optimum ratio of the jet and craft speeds is automatically obtained.

With the nozzle-like annular duct construction of the character already referred to it is necessary to feed the additional water or other medium likewise by means of an annular duct system which overlies the first annular duct. In such a case the enlarged section of the guide ring wall is in some cases already completely or in part occupied by the mouth of the annular duct and consequently the mouth of the annular duct for the additional medium cannot lie entirely at that point but must lie wholly or partly behind it in the enlarged part.

Technical experiments have confirmed the improvement in the thrust by means of these devices with a guide ring with a considerably reduced inlet part, or in the absence of such an inlet part, in towing and in the free travel of a free screw propeller surrounded by a casing.

Furthermore it should be stated that the invention is applicable analogously to an air screw propeller.

Constructional examples of the invention which have proved desirable in practice are described hereinafter as applied to ship propeller screws, with reference to the accompanying drawings, wherein:

FIG. 1 is a longitudinal sectional view of one embodiment;

FIG. 2 is a side elevation view of another embodiment;

FIG. 3 is a longitudinal sectional view of a third embodiment;

FIG. 4 is a cross sectional view along the line A-B in FIG. 3;

FIG. 5 shows a further embodiment of a guide ring in a longitudinal sectional view along the line C-D in FIG. 6, and

FIG. 6 is a partial end elevation view of FIG. 5.

In all embodiments of the invention, the guide ring consists of an outer circular wall and an inner circular wall and the movement of the ship or aircraft is assumed to be in the direction of the arrow F. In FIG. 1, the outer circular wall of the guide ring 1 is shown at 2 and the inner circular wall at 3. Longitudinally extending ducts 4 are disposed between these concentric circular walls with inlet openings 5 and outlet openings 6 for the water or air, respectively. The inlet openings 5 are disposed in the inner wall 3 and the ducts 4 terminate in the outlet openings 6 externally of the outer circular wall 2. The peripheral path of the outer tips of the screw propeller 7 lies in the region of the front parts of the inlet openings 5, preferably at the front edge thereof.

The construction of the guide ring 101 according to FIG. 2 differs from the embodiment of FIG. 1 essentially by the fact that the outlet openings 106 of the ducts 104 open into the inner circular wall 103.

In the embodiment according to FIGS. 3 and 4 an annular space 204 is provided between the outer circular wall 202 and the inner circular wall 203. This annular space 204 takes the place of the ducts 4 and 104 in FIGS. 1 and 2 respectively. The two concentric circular walls 202a, 203a are supported one from the other by radial fins 8 of which four are shown in FIG. 4. Also with this embodiment the periphery of the screw propeller 207 lies in the region of the forward edge of the annular duct 204, and the annular outlet opening 206 is arranged in the inner wall 203 and is spaced inwardly from the rear end of the guide ring 201.

In the embodiment of the invention according to FIGS. 5 and 6, the guide ring 301 has outer and inner circular walls 302 and 303 respectively. The guide ring 301 is provided with a reduced inlet for which purpose the ring 301 is provided preferably with a rounded inwardly extending edge 9. Between the concentrically spaced outer wall 302 and inner wall 303 the ducts 304 are arranged, for example in the form of a lengthwise extending series of tubes which at the same time support the two circular walls 302, 303 one from the other. The inlet openings 305 and the outlet openings 306 of the ducts 304 open into the inner circular wall 303. Furthermore, the outlet openings 306 open into an inwardly facing portion of the guide ring 301 between the axially spaced inlet portions of the walls 302 and 303.

Additional ducts 10 are provided between the ducts or tubes 304 and serve as additional water pipes having inlet openings 11 in the outer wall 302 between the inlet and outlet openings of the ducts 304, while the outlet openings 12 of the ducts 10 terminate at the inwardly directed end of the ring 301 formed by the two concentric wall portions 302 and 303. The screw propeller 307 is located in the region of the inlet openings 305 of the ducts 304 and a pear-shaped guide body 13 extends axially from a point outside of the outlet of the guide ring 301 to a point within the guide ring, in fact, it extends to a point adjacent the screw propeller 307.

In all embodiments of the invention the double walled guide ring has a smoothly contracting inlet portion through which the water is propelled by the action of the screw propellers 7, 207 and 307 respectively. The screw propeller forces the water into a ductway which has a minimum cross-sectional area at a point lying beyond the screw propeller and then expands in a smooth and progressive manner. The inlets of the ductways 4, 204 and 304 respectively, lie immediately beyond the tips of the screw propeller, but at a portion of the ductway in advance of the point where the minimum cross section is reached, while the outlets of the ductways 4, 204, 304 are located at or towards the outer end of the guide ring where the diameter is somewhat greater than the minimum diameter.

The outer configuration of the guide ring is preferably also of smoothly curved form and embodies a maximum diameter portion near the leading end, smoothly tapering towards a minimum diameter portion at the rear end.

THE EMBODIMENTS OF THE INVENTION IN WHICH AN EXCLUSIVE
PROPERTY OR PRIVILEGE IS CLAIMED ARE DEFINED AS FOLLOWS:

1. In a screw propeller propulsion device, comprising a screw propeller for driving a craft in a forward direction, a guide ring having front and rear ends surrounding the propeller and extending in a direction opposite to the direction of propulsion, inner and outer walls on said guide ring forming a ductway therebetween, said inner wall being provided with an inlet opening adjacent the front end of said guide ring and in communication with the interior of said ring, said screw propeller being disposed in said guide ring with its peripheral edges adjacent said inlet opening and disposed forwardly thereof, said ductway being provided with an outlet adjacent the rear end of said guide ring.

2. In a screw propeller propulsion device as set forth in claim 1, wherein said inlet opening is provided in the inner wall of said guide ring at a point lying immediately beyond the periphery of the screw propeller and said outlet is disposed toward the rear portion of said guide ring.

3. In a screw propeller propulsion device as set forth in claim 1, in which the inner wall provides a fluid flow ductway in which certain portions are reduced to a minimum and are increased to greater dimensions, said screw propeller being disposed in advance and forwardly of said reduced portions and said inlet openings being disposed adjacent the front end of said guide ring and between said screw propeller and said certain reduced minimum portions, and outlet openings at the rear end of said guide ring rearwardly of said certain reduced portions.

4. In a screw propeller propulsion device, a guide ring of double walled construction having spaced inner and outer walls forming a fluid passage therebetween, said guide ring being provided with a central passage, a screw propeller mounted in said passage with its axis extending longitudinally thereof, said inner wall being provided with inlet openings adjacent the front end of said ring and lying at a point transversely of the axis of the propeller adjacent the periphery thereof and within a radial plane containing the tips of

the propeller blades, said inner wall being provided with an internal diameter approximating the diameter of the propeller, and said guide ring being provided with outlet openings at the rear thereof, said inlet and outlet openings being in communication with a common annular duct formed within the guide ring and being arranged in approximately the rear third part of said ring.

5. In a screw propeller propulsion device as set forth in claim 4, in which said inlet and outlet openings are formed by a series of equidistantly spaced longitudinally extending slots in the inner wall extending in a direction parallel with the direction of the propeller shaft axis, said openings being disposed behind and rearwardly of the periphery of said propeller.

6. In a screw propeller propulsion device as set forth in claim 4, in which said inlet and outlet openings are formed by annular slots arranged forwardly and rearwardly of said guide ring.

7. In a screw propeller propulsion device as set forth in claim 4, in which said inner wall is reduced in diameter adjacent its central protion which is tapered forwardly to the inlet portion of said passage with said reduced wall portion being arranged rearwardly of the screw propeller, said inner wall being increased in diameter rearwardly of said decreased diametral portion with the outlet openings arranged intermediate said reduced diametral portion and the end of said ring.

8. In a screw propeller propulsion device as set forth in claim 4, including an additional duct system for additional fluid having inlet openings in the outer wall and outlet openings in alignment with the outlet openings of said common duct, said second duct system being formed of an annular duct which overlies the common duct in such a manner that its outlet opening lies directly behind a stepped portion in the enlarged rear end of said guide ring thus forming a guide body extending coaxially of the screw propeller axis and projecting rearwardly of a flattened hub thereof.

9. In a screw propeller propulsion device as set forth in claim 8, in which said guide ring is provided with a maximum external diameter which is

disposed rearwardly to form a tapered portion terminating adjacent said outlet and which is of maximum diameter adjacent the forward end of the ring and the reduced diametral portion of said inner wall.

735219

SCREW PROPELLED PROPULSION DEVICES

Fig.1.

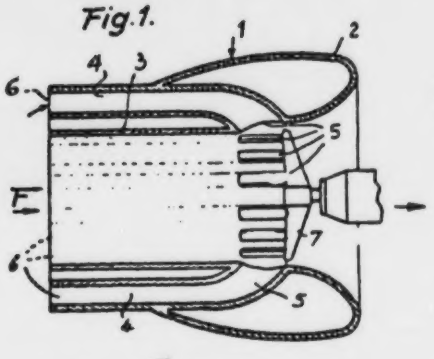
1
2
4
3
6
5
F
7
6
5
4

Fig.2.

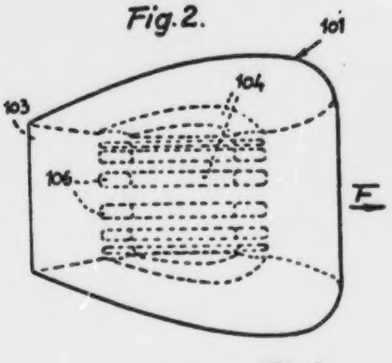
101
104
103
106
F

Fig.3.

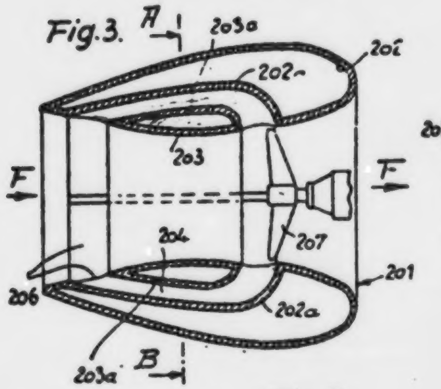
A
203a
202
201
203
F
F
204
207
201
206
202a
203a
B

Fig.4.

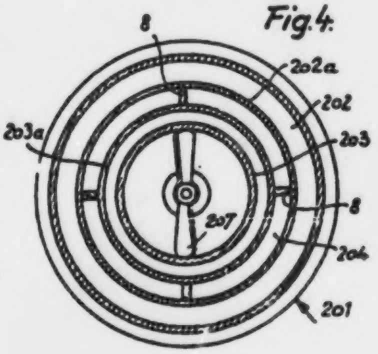
8
202a
202
203a
203
8
207
204
201

Fig.5.

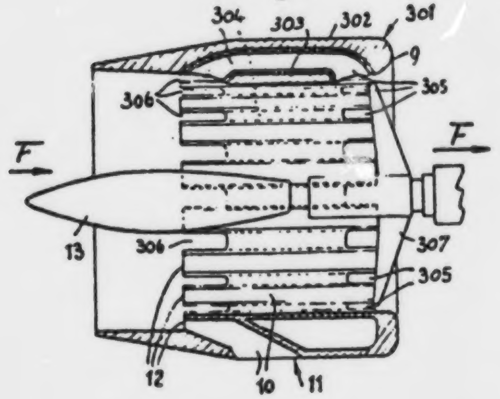
304
303
302
301
9
305
306
F
F
13
306
307
305
12
10
11

Fig.6.

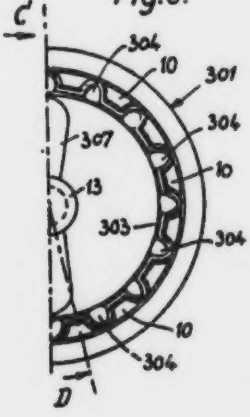
C
304
10
301
304
307
13
10
303
304
10
304
D

CANADA
THE PATENT OFFICE

PATENT No. 509,171 ISSUED JAN. 18, 1955

Protecting Means for Propellers

Nils J. Liasen, Alesund, Norway
Application March 11, 1952, Serial No. 628,098
1 Claim

1

The present invention relates to protecting means for propellers for preventing ice or other swimming objects from striking the propeller blades.

The protecting means according to the invention is of the type in which fins, the edges of which incline outwardly from their forward to their aft end, are provided on the hull forward of the propeller. In known protecting means of this type the fins have not been arranged in such a way that effective protection was secured for all parts of the propeller.

The invention has for its object a protecting means of the said type in which the fins are arranged and dimensioned so that they provide safe protection of the propeller for its whole area, and besides, as proved by model tank tests, not or only to a small degree influence the efficiency of the propeller and the resistance of the ship.

According to the invention two or more fins or pairs of fins are arranged one above the other. The fins are suitably arranged parallel or approximately parallel one with the other and somewhat sloping downwards, and each fin is dimensioned so that it at its aft edge extends outwards in alignment with the circumscribed circle of the propeller. Hereby the propeller also is protected against objects which extend comparatively deep into the water, for instance against ice patches in vertical or inclined position. In view of the fact that the fins owing to their shape push objects rammed outwards, it is not necessary that the outer edges of the fins extend fully in alignment with the circumscribed circle of the propeller. The fins preferably are shaped approximately in accordance with the stream lines of the water along the ship's hull.

The drawing illustrates an embodiment of the protecting means according to the invention with three pairs of fins arranged one above the other.

Figures 1, 2 and 3 illustrate part of the aft end of the ship with the protecting means as seen from the side, from behind and from above, respectively.

In the drawing 1 is the aft end of the ship,

2

2 the propeller, and 3 the rudder. In order to make the drawing clearer the rudder is not shown in Figure 2.

The protecting means consists of the fins 4, 5 and 6 which are arranged in pairs, one above the other, approximately parallel and sloping downwards. As it appears most clearly from Figure 2, the fins are so dimensioned that they at their aft end extend out about in alignment with the circumscribed circle of the propeller 7, or in other words, to a distance from the centre line of the propeller equal or approximately equal to the radius of the circumscribed circle of the propeller. As it appears, the whole propeller area thereby will be well protected. The height of the lower situated fins as a rule will be somewhat smaller than of the higher situated fins.

The embodiments of the invention in which an exclusive property or privilege is claimed are defined as follows:

Protecting means for propellers comprising fin members carried by the hull forward of the propeller and having their outer edges inclined outwardly from their forward to their aft end, characterized therein that at least two such fin members are provided on each side of the hull, one above the other and approximately parallel one with the other, each of the fins being so dimensioned that its aft end extends out approximately in alignment with the circumscribed circle of the propeller.

FETHERSTONHAUGH & CO.,
70 Gloucester St.,
Ottawa, Ont.,
Patent Agent of the Applicant.

Edmond Cloutier, C.M.G., O.A., D.S.P., Queen's Printer and Controller of Stationery, Ottawa, 1954

509171

Fig. 1

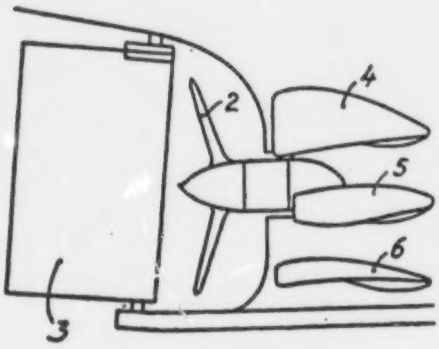

Fig. 2

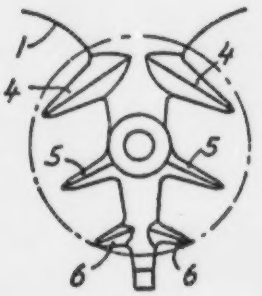

Fig. 3

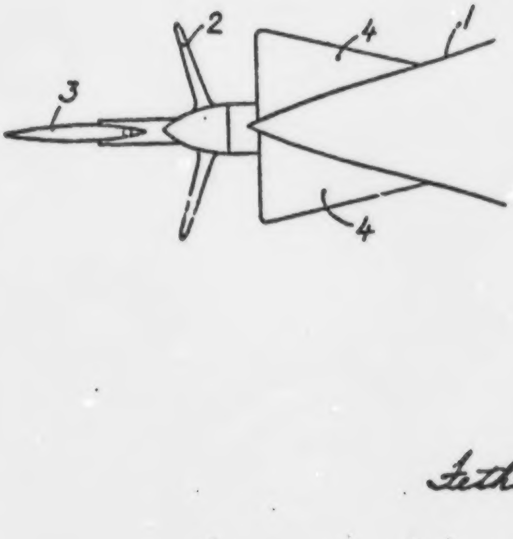

INVENTOR
NILS JOHANNES LJAAEN
PATENT AGENTS

Fetherstonhaugh & Co

⑪ Ⓐ **No.** 981118

㊺ **ISSUED** Jan. 6, 1976

(52) **CLASS** 115-30
C.R. CL.

⑲ (CA) CANADIAN PATENT

(54) PROPELLER GUARD

(72) Liaaen, Nils J., 6000 Ålesund, Norway

Granted to A.M. Liaaen A/S, 6000 Ålesund, Norway

㉑ **APPLICATION No.** 176,198
㉒ **FILED** July 11, 1973

㉚ **PRIORITY DATE** July 12, 1972 (2484/72) Norway

No. OF CLAIMS 6

DISTRIBUTED BY THE PATENT OFFICE, OTTAWA.
CCA-274 (2-74)

The present invention relates to a propeller guard for seagoing vessels.

For the purpose of increasing the propulsion force of a propeller, it is well known to provide the propeller with a surrounding nozzle in order thereby to obtain a most possible stable water flow to the propeller and most possible quiet propulsion conditions with a low vibration level and noise level. Such purposes are of particular interest to tugs, trawlers and other fishing vessels, both with regard to convenience and out of catch technical reasons. Obviously, such conditions are also relevant to other vessel types than those mentioned.

However, the provision of propeller nozzles also implies weaknesses. A propeller which is surrounded by a nozzle provides a greater suction effect of the water flow in front of the propeller than a propeller without a nozzle. This entails that foreign bodies may easily be drawn into the nozzle and cause damages by jamming between the nozzle and the propeller proper.

Usually, such nozzles are secured to the vessel hull at the top edge of the nozzle and to the vessel heel at the lower edge of the nozzle. This implies that nearly half the circumference of the nozzle is freely projecting into the water flow to both sides of the propeller, a fact which obviously means a structural weakness. The consequence is that the nozzle may easily be damaged, in particular when operating in ice. Such damages to the nozzle ring proper may be of decisive consequences to the reliability of service of the vessel. The consequence is that propeller nozzles, in spite of their great advantages, have scarcely been applied to vessels operating in the Arctic.

The object of the present invention is a guard to a propeller which is surrounded by a fixed nozzle, against the damaging effects of foreign bodies, in particular ice, use being made of such fins which since long have been known for the protection of propellers. Such fins are secured to the

*

vessel hull at both sides of the same and they are so shaped that the fore edge of each fin slopes outwardly from fore to aft, so that a foreign body which approaches the side of the vessel is guided outwardly sideways and consequently passes outwardly of the propeller.

The object of the invention is a combination of the two arrangements, both known per se, the aft edge of each fin being secured to the fore edge of the propeller nozzle. Hereby, not only the advantages of each individual of the two arrangements reffered to above are obtained, but also that the nozzle is by far better supported relatively to the hull than in previously known arrangements, so that the nozzle arrangement may also be made use of at fishing or catch where the advantages of the same are of a particularly great interest also in ice filled waters.

Further features of the invention will appear from the following description and the enclosed drawing which illustrates an example of how the guard may be constructed.

In the drawing, Figure 1 is a side view of the stern of a vessel provided with a guard according to the invention.

Figure 2 is a sectional view taken along the line A-A in Figure 1, seen in the direction of the arrows.

Figure 3 is a top view of the guard, in the top portion as seen from above towards the top fin, in the lower portion as seen from above towards the middle one of the three fins which are shown in Figure 1.

In the drawing, 1 is the stern of the vessel, provided with a heel 2 and rudder 3. 4 is the propeller which is surrounded by a nozzle 5 which is mounted co-axially to the propeller 4 and has an inner diameter which at the propeller is only slightly greater than the external propeller diameter, but flares slightly at the fore edge 6. The nozzle 5 is, in the conventional manner, secured to the stern at 7 and to the heel 2 at 8.

A number of projections, fins, 9, 10 and 11 are arranged to either side of the stern 1, foremost secured to the hull and at or adjacent to the aftmost point secured to the fore edge 6 of the nozzle 5, so that the latter, in addition to being secured at top and bottom to the vessel, is also connected to the same at a number of points to either side of the fore-and-aft line. As shown in the drawing, each fin is falling off from the foremost end, both alongships and athwartships, so that the aftmost point of each fin, which is secured to the propeller nozzle is situated lower and further outwards to the side than the connection to the hull. Consequently, foreign bodies, such as ice flakes abutting against the side of the vessel are deviated outwardly and downwardly relatively to the fore-and-aft line and guided outside of the nozzle 5, so that they are prevented from entering the same and cause damage. The fins to either side of the hull are shown approximately parallel for the purpose of better guiding the foreign bodies. As shown in the top portion of Figure 3, the top fin 9 may be made in the form of a stay which extends between the hull and a point relatively high up on the aft nozzle circumference, whereas the remaining fins 10, 11 are made with a full sectional area in the direction of water flow and secured to the nozzle 5 at the circumference of the inlet to the same.

As shown in dotted lines in Figure 1, a tube 12 may be arranged extending from inside the hull to a point near to the lowermost point of the nozzle for the supply of vapour or hot gas, such as exhaust gas, for the purpose of loosening ice which might have fastened in the nozzle.

THE EMBODIMENTS OF THE INVENTION IN WHICH AN EXCLUSIVE PROPERTY OR PRIVILEGE IS CLAIMED ARE DEFINED AS FOLLOWS:

1. A propeller guard for the propeller of a seagoing vessel, comprising a nozzle for securing to a vessel's hull and to surround said vessel's propeller, and at least two fins for securing by their fore ends to said hull on respective sides of the hull, the fins being so shaped that their fore edges slope outwardly from fore to aft, the aft ends of the fins being secured to the fore end of the nozzle.

2. A guard as claimed in claim 1, in which additional fins are secured to the sides of said hull, the fins on respective sides being arranged with respect to one another so that they are substantially parallel and slope downwardly from the hull rearwardly towards the fore end of the nozzle.

3. A guard as claimed in claim 1 or 2, wherein a top fin on each side of the vessel comprises a stay extending between the hull and the fore end of the nozzle.

4. A guard as claimed in claim 1, in combination with a tube which, in use, extends from the interior of the hull to the fore end of the nozzle for the supply of vapour or hot gas.

5. A combination as claimed in claim 4, wherein the tube extends to the vicinity of the lowermost point of the fore end of the nozzle.

6. A vessel to which is secured a propeller guard as claimed in claim 1, 2 or 4.

FIG.1.

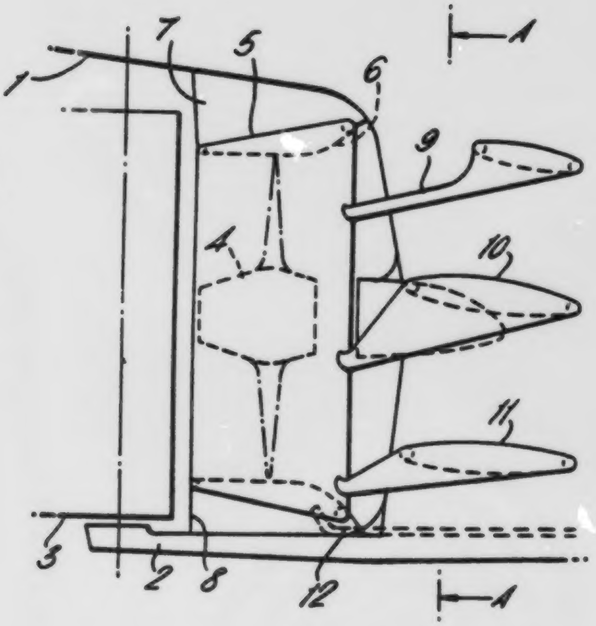
A
1
7
5
6
9
4
10
11
3
2
8
12
A

FIG.2.

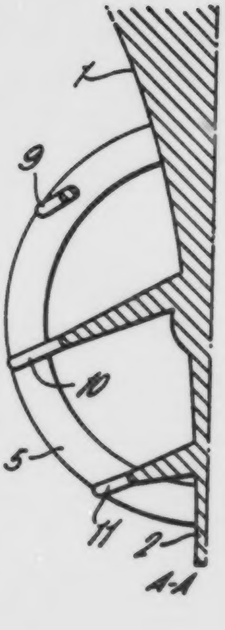
1
9
10
5
11
2
A-A

FIG.3.

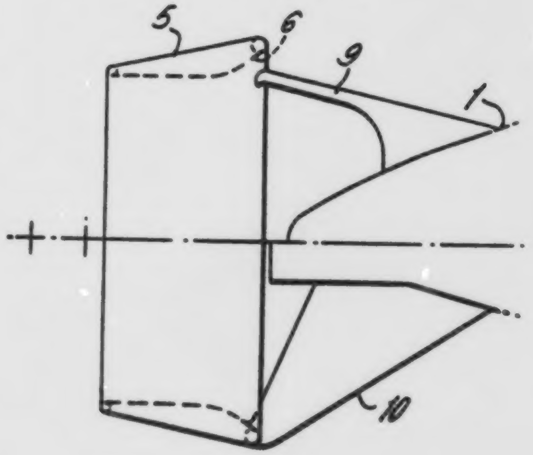

⑪ ⑫ No. 910732

㊺ ISSUED Sep. 26, 1972

(52) CLASS 115-15
C.R. CL.

⑲ CANADIAN PATENT

(54) MULTIPLE PROPELLER DUCTED SYSTEM

David J. Doust, Montreal, Quebec, Canada

㉑ APPLICATION No. 084,721
㉒ FILED June 4, 1970

㉚ PRIORITY DATE June 9, 1969 (29,070/69) G. B.

No. OF CLAIMS 12

This invention relates to a new and improved propulsion and steering apparatus for use with waterborne, semi-submerged or fully submerged vessels.

Conventional propellers working outside of a ship's hull can be adversely affected by the following factors:

a) Breakdown of flow into the propeller or propellers, especially in the case of full-bodied vessels such as tankers, ore and bulk carriers.

b) Vibration of the hull structure due to propeller-excited pulsations arising from the flow irregularities exaggerated by item (a);

c) Loss of propulsive efficiency at high thrust loadings, rates of rotation and input shaft powers which physically restrict the speed performance of large vessels and largely determine the choice between single, twin or multiple combinations;

d) Loss of manoeuvrability and rudder action due to the blanking effect of the after body shape on the flow into the rudders;

e) Loss of stopping ability and reverse propeller thrust on the vessel, making the problem of stopping and taking avoiding action very difficult in the case of super-tankers and other large vessels;

f) Liability of damage to propeller or propellers working outside the confines of the hull surface, due to contact by ice, floating hazards or other vessels.

According to the present invention, there is provided a ducted propulsion system for waterborne, semi-submerged or fully submerged vessels comprising a ducted system having two or more intake ducts which open below the mid depth of the vessel, and which merge into a specially shaped non-circular composite duct which generally extends in the fore and aft direction of the vessel, propeller means mounted independently in said composite duct and adapted to induce a flow of water through said system of ducts to propel said vessel, said propeller means comprising two or more propellers or impellers each with its own independent shafting, bearings and supporting structure.

By fitting such a series of two or more propellers or impellers, longitudinally spaced along the composite duct, it is possible to increase the total power absorption of the overall propulsion system without the attendant disadvantages of multi-conventional propeller systems exposed outside of the hull surface of the vessel.

Due to the configuration of the composite duct, it is also possible to provide for power absorption from the main propulsion machinery in excess of that which can be absorbed by a single propeller working in a circular duct, thus resulting in increased thrust available for propulsion of the vessel.

The mechanical complications of co-axially mounted, contra-rotating propellers are also largely overcome by driving the multi-stage series of propellers independently and mounting them non-coaxially in the composite duct.

The invention will be further described by way of example only with reference to the embodiments illustrated in the accompanying drawings, wherein:

Fig. 1 is a schematic drawing of the duct system;

Fig. 2 is a sectional detail view of the inlet section of the duct;

Fig. 3 is a sectional detail view of the inlet grid;

Fig. 4 is a sectional detail plan view of the inlet fairing;

Fig. 5 is a sectional view on the line 5-5 of Fig. 4;

Fig. 6 is a sectional detail plan view of the valve section of the duct;

Fig. 7 is a sectional view on the line 7-7 of Fig. 6;

Fig. 8 is a sectional detail plan view of the transition section of the duct;

Fig. 9 is a series of section views on the line V-V, W-W and X-X of Fig. 8;

Fig.10 is a sectional detail plan view of the merging section of the duct;

Fig.11 is a sectional view on the line 11-11 of Fig. 10;

Fig.12 is an isometric view of the merging section;

Fig.13 is a sectional plan view of the impeller section of the duct;

Fig.14 is a detail of the shaft support;

Fig.15 is a sectional view on the line 15-15 of Fig.13;

Fig.16 is a sectional plan view of a modified impeller section of the duct;

Fig.17 is a detail of the shaft supporters;

Fig.18 is a sectional view on the line 18-18 of Fig. 16;

Fig.19 is a sectional view on the line 19-19 of Fig. 16;

Fig.20 is a sectional plan view of the diffuser section;

Fig.21 is a series of sectional views on the lines P-P, Q-Q and T-T of Fig. 20;

Fig.22 is a sectional plan view of the rudder section;

Fig.23 is a sectional view on the line 23-23 of Fig.22;

Fig.24 is a detail view of the exit grid bars;

Fig.25, 26 & 27 illustrate various methods of noise and vibration attenuation.

Referring to the drawings, a vessel 11 is provided with a ducted propulsion system comprising two intake ducts 12 opening from the sides of the vessel and extending inwards and aft to merge into a common composite duct 13 the exit end of which opens into a rudder section or expansion nozzle 14. A third intake duct opening from the bottom of the vessel may be provided if desired; however, such a duct is not shown in the drawings.

Each intake duct is of non-circular cross-section with special triangulated recessing provided at their after extremities to avoid high entry hydraulic losses in the overall system. Each of the intake ducts 12 is also provided with conventional flow restricting means of substantially rectangular cross-section, to vary the effective flow of water, through said ducts by varying the cross-sectional area of the ducts.

In order to increase the permissible power input to a particular vessel and without the complication of conventional multiple/twin-screw shafts (A-bossings) exposed outside of the ship surface, two or more impellers may be mounted non-coaxially mounted within the common duct 13. Note that with the composite duct system indicated, impeller clearances are much less critical than for a regular duct and concentric coaxial impeller, and produces improvements in propulsion efficiency of between 5% and 10% relative to a single impeller.

The propellers are mounted in the mid portion of the composite duct 13, these propellers are spaced longitudinally at intervals in the duct.

Each propoller or impeller is separately mounted on a shaft and may be driven independently or through a common gear box or propulsion motor, depending on the particular application of the system.

Greatly increased lateral control of the vessel when going astern is achieved by throttling the flow in either of the Y intake ducts 12. This can be further improved by the use of controlled pitch impellers.

Figure 1 is a diagrammatic layout of the ducted propulsion system or as it is called the "YPASS Propulsion System". The various sections are designated in Figure 1 as follows:

Section "A" - Inlet Section

Section "B" - Valve Section

Section "C" - Transition Section

Section "D" - Merging Section

Section "E" - Impeller Section

Section "F" - Diffuser Section

Section "G" - Rudder Section

Each of these sections is described separately.

INLET SECTION

The duct inlet is illustrated in Figure 2. The width of the duct is shown as "a". Inlet grids 14 are spaced across the front of the inlet 15. These grids protect the inlet ducts from ice or submerged objects. Details of the cross-section of the grids are shown in Figure 3. It has been found that to avoid high frictional losses the width "b" of the triangular grid preferably is from about 0.1 inches to about 0.1a and the spacing between the grid bars is preferably from about 0.1a to about "a".

It has been determined that conic development recesses give the minimum friction entry losses into such a system. The angle of entry "α" of the recessed cone fairing 16 which is shown in Figures 2 and 4 may vary from about 0° to about 60° with the optimum angle varying from about 10° to 40° depending on the local lines of the vessel in way of the ducted inlet. A good average design value appears to be about 30° for a vessel of average after body fullness. The dimension "d" which is the depth of the inlet fairing 16 may vary from about 0 to about 0.5a. Figure 5 illustrates the cross-section of the inlet fairing 16 taken on the line 5-5 on Figure 4.

VALVE SECTION

The valve section of the duct is illustrated in Figure 6. The valve 17 is shown in the open position in full lines and in the closed position in broken lines. Figure 7 is a detail of the valve 17 and shows the valve mounted on a shaft 18 which is supported from above. The valve 17 could, of course, be mounted on a shaft passing through the duct to give a top and bottom support for the valve. This can be done as desired. If desired, the corners of the duct can be rounded. The value of "e" which is the radius of the corners of the duct in the valve section should be selected to be in the range of from about 0 to less than $0.5\sqrt{a^2+h^2}$ where "a" is the width of the duct and "h" is the height of the duct at the valve section.

TRANSITION SECTION

The transition section of the duct which is located between the valve section and the merging section is illustrated in Figures 8 and 9. It has been found advantageous in order to efficiently control the flow of water without causing choking at the intersection to limit the radius "j" of the corner of this section by the following formula:

$$J = e + \left[\frac{(0.5h - e)\ell}{L}\right]$$

The length transition section "L" is greater than the width of the duct "a".

Figure 9 shows the manner which the cross-section of the transition section changes from a more or less rectangular section at "x" to a section which has a flat surface on one side and a semi-circular surface at the other. At the point at which the transition section joins the valve section, at line X-X, the cross-section of the duct is rectangular with the corner radius being equal to "e" which was defined above. Moving along the transition section the surface of the duct on the inside or on the Y side does not change. In other words, it remains flat with small radius corners. The surface of the duct on the outside of the Y gradually changes into a curved section, the radius of which is determined by the formula given above. At the point at which the transition section joins the merging section, the outer surface of the duct is semi-circular.

MERGING SECTION

The merging section in which the two separate inlet ducts 12 merge into a common duct 13 is illustrated in Figures 10, 11 and 12. The ratio of the area of the inlet ducts in relation to the area of the common ducts is dependent of the speed of advance of the vessel, its size and shape. Generally, it has been found that the width of the common duct "w" should be greater than "a", the width of the single duct. In addition, it has also been found that the cross-sectional area of the composite duct must not be greater than the combined cross-sectional areas of the inlet ducts.

For optimum results, the angle "β" which is the angle that the centre line of the separate inlet ducts makes with the centre line of the vessel, should be selected to be in the range of from about 20° to about 60°. The width of the joining piece "k" between the two ducts, should be equal to or less than "w", the width of the common duct. This joining piece 39 is a watertight structural member which is flat to simplify mounting of the impeller shaft stuffing boxes and bearings. A fairing piece 40 which need not be watertight is located aft of the joining piece 39 to streamline the flow of water through the ducts.

IMPELLER SECTION

The impeller section is shown in Figures 13 to 19. Figure 13 is a plan view of an impeller section in which there are located two impellers 20. The impellers may be staggered one in front of the other as is shown or they may be mounted side by side. Each impeller is driven by its own independent shaft. The shafts are supported on shaft supports 21 which are shown in detail in Figure 14. The impellers 20 would normally be operated so that the impellers were contra-rotating and were out of phase with each other. The clearance which has been found on these very large impellers is surprisingly little and a maximum of three inches has been found to be required. Usually considerably less than this is needed.

To reduce the wear of the walls of the duct, wear inserts 22 are inserted into the walls of the duct at those places at which the propellers come close to the walls and at which wear would normally be quite high.

It has been found that the number of blades in the propeller can be varied considerably depending on the type of vessel in which the ducted propulsion system is used. Usually, the number of blades varies from about 3 to 7.

Figure 16 illustrates an impeller section in which there are 3 impellers 23, each mounted on its own independent drive shaft. In this case, the impellers are staggered so that two are along side of one another and the centre one is placed forward of the other two.

In such an arrangement, the shaft supports 24, which are illustrated in Figure 17, would normally be located above and below the shaft. Wear inserts 25 may be fitted about the periphery of the duct in line with the impellers which are located in a side-by-side arrangement. Additional wear inserts 26 may be located at the top and bottom of the duct as is illustrated in Figure 18 at the point at which the forward impeller approaches the surface of the duct.

Figure 19 shows the arrangement of the three impellers, two of which operate in a clockwise direction and the third impeller operates in a counter-clockwise direction. The propellers are mounted on the shaft so that they are out of phase with each other.

The cross-section of the duct in the impeller section is illustrated in Figure 19. The two side walls are semi-circular to fit the contour of the impellers or propellers mounted within them. The top and bottom surfaces are flat.

DIFFUSER SECTION

Figures 20 and 21 show the diffuser section and illustrate how the duct cross-section varies at this section. The side walls of the duct in the impeller section are semi-circular and the top and bottom walls are flat. In the diffuser section the cross-section becomes rectangular. At the start of the diffuser section the radius in the corners is h/2 where "h" is the height of the duct. At the end of the diffuser section, the cross-section of the duct is rectangular. The radius at the corners gradually changes and is determined by the formula $x = \left(\frac{h}{2}\right)\left(\frac{u}{H}\right)$ where "h" is the length of the diffuser section and "u" is the distance from the end of the diffuser section to the point at which the radius is to be calculated. The length of the diffuser section is shown as "H".

RUDDER SECTION

The rudder section is illustrated in Figures 22, 23 and 24. As will be seen from a study of Figure 22, a plurality of rudders 30 are employed. Increased steering effect when running ahead can be provided by means of the cascading effect of three or four or more rudders operating in tandem. The benefits of tandem rudder arrangement is further increased by the use of controlled pitch impellers. The cross-section at the rudder section is shown in Figure 23 and is rectangular.

A series of grids are spaced across the aft end of the duct to protect the rudders. Details of the grid bars are given in Figure 24. The number of rudders used varies greatly again with the type of vessel. It is envisaged that anywhere from two to ten rudders can be used to advantage.

NOISE AND VIBRATION ATTENUATION

The ducted propulsion system of the present invention can be modified to modulate the noise emission external to the ship. Various ways of doing this are shown in Figures 25, 26 and 27.

Figure 25 illustrates one method by which noise and vibration may be controlled. The left-hand side of the figure is a cross-section of the ship with the hull 32 being shown and the duct wall 33. The right-hand part of the drawing is a longitudinal cross-section and the transverse members 35 are shown. Damping material 36 can be adhered to the exterior surface of the duct walls 33 in order to reduce the noise and vibration.

Figure 26 again shows a cross-section of the duct, the left-hand side of the drawing being a section across of the ship and the right-hand side of the drawing being a longitudinal cross-section. Acoustic absorptive material 37 is adhered to the exterior walls of the duct 33, the hull 32 and the transverse members 35 to provide noise and vibration control.

Figure 27 illustrates the use of acoustic insulation. In this case, the void between the hull 32 and the duct 33 is filled with acoustic insulation 38 again to reduce noise and vibration.

A

The embodiments of the invention in which an exclusive property or privilege is claimed are defined as follows:

1. A ducted propulsion system for waterborne, semi-submerged or fully submerged vessels comprising a ducted system having two or more intake ducts which open below the mid depth of the vessel , and which merge into a specially shaped non-circular composite duct which generally extends in the fore and aft direction of the vessel, propeller means mounted independently in said composite duct and adapted to induce a flow of water through said system of ducts to propel said vessel, said propeller means comprising two or more propellers or impellers each with its own independent shafting, bearings and supporting structure.

2. A ducted propulsion system for waterborne, semi-submerged or fully submerged vessels comprising a duct system having two or more intake ducts which open below the mid depth of the vessel and which merge into a composite duct generally extending in the fore and aft direction of said vessel, each of said inlet ducts consisting of:

an Inlet Section
a Valve Section, and
a Transition Section

said inlet section having a recessed cone fairing at its after end which makes an angle of less than 60° with the hull, and a plurality of grids spaced across the inlet,
said valve section having a valve adapted to throttle, the flow of water through said inlet duct and
said transition section having a cross-section which gradually changes from the cross-section of the valve section to the cross-section of the merging section,
said inlet ducts join together to form a single composite duct at the merging section, the angle between said separate inlet ducts and the centre line of the ship being in the range of from about

20° to about 60°,

said composite duct consisting of an impeller section in which there is mounted propeller means adapted to induce a flow of water in said duct system, said propeller means comprising two or more propellers or impellers each having its own independent shafting, bearing and supporting structure, the side walls of the duct forming said impeller section being semi-circular and the top and bottom being flat,

a diffuser section in which the cross-section of the duct changes gradually from that of the impeller section to a rectangular cross-section and

a rudder section having a rectangular cross-section adapted to house a plurality of rudders and a series of grids spaced across the aft end of said duct.

3. The ducted propulsion system as claimed in claim 1 and 2 having two inlet ducts which open from the sides of the vessel.

4. The ducted propulsion system as claimed in claims 1 and 2 in which there are three inlet ducts, two opening from the sides of the vessel and one opening from the bottom of the vessel.

5. The ducted propulsion system as claimed in claims 1 and 2 in which the cross-sectional area of the composite duct is not greater than the combined cross-sectional areas of said inlet ducts.

6. The ducted propulsion system as claimed in claim 2 in which said recessed cone fairing makes an angle of between 10° and 40° with the hull.

7. The ducted propulsion system as claimed in claims 1 and 2 in which there are two impellers mounted in a side by side relationship.

8. The ducted propulsion system as claimed in claims 1 and 2 in which there are two impellers which are mounted one in front of the other in a staggered relationship.

9. The ducted propulsion system as claimed in claims 1 and 2 in which there are three impellers, two of which are mounted alongside of each other and the third is mounted between the other two and out of line with them.

10. The ducted propulsion system as claimed in claims 1 and 2 in which the impellers are contra-rotating.

11. The ducted propulsion system as claimed in claim 2 in which the number of rudders is from two to ten.

12. The ducted propulsion system as claimed in claims 1 and 2 in which sound and vibration absorptive material is placed about the ducts to modulate noise emission.

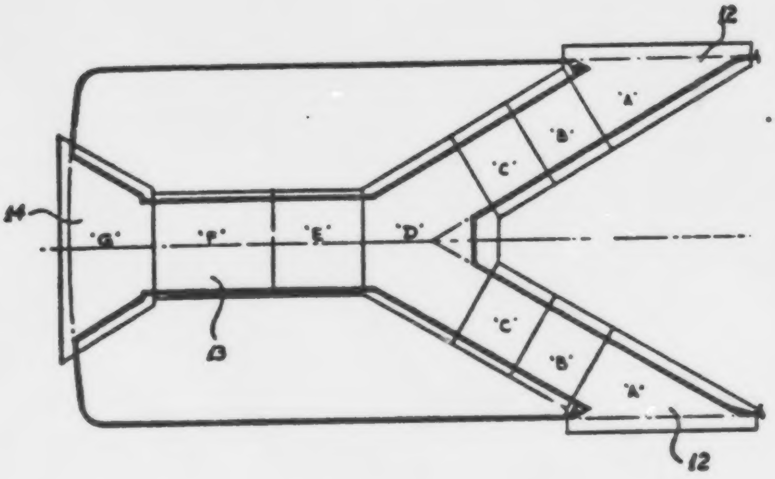
12
'A'
'B'
'C'
14
'G'
'F'
'E'
'D'
13
'C'
'B'
'A'
12

FIG. 1

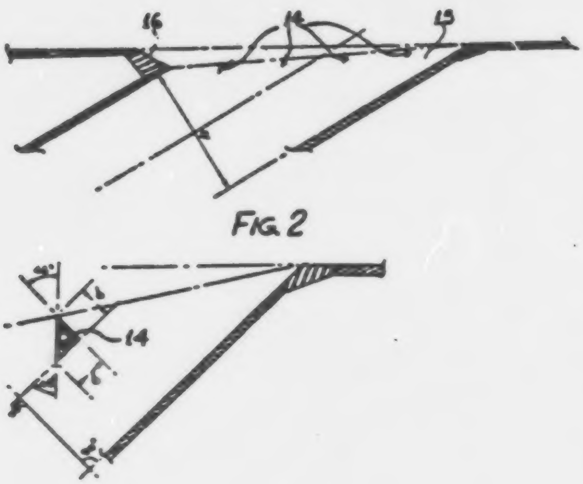

FIG. 2

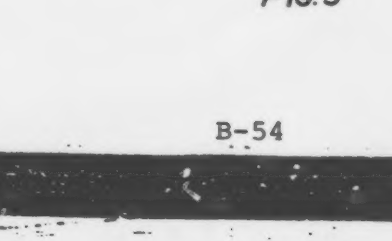

FIG. 3

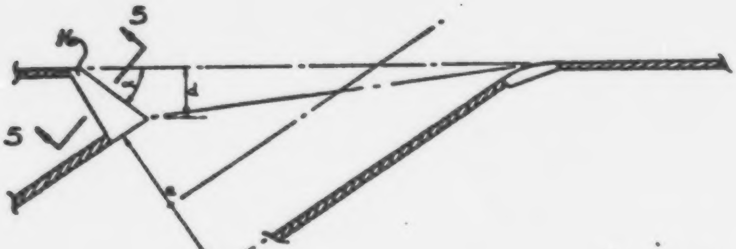

FIG. 4

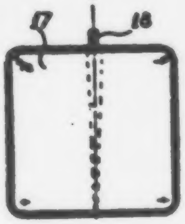

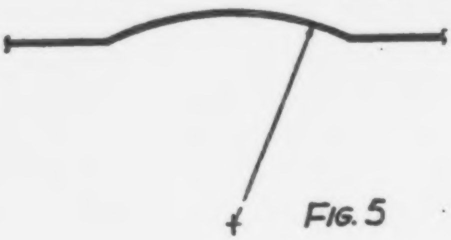

FIG. 5

FIG. 7

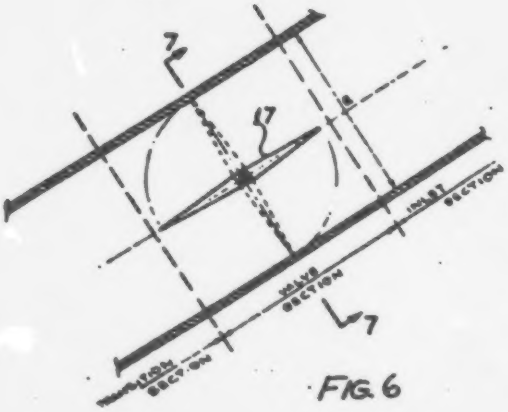
7
17
INLET SECTION
VALVE SECTION
7
TRANSITION SECTION

FIG. 6

910732
9-3

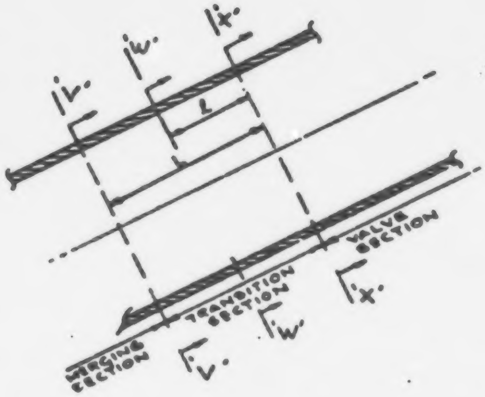
'V'
'W'
'X'
L
MERGING SECTION
TRANSITION SECTION
VALVE SECTION
'V'
'W'
'X'

FIG. 8

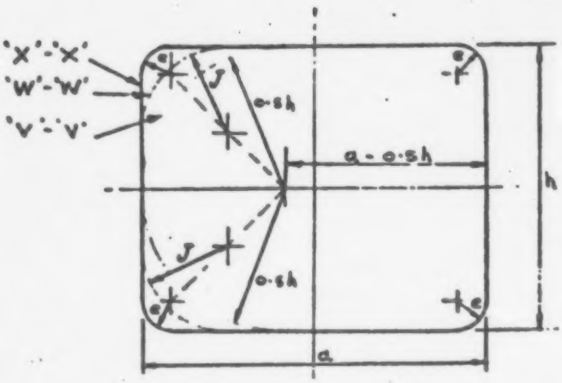
'X'-'X'
'W'-'W'
'V'-'V'
e
J
0.5h
a - 0.5h
h
J
0.5h
e
e
e
a

FIG. 9

910732
7-4

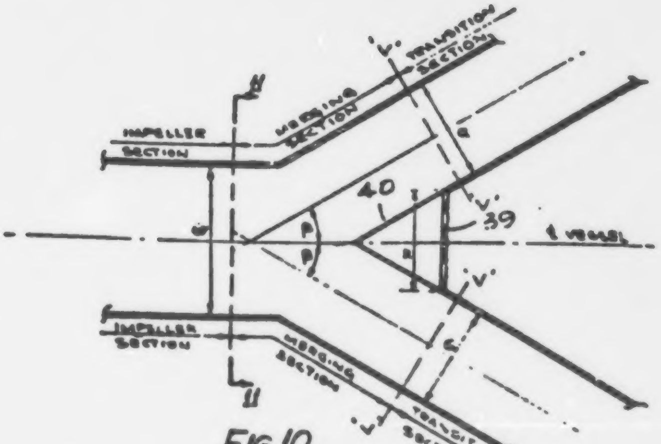
IMPELLER SECTION
MERGING SECTION
TRANSITION SECTION
IMPELLER SECTION
MERGING SECTION
TRANSIT ION SECTION
V
V
V
V
40
39
℄ VESSEL
β
β
11
11

FIG.10

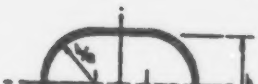

FIG.11

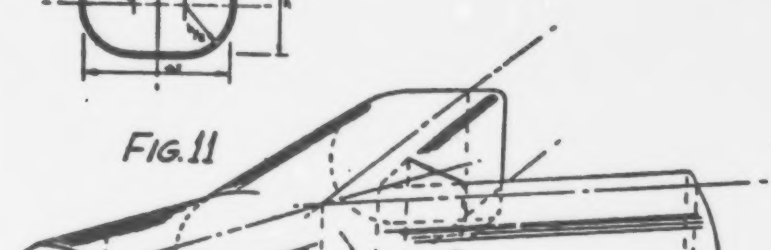

FIG.12

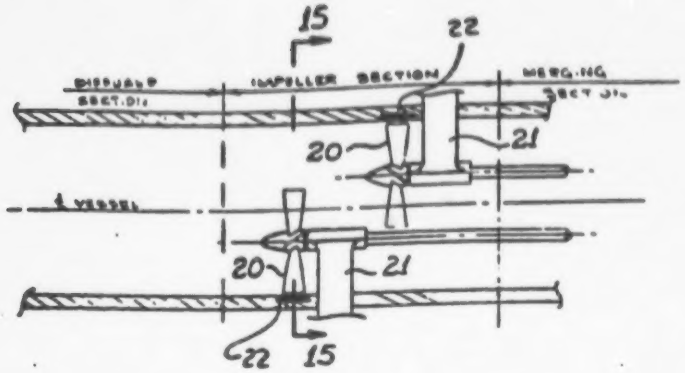
15
22
DIFFUSER SECTION
IMPELLER SECTION
MERGING SECTION
20
21
℄ VESSEL
20
21
22
15

FIG. 13

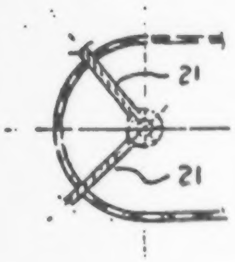

FIG. 14

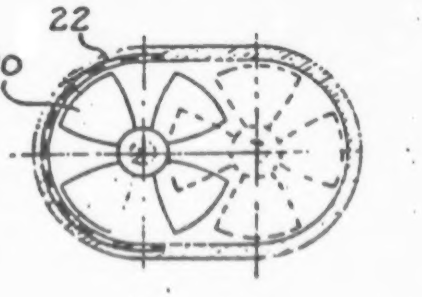

FIG. 15

910732
9-6

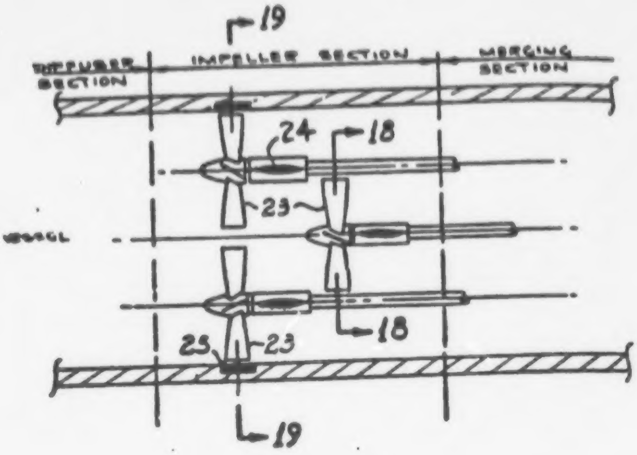
19
DIFFUSER SECTION
IMPELLER SECTION
MERGING SECTION
24
18
23
23
℄ VESSEL
18
25
23
19

FIG. 16

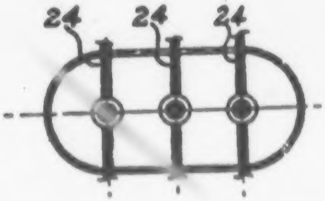

FIG. 17

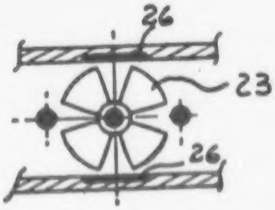

FIG. 18

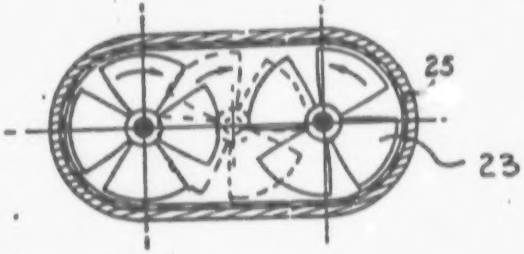

FIG. 19

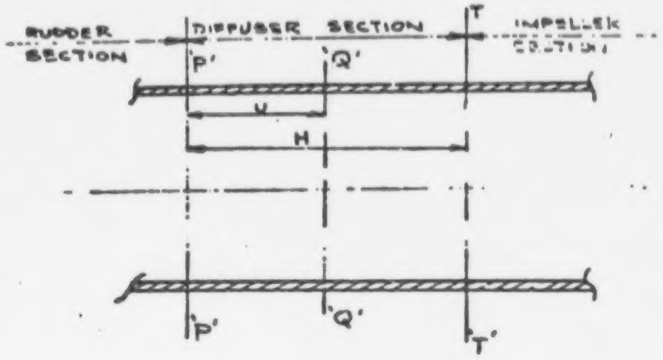
RUDDER SECTION
DIFFUSER SECTION
T
IMPELLER SECTION
'P'
'Q'
U
H
'P'
'Q'
'T'

FIG.20

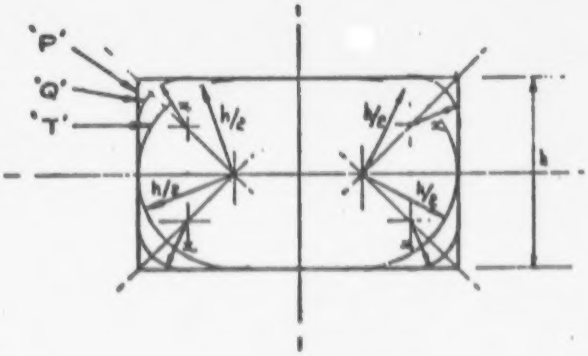
'P'
'Q'
'T'
h/2
h/2
h/2
h/2
h

FIG. 21

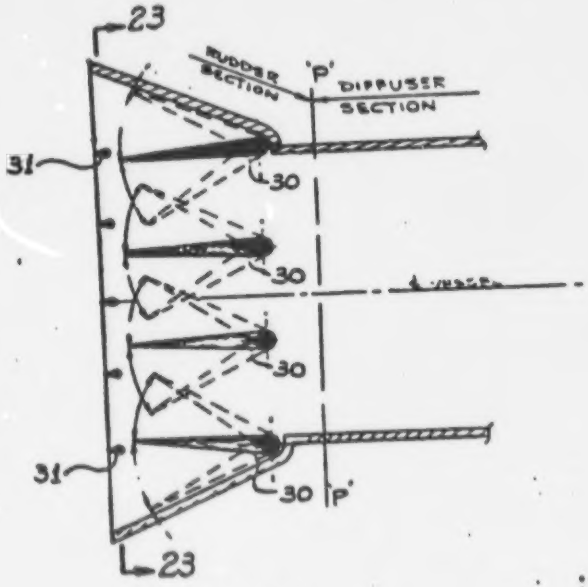
23
RUDDER SECTION
'P'
DIFFUSER SECTION
31
30
30
℄ VESSEL
30
31
30
P'
23

FIG. 22

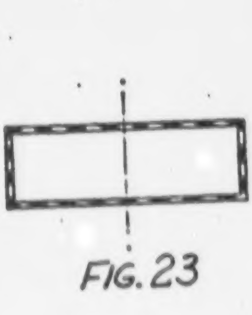

FIG. 23

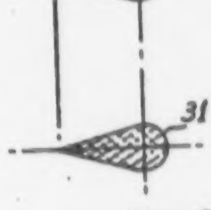

FIG. 24

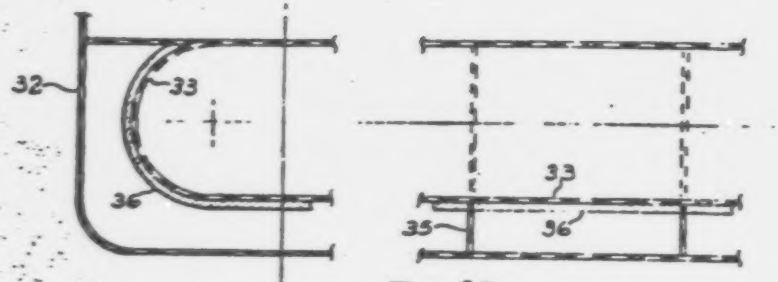
32
33
36
33
36
35

FIG. 25

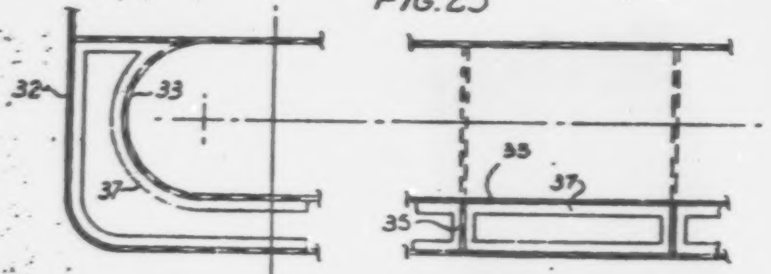
32
33
37
35
37
35

FIG. 26

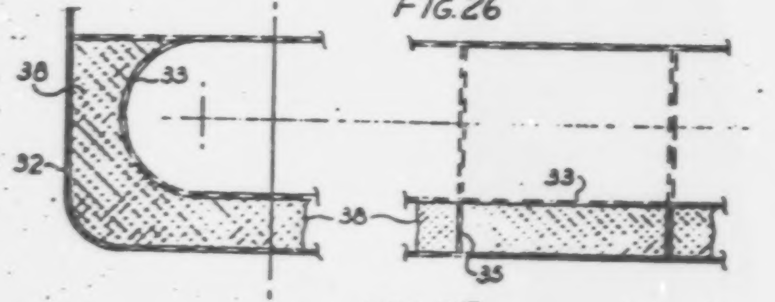
38
33
32
38
33
35

FIG. 27

Volume

2

TP 2704

Prepared For The
TRANSPORTATION DEVELOPMENT CENTRE
Transport Canada

Davis Engineering
consulting engineers

CA1
C
v.
c.

MM

Library and Information Centre / Centre de Documentation (GSLA)
RECEIVED — REÇU LE
AUG 7 1983
Transport Canada / Transports Canada

CA1
DTC801-
80
P661
v.
2
c.2
41.D

386432

PROTECTION OF PROPELLERS IN ICE

VOLUME 11

"DETAIL DESIGN OF PROTECTION SCHEMES"

Prepared For:

TRANSPORTATION DEVELOPMENT CENTRE
TRANSPORT CANADA

Prepared By:

DAVIS ENGINEERING LIMITED
CONSULTING ENGINEERS
OTTAWA, CANADA

AUTHORS: Dr. M.F. George
Mr. F.R. Livingstone

JUNE 1981

REPORT DOCUMENTATION FORM

1. Transport Canada Report No. TP 2704	2. TDC Project No. 8951	3. Recipient's Catalogue No.

4. Title and Subtitle PROTECTION OF PROPELLERS IN ICE VOLUME II - DETAIL DESIGN OF PROTECTION SCHEMES	5. Report Date JANUARY 1983 6. Performing Organization Report No. C323
7. Author(s) Dr. M.F. George Mr. F.R. Livingstone	8. Transport Canada File No. D500-566-1
9. Performing Organization Name and Address Davis Engineering Limited, 1481 Cyrville Road, Ottawa, Ontario K1B 3L7	10. DSS File No. 18 ST.T8200-8-8557 11. DSS or Transport Canada Contract No. 0ST79-00047
12. Sponsoring Agency Name and Address Transportation Development Centre, 1000 Sherbrooke Street West, Montreal, Quebec H3A 2R3	13. Type of Report and Period Covered TECHNICAL 14. Sponsoring Agency Code TDC 8951
15. Supplementary Notes	16. TDC Project Officer R.H.F DILLON

17. Abstract

Design details are given for a propeller protection scheme for a triple-screw 150,000 SHP icebreaker.

The propellers are located in tunnels and structural design drawings are given for the tunnels, propeller duct, and ice guards.

A design for a 50,000 SHP controllable pitch propeller operating in a duct is developed. The propulsion shafting and outboard bearing design are also developed.

Various manoeuvring devices are investigated and a design given for a fully protected in-hull rudder.

Finally, a model test program for evaluating the concept is presented.

18. Key Words Ship, Icebreaker, Propeller, Blade, Protection, Guard, Ice.	19. Distribution Statement Limited number of copies available from sponsoring agency.

20. Security Classification (of this report) Unclassified	21. Security Classification (of this page) Unclassified	22. No. of Pages	23. Price

TDC CDT 79-005

FORMULE DE DOCUMENTATION POUR RAPPORT

1. Nº du rapport Transports Canada TP 2704	2. Nº de l'étude — CDT 8951	3. Nº de catalogue du destinataire
4. Titre et sous-titre PROTECTION OF PROPELLERS IN ICE - VOLUME II - DETAIL DESIGN OF PROTECTION SCHEMES		5. Date du rapport janvier 1983 6. Nº du rapport de l'organisme exécutant C323
7. Auteur(s) Dr. M.F. George Mr. F.R. Livingstone		8. Nº de dossier Transports Canada D1460-137
9. Nom et adresse de l'organisme exécutant Davis Engineering Limitée 1481 Cyrville Road Ottawa (Ontario) K1B 3L7		10. Nº de dossier — ASC 18ST.T8200-8-8557 11 Nº de contrat — ASC ou Transports Canada 0ST79-00047
12. Nom et adresse de l'organisme parrain Centre de développement des transports (CDT) 1000 o., rue Sherbrooke Suite 2421 Montréal (Québec) H3A 2R3		13. Genre de rapport et période visée Technique 14 Code de l'organisme parrain CDT 8951
15. Remarques additionnelles		16. Agent de projet — CDT R.H.F. Dillon

17. Résumé

Ce rapport traite de certains détails concernant l'étude d'un système de protection pour bloc propulsif à 3 hélices destiné à un brise-glace d'une puissance à l'arbre de 150 000 Hp.

Il présente les plans d'étude structurelle des carénages, tuyères et protections qui forment ce système.

Le concept d'un bloc formé d'une hélice à pas variable de 50 000 Hp et de son carénage y est proposé, ainsi que l'arbre de propulsion et le palier extérieur correspondants.

En outre, il y est question de divers dispositifs de manoeuvre et du concept relatif à un gouvernail intégré à la coque, assurant ainsi la protection complète de celui-ci.

Enfin, il propose un programme d'essais sur modèle visant à évaluer le concept suggéré.

18. Mots-clés Navire, brise-glace, hélices, pales, protections, carénages, glaces	19 Diffusion Le CDT dispose d'un nombre limité d'exemplaires

20. Classification de sécurité (de ce rapport) non-classifié	21. Classification de sécurité (de cette page) non-classifiée	22 Nombre de pages	23. Prix

TABLE OF CONTENTS

PAGE:

LIST OF FIGURES iv
LIST OF TABLES vii
VOLUME I - SUMMARY viii
EXECUTIVE SUMMARY ix

1.0 INTRODUCTION 1

2.0 RECOMMENDED PROPELLER PROTECTION SCHEMES 4

- 2.1 Triple-Screw Ship 4
- 2.2 Twin-Screw Ship 8
- 2.3 Single-Screw Ship 8

3.0 DESIGN & STRUCTURAL DETAILS OF THE TRIPLE SCREW CONCEPT, POLAR7A (150,000 SHP POLAR7) 9

- 3.1 General 9
- 3.2 Principle Dimensions of POLAR7A 10
- 3.3 Shell Plating 10
- 3.4 Proposed Internal Arrangement 12
- 3.5 Preliminary Principle Scantlings 13

4.0 PROPELLERS FOR POLAR7A - DESIGN & PERFORMANCE 34

- 4.1 Preliminary Design Data for the Triple-Screw 150,000 HP POLAR7 (POLAR7A) 36
  - 4.1.1 Propeller Particulars 37
  - 4.1.2 Openwater Characteristics 39
- 4.2 Propeller Installation/Removal 52
  - 4.2.1 General 52
  - 4.2.2 Installation/Removal of CP In-Hull Propellers 55

TABLE OF CONTENTS (Cont'd)

PAGE:

5.0 PROPULSION SHAFTING 62

5.1 General 62
5.2 Shafting Dimensions 62
5.3 Shafting Preliminary Stress Analysis 65
5.4 Shafting Dimensions by the Classification Society Regulations 68
5.4.1 Canadian Regulations CASPPR 68
5.4.2 Lloyds 1975, Ice Class 1* 69
5.4.3 Finnish-Swedish Ice Class 1A Super 71
5.4.4 ABS - Class IAA 73
5.4.5 Conclusions 76
5.5 Strut and Sterntube Bearings 78
5.6 Whirling Frequency Analysis 79

6.0 MANEUVERING DEVICES 81

6.1 Types of Maneuvering Devices 81
6.1.1 Rudders 82
6.1.2 Bow Rudders 83
6.1.3 Thruster Units 84
6.1.4 Steering Nozzles 88
6.1.5 Rudder - Nozzle Combination 89
6.2 Protection of Maneuvering Devices 90
6.2.1 Protection of Rudder & Steering Gear 90
6.2.2 CASPPR - Rudder and Steering Gear 96
6.2.3 Protection of Thruster Units 98
6.3 Recommended Manoeuvering Device POLAR 7A - In-hull Stern Rudders 102
6.4 Rudder Area and Force 104
6.4.1 General 104
6.4.2 Rudder Area 105
6.4.3 Rudder Force 106

TABLE OF CONTENTS (Cont'd)

PAGE:

6.0 MANEUVERING DEVICES (Cont'd)

6.5 Rudder Arrangement & Structural Details 109

6.5.1 General Description 109

6.5.2 Rudder Scantlings 110

REFERENCES 114

APPENDIX A - Proposed Test Plan 116

LIST OF FIGURES

FIGURE NO.:	DESCRIPTION:	PAGE:
2.1	Simplified Lines Plan with Device Fitted	5
2.2	Twin Screw Modified PIERRE RADISSON with Protection Device in Place	6
2.3	Single Screw MV ARCTIC with Protection Device in Place	7
3.1	CASPPR Hull Design Thickness of Shell Plating	11
3.2	Forebody Section	15
3.3	Midship Section	16
3.4	Duct and Stern Guard Detail	17
3.5(a)	Bottom Guard Unit and Sidewall Detail (Circular Guards)	18
3.5(b)	Structural Detail of Supporting and Bottom Guards (Tear-drop Guard)	19
3.6	Shafting Arrangement	20
3.7	A-Bracket Casting	21
3.8	Detail of Upper Corner of Side Wall (A-Bracket)	22
3.9	Circular Duct Section (Duct L.E. Casting)	23
3.10	Supporting Frame for Guards	24
3.11	Stern Guards	25
3.12	Rudder Arrangement	26
4.1	K_a^{-4-55} Screw Series in an Axial Cylinder for V = 2 Knots (Not Corrected for CCP and Tip Clearance)	40
4.2	K_a^{-4-55} Screw Series in an Axial Cylinder for V = 16 Knots (Not Corrected for CCP and Tip Clearance)	41

LIST OF FIGURES (Cont'd)

FIGURE NC.:	DESCRIPTION:	PAGE:
4.3	Results of Open Water Tests with the K_a^{-4-55} Screw Series in an Axial Circular Cylinder	42
4.4	Open Water Efficiency for a CCP, K_a^{-4-55}, in an Axial Cylinder	47
4.5	Thrust vs. R.P.M. at Constant Ship Speed	48
4.6	Thrust Coefficient vs. Torque Coefficient for B4-55 at Zero Speed of Advance	50
4.7	Propeller Tailshaft Withdrawal	53
4.8	Propeller Removal	54
4.9	Removal of Propeller Blades in a Ducted CP Propeller Arrangement	56
4.10	Scheme I	57
4.11(a)	Stern Guards (Scheme II-A)	59
4.11(b)	Stern Guards (Scheme II-B)	60
5.1	Shafting Main Dimensions	63
5.2	Sketch of Shafting Arrangement for the Computer Program	64
5.3	Shaft Stress Results, Position 1	66
5.4	Shaft Stress Results, Position 2	67
5.5	Whirling Frequency Results	80
6.1	General Layout of a Thruster Unit	85
6.2	Rudder Locking Pin for Astern Operation by Arctic Class Vessels (Ref. 17)	92
6.3	Possible Reinforcement for an Arctic-Type Rudder	94

LIST OF FIGURES (Cont'd)

FIGURE NO.:	DESCRIPTION:	PAGE:
6.4	KIGORIAK	99
6.5	Attachment of Closing Side of Double Plate Rudder	113

LIST OF TABLES

TABLE NO.:	DESCRIPTION:	PAGE:
4.1	K_a^{-4-55} Screw Series in an Axial Cylinder Corrected for CP and Tip Clearance	
5.1-A	Solid Shafts	
5.1-B	Hollow Shafts (I.D. = 0.6 O.D.) with the Same Section Modulus as in Table 5.1-A	

VOLUME I - SUMMARY

As a first phase of our investigation of Protection of Propellers In Ice, we have produced a Volume I report entitled "Assessment of Protection Schemes". The report presents a theoretical appraisal of published and unpublished protection schemes applicable to single and multi-screw ice class ships.

The major concepts identified and investigated were ducts, ring propellers, deflecting fins, bilge keels, propeller cages, open or partial tunnels, and in-hull propulsion systems. Various devices within each concept were developed and each device was critically reviewed on the basis of its anticipated, or when possible, demonstrated capabilities for protecting a propeller from ice damage and, in addition, for its effects on propulsive efficiency. A description of each concept was provided followed by an assessment of its worth as a propeller protection device. Some assessment was largely qualitative in nature since very little information was available either experimentally or derived from actual operating experience.

Finally in the Volume I report, conclusions were drawn with regard to the most suitable and effective devices to be recommended for Arctic Class vessels. These recommendations with regard to the protection devices for single-screw, twin screw, and triple-screw ships are reproduced in Section 2.0 of this report.

EXECUTIVE SUMMARY

This report presents the design details for a triple-screw 150,000 SHP icebreaker with full propeller protection.

The protection scheme consists of placing each propeller in a tunnel which is open along the bottom. A grid on the inlet prevents the ingress of large pieces of ice.

The design of the tunnels and ducts in which the propellers operate, is given in detail. The strength requirements with respect to the Classification Society Rules are examined. The design and installation of the ice guards (inlet/outlet grids) is also addressed.

The basis for selecting a four bladed controllable pitch propeller absorbing 50,000 HP is discussed. This 6500 mm diameter propeller produces close to 300 tons thrust at the near-bollard pull condition. The method of installing and removing the propellers from the tunnels is described.

A design for the propulsion shafting is given and a comparison made with the various Classification Society Rules. Due to the protection scheme, the propeller and shafting have been designed for Arctic Class 2 rather than Arctic Class 7 which results in a considerable reduction in size and thus in cost for these components.

Various types of manoeuvring devices are discussed and a design developed for a fully protected in-hull rudder.

Finally, based on the design presented in this report, a model test program is presented for evaluation of the concept.

1.0 INTRODUCTION

Arctic shipping has attracted considerable interest recently in connection with the exploration for energy related natural resources. With the increased offshore drilling operations in the northern waters exploring for both oil and natural gas, the need for capable Arctic-Class supply vessels and LNG [illegible]riers to operate in the Arctic environment has become a necessity for such operations to be successful. Before such vessels can be successfully designed, however, details of the environment is which they operate must be known.

A variety of ice conditions are found in Canadian Arctic waters, ranging from hard multi-year ice (having very high strength, approximately 3,000 psi in compression and 250 psi in tension) to slush ice. Free icebergs and small and large ice islands are also common.

Ice-class vessels are either Icebreakers or vessels with icebreaking capabilities.

Icebreakers* can generally be grouped into three types: harbour icebreakers (small vessels designed to cut homogeneous sheets of light harbour and river ice); non-polar icebreakers (larger vessels designed to assist shipping in moderate ice conditions); and polar icebreakers (vessels designed to operate in heavy ice conditions as in the Arctic, Antarctic, and Siberia.

---

* Icebreaker is defined by Arctic Waters Pollution Prevention Act (Canada) as "a ship specially designed and constructed for the purpose of assisting the passage of other ships through ice".

The term "POLAR N", with N varying between 3 and 10, was introduced by ASPPR to describe the capability required of a vessel to operate in a specific ice zone regardless of the prime function of the vessel.

Throughout this report, the term "icebreaker" will be referring to this type of POLAR class vellel, such as the 150,000 S.HP POLAR 7 icebreaker (POLAR7A) used in our investigation to study the effectiveness of the propeller protection scheme for a triple-screw ship.

The design of a successful vessel to operate in such a harsh environment as the Arctic, involves numerous design problems. Principles used in conventional ship design for resistance and power predictions, hull strength requirements, and propulsion system design are no longer applicable to ice-class ships and special techniques must be applied.

Techniques presently used in design are based on operational experience and on model testing. For example, MANHATTAN in 1969, as a test vehicle, answered many questions and was successful in her goal of establishing and validating information with regard to ice-class vessels. Such information is a great asset in the design and development of icebreakers.

Classification Society regulations increase the strength of components subject to ice loading. Another approach to reduce the "high risk factor" of such vessels is to protect the vulnerable items from damage by ice. Damage to propellers, shafts, and rudders in particular, carries severe consequences in assessing the reliability of these vessels.

The protection of propellers from ice, is the main objective of this study. Volume I(3) of this study described the different protection devices for single, twin and triple-screw vessels, whereas this report, Volume II, discusses the implementation, both structurally and hydrodynamically, of the recommended protection device to the proposed 150,000 SHP POLAR 7 triple-screw icebreaker (POLAR7A). Section 2.0 describes the recommended propeller protection schemes for the single, twin, and triple-screw ships. Section 3.0 gives details of the design of the protection concept for the triple-screw case. Propeller design and performance for POLAR7A are discussed in Section 4.0, and the propulsion shafting system in Section 5.0. Manoeuvring devices are discussed in Section 6.0 together with the design, arrangement, and structural details of the recommended manoeuvring device (protected in-hull stern rudders). Finally, the proposed test plan to be carried out to evaluate the scheme experimentally is given in Appendix A.

2.0 RECOMMENDED PROPELLER PROTECTION SCHEMES

In Volume 1 Report (3) of this study, conclusions were drawn with regard to the most suitable and effective propeller protection devices for Arctic class vessels. These schemes are summarized below.

2.1 Triple-Screw Ship

An in-hull propulsion scheme is proposed in which the three propellers are totally enclosed in separate tunnels with guarded bottom intakes. Four different arrangements of such a scheme for a triple-screw ship are shown in figures 31 to 34 inclusive in the Volume 1 Report (3). They were developed using as a basis the hull form of the 90,000 SHP POLAR 7 (7) enlarged by a linear scale factor to allow the new hull to absorb the proposed 150,000 SHP with some margin for the protection arrangement. In the first arrangement the basic hull form was used without any modifications. Typical propeller locations for a triple-screw ship were adopted. In the second arrangement the aft body shape was altered in order to accommodate the tunnels with the propellers in one plane. For the third arrangement, the aft end of the tunnel was made flush with the ship's hull to improve the performance in astern operation. In the fourth arrangement, a squared-off transom stern was used together with a wall-sided hull form. In the above four arrangements the tunnel exits are fitted with removable guards. The fourth arrangement, shown in Figure 2.1, is considered to be the most promising concept for a triple-screw vessel. Its performance will be investigated experimentally by model testing. The design and structual details of this concept are given in Section 3.0.

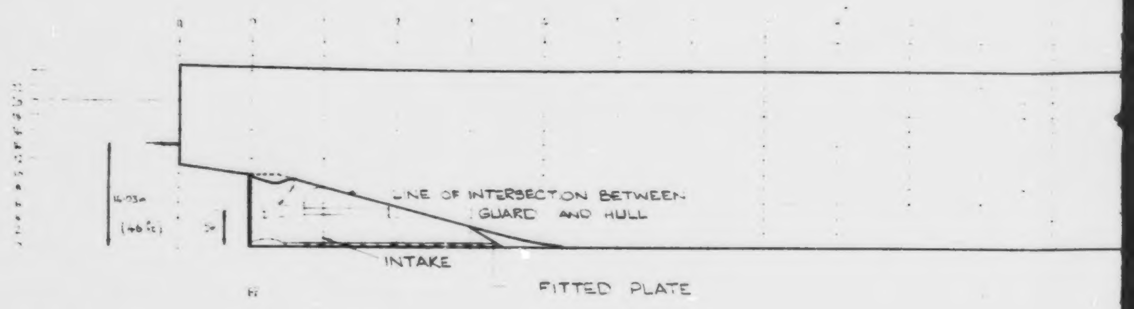
14·23m
(46 ft)
LINE OF INTERSECTION BETWEEN
GUARD AND HULL
INTAKE
FITTED PLATE

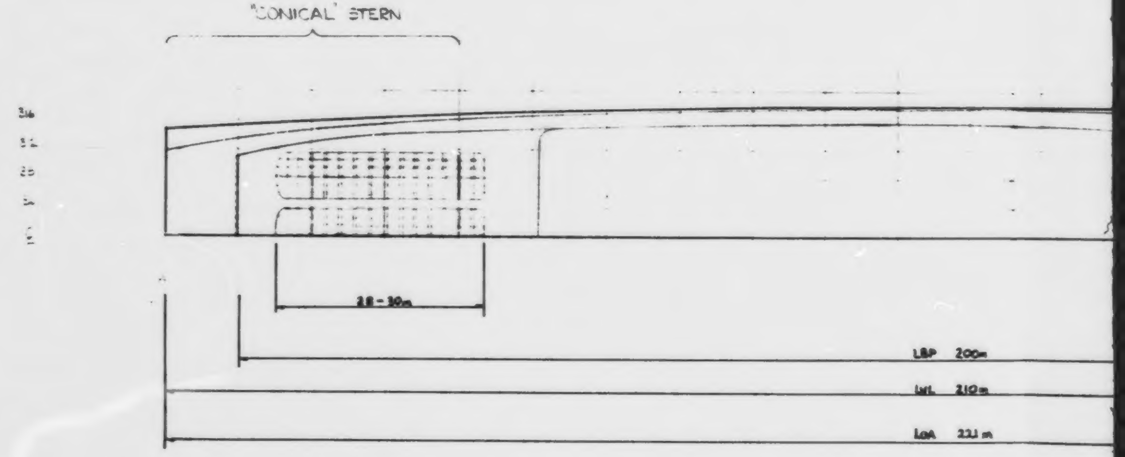
'CONICAL' STERN
28 - 30m
LBP 200m
LWL 210m
LOA 221 m

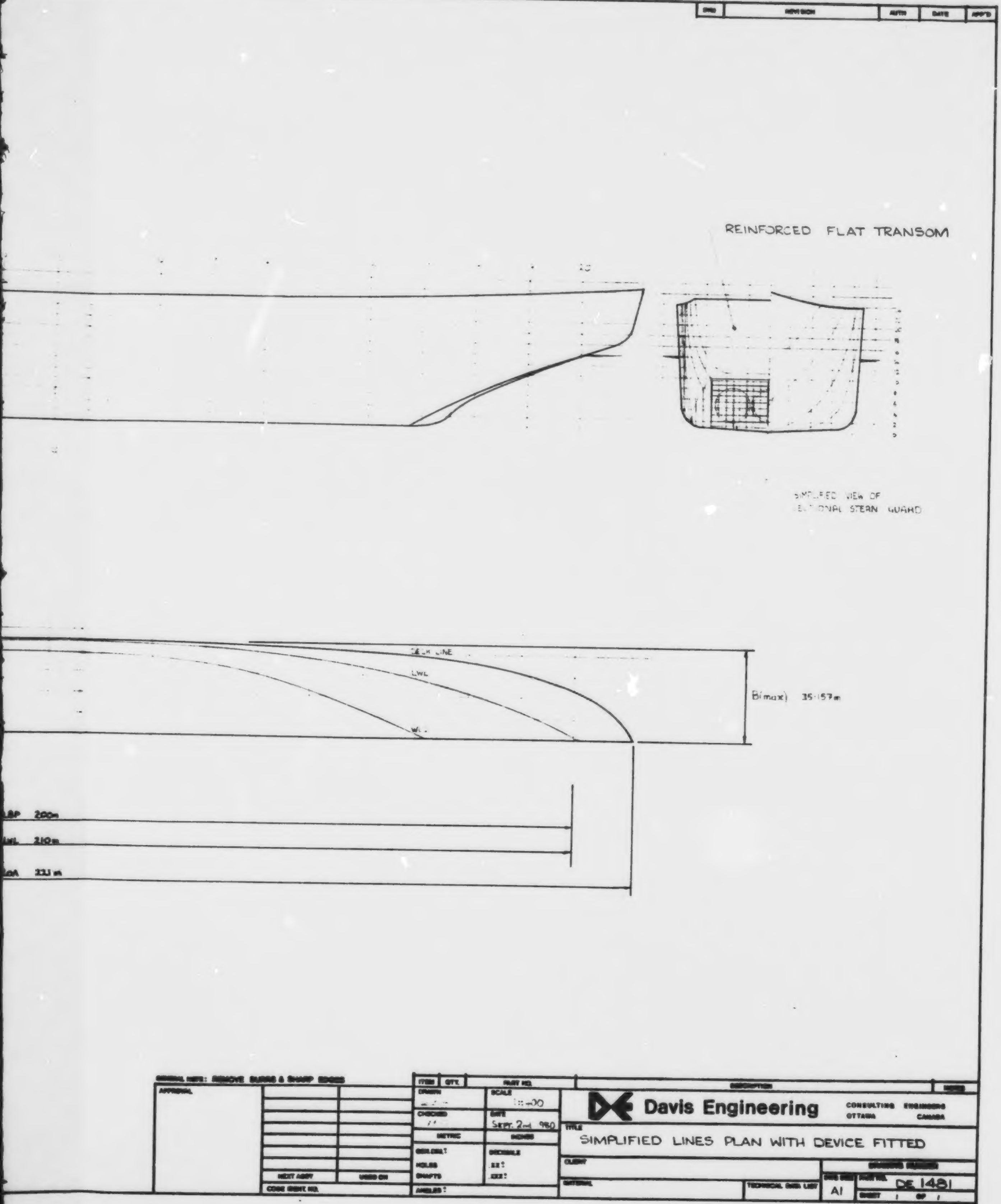

REINFORCED FLAT TRANSOM
20
SIMPLIFIED VIEW OF
SECTIONAL STERN GUARD
DECK LINE
LWL
WL
B(max) 35·157m
LBP 200m
LWL 210m
LOA 221m
GENERAL NOTE: REMOVE BURRS & SHARP EDGES
APPROVAL
NEXT ASSY
USED ON
CODE IDENT NO.
ITEM
QTY
PART NO.
DESCRIPTION
NOTES
DRAWN
SCALE
1:400
CHECKED
DATE
Sept. 2nd 980
METRIC
INCHES
DECIMALS
HOLES
.XX
SHAFTS
.XXX
ANGLES
Davis Engineering
CONSULTING ENGINEERS
OTTAWA CANADA
TITLE
SIMPLIFIED LINES PLAN WITH DEVICE FITTED
CLIENT
MATERIAL
TECHNICAL DATA LIST
DRAWING NUMBER
A1
DE 1481
SHEET 1 OF 1

FIGURE 2.1 - Simplified Lines Plan with Device Fitted

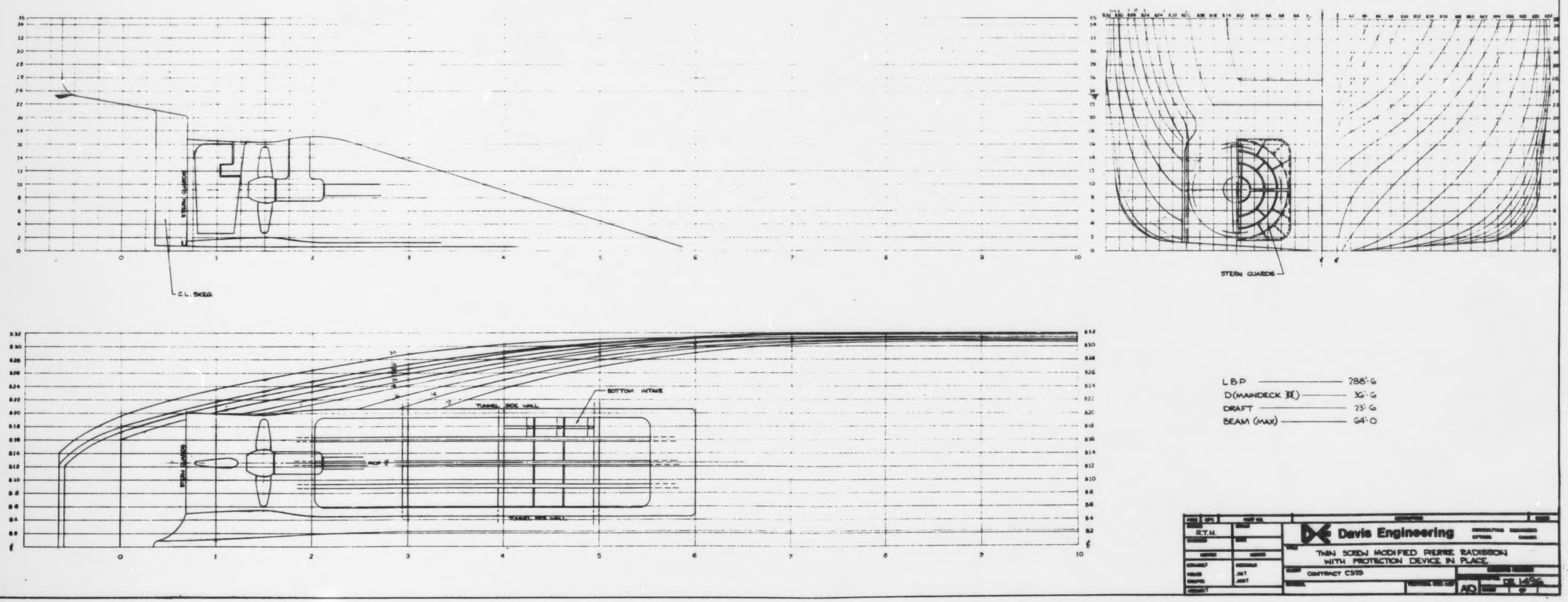
STERN GUARDS
C.L. SKEG
BOTTOM INTAKE
TUNNEL SIDE WALL
PROP ℄
LBP 288'-6
D(MAINDECK II) 36'-6
DRAFT 23'-6
BEAM (MAX) 64'-0
R.T.H.
Davis Engineering
TWIN SCREW MODIFIED PIERRE RADISSON WITH PROTECTION DEVICE IN PLACE
CONTRACT CS29
AD
DE 1496

FIGURE 2.2 - Twin Screw Modified PIERRE RADISSON with Protection Device in Place

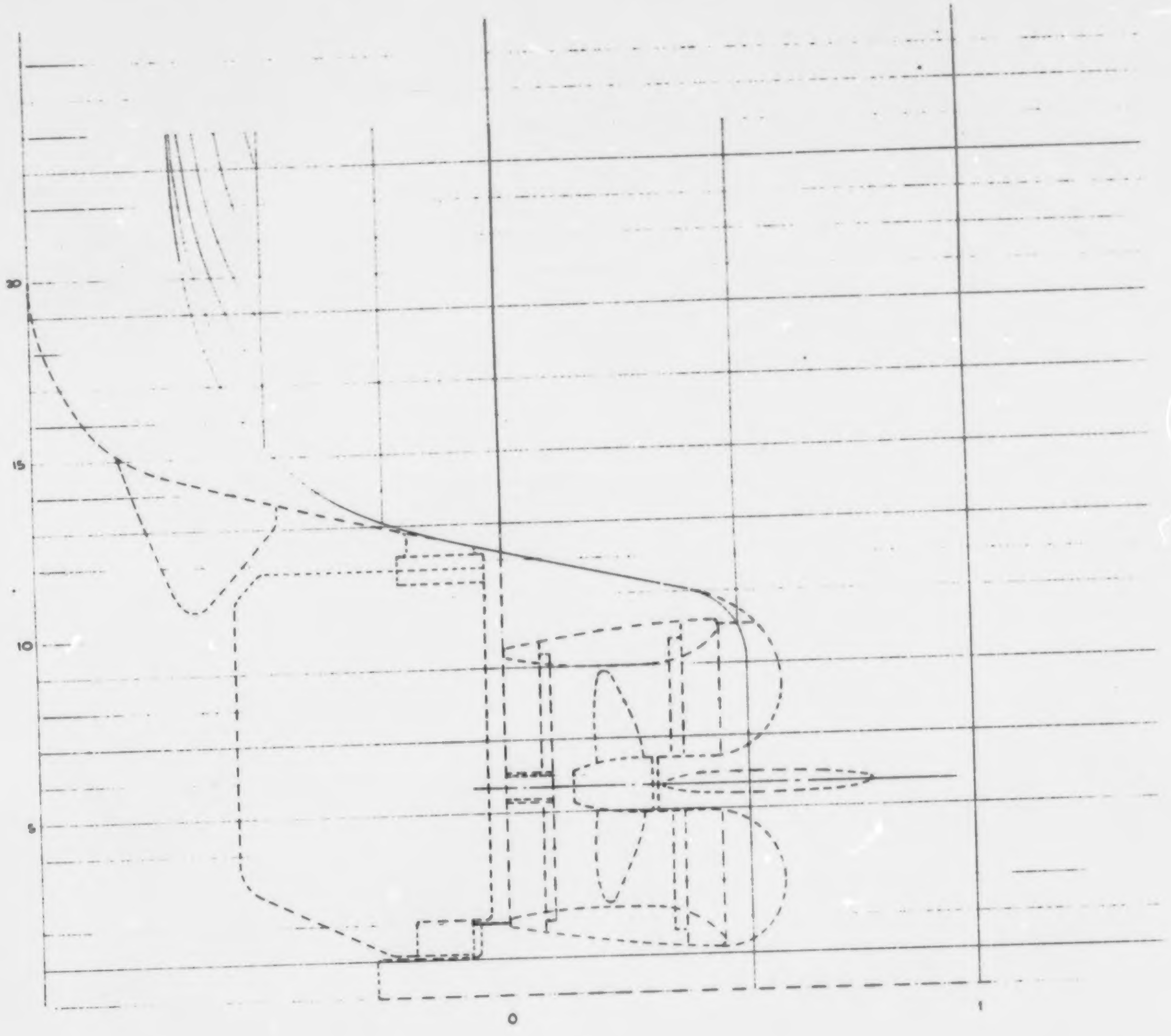

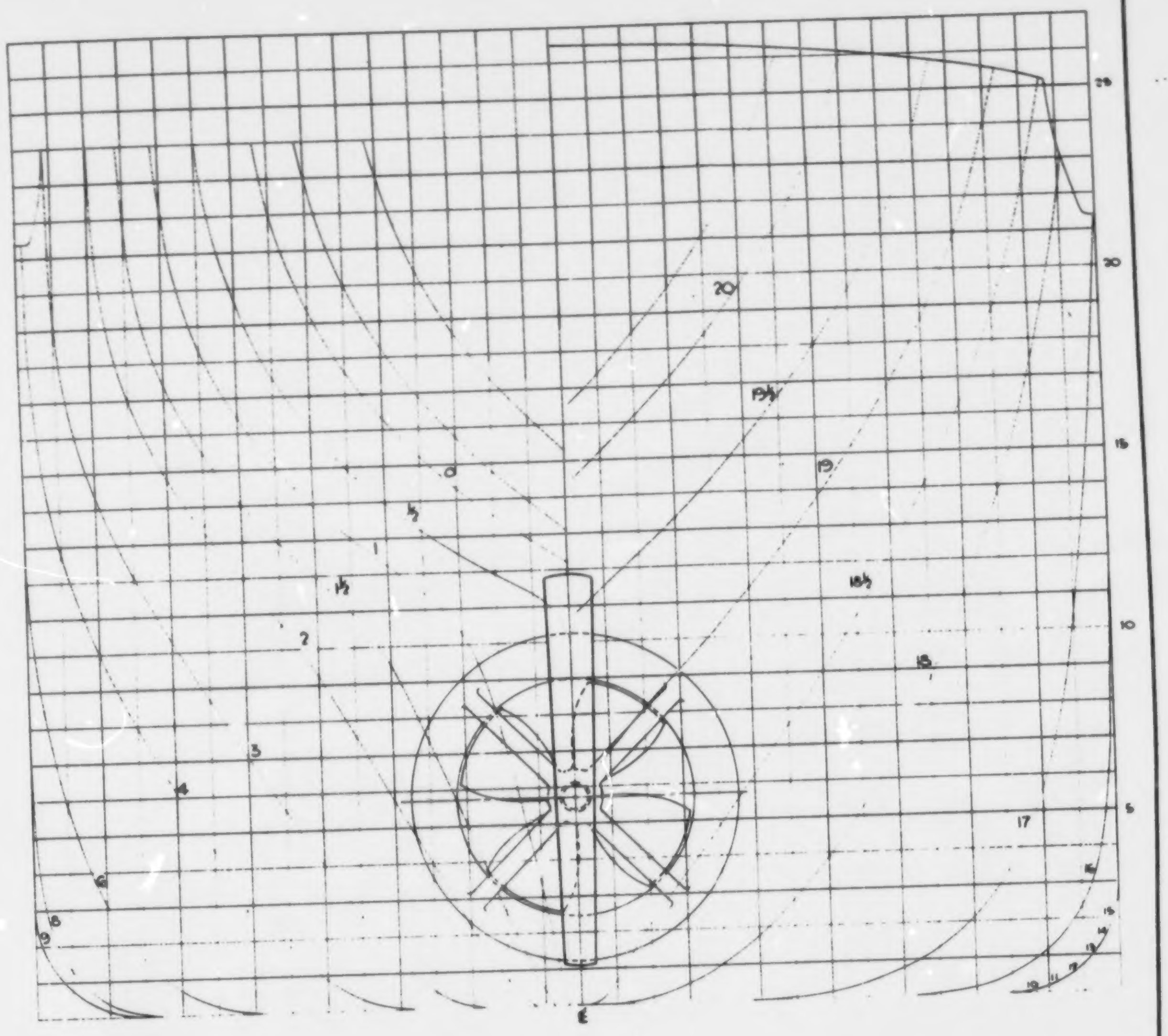
20
19½
19
18½
18
17
0
½
1
1½
2
3
4
25
20
15
10
5
℄

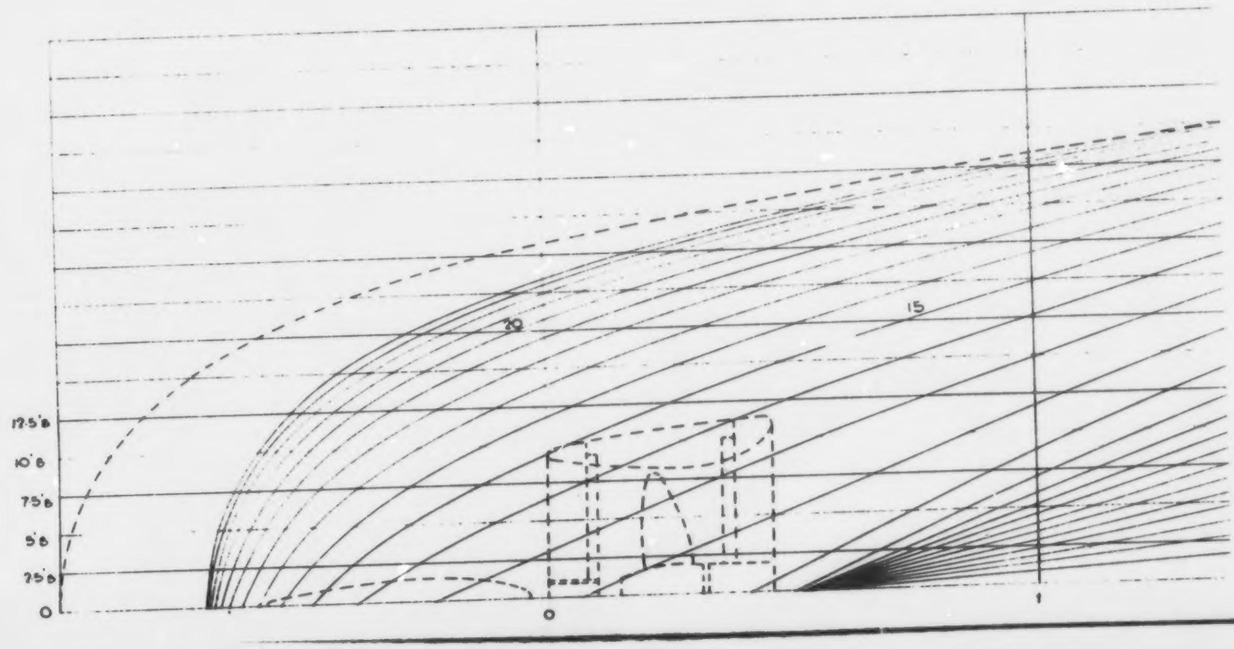
20
15
12.5'
10'
7.5'
5'
2.5'
0
0
1

LBP	196·60 M
DRAUGHT (MOULDED)	22·86 M
DEPTH (MOULDED)	15·24 M
BEAM (MOULDED)	10·97 M

FIGURE 2.3 - Single Screw MV ARCTIC with Protection Device in Place

Davis Engineering

SINGLE SCREW MV ARCTIC
WITH PROTECTION DEVICE IN PLACE

RTH

CONTRACT C373

A1

DE 1499

2.2 Twin-Screw Ship

The in-hull propulsion scheme was also considered the most appropriate for the twin screw ship.

The simplified lines plan for a twin-screw ship is shown in drawing no. DE1496 (Figure 2.2). The hull form was developed using as a basis the hull form of PIERRE RADISSON. Each propeller is enclosed in a separate tunnel with guarded bottom intake. The tunnel exits are fitted with removable guards to facilitate removal and maintenance of propeller, shafts, bearings, etc.

2.3 Single-Screw Ship

The recommended protection scheme for a single-screw ship consists of a strong double flared nozzle with deflector fins on the bossing and skeg as shown in drawing no. 1499 (Figure 2.3). The trailing part of the nozzle is fitted with removable guards. The lines plan for a single-screw ship with the device in place is shown in Figure 2.3. The hull form is that of MV ARCTIC.

3.0 DESIGN & STRUCTURAL DETAILS OF THE TRIPLE SCREW CONCEPT, POLAR7A (150,000 SHP POLAR7)

3.1 General

The 150,000 HP triple-screw POLAR7 icebreaker (POLAR7A) proposed for the study of the in-hull protection schemes is similar to that of the 90,000 HP POLAR7 (7), but enlarged by a linear factor of 15% to allow the new hull to absorb the available 150,000 HP. A protection margin of 10 - 12% of the power was assumed. Figure 2.1 shows the simplified lines plan with the protection device in place. The bow is an MIT type with an angle of 16 degrees to the vertical at the waterline, increasing underwater to 27 degrees at the keel. The aft body is made fuller in comparison with conventional icebreakers in order to allow for the installation of the protection device, but at the same time provide smooth and continuous waterlines without abrupt changes. Areas of concave section and of high double curvature have been eliminated. The Reamer concept has not been adopted in this design to avoid the additional ice resistance caused by it. Water lubrication along the entire length of the vessel can be used to improve her ice performance.*

In the following sections the construction requirements of the ASPPR, or equivalent regulations, are complied with as closely as possible. Design of the protection guards will be based on a simple and direct impact load.

---

*This technique is somewhat similar to that employed on the Russian icebreakers "Leonid Krasin" (8850 tons, 10,000 HP) and "Lenin" (5150 tons, 7,500 HP) (9). On these icebreakers, however, the warm water is sprayed onto the ice at the bow.

3.2 Principle Dimensions of POLAR7A

Midship-Fwd: as POLAR7 lines for forebody

Midship-Aft: parallel side walls with squared off transom stern

LOA - 221 m
LBP - 200 m
LWL - 210 m
B_m (W.L.) - 35.157 m
T_m - 14.03 m
D_m - 24 m at midship to forecastle deck
Counter Height - 3.50 m
Prop Centreline - 3.00 m fwd. of stn. 0, 4.5 m above baseline
Sheer - 1.75 m fwd., 0.875 m aft.
Counter Angle - 15°
Tunnel Length - 25.00 m from LE of duct
Tunnel Angle - 20°
Duct LENGTH - 7.5 m
DIA (LE) - 8.70 m
DIA (TE) Inner - 7.45 m
Counter Length - 10 m
Height to Base of Counter - 9.35 m

3.3 Shell Plating

The calculated thickness of shell plating in each area, according to ASPPR, is shown in Figure 3.1. The assumed ice pressure is as follows.

Arctic Class 7 Ice Pressures (psi)

Bow Area	Lower Bow Area	Midbody Area	Lower Transition Area	Upper Transition Area	Stern Area
1400	7	850	600	420	1050

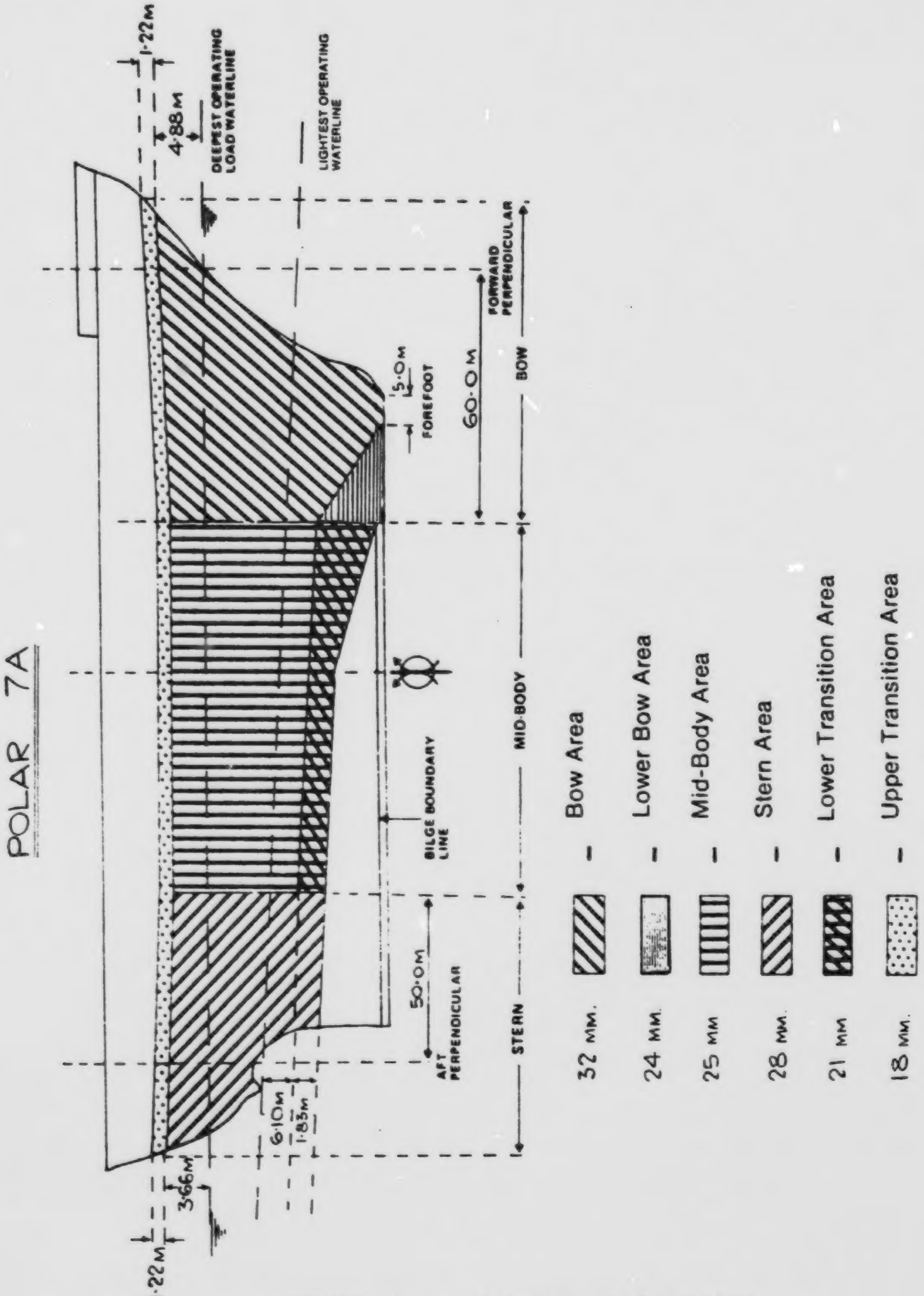
POLAR 7A
1·22M
4·88M
DEEPEST OPERATING LOAD WATERLINE
LIGHTEST OPERATING WATERLINE
FORWARD PERPENDICULAR
BOW
60·0M
5·0M
FOREFOOT
MID-BODY
BILGE BOUNDARY LINE
STERN
50·0M
AFT PERPENDICULAR
6·10M
1·83M
3·66M
1·22M
32 MM. – Bow Area
24 MM. – Lower Bow Area
25 MM – Mid-Body Area
28 MM. – Stern Area
21 MM – Lower Transition Area
18 MM. – Upper Transition Area

FIGURE 3.1 CASPPR Hull Design
Thickness of Shell Plating

3.4 Proposed Internal Arrangement

AT MIDSHIPS:	a)	Three Decks:	- weather deck - main deck - lower deck
	b)	Double Bottom:	- floors at main frames - keel plate - centerline girder - two intercostal side girders each side
	c)	Transverse Subdivision:	- centerline bulkhead to weather deck
OVERALL:	a)	Longitudinal Subdividion:	- watertight transverse bulkheads (subject to flooding requirements) - forward collision bulkhead - aft collision bulkhead
	b)	Longitudinal Structure:	- side stringers - stiffners on all decks - centreline girder and side girders - hatch side girders
	c)	Transverse Structure:	- bulb angle plate frames keel to lower deck lower deck to main deck main deck to weather deck - D.B. floors - hatch end beams - deck transverse beams

GENERAL:

- engine room aft
- fore peak division
- aft peak division
- cast stem and stern frames
- three tunnels with circular duct sections
- bottom and stern guards
- shafting, bearings, and struts
- rudders
- bow thrusters

3.5 Preliminary Principle Scantlings

The scantlings were obtained according to the Canadian Regulations (CASPPR) for Class 7 vessels. Cross reference was made with other regulations such as Lloyds, ABS, and DNV for some structural members, and the highest scantlings were adopted.

Since the stern and the afterbody sections are new in a sense that they are non-standard for these types of vessels, efforts were made to relate their design to relevant items for conventional ships wherever possible. For some items, however, simple design procedures were followed to determine their main dimensions, shapes, etc.

The main scantlings of each item are shown in the corresponding drawings as follows:

Item:	Drawing No.:	Figure No.:
- Fore Body Arrangement		3.2
- Midship Section Scantlings		3.3
- Tunnel Arrangement & Construction	DE 1483	3.4

Item:	Drawing No.:	Figure No.:
- Side Walls (skirts) Details	DE 1483	3.4
	DE 1484	3.5
- Shafting Arrangement	DE 1492	3.6
- A-Bracket Casting	DE 1490	3.7
	DE 1483	3.4
- Detail of UPPER Corner of Side Wall (A-Bracket)	DE 1489	3.8
- Circular Duct Section (Duct L.E. Casting)	DE 1488	3.9
- Supporting Frame for Guards	DE 1482	3.10
- Bottom Guards	DE 1484	3.5
- Stern Guards	DE 1485	3.11
- Rudder Arrangement	DE 1495	3.12

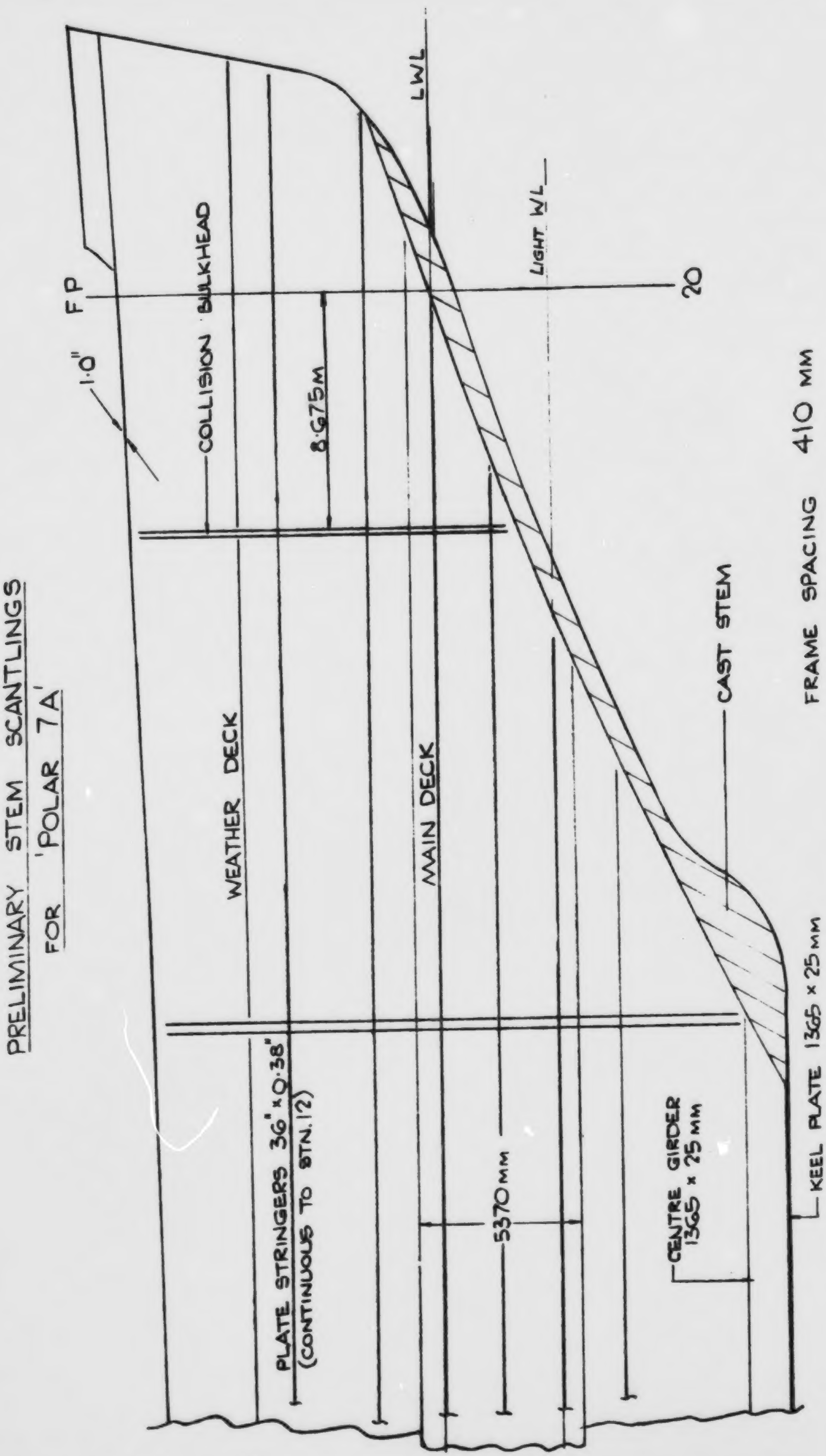
PRELIMINARY STEM SCANTLINGS
FOR 'POLAR 7A'
WEATHER DECK
MAIN DECK
COLLISION BULKHEAD
8.675M
1.0"
FP
LWL
LIGHT WL
20
CAST STEM
FRAME SPACING 410 MM
PLATE STRINGERS 36" x 0.38"
(CONTINUOUS TO STN. 12)
5370MM
CENTRE GIRDER
1365 x 25 MM
KEEL PLATE 1365 x 25 MM

FIGURE 3.2 Forebody Section

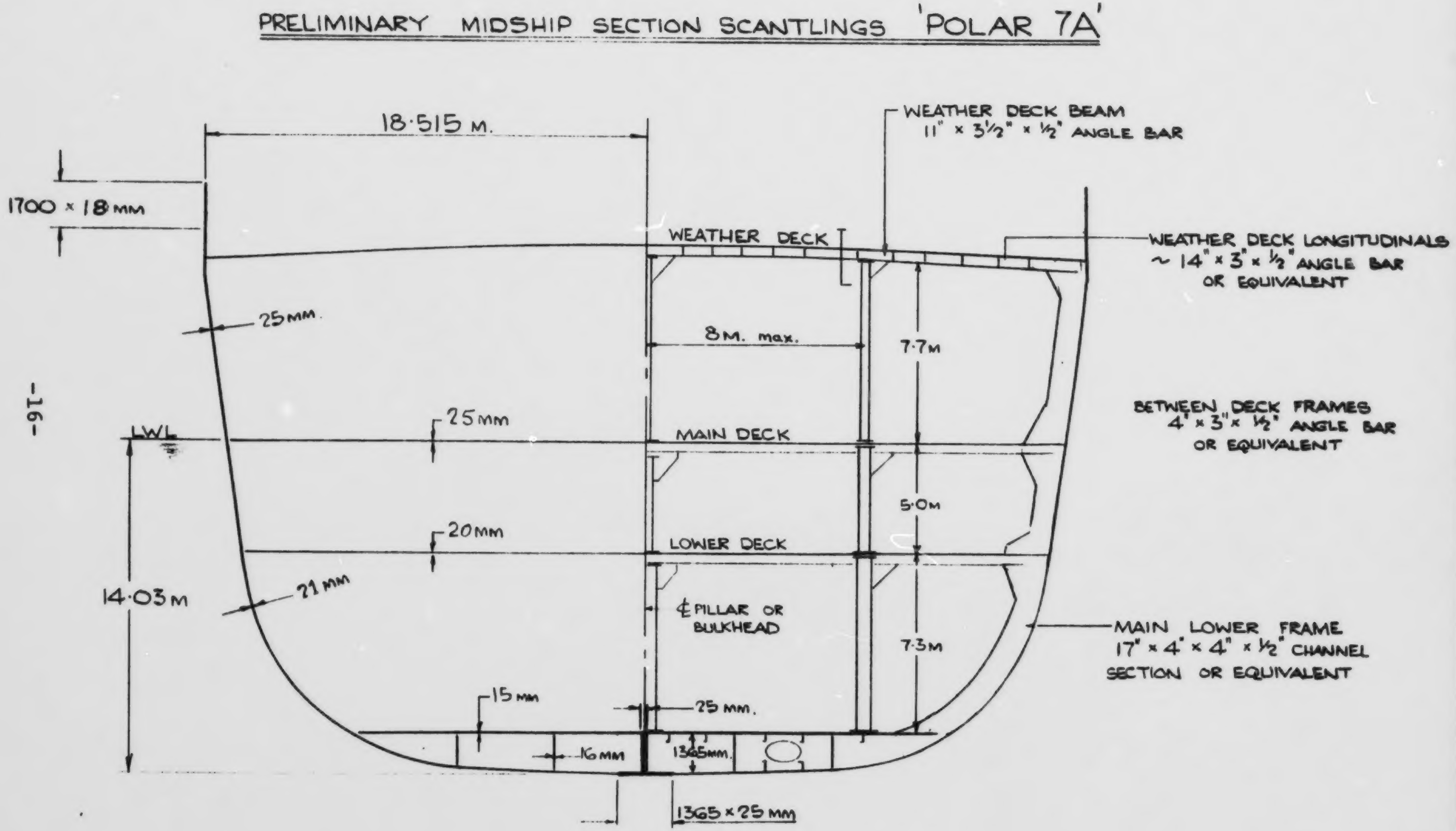
PRELIMINARY MIDSHIP SECTION SCANTLINGS 'POLAR 7A'
18·515 M.
1700 × 18 MM
WEATHER DECK BEAM
11" × 3½" × ½" ANGLE BAR
WEATHER DECK
WEATHER DECK LONGITUDINALS
~ 14" × 3" × ½" ANGLE BAR
OR EQUIVALENT
25 MM.
8 M. max.
7·7 M
BETWEEN DECK FRAMES
4" × 3" × ½" ANGLE BAR
OR EQUIVALENT
LWL
25 MM
MAIN DECK
5·0 M
20 MM
LOWER DECK
14·03 M
21 MM
℄ PILLAR OR
BULKHEAD
7·3 M
MAIN LOWER FRAME
17" × 4" × 4" × ½" CHANNEL
SECTION OR EQUIVALENT
15 MM
25 MM.
16 MM
1365 MM.
1365 × 25 MM

FIGURE 3.3 MIDSHIP SECTION

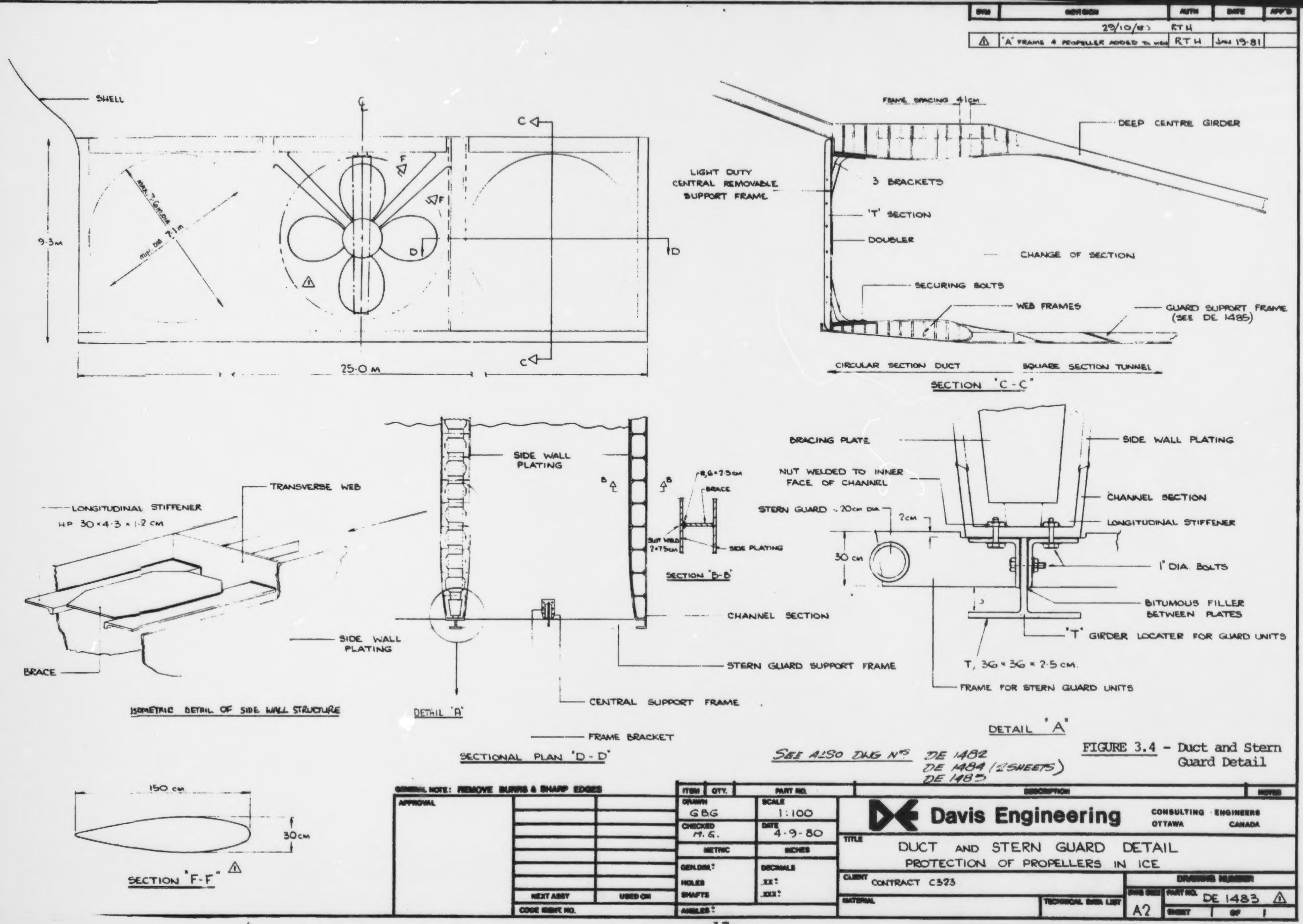
SHELL
C
C
C
F
F
D
D
max. 7.6m DIA
min. DIA 7.1m
9.3m
25.0 m
FRAME SPACING 41cm
DEEP CENTRE GIRDER
LIGHT DUTY CENTRAL REMOVABLE SUPPORT FRAME
3 BRACKETS
'T' SECTION
DOUBLER
CHANGE OF SECTION
SECURING BOLTS
WEB FRAMES
GUARD SUPPORT FRAME (SEE DE 1485)
CIRCULAR SECTION DUCT
SQUARE SECTION TUNNEL
SECTION 'C-C'
TRANSVERSE WEB
LONGITUDINAL STIFFENER
H.P. 30 × 4.3 × 1.2 cm
SIDE WALL PLATING
BRACE
ISOMETRIC DETAIL OF SIDE WALL STRUCTURE
SIDE WALL PLATING
B
B
R,6 = 7.5cm
BRACE
SLOT WELD 7×75cm
SIDE PLATING
SECTION 'B-B'
CHANNEL SECTION
STERN GUARD SUPPORT FRAME
CENTRAL SUPPORT FRAME
FRAME BRACKET
DETAIL 'A'
SECTIONAL PLAN 'D-D'
BRACING PLATE
SIDE WALL PLATING
NUT WELDED TO INNER FACE OF CHANNEL
CHANNEL SECTION
STERN GUARD 20cm DIA
2cm
LONGITUDINAL STIFFENER
30 cm
1" DIA BOLTS
BITUMOUS FILLER BETWEEN PLATES
'T' GIRDER LOCATER FOR GUARD UNITS
T, 36 × 36 × 2.5 cm
FRAME FOR STERN GUARD UNITS
DETAIL 'A'
150 cm
30cm
SECTION 'F-F'

SYM	REVISION	AUTH	DATE	APP'D
	29/10/80	RTH		
⚠	"A" FRAME & PROPELLER ADDED TO VIEW	RTH	JAN 19-81	

SEE ALSO DWG Nos DE 1482
DE 1484 (2 SHEETS)
DE 1485

FIGURE 3.4 - Duct and Stern Guard Detail

GENERAL NOTE: REMOVE BURRS & SHARP EDGES

DRAWN: GBG
SCALE: 1:100
CHECKED: M.G.
DATE: 4-9-80

Davis Engineering
CONSULTING ENGINEERS
OTTAWA CANADA

TITLE: DUCT AND STERN GUARD DETAIL
PROTECTION OF PROPELLERS IN ICE

CLIENT: CONTRACT C323

DWG SIZE: A2
PART NO. DE 1483 ⚠
SHEET 1 OF 1

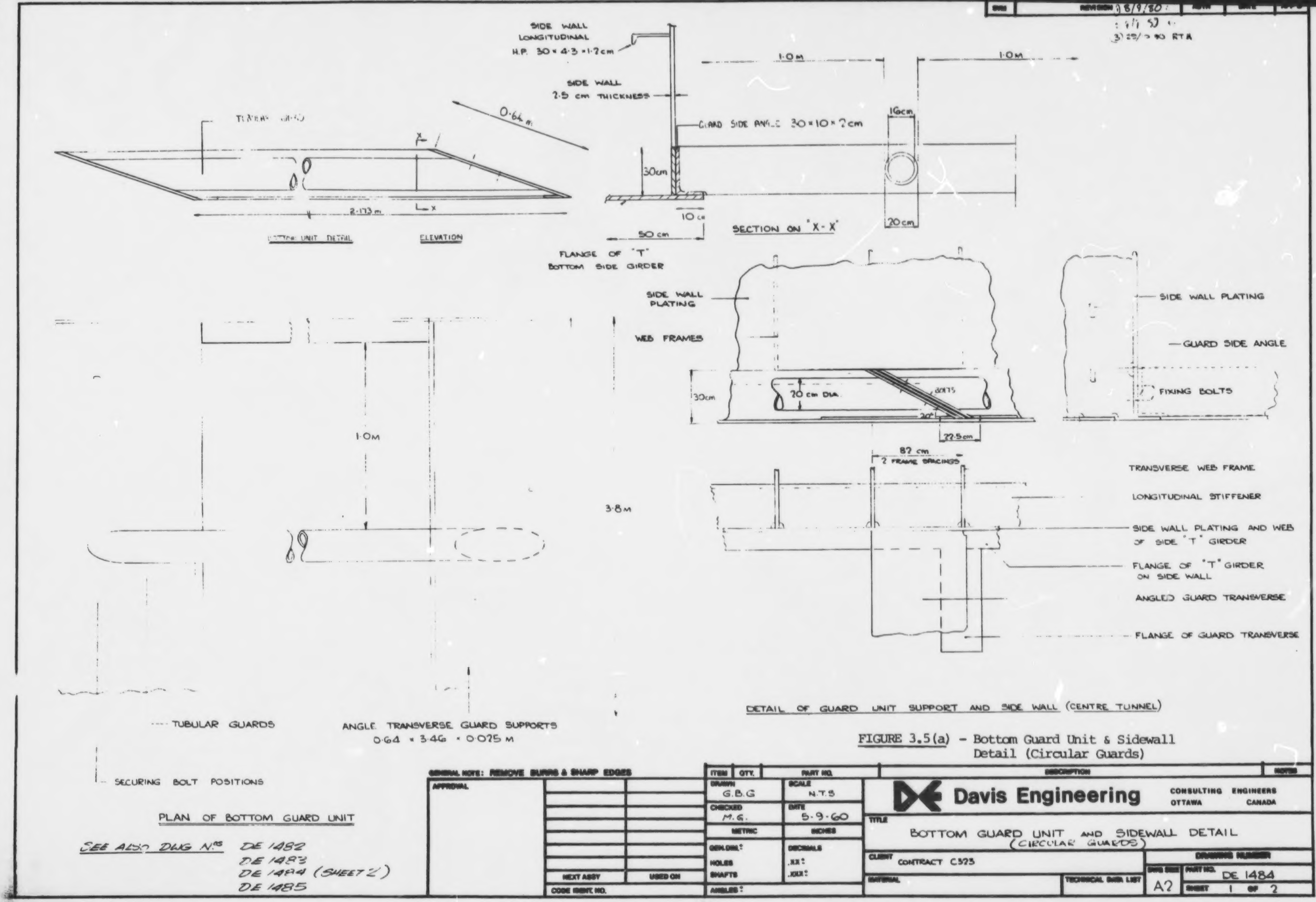
REVISION 1) 8/9/80
2) 4/1 83
3) 25/7 80 RTA
SIDE WALL LONGITUDINAL H.P. 30 × 4·3 × 1·2cm
SIDE WALL 2·5 cm THICKNESS
TUBULAR GUARD
0·64 m
X
X
2·173 m
BOTTOM UNIT DETAIL
ELEVATION
GUARD SIDE ANGLE 30 × 10 × 2cm
30cm
10 cm
50 cm
FLANGE OF "T" BOTTOM SIDE GIRDER
SECTION ON "X - X"
1·0 m
1·0 m
16cm
20cm
SIDE WALL PLATING
WEB FRAMES
30cm
20 cm DIA.
BOLTS
20°
22·5cm
SIDE WALL PLATING
GUARD SIDE ANGLE
FIXING BOLTS
87 cm
2 FRAME SPACINGS
TRANSVERSE WEB FRAME
LONGITUDINAL STIFFENER
SIDE WALL PLATING AND WEB OF SIDE "T" GIRDER
FLANGE OF "T" GIRDER ON SIDE WALL
ANGLED GUARD TRANSVERSE
FLANGE OF GUARD TRANSVERSE
DETAIL OF GUARD UNIT SUPPORT AND SIDE WALL (CENTRE TUNNEL)
1·0m
3·8m
TUBULAR GUARDS
ANGLE TRANSVERSE GUARD SUPPORTS 0·64 × 3·46 × 0·075 M
SECURING BOLT POSITIONS
PLAN OF BOTTOM GUARD UNIT
SEE ALSO DWG No'S DE 1482
DE 1483
DE 1484 (SHEET 2)
DE 1485
GENERAL NOTE: REMOVE BURRS & SHARP EDGES
APPROVAL
NEXT ASSY
USED ON
CODE IDENT. NO.
ITEM
QTY.
PART NO.
DESCRIPTION
NOTES
DRAWN G.B.G
SCALE N.T.S
CHECKED M.G.
DATE 5·9·60
METRIC
INCHES
GEN. DIM.:
HOLES
SHAFTS
ANGLES:
DECIMALS
.XX:
.XXX:
Davis Engineering
CONSULTING ENGINEERS
OTTAWA CANADA
TITLE BOTTOM GUARD UNIT AND SIDEWALL DETAIL (CIRCULAR GUARDS)
CLIENT CONTRACT C323
MATERIAL
TECHNICAL DATA LIST
DRAWING NUMBER
DWG SIZE A2
PART NO. DE 1484
SHEET 1 OF 2

FIGURE 3.5(a) - Bottom Guard Unit & Sidewall Detail (Circular Guards)

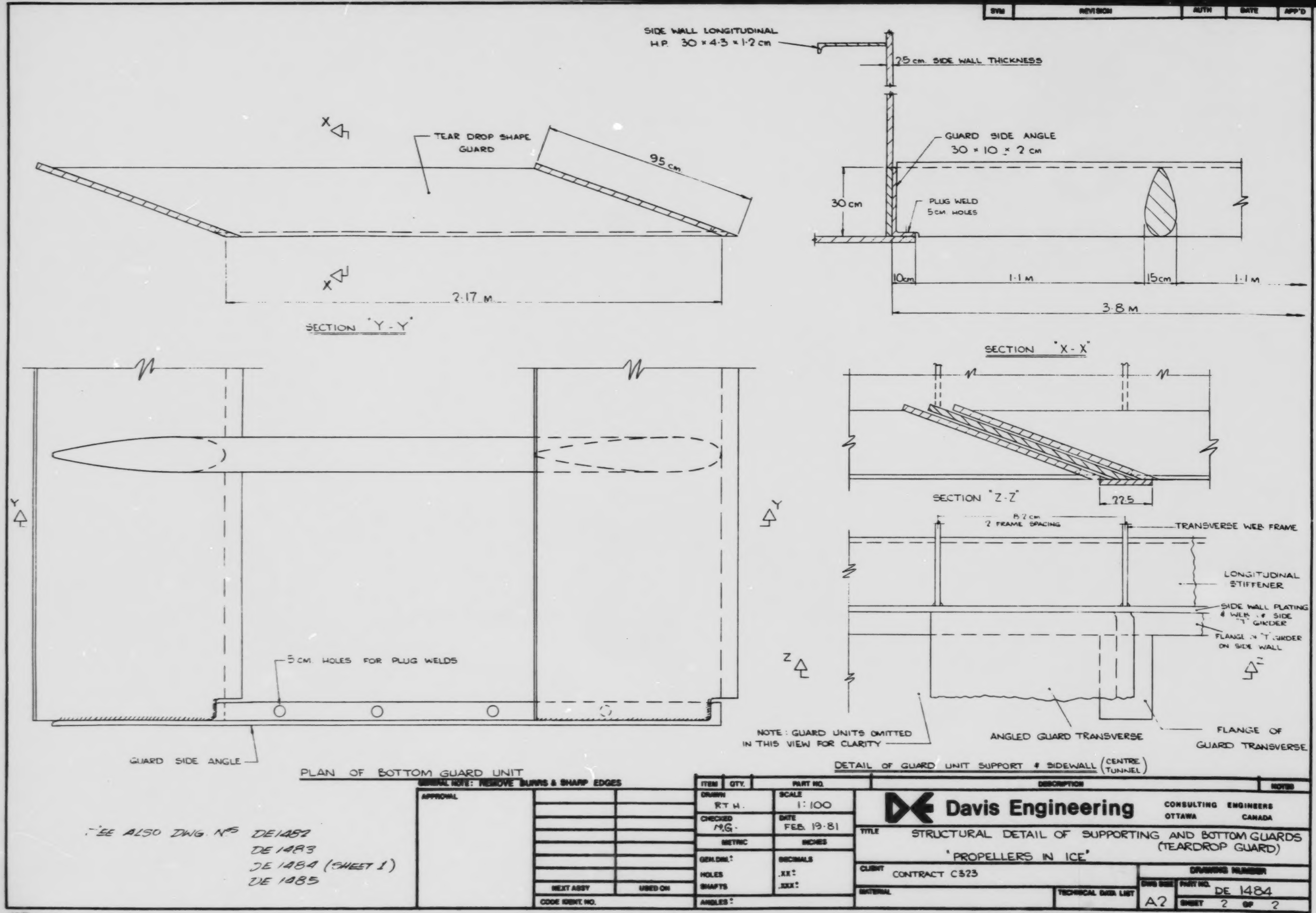
SYM
REVISION
AUTH
DATE
APP'D
SIDE WALL LONGITUDINAL
H.P. 30 × 4·3 × 1·2 cm
2.5 cm. SIDE WALL THICKNESS
GUARD SIDE ANGLE
30 × 10 × 2 cm
30 cm
PLUG WELD
5 cm HOLES
10cm
1·1 M
15cm
1·1 M
3·8 M
X
TEAR DROP SHAPE
GUARD
95 cm
X
2·17 M
SECTION "Y - Y"
SECTION "X - X"
SECTION "Z-Z"
22.5
8.2 cm
2 FRAME SPACING
TRANSVERSE WEB FRAME
LONGITUDINAL
STIFFENER
SIDE WALL PLATING
& WEB OF SIDE
"T" GIRDER
FLANGE OF "T" GIRDER
ON SIDE WALL
Y
Y
Z
Z
5 CM. HOLES FOR PLUG WELDS
NOTE: GUARD UNITS OMITTED
IN THIS VIEW FOR CLARITY
ANGLED GUARD TRANSVERSE
FLANGE OF
GUARD TRANSVERSE
GUARD SIDE ANGLE
PLAN OF BOTTOM GUARD UNIT
DETAIL OF GUARD UNIT SUPPORT & SIDEWALL (CENTRE TUNNEL)
GENERAL NOTE: REMOVE BURRS & SHARP EDGES
APPROVAL
NEXT ASSY
USED ON
CODE IDENT. NO.
ITEM
QTY.
PART NO.
DESCRIPTION
NOTES
DRAWN
RT H.
SCALE
1:100
CHECKED
M.G.
DATE
FEB. 19·81
METRIC
INCHES
GEN.DIM.:
DECIMALS
HOLES
.XX:
SHAFTS
.XXX:
ANGLES:
Davis Engineering
CONSULTING ENGINEERS
OTTAWA CANADA
TITLE
STRUCTURAL DETAIL OF SUPPORTING AND BOTTOM GUARDS
(TEARDROP GUARD)
'PROPELLERS IN ICE'
CLIENT
CONTRACT C323
MATERIAL
TECHNICAL DATA LIST
DRAWING NUMBER
DWG SIZE
A2
PART NO.
DE 1484
SHEET 2 OF 2
SEE ALSO DWG. Nos DE1482
DE 1483
DE 1484 (SHEET 1)
DE 1485

FIGURE 3.5(b) - Structural Detail of Supporting & Bottom Guards (Tear-drop)

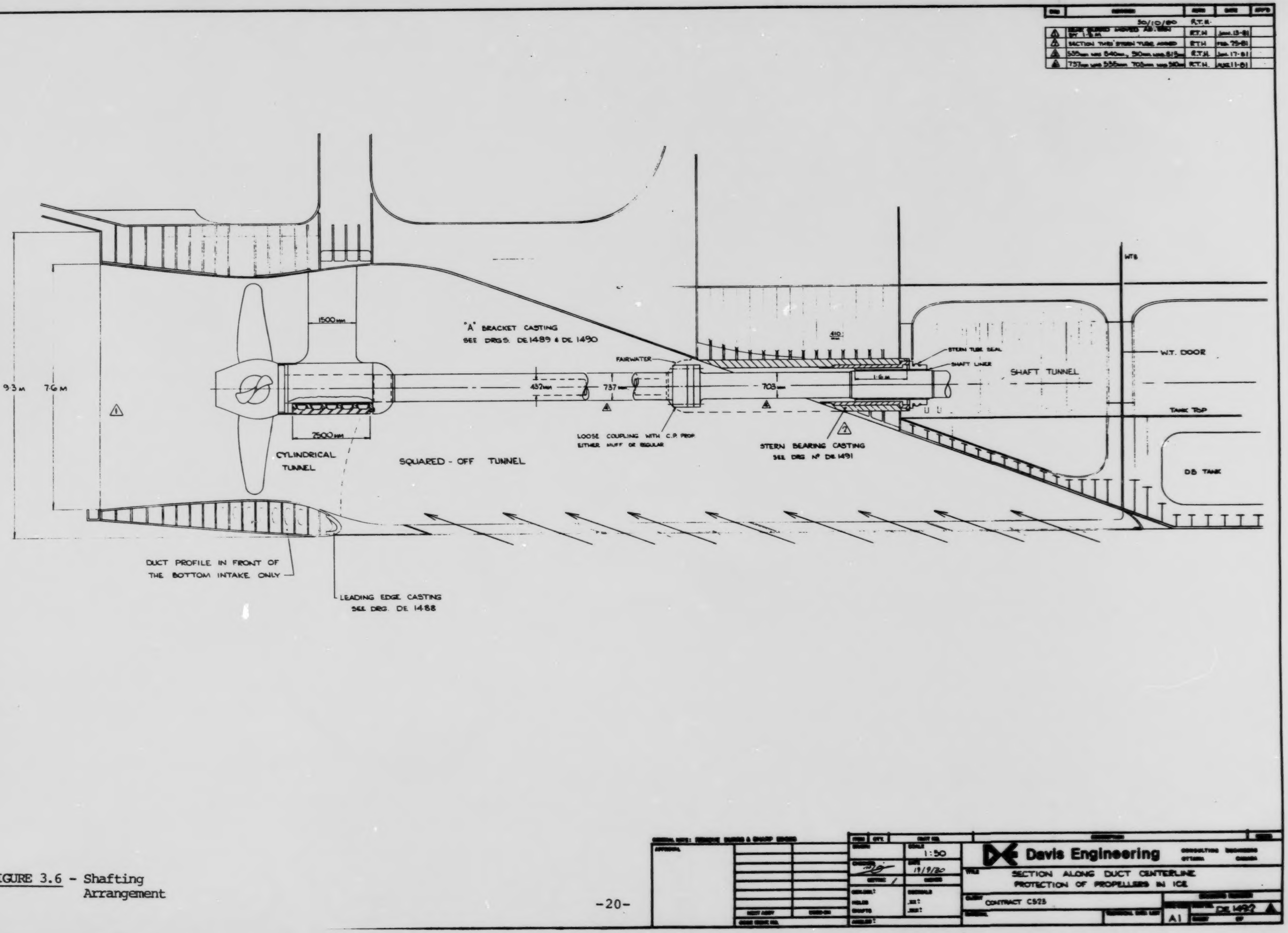

30/10/80 R.T.H.
SECTION THRU STERN TUBE ADDED R.T.H FEB. 25-81
535mm was 540mm, 510mm was 815mm R.T.H. Jan. 17-81
737mm was 535mm 703mm was 510mm R.T.H. AUG 11-81
R.T.H Jan. 13-81
9.3 M
7.6 M
1500 mm
2500 mm
"A" BRACKET CASTING
SEE DRGS. DE 1489 & DE 1490
FAIRWATER
432 mm
737 mm
703 mm
1.6 M
410
STERN TUBE SEAL
SHAFT LINER
SHAFT TUNNEL
WTB
W.T. DOOR
TANK TOP
DB TANK
LOOSE COUPLING WITH C.P. PROP
EITHER MUFF OR REGULAR
STERN BEARING CASTING
SEE DRG Nº DE 1491
CYLINDRICAL
TUNNEL
SQUARED - OFF TUNNEL
DUCT PROFILE IN FRONT OF
THE BOTTOM INTAKE ONLY
LEADING EDGE CASTING
SEE DRG. DE 1488
1:50
19/9/80
Davis Engineering
SECTION ALONG DUCT CENTERLINE
PROTECTION OF PROPELLERS IN ICE
CONTRACT C523
A1
DE 1492

FIGURE 3.6 - Shafting Arrangement

REV	REVISION	AUTH	DATE	APP'D

CONSTRUCTION SEQUENCE OF STERN UNIT

1. ALIGN AND LAY UP CAST DUCT LEADING EDGES
2. LAY UP SIDE WALL BOTTOM PLATING (KEEL PLATES) (4 OFF)
3. BUILD UP SIDE WALLS INCLUDING TRANSVERSE WEBS AND LONGITUDINAL STIFFENERS
4. COMPLETE DUCT PLATING
5. POSITION 'A' BRACKET AND WELD TO TRANSVERSE WEBS AND SIDE SHELL PLATING
6. LAY UP TRANSVERSE FRAMES - WELD TO 'A' BRACKETS
7. POSITION STERN FRAME CASTING
8. WELD STERN FRAME TO TRANSVERSE FRAMING AND 'A' BRACKETS
9. POSITION CAST STERN BEARING
10. WELD STERN BEARING TO STERN FRAMES, LONGITUDINALS AND DEEP FLOORS
11. COMPLETE FRAMING AND STRINGERS.
12. CONTINUE IN NORMAL SEQUENCE UNTIL UNIT IS COMPLETE.

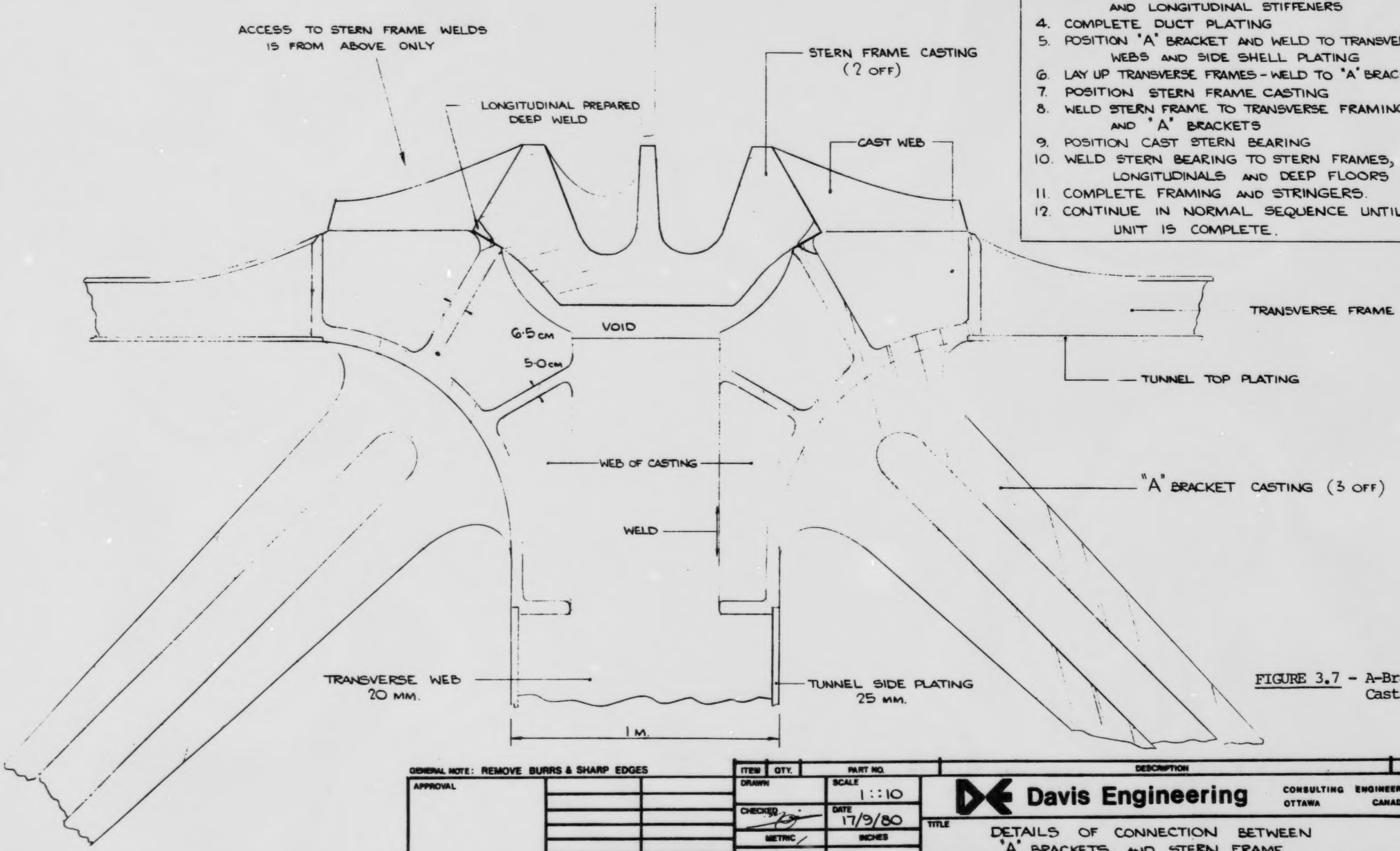
ACCESS TO STERN FRAME WELDS IS FROM ABOVE ONLY
LONGITUDINAL PREPARED DEEP WELD
STERN FRAME CASTING (2 OFF)
CAST WEB
TRANSVERSE FRAME
TUNNEL TOP PLATING
6·5 CM
5·0 CM
VOID
WEB OF CASTING
WELD
"A" BRACKET CASTING (3 OFF)
TRANSVERSE WEB 20 MM.
TUNNEL SIDE PLATING 25 MM.
1 M.

FIGURE 3.7 - A-Bracket Casting

SEE ALSO DWG. Nº DE 1489

GENERAL NOTE: REMOVE BURRS & SHARP EDGES		ITEM	QTY.	PART NO.
APPROVAL		DRAWN	SCALE 1::10	
		CHECKED	DATE 17/9/80	
		METRIC ✓	INCHES	
		GEN.DIM.:	DECIMALS .XX:	
		HOLES	.XXX:	
NEXT ASSY	USED ON	SHAFTS		
CODE IDENT. NO.		ANGLES:		

DESCRIPTION | NOTES

Davis Engineering
CONSULTING ENGINEERS
OTTAWA CANADA

TITLE DETAILS OF CONNECTION BETWEEN 'A' BRACKETS AND STERN FRAME

CLIENT CONTRACT C323

MATERIAL

TECHNICAL DATA LIST

DRAWING NUMBER
DWG SIZE A2
PART NO. DE 1490
SHEET 1 OF 1

SYM | REVISION | AUTH | DATE | APP'D

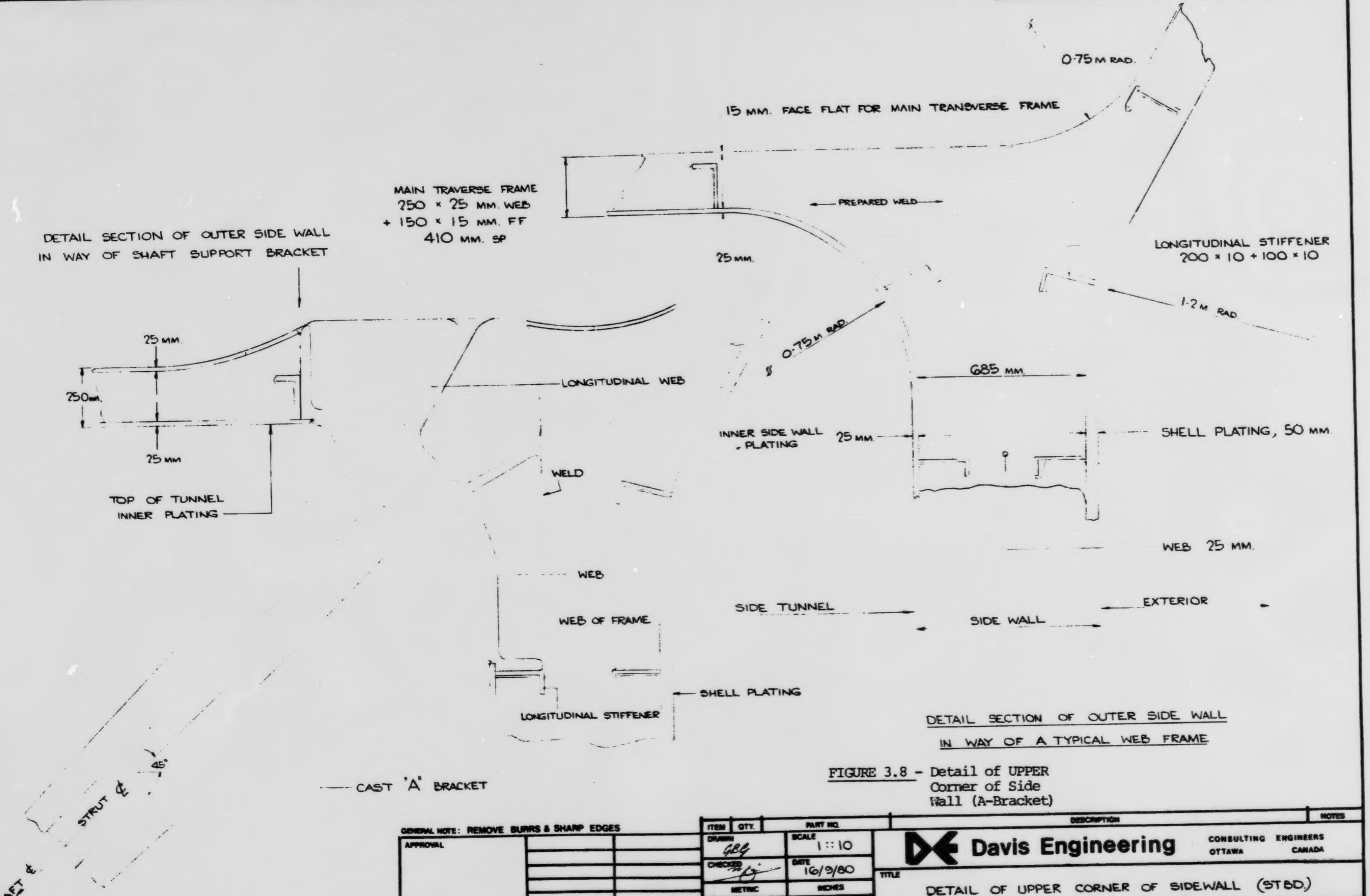
0·75 M RAD.
15 MM. FACE FLAT FOR MAIN TRANSVERSE FRAME
MAIN TRAVERSE FRAME
250 × 25 MM. WEB
+ 150 × 15 MM. FF
410 MM. SP
PREPARED WELD
DETAIL SECTION OF OUTER SIDE WALL
IN WAY OF SHAFT SUPPORT BRACKET
25 MM.
LONGITUDINAL STIFFENER
200 × 10 + 100 × 10
1·2 M RAD
25 MM.
0·75 M RAD
250 MM.
LONGITUDINAL WEB
685 MM.
INNER SIDE WALL
PLATING
25 MM.
SHELL PLATING, 50 MM.
25 MM
WELD
TOP OF TUNNEL
INNER PLATING
WEB 25 MM.
WEB
WEB OF FRAME
SIDE TUNNEL
SIDE WALL
EXTERIOR
SHELL PLATING
LONGITUDINAL STIFFENER
45°
CAST 'A' BRACKET
STRUT ℄
TO SHAFT ℄

DETAIL SECTION OF OUTER SIDE WALL
IN WAY OF A TYPICAL WEB FRAME

FIGURE 3.8 - Detail of UPPER Corner of Side Wall (A-Bracket)

SEE ALSO DWG. # DE1490

GENERAL NOTE: REMOVE BURRS & SHARP EDGES

APPROVAL

NEXT ASSY | USED ON

CODE IDENT. NO.

ITEM | QTY. | PART NO. | DESCRIPTION | NOTES

DRAWN GBG
SCALE 1 :: 10
CHECKED
DATE 16/9/80
METRIC | INCHES
GEN. DIM. ±
DECIMALS .XX ± .XXX ±
HOLES
SHAFTS
ANGLES ±

Davis Engineering CONSULTING ENGINEERS OTTAWA CANADA

TITLE DETAIL OF UPPER CORNER OF SIDEWALL (STBD)

CLIENT CONTRACT C323

MATERIAL

TECHNICAL DATA LIST

DRAWING NUMBER
DWG SIZE A2
PART NO. DE 1489
SHEET 1 OF 1

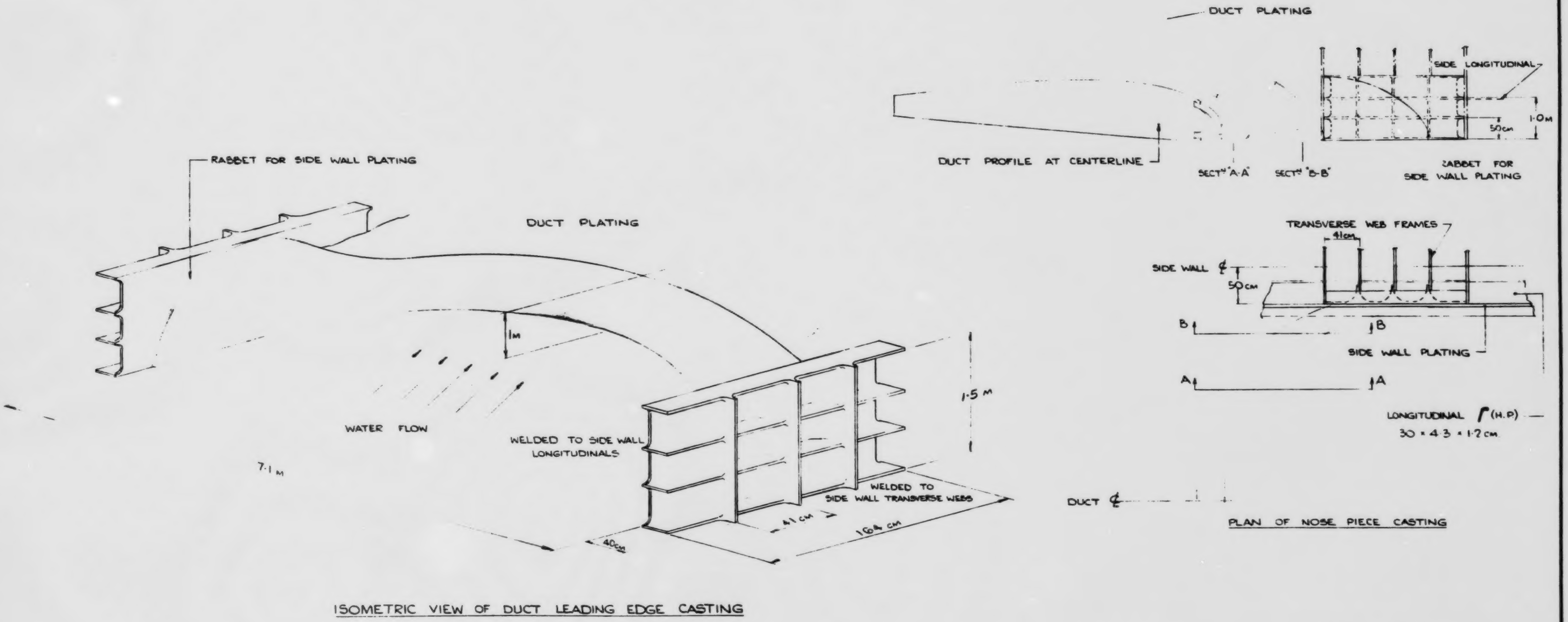
DUCT PLATING
SIDE LONGITUDINAL
1·0M
50cm
DUCT PROFILE AT CENTERLINE
SECTN "A-A"
SECTN "B-B"
RABBET FOR SIDE WALL PLATING
TRANSVERSE WEB FRAMES
41cm
SIDE WALL ℄
50cm
B
B
SIDE WALL PLATING
A
A
LONGITUDINAL Γ (H.P)
30 × 4·3 × 1·2cm
DUCT ℄
PLAN OF NOSE PIECE CASTING
RABBET FOR SIDE WALL PLATING
DUCT PLATING
1M
1·5 M
WATER FLOW
WELDED TO SIDE WALL LONGITUDINALS
WELDED TO SIDE WALL TRANSVERSE WEBS
7·1 M
41 cm
164 cm
40cm
ISOMETRIC VIEW OF DUCT LEADING EDGE CASTING

NOTE: BUILDING OF STERN UNIT OF SHIP SHOULD COMMENCE WITH THESE CASTINGS (3-OFF)

FIGURE 3.9 - Circular Duct Section (Duct L.E. Casting)

GENERAL NOTE: REMOVE BURRS & SHARP EDGES

ITEM	QTY.	PART NO.	DESCRIPTION	NOTES

APPROVAL

NEXT ASSY | USED ON

CODE IDENT. NO.

DRAWN G.B.G.

SCALE 1:100

CHECKED

DATE 12-9-80

METRIC | INCHES

GEN.DIM.:

DECIMALS

HOLES

.XX:

SHAFTS

.XXX:

ANGLES:

Davis Engineering
CONSULTING ENGINEERS
OTTAWA CANADA

TITLE GENERAL VIEW OF DUCT LEADING EDGE CASTING
PROTECTION OF PROPELLERS IN ICE

CLIENT CONTRACT C323

MATERIAL

TECHNICAL DATA LIST

DRAWING NUMBER

DWG SIZE A2

PART NO. DE 1488

SHEET 1 OF 1

29.10.80	R.T.H.		
3	3 POSSIBLE ARRANGEMENTS FOR BOTTOM GUARD SHOWN	R.T.H	FEB.16-81

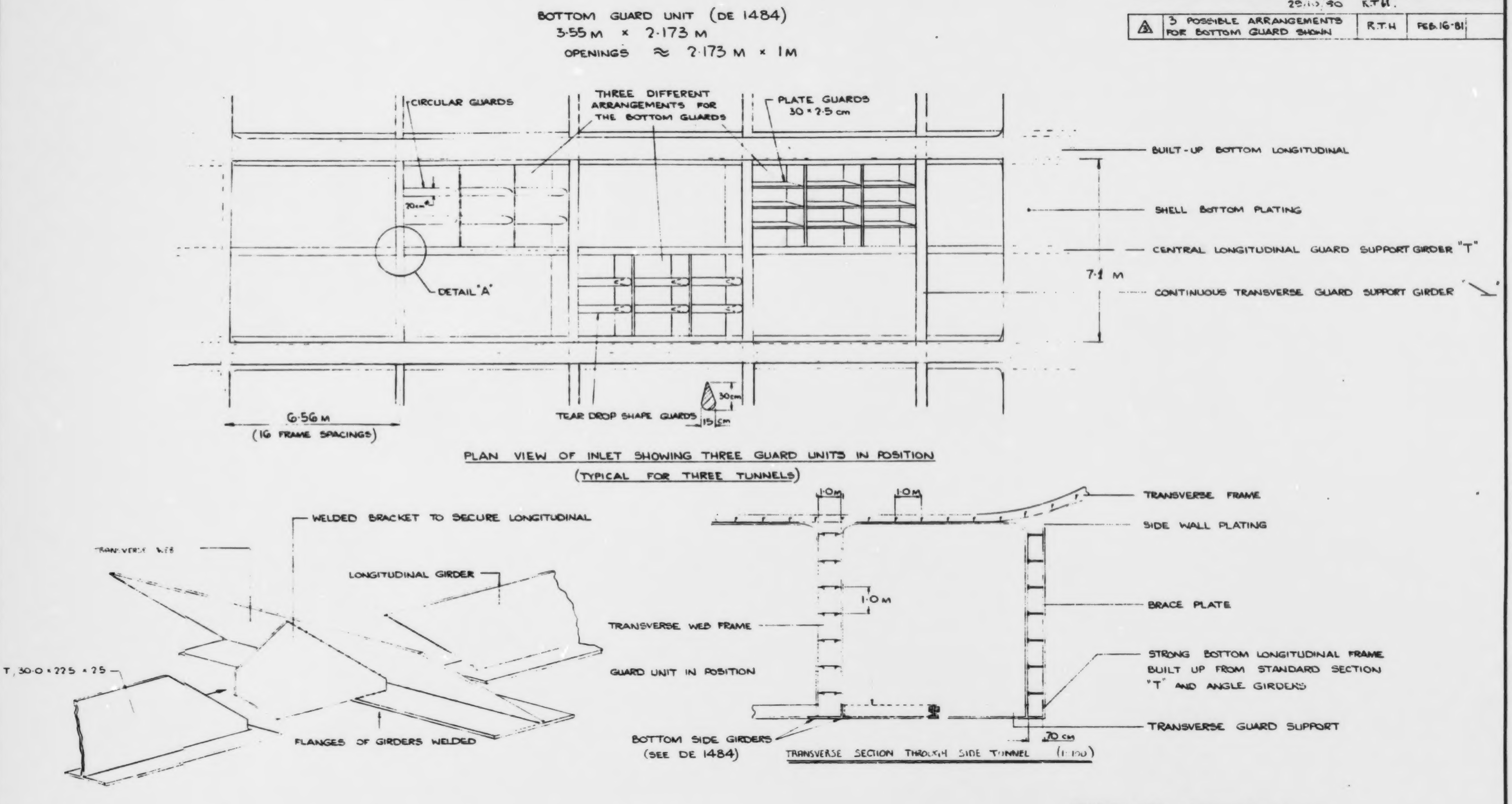
BOTTOM GUARD UNIT (DE 1484)
3.55 M × 2.173 M
OPENINGS ≈ 2.173 M × 1 M
CIRCULAR GUARDS
THREE DIFFERENT ARRANGEMENTS FOR THE BOTTOM GUARDS
PLATE GUARDS 30 × 2.5 cm
20 cm
DETAIL 'A'
BUILT-UP BOTTOM LONGITUDINAL
SHELL BOTTOM PLATING
CENTRAL LONGITUDINAL GUARD SUPPORT GIRDER "T"
7.1 M
CONTINUOUS TRANSVERSE GUARD SUPPORT GIRDER
30 cm
15 cm
TEAR DROP SHAPE GUARDS
6.56 M
(16 FRAME SPACINGS)
PLAN VIEW OF INLET SHOWING THREE GUARD UNITS IN POSITION
(TYPICAL FOR THREE TUNNELS)
WELDED BRACKET TO SECURE LONGITUDINAL
TRANSVERSE WEB
LONGITUDINAL GIRDER
T, 30.0 × 22.5 × 2.5
FLANGES OF GIRDERS WELDED
1.0 M
1.0 M
TRANSVERSE FRAME
SIDE WALL PLATING
1.0 M
BRACE PLATE
TRANSVERSE WEB FRAME
GUARD UNIT IN POSITION
STRONG BOTTOM LONGITUDINAL FRAME BUILT UP FROM STANDARD SECTION "T" AND ANGLE GIRDERS
BOTTOM SIDE GIRDERS (SEE DE 1484)
TRANSVERSE GUARD SUPPORT
70 cm
TRANSVERSE SECTION THROUGH SIDE TUNNEL (1:100)
DETAIL 'A' — ISOMETRIC VIEW OF LONGITUDINAL/TRANSVERSE CONNECTION (N.T.S.)

FIGURE 3.10 - Supporting Frame for Guards

GENERAL NOTE: REMOVE BURRS & SHARP EDGES

DRAWN	G.B.G.
SCALE	1:100
CHECKED	M.G.
DATE	2-9-80

Davis Engineering CONSULTING ENGINEERS OTTAWA CANADA

TITLE STRUCTURAL DETAIL OF SUPPORTING FRAME FOR GUARD UNITS

CLIENT CONTRACT C323

DWG SIZE A2 PART NO. DE 1482 3

SHEET 1 OF 1

SEE ALSO DWG Nos DE 1483
DE 1484 (2 SHEETS)
DE 1485

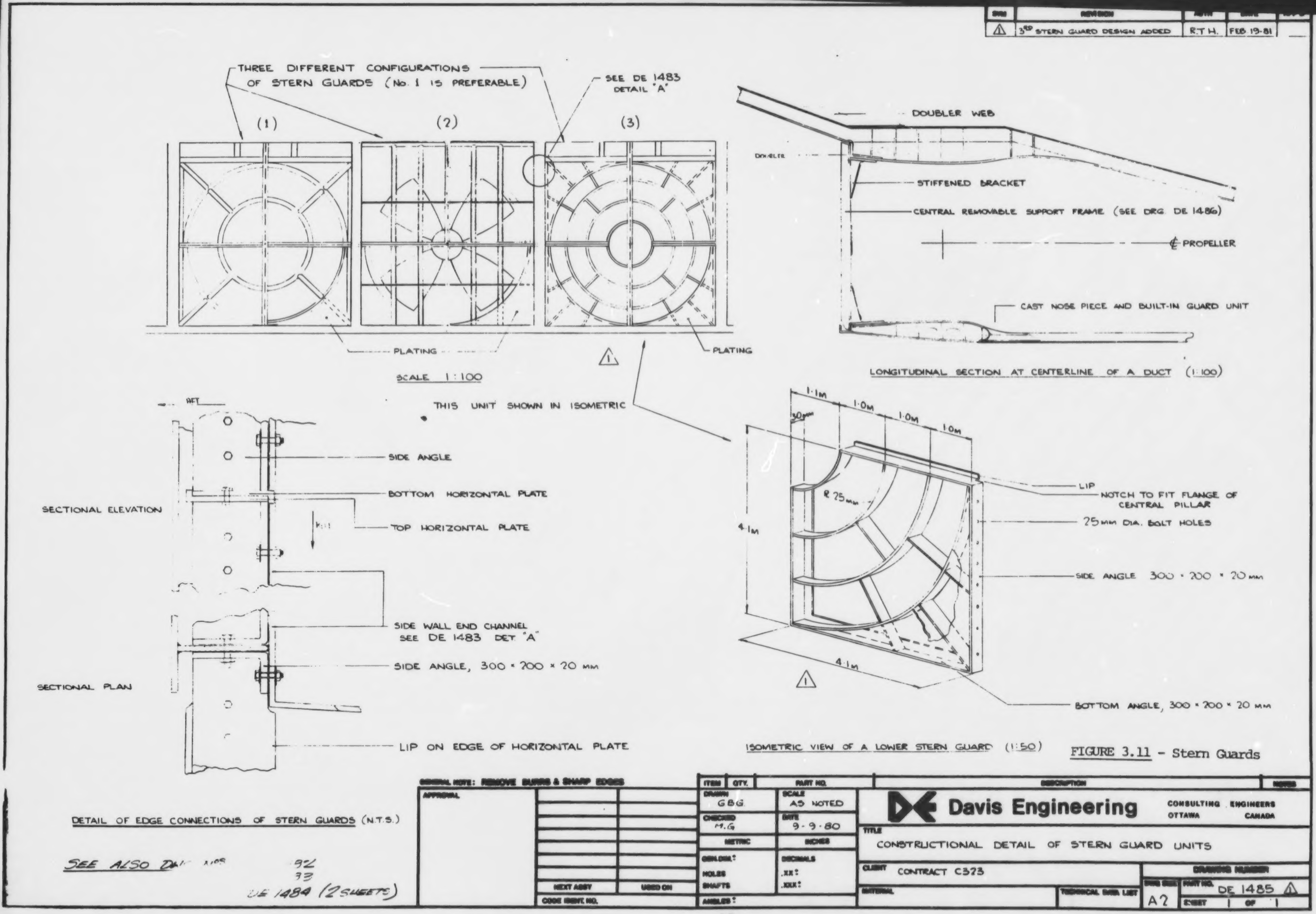
REVISION
1 3RD STERN GUARD DESIGN ADDED R.T.H. FEB 19-81
THREE DIFFERENT CONFIGURATIONS OF STERN GUARDS (No. 1 IS PREFERABLE)
SEE DE 1483 DETAIL 'A'
(1)
(2)
(3)
PLATING
PLATING
SCALE 1:100
DOUBLER WEB
DOUBLER
STIFFENED BRACKET
CENTRAL REMOVABLE SUPPORT FRAME (SEE DRG DE 1486)
℄ PROPELLER
CAST NOSE PIECE AND BUILT-IN GUARD UNIT
LONGITUDINAL SECTION AT CENTERLINE OF A DUCT (1:100)
AFT
THIS UNIT SHOWN IN ISOMETRIC
SIDE ANGLE
BOTTOM HORIZONTAL PLATE
SECTIONAL ELEVATION
TOP HORIZONTAL PLATE
SIDE WALL END CHANNEL SEE DE 1483 DET 'A'
SIDE ANGLE, 300 × 200 × 20 MM
SECTIONAL PLAN
LIP ON EDGE OF HORIZONTAL PLATE
DETAIL OF EDGE CONNECTIONS OF STERN GUARDS (N.T.S.)
SEE ALSO DA[illegible] NOS 92
93
DE 1484 (2 SHEETS)
1.1M
1.0M
1.0M
1.0M
30MM
R 25MM
4.1M
4.1M
LIP
NOTCH TO FIT FLANGE OF CENTRAL PILLAR
25MM DIA. BOLT HOLES
SIDE ANGLE 300 × 200 × 20 MM
BOTTOM ANGLE, 300 × 200 × 20 MM
ISOMETRIC VIEW OF A LOWER STERN GUARD (1:50)
GENERAL NOTE: REMOVE BURRS & SHARP EDGES
APPROVAL
NEXT ASSY
USED ON
CODE IDENT. NO.
ITEM
QTY.
PART NO.
DESCRIPTION
NOTES
DRAWN GBG
SCALE AS NOTED
CHECKED M.G
DATE 9-9-80
METRIC
INCHES
GEN.DIM.±
DECIMALS
HOLES
.XX±
SHAFTS
.XXX±
ANGLES±
Davis Engineering
CONSULTING ENGINEERS
OTTAWA CANADA
TITLE
CONSTRUCTIONAL DETAIL OF STERN GUARD UNITS
CLIENT CONTRACT C373
MATERIAL
TECHNICAL DATA LIST
DRAWING NUMBER
DWG SIZE A2
PART NO. DE 1485
SHEET 1 OF 1

FIGURE 3.11 - Stern Guards

SYM	REVISION	AUTH	DATE	APP'D
△1	RUDDER SIZE REDUCED. STRUT BEARING SHORTENED	R.T.H.	FEB.17-81	
△2	GENERAL REVISION -STRUT BEARING	R.T.H	FEB.26-81	
△3	SECTIONS "X-X","Y-Y" & "Z-Z" ADDED	R.T.H.	MAR.26-81	

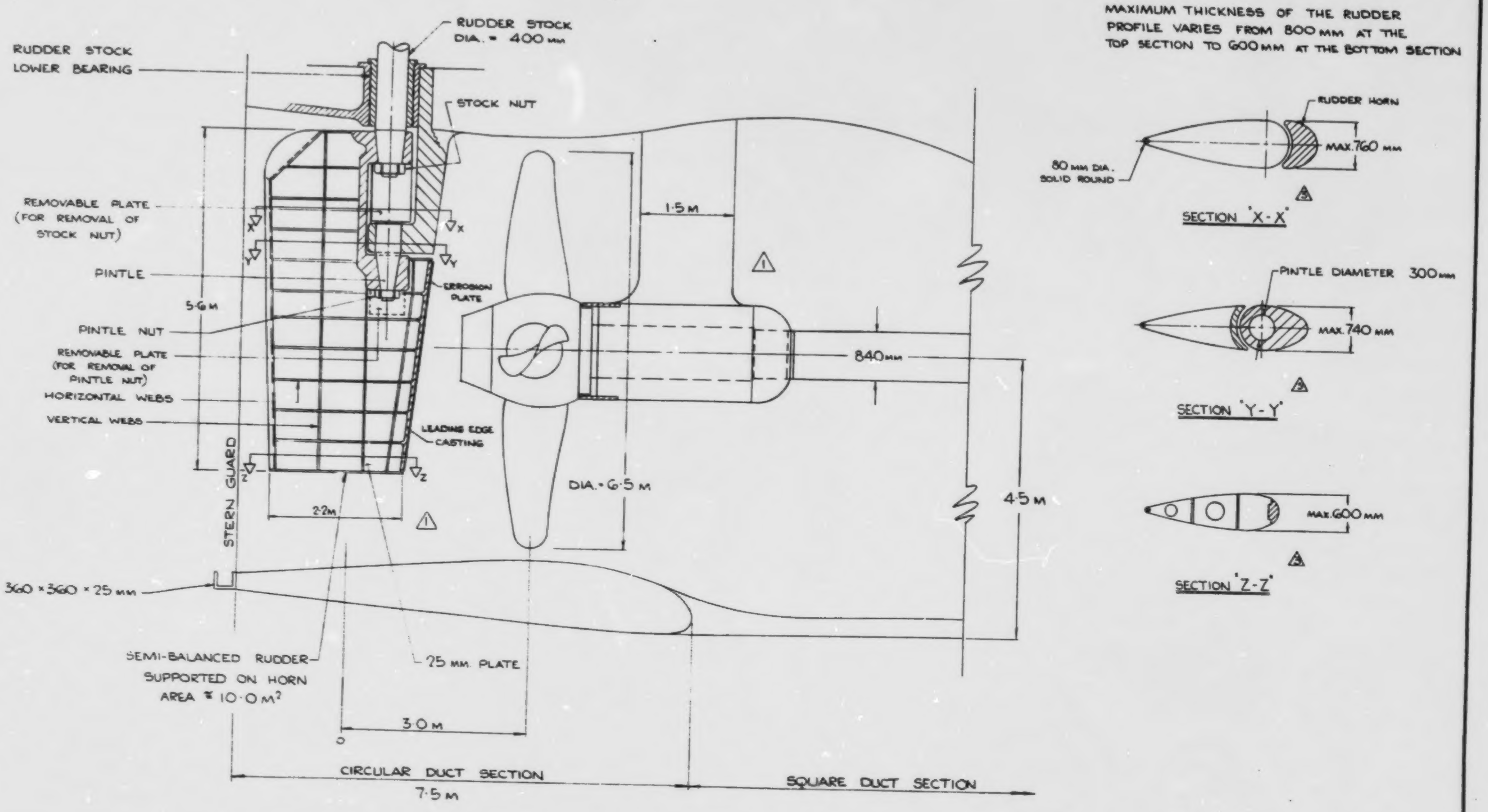
MAXIMUM THICKNESS OF THE RUDDER PROFILE VARIES FROM 800 MM AT THE TOP SECTION TO 600 MM AT THE BOTTOM SECTION
RUDDER STOCK DIA. = 400 MM
RUDDER STOCK LOWER BEARING
STOCK NUT
REMOVABLE PLATE (FOR REMOVAL OF STOCK NUT)
PINTLE
5·6 M
PINTLE NUT
REMOVABLE PLATE (FOR REMOVAL OF PINTLE NUT)
HORIZONTAL WEBS
VERTICAL WEBS
EROSION PLATE
LEADING EDGE CASTING
X
Y
Z
STERN GUARD
2·2 M
△1
1·5 M
840 MM
DIA. = 6·5 M
4·5 M
360 × 360 × 25 MM
SEMI-BALANCED RUDDER SUPPORTED ON HORN AREA ≅ 10·0 M²
25 MM PLATE
3·0 M
CIRCULAR DUCT SECTION
7·5 M
SQUARE DUCT SECTION
RUDDER HORN
80 MM DIA. SOLID ROUND
MAX. 760 MM
△3
SECTION 'X-X'
PINTLE DIAMETER 300 MM
MAX. 740 MM
SECTION 'Y-Y'
MAX. 600 MM
SECTION 'Z-Z'

FIGURE 3.12 - Rudder Arrangement

GENERAL NOTE: REMOVE BURRS & SHARP EDGES
APPROVAL
NEXT ASSY
USED ON
CODE IDENT. NO.
ITEM
QTY.
PART NO.
DRAWN R.T. H.
SCALE 1:50
CHECKED
DATE JAN. 8-81
METRIC
INCHES
GEN.DIM.±
HOLES
SHAFTS
ANGLES ±
DECIMALS
.XX ±
.XXX ±
DESCRIPTION
NOTES
Davis Engineering
CONSULTING ENGINEERS
OTTAWA CANADA
TITLE RUDDER ARRANGEMENT (SINGLE PINTLE)
PROTECTION OF PROPELLERS IN ICE
CLIENT CONTRACT C323
MATERIAL
TECHNICAL DATA LIST
DRAWING NUMBER
DWG SIZE A2
PART NO. DE 1495 △3
SHEET 1 OF 1

Some of the design features and criteria of the proposed hull for the triple screw case are highlighted below.

*Framespacing: The minimum spacing was established at 410 mm (16 inches) in order to provide accessibility for welding either in prefabrication or in situ. Web frames were located on every second frame. Longitudinal framing in the double bottom spaced about 900 mm apart, mainly for accessibility in making repairs within the double bottom.

*Framing: Mixed framing was used but mainly transverse. The bow and stern structures were transversely framed. This allows the hull some flexibility in the longitudinal direction.

*Tunnel Shape: The one-dimensional flow analysis for an in-hull propulsion system was shown in Appendix A, Volume 1. The performance of the in-hull propulsion system was shown to be influenced by the tunnel slope θ. However, requirements such as: length of the tunnel circular/section, fitment of the squared-off transom, the intake area in relation to the propeller disk area, bottom guards and supporting frames, overall length, etc., affected the choice of the tunnel slope θ. The tunnel slope was taken as 20 degrees which allows a bottom intake open area (corrected for the blockage of the guards) of about 4 - 5 times the propeller disk area and a tunnel circular section of about 7.5 m long to allow for the rudder to be fitted behind the propeller.

*Strut: Two options were considered for the location of the strut; viz., forward or aft of the propeller. In placing the strut aft, the strut would benefit from the high jet stream by converting some of the lost energy to useful thrust. Due to the difficulties however, of installing and removing the propeller with the strut aft, it was decided to locate the strut in the forward position.

*Bottom Guards: A number of options were considered with regard to both the configuration and method of manufacture for the bottom guards. Shapes such as fish tail, flat scoop, circular and tear-drop section were among those configurations. Bearing in mind the frictional and drag losses of these guards and assuming that the flow is more or less unidirectional at the bottom intake, it was decided to adapt the tear-drop like section for testing at this stage. The circular configuration may be tested and compared with the tear-drop section to determine the effect of the shape on the overall performance.

With regard to the method of manufacture, it was decided to build the bottom guards in units, each of about 3 x 6 meters in a box type frame which then could be welded to the longitudinal and transverse bottom supporting structure. Additional transverse members were also used to reduce the effective length of the bottom guards. This resulted in a mesh structure with openings of about 1 m x 2 m which would allow a piece of ice of about "3 ft." in two dimensions to pass through.

The main advantage of constructing the bottom guards in units is considered to be easy handling during assembly and the replacement in case of damage. Whether to cast or fabricate the bottom guard units was also considered. Some inquiries were made with leading steel casting suppliers for their recommendations. All indicated that casting of such units would not be practical and most uneconomical. The only way to produce them in a foundary would be to cast the side sections, weld together and then weld-in the guards; a process which is in reality fabrication. Therefore, the general recommendation for the manufacture of these guard units is steel fabrication. The material could be carbon steel A36 for the side sections and A53 for the guards (rolled section).

The strength calculation for the bottom guards was based on a localized high impact loading. The worst case is when a large fragment of ice at a higher velocity than the ship, hits the guard system and the impact load is carried by just one member of the grillage. If we assume a piece of (broken) ice has a dimension in three directions equivalent to that of the representative ice thickness (say about 2 meters), then the weight of this piece of ice is about 8000 kg. Now, based on observations made earlier on ice flow around model icebreakers, the induced velocities seem to cause the broken ice to move much faster than the ship.

If one assumes that the continuous icebreaking speed is about 4 knots, then it is reasonable to assume that the broken ice attains a speed of about 6 knots by the time it reaches the bottom grill. Assuming also that the acceleration is uniform, and the ice piece travels about 190 meters (which is the approximate distance between the bow and the centre of the bottom intake) in 60 seconds, then the impact load can be derived from Newton's second law as follows:

$$\text{Force} = m \; \frac{dv}{dt}$$

with the acceleration $\frac{dv}{dt} = \frac{6 - 4}{60} * 0.5144 = 0.017 \text{ m/sec}^2$

$$\text{Impact force} = \frac{8000}{9.81} * 0.017$$

$$\cong 14 \text{ kg.}$$

If the ice pieces are following the streamlines, then the impact load is in fact directed at an angle to the horizontal equal to that of the tunnel deflected flow, which is about 20°. Therefore

$$\text{Impact load} = 14 \times \sin 20$$

$$= 4.78 \text{ kg.}$$

The impact load is quite low as one would expect due to the low acceleration and low speeds. Another approach can be followed to estimate the impact load by writing Newton's second law in its original form

$$F \; \Delta \; T = \Delta(mv)$$

where F = external force, ΔT = time interval during which "F" acts, and $\Delta(mv)$ = change of momentum of the system.

Then: Force per unit time = $\Delta(mv)$

$$= \frac{8000}{9.81} * 6 * 0.5144 * \sin 20$$

Force (impact load) = 860.8 kg./unit time

This force can be applied as a static load to design the bottom guards.

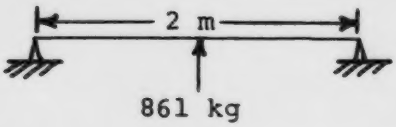

For simply supported case

$$\sigma = \frac{MY}{I}, \quad M_{\text{max.}} = 430.5 \text{ kg. m}$$

$$\sigma = \text{allowable tensile strength}$$
$$\cong 4.7 \times 10^7 \text{ kg./m}^2$$

$$\text{minimum section modulus} = \frac{M}{\sigma}$$

$$= \frac{430.5}{4.7 \times 10^7} \times 10^6 \text{ cm}^3$$

$$= 92 \text{ cm}^3$$

A hollow tubular section of 200 mm O.D. and 150 mm I.D. and a tear-drop-like section of 300 mm x 150 mm provide section moduli of 537 cm^3 and 714 cm^3 respectively.

* Duct Shape: The tunnel consists of two sections; the square section and the circular duct section. The bottom sector of the duct resembles the profile of NSMB duct 1917 at the centreline. The leading edge thickness increases with increasing distance from the duct centreline. The outer surface of the bottom sectors was made flat to coincide with the horizontal plane of the bottom intake. The general view of the leading edge casting is shown in Figure 3.9 (DE 1488). The overall length of the circular duct section is about 7.5 meters with the centreline of the propeller at about 2.7 meters abaft the duct leading edge.

The idea behind this shape of the duct is to accelerate the flow at the propeller disk, and to create an additional net forward thrust by the duct bottom sector. As a result, more thrust is achieved for a given total power or for a required total thrust, the heavily loaded propeller is unloaded.

* Stern Guards: The general criteria considered for the design of the bottom guards were also considered for the stern guards. The latter, however, are subjected to less severe loading than the bottom guards unless, of course, the ship is moving astern in solid ice.

The stern guards would have to be removable for the installation/removal of the rudder and propeller. In order to provide extra strength for the stern guards, a vertical removable supporting member was installed.

Three different configurations of stern guards were investigated; viz. circular tubular guards (configuration (1)), arrangement similar to that of the bottom guards (configuration (2)), and circular flat plate guards (configuration (3)). They are shown in Figure 3.11 (DE 1485). Configuration 3 was considered as the best compromise among the three configurations. It is simpler to manufacture compared with arrangement 1, and does not result in small peripheral areas (pocket areas) compared with arrangement 2.

The stern guards are built in four units with "lips" on the edge of the horizontal plates of each unit as shown in drawing no. DE1485. The recommendation with regard to fabrication for the bottom guard units would also apply to the stern guard units. Each unit is about 4.1 x 4.1 meters in a box type frame which then could be bolted rigidly to the vertical walls (side skirts) and horizontal channels at the tunnel exit. (See drawing nos. DE1483 - Figure 3.4). Frictional and drag losses for a successful stern guard design must be kept to a minimum, and can be arrived at by model testing of different configurations and shapes.

Consideration was given to the possibility of installing a bearing aft of the propeller and using the structure of the bottom half of the stern guards for support. However, with the development of the in-hull rudder arrangement, the idea was abandoned.

Finally, an important criterion was considered carefully in the design of the stern guards; this is with regard to the openings between the guards in comparison to that of the bottom intake. Smaller areas would result in ice pieces being accumulated inside the tunnel behind the propeller, whereas larger areas would result in trapping ice pieces inside the tunnel and on the top of the bottom guards in astern operations and consequently clogging the bottom intake. A compromise was made which resulted in the configuration shown in Figure 3.11.

4.0 PROPELLERS FOR POLAR7A - DESIGN & PERFORMANCE

The design of a standard series propeller for a normal type of ship is by no means difficult. Design charts and cavitation diagrams are available which are based on extensive open water testing of parametric series carried out in a number of experimental establishments pioneered by the NSMB. By using these charts the propeller can be designed to absorb a given delivered horsepower at a given speed of advance, to run at a stipulated rate of revolution or at a rate of rotation selected from a stipulated range of values. If the rate of rotation is specified then the diameter can be chosen to correspond to the advance coefficient at which the screw efficiency is the maximum, i.e., the optimum diameter can be chosen; providing that its value is not greater than that determined by aperture size. Alternatively, if the screw diameter is specified, then the rate of rotation is selected within the stipulated range so that its value corresponds to the advance coefficient at which the propeller efficiency is maximum, i.e., the optimum rate of rotation can be chosen.

The difficulty of the procedure increases exponentially with the difficulty of the intended operating conditions of the ship, i.e., with the special requirements which the propulsion system should maintain. In such cases, the propeller is specially designed to suit specified requirements and its predicted performance needs to be substantiated experimentally by open water and self-propulsion tests. Propellers for icebreakers are of particular interest in the present investigation. The overall performance of an icebreaker depends to a great extent on the propeller characteristics in not only design but off-design conditions.

The ability of the propeller to produce sufficient thrust at relatively low speeds is of prime importance. The mission profile of an icebreaker can be used to optimize propeller performance over a range of operating conditions, resulting in some reduction in efficiency during icebreaking.

Icebreaking in a continuous mode for Arctic Class vessels is conducted at slow speed in close proximity to a bollard condition (say about 3 knots). Therefore it is reasonable to design the propulsion device for these vessels bearing in mind the requirement of maximum thrust* at bollard pull. Factors such as maximum permissible diameter**, propeller/hull interaction, propulsion arrangement (e.g., ducts, protection arrangement), pitch distribution**, increased blade thickness (by strength considerations), and ice torque (for unprotected propellers) are just a few of the factors which affect the performance of the final design.

The mission profile of the proposed POLAR7A icebreaker may be as follows, based on information supplied by the Canadian Coastguard:

Full Power	150,000 HP	30% of time	180 hours/month
2/3 Power	100,000 HP	20% of time	120 hours/month
1/3 Power	50,000 HP	30% of time	180 hours/month
Cruising	25,000 HP	20% of time	120 hours/month

However, propeller design at near-bollard pull condition should be aimed at.

---

* The total thrust is equal to the total icebreaking resistance (low speed).

** Increasing the pitch and decreasing the diameter from open water values generally improves the performance of the propeller in ice (19).

4.1 Preliminary Design Data for the Triple-Screw 150,000 HP POLAR7 (POLAR7A)

With the protection arrangement in place, the three propellers are enclosed in separate tunnels, and thus their mutual interactions are kept to a mimimum.

Having equal power distributions (50,000 HP/propeller) it is reasonable, at this stage, to suggest three identical propellers with the same particulars, same R.P.M., and same direction of rotation. The resistance and self-propulsion tests, together with the wake survey, will clearly substantiate or refute the above suggestion. The results of the wake measurements, in particular, will have a direct impact on the final design of the propeller.

In the meantime, since no information is available with regard to the wake contours, LIPS have received from NSMB the wake distribution of a triple-screw push boat equipped with nozzles and used the data in their preliminary design.

A problem area which had to be resolved was that of tip clearance. Lips had originally suggested a tip clearance of at least 25% of propeller diameter in order to avoid trapping small pieces of ice between the blade tips and the tunnel A 2-meter clearance suggested by Lips for a 6.2 m propeller was certainly an overestimation and had to be reviewed carefully.

There are a number of factors affecting the choice of the tip clearance for our design. It is known that in order to achieve the full hydrodynamic benefits of a ducted propeller system, the tip clearance must be kept to a minimum, say within the thickness of the boundary layer developed on the inside of the duct. A tip clearance of about 1% of propeller diameter is commonly used for ducted propellers.

Another critical factor in fixing the tip clearance is that concerned with propeller/hull vibration. In a heavily loaded propeller absorbing 50,000 HP, propeller induced vibrations are likely to be severe and may be transmitted to the hull if the tip clearance is too small.

Considering these factors, beside the requirements of having enough clearance to protect the blade tips from wedged ice pieces, it has been suggested to use a tip clearance of five times that commonly used for Kort-Nozzles, i.e., 5% of propeller diameter. After lengthy consultation between LIPS and DAVIS ENGINEERING, a radial tip clearance of 300 mm was agreed upon for a propeller diameter of 6500 mm, bearing in mind that the in-hull propulsion system reflects the nozzle concept more than an open propeller.

4.1.1 Propeller Particulars

After careful consideration, three identical propellers with the following particulars were chosen by LIPS:

- propeller diameter: 6500 mm
- blade contour: Kaplan type - CPP

- blade area ratio: approximately 0.60
- number of blades: 4
- mean design pitch/diameter ratio: approximately 0.820
- pitch distribution: pitch at tip/mean pitch = 1.00
  - pitch at 0.85 radius/mean pitch = 1.03
  - pitch at 0.70 radius/mean pitch = 1.02
  - pitch at 0.50 radius/mean pitch = 0.97
  - pitch at 0.30 radius/mean pitch = 0.72
- hub diameter ratio: approximately 0.29
- tip clearance: 300 mm

The propeller diameter of 6500 mm was based on two considerations, namely, dimensional constraints on the ship's beam, and optimum performance taking into account a speed of 2 and 16 knots as specified for the icebreaking and free-running modes respectively. Preliminary calculations have indicated that small changes from the speed of 2 knots, (zero and 4 knots), will hardly influence the thrust values.

An increase in the number of blades usually results in a small decrease in the propeller efficiency in the free-running condition. With a propeller diameter of 6500 mm, which is below the optimum, it is possible to increase the thrust by about 2.5% by using a five-bladed propeller instead of the four-bladed one. However, other considerations such as vibration problems, cost, and weight would have to be taken into account before finally choosing the number of blades. Meanwhile, a four-bladed propeller has been selected.

The blade area ratio of 0.55 was determined by cavitation considerations. Calculations have shown that an increase in the blade area ratio will have a minor effect on thrust in the bollard condition.

4.1.2 Openwater Characteristics

At this stage, with no information available with regard to the propulsion characteristics of such an in-hull propulsion system, it is reasonable to base the calculations on a similar propeller in an axial cylinder. Propeller/tunnel interaction, the effect of tip clearance, the difference in efficiency between a fixed pitch and a controllable pitch propeller, and finally the net forward thrust due to the tunnel aerofoil segment can hardly be predicted without model testing. Some of these effects can be allowed for by assuming similar working conditions between the proposed propulsion device and a ducted propeller.

Figure 4.1 shows the thrust versus propeller diameter for different absorbed powers at a speed of 2 knots and 150 R.P.M. The open water efficiency of the NSMB Ka k/a 4-55 screw series in an axial cylinder is shown in Figure 4.2 for different propeller diameters and different absorbed powers at a speed of 16 knots and 150 R.P.M. The results of Figures 4.1 & 4.2 were supplied by LIPS and these are not corrected for CPP or tip clearance.

Although the icebreaking speed of 2 knots seems to be a little low for the available power and the class designated to the icebreaker, it is nevertheless a reasonable speed and the resistance and self-propulsion tests will shed more light on the thrust requirements.

The NSMB results of open water tests with the Ka 4-55 in an axial circular cylinder is shown in Figure 4.3. With the available 50,000 HP per shaft, 150 R.P.M., and 6500 mm propeller, the torque coefficient k_Q is 0.0315 at near-bollard pull condition (not

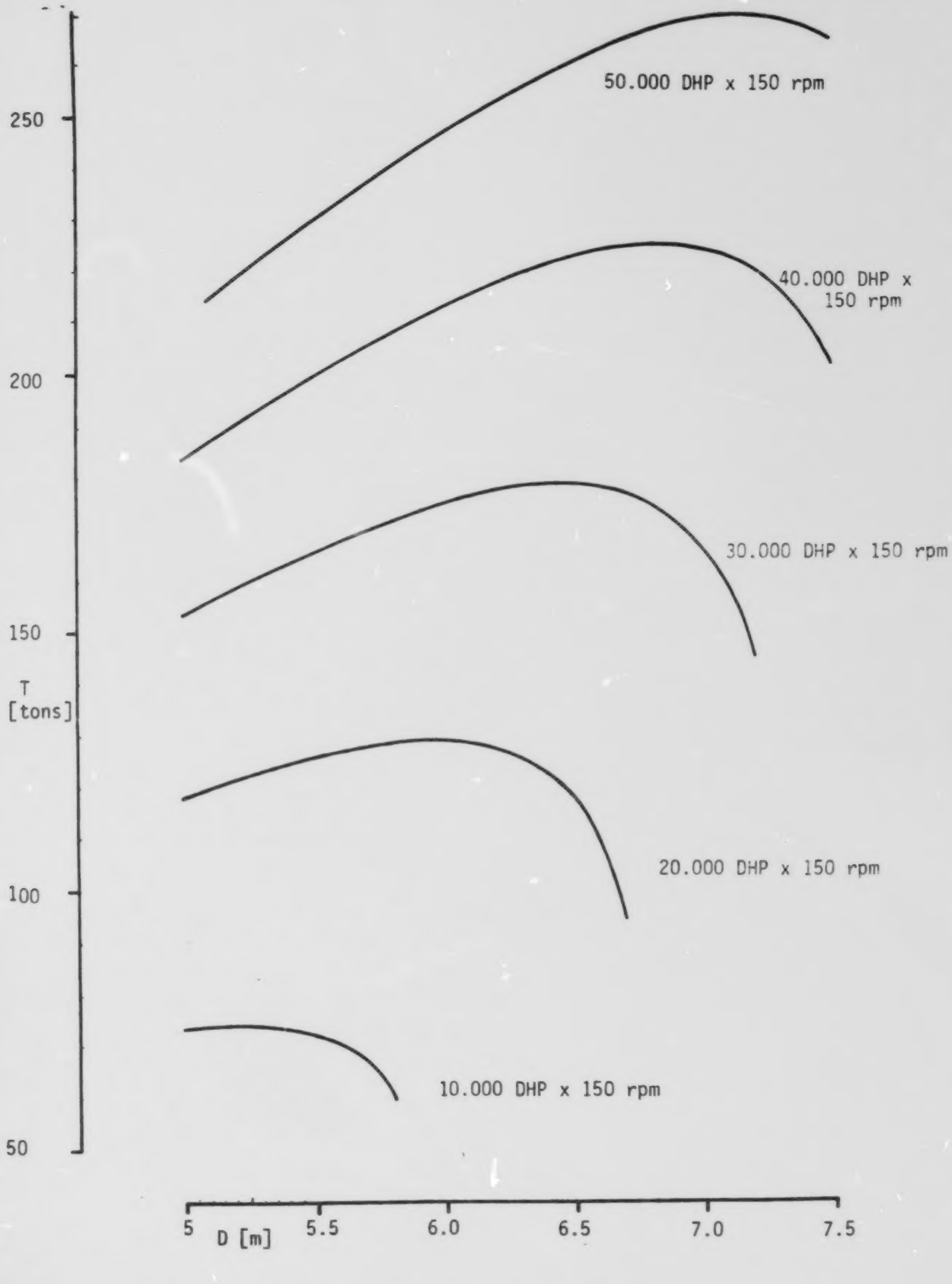

FIGURE 4.1 K_a-4-55 Screw Series in an Axial Cylinder For V=2 Knots (Not Corrected for CPP and Tip Clearance)

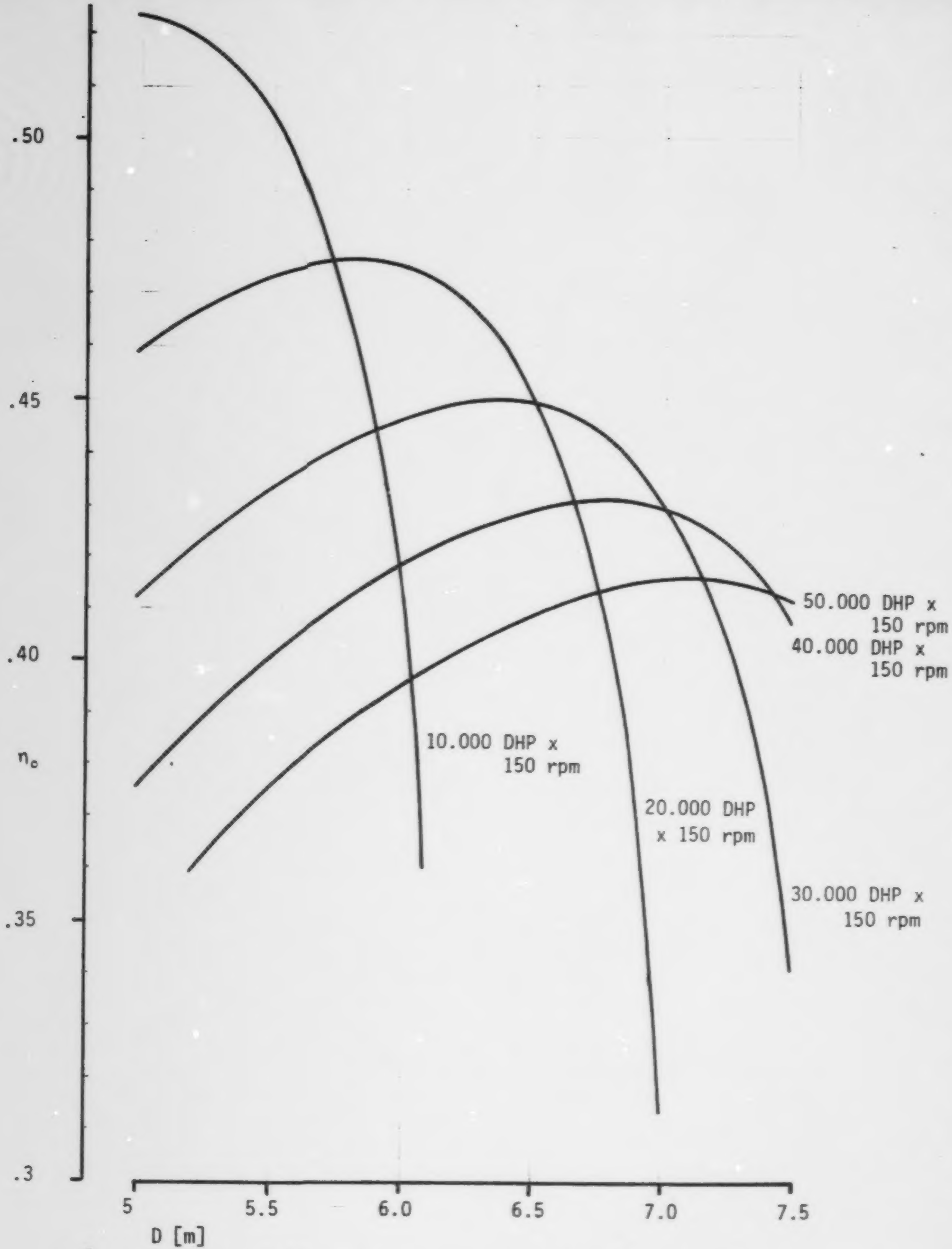

FIGURE 4.2 - K_a^{-4-55} Screw Series in an Axial Cylinder V=16 (Not Corrected for CPP and Tip Clearance)

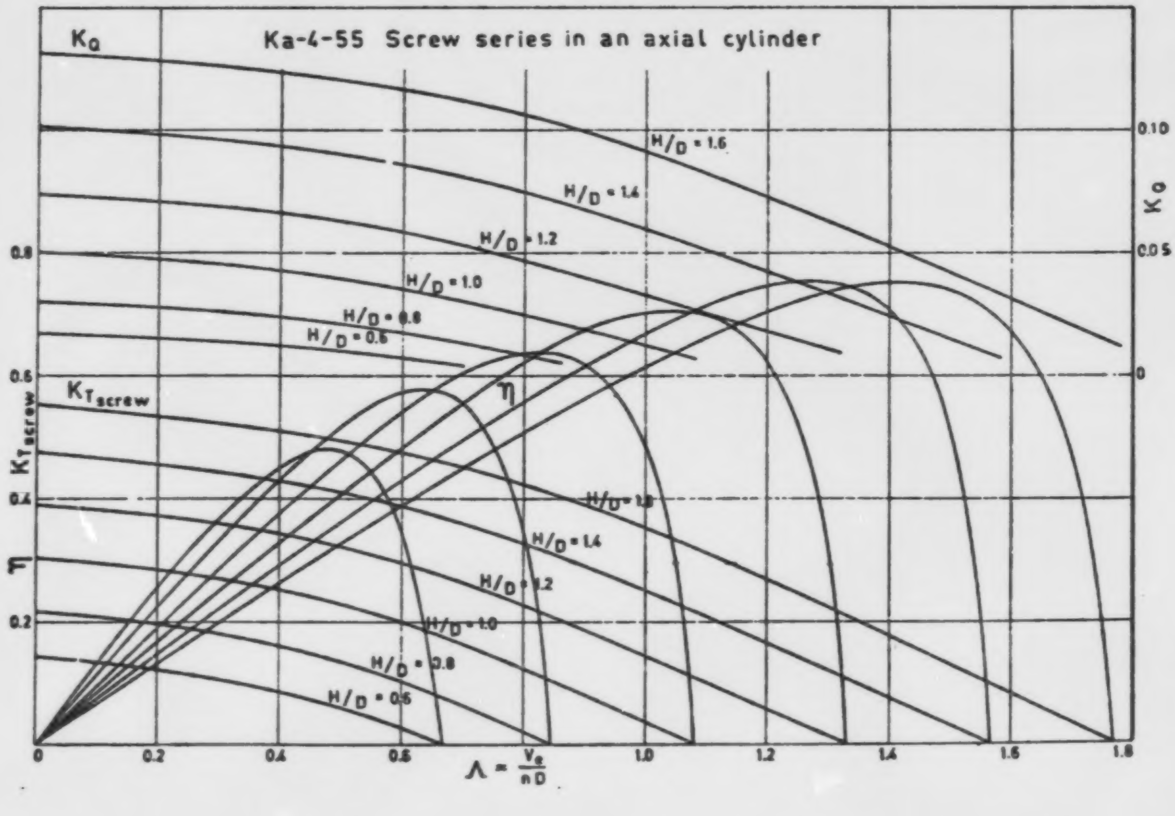

FIGURE 4.3 RESULTS OF OPEN WATER TESTS WITH THE K_a-4-55 SCREW SERIES IN AN AXIAL CIRCULAR CYLINDER

corrected for CPP and tip clearance). The thrust coefficient, k_T in this case is 0.225 and the thrust is about 262 tons; which is in agreement with LIPS' prediction of 260 tons (Figure 4.1).

Two corrections are required to allow for the tip clearance and the difference in performance of a fixed pitch and a controllable pitch propeller. Since the proposed propulsion device is neither a typical ducted propeller nor an open one (although it might reflect the former concept), one should investigate the effect of tip clearance on the thrust produced by the propeller itself in both cases, i.e., with and without duct.

For normal operating conditions it is known that for what may be regarded as reasonable ranges of tip clearance, the propeller thrust decreases with increasing clearance for low power coefficient (based on ship velocity) and increases with increasing clearance for higher power coefficient (heavily loaded). For large tankers, for example, with a typical power coefficient[†] $(P/\frac{1}{2}\rho AV^3)$ between 8 - 12, the total thrust, propulsion efficiency, and duct thrust decreases with increasing tip clearance whereas the propeller thrust increases slightly.

The other required correction to the open water tests is that with regard to the use of a controllable pitch propeller instead of a fixed pitch one. As one would expect, using a controllable pitch propeller would improve the performance over all the range or working conditions, with efficiencies usually a little below the maxima for fixed pitch propellers. With the propeller diameter fixed at 6500 mm and a tip clearance of 300 mm, Table 4.1 shows the predicted thrust at different R.P.M. with different pitch ratio

---

[†] For bollard pull condition, comparison should be based on torque coefficient rather than power coefficient, i.e., on R.P.M. rather than V.

- absorbed power: 50.000 DHP

V_s (kn.)	100 rpm		110 rpm		120 rpm		130 rpm		140 rpm		150 rpm	
	P/D	T (tons)	P/D	T (tons)	P/D	T (tons)	P/D	T (tons)	P/D	T (tons)	P/D	T (tons)
0	1.439	216.7	1.250	220.3	1.107	222.8	.992	224.6	.897	225.7	.817	225.9
2	1.440	220.9	1.252	224.5	1.108	226.6	.994	227.9	.900	228.6	.821	228.5
4	1.444	223.3	1.256	226.9	1.113	228.7	.999	229.7	.905	230.0	.826	229.6
6	1.452	224.6	1.264	228.3	1.121	229.8	1.006	230.4	.912	230.2	.833	229.9
8	1.464	225.1	1.275	228.7	1.131	230.1	1.015	230.4	.921	230.2	.841	229.4
10	1.479	225.0	1.290	228.6	1.144	229.8	1.027	229.9	.931	229.5	.851	228.5
12	1.497	224.2	1.306	227.8	1.159	228.8	1.041	228.7	.944	228.1	.862	226.9
14			1.326	226.2	1.177	227.1	1.057	226.8	.959	226.0	.875	224.6
16			1.348	224.4	1.197	225.2	1.075	224.7	.975	223.7	.890	222.1

- absorbed power: 40.000 DHP

0	1.289	189.3	1.126	191.7	1.000	193.4	.897	194.5	.811	194.6	.735	193.4
2	1.290	192.8	1.128	195.0	1.002	196.2	.900	196.8	.815	196.7	.742	195.4
4	1.295	194.9	1.133	196.7	1.008	197.6	.906	197.9	.821	197.5	.748	196.1
6	1.305	195.8	1.142	197.5	1.016	198.0	.914	198.0	.829	197.4	.756	196.0
8	1.318	195.9	1.154	197.4	1.026	197.8	.924	197.5	.838	196.7	.764	195.2
10	1.335	195.5	1.169	196.9	1.040	197.0	.936	196.5	.849	195.6	.775	193.9
12	1.354	194.4	1.187	195.6	1.056	195.6	.950	194.9	.862	193.7	.786	191.9
14	1.377	192.6	1.208	193.7	1.075	193.5	.967	192.6	.877	191.2	.800	189.3
16	1.402	190.6	1.231	191.7	1.096	191.2	.986	190.1	.894	188.5	.816	186.4

- absorbed power: 30.000 DHP

0	1.125	158.3	.988	159.8	.878	160.6	.786	160.5	.707	158.8	.634	155.0
2	1.128	160.9	.991	161.9	.882	162.3	.792	162.0	.714	160.3	.645	156.9
4	1.134	162.1	.997	162.8	.889	162.9	.799	162.3	.722	160.7	.654	157.6
6	1.145	162.4	1.007	162.9	.898	162.7	.808	161.9	.731	160.3	.663	157.3
8	1.159	162.1	1.020	162.3	.909	161.9	.818	160.9	.741	159.2	.673	156.3
10	1.177	161.2	1.036	161.2	.923	160.6	.831	159.5	.752	157.6	.684	154.8
12	1.198	159.7	1.055	159.5	.940	158.7	.846	157.4	.766	155.4	.696	152.6
14	1.223	157.6	1.077	157.2	.960	156.2	.864	154.7	.782	152.6	.711	149.7
16	1.251	155.3	1.102	154.7	.982	153.5	.884	151.8	.801	149.5	.728	146.5

TABLE 4.1 K_a-4-55 Screw Series in an Axial Cylinder Corrected for CP and Tip Clearance

- absorbed power: 20.000 DHP

V_s (kn.)	100 rpm		110 rpm		120 rpm		130 rpm		140 rpm		150 rpm	
	P/D	T (tons)	P/D	T (tons)	P/D	T (tons)	P/D	T (tons)	P/D	T (tons)	P/D	T (tons)
0	.936	122.3	.822	122.6	.727	121.9	.642	118.7	.560	112.1	.460	95.6
2	.940	123.6	.828	123.6	.735	122.6	.654	120.0	.578	114.7	.497	103.7
4	.948	123.9	.836	123.6	.744	122.5	.664	120.1	.592	115.6	.518	106.8
6	.960	123.4	.847	122.9	.754	121.8	.675	119.5	.603	115.2	.533	107.8
8	.976	122.4	.861	121.7	.767	120.4	.687	118.1	.615	114.2	.546	107.4
10	.995	120.9	.878	120.1	.782	118.6	.701	116.4	.628	112.6	.559	106.1
12	1.019	118.9	.898	117.9	.800	116.3	.717	113.9	.642	110.1	.573	104.0
14	1.046	116.4	.923	115.1	.822	113.4	.736	110.9	.660	107.2	.589	101.2
16	1.076	113.8	.950	112.2	.847	110.2	.759	107.6	.681	103.8	.609	98.1

- absorbed power: 10.000 DHP

0	.675	75.7	.572	71.4	.442	57.6	.425	49.6				
2	.688	76.1	.593	72.8	.493	64.6	.449	51.2				
4	.700	75.7	.608	72.8	.518	66.4	.469	50.8				
6	.715	74.6	.622	71.9	.535	66.4	.494	49.6				
8	.732	73.0	.638	70.4	.551	65.3	.525	48.2				
10	.755	70.9	.658	68.3	.569	63.5	.562	46.4				
12	.782	68.4	.682	65.7	.592	61.1						
14	.815	65.4	.712	62.7	.620	58.3						
16	.852	62.2	.747	59.4	.654	55.3						

TABLE 4.1 (Cont'd) K_a-4-55 Screw Series in an Axial Cylinder Corrected for CP and Tip Clearance

settings to absorb a given power as a function of ship speed in open water and in ice conditions. The table was produced by LIPS and based on corrected data taking into account the change in performance due to CPP and the increased tip clearance.

Figure 4.4 shows the design data compiled from Figure 4.1 and Table 4.1 for a ship speed of 16 knots. It is clear that the improvement in the open water efficiency achieved by using a CP propeller is greater than the loss due to the increased tip clearance. The maximum open water efficiency is about 54%.

Figure 4.5 is a graphic presentation of the corrected open water data given in Table 4.1. The maximum thrust (as a design criterion for the propulsion of an icebreaker) which can be produced by a 6500 mm k_a 4-55 propeller in an axial cylinder with tip clearance of 300 mm is about 230 tons at 140 R.P.M. and ship speed of 4 knots[††]. The mean pitch ratio in this case is 0.905. The propeller thrust at near-bollard pull conditions was decreased by about 13%, according to LIPS' results, to allow for the CPP and the increased tip clearance. The decrease of propeller thrust due to the increased tip clearance, as indicated by LIPS, requires further investigation. As previously mentioned, the propeller thrust may be increased or decreased with increasing tip clearance depending on the power coefficient. To investigate this point further let us consider the propeller with and without the duct at near-bollard pull condition. First of all, since the Kaplan type propeller series k_a is specially designed to operate in ducts, its open water test results do not exist. The propeller is replaced by a 6500 mm of the series B4-55 just for the purpose of the demonstration. Figure 4.6 shows the relationships between the propeller thrust coefficient for B4-55,

---

[††] $k_Q = 0.0387$, $k_T = 0.226$

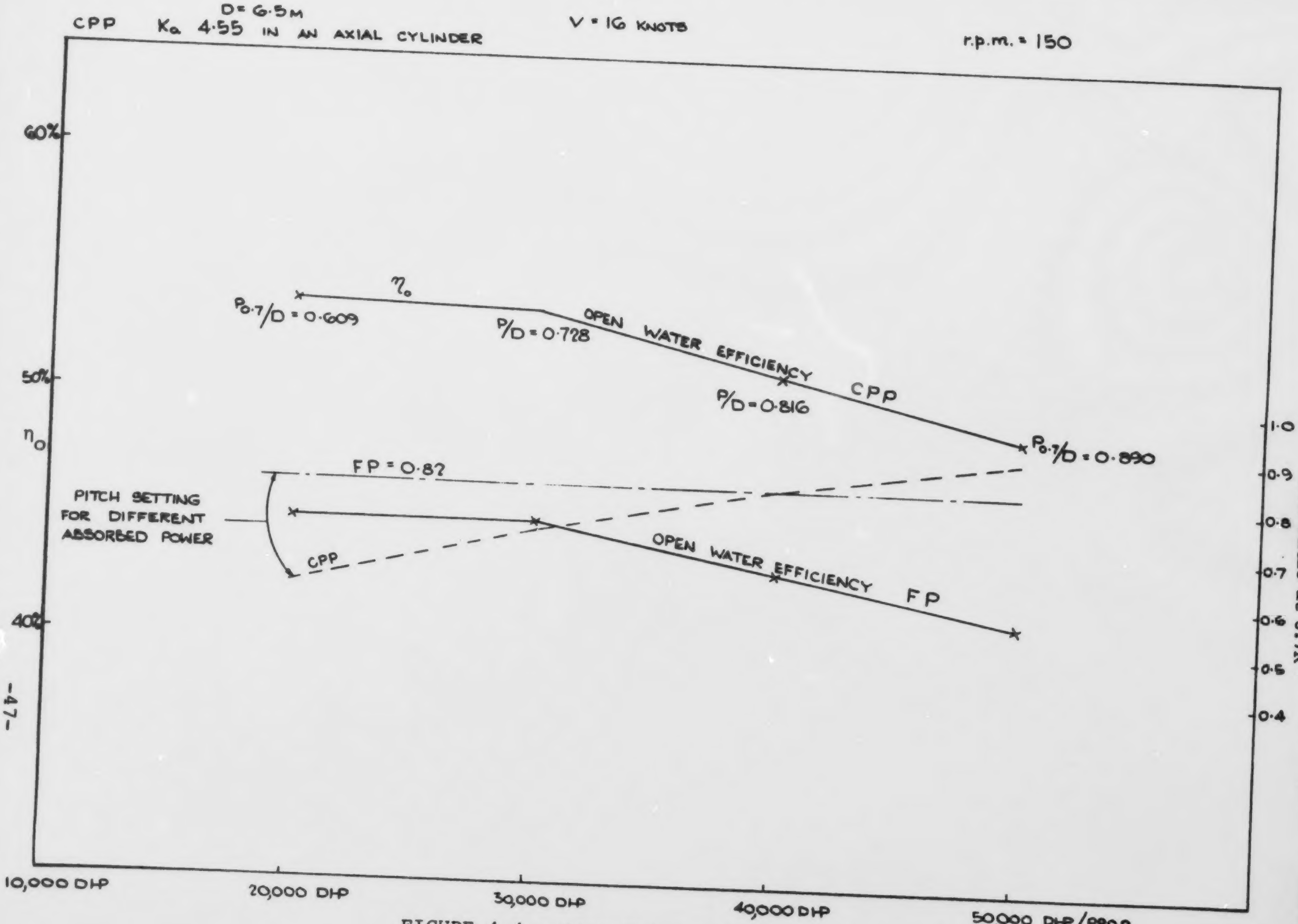

FIGURE 4.4 - Open Water Efficiency for a CPP, K_a-4-55, in an Axial Cylinder

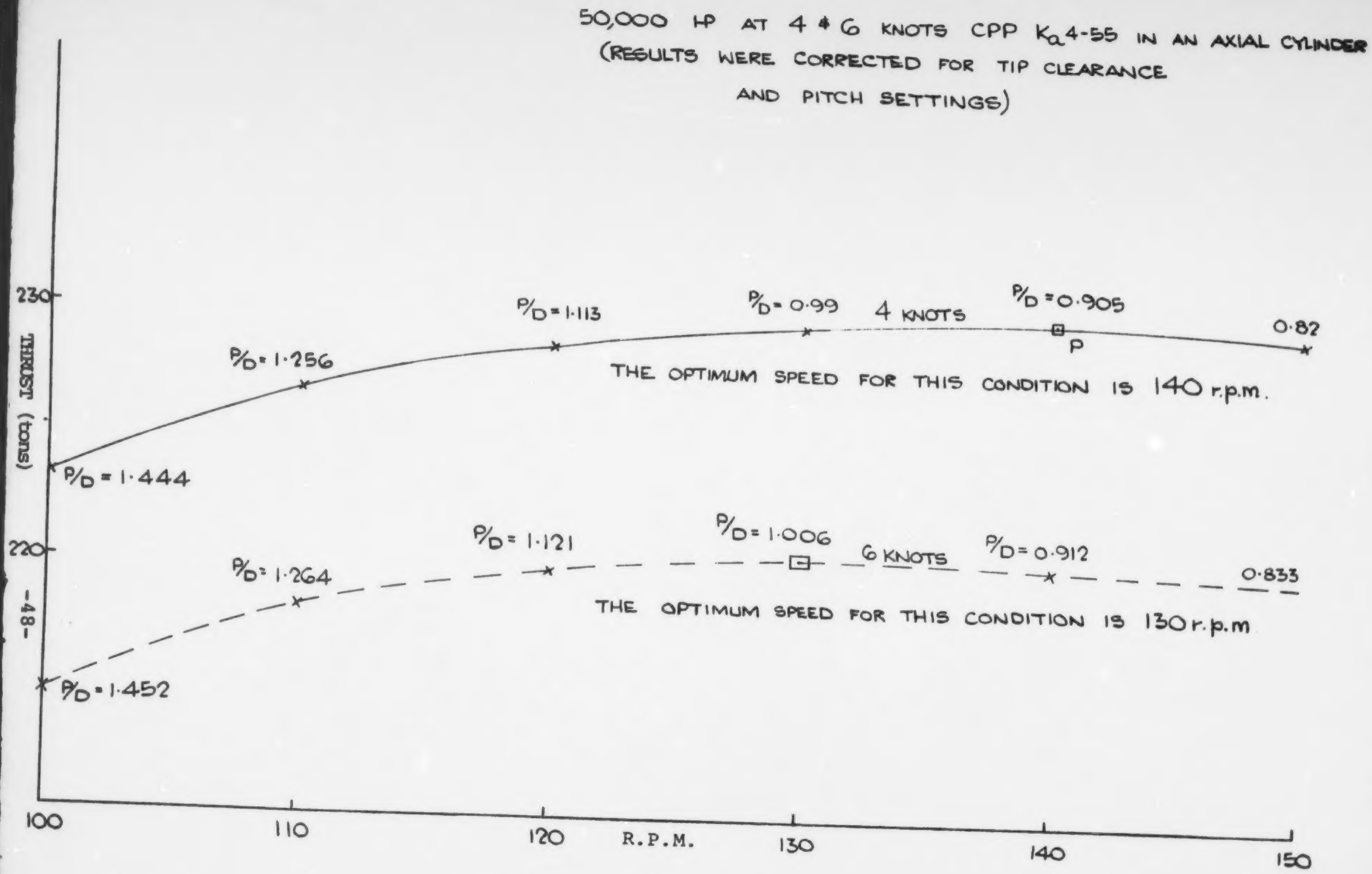

FIGURE 4.5 - Thrust vs. R.P.M. at Constant Ship Speed

with and without duct 19, versus torque coefficient at bollard pull condition. These relationships are based on the NSMB open water test results.

It is clear from Figure 4.6, that at zero velocity, propeller thrust is higher for the open case compared with the same propeller inside a duct for the same torque coefficient.* The increase in propeller thrust as a result of a very large tip clearance (i.e., open propeller) varies between 40% and 20%, with the lower percentage at higher torque coefficients.

So, for the proposed preliminary design, with $k_Q = 0.0387$ (50,000 HP, N = 140 R.P.M., and 6500 mm diameter) and by replacing the Kaplan type by the B Series (for the sake of the demonstration only) the following open water characteristics can be expected:

Propeller thrust coefficient k_T(open) = 0.3315
Propeller thrust coefficient k_T(ducted) = 0.237
zero speed

Therefore,

Propeller thrust(open) = 336.7 tons (P/D = 0.77)
Propeller thrust(ducted) = 240.7 tons (P/D = 0.84)

With a radial tip clearance ratio of about 4.2%, the predicted propeller thrust should lie between these two figures, i.e., between 240.7 and 336.7 tons (B 4-55). Now, with k_a 4-55 screw in an axial cylinder, the propeller produces 262 tons (as previously predicted) at bollard pull, and one should expect an increase in the propeller thrust with increasing tip clearance for the same power absorbed; with analogy to the foregoing discussion of the B 4-55 propeller.

---

* Obviously, the propeller pitch has to be adjusted so that the propeller absorbs the same power at the same R.P.M.

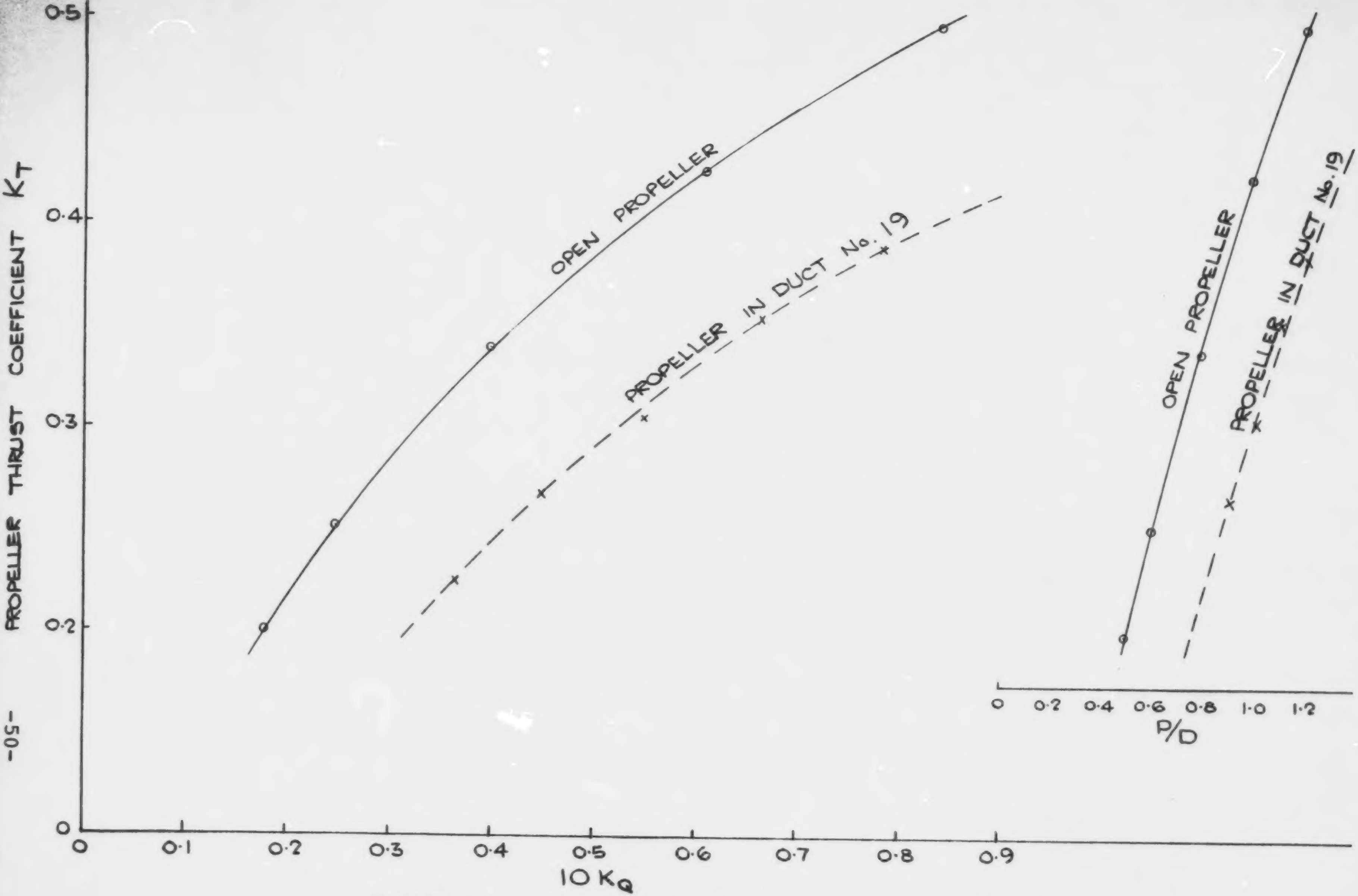

FIGURE 4.6 - Thrust Coefficient vs. Torque Coefficient for B4-55 at zero speed of Advance

The expected increase in thrust at bollard can be substantiated even further by the fact that the duct in the proposed propulsion device is countersunk over about 270° of its periphery. According to the NSMB tests, the thrust/power ratio of the ducted propulsion system at bollard increases as the countersunk angle increases (3).

In conclusion, a propeller of the series k_a 4-55, diameter 6500 mm, P/D = 0.82 - 0.95, N = 140 - 150 R.P.M., and absorbing 50,000 HP combined with 19A duct countersunk over about 270° of its circumference and accommodating the propeller with 300 mm tip clearance, would produce close to 300 tons total thrust at near-bollard pull condition (icebreaking mode). The icebreaking continuous speed will then be about 3 - 4 knots. Thrust in order of magnitude of 400 tons at 4 - 5 knots for 50,000 HP can be achieved with a propeller diameter of about 13.0 meters and R.P.M. of about 40. (LIPS).

4.2 Propeller Installation/Removal

4.2.1 General

For ducted propeller installations, the relatively small clearance between the propeller and duct make the fitting and removal of the propeller a matter requiring close consideration. Having the rudder behind the duct also complicates the installation/removal procedure. One solution is to use a propeller with detachable blades.* For larger propellers, however, the detachable blades will weight several tons and thus, will be in themselves difficult to remove from the duct unless a special arrangement is employed. An alternative solution to this problem is to withdraw the tailshaft and propeller aft until it is clear of the duct, as shown in Figure 4.7. ** Suitable lifting eyebolts on the shell plating could then be arranged to take the weight of the propeller while the shaft is withdrawn inboard, the propeller being released from the shaft by hydraulic means.

Another arrangement for propeller removal is shown in Figure 4.8. It consists of fitting a lifting beam attached to the hull forward of the propeller, and to the rudder skeg aft of the propeller. Steel slinging plates fixed to the forward and aft ends of the propeller would then permit the propeller to be removed aft with a suitable carriage.

---

* Detachable bladed propeller is more costly than a fixed bladed propeller and would also have a larger boss-diameter ratio giving 1½% to 2% less in efficiency.

** Symposium on ducted propeller, RINA, 1973, Paper No. 6 by A. Emerson et. al.

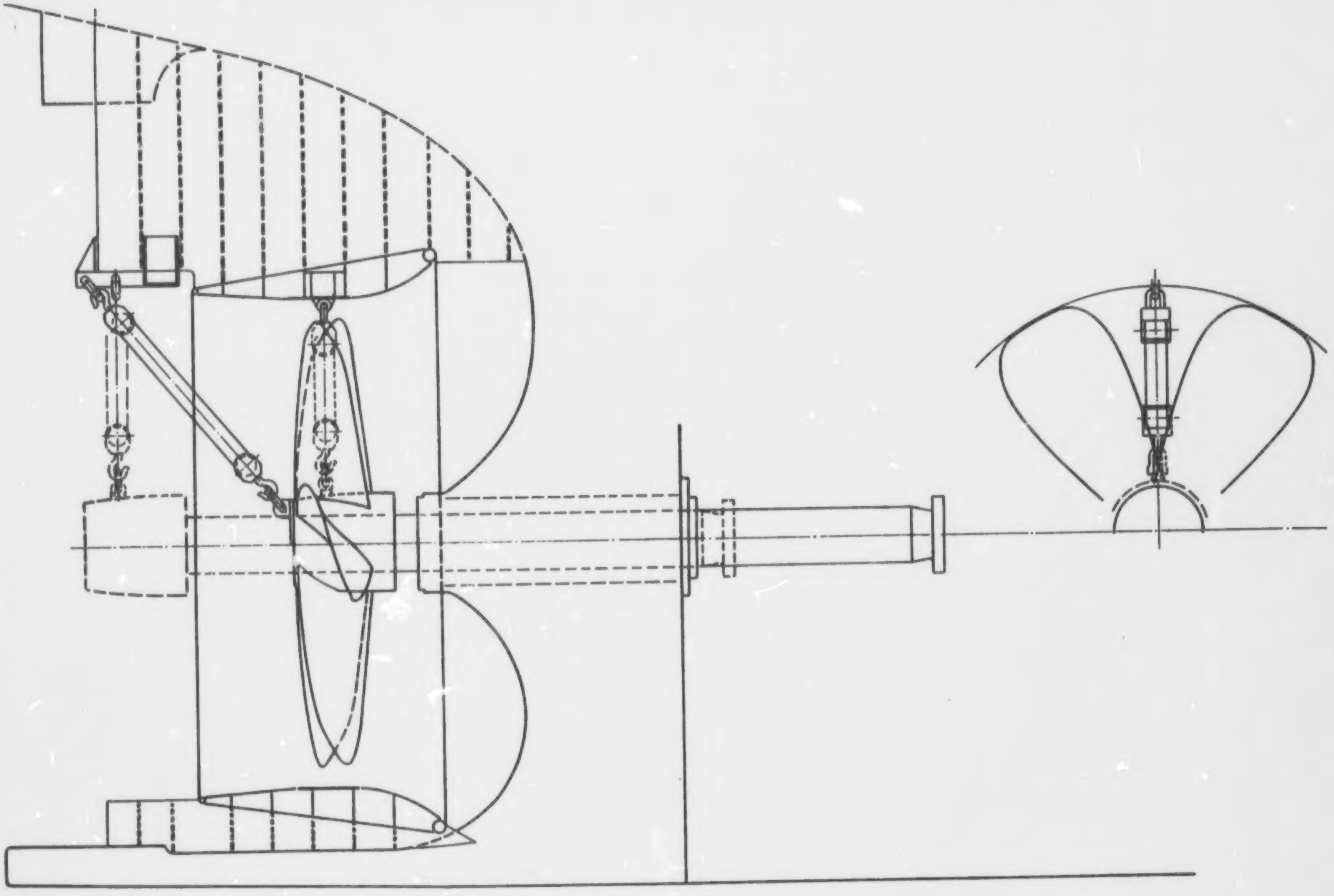

FIGURE 4.7 PROPELLER TAILSHAFT WITHDRAWAL

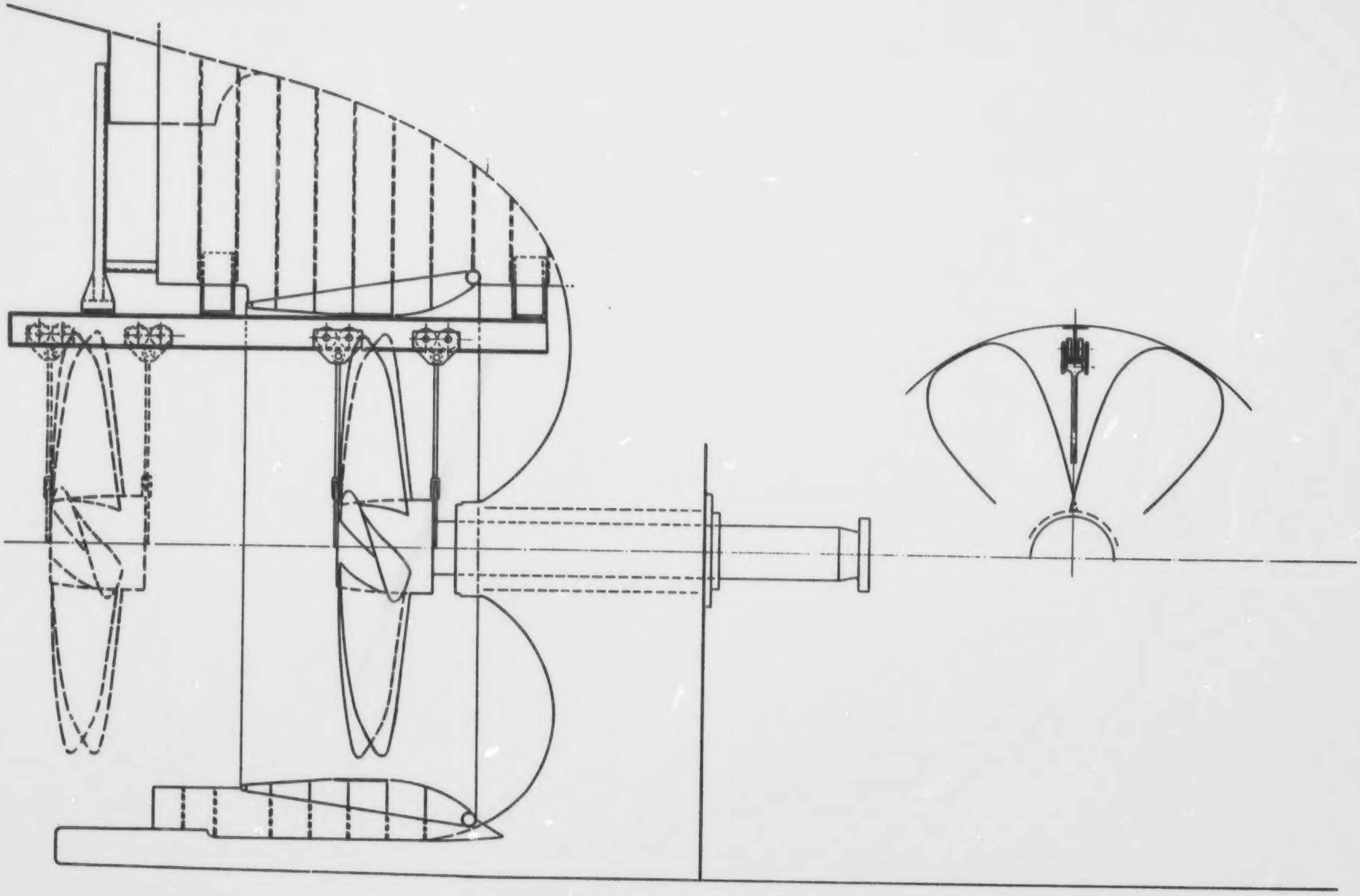

FIGURE 4.8 PROPELLER REMOVAL

For a controllable pitch propeller inside a duct, it is normal practice to remove the blades only, and to leave the hub intact and not disturb the mechanical and hydraulic systems. Figure 4.9* illustrates the dismounting of one blade in a four-blade CP propeller. The steps can be summarized as follows:

- bring blade to 12 o'clock position for unlocking and loosening of blade bolts;
- replace four bolts by eyebolts as shown in the sketch (Figure 4.9);
- arrange sufficient hoisting facilities;
- turn blade to 6 o'clock position for removal of the blade.

The assembly of the propeller can be carried out in the reverse sequence.

4.2.2 Installation/Removal of CP In-Hull Propellers

The blades of the CP propeller in the proposed in-hull propulsion system can be removed by similar schemes to that suggested and used by LIPS. Two schemes are suggested, one with and one without, the removal of the rudder.

Scheme I

Figure 4.10 illustrates the removal arrangement. The following instructions have to be followed.

- the stern guards are removed;
- the rudder is removed;
- an I-beam is supported and fixed at one end to the base of the rudder horn and the other end supported vertically to the transom;

---

* LIPS Drawing A308783/0900139

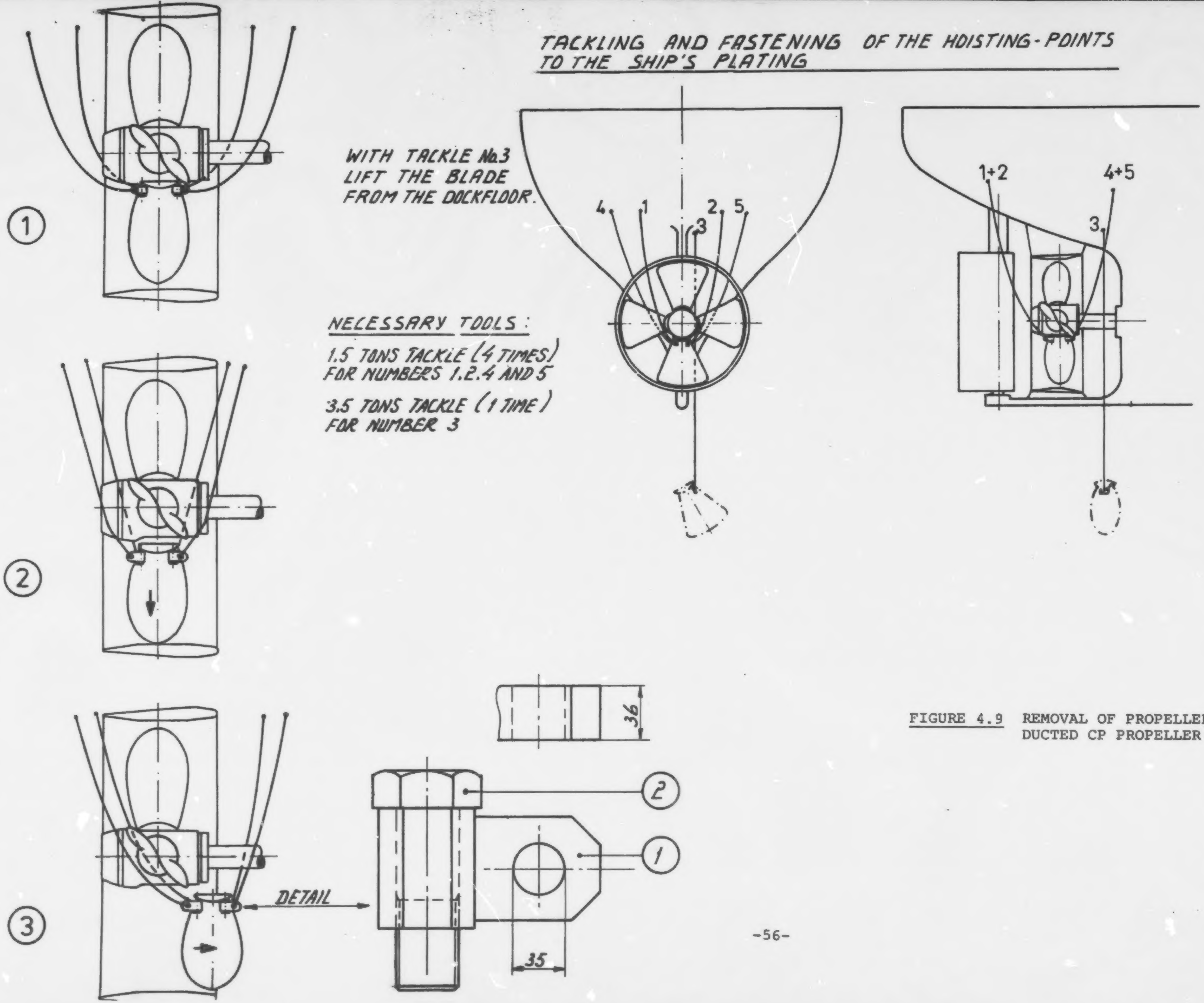
TACKLING AND FASTENING OF THE HOISTING-POINTS TO THE SHIP'S PLATING
①
②
③
4
1
2
5
3
1+2
4+5
3
DETAIL
36
35
2
1

WITH TACKLE No.3 LIFT THE BLADE FROM THE DOCKFLOOR.

NECESSARY TOOLS:

1.5 TONS TACKLE (4 TIMES) FOR NUMBERS 1.2.4 AND 5

3.5 TONS TACKLE (1 TIME) FOR NUMBER 3

FIGURE 4.9 REMOVAL OF PROPELLER BLADES IN A DUCTED CP PROPELLER ARRANGEMENT

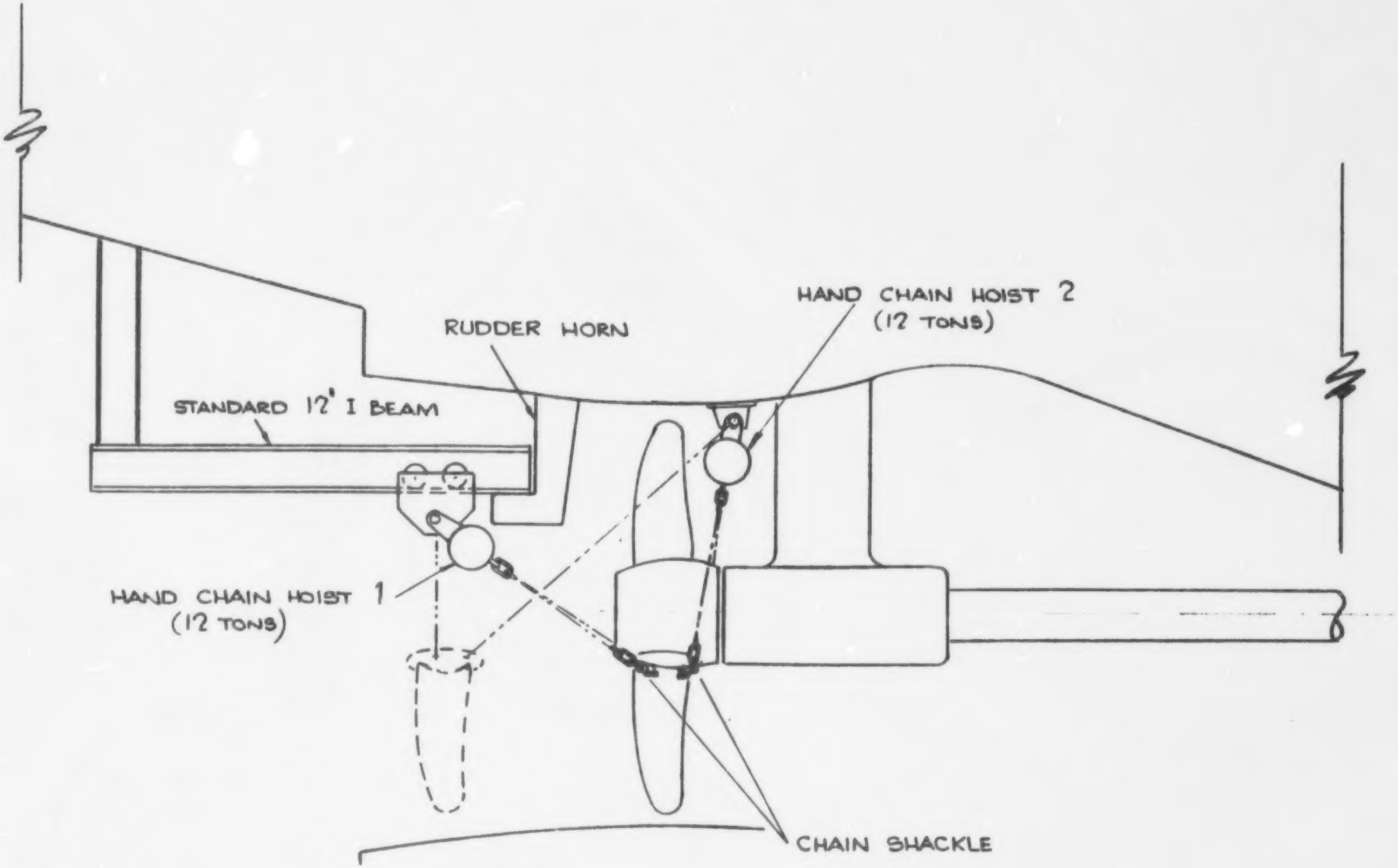
HAND CHAIN HOIST 2
(12 TONS)
RUDDER HORN
STANDARD 12' I BEAM
HAND CHAIN HOIST 1
(12 TONS)
CHAIN SHACKLE

FIGURE 4.10 SCHEME I

- two chain hoists * are required; hoist 1 (≈ 12 tons capacity) of the trolley-type fitted onto the beam, and hoist 2 (≈ 10 tons capacity)with a clevis-connection attached to an eyebolt on the tunnel shell plating;
- each hoist is fitted with a suitable latched hook which is in turn fitted with double sling chains attached to chain shackles;
- bring the blade to a 12 o'clock position for unlocking and loosening of blade bolts;
- choose four bolts; two on each side of the blade and replace them by eyebolts similar to that shown in Figure 4.9;
- turn blade to a 6 o'clock position and attach the chain shackles to the eyebolts;
- control the lift length of each hoist and detach the blade from the hub completely; and,
- bring the loose blade under hoist 1 and move it clear of the tunnel.

For assembly, the above steps are to be carried out in reverse sequence.

Scheme II

Two arrangements have been suggested for propeller blade removal without removing the rudder. Figures 4.11A and 4.11B illustrate the two arrangements (Scheme II-A and Scheme II-B). The following instructions have to be followed for Scheme II-A:

- remove stern guards;
- bring blade to 12 o'clock position for unlocking and and loosening of blade bolts;

---

* Electric wire rope hoists can be used instead, however, they may not be suitable due to their weight and dimensions in a restricted space. For example, an R-W type hoist of 10 ton capacity weighs about 1 ton and its overall length is about 6½ ft.

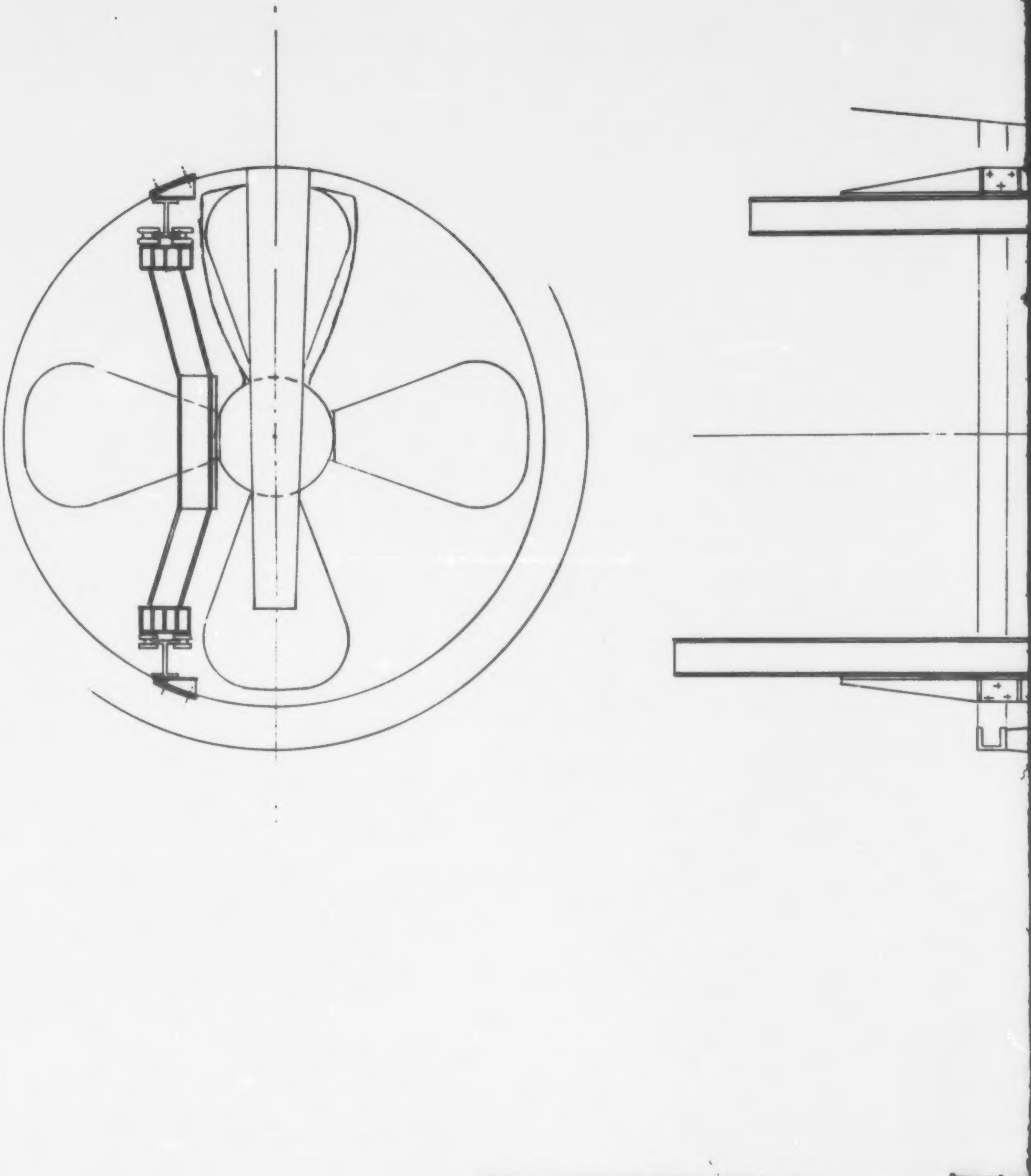

GENERAL NOTE: REMOVE BURRS & SHARP EDGES

APPROVAL			ITEM
			DRAWN
			CHECKED M.C
			METR
			GEN.DIM.:
			HOLES
	NEXT ASSY	USED ON	SHAFTS
	CODE IDENT. NO.		ANGLES:

SYM | REVISION | AUTH | DATE | APP'D

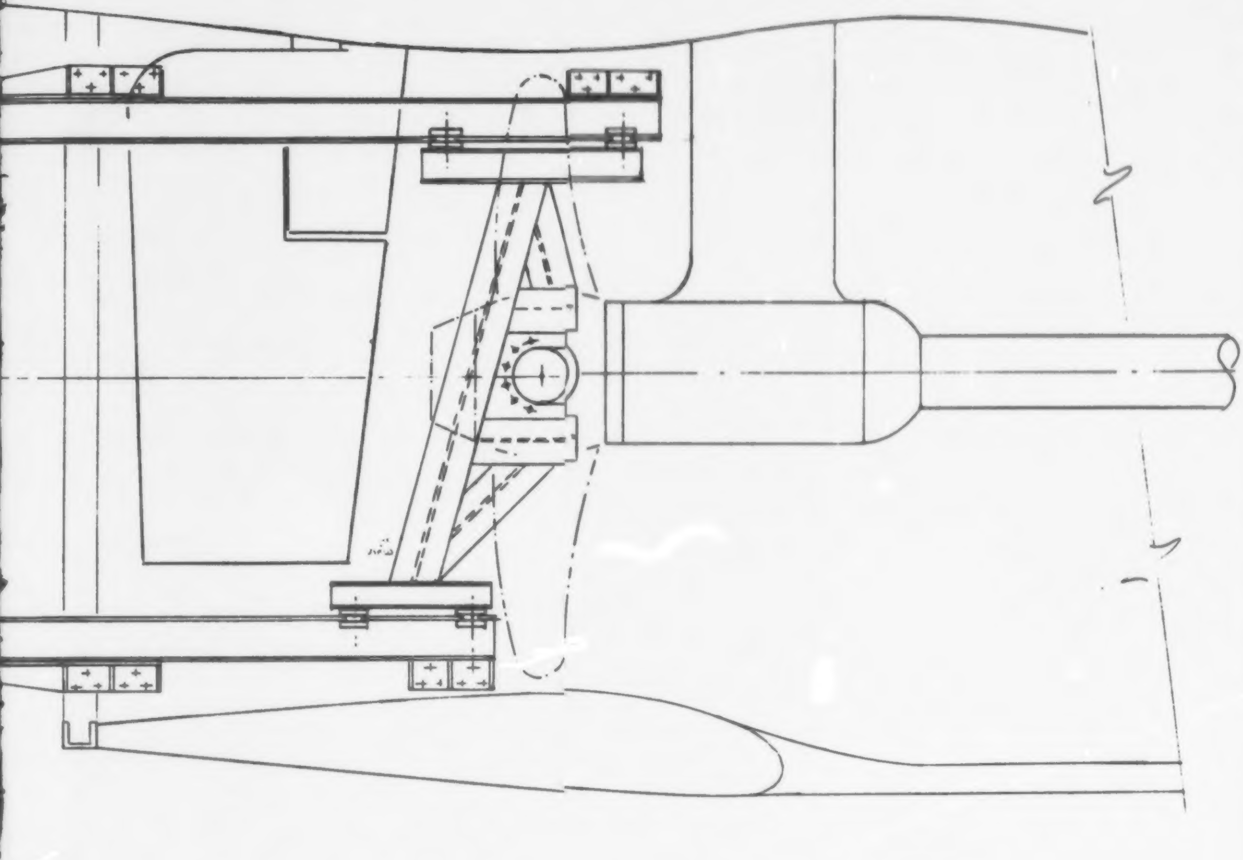

FIGURE 4.11(a) - Stern Guards
(Scheme II-A)

ITEM | QTY. | PART NO. | DESCRIPTION | NOTES

DRAWN
SCALE 1:50
CHECKED M.G.
DATE 22 JUN 81
METRIC
INCHES
GENERAL:
DECIMALS
HOLES
.XX:
SHAFTS
.XXX:
ANGLES:

Davis Engineering
CONSULTING ENGINEERS
OTTAWA CANADA

TITLE PROPELLER BLADE REMOVAL - SCHEME II-A

CLIENT CONTRACT C325
MATERIAL
TECHNICAL DATA LIST
DRAWING NUMBER
DWG SIZE
PART NO. DE 1497
SHEET OF

- turn blade to 6 o'clock position and remove the bolts covering 180^0 sector from the vertical;
- attach 2 I-beams and sufficient hoisting facilities as shown in the sketch Figure 4.11A (drawing No. DE 1497);
- turn the blade to 9 o'clock position;
- secure the blade to the supporting structure by bolts;
- detach the blade completely from the hub;
- move the supporting structure till the blade is clear of the tunnel.

The main disadvantage of this arrangement lies in the high rigidity of the supporting structure which leaves no room for practical tolerances in the assembly.

A more flexible arrangement is shown in Figure 5.11B (drawing No. DE1498) (Scheme II-B). The following instructions have to be followed:

- support blade in 3 o'clock position;
- arrange two hoists on duct side plating;
- unlock and remove bolts;
- pull blade radially to clear hub;
- rotate blade 90^0 in plan view by controlling the side hoist pull;
- use the main travelling hoist to move the blade (base first) from the tunnel.

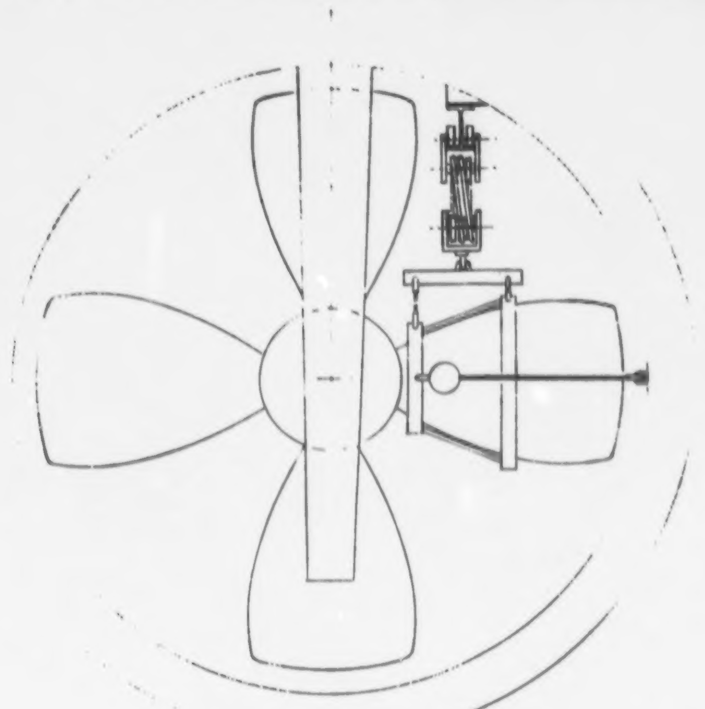

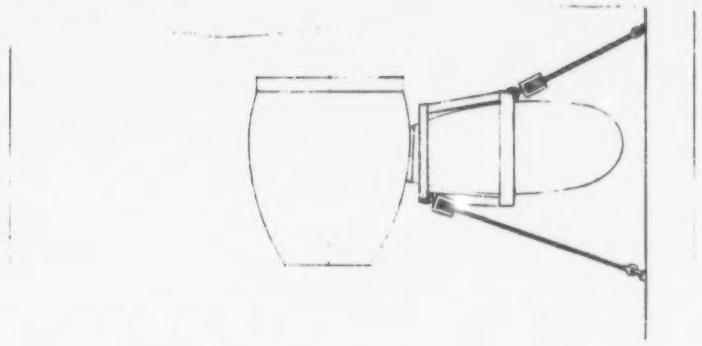

PART PLAN VIEW

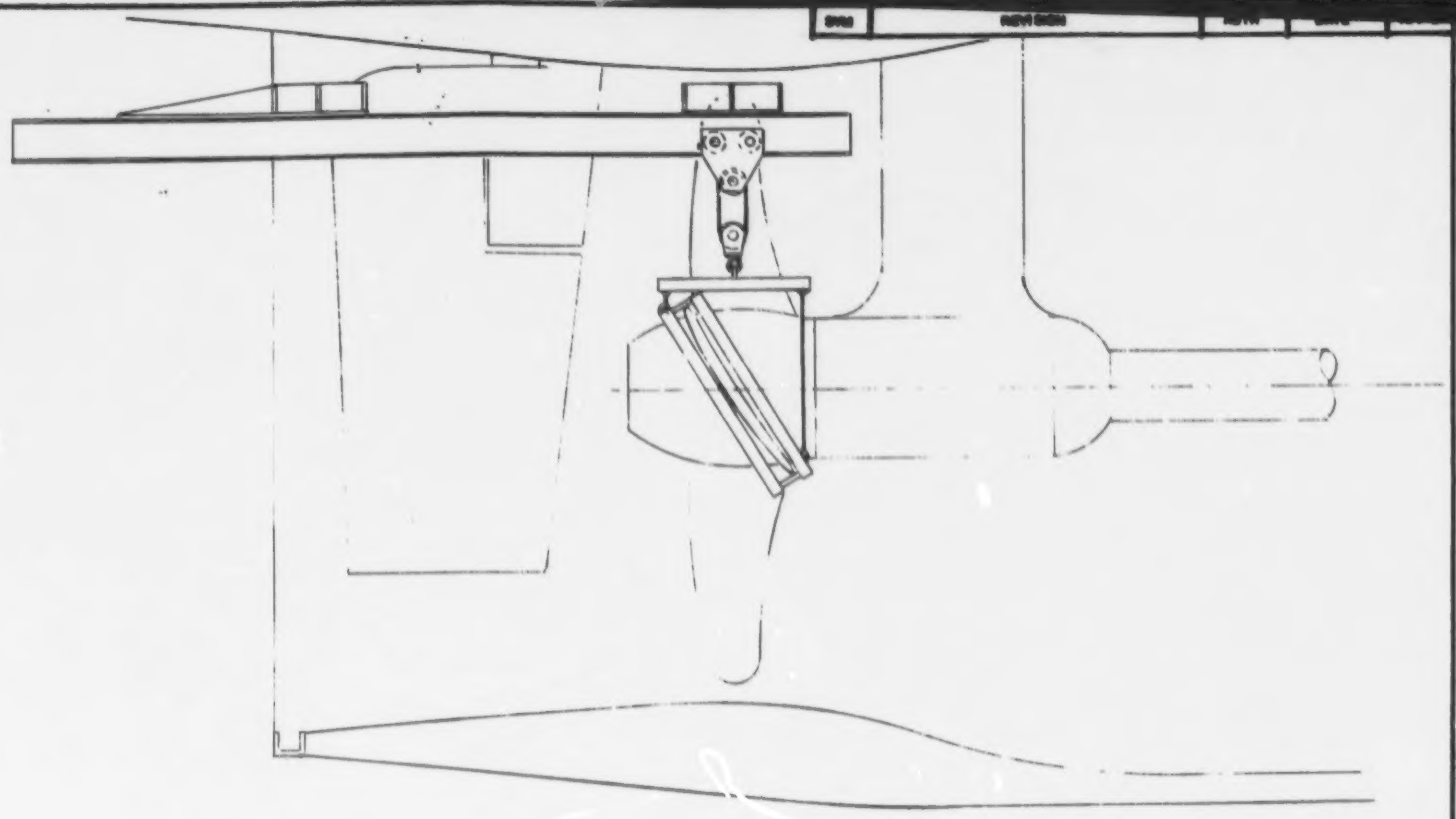

SIDE ELEVATION

1. SUPPORT BLADE IN 3 OCLOCK POSITION AS SHOWN
2. ARRANGE TWO HOISTS ON DUCT SIDE PLATING AS SHOWN IN PLAN VIEW
3. UNLOCK & REMOVE BLADE BOLTS
4. PULL BLADE RADIALLY TO CLEAR HUB
5. ROTATE BLADE 90° IN PLAN VIEW BY CONTROLLING THE SIDE HOIST PULL
6. USE THE MAIN TRAVELLING HOIST TO MOVE THE BLADE (BASE FIRST) FROM THE TUNNEL

FIGURE 4.11(b) - Stern Guards
(Scheme II-B)

GENERAL NOTE: REMOVE BURRS & SHARP EDGES

APPROVAL

NEXT ASSY | USED ON

CODE IDENT. NO.

ITEM | QTY. | PART NO. | DESCRIPTION | NOTES

DRAWN

SCALE N.T.S.

CHECKED

DATE 27.4.81.

METRIC | INCHES

GEN. DIM. ±

DECIMALS

HOLES

.XX ±

SHAFTS

.XXX ±

ANGLES ±

Davis Engineering

CONSULTING ENGINEERS
OTTAWA CANADA

TITLE PROPOSED METHOD OF PROPELLER REMOVAL
SCHEME II-B

CLIENT CONTRACT C323

MATERIAL

TECHNICAL DATA LIST

DRAWING NUMBER

DWG SIZE

PART NO. DE 1498

SHEET OF

- turn blade to 6 o'clock position and remove the bolts covering 180^0 sector from the vertical;
- attach 2 I-beams and sufficient hoisting facilities as shown in the sketch Figure 4.11A (drawing No. DE 1497);
- turn the blade to 9 o'clock position;
- secure the blade to the supporting structure by bolts;
- detach the blade completely from the hub;
- move the supporting structure till the blade is clear of the tunnel.

The main disadvantage of this arrangement lies in the high rigidity of the supporting structure which leaves no room for practical tolerances in the assembly.

A more flexible arrangement is shown in Figure 5.11B (drawing No. DE1498) (Scheme II-B). The following instructions have to be followed:

- support blade in 3 o'clock position;
- arrange two hoists on duct side plating;
- unlock and remove bolts;
- pull blade radially to clear hub;
- rotate blade 90^0 in plan view by controlling the side hoist pull;
- use the main travelling hoist to move the blade (base first) from the tunnel.

5.0 PROPULSION SHAFTING

5.1 General

A sketch of the shafting arrangement is shown in Figure 5.1 and a detailed arrangement in Figure 3.6 (DE 1492). The shafting sections are connected by means of either solid flange couplings or removable flange couplings. The outboard shafting is supported in water lubricated strut and sterntube bearings and the line-shaft in regular thrust and plummer bearings.

5.2 Shafting Dimensions

As the outboard shafting and propellers are protected, design to full Arctic Class 7 requirements is not necessary. Arctic Class 2 requirements, therefore, have been used in the shafting design to provide the necessary strength against the impact of the ice allowed through the bottom grills.

Also, as it is proposed to use CP propellers, hollow shafting will be required to accommodate the pitch change hydraulics. The Finnish-Swedish Ice Class Rules require that if the inner diameter exceeds 0.4d, then the outer diameter must be increased so that the section modulus is not less than for a solid shaft.

The shafting will be sized using a basic stress analysis approach and then it will be checked against the Classification Society Regulations.

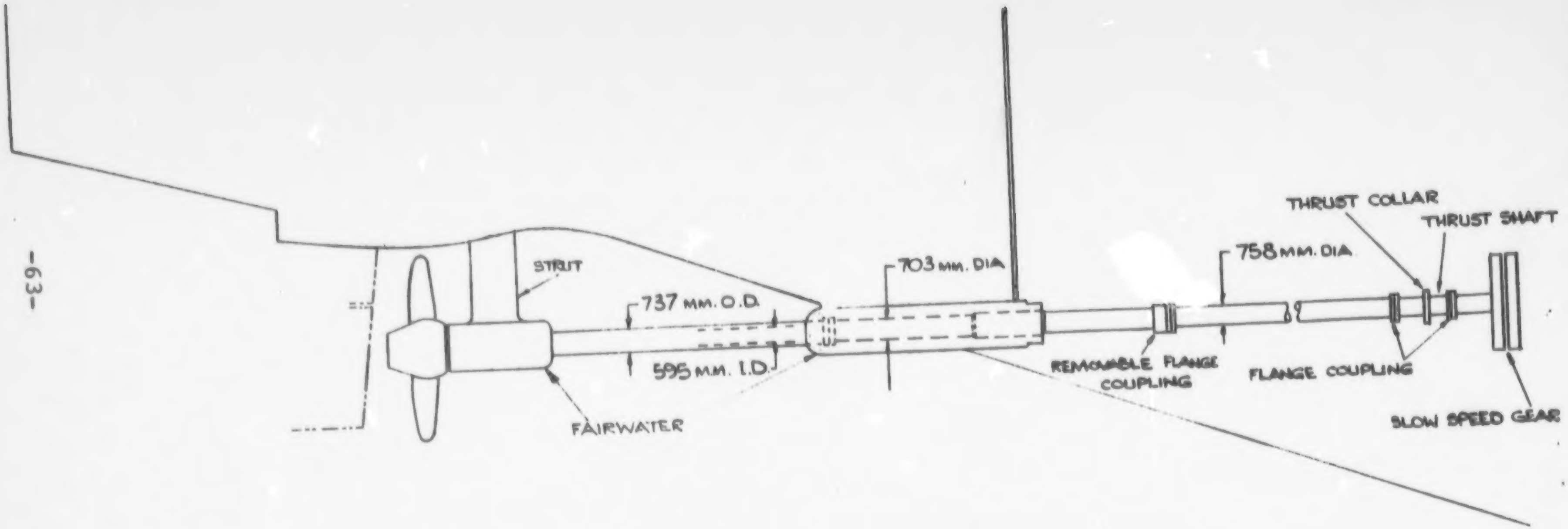
THRUST COLLAR
THRUST SHAFT
703 MM. DIA
758 MM. DIA
STRUT
737 MM. O.D.
595 MM. I.D.
FAIRWATER
REMOVABLE FLANGE COUPLING
FLANGE COUPLING
SLOW SPEED GEAR

FIGURE 5.1 SHAFTING MAIN DIMENSIONS

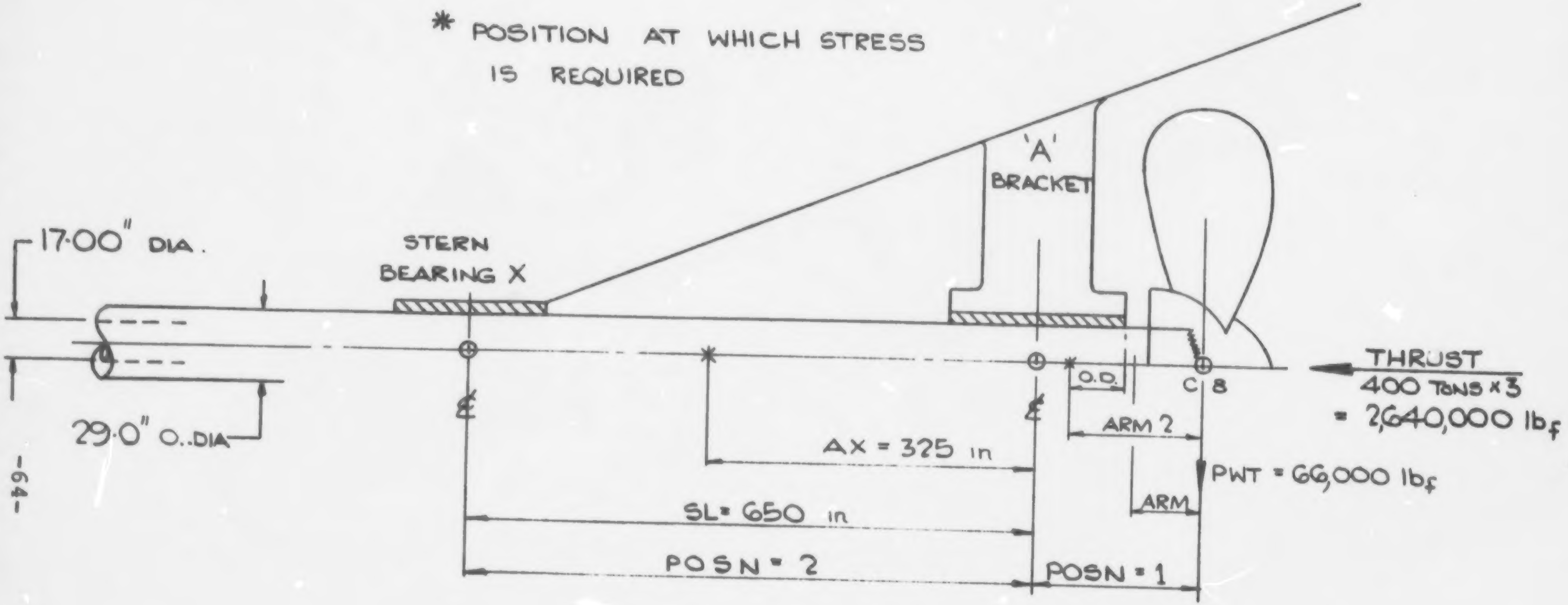
* POSITION AT WHICH STRESS IS REQUIRED
17.00" DIA.
29.0" O..DIA
STERN BEARING X
'A' BRACKET
O.D.
C 8
THRUST
400 TONS x 3
= 2,640,000 lbf
ARM 2
PWT = 66,000 lbf
ARM
AX = 325 in
SL = 650 in
POSN = 2
POSN = 1

NOTE
BEARING AT X COULD BE AN ADDITIONAL 'STRUT' BEARING ON LONG SHAFT SHIPS.

FIGURE 5.2 - Sketch of the Shafting Arrangement for the Computer Program

5.3 Shafting Preliminary Stress Analysis

The method used here in calculating the stresses in the propulsion shaft is that outlined in the BuShips Design Data Sheet DSS4301 (Jan. 1960).

Calculations of "steady" and "alternating" stresses are carried out. The bending stress multiplied by the estimated stress concentration factor (SCF) yields the maximum bending stress, and this should not exceed 6000 psi. The design torque is taken as 20% in excess of full power torque. The factor of safety is determined by combining the steady and alternating stress. The fatigue limit and yield stress are assumed 34,000 and 49,000 psi respectively.

A FORTRAN program was written and run out on our PDP11/03 computer to perform the above computations. Figure 5.2 shows a sketch of the arrangement with the different variables required by the program. The output results of two runs (two different stress points, one between the propeller and 'A' bracket and the other at midspan between the 'A' bracket and the sterntube bearings) are shown in Figures 5.3 and 5.4. The maximum bending stresses at the two selected sections are 5906 psi and 1381 psi which are less than the maximum allowable bending stress of 6000 psi. The factors of safety are 2.4 and 3.4 for the two outboard sections. A tailshaft O.D. of 737 mm (29.0 inches) and I.D. of 432 mm (170 inches) was required to achieve these safety factors.

```
07-AUG-81                                                          15:27:05
                     SHAFT STRESS ANALYSIS
                     ---------------------

 INPUT DATA
 ----------

    SHAFT OD:  29.000 inch  SHAFT ID:  17.000 inch  PROP.WT.:  66000.0  lbf
    ARM1:    40.625  inch    ARM2:    71.875  inch    POSN: 1.
    THRUST: 2640000.00 lbf  SHP:    50000.00         RPM:    150.00
    NO. SHAFTS: 3.

    STRESS CONC. FACTORS   FATIGUE LIMIT: 34000.00 BEARING SPAN(SL):  650.000
     KB:1.68    KT:1.31    YIELD POINT: 49000.00   AX:   25.000

 RESULTS
 -------

    SHEAR STRESS       THRUST PER SHAFT                 STEADY RESULTANT
        5968.               880000.                          12107.

    BENDING STRESS          ALTERNATING RESULTANT   SAFETY FACTOR
        5906.                5958.                    2.3679
```

FIGURE 5.3 - Shaft Stress Results,
Position 1

```
07-AUG-81                                                        15:27:48
                    SHAFT STRESS ANALYSIS
                    ---------------------

 INPUT DATA
 ----------

    SHAFT OD:  29.000 inch  SHAFT ID:  17.000 inch  PROP.WT.:  66000.0 lbs
    ARM1:    40.625 inch    ARM2:    71.875 inch    POSN: 2.
    THRUST: 2640000.00      SHP:    50000.00        RPM:    150.00
    NO. SHAFTS: 3.

    STRESS CONC. FACTORS   FATIGUE LIMIT: 34000.00 BEARING SPAN(SL):  650.000
     KB:1.68     KT:1.31   YIELD POINT: 49000.00   AX:  325.000

 RESULTS
 -------

    SHEAR STRESS        THRUST PER SHAFT                STEADY RESULTANT
       5966.                 880000.                         12107.

    BENDING STRESS           ALTERNATING RESULTANT     SAFETY FACTOR
       1381.                  1587.                      3.4042
```

FIGURE 5.4 - Shaft Stress Results, Position 2

5.4 Shafting Dimensions by the Classification Society Regulations

5.4.1 Canadian Regulations CASPPR

*Propeller Shaft

$$d = 1.15\sqrt[3]{\frac{S_u WT^2}{S_y}} \quad \text{cm}$$

S_u = ultimate tensile stress of propeller material
≃ 100,000 psi

S_y = yield stress of the propeller shaft
≃ 49,000 psi

$$WT^2 = \frac{2108}{S(0.65 + 0.7P)} \left(\frac{272H}{RN} + 23.45M\right) \text{cm}^2$$

M = ice torque
= MD^2
≃ $30.1\ (6.5)^2$ = 1271.7 Kn.m (Class 7)
≃ $17.7\ (6.5)^2$ = 747.8 Kn.m (Class 2)

H = S.HP in K. Watts
= 50,000 * 0.746
= 37300 KW

R = 150 r.p.m.

N = No. of blades
= 4

P = mean pitch ratio
= 0.7
S = 100,000 psi
= 689.3 megapascal
WT^2 = 125360.22 cm^3 (Class 7)
= 49225 cm^3 (Class 2)
Therefore d = 730 mm (Class 7)
= 533 mm (Class 2)

*Intermediate and Thrust Shafts

$$d = \sqrt{\frac{D^2\ S\ WP}{C\left(\frac{D^2}{H^2} + 2\right)}} \text{ inches}$$

"d" is to be increased by 20% for Class 7 and by 8% for Class 2

"d" need not be increased more than 73.0 mm (Class 7) or 53.5 mm (Class 2)

d (intermediate shaft) = 690 mm)
d (thrust shaft) = 650 mm) Class 7

and

d (intermediate shaft) = 500 mm)
d (thrust shaft) = 520 mm) Class 2

5.4.2 Lloyds 1975, Ice Class 1*

*Intermediate and Thrust Shaft Diameters

The intermediate shaft diameters for Ice Class 1 are to be increased by 12% above the value given by

$$d = 25.4\ C\ \sqrt[3]{\frac{H}{R}\left(\frac{60}{T+16}\right)} \text{ mm}$$

H = 50,000 HP

$R = 150$ r.p.m.

T = minimum tensile strength

$\approx 44 \text{ Kg} / \text{mm}^2$

$C = 3.5$ (for turbines and electric propelling motors)

Therefore $d = 616.4$ mm

Therefore

$d_{\text{intermediate}}$ (for ICE CLASS 1*) $= 1.12 \times 616.4 = 690.4$ mm

and for the thrust shaft diameter

$$d_{\text{thrust}} = 1.1 \times d_{\text{intermediate}} = 759.4$$

*Screw Shaft

The diameter of the propeller shaft is not to be less than given by the following formula.

$$\begin{aligned} d &= cd \\ &= 1.236 * 616.4 \\ &= 761.4 \text{ mm} \end{aligned}$$

The diameter of the screw shaft for Ice Class 1* is increased by 20%.

$$d_s = 1.2 * 761.4 = 913.7 \text{ mm}$$

5.4.3 Finnish-Swedish Ice Class 1A Super

Screw Shaft Diameter

$$d_s = 11.5 \sqrt[3]{\frac{\sigma_b . Ct^2}{\sigma_y}} \text{ mm}$$

$$Ct^2 = \frac{2.15}{\sigma_b \ (0.65 + 0.7 \ H/D)} \quad \left(20{,}000 \ \frac{S.\ HP}{Z.N} + 23000 \ M\right)$$

$$M = m \ D^2$$

$$= 2.15 \ (6.5)^2 = 90.84$$

$$\text{Therefore} \quad Ct^2 = \frac{2.15}{\frac{100000}{14.7 \times 100} \quad (0.65 + 0.49)} \quad \left(20{,}000 \ \frac{50{,}000}{4 \times 150} + 23000 \times 90.84\right)$$

$$= 104129.8$$

$$\text{Therefore} \quad d_s = 625.6 \text{ mm}$$

$$\text{Therefore} \quad d_s \ (\text{Ice Class 1A Super}) = 1.2 * \ 625.6 = 750 \text{ mm}$$

Intermediate and Thrust Shafts

The intermediate shaft diameter for Ice Class 1A Super is to be increased by 10% from that required by the rules.

$$d_{\text{intermediate}} = 1.1 * 625.6$$

$$= 699.2 \text{ mm}$$

$$d_{\text{thrust}} = 1.1 * d_{\text{intermediate}}$$

(d_{thrust} need not be increased more than 710 mm)

Therefore $d_{thrust} = 1.1 * 688.2$

$= 757$ mm

taken $= 710$ mm

5.4.4 ABS - Class IAA

* The Line and Thrust Shafts

The least diameter of line shafts and thrust shafts using Grade 2 steel, as determined from the following equations is to be increased by at least 10% for class IAA.

$$d = c^{3} \sqrt{H/R} \quad \text{mm}$$

H = SHP at rated speed 50,000 HP

R = 150 r.p.m.

C = 89.0 lineshaft
  = 101.5 thrust shaft

Therefore,

$$d_{\text{lineshaft}} = 89^{3} \sqrt{50000/150} = 617 \text{ mm}$$

$$d_{\text{thrust shaft}} = 101.5^{3} \sqrt{50000/150} = 704 \text{ mm}$$

The shafts are to be increased by 10% for Class IAA

$$d_{\text{lineshaft}} = 1.1 * 617 = \underline{\underline{680}} \text{ mm}$$

$$d_{\text{thrust shaft}} = 1.1 * 704 = \underline{\underline{774}} \text{ mm}$$

* Intermediate Shafts

- including stern tube shaft and any other shafts between the thrust shaft and propeller shaft.

The least diameter is $1.2 * d_{\text{lineshaft}} = 1.2 * 680$

$$= \underline{\underline{815}} \text{ mm}$$

and if, for the stern tube shaft, it is sea-water lubricated, then the diameter of the stern tube shaft is not to be less than $1.23 \times d_{\text{lineshaft}} = 835$ mm

* Tail Shaft (propeller shaft)

least diameter $= 1.236\, d_{\text{lineshaft}}$

$= 1.236 \times 679$

$= \underline{\underline{840}}$ mm

* Propeller Weight

$W = kD^3\ (\text{MWR})\ (\text{BTF})$ lb. (manganese bronze)

k = constant = 0.26

D = propeller diameter (inches)

MWR = mean width ratio

$$= \frac{\text{developed area per blade}}{D\ (\text{blade radius} - \text{hub radius})} \approx 0.332$$

BTF = blade thickness fraction

$$= \frac{\text{max. blade thickness extrapolated to shaft axis}}{D} \approx 0.045$$

Therefore W = 30,000 kg

The propeller weight given by KAMEWA for a 4-blade, 6.5 m CP propeller is 32,000 kg.

Couplings and Bolts

The minimum diameter of the shaft coupling bolts is:

$$d = 0.57 \sqrt{D^3/Nr} \quad \text{mm}$$

D = shaft diameter in mm

N = number of bolts fitted in one coupling

r = radius of pitch circle in mm

Now, for shafts say 840 mm, and use 8 bolts with a pitch circle radius of say $1.05 \frac{D}{2} = 882$ mm

Therefore,

$$d = 0.57 \sqrt{840^3/(8 * \frac{1.05 * 840}{2}} \quad = \quad 234 \text{ mm}$$

Notes:

When couplings are separate from the shaft, provision is to be made to resist the stern pull.

The thickness of lineshaft coupling flanges is not to be less than the minimum diameter of the coupling bolts, i.e. 240 mm.

The fillet radius at the base of the flange is not to be less than 1/8 of the shaft diameter, i.e., 110 mm.

5.4.5 Conclusions

Table 5.1 indicates the wide variation in the Classification Society requirements for Arctic Class 7 or equivalent solid and hollow shafting.

With the propulsion system fully protected by the proposed propeller protection scheme, it is reasonable to suggest compliance with the strength requirements of the CASPPR for a lower Arctic Class, e.g., Arctic Class 2. The shafting dimensions for this case are also shown in Table

It must be noted that the section modulus of the propeller shaft, for example, as obtained by the stress analysis calculations is about 2.3 times that required by the CASPPR Class 2. The bearing span, bending moment distribution along the propeller shaft, propeller weight, and specified allowable stresses are the main factors behind this discrepancy. At this stage of design, the dimensions obtained by the stress analysis calculations are adopted, with the other components of shafting being scaled up by the same ratio.

If the requirements of CASPPR for Ice Class 2 were complied with instead of Ice Class 7, due to the protection scheme, a reduction of over 30% could be achieved in the shafting dimensions, as shown in Table 5.1.

	CASPPR Arctic Class 7	ABS Ice Class 1AA	Lloyds Ice Class 1*	Finish - Swedish Ice Class 1A Super	CASPPR Arctic Class 2
Propeller Shaft (mm)	730	840	914	710	535
Intermediate Shaft (mm)	650	815	691	689	510
Line Shaft(mm)	650	680	710	689	510
Thrust Shaft (mm)	690	775	760	710	525

TABLE 5.1-A SOLID SHAFTS

	O.D.	I.D.	O.D.	I.D.	O.D.	I.D.	O.D.	I.D.	O.D.	I.D.
Propeller Shaft (mm)	765	459	880	528	958	574	744	447	561	337
Intermediate Shaft (mm)	681	409	854	513	724	435	722	433	535	321
Line Shaft (mm)	681	409	713	428	744	447	722	433	535	321
Thrust Shaft (mm)	723	434	812	487	796	478	744	447	550	323

TABLE 5.1-B HOLLOW SHAFTS (I.D. = 0.6 O.D.) WITH THE SAME SECTION MODULUS AS IN TABLE 5.1-A

5.5 Strut and Sterntube Bearings

The arrangement of the strut and sterntube bearings is shown in Figure 3.6 (DE 1492). It is proposed that both bearings be water lubricated, thus avoiding any possibility of pollution due to leakage from oil lubricated bearings.

Split bronze bearing bushes retain the bearing elements which can be configured in either conventional segmental staves or as four pads. Phenolic composition staves are readily available under several proprietary names and are proposed for this installation. The bore of the bush would be accurately machined in the first instance so that bearing staves can be fitted without the need for further boring to maintain alignment or provide running clearances.

A full shafting arrangement of inboard and outboard bearings would be required to allow calculations to be completed to determine accurate bearing loads. From a survey of previous designs, a guideline of twice the propeller weight gives an approximation to the strut bearing load. Using a bearing pressure of 55 tons/m^2 (80 lb/in^2) and a load of 60 tons, the required area is 1.1 m^2. For a diameter over the liner of 765 mm, the bearing effective length required is 1441 mm, which is approximately an L/D ratio of two. As is generally the case, the requirements for the strut dimensions increase the length of the barrel beyond the requirements for the bearing. For the sterntube bearing, an L/D ratio of one keeps bearing pressures well within design limits.

5.6 Whirling Frequency Analysis

Whirling vibration of propulsion shafting has received considerable attention in recent years. Most of the recent analytical methods include some critical parameters such as the stiffness of the thrust bearing and the size of the masses attached to the shaft in the vicinity or on the other side of the thrust block.

Detailed methods can be found in a number of publications, but for the purpose of preliminary calculations in the present design stage of the propulsion shafting system, a simple approach based on the Panagopulos method will serve our purpose.

The shaft is assumed of uniform diameter of density 0.28 lb/in^3 and modulus of elasticity of 30×10^6 psi. The bearings are considered infinitely stiff. The after (strut) bearing is considered a simple support and the forward bearing a fixed support. Figure 5.6 shows the printout of the results. The critical whirling natural frequency is 256.9 r.p.m. which is well above the shaft design speed of 150 r.p.m. Thus the proposed bearing span is acceptable.

```
07-AUG-81                                                        15:29:28


                    WHIRLING FREQUENCY ANALYSIS
                    ---------------------------


        INPUT DATA
        ----------

        PROP. WT.=66000.0  lbf          PROP. DIAM.= 256.000  inch
        OUTER SHAFT DIAM.=29.0 inch     INNER SHAFT DIAM.=17.0 inch
        PROP. OVERHANG= 40.625 inch     BEARING SPAN=650.000  inch
        DENSITY=  0.280  lb/inch³       MOD OF ELASTICITY= 0.30E+08 psi


        OUTPUT DATA
        -----------

        SHAFT FLEXURAL RIGIDITY =  0.91856E+12
        PROP ANGULAR INERTIA EFFECT =   92259768.0000
        PROP VERTICAL MOTION EFFECT =   83591784.0000
        SHAFT MASS EFFECT =  0.42197E+12

                THE WHIRLING FREQUENCY IS    0.256914E+03
```

FIGURE 5.5 - Whirling Frequency Results

6.0 MANEUVERING DEVICES

6.1 Types of Maneuvering Devices

The requirements for good maneuverability of an icebreaker are clearly much more demanding than those for ordinary merchant ships. The icebreaker often encounters heavy ice that is sometimes impossible to negotiate, even at full power. In this situation, the icebreaker will ram at full power, reverse until it is free and then ram again. The process will continue until the icebreaker is able to proceed. The ice condition may be so severe (iceberg or ice island) that the icebreaker will be forced to change course.

Another situation requiring good maneuverability is the case when the icebreaker is cutting free ships that are immobilized in the ice. In this situation the icebreaker will move in a seesaw manner around the ship until the ice is loose enough for the ship to get started again.

As indicated abcve, a fundamental requirement in a polar icebreaker is the ability to readily proceed astern and this may not be always through precut ice. Rudders,if unprotected, become very vulnerable to ice damage when the vessel is going astern. The rudder size, strength and protection involve at best a compromise. The hull shape of an icebreaker normally would require a proportionally larger rudder. The desired dimensions of a rudder can rarely be obtained since it must be located below the ice belt to minimize the danger of hitting solid ice when backing. Furthermore, the fore and aft dimensions must be limited to reduce the rudder torque when backing with the rudder off centre.

A full ice horn (or ice shoe) is sometimes constructed to provide partial protection for the rudder. However, damaged rudders, twisted rudderstocks and damaged steering gears are common occurrences to icebreakers while backing in heavy ice.

6.1.1 Rudders

The MANHATTAN was equipped with twin rudders, one abaft each of her twin 23 feet diameter propellers. A metal pad was fitted between the upper edge of the rudders and the hull to prevent ice from jamming them. The rudders were of a floating type and were canted outwards at an angle of 15 degrees from the vertical. The fitment of the metal pad mentioned above restricted the rudder angles to 5 degrees in ice. With this maneuvering arrangement, her maneuverability was judged to be very good for her size (124,000 DWT). At 5 degrees helm and 12 knots in light ice conditions, her tactical diameter was about two miles (1). Her maneuverability, however, in 6-8 feet of "broken" ice was poor for several reasons. Manhattan's speed under these conditions was about 6 to 7 knots and frequently, less. Also, her helm was restricted to 5 degrees because of the limitation of ice protection fitments and her beam to length ratio was unfavourable (1/6) for course alterations in ice (shortest possible length is required). Another reason was the low power/displacement ratio of about 0.3 which is about ten times smaller than what is usually recommended for polar icebreakers.

A basic development in the design of the steering gear for a POLAR 10 icebreaker has been suggested in reference (10).

The design incorporates an explosive-type relief valve which will release the rudder and allow movement to the "hard over" position against stops mounted on the ship's hull in only 1/10 second.

6.1.2 Bow Rudders

For the sake of completeness, the "bow rudder" concept is discussed briefly below as a possible maneuvering device, although its application for icebreakers is certainly out of the question.

It is known that if a lateral force is applied at a "neutral" point, a ship follows a straight path at angle of attack which depends on the magnitude of the force. Thus, it would be of considerable use to a navigator if he could cause a force to be applied at any selected point along the ship's length, i.e. he could control ship's head and path independently. This could be achieved if control surfaces were fitted at both ends of the ship. Also, if the only rudders fitted are those aft, there is a greater danger that damage could render the ship uncontrollable.

Against these considerations, it must be remembered that because the neutral point is fairly well forward (about one-sixth of the length of the ship abaft the bow), forward rudders at the bow are relatively much less effective. Neither can they benefit from the effects of the screw race (for a rudder behind the propeller, the inflow velocity is usually augmented by 30% over the ship's ahead speed). Unless they are well forward and therefore exposed to damage, the flow conditions over the bow rudder are unlikely to be good.

These factors generally outweigh the possible advantages given above and only a few bow rudders as such are fitted to ships in service. For icebreakers, one always tries to keep risks to a minimum, and fitting a bow rudder for such vessels will undoubtedly increase that risk and may result in serious forebody damage unless the rudder is fitted well below the underside of the ice sheet where it will then be less effective. The bow rudder also interferes with the bow operation as a smooth cutting tool. The idea, therefore, will not be considered further.

6.1.3 Thruster Units

At low or zero ship speed, the rudder has little or no effect as a maneuvering device, and therefore a complementary device to the rudder is required to improve the ship's maneuverability.

The thruster unit is a propelling device installed in the bow and /or the stern of a ship to produce a force in the transverse direction.

Thruster units are by no means a new concept for ship maneuvering. The technique had been known for more than a century, although it did not come to a practical application until the early 1950's.

Typically, such a device is a propeller (4-bladed fixed or controllable pitch) in a transverse tunnel. The general layout of a thruster unit is shown in Figure 6.1. The main components of the unit are:

1. Bevel gear: specially designed with ever-increasing power transmission capabilities.

2. Rolling-contact bearings: necessary to maintain the proper alignment of bevel gears. Materials and method of manufacture are critical parameter of the design.

Type FM is equipped with a fixed pitch propeller. Type CM is equipped with a controllable pitch propeller.

These types cover a horse-power range from 70 HP for FM 1 up to 2500 HP for CM 16 and FM 16.

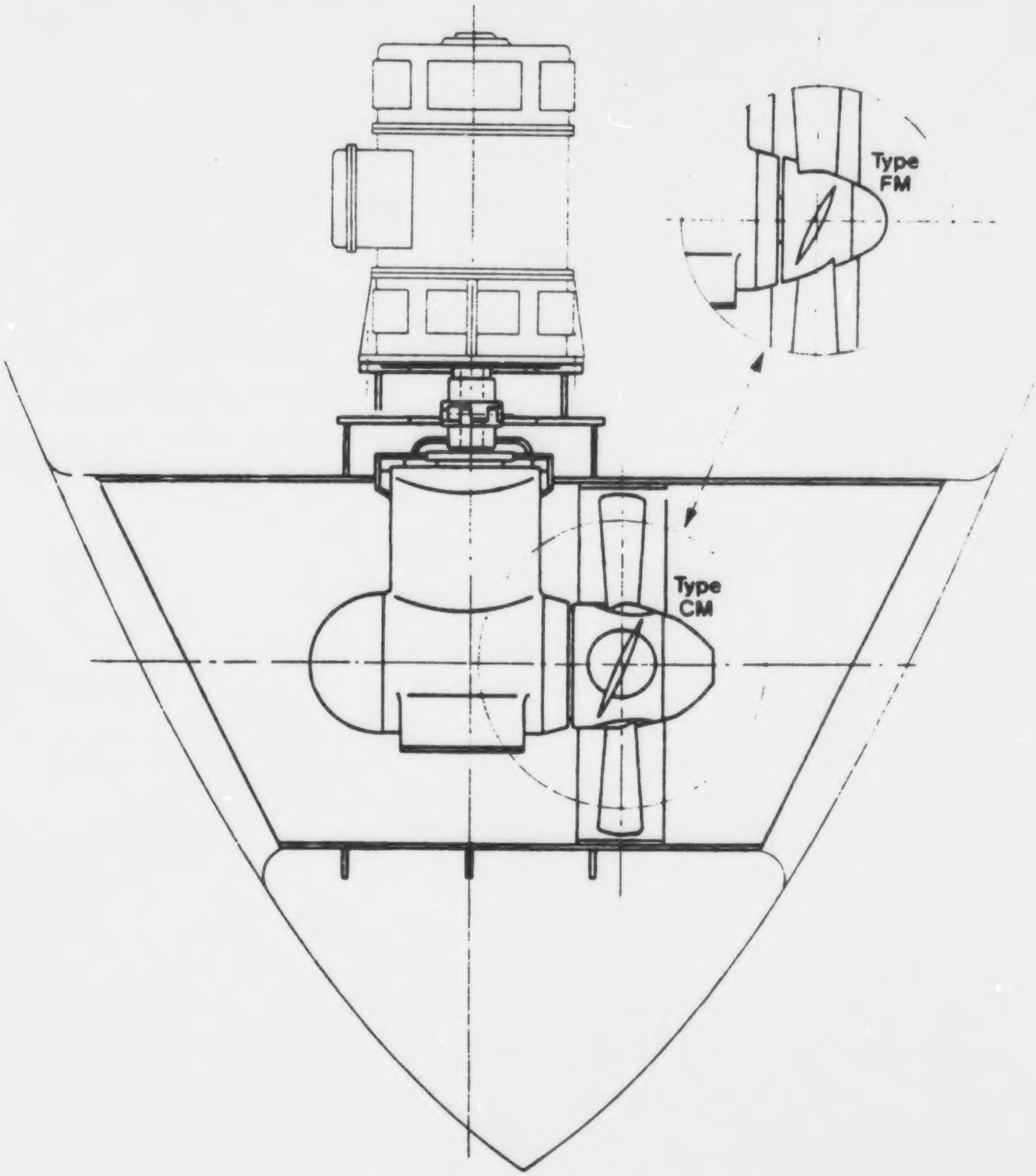

FIGURE 6.1 - General Layout of a Thruster Unit

3. Seals: Lip seal technology developed by mid 1950's is widely used in today's applications.

4. Tunnel: the tunnel is reinforced with rings and must be welded into the structural members of the ship. Normally the tunnel is fitted with a seating on top to which the driving motor can be fitted. Lips use a stainless steel ring welded in the tunnel in way of the propeller.

5. Prime mover and Propeller Unit: the selection of prime mover and propeller design are closely interelated. In a recent KaMeWa thruster installation (2200 HP bow thruster, and 1500 HP stern thruster for a 265,000 tdw tanker) the controllable pitch propeller is driven by an electric motor mounted vertically. The driving shaft is coupled using an elastic coupling. The motor is constant speed, non-reversing type. Any type of uni-directional constant speed prime mover can be used, e.g. diesel engines, gas turbines, hydraulic motors, or alternators. Lips transverse propeller (thruster) can be mounted with the driving shaft vertical or horizontal. Lips have used both fixed and controllable pitch propellers in their thruster installations. The fixed pitch propeller unit can be driven by diesel engines or gas turbines with reverse reduction gear, dc electric motors with stepped speed control or diesel-electric installation system. Ref. (16) recommended contra-rotating propeller system for thruster units.

The design specifications and dimensions of a thruster unit vary from one application to another. The thrust required by the transverse propeller is a function of the above and under-water lateral areas and the type of ship (passenger ship, tug, tanker or icebreaker). For a passenger ship, the above-water lateral area is often three times the under-water area due to the relatively large super-structure. The thrust is usually based in this case on the above-water area.

For icebreakers, the vessel is deep-draughted and consequently, the lateral under-water area could be twice or more times the above-water area. For these vessels, it is reasonable to base the thrust required by the transverse thruster on the under-water area. The thrust ratio suggested and used by Lips is 5 - 9 kg/m^2 * (14). The horse power of the driving system is about 85 HP/ton thrust (or 100 HP/1.2 ton thrust). The diameter of the tunnel ranges between 545 mm for FM1 Lips (75 HP) to about 2755 mm for FM16 or CM 16 Lips (2500 HP). The tunnel wall thickness ranges between 8 mm and 20 mm for FM1 and FM16 or CM16 respectively. The design of the KaMeWa steering propeller (transverse thruster) differs slightly from that of Lips. It consists of a controllable pitch propeller driven by a prime mover supplying a power of about 100 HP per ton thrust. KaMeWa uses a thrust ratio of 3-8 kg/m^2 in their designs. The tunnel diameter ranges between 1106 mm (for 350 HP) to 3300 mm (for 3500 HP) with standard electric motor voltages of 3*380V/50 cycles, 3*440V/60 cycles or 3*550V/60 cycles. The tunnel wall thickness ranges between 22 mm and 35 mm (15).

---

* Usually, for each type of ship, there are two ratios to estimate the required thrust per unit projected lateral area; one based on the above-water area and the other on the under-water area. These ratios were obtained from both model tests and full scale measurements. For each design the two ratios may be tried and the greater of the two should be adhered to.

6.1.4 Steering Nozzles

The steering nozzle is a maneuvering device which is integrated with the propulsion system. It is in a sense a duct which can be rotated around the propeller plane. The duct can be designed so that the advantages of a flow accelerating nozzle are obtained, particularly that with regard to thrust augmentation at near-bollard pull conditions. In addition, the steering nozzle can provide superior turning forces by diverting the entire jet stream. For applications in ice, the exclusion of the rudder is certainly an advantage. In addition, since the performance of a ducted propeller is extremely sensitive to its position on a particular hull, there is a clear indication of the benefits to be derived from the steering duct which gives more flexibility in the positioning of the duct relative to the hull.

The prime disadvantages of the device lies in the higher vulnerability of the nozzle to damage. Furthermore, adequate propeller protection in ahead and astern operations is not possible with the steering nozzle arrangement. Partial protection may be provided by ice knives and deflector rings mounted ahead of the steering nozzle (17).

At high speeds and when going astern, this type of system becomes less effective, because of increased drag, loss of propulsive efficiency and increased risk of nozzle and/or propeller damage by ice.

6.1.5 Rudder - Nozzle Combination

To render the steering nozzle more effective, a rudder may be fitted to the nozzle and thus, can be rotated with it as one unit around the propeller plane.

Although the rudder lies in an already deflected flow, it can still produce a lateral force which contributes to the turning momentum and thus, improves the overall maneuverability of the vessel. The creation of such a lateral force on the lifting surface (i.e. rudder) requires some explanation. In a potential flow, the rudder with zero angle of incidence does not produce a lift force. However, due to the propeller/rudder interaction, different pressure distributions are created on both sides of the rudder. The resulting net pressure multiplied by the rudder area constitute the lateral force. Since the magnitude and direction of this force depends on the propeller direction of rotation, therefore, a rudder/nozzle maneuvering device with propeller rotating in one direction (CPP) will be more effective in steering the vessel to one side than to the other. With a fixed pitch propeller, this effectiveness of the maneuvering device is reversed when the ship is going astern.

Although the rudder/nozzle maneuvering device may be attractive for some applications, it is certainly not for Arctic class vessels. The vulnerability of both the nozzle and the rudder to ice damage makes the device unsuitable for ice operations.

6.2 Protection of Maneuvering Devices

Among the various types of maneuvering devices discussed in the previous section, stern rudders and thruster units (bow and/or stern) are clearly the most promising devices applicable to Arctic class vessels provided that adequate protection schemes can be implemented. This section is concerned with the protection requirements of such arrangements.

6.2.1 Protection of Rudder and Steering Gears

Unprotected rudders of Arctic class vessels are most likely to sustain serious damage especially when the ship is going astern in solid or even precut ice. Canada's Arctic Shipping Pollution Prevention Regulations does not specify the ice conditions that a particular class of Arctic vessel is supposed to operate under, neither does it make reference to speed of advance under which ice is broken. Failure to select the proper speed of advance will certainly result in extensive damage to the hull and appendages (rudder) in particular regardless of the extra heavy scantlings called for by ASPPR. Therefore, high Arctic class vessel steering gear and/or rudder may be irreversibly damaged in such a hostile environment and the vessel rendered uncontrollable. A positive means to avoid the serious consequences of such a failure is to install auxiliary steering gear capable of being readily connected to the tiller and commissionable from the wheelhouse immediately when failure of the main unit is discovered. Although ASPPR calls for such an installation, MV ARCTIC, for example, is not equipped with an auxiliary steering gear (17). It is reasonable to suggest that this requirement by ASPPR might not be necessary or applicable to low Arctic class vessels such as MV ARCTIC (Class 2).

The auxiliary steering gear mentioned above replaces the main unit in case the latter sustains failure or damage. There are, in addition, some devices which can still be installed to reduce the risk of damage in the first place. A shock-sensing device for steering gear can be used to monitor shock transmitted to the rudder stock and steering gear. A hydraulic oil dump valve can be incorporated, as in the case of KIGORIAK Class 3 icebreaker, to allow the rudder to move from centre to hard over in the event of severe ice torque, thus protecting the stock and/or steering gear. The duration of such movement was estimated as 1/10 second (10)*. There are two major problems in designing such relief valves. First, since the steering gear in heavy duty vessels (icebreakers) are of the electrohydraulic type, the pressure build-up of the fluid has to be appreciable before the relief valve operates. Therefore, rudder, rudder stock, and steering gear may sustain damage before excess pressure in the hydraulic circuits is relieved. Second, sensing accurately when the hydraulic pressure has to be relieved is absolutely essential in the design of the circuit. Further, monitoring a system which will dump an appropriate volume of oil instantaneously to prevent damage to the steering components has yet to be accomplished satisfactorily (17).

Using a relatively small diameter retractable locking pin seems an inexpensive and practical way to protect the rudder when the ship is going astern (see Fig. 6.2). The rudder is brought to the centre and the power is disconnected from the steering gear before the pin is inserted. Some designers, however, consider the centre locking pins to be hazardous as they increase the danger that the rudder stock might twist. Dome Petroleum, for example, ruled out any form of internal stopper since extensive damage has been done to the rudders and steering gears of Dome vessels fitted with internal stopper systems (6).

---

*This figure has to be proven in the actual operating conditions.

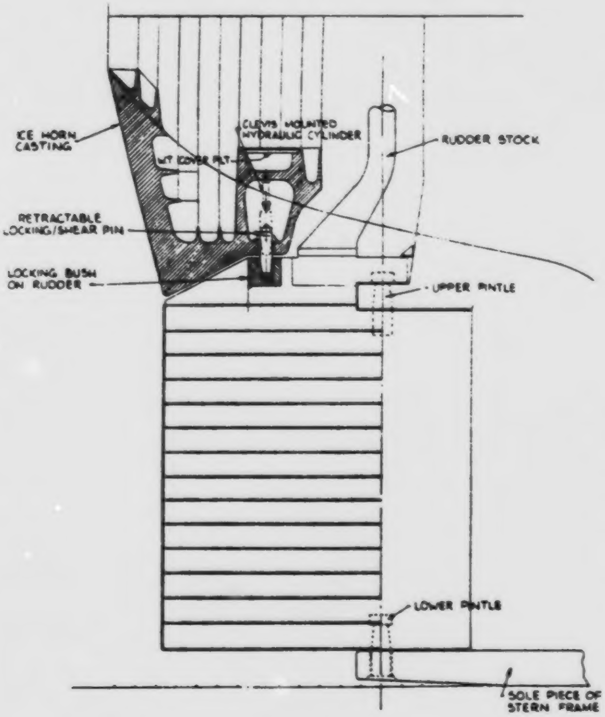
ICE HORN CASTING
CLEVIS MOUNTED HYDRAULIC CYLINDER
RUDDER STOCK
WT COVER PLT
RETRACTABLE LOCKING/SHEAR PIN
LOCKING BUSH ON RUDDER
UPPER PINTLE
LOWER PINTLE
SOLE PIECE OF STERN FRAME

FIGURE 6.2 - Rudder Locking Pin for Astern Operation by Arctic Class Vessels (Ref. 17)

All Arctic class vessels according to Canada's Arctic Shipping Pollution Prevention Regulations "CASPPR" must be provided with an ice horn (or ice knife) to protect the rudder from damage by ice (see Figure 6.2). Ice should be prevented from wedging between the top of the rudder and the ship's hull.

The above-mentioned emergency systems and protection devices namely auxiliary steering gears, relief valves, locking pins and ice horns cannot prevent the rudder from sustaining ice impacts in a manner which would produce excessive torque on the rudderstock. Therefore, the CASPPR requires that scantling of rudders, rudderposts, rudderstocks, pintles and steering gear of every Arctic class vessel must be based on a higher design speed specified by the regulations for each Arctic class. The design of the different components of a steering system for an Arctic Class 7 vessel, for example, must be based on a speed of 26 knots as required by CASPPR (18).

Finally, the rudder must be reinforced in direct proportion to the ice reinforcement required for the stern area plating. The weakest section of a conventional rudder lies in way of its trailing edge. One possible reinforcement for an arctic-type rudder is that shown in Figure 6.3 (modified from Ref. 17). The conventional round bar forming the trailing edge is replaced by a heavy cast section oriented vertically. The horizontal stringers are extended beyond the aerofoil contour and terminate at the forward end of the trailing edge casting. The side platings are rounded at the trailing edge to produce a "fishtail". This configuration enhances the hydrodynamic characteristics of the rudder for a number of reasons (17). The extended horizontal stringers, for example, arrest the secondary flow across the sides of the rudder and by doing so, the normal force is increased. In addition, the fishtail endings produce a high lift coefficient. As a result, course stability is improved while smaller helm angle can be employed to maintain a given course.

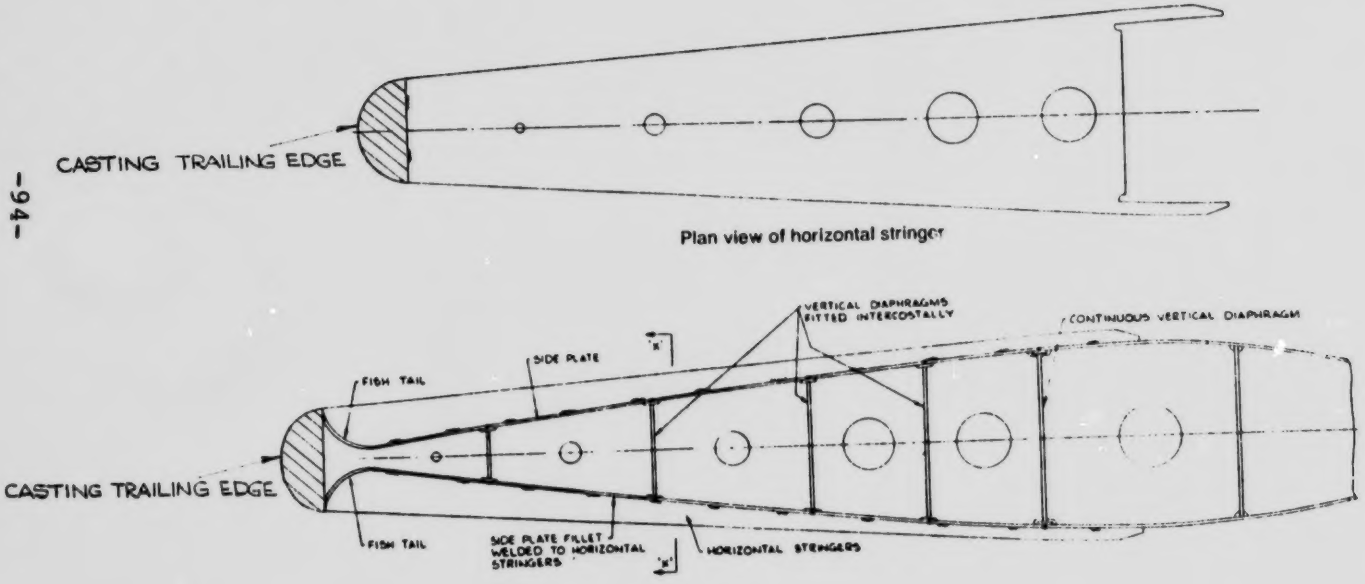
CASTING TRAILING EDGE
Plan view of horizontal stringer
VERTICAL DIAPHRAGMS FITTED INTERCOSTALLY
CONTINUOUS VERTICAL DIAPHRAGM
FISH TAIL
SIDE PLATE
'X'
CASTING TRAILING EDGE
FISH TAIL
SIDE PLATE FILLET WELDED TO HORIZONTAL STRINGERS
'X'
HORIZONTAL STRINGERS

FIGURE 6.3 - Possible Reinforcement for an Arctic-Type Rudder

Past icebreaker designs have incorporated a flap rudder amidships with a small area. This, however, does not lend itself to the high maneuverability which is desirable for icebreakers. For a triple-screw vessel, a semibalanced rudder is a better choice. Tests (13) have shown a significant difference in maneuvering characteristics between semibalanced and flapped rudders. Locating the rudder in the propeller flow will also increase directional stability which is poor for icebreaker forms. Protection of the rudder against ice impact and ice jamming is also important. An ice shoe to protect the upper surfaces of the rudder during backing should be built into the stern.

6.2.2 CASPPR - Rudder and Steering Gear

The requirements of the Canadian regulations are as follows: (18, item 11).

1. Rudders, rudderposts, rudderstocks, pintles and steering gear of every Arctic class ship shall comply with the Hull Construction Regulations.

2. When calculations are being made for the strength of the rudders, rudderposts, rudderstocks, pintles and steering gear referred to in subsection 1, the speed of an Arctic class ship shall be deemed to be the speed set out as shown in the following Table.

Arctic Class	1	1A	2	3	4	6	7	8	10
Speed, knots	16	18	20	22	22	24	26	26	26

3. Where it can be shown that the maximum operating load on a rudder of a ship is greater than the load calculated by using the speed set out in the above table, the rudder, rudderpost, rudderstock, pintles and steering gear shall be designed for the higher load.

4. The main steering gear of an Arctic class ship shall be fitted with a shock absorbing device and shall be capable of moving the rudder from 35 degrees on one side to 30 degrees on the other in $\sqrt{2L}$ seconds, where L is in feet.

5. Every Arctic Class ship shall, in addition to a main steering gear, be fitted with an auxiliary steering gear capable of being readily connected to the tiller and, in the case of a ship with twin rudders operated by a single steering gear, shall be equipped so that each rudder can be readily disconnected and secured.

6. Every Arctic Class ship shall be fitted with ice horns directly abaft each rudder in such a manner that:

   a) the upper edge of the rudder is protected within two degrees port and starboard of mid-position when going astern; and

   b) ice is prevented from wedging between the top of the rudder and the ship's hull.

7. The rudder sideplating for every Arctic class ship shall be reinforced for ice in direct proportion to the ice reinforcement for the stern area plating.

6.2.3 Protection of Thruster Units

For icebreakers, where the icebreaking velocity (continuous velocity) is relatively low, usually about 3 knots for a successful design (13), the rudder has little or no effect. The dimensional constraints and clearances required at the afterbody of an icebreaker do not usually allow an effective protection system to be applied to a normal size rudder.

Bow and/or stern transverse thruster units, similar to those fitted to normal ships, are considered to be a promising solution to the above-mentioned difficulties encountered by icebreakers. As previously mentioned, they are complementary devices to the rudder, which in this case may be reduced in size to be accommodated in a reasonable protection system (Section 6.3).

KIGORIAK, an Arctic Class 3 icebreaker, is fitted with a bow and a stern thruster unit (Lips design). The prime function of these thrusters for KIGORIAK is to facilitate the dynamic positioning of the tug as a requirement for anchor handling operations. It was reported (6) that these thruster units are capable of holding KIGORIAK reasonably steady in open water in 30 knot beam winds.

These thrusters are located in the box keel as shown in Figure 6.4. There is no data available as to the performance of KIGORIAK thrusters at low or zero speed of advance in ice-covered waters.

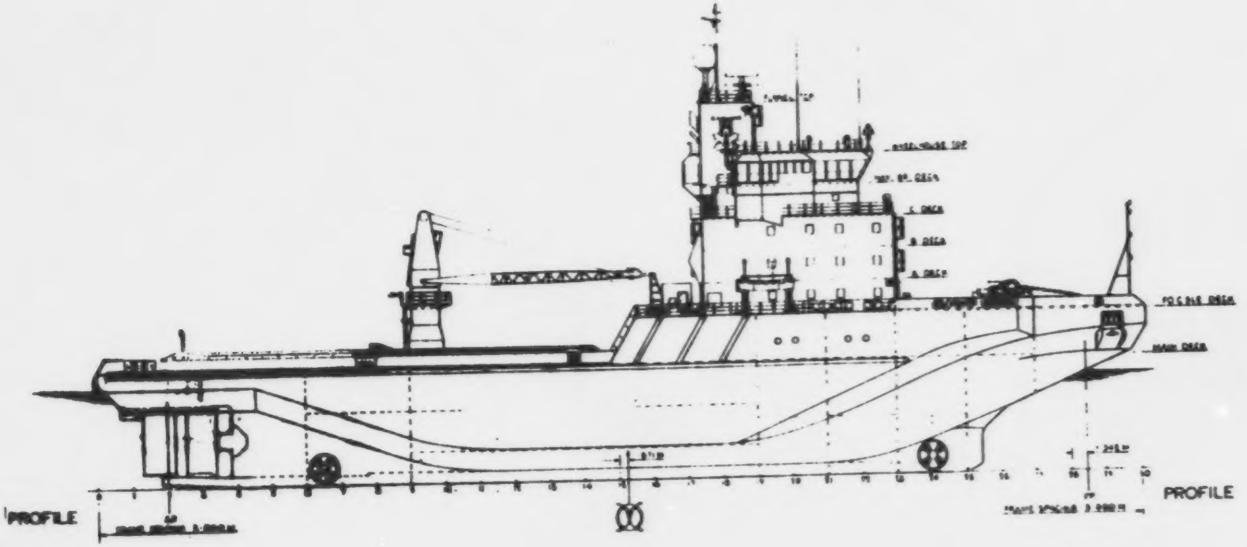
C DECK
B DECK
A DECK
FO'C'SLE DECK
MAIN DECK
PROFILE
PROFILE

FIGURE 6.4 KIGORIAK

However, it is believed, based on model data of thrusters in open waters, that their effect may be seriously reduced when the ship has forward speed. The fall in side force may amount to nearly 50% at 2 knots; 40% occurring between 1 and 2 knots. In this case, if the bow and stern thrusters are identical, then one would expect the stern unit to be more effective than the one at the bow. This is as a result of the lower water velocity at the after body due to the wake effect. The foregoing observations can realistically be generalized to include operation in light and moderate ice conditions provided that the thruster units are fitted well below the surface; as in the case of KIGORIAK , for example.

For higher class icebreakers, however, factors such as special hull design or special bow shape (e.g. unconventional hull form), propeller protection scheme (e.g. in hull propulsion system) and operational conditions (e.g. heavy ice) should be considered carefully in the strength requirements of the thruster components and in the general arrangement of the unit. Propeller blades, tunnel wall, bevel gear (gear box) strength, hub and driving shaft pitch mechanism (for CP propellers), propeller motor seating structure and propeller streamlined stays would have to be extra strong for this type of vessel if the thruster unit is not protected. The radial tip clearance between the blade tips and the inner surface of the tunnel is about 0.5% of the diameter of a thruster unit fitted into normal vessels.

The bow thruster must be located as far forward and as near the keel as possible to be more effective. If it is too far forward, however, it will interfere structurally with the specially designed bow and thus, reduce the effectiveness of the latter and, as a result, reduce the icebreaking capability of the vessel.

Also, placing it too deep might result in some structural problems beside increasing its vulnerability to damage by grounding in heavy ice which is likely to happen more frequently in higher Arctic zones. Such damage may result in serious hull damage and may incapacitate the icebreaker. Another consideration is the submergence of the thruster tunnel to operate satisfactorily and free of cavitation, the tunnel centreline should be located at least one diameter below the water surface. For operation in ice covered waters, the submergence should be measured from the underside of the ice sheet. Usually the location of a thruster unit is a compromise based on the manoeuvering requirements and the icebreaking capability of the vessel.

From the foregoing observations, it is clear that some kind of protection is required for thrusters fitted to higher Arctic class vessels to ensure safety of operation. The obvious arrangement would be that of protection guards fitted at the inlet and outlet of the thruster tunnel to protect the propeller from getting in contact with large fragments of ice. These guards could be similar to the stern guards used for the main propeller/rudder arrangement in our proposed in-hull propulsion systems(3). These protection guards could be made flush with the hull surface so that the additional resistance caused by them would be kept to a minimum.

The radial clearance for the icebreaker application should certainly be higher than the 0.5% diameter commonly used for normal ship thrusters. With the thruster protection arrangement in place, the tunnel inflow will still contain small pieces of ice, the size of which depends on the openings in the grillage structure of the protection system. Tip clearance should be large enough to allow such pieces to pass freely. A gap of about 2.5% diameter is reasonable for icebreaker applications.

Finally, to reduce the cross flow when the thruster unit is not in operation, a controllable pitch propeller is recommended.

6.3 Recommended Manoeuvering Device for POLAR 7A - In-hull Stern Rudders

The most vulnerable items to ice damage in an icebreaker are the outboard components of the propulsion systems (i.e., propeller, nozzle, strut bearing, etc.) and the steering system (i.e., rudder, rudderpost, rudder stock, steering gear, etc.). Propeller protection schemes were discussed in Volume I report (3).

To comply with safety (or protection) requirements of the steering system, two fundamentally different approaches can be outlined.

First Indirect protection schemes which aim at protecting the rudder system and steering gear system from damage due to ice impact during ahead and astern operations. This scheme requires:

- reinforced rudder(s);
- heavy scantlings of rudderpost, rudderstock, pintles, and steering gear;
- auxiliary steering gear;
- shock-sensing relief valve or locking pin, and
- ice horn(s)

Second Direct protection schemes which aim at preventing the rudder system from contacting large fragments of ice.

The first scheme has been dealt with extensively in the foregoing sections.

The second scheme, direct protection, involves the enclosure of each rudder in a tunnel which is protected by guards at both ends. By doing so, the rudder system and steering system are fully protected. Figure 3.12 (Drawing DE 1495) shows such a rudder arrangement together with the in-hull propulsion system for one shaft of the proposed triple-screw 150,000 SHP POLAR 7 icebreaker. Three semi-balanced identical rudders are recommended, one in each tunnel. Each rudder is placed in the propeller race with enough clearance between the blades and the horn and between the rudder trailing edge and the tunnel stern guards. The ice impact loads are expected to be mitigated considerably for such an arrangement with guards fitted to the intake and discharge apertures. The prime function of fitting these bottom and stern guards is to eliminate ice milling of the propeller, and to reduce ice ingestion and ice impact loads on both the propeller and rudder system in ahead and astern operations. The grill fitted to the bottom intake need not be as robust as the grill used aft of the rudder, since impact between ice pieces and bottom grill will be less severe. The rudder structural details are given in Section 6.5.

Finally, it must be noted that since the recommended arrangement provides an adequate protection to the rudder system, it is possible to apply the Class 2 standards in the design without sacrificing reliability in service.

6.4 Rudder Area and Force

6.4.1 General

The area of the rudder is usually determined as an arbitrary proportion to the under water central area given by L * T where L is LBP and T is draft. For merchant ships over 400 feet long the area of the rudder is about 2% L*T. For smaller ships, it may increase to about 3% for a 100 ft. ship. Sea-going tugs may have a rudder area of 4% and harbour tugboats could have a rudder area of 6 to 8%.

From the hydrodynamic point of view, a deep narrow rudder is more effective than a shallow wide rudder of the same area. The steering qualities of the hull itself have as much to do with manoeuverability as does the size of rudder.

In addition to rudder area and shape, the transverse location of the rudder is of considerable importance. A rudder located in a propeller race encounters high flow velocities and consequently, develops greater lift than a rudder outside the propeller race.

Rudders for icebreakers, however, encounter more severe loads due to ice impact and open water design rules should be regarded as guidelines only, subject to modifications. More important, there are clear indications in the literature that strength specifications for rudders and steering gear systems for ice-class vessels are understated by the shipping classification societies. The rules requirements, however, will be followed with reasonable changes until field tests verify the proper design.

Finally, it is worth stating that for an icebreaker fitted with a suitable rudder protection system, the strength requirements for a lower ice class can be complied with instead.

6.4.2 Rudder Area

The principal dimensions of the proposed 150,000 SHP POLAR 7 icebreaker (POLAR 7A) are given in Section 3.4 and the recommended in-hull rudder arrangement is discussed in Section 6.3.

For open water with L = 200 m and T = 14.03 m, the rudder area of 2% will be 56.12 m^2. DET NORSKE VERITAS (DNV) 1975, on the other hand, requires the rudder area to be derived from the expression:

$$\text{Rudder area} = \frac{TL}{100} \left(1 + 25 \left(\frac{B}{L}\right)^2\right) \ m^2$$

T = draft 14.03 m

B = beam 35.157 m

L = LBP 200 m

Therefore, rudder area = 49.7 m^2

This rudder area is to be used with an augmented propeller race velocity of 1.3 times ship's ahead speed. With the recommended in-hull rudder arrangement, the propeller jet velocity is likely to be much higher than that for an open rudder. Therefore, it is reasonable to apply a smaller rudder area of about 30m^2 with the velocity of water past the rudder of about 1.75 times ship speed in order to produce the same turning moment. Since three rudders are used, one behind each propeller, then each rudder area is about 10 m^2.

6.4.3 Rudder Force

The rudder being of streamlined cross-section will be acted upon by a lift and drag force when held at an angle of attack relative to the flow of water. In order to improve the manoeuverability of a ship, the rudder must be designed to produce maximum lift for minimum drag.

The lift developed depends upon:

- The cross-sectional shape;
- The area of the rudder;
- The profile shape of the rudder and, in particular, the aspect ratio of the rudder, i.e. the ratio of the depth of the rudder to its chord length;
- The square of the velocity of the water past the rudder;
- The density of water;
- The angle of attack.

The basic dynamic flow formula of forces on rudders is given by

$$F_R = C_R \frac{\ell}{2} A_R V_R^2$$

where C_R is the total force coefficient for angle of attack.

Many formulae have been suggested for calculating the forces on the rudders.

(a) Reference (16) gives rudder force by one of the older formulae as:

$F_R = 577\ A_R\ {V_R}^2 \sin(\delta_R)$ Newtons

A_R = rudder area = 10 m^2

V_R = the velocity of water past the rudder (allowance must be made for the propeller race and the protection arrangement in augmenting the ship's ahead speed)

$\approx$ 1.3 ship speed

= 1.3 * 16 = 20.8 knots = 10.7 m/sec

δ_R = stall angle (hard-over angle) = 35^o

$F_R \approx$ 38.6 tons

(b) Another formula given in the same reference (16) for ahead motion:

$F_R = 21.1\ A_R\ {V_{ship}}^2\ \delta_R$ Newtons

$A_R = 10\ m^2$, V_{ship} = 8.23 m/sec (16 knots), $\delta_R = 35^o$

Therefore, ahead motion force $\approx$ 51 tons

For astern motion:

$F_R = 19.1\ A_R\ {V_{ship}}^2\ \delta_R$ Newtons

$\approx$ 46 tons

(c) Baker and Bottomley formula:

$F_R = 18.0\ A_R\ V^2{}_R\ \delta_R$ Newtons, V_R in m/s

$\simeq$ 43 tons

(d) Ship design and construction, SNAME:

$F_R = 196\ A_R\ V^2$ Newtons, V = ship speed in knots

$\simeq$ 50 tons

(e) DNV, 1975, Section 18,B:

$F_R = 5(H^2{}_R + 2A_R)V^2\ k_g$, V = ship speed in knots

where,

H = rudder mean height $\ngtr \sqrt{2A_R} = 4.47$

$F_R \simeq 51$ tons

(f) CASPPR:

When calculations are being made for the strength of the rudders, the speed of an Arctic Class ship shall be deemed to be the speed set out in Section 6.2.2 for the same class number.

For the proposed POLAR Class 7 icebreaker, the design speed according to CASPPR should be 26 knots. However, with the rudder fully protected, it is reasonable to suggest, as previously mentioned, to base the strength calculations on a lower Arctic class, e.g., Arctic Class 2. The design speed in this case will be 16 knots.

6.5 Rudder Arrangement and Structural Details

As previously stated, with the rudders fully protected in in-hull tunnels, the current open-water practice, together with minimum ice strengthening requirements, can be adopted without sacrificing reliability in service.

6.5.1 General Description

Figure 6.5 (Drawing DE 1495) shows the general arrangement of the proposed rudder/propeller/tunnel configuration in one of the three tunnels.

The rudder is of a semi-balanced type supported on horn using one pintle. Bearings can be made either of reinforced laminated phenolics or white metal. In order to reduce friction and consequently, reduce steering gear size, it is possible to install anti-friction rudderstock inboard bearings. Such bearings would degrade rapidly in sea water and must be protected by carefully designed seals if used at the hull (e.g. rudder-stock lower bearing) or outboard (e.g. pintle) so that bearings can be kept in oil or grease with no sea water intrusion. The tapered fit between the rudder and rudderstock, plus the nut at the bottom of the rudderstock, provide structual continuity.

The keys at the lower end of the rudderstock transmit the torque. An erosion plate is shown at the rudder leading edge below the fixed rudder horn for resisting possible cavitation impingement from the propeller trailing vortex system and also for providing additional protection against impact by small ice pieces contained in the propeller slipstream. The external rudder stopper provides metal-to-metal contact to protect the steering system in case of damage. The rudder horn is a casting and provides support for the pintle.

The dimensions and clearances of the schemes, as shown in the same drawing (DE 1495), are carefully chosen to permit disassembly in a drydock. Removable plates are used below the pintle nut and stock nut to facilitate the disassembly.

An NACA 00XX airfoil section is adopted for the rudder with a leading edge casting and a round bar forming the trailing edge. The maximum thickness (XX) is taken as 22% of the length at the top and 15% at the bottom connected by straight lines in between. The maximum thickness of these symmetrical NACA 4-digit series occurs 30% aft of the leading edge.

The structure of the rudder consists of vertical and horizontal webs covered by plating. The internal surfaces are to be covered by a corrosion-resistant coating.

6.5.2 Rudder Scantlings

The Canadian Arctic Shipping Pollution Prevention Regulations (CASPPR), for rudders and steering gears, are given in Section 6.2.7.

The following is the summary of the calculation:

Rudder force $N = 50,000$ kg.
Rudder torque $Q = 1.38\times10^{6}$ kg.
$d = 230$ mm
$d_v = 234$ mm
Rudder plating thickness = 22 mm

S = smaller distance between the horizontal or the vertical web plates
= 400 mm

The strength requirements by Lloyds Register of Shipping yields

d = 285 mm (ahead)
= 189 mm (astern)

Rudder plating thickness t = 13.5 mm

Lloyds Ice Class 1*, for unprotected rudders, requires that in no case should the design speed be taken less than 20 knots (similar to DNV, Class 1A*). The diameter of the rudderstock at and below the lowest bearing is calculated as d = 390 mm. The minimum thickness of rudder plating is calculated as t = 17 mm.

With regard to rudder side plating, the CASPPR requires that for every Arctic class ship, it should be reinforced for ice in direct proportion to the ice reinforcement required for the stern area plating. The thickness of the shell plating, as required by CASPPR, should not be less than the spacing of the main frames multiplied by a factor. To comply with CASPPR, the shell plating thickness at the aftbody of an Arctic Class 7 icebreaker should not be less than 19.8 mm, assuming ice pressure of 1050 psia, material yield stress of 200,000 psi, and frame spacing of 410 mm. The rudder side plating, therefore, should not be taken less than 19.8 mm thick.

On the other hand, the Finnish-Swedish Regulations require that the minimum thickness of rudder plating, and horizontal and vertical webs in the ice belt region is to be taken as for the shell plating in the aft region. The thickness of the shell plating, however, according to the Finnish-Swedish Regulations depends on the type of framing. With transverse framing, the minimum thickness is at least 17 mm (ordinary steel of 24.0 kg/mm^2 yield stress) or at least 8.5mm (high tensile steel of 140.0 kg/mm^2 yield stress). The thickness of the shell plating associated with longitudinal framing is calculated as 17.3 mm and 8.4 mm for the two types of steel respectively.

From the above calculations, the diameter of the rudderstock is taken as 400 mm and the rudder side plating and horizontal and vertical webs are taken as 25 mm thick to comply with the different requirements of the various Rules. The spacing of the horizontal and vertical webs is taken as 400 mm. Finally, the closing side of the rudder plating must be welded entirely from the outside, and approved practice for that is shown in Figure 6.5.

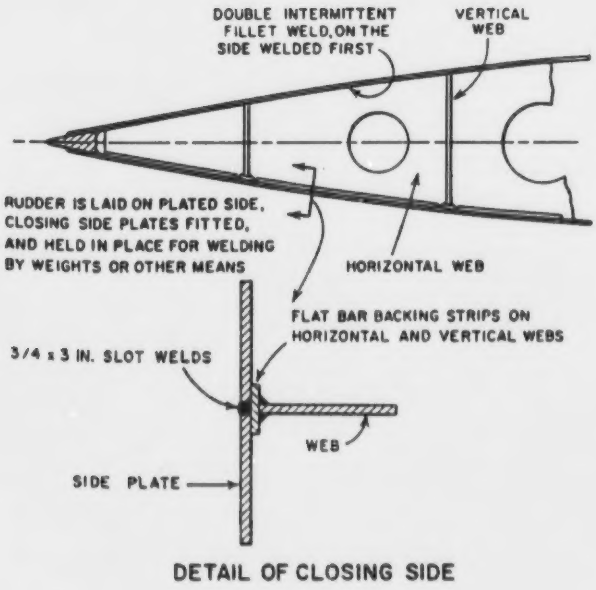
DOUBLE INTERMITTENT FILLET WELD, ON THE SIDE WELDED FIRST
VERTICAL WEB
RUDDER IS LAID ON PLATED SIDE, CLOSING SIDE PLATES FITTED, AND HELD IN PLACE FOR WELDING BY WEIGHTS OR OTHER MEANS
HORIZONTAL WEB
FLAT BAR BACKING STRIPS ON HORIZONTAL AND VERTICAL WEBS
3/4 x 3 IN. SLOT WELDS
WEB
SIDE PLATE
DETAIL OF CLOSING SIDE

FIGURE 6.5 - Attachment of Closing Side of Double Plate Rudder

REFERENCES

1. "Report on the Voyage in the Canadian Arctic of CCGS JOHN A. MACDONALD, Summer 1969, (MANHATTAN'S JOURNEY)", by Stolee, E.

2. "Ice Tech 75", Sumposium on Icebreaking and Related Technologies, Montreal, April, 1975.

3. "Protection of Propellers In Ice", Volume 1 - Assessment of Protection Schemes. Prepared by Davis Engineering Ltd., for Transport Canada Research and Development Centre, TP2704, August 1980.

4. "The Design and Building of Icebreakers", by Watson, A., Inst. Marine Engineers, V. 71, No. 2, p. 37-65, Februrary 1959.

5. "Application of Nuclear Power to Icebreakers", by Lank, S.W., and Oakley, O.H., Presented at the spring meeting on the St. Lawrence Seaway, June 1959, of the Society of Naval Architects and Marine Engineers.

6. "The CANMAR KIGORIAK - HULL 1132", by John Shepherd,Saint John Shipbuilding & Dry Dock Co., Ltd., Saint John, N.B., 1980.

   "Advanced Hull Design for New Dome Petroleum Icebreaker, Harbour & Shipping, November 1979.

7. "Resistance, Self Propulsion and Wake Survey Experiments with a Model of a Triple Arctic Class "7" Icebreaker, Model "299", NRC, LTR-SH-196, September 1976.

8. "The Development of Arctic Sea Transportation", by Edwards, R.T., Jr., MTS Journal, Volume 4, No. 5, 1969-1970.

9. "Icebreakers and their Design", by Jan-Erik Jansson, European Shipbuilding, No. 6, 1956.

10. "AML-Arctic Class 10 Icebreaker - Research, Design and High Risk Components", Dome Petroleum Ltd., Calgary, Alberta, March, 1978.

11. "Development of Ice-Breaking Vessels for the U.S. Coast Guard", by Johnson, H.F. Trans-SNAME, 1946, Vol. 54, pp. 112-151.

12. "Construction of the POLAR STAR - A Shipyard View Through Launch", by Wm. R. Nodell, Lockheed Shipbuilding & Construction Co., U.S.A. , 1974.

13. "The Design of Polar Icebreakers" by L.C. Melberg, J.W. Lewis, R.T. Edwards, R.G. Taylor and R.P. Voelker.

14. "Lips Transverse Thruster Reference Lists" - Lips Publication, Drunen, Holland.

15. "KaMeWa Steering Propellers", M-288-E.9.1976, Sweden.

16. "Basic Ship Theory", Volume 2, by K.J. Rawson and E.C. Tupper.

17. "Design of Steering Gears, Rudders, Rudderstocks, and Propeller Protection for Canadian Arctic Class Vessels", by N.V. Laskey, Marine Technology, Vol. 17, No. 3, July, 1980, pp. 267-280.

18. "Canada's Arctic Shipping Pollution Prevention Regulations" - CASPPR, Chapter 353.

19. "On Propulsion of Icebreakers", by K. Airaksinen and M. Marttila, Oy Wartsila A.B., Helsiniki, Finland, 1976.

20. "Longitudinal Stiffness Analysis for the Propulsion Shafting Systems of the Polar Class Icebreakers", by L. Vassilopoulos and F.M. Hamilton, Naval Engineering Journal, April 1980.

21. "Externally Pressurized Stern Tube Bearing" by R.H.F. Dillon, Transport Canada Research and Development Centre (TDC), July 1979.

22. "ICE TECH '81", STAR Symposium, SNAME, Ottawa, June 1981

APPENDIX A

Proposed Test Plan

15.12.1980
Revised 5.1.1981

PROTECTION OF PROPELLERS IN ICE

Proposed Test Plan

In light of the discussion we had at NRC on Friday, December 12, 1980,(those present were: Mr. Livingstone, Mr. Michaelidis, and Dr. George) the following model construction and test plan is proposed.

(1) Digitizing and fairing the lines plans for the triple screw model by NRC will start mid January, 1981. Time allocated for this activity is roughly two weeks.

(2) Model cutting, smoothing, painting and manufacture of the appendages (perspex or similar) followed by fixing shafts and dynamometers, manoeuvring devices, etc. This activity will take about six weeks to complete.

(3) 1st Stage of Testing: Model 299A

(a) Free running resistance tests in open water, ahead and astern, with the protection device in place and all other appendages as well, such as propeller shafts, rudders, bottom and stern guards, ... etc.

(b) Nominal wake survey at the three propeller locations. Spherical head Pitot tubes are used to measure the three velocity components (axial, tangential, and radial components). This is essential for LIPS to refine their propeller design. The wake survey should be carried out for two speeds corresponding to the following:

i) open water speed of about 16 knots; and,
ii) speed in ice condition of about 4 - 5 knots.

(c) Review results from resistance tests and assess performance of propeller protection device. Re-run resistance tests with revised design of guards, if required.

(4) 2nd Stage of Testing:

(a) With the wake survey results from the first stage of experiments, LIPS will be able to define their propeller design package. The package should include number of blades, blade series, propeller diameter, hub diameter ratio, thickness and camber distribution, rake and skewback, thickness fraction ratio, propeller drawings, propeller open water characteristics in design and off-design conditions, cavitation number and propeller submergence, and any other propeller-related data such as direction of rotation for the three propellers, propeller estimated weight, ... etc.

(b) NRC will manufacture three propellers in accordance with the data supplied by LIPS.

(c) Self-propulsion tests both in open water and in simulated ice conditions will be carried out in both ahead and astern directions.

(d) Ice flow is photographed for some selected runs.

(5) Summary of the results obtained from the two stages of experiments.

(a) Nominal wake distribution (mainly axial and tangential) at the three propeller locations and mean nominal wake fraction.

(b) Model resistance and self-propulsion data, effective horsepower, QPC, thrust deduction factor, relative rotative efficiency (for the same thrust).

(c) Mean value of the effective wake fraction.

(d) Ice flow observation for same selected runs of the free running and self-propulsion tests.

(6) 3rd and Final Stage of Testing:

*In the light of the test results of the first and second stages, any necessary modifications suggested during the course of the experiments should be implemented at this stage. Some modifications might be essential to improve the overall performance of the model. For example, altering intake/propeller area ratio, or redesign the bottom grillage if the passage ways seem to be blocked by ice, or rearrange the longitudinal and transverse guards to increase the effectiveness in dispersing the ice pieces. Major alterations will be avoided to minimize the overall cost.

CA1
DTC 801
80
P661
V. 2
C. 2

MM

Library and Information Centre / Centre de Documentation (GSLA)
RECEIVED - REÇU LE
APR 7 1983
Transport Canada | Transports Canada

General Remarks

*The propellers must be modelled according to the full scale data supplied by LIPS.

For two geometrically similar propellers ($\lambda = 46$):

$$T_m = T_s \frac{\rho_2}{\rho_s} \frac{V^2{}_m}{V^2{}_s} \frac{D^2{}_m}{D^2{}_s}$$

$$= T_s \frac{\rho_m}{\rho_s} \frac{V^2{}_m}{V^2{}_s} 1/\lambda^2$$

and if the model and full size propeller are working at the same Froude number, then,

$$T_m = T_s \frac{\rho_m}{\rho_s} 1/\lambda^3$$

and if they have the same advance coeff, then:

$$N_m = N_{ship} \sqrt{\lambda}$$

So, for a 6.5 meter full scale propeller, running at 150 r.p.m., the self-propulsion of 1:46 scale model will be carried out with 14.13 cm propeller rotates at about 1017 r.p.m.

Volume

3

TP 2704

Prepared For The
TRANSPORTATION DEVELOPMENT CENTRE
Transport Canada

[illegible] Engineering [illegible]
consulting engineers

v.

Library and Information Centre/
Centre de Documentation (GSLA)
RECEIVED - REÇU LE
APR 7 1983
Transport Canada / T.

CA1
DTC801-
80
P661
v.
3
C. 1

41.D

386444

PROTECTION OF PROPELLERS IN ICE

VOLUME III

TEST RESULTS, ANALYSIS, AND DISCUSSION

Prepared For:

TRANSPORT DEVELOPMENT CENTRE
TRANSPORT CANADA

Prepared By:

DAVIS ENGINEERING LIMITED
CONSULTING ENGINEERS
OTTAWA, ONTARIO

AUTHORS: Dr. M. F. George
Mr. F. R. Livingstone

JANUARY 1983

REPORT DOCUMENTATION FORM

1. Transport Canada Report No. TP 2704	2. TDC Project No. 8951	3. Recipient's Catalogue No.
4. Title and Subtitle PROTECTION OF PROPELLERS IN ICE VOLUME III - TEST RESULTS, ANALYSIS AND DISCUSSION		5. Report Date JANUARY 1983 6. Performing Organization Report No. C323
7. Author(s) F.R. Livingstone, M.F. George		8. Transport Canada File No. D500-566-1
9. Performing Organization Name and Address Davis Engineering Ltd. 1481 Cyrville Rd., Ottawa, Ontario. K1B 3L7		10. DSS File No. 18 ST.T8200-8-8557 11. DSS or Transport Canada Contract No. OST79-00047
12. Sponsoring Agency Name and Address Transportation Development Centre 100 Sherbrooke Street, West, Montreal, Quebec H3A 2R3		13. Type of Report and Period Covered TECHNICAL 14. Sponsoring Agency Code TDC 8951
15. Supplementary Notes		16. TDC Project Officer R.H.F. DILLON

17. Abstract

This report analyses the results obtained from a series of ship model tests designed to evaluate the performance of a Propeller Protection scheme for Polar Class Icebreakers.

A conventional triple-screw Icebreaker hull form with no protection was designated as the "Parent Model" for comparison purposes. Based on a design described in the Volume I and Volume II reports, a model incorporating full propeller protection was constructed and tested.

Initial tests showed that the model had high resistance compared to the parent model. A series of resistance tests were then conducted and recommendations made for reducing the resistance.

Self-propulsion tests were also conducted and a comparison of the QPC's showed that up to 12 knots the model with protection had a higher QPC than the parent but this reversed at higher ship speeds.

The series of model tests highlighted the problem areas associated with providing complete propeller protection. However, the assessment of performance is very dependent on the ship speeds considered and thus the mission profile of the vessel.

18. Key Words Ship, Icebreaker, Propeller, Blade, Protection, Guard, Ice	19. Distribution Statement Limited number of copies available from sponsoring agency

20. Security Classification (of this report) Unclassified	21. Security Classification (of this page) Unclassified	22. No. of Pages	23. Price —

TDC/CDT 79-005

FORMULE DE DOCUMENTATION POUR RAPPORT

1. Nº du rapport Transports Canada
TP 2704

2. Nº de l'étude — CDT
8951

3. Nº de catalogue du destinataire

4. Titre et sous-titre
PROTECTION OF PROPELLERS IN ICE
Volume III - Test Results, Analysis and Discussion

5. Date du rapport
janvier 1983

6. Nº du rapport de l'organisme exécutant
C323

7. Auteur(s)
R.F. Livingstone, M.F. George

8. Nº de dossier Transports Canada
D1460-137

9. Nom et adresse de l'organisme exécutant
Davis Engineering Ltd.
1481 Cyrville Road
Ottawa (Ontario)
K1B 3L7

10. Nº de dossier — ASC
18ST.T8200-8-8557

11. Nº de contrat — ASC ou Transports Canada
0ST79-00047

12. Nom et adresse de l'organisme parrain
Centre de développement des transports (CDT)
1000 o., rue Sherbrooke
Suite 2421
Montréal, Québec H3A 2R3

13. Genre de rapport et période visée
Technique

14. Code de l'organisme parrain
CDT 8951

15. Remarques additionnelles

16. Agent de projet — CDT
R.H.F. Dillon

17. Résumé

Ce rapport analyse les résultats d'une série d'essais sur modèles réduits visant à mesurer le rendement d'un système pour la protection des hélices des brise-glace de cote arctique.

Une carène de brise-glace de type classique, équipée d'un bloc propulsif à 3 hélices sous aucune protection, a été étudiée pour servir de "témoin". Un modèle du concept décrit dans les tomes I et II, et comportant le système de protection préconisé, a été réalisé et essayé.

Les premiers essais avaient révélé que le modèle offrait une résistance à la marche supérieurs à celle du modèle témoin. Des essais ont donc été conduits pour mesurer cette résistances, et des moyens ont été proposés en vue de la réduire.

Des essais sur modèle automoteur ont également été faits et, par comparison du rendement propulsif obtenu, il a été constaté que le rendement du modèle protégé était supérieur à celui du témoin jusqu'à la vitesse de 12 noeuds mais, qu'au-delà, cette tendance s'inversait.

Ces essais sur modèle ont permis de cerner les difficultés reliées au système de protection totale du bloc propulsif. Cependant, le rendement reste tributaire des vitesses de marche du navire et, par conséquent, du rôle que celui-ci est appelé à jouer.

18. Mots-clés
Navire, brise-glace, hélice, pale, protection, carénage, glaces

19. Diffusion
Un nombre limité d'exemplaires est disponible au CDT

20. Classification de sécurité (de ce rapport)
non-classifié

21. Classification de sécurité (de cette page)
non-classifiée

22. Nombre de pages

23. Prix

CDT TDC 79-005

TABLE OF CONTENTS

LIST OF SYMBOLS
LIST OF TABLES
LIST OF FIGURES
EXECUTIVE SUMMARY

1.0 INTRODUCTION

2.0 DESCRIPTION OF MODELS

3.0 TEST PROGRAM

4.0 WAKE SURVEY: MODELS 299 AND 299B

- 4.1 General
- 4.2 Test Results
- 4.3 Discussion

5.0 RESISTANCE TESTS: MODELS 299 to 299E

- 5.1 General
- 5.2 Test Results
- 5.3 Discussion of Resistance Experiments
  - 5.3.1 Model 299
  - 5.3.2 Model 299B
  - 5.3.3 Model 299C
  - 5.3.4 Model 299D (Bare Hull)
  - 5.3.5 Model 399E

LIST OF SYMBOLS

BP	Taylor's propeller coefficient based on delivered horsepower
CA	Ship model correlation allowance
CDVOL	Power-displacement coefficient
CR	Specific residuary resistance coefficient
CTM(59)	Specific total resistance coefficient for the model at temperature 59° F
$CT-R(t_3)$	Coefficient of thrust excess in propulsion test at temperature t_3 °F (= applied towing force/$1/2\rho Sv^2$)
CTS	Specific total resistance coefficient for the ship
CTVOL	Resistance displacement coefficient $(R/1/2\rho v^2\nabla^{2/3})$
D	Propeller diameter
DELTA	Taylor's advance coefficient
ETAD, η_D	Quasi-propulsive coefficient
ETAH, η_H	Hull efficiency
ETAO, η_O	Propeller efficiency in open water
ETAR, η_R	Relative rotative efficiency
FN	Froude number $(v/\sqrt{gL})$
FNVOL	Speed-displacement coefficient $(= v/\sqrt{g\nabla^{1/3}})$
FP	Pull or towing force
G, g	Acceleration due to gravity
JOM, J	Advance coefficient of model test propeller in open water test
JOS	Advance coefficient for ship propeller in open water test

JP	Apparent advance coefficient for model in propulsion test
KQOM, KQ	Propeller torque coefficient of model test propeller in open water test
KQOS	Propeller torque coefficient for ship propeller in open water
KQP	Propeller torque coefficient in propulsion test
KTOM, KT	Propeller thrust coefficient of model test propeller in open water test
KTOS	Propeller thrust coefficient for ship propeller in open water
KTP	Propeller thrust coefficient in propulsion test
L	Length on waterline
LCB	Longitudinal position of the centre of buoyancy from midships of L, per cent of L
n	Propeller revolutions per second
NS	Shaft revolutions for ship, RPM
NVOL	Shaft revolution made dimensionless with respect to displacement (= $n\ \nabla^{1/3} g$)
P	Propeller nominal pitch
PD	Delivered power, horsepower
PDVOL	Delivered power-displacement coefficient (speed eliminated) (= $PD \times 550/\rho g^{3/2} \nabla^{7/6}$)
PE	Effective power, horsepower
S	Wetted surface area
TH	Thrust
THDF, t	Thrust deduction fraction
TAU	Resistance per unit displacement (= $R/\rho g \nabla$)
TAUR	Residuary resistance per unit displacement

TAUT	Thrust per unit displacement
V	Ship speed, knots
v	Speed
WFT, W_T	Taylor wake fraction
ZETO	Static thrust coefficient $(= T/(\rho\pi/2)^{1/3}P_D{}^{2/3})$
∇	Volume of displacement
ρ	Mass density of water

LIST OF TABLES

Table No.:	Title of Table:
2.1	Hydrostatic Particulars for Full Sized Ship, $\lambda = 46$
2.2	Propeller Description
3.1	Test Program
5.1	Results of Resistance Experiments Design, Model 299
5.2	Results of Resistance Experiments with Grills (Ahead) Model 299B
5.3	Results of Resistance Experiments with Grills (Astern) Model 299B
5.4	Results of Resistance Experiments without Grills (Ahead) Model 299B
5.5	Results of Resistance Experiments without Grills (Astern) Model 299B
5.6	Results of Resistance Experiments Design, Model 299C
5.7	Results of Resistance Experiments Bare Hull, Model 299D
5.8	Results of Resistance Experiments, Model 299E
5.9	Comparison of Effective Power at Three Selected Speeds
6.1	Results of Open Water Tests Propeller 56 L, R, C, Model 299
6.2	Results of Open Water Tests Propeller 74 L, R, C, Models 299C, 299E
7.1	Results of Propulsion Experiments Propeller No. 56 L, R, and C, Model 299
7.2	Results of Propulsion Experiments Propeller No. 56 L, R, and C, Model 299
7.3	Results of Propulsion Experiments Propeller No. 56 L, R, C, Model 299
7.4	Results of Propulsion Experiments Propeller No. 56 L, R, C, Model 299

7.5 Results of Propulsion Experiments Propeller No. 56 L, R, C, Model 299

7.6 Results of Overload Experiments Propeller No. 56 L, R, C, Model 299

7.7 Results of Overload Experiments Propeller No. 56 L, R, C, Model 299

7.8 Results of Overload Experiments Propeller No. 56 L, R, C, Model 299

7.9 Results of Overload Experiments Propeller No. 56 L, R, C, Model 299

7.10 Results of Propulsion Experiments Propeller No. 74 L, R, C, Model 299C

7.11 Results of Propulsion Experiments Propeller No. 74 L, R, C, Model 299C

7.12 Results of Propulsion Experiments Propeller No. 74 L, R, C, Model 299C

7.13 Results of Propulsion Experiments Propeller No. 74 L, R, C, Model 299C

7.14 Results of Propulsion Experiments Propeller No. 74 L, R, C, Model 299C

7.15 Results of Overload Experiments Propeller No. 74 L, R, C, Model 299C

7.16 Results of Overload Experiments Propeller No. 74 L, R, C, Model 299C

7.17 Results of Overload Experiments Propeller No. 74 L, R, C, Model 299C

7.18 Results of Overload Experiments Propeller No. 74 L, R, C, Model 299C

7.19 Results of Propulsion Experiments Propeller No. 74 L, R, C, Model 299E

7.20 Results of Propulsion Experiments Propeller No. 74 L, R, C, Model 299E

7.21 Results of Propulsion Experiments Propeller No. 74 L, R, C, Model 299E

7.22 Results of Propulsion Experiments Propeller No. 74 L, R, C, Model 299E

7.23 Results of Propulsion Experiments Propeller No. 74 L, R, C, Model 299E

7.24 Results of Overload Experiments Propeller No. 74 L, R, C, Model 299E

7.25 Results of Overload Experiments Propeller No. 74 L, R, C, Model 299E

7.26 Results of Overload Experiments Propeller No. 74 L, R, C, Model 299E

7.27 Results of Overload Experiments Propeller No. 74 L, R, C, Model 299E

7.28 Maximum Speed at Full Power in Clear Water

7.29 Comparison of Delivered Power at Three Selected Speeds

7.30 Comparison of Relative Rotative Efficiency, at 16 Knots

7.31 Effective Mean Wake Fraction, WFTT, at 16 Knots

7.32 Comparison of Thrust Deduction Factors, THDF, at 16 Knots

7.33 Summary Table

7.34 Comparison of Hull Efficiency at 16 Knots

7.35 Comparison of Propulsion Factors, at 16 Knots

A-1 Harmonic Analysis of the Wake Components, Centre Propeller, Model 299B

A-2 Harmonic Analysis of the Wake Components, Centre Propeller, Model 299B

A-3 Harmonic Analysis of the Wake Components, Centre Propeller, Model 299B

A-4 Harmonic Analysis of the Wake Components, Centre Propeller, Model 299B

A-5 Harmonic Analysis of the Wake Components, Wing Propeller, Model 299B

A-6 Harmonic Analysis of the Wake Components, Wing Propeller, Model 299B

A-7 Harmonic Analysis of the Wake Components, Wing Propeller, Model 299B

A-8 Harmonic Analysis of the Wake Components, Wing Propeller, Model 299B

B-1 Resistance Prediction of Full Scale Grills

C-1 Hydrostatics for Full Scale Ship, Scale : 46, Model 299F

C-2 Propeller Description, Model Propeller 74 L, R, C

C-3 Results of Resistance Experiments, Model 299F

C-4 Results of Propulsion Experiments, Propeller No. 74 L, R, C, Model 299F

C-5 Results of Propulsion Experiments, Propeller No. 74 L, R, C, Model 299F

C-6 Results of Propulsion Experiments, Propeller No. 74 L, R, C, Model 299F

C-7 Results of Propulsion Experiments, Propeller No. 74 L, R, C, Model 299F

C-8 Results of Propulsion Experiments, Propeller No. 74 L, R, C, Model 299F

C-9 Results of Overload Experiments, Propeller No. 74 L, R, C, Model 299F

C-10 Results of Overload Experiments, Propeller No. 74 L, R, C, Model 299F

C-11 Results of Overload Experiments, Propeller No. 74 L, R, C, Model 299F

C-12 Results of Overload Experiments, Propeller No. 74 L, R, C, Model 299F

C-13 Comparison of Speed at Design Power

LIST OF FIGURES

Figure No.:	Figure Title:
2.1	Model 299, $\lambda = \sim$ Body Plan
2.2	Model 299, $\lambda = \sim$ Lines Plan
2.3(a)	Model 299 - Bow View
2.3(b)	Model 299 - Stern View
2.4	Model 299B Body Plan
2.5	Model 299B Lines Plan and Profiles
2.6	Model 299B with Wake Rake in Place (Stern View) Model 299B with Wake Rake in Port Nozzle (View from Rear)
2.7	Model 299C Lines Plan and Profile (Stern)
2.8	Model 299C - Stern View
2.9	Model 299D (Bare Hull) - Stern View
2.10	Model 299E, Nozzles and Skegs Looking Aft Model 299E, Nozzles and Skegs Looking Forward
2.11	Model 299B, Bottom Grills and Skegs
2.12	Model 299B, Nozzles and Rear Ice Guards
4.1	View Looking Aft
4.2	Effective Wake Contours Measured at a Position Slightly Ahead of the Centre Propeller (1-1-1 Power Distribution)
4.3	Effective Wake Contours Measured at a Position Slightly Ahead of the Wing Propeller (1-1-1 Power Distribution)
4.4	Model 299B Centre Propeller, 16 KT, Axial Component
4.5	Model 299B Centre Propeller, 16 KT, Tangential Component
4.6	Model 299B Centre Propeller, 16 KT, Radial Component
4.7	Model 299B Wing Propeller, 16 KT, Axial Component

4.8 Model 299B Wing Propeller, 16 KT, Tangential Component

4.9 Model 299B Wing Propeller, 16 KT, Radial Component

4.10 Model 299B Centre Propeller Axial Wake Contour, 16 Knots

4.11 Model 299B Centre Propeller Flow Vectors in Propeller Plane, 16 Knots

4.12 Model 299B Port Propeller Axial Wake Contour, 16 Knots

4.13 Model 299B Port Propeller Flow Vectors in Propeller Plane, 16 Knots

5.1 Model 299 Ship Effective Horsepower

5.2 Model 299B Model Resistance Coefficients (Ahead)

5.3 Model 299B Model Resistance Coefficients (Astern)

5.4 Model 299B EHP (Ahead)

5.5 Model 299B EHP (Astern)

5.6 Resistance Test, Ahead

5.7 Model 299D (Bare Hull), $S = 48.78\ ft^2$

5.8 ITTC Skin Friction Line

5.9 Model 299B Body Plan

5.10 Model 299B Load Waterline

5.11 Model 299B Sheer View

6.1 Propellers 56 L & R Average Results of Open Water Tests

6.2 Model Propellers 74 L, R, C, Mean of Open Water Tests

7.1(a) Model 299 DHP, EHP, and RPM for Ship in Clear Water at Self-Propulsion Points

7.1(b) Comparison of Ship Open Water Performance

7.1(c) Comparison of Clear Water Performance, Models 299, 299C, and 299E

7.2	Comparison of Quasi-Propulsive Coefficient
7.3(a)	Comparison of Propulsion Factors
7.3(b)	Comparison of Propulsion Factors
7.4	Comparison of Wake Fraction
7.5	Comparison of Thrust Deduction Factors
7.6	Thrust Versus Ship Speed
7.7	Model 299, Towing Force in Overload Experiments at Indicated Ship Speeds
7.8	Model 299C, Towing Force in Overload Experiments
7.9	Model 299E, Towing Force in Overload Experiments
7.10	Model 299, Thrust Deduction in Overload Experiments
7.11	Model 299C, Thrust Deduction in Overload Experiments
7.12	Model 299E, Thrust Deduction in Overload Experiments
7.13	Comparison of Bollard Pull (at Zero Speed)
8.1	Model 299E, Streamflows on Outside of Skegs
8.2	Model 299E, Streamflows on Inside of Skegs and Nozzles
8.3	Model 299E, Streamflows on Tunnel Roof and Top of Nozzles
8.4	Model 299E, Streamflows on the Aft Body
9.1	Models 299E, 299F
B-1	Resistance Prediction of Full Scale Grills
B-2	Grills Resistance as the Difference of the Model Total Resistance Coefficients of Both With and Without the Grills
C-1	Comparison of Ship Open Water Performance
C-2	Model 299F, Propulsion Factors in Clear water
C-3	Model 299F, Propulsion Factors in Clear water
C-4	Model 299F, Towing Force in Overload Experiments

C-5 Model 299F, Thrust Deduction in Overload Experiments
C-6 Towing Forces in Overload Experiments
C-7 Comparison of Pull at Design Power

EXECUTIVE SUMMARY

This report analyses the results obtained from a series of ship model tests designed to evaluate the performance of a propeller protection scheme for Polar Class icebreakers.

A conventional triple-screw icebreaker hull form with no protection was designated as the "parent model" for comparison purposes (Model 299). Based on a design described in the Volume I and Volume II reports, a model incorporating full propeller protection was constructed and tested in the tank at the National Research Council (Model 299B).

Tank tests on Model 299B indicated excessively high resistance. To determine the main source of this added resistance a series of resistance tests were carried out in which the protecting grills were removed, the stern shape changed, and finally, all appendages removed. Paint tests were also conducted to determine areas of flow separation in the tunnels. It was concluded that to reduce the resistance the following would be required.

(a) The sectional areas in the afterbody would have to be reduced, i.e., finer ship lines are required. This would require lengthening the ship.

(b) The tunnels would have to be redesigned to:

- improve entry conditions;
- reduce flow separation; and,
- improve flow into ducts.

(c) The grill resistance could be improved by a redesign although it was considered that the scale factor was a problem resulting in higher resistance predictions.

A series of self-propulsion tests were conducted for Model 299B and its derivatives, i.e., Models 299C, 299D, 299E, and 299F. A comparison of the quasi-propulsive coefficient (QPC), defined as the ratio of the effective power to the delivered power, for the various models showed that up to 12 knots they had a higher QPC than the parent model but this reversed at higher ship speeds.

In Model 299E the outside rectangular shape of the ducts was replaced by circular shaped ducts. This resulted in improved performance due to the thrust generated by the ducts. As only stock propellers, based on truncated B-Series, were used in the tests some loss in efficiency can be attributed to the propellers. At 16 knots the QPC of Model 299E was 0.411 compared to 0.462 for Model 299. The lower QPC for Model 299E was due to a lower hull efficiency, in which gains in thrust deduction factor were lost due to a high negative wake factor.

The series of model tests highlighted the problem areas associated with providing complete propeller protection. A significant improvement in performance will be achieved by implementing the recommendations listed above. The assessment of the performance is very dependent on the ship speeds considered and thus the mission profile of the vessel. At icebreaking speeds the guarantee of operational reliability outweighs the increase in horsepower required.

1.0 INTRODUCTION

The main objective of the study is to design a device that protects the propeller of a polar class icebreaker from damage by ice. In pursuing the study, three phases became apparent.

Phase I was concerned with a theoretical appraisal of published and unpublished propulsion protection systems. The major concepts identified and investigated included: nozzles; ring propellers; deflecting fins; bilge keels; propeller cages; open partial tunnels; and in-hull propulsion systems. Various devices within each concept were developed and critically reviewed. Conclusions were drawn with regard to the most suitable and effective devices for use in heavy ice. To conclude that phase a report was written entitled "Protection of Propellers In Ice - Volume I - Assessment of Protection Schemes", TP 2704, August, 1980.

Phase II of the study was concerned with the detail design of protection schemes, specifically that associated with the proposed in-hull propulsion system for a triple-screw POLAR 7 icebreaker. Topics such as: hull strength requirements; propeller designs and performance; propulsion shafting; maneuvering devices including the proposed in-hull stern rudders; and rudder arrangement and structural details were studied. To conclude Phase II of the study, a report was written entitled "Protection of Propellers In Ice - Volume II - Detail Design of Protection Schemes", TP 2704, June, 1981. The present report, Volume III, is concerned with Phase III of the study. It deals with the model test results, discussions, and conclusions.

2.0 DESCRIPTION OF MODELS

The lines plans of a triple-screw icebreaker (POLAR 7A) incorporating the proposed in-hull propulsion scheme were developed using as a basis the hull form of the Canadian Coast Guard's 90,000 SHP POLAR 7 enlarged by a linear scale factor (15%) to allow the new hull to absorb the proposed 150,000 SHP with some margin for the protection arrangement.

The lines plans of the forebody of the enlarged hull were similar to those of the parent hull form (Model 299) while for the aftbody, the lines plans were modified to accommodate the protection device. This modification resulted in a squared-off transom stern together with a wall-sided hull form (Model 299B).

Model 299, the parent model, is considered to represent a 1/46 scale of the full sized ship, as does Model 299B incorporating all the proposed protection appendages. Figures 2.1 to 2.6 show the lines and appendages of Model 299 and Model 299B.

Model 299C is identical to Model 299B except for the transom stern which was replaced with a rounded (cruiser type) stern in accordance with our design modifications shown in Figures 2.7 and 2.8.

Model 299D is the bare hull of Model 299C with all appendages removed. A stern view of Model 299D is shown in Figure 2.9.

Model 299E (Figure 2.10) represents modifications made to Model 299C, which consisted of removing the bottom grills, the stern guards, and the side walls separating the propeller tunnels, and also fairing the ducts.

Finally, Model 299F represents a further modification to Model 299E, which consisted of refitting the tunnel separating walls. Test results, analysis, and discussion on Model 299F were not complete at the time of writing of this report and therefore are presented separately in Appendix C.

Model 299B, later modified to Model 299E, was made of wood and finished with gloss paint. To simulate turbulence, the model was fitted with a tripwire, 1 mm in diameter, parallel to the stern profile at a distance of 360 mm from the leading edge. This distance combined with the degree of turbulence present in the tank assures transition into turbulent flow, even at a speed as low as 7 knots equivalent full scale (1).

Figures 2.11 and 2.12 show the bottom grills, skegs, nozzles, and stern guards.

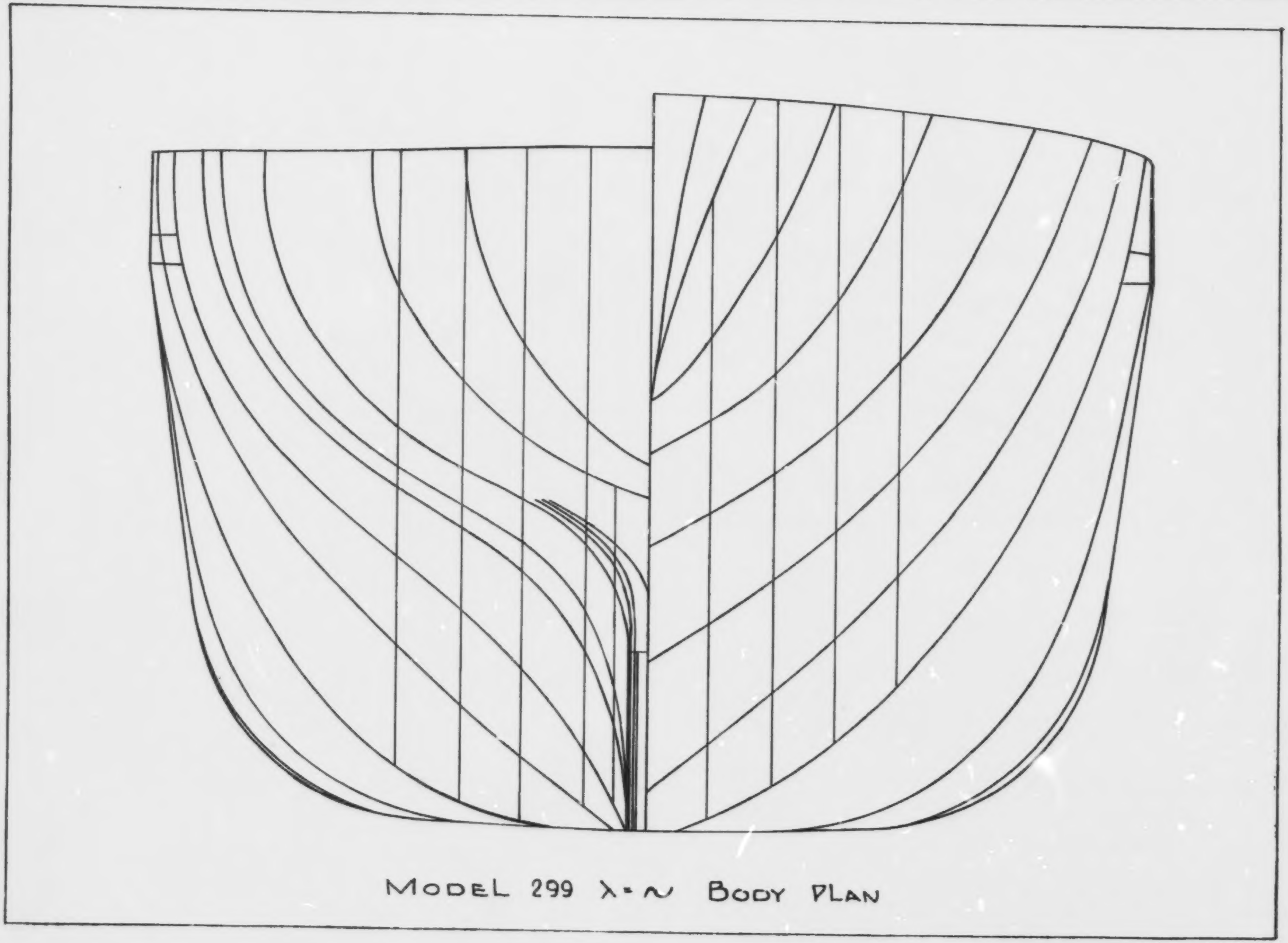
MODEL 299 λ = ∾ BODY PLAN

FIGURE 2.1 MODEL 299 BODY PLAN

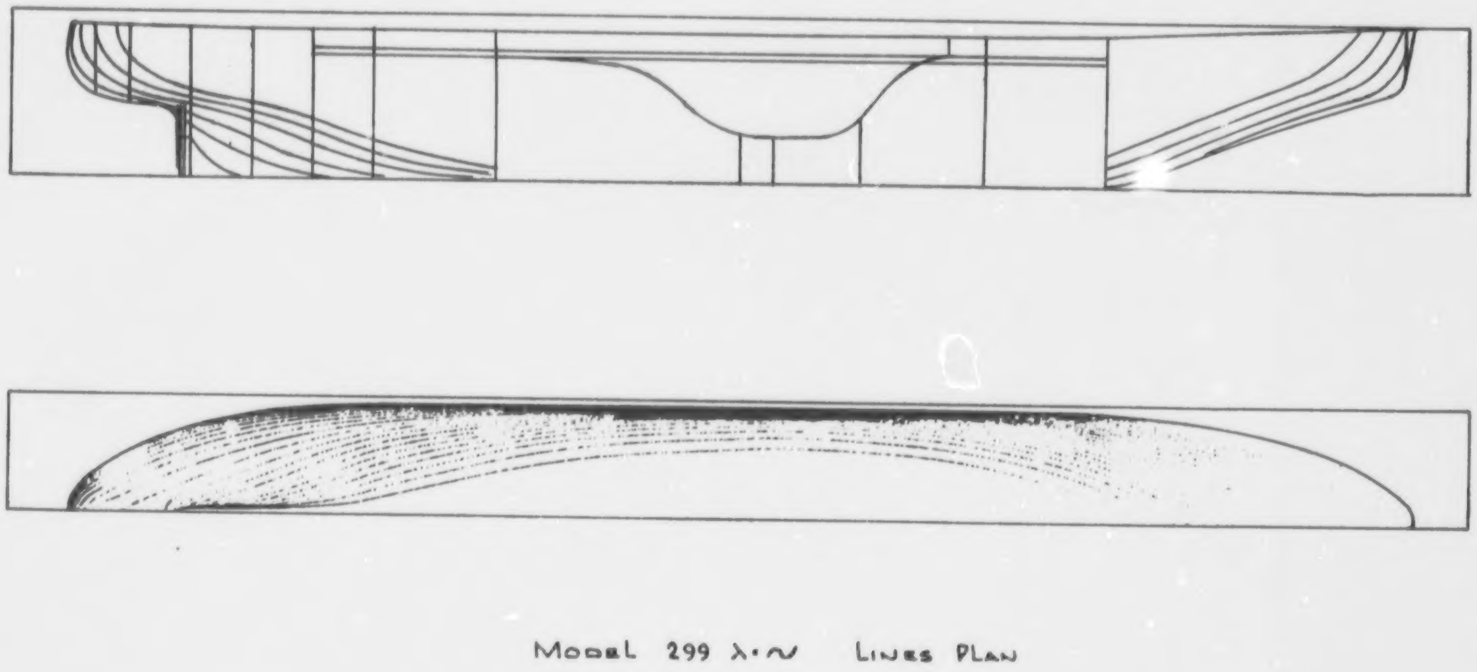
Model 299 λ·~ Lines Plan

FIGURE 2.2 MODEL 299 LINES PLAN

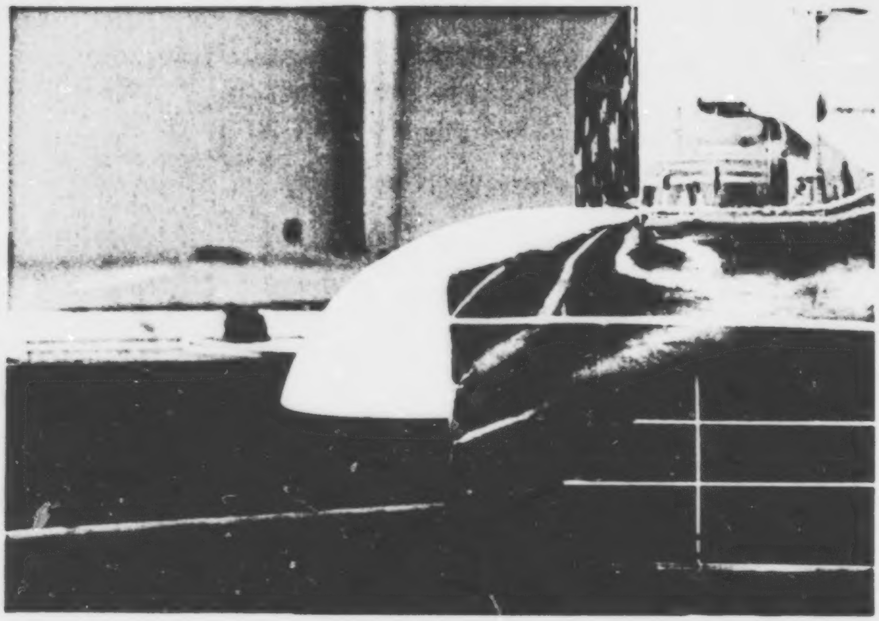

FIGURE 2.8 MODEL 299C -
STERN VIEW

FIGURE 2.9 MODEL 299D -
(BARE HULL)
STERN VIEW

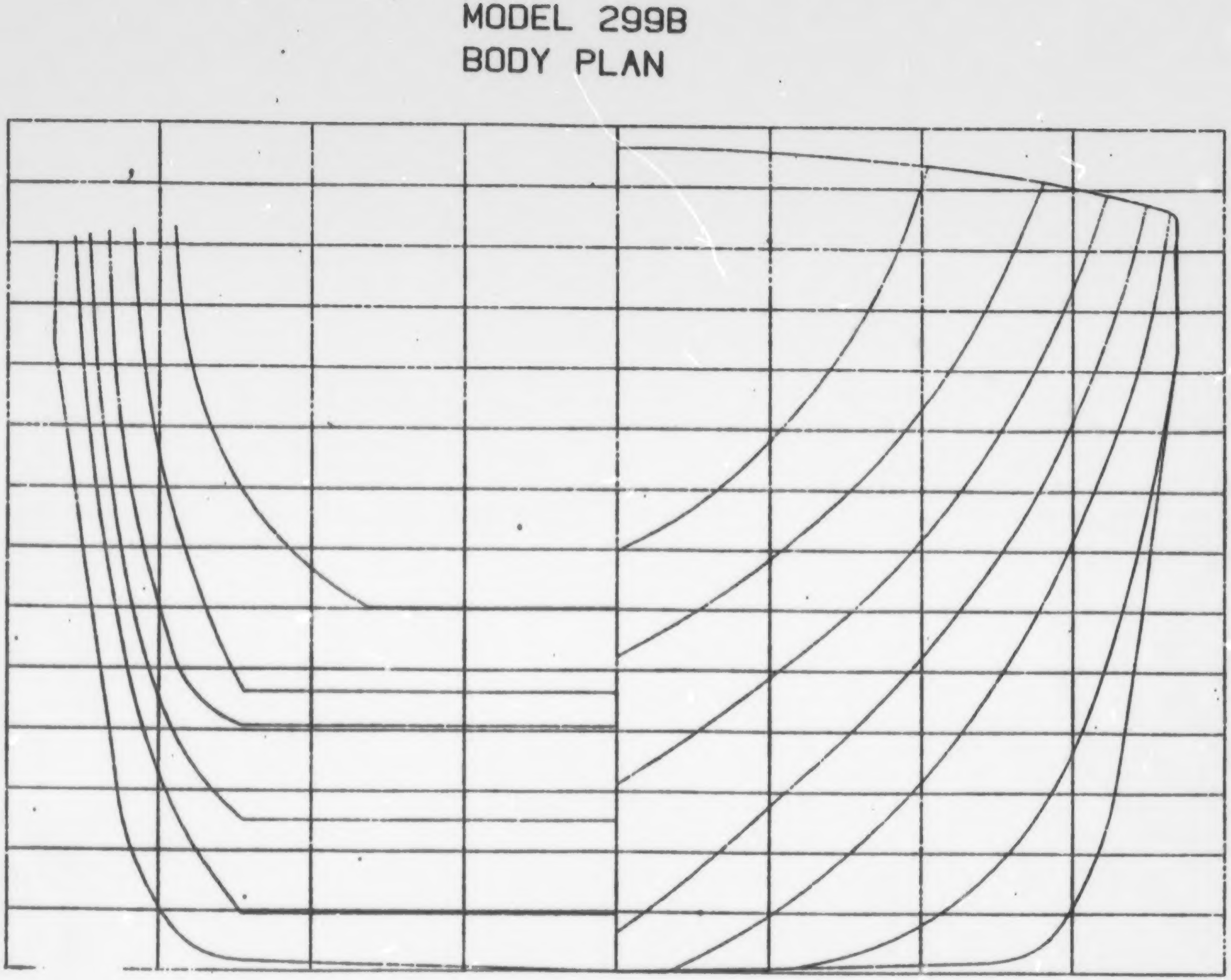
MODEL 299B
BODY PLAN

FIGURE 2.4 MODEL 299B BODY PLAN

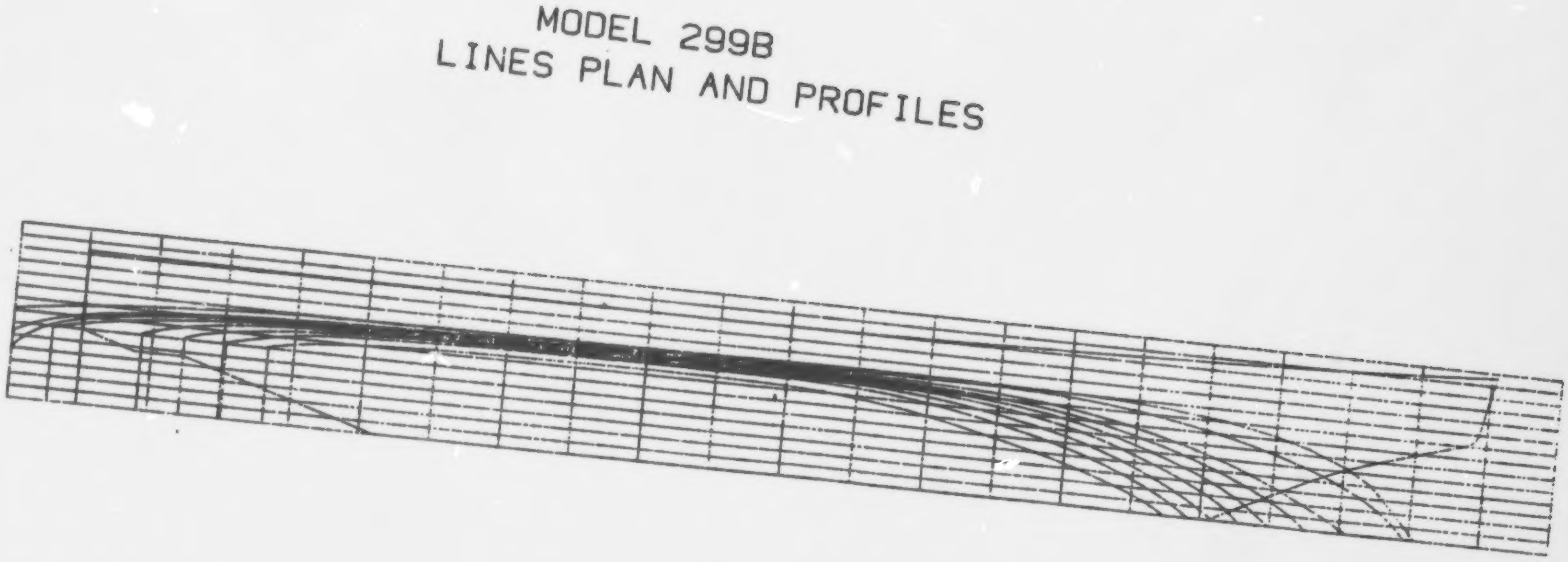
MODEL 299B
LINES PLAN AND PROFILES

FIGURE 2.5 MODEL 299B LINES PLAN AND PROFILES

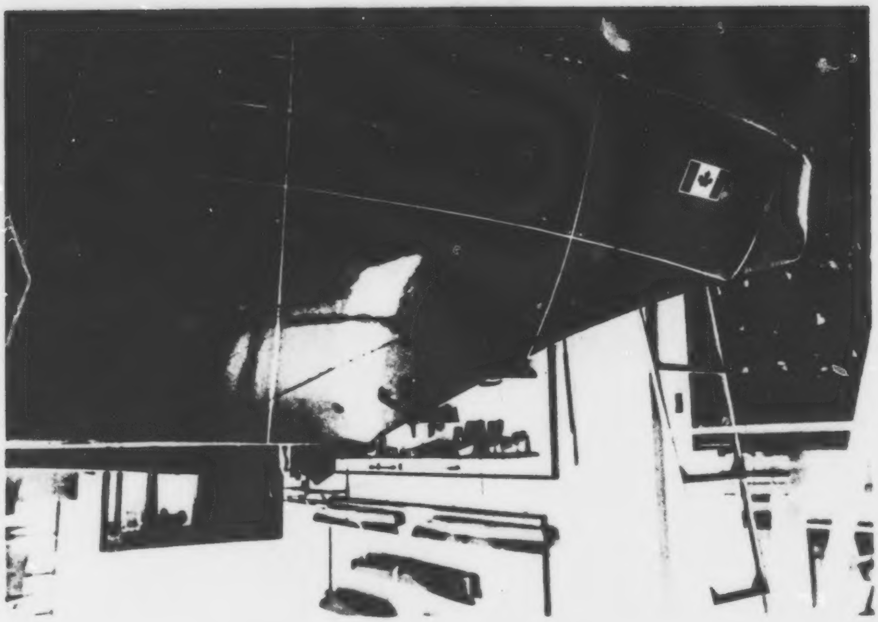

FIGURE 2.3a MODEL 299 -
BOW VIEW

FIGURE 2.3b MODEL 299 -
STERN VIEW

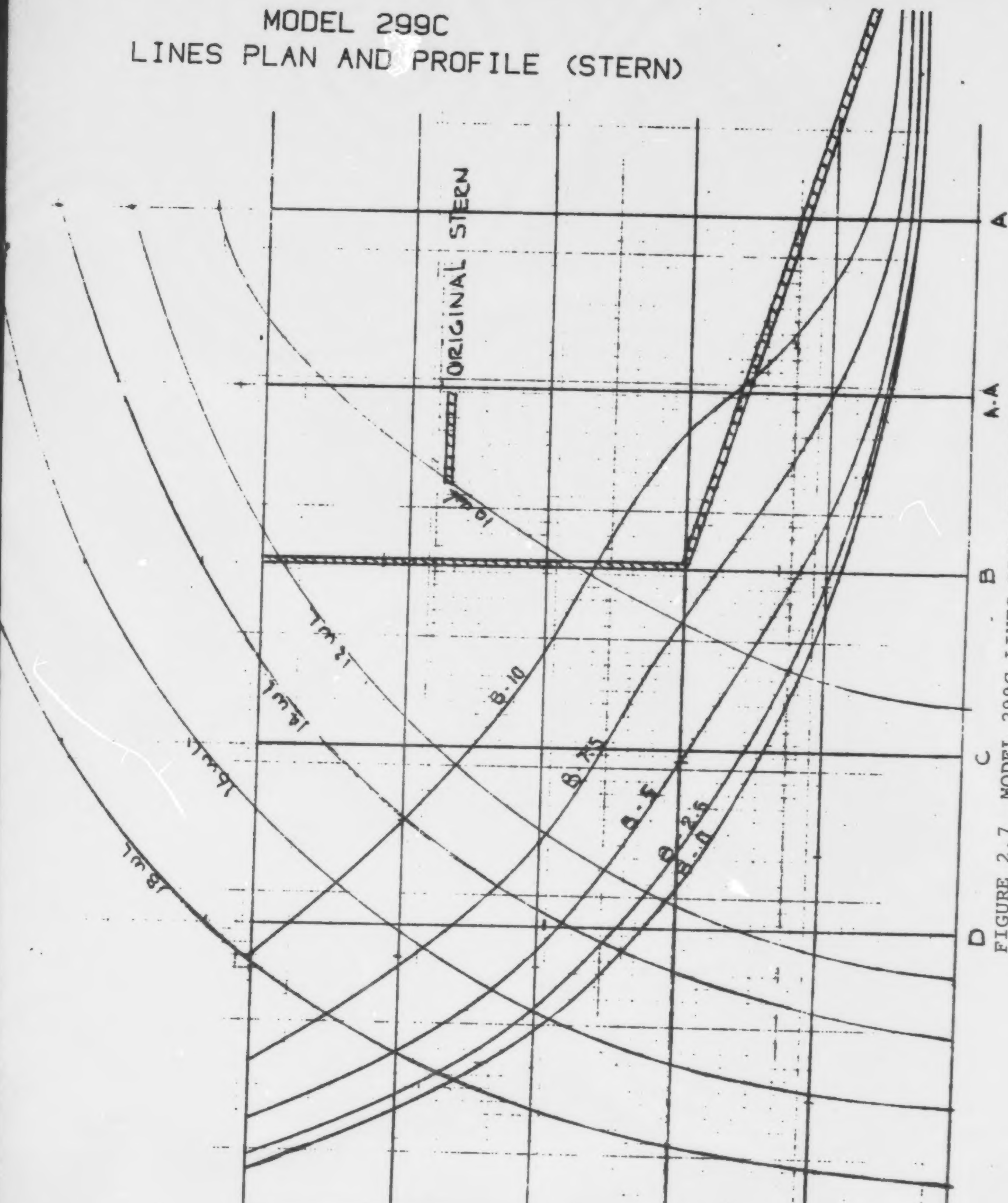
MODEL 299C
LINES PLAN AND PROFILE (STERN)
ORIGINAL STERN
A
A.A
B
C
D
10 wl
12 wl
14 wl
16 wl
18 wl
B.10
B.7.5
B.5
B.2.5
B.0
18 wl.
16 wl.
14 wl.
12 wl.
10 wl.
8 wl.

FIGURE 2.7 MODEL 299C LINES PLAN AND PROFILE (STERN)

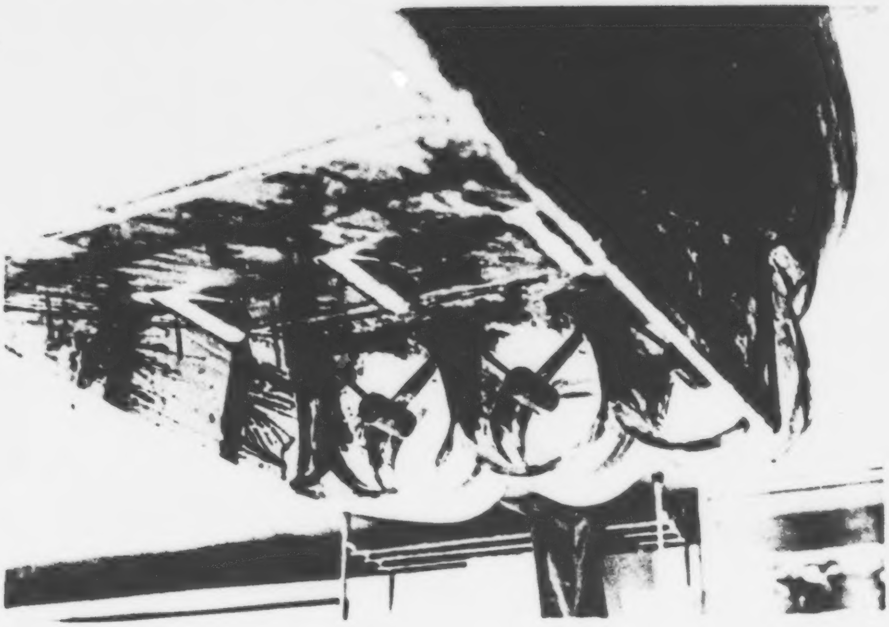

MODEL 299E, NOZZLES AND
SKEGS
LOOKING AFT

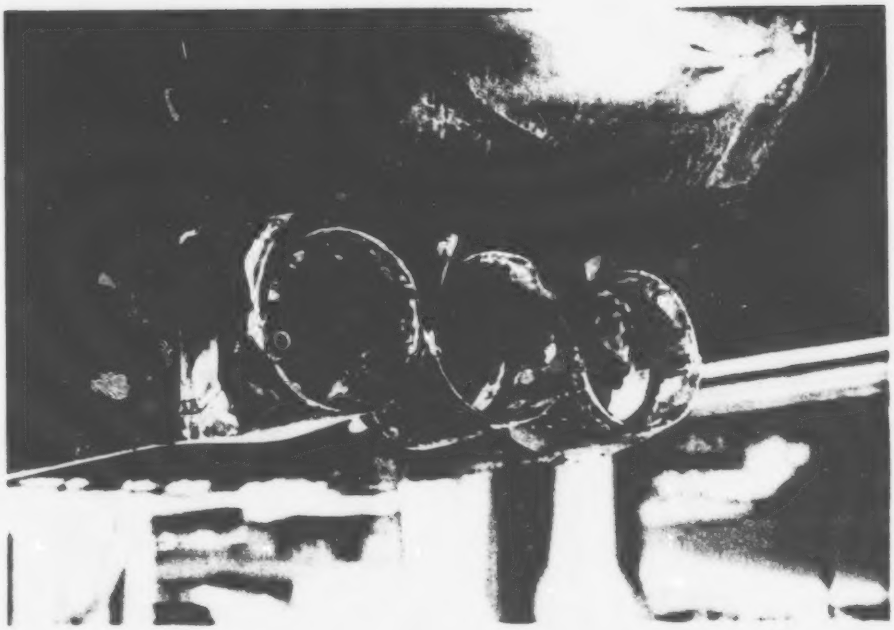

MODEL 299E, NOZZLES AND
SKEGGS
LOOKING FORWARD

FIGURE 2.10

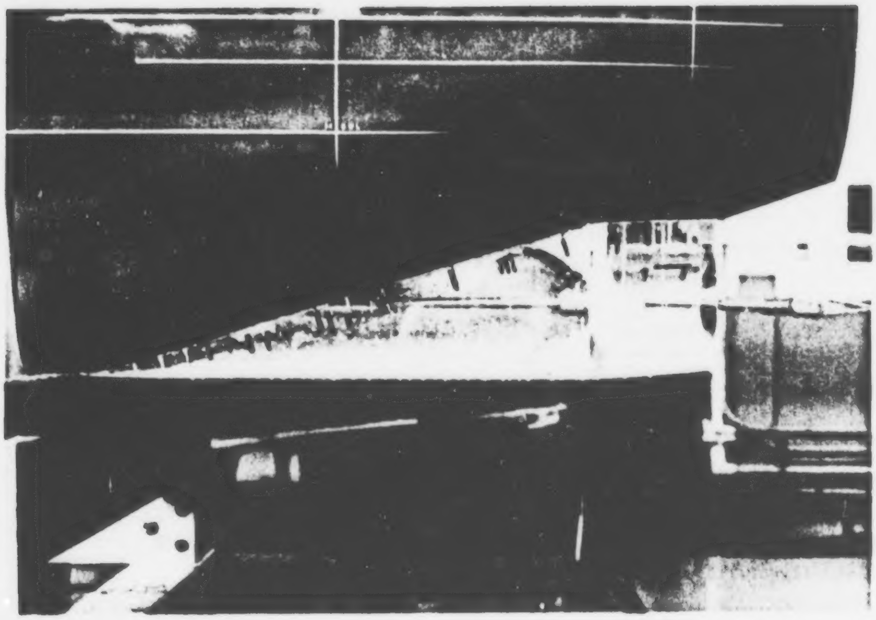

MODEL 299B WITH WAKE RAKE
IN PLACE
(STERN VIEW)

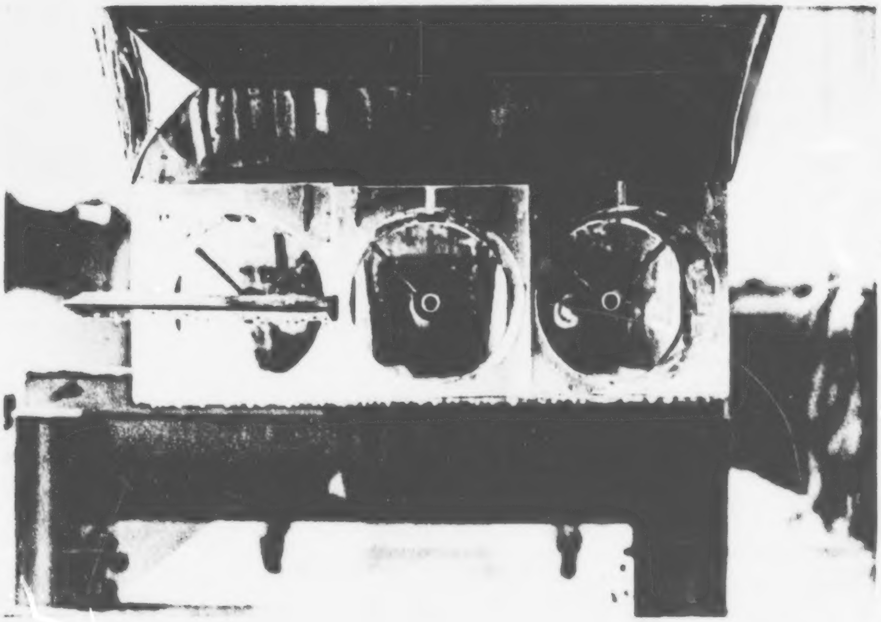

MODEL 299B WITH WAKE RAKE
IN PORT NOZZLE
(VIEW FROM REAR)

FIGURE 2.6

MODEL 299B
BOTTOM GRILLS AND SKEGS

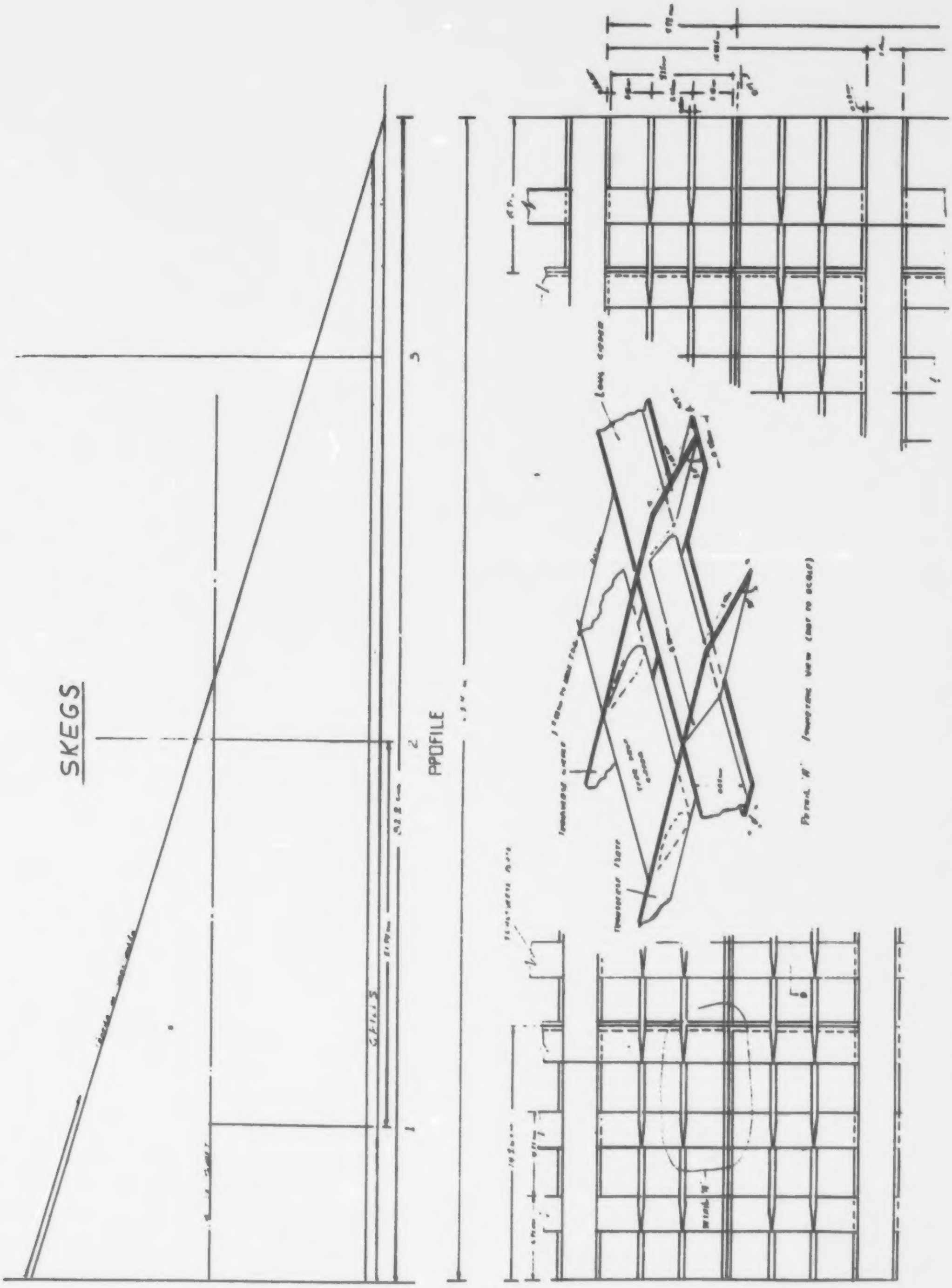
SKEGS
PROFILE
GRILLS
1
2
3

FIGURE 2.11 MODEL 299B BOTTOM GRILLS AND SKEGGS

MODEL 299B
NOZZLES AND REAR ICE GUARDS

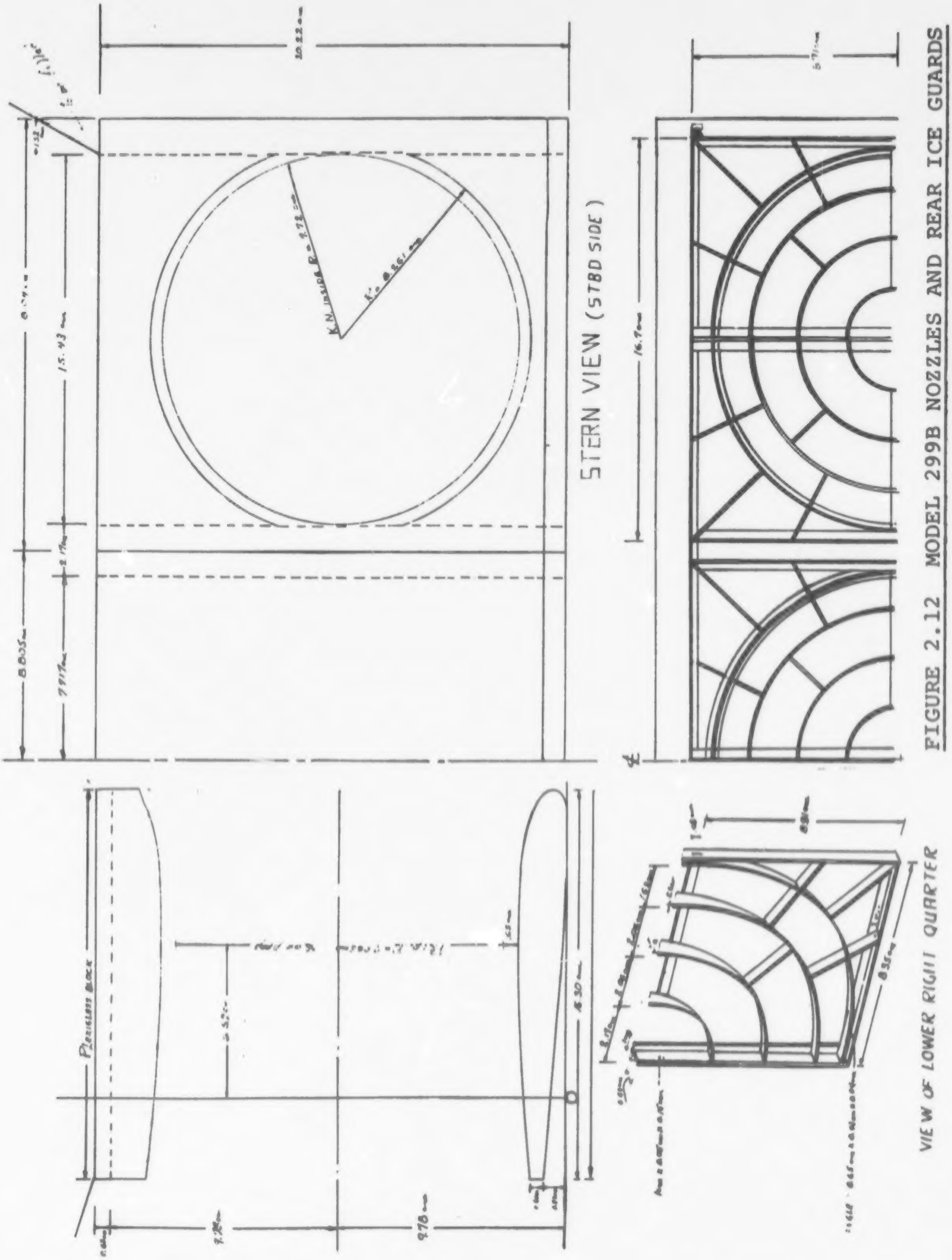
10.22 in
15.43 in
16.7 in
8.005 in
9.78
9.78
STERN VIEW (STBD SIDE)
VIEW OF LOWER RIGHT QUARTER

FIGURE 2.12 MODEL 299B NOZZLES AND REAR ICE GUARDS

Full hydrostatic particulars for the models are given in Table 2.1. It must be pointed out that due to the nature of the protection device and the subsequent modifications in the appendages both the displacement and the wetted surface area vary considerably among the different models. For example, Model 299C has about 44% larger wetted surface area and about 23% larger displacement compared with the parent Model 299. Such variations in the hydrostatic particulars for the models make a direct comparison less accurate; a fact which will be considered in the analysis of the test results.

Finally, for the self-propulsion tests, Model 299 was fitted with two R.H. propellers and one L.H. propeller with particulars given in Table 2.2. For Models 299B to 299E, the propellers used were manufactured from stock blades of B-Series with squared-off tips to resemble the Kaplan type. The particulars of these propellers compared with the design are also given in Table 2.2.

Although there was no complete similarity between the design and the manufactured propellers, they were considered acceptable at this early stage of design, provided that the open water performance characteristics of the manufactured propellers are obtained.

		M-299 (With Appendages)	M-299B (With Grills)	M-299B (No Grills)	M-299C (With Grills)	M-299D (Bare Hull)	M-299E (With Appendages)
Length Between Perpendiculars (L_{BP})	(M)	199.53	200.0	200.0	200.0	200.00	200.0
Length on Waterline (L_{WL})	(M)	208.70	210.0	210.0	216.43	216.43	216.43
Waterline Beam at Midships (B)	(M)	35.16	35.16	35.16	35.16	35.16	35.16
Draft at Midships (H)	(M)	14.032	14.032	14.032	14.032	14.032	14.032
Trim, Positive Stern Down	(M)	0	0	0	0	0	0
Volume of Displacement	(M^3)	55,607	68,217	68,198	68,647	67,286	68,163
Displacement (S.W.)	(KN)	560,512	687,620	687,427	691,954	678,228	687,073
Wetted Surface Area	(M^2)	9,030	12,865	11,617	12,971	9,589	11,090
Area of Maximum Station	(M^2)	435.7	435.7	435.7	435.7	435.7	435.7
Block Coefficient (C_B)	(-)	0.537	0.691	0.691	0.696	0.682	0.691

TABLE 2.1 - HYDROSTATIC PARTICULARS FOR FULL SIZED SHIP λ - 46

	MODEL PROPS 56L,R,C FOR SHIP MODEL 299	PROP DESIGN PARTICULARS FOR SHIP MODELS 299B,C,E	MODEL PROPS 74L,R,C FOR SHIP MODELS 299B,C,E
Scale	46	46	46
Prop. Diam. (mm)	7250	6500	6826*
Pitch at 0.7 R (mm)	4640	5330	5710
P/D	0.64	0.82	0.836
B.A.R.	0.45	0.60	0.413
Design	Wageningen B-Series	Kaplan K_a-Series	B-Series with Squared-off Tips
No. of Blades	4	4	4
Hub Ratio	0.30	0.29	0.29
Tip Clearance (mm)	---	300	138*

* The propeller diameter for the self-propulsion tests had to be increased to compensate for the difference in the B.A.R. between the NRC stock blades and the design value so that the new propeller would produce the same bollard pull thrust. The radial tip clearance in this case was 3 mm (model scale).

TABLE 2.2 - PROPELLER DESCRIPTION

3.0 TEST PROGRAM

As in most Research and Development projects, the test program of the present study was originally developed on the basis of the best information available. As the work progressed, new information became available and, as a result, changes were made in the test program to shed more light on problem areas and provide guidance for possible solutions.

The test program included Models 299, 299B, 299C, 299D, and 299E. The description of these models was given in Section 2.0. The experiments covered a wide range of activities namely wake survey, resistance tests ahead and astern, propeller open water tests, self-propulsion tests, and overload experiments. All tests were carried out in clear water. Table 3.1 shows the experiments carried out for each model. Appendages included in the experiments were: propeller shafts, dummy hubs, A-brackets, protection devices, rudders, and bottom grills and stern guards.

	M-299 WITH APPEND	M-299B WITH ALL APPEND	M-299B ALL APPEND WITHOUT GRILLS	M-299C WITH ALL APPEND	M-299D BARE HULL	M-299E WITH APPEND
Wake Survey	X	X				
Resistance Tests, Ahead	X	X	X	X	X	X
Resistance Tests, Astern		X	X			
Propeller Open Water Tests	X			X		
Self-Propulsion Tests	X			X		X
Overload Tests	X			X		X
Flow Tests						X

TABLE 3.1 - TEST PROGRAM

4.0 WAKE SURVEY: Models 299 and 299B

4.1 General

Two different rakes of pitot tubes and two different arrangements were used for the two models.

With Model 299, for an axial wake survey, a rake of eight pitot tubes, appropriately spaced was placed slightly ahead of the propeller plane (approximately 14 inches equivalent full scale, ahead of the most forward point of the propeller blades leading edge). The rake was indexed as to allow a rotation of 5 - 15 degrees in the range of 0 - 360 degrees. Each tube was connected via a scanivalve to a differential pressure transducer, the signal of which together with that of the speed of the carriage was entered into the computer system for subsequent analysis.

For each run, the model was accelerated with its own propellers (56 L,R,C) to the equivalent speed of 18 knots, and allowed a few seconds to settle before the recording started.

The other rake was used with Model 299B and consisted of five tubes. However, four only were used due to the restriction imposed by the nozzles. This rake was mounted so that the heads of the probes lay in the propeller plane and could be rotated 360 degrees. The non-dimensional radii for these heads, with reference to the inside radius of the nozzle at the plane of the propeller (taken as 3550 mm full scale) were as follows:

$$r/R_{max} = 0.311,\ 0.492,\ 0.674,\ 0.855.$$

The pitot tubes in this rake were of a spherical type which is capable of measuring the three (axial, tangential, radial) speed components. To do so, each head was connected to four transducers measuring the differential pressures between the centre hole and the four outer holes.

For each run, Model 299B was towed at a constant speed, equivalent to 16 knots full scale, then the rake was rotated, in steps, for the next run. This was repeated until a complete rotation of the rake was achieved.

Time averaged values of the transducers signals were used to obtain the corresponding speed components. Figure 4.1 shows a typical installation of a three component wake rake.

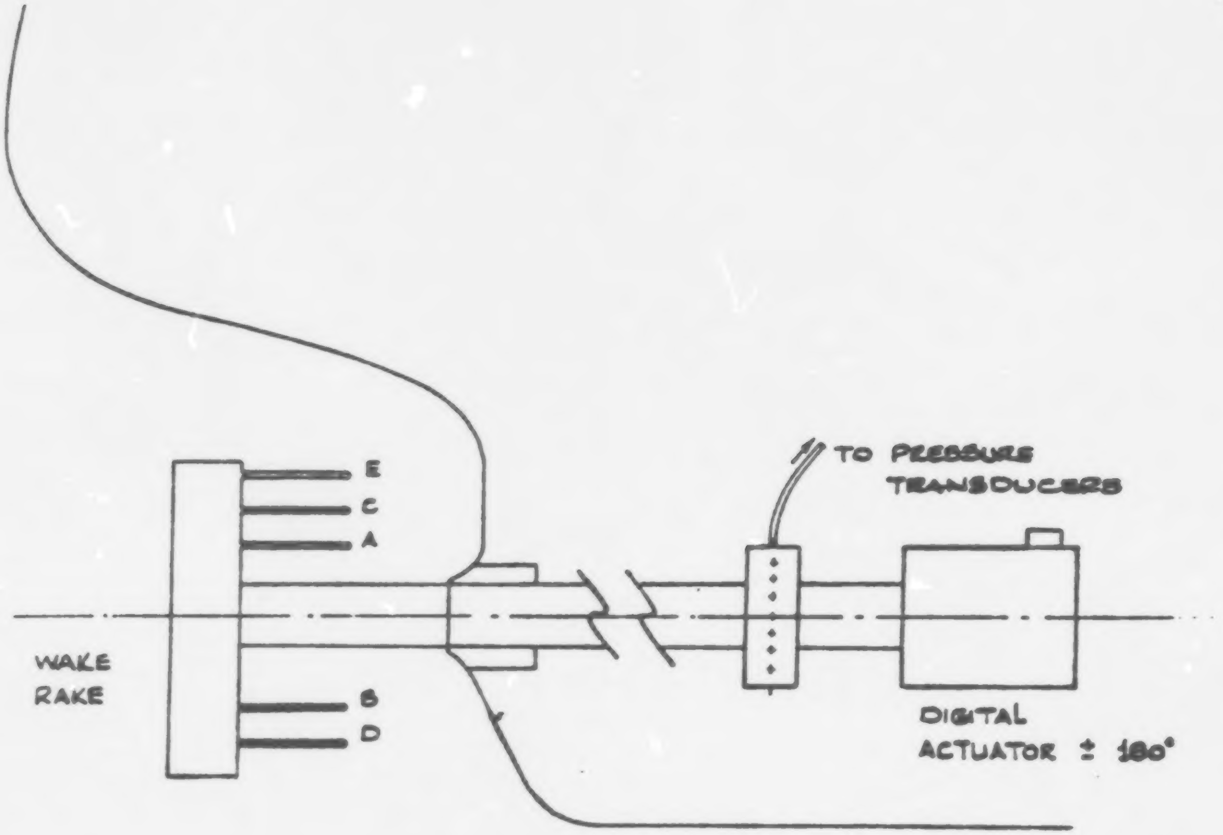
E
C
A
B
D
WAKE
RAKE
TO PRESSURE
TRANSDUCERS
DIGITAL
ACTUATOR ± 180°

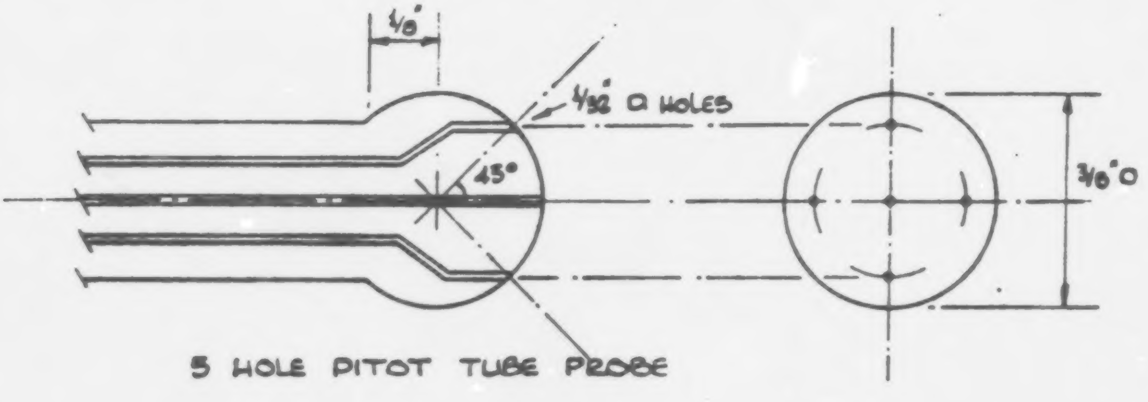
1/8"
1/32" Ø HOLES
45°
3/8" Ø

5 HOLE PITOT TUBE PROBE

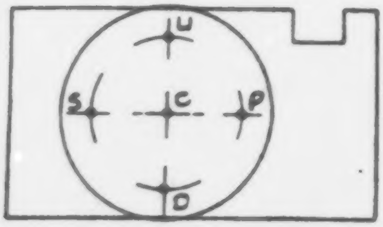

VIEW LOOKING AFT

FIGURE 4.1

4.2 Test Results

The effective axial wake survey of the parent Model 299 was carried out by NRC prior to the present study. Figures 4.2 and 4.3, reproduced from Ref. (5), show the effective wake contours of the center and wing propellers of Model 299.

The nominal wake survey of Model 299B (present study) was carried out as follows. After an initial period in which the towed model reached a reasonable steady state, all pressure channels together with the speed of the carriage were continuously scanned at a rate of 20 samples per channel per second and the information stored on digital magnetic tapes for subsequent analysis.

The magnetic tapes were later read into the NRC Laboratory's main computer and some basic analyses and fairing were carried out. Figures 4.4 to 4.9 show the axial, tangential, and radial components for the center and wing propellers at 16 knots equivalent full scale. The tangential component is positive counterclockwise looking at the propeller from aft, while the radial component is taken positive towards the center of the propeller. From these figures, the wake contours and the flow vectors are shown in Figures 4.10 to 4.13.

Based on the harmonic equation

$$\frac{V(\theta)}{\bar{V}} = C_o + \sum_{k=1}^{N} C_k \sin(k\theta + \phi_k)$$

the coefficients and phase angles were obtained. Tables A.1 to A.8, Appendix A, give this information.

Finally, although these wake data are for Model 299B, Model 299C is expected to have an identical wake field.

4.3 Discussion

The objective of a wake survey is usually three-fold. First, it helps in identifying problem areas related to hull design and/or appendages. Flow separation as well as areas of concentrated wake or excessive velocity gradients can be identified from the results. Second, a better estimation of the mean wake fraction over the entire propeller disk can be obtained and consequently a better prediction of the propulsive efficiency. Third, a wake adapted - radially, circumferentially, or both - propeller can be designed to give better performance (e.g., higher efficiency, lower cavitation risk, and lower noise radiation). In the present study, however, the first two objectives were the prime concern.

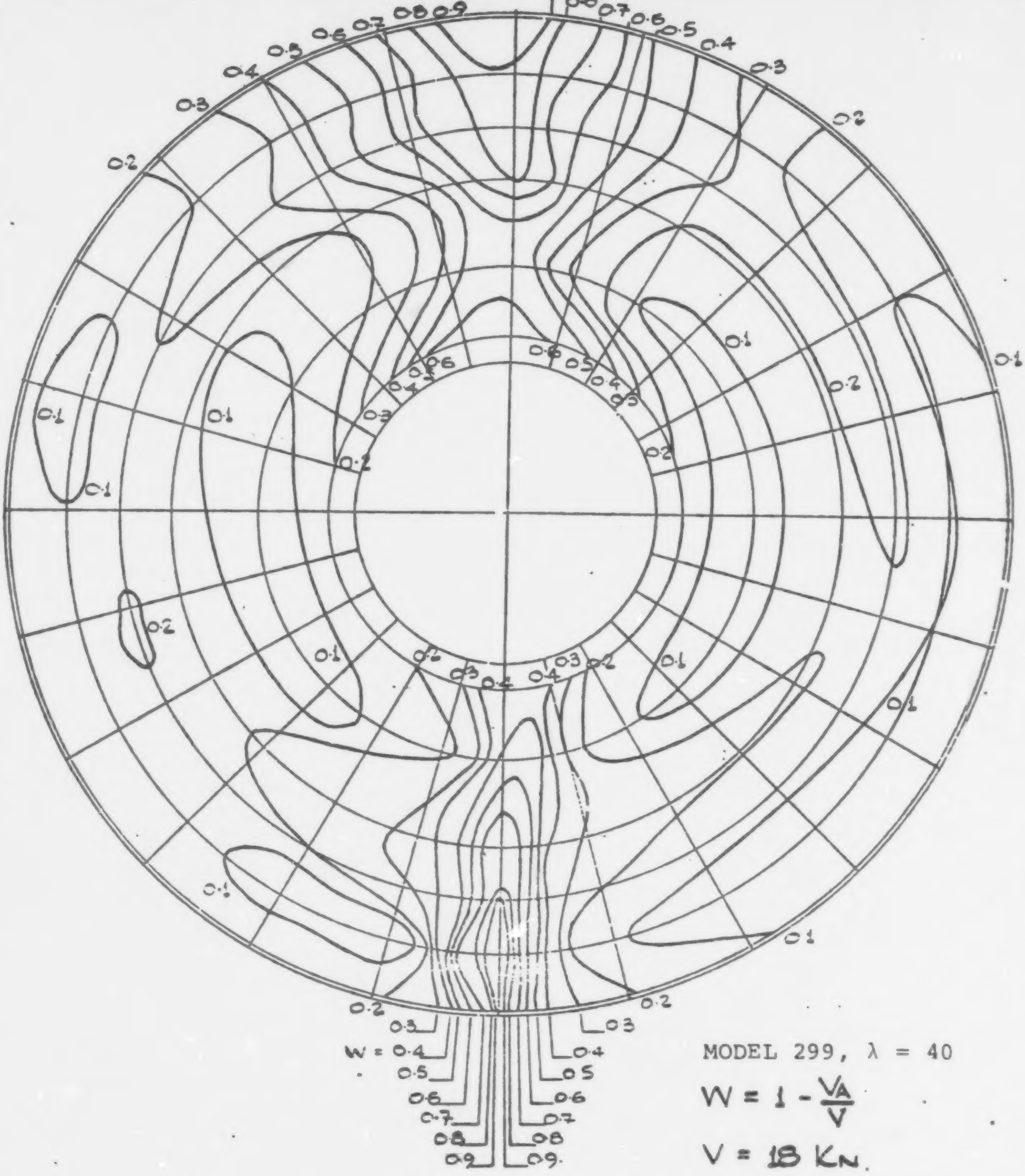

EFFECTIVE WAKE CONTOURS MEASURED AT A POSITION SLIGHTLY AHEAD OF THE CENTRE PROPELLER

(1-1-1 POWER DISTRIBUTION)

FIGURE 4.2 MODEL 299, λ = 40

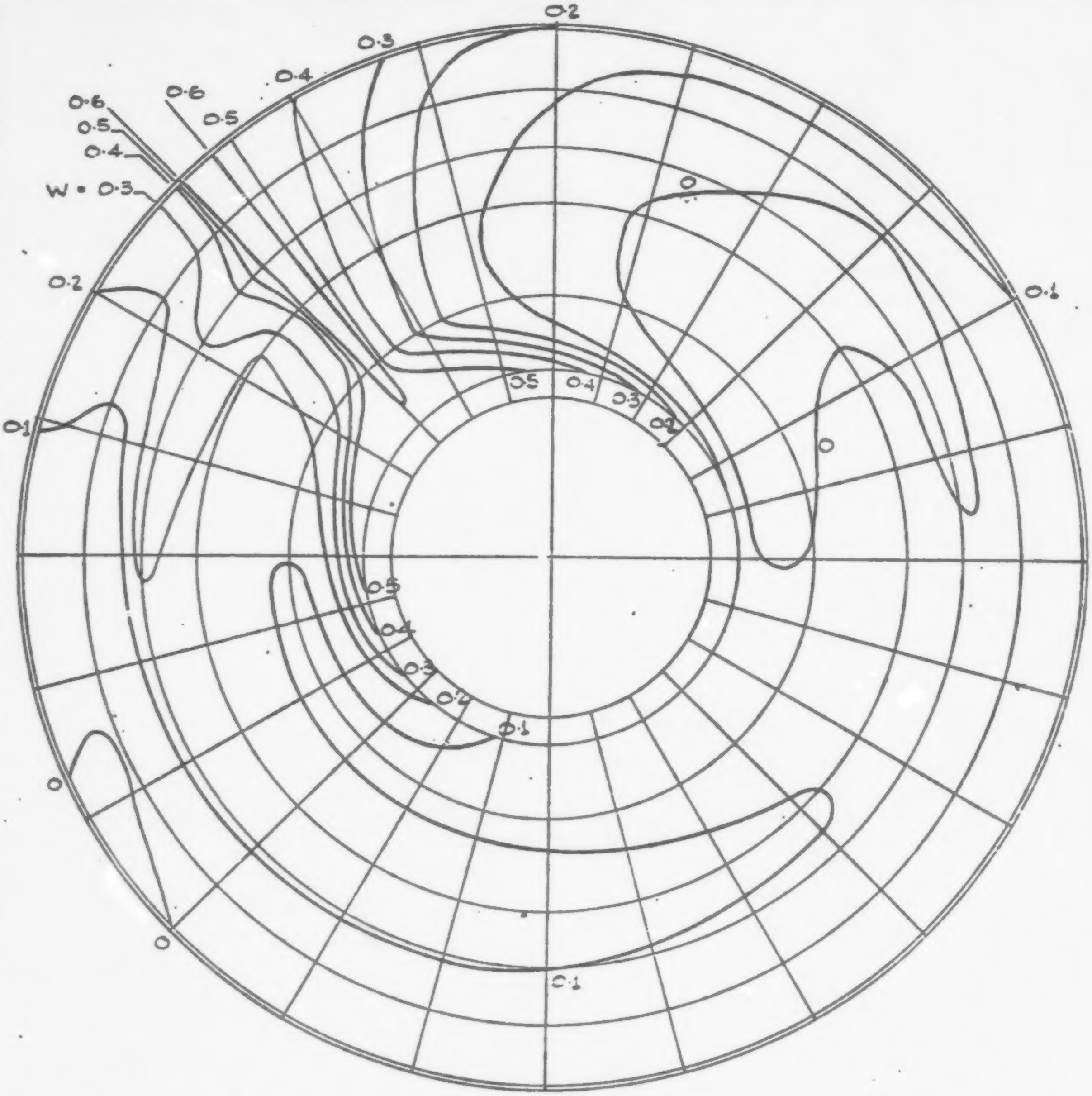

MODEL 299, λ = 40

$W = 1 - \frac{V_A}{V}$

V = 18 Kn

EFFECTIVE WAKE CONTOURS . MEASURED AT A POSITION SLIGHTLY AHEAD OF THE WING PROPELLER.

(1-1-1 POWER DISTRIBUTION)

FIGURE 4.3 MODEL 299, λ = 40

The results of the wake survey carried out with the original hull form, i.e., Model 299, were presented in the preceding section for completeness. No comparison should be attempted between the wake surveys of Model 299 and Model 299B for a number of reasons. First, the nature of the measurements was different. While the effective wake results were presented for Model 299 (5), the nominal wake values were measured for the proposed design, i.e., Model 299B. Second, the equivalent full scale speeds for both models were not the same. These speeds are 19.3* knots and 16 knots for Models 299 and 299B respectively. Thus one can only analyse the results of the two models separately.

The effective wake contours of Model 299, Figures 4.2 and 4.3, show high concentration of wake behind the bossings for the wing propellers and even more behind the skeg for the center propeller. Speed gradients of this magnitude could result in propeller excited vibrations, noise radiation, and cyclic cavitation changes. The results of the three-component wake survey for Model 299B are shown in Figures 4.4 to 4.9. The coefficients and phase angles from the harmonic analysis are given in Tables A.1 to A.8, Appendix A. For the center propeller all axial and radial components have a phase of 90^o which indicates a symmetry about 0^o - 180^o (vertical line) on the propeller disk. In the case of the tangential components, the phase angle is zero which indicates an anti-symmetry about the 0^o - 180^o line. For the wing propeller, there is no symmetry or anti-symmetry for any component since the phase angle is random. Figures 4.10 to 4.13 clearly illustrate the above features. The nominal wake contours for the center propeller (Figure 4.10) indicate that there are no sharp speed gradients of any significant magnitude except for the two spots behind the two arms of the A-bracket. For the wing propellers (Figure 4.11) two additional areas of deficiency in the axial flow can be seen; one in the 0^o position, and the other in the 140^o position for the port propeller (220^o position for the starboard propeller) resulting very likely from the effect of the outer skegs on the flow into the nozzle. For both propellers, center and wing, areas of overvelocities are created around the 180^o position due to the effect of the nozzles.

---

* The original hull form represented by 1:40 scale Model 299 was run at a constant speed corresponding to 18 knots full scale. For the same model to represent 1:46 full scale, the wake results are thus related to approximately 19.3 knots.

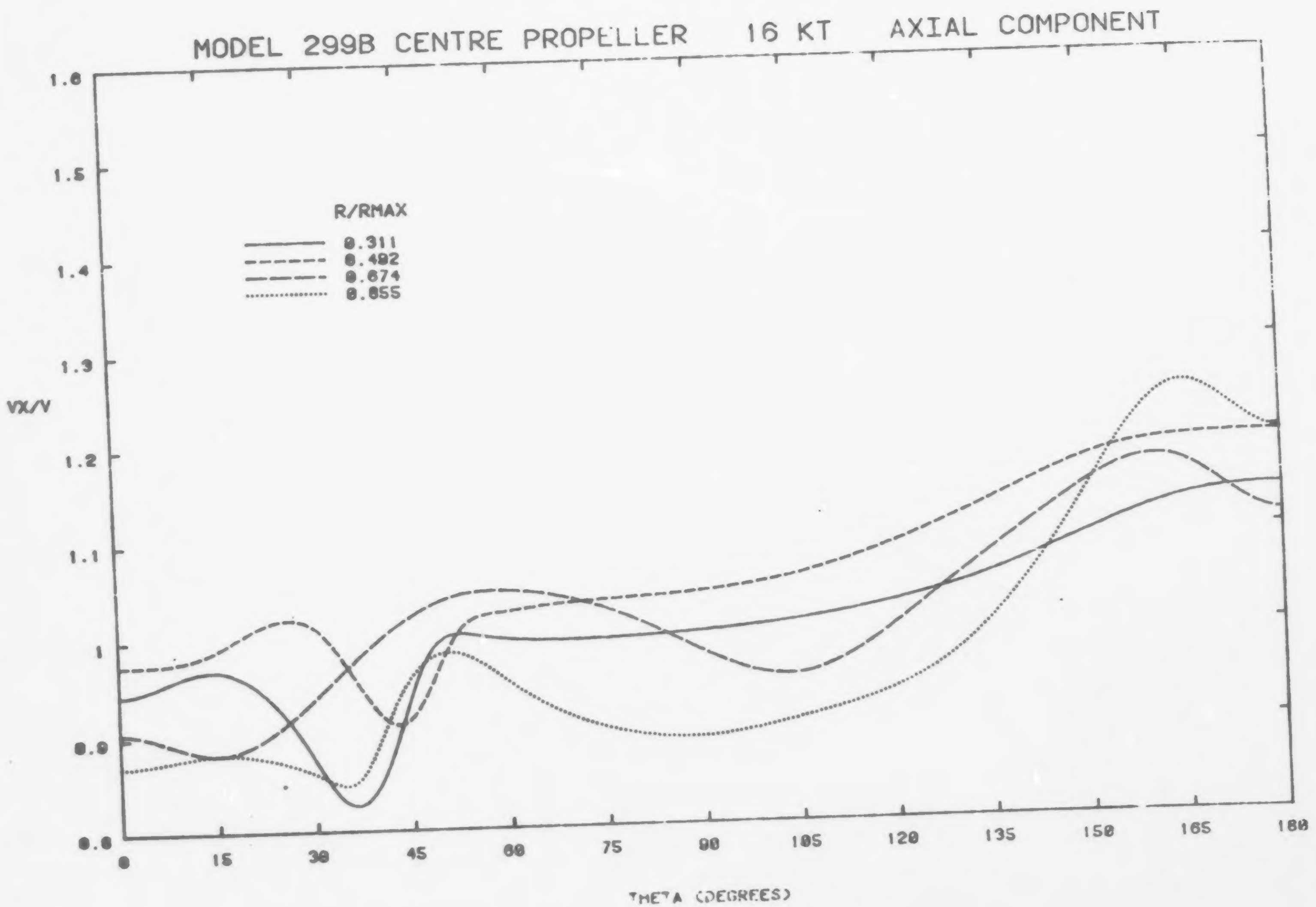

FIGURE 4.4 MODEL 299B CENTRE PROPELLER 16KT AXIAL COMPONET

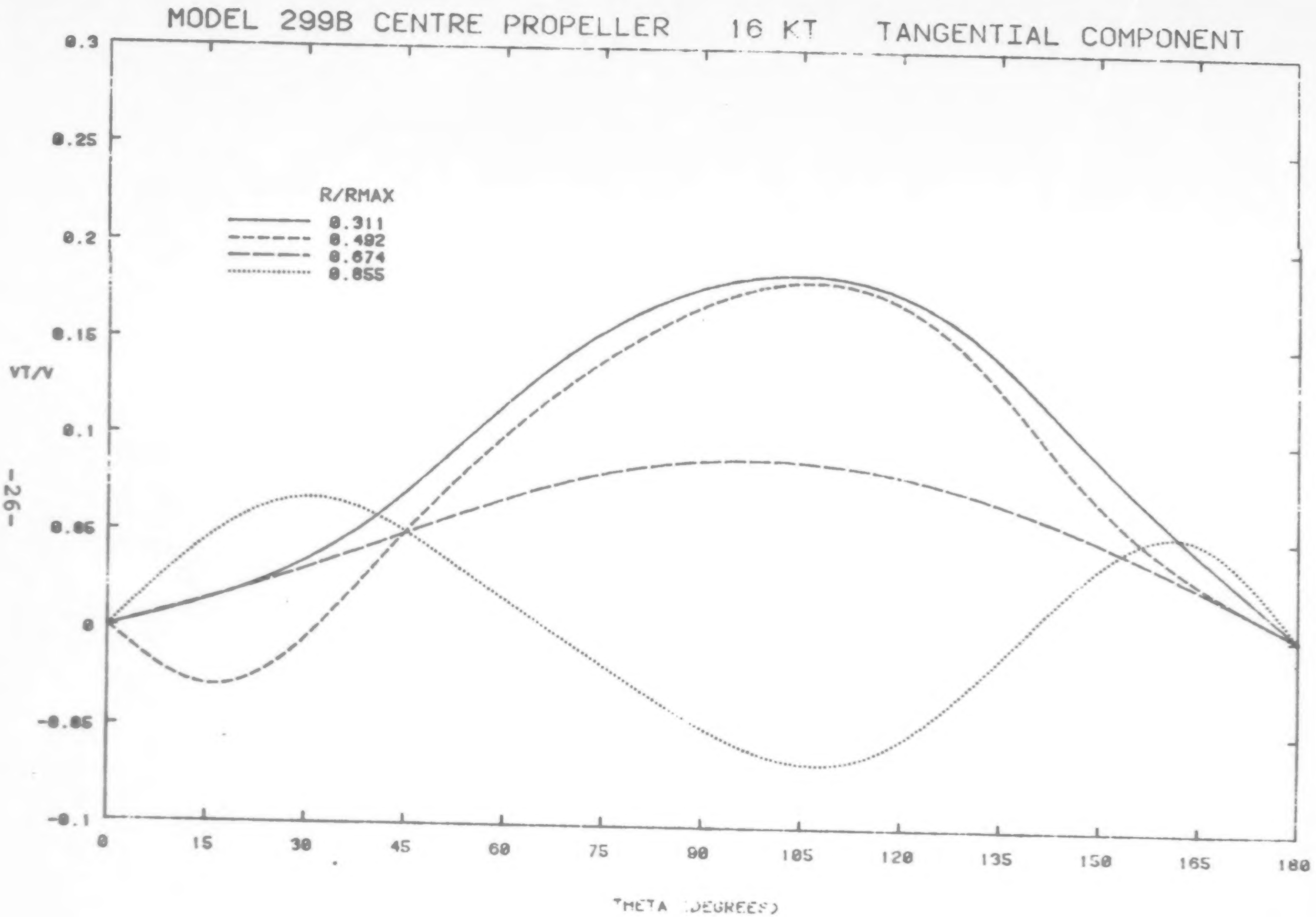

FIGURE 4.5 MODEL 299B CENTRE PROPELLER 16KT TANGENTIAL COMPONET

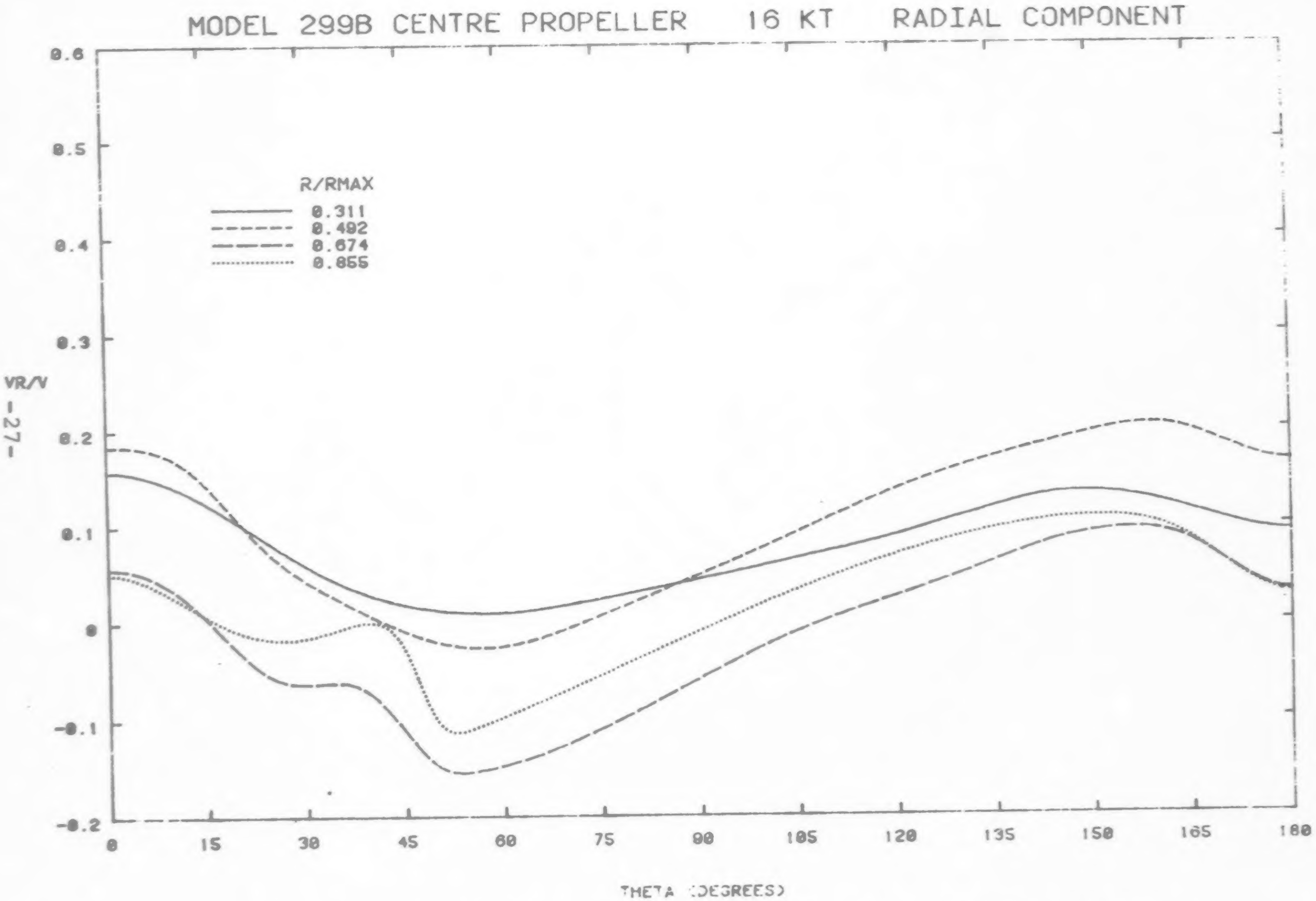

FIGURE 4.6 MODEL 299B CENTRE PROPELLER 16KT RADIAL COMPONENT

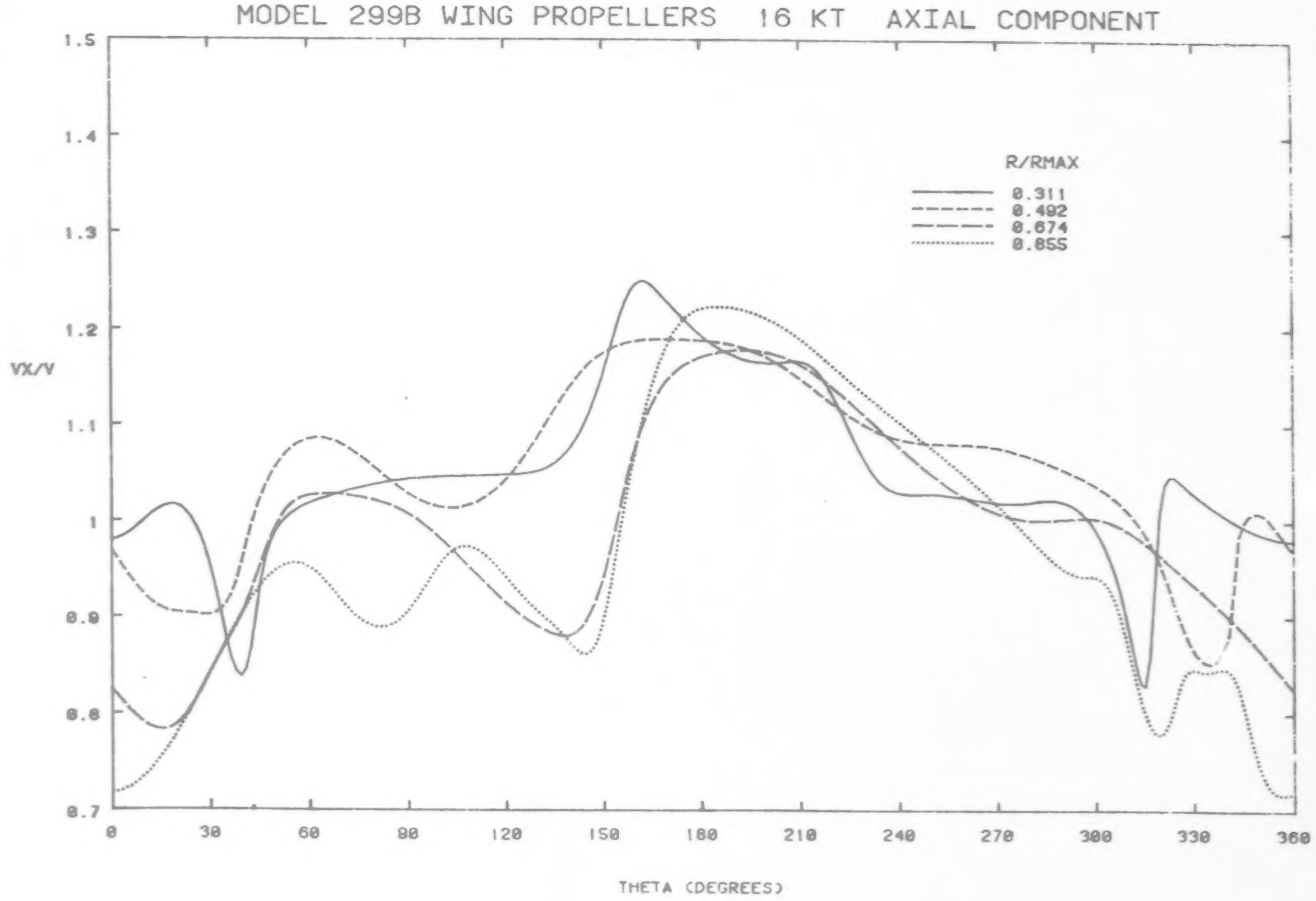

FIGURE 4.7 MODEL 299B WING PROPELLERS 16 KT AXIAL COMPONENT

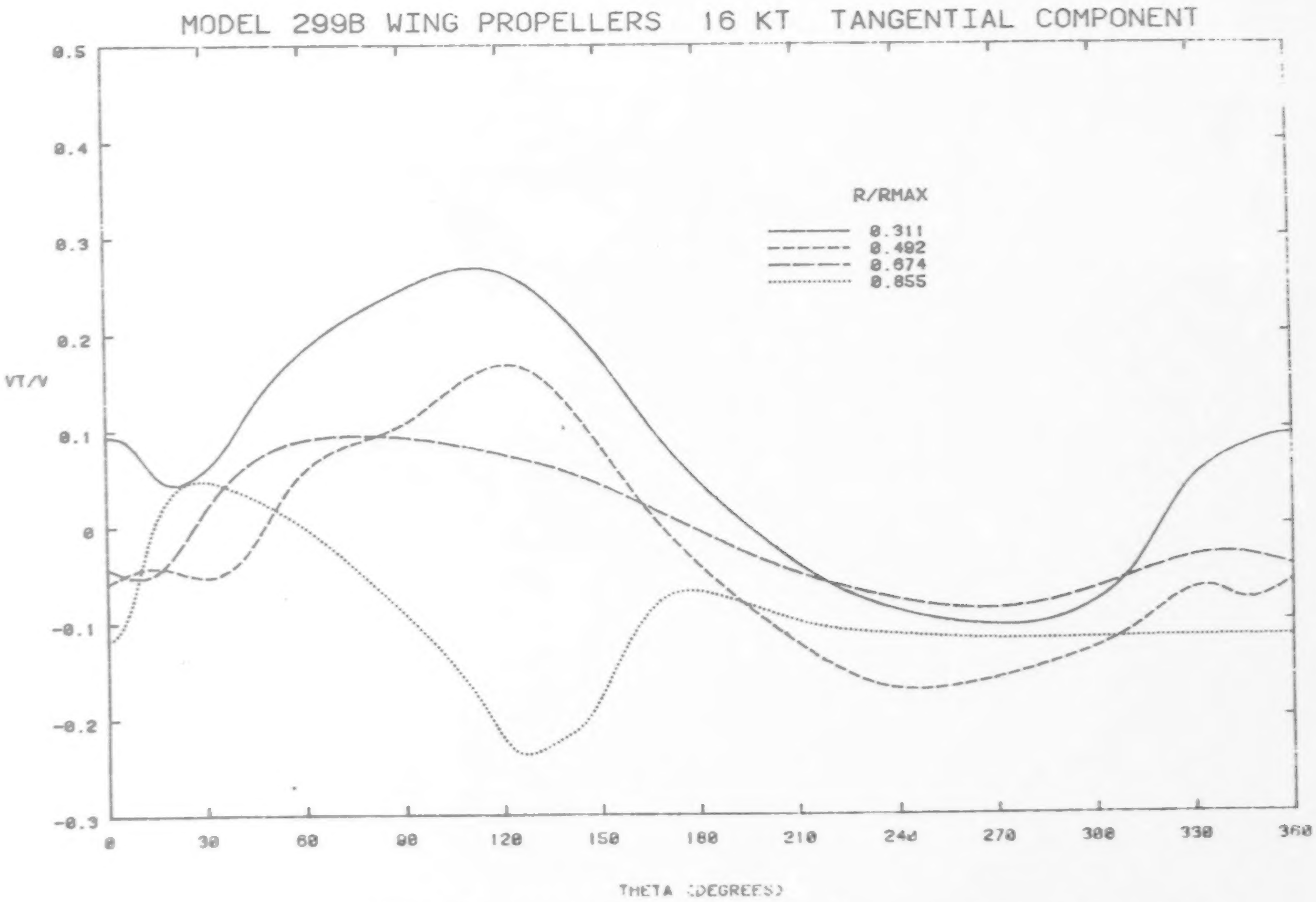

FIGURE 4.8 MODEL 299B WING PROPELLERS 16KT TANGENTIAL COMPONENT

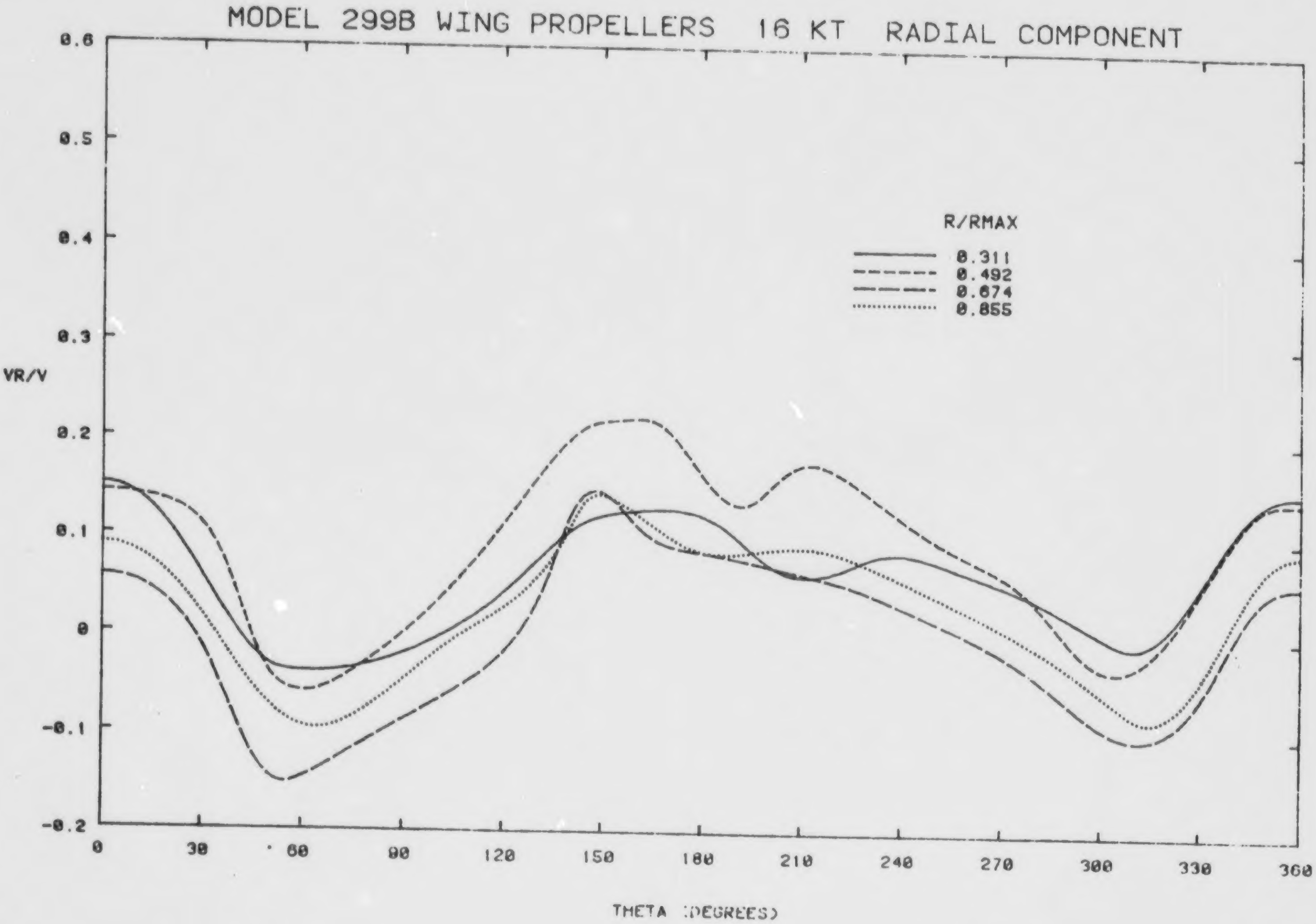

FIGURE 4.9 MODEL 299B WING PROPELLERS 16 KT RADIAL COMPONENT

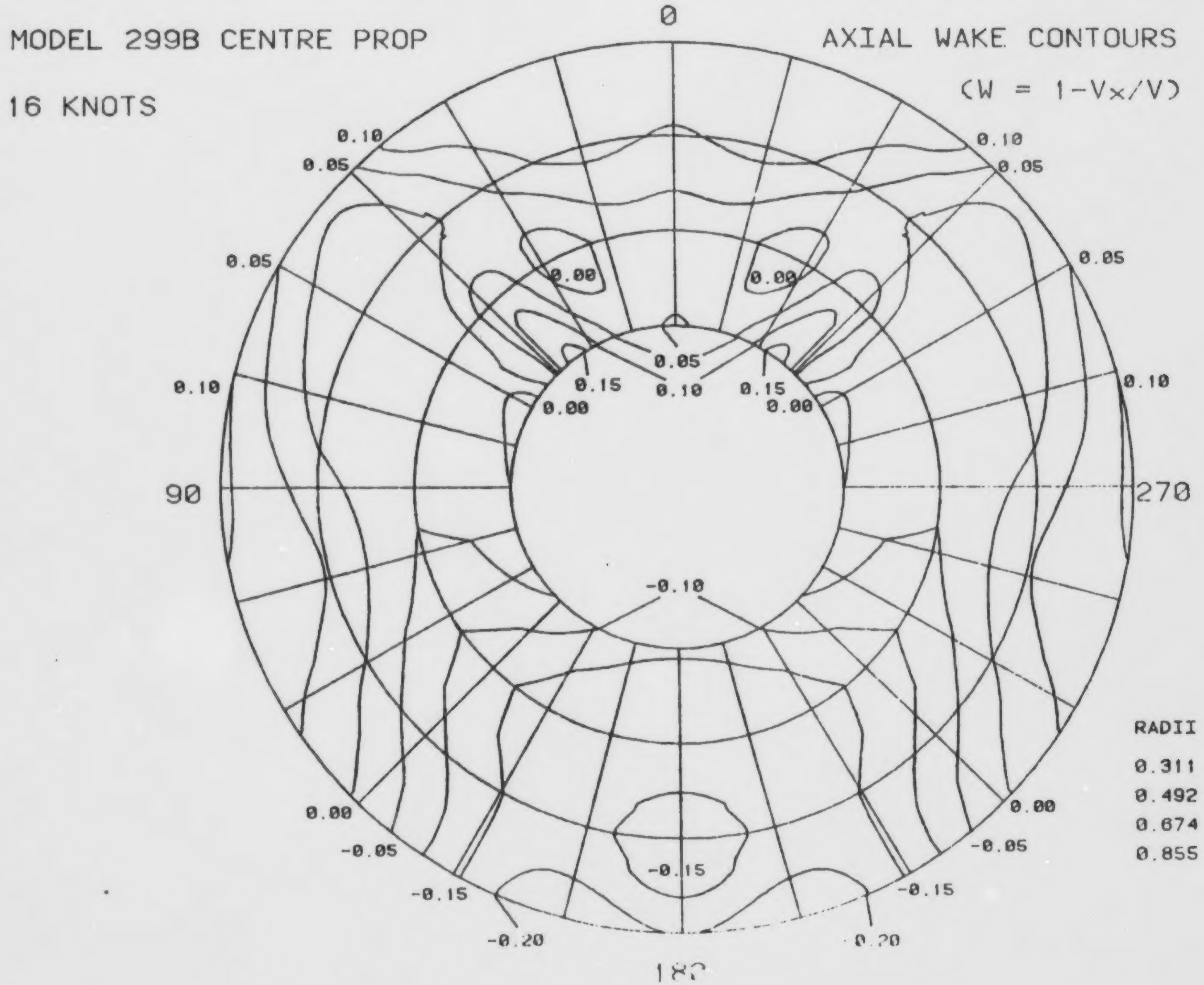

FIGURE 4.10 MODEL 299B CENTRE PROP. 16 KNOTS

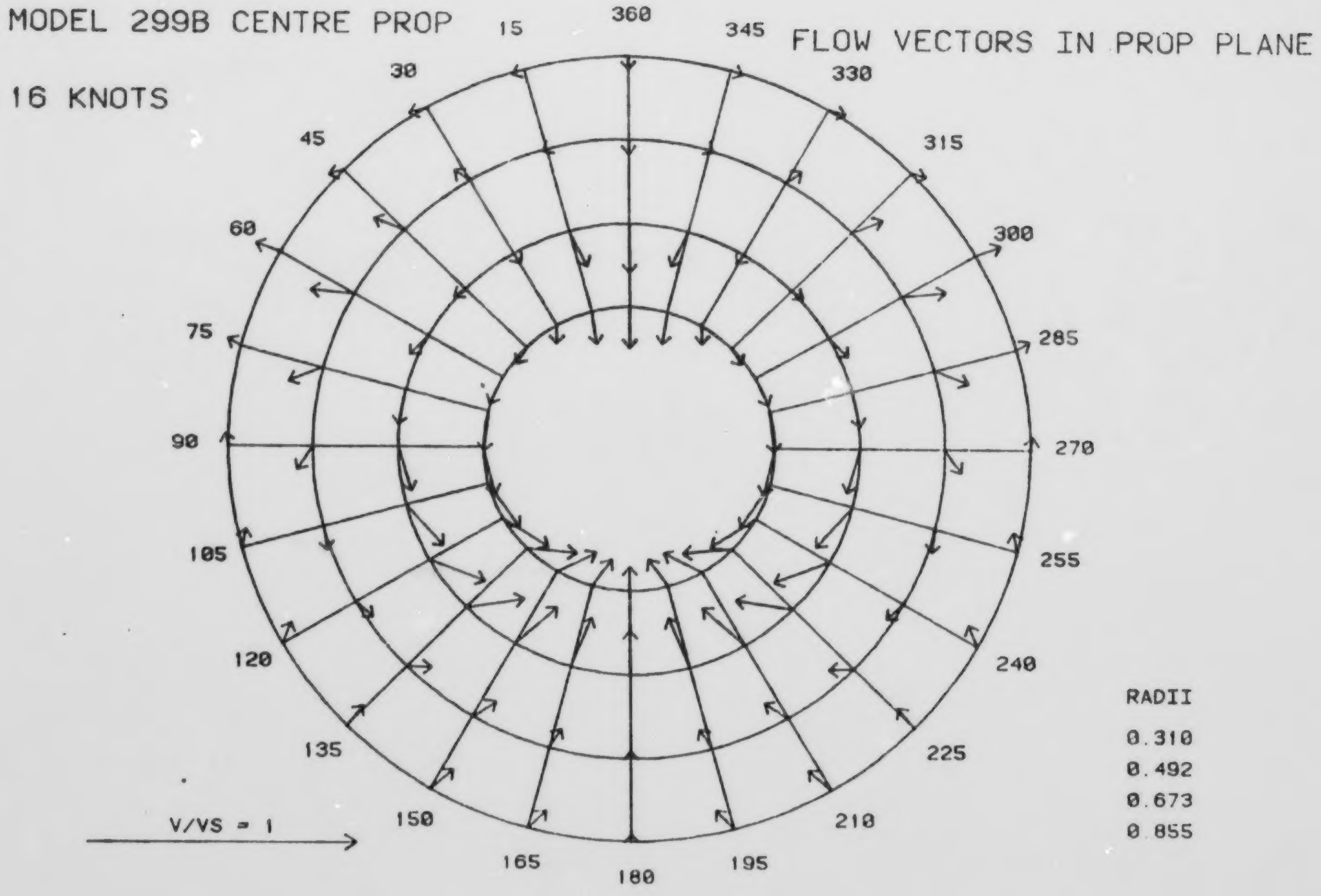

FIGURE 4.11 MODEL 299B CENTRE PROP. FLOW VECTORS IN PROP PLANE

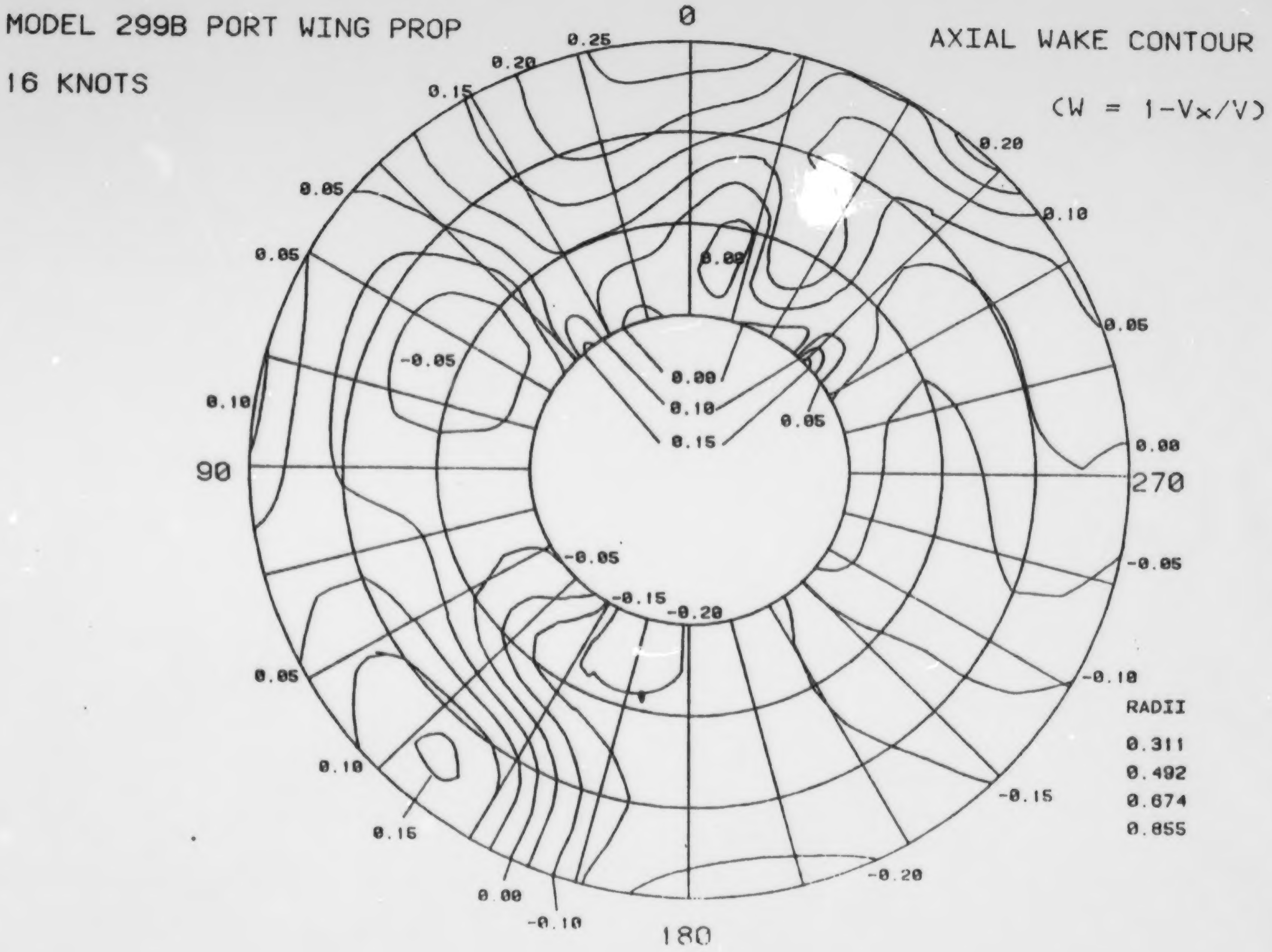

FIGURE 4.12 MODEL 299B PORT WING PROP AXIAL WAKE CONTOUR 16 KNOTS

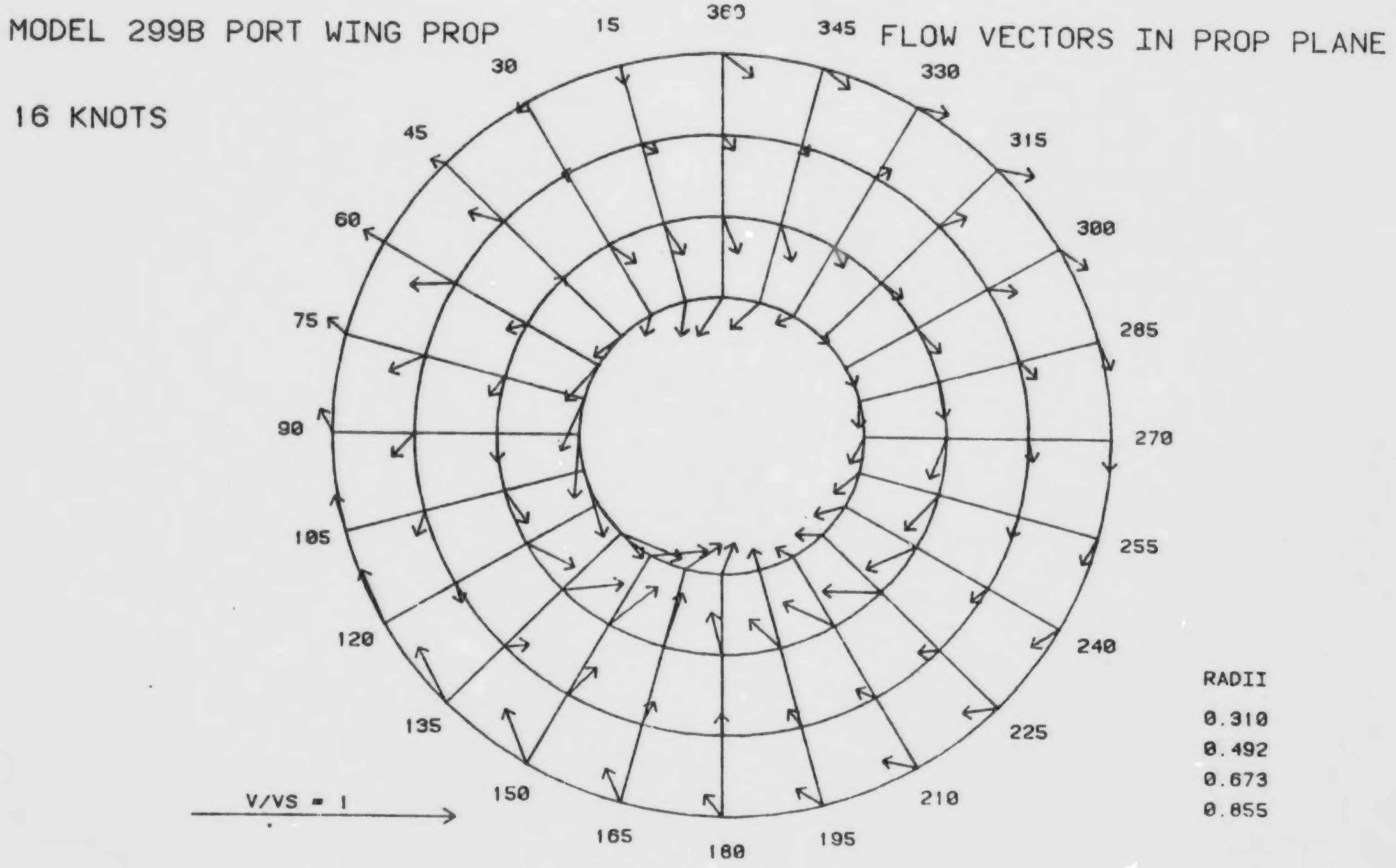

FIGURE 4.13 MODEL 299B PORT WING PROP FLOW VECTORS IN PROP PLANE 16 KNOTS

The axial nominal wake contours, such as those shown in Figure 4.10, can be utilized in two ways in the preliminary propeller design. A circumferential mean wake factor for any radius can be obtained by integrating the wake velocity over the angular position for that radius. These factors may then be used to design a wake-adapted propeller. Alternatively, these factors may be averaged over the disk and a "mean wake fraction" is then obtained and used in the propeller design. The latter approach was adopted in the preliminary design of the propellers in the present project. However, since optimum propeller performance at a speed of 4 knots as well as 16 knots (according the suggested mission profile of POLAR 7A; see Section 5.0, Volume II, Protection of Propellers in Ice - Detail Design of Protection Schemes) should be achieved, the variation of the mean wake fraction with speed must be considered. A wake survey at a speed of 4 knots equivalent full scale was not carried out since errors associated with low speed measurements are usually large. Therefore, the wake distribution, obtained at a speed of 16 knots equivalent full scale, would have to be the basis for predicting the distribution at different speeds, and in particular at an equivalent speed of 4 knots full scale. One can consider the "wake" as a combination of various kinds of wake flows namely: potential wake, viscous wake, pre-separation wake*, full separation eddying wake, and wave wake, (and propulsion device jet wake in the case of effective wake measurements). Of the above forms of wake, the potential flow itself, neglecting surface waves, does not change pattern with speed since wake and other velocities retain their proportions to the body speed, V, regardless of the magnitude of their velocity. The boundary layer thickness increases as the speed decreases and as a result the viscous wake decreases. The shape and position of separation zones may change with speed. The Velox wave system around the ship changes with speed and therefore corresponding changes occur in the orbital velocity at any given point depending on the positions of the adjacent crests and troughs relative to that point.

When the above wake variations are averaged over the propeller disk, the net result is a wake fraction that can be assumed fairly constant with speed (Ref. 6, pp. 194). Therefore, the wake survey conducted at 16 knots equivalent full scale was considered as a representation of the nominal wake distribution at any speed including the 4 knots.

Obviously, it is by no means sufficient to have information concerning only the axial (fore and aft) nominal wake fraction representing the local speeds of advance. The graphical method,

---

* This is strictly speaking a viscous wake. However, as it is caused by a longitudinal pressure gradient, involving an increase of pressure with distance downstream, rather than directly by friction between the liquid and the solid surface, it is given a special name.

Figures 4.11 and 4.13 for the center and wing propellers respectively, embodies projections of the actual velocity vectors in the propeller plane. These figures give an excellent visual representation of the flow over the propeller plane by furnishing directly all the quantitative information derived from the model tests. Figure 4.11 indicates that the flow is axisymmetric over the entire disk of the center propeller. It is generally inward over most of the disk except at the top sector from about 0.65 R upwards where the flow is outwards. It is more likely that we are dealing with a separated flow resulting from the possible adverse pressure gradient along the tunnel roof.

By the same token, Figure 4.13 for the wing propeller (portside) indicates that the flow over the imaginary propeller disk is not symmetric. The flow in the outer radii seems to contain some swirl or rotational motion whereas the flow in the inner radii does not have any clear feature that can be assigned to it. The bottom right hand quarter, however, seems to have a relatively better flow than that over the other three quarters. Flow separation and eddying wake over the top half of the disk ($\theta = 270^\circ$ to $\theta = 90^\circ$) cannot be either substantiated or ruled out at this stage; a fact that must be accounted for in the analysis of the test results in general and the propulsion tests in particular. As a guide line, the wake velocity inside a separation zone is predominantly forward.

Finally, it must be realized that whatever the type of propulsion device used, it integrates the multitudinous relative-velocity vectors of the complex flow through all parts of the disk (or the thrust-producing area) in remarkably efficient fashion, as long as no separation zone exists.

5.0 RESISTANCE TESTS: Models 299 to 299E

5.1 General

A description of the models was given in Section 2.0. For the resistance tests, the propellers were replaced with dummy hubs while the model was ballasted to the correct draft and displacement and attached to the carriage with a pair of guides allowing freedom to surge, heave, and pitch. The model was towed from a point in the extension of the centerline of the center shaft and accelerated successively to constant speeds over the range of 5 to 24 knots equivalent full scale (except for Model 299, the speed range covered was 3 to 30 knots). The effective model speeds through water were obtained by using a blockage correction (NRC). The resistances were measured with a DC input and DC output differential transformer type transducer, the signal of which, together with that of the carriage speed, was entered into a computer system installed on the carriage. The system has a 32 channel multiplexer and variable sampling rates. For these tests, the rate was selected to 20 samples per channel per second.

5.2 Test Results

Predictions for the full scale were made from the test results for the salt water at 15° C (59° F) using the I.T.T.C. 1957 skin friction line together with correlation allowances of 0, 0.0003, and 0.0004. However, due to the considerable differences in the hull form of the models, it was decided to only present the results, and later on make the comparisons, based on model/ ship correlation allowance equal to 0.

Predictions of the effective horsepowers for the full scale POLAR 7 hull form, based on the results of resistance experiments on parent Model 299 with scale factor 1:46, are shown in Table 5.1. Similarly, predictions based on the results of Models 299B, 299C, 299D, and 299E are given in Tables 5.2 to 5.8. The definition of the different coefficients used in the tables and throughout the report are defined under "List of Symbols" at the beginning of the text.

5.3 Discussion of Resistance Experiments

The results of the parent Model 299 are used as the base for comparison. As indicated in Section 2.0, the models have, unavoidably, different hydrostatic particulars which make a direct comparison less accurate. Variations in the displacement and the wetted surface area, in particular, affect the resistance and the propulsion characteristics of the ship. However, if one consid-

```
                              RESULTS OF RESISTANCE EXPERIMENTS
MODEL NO. 299                            DESIGN                            
L =  654.60 FT.                        T =  44.02 FT.                     TEST DATE  02-JUN-80
SHIP PREDICTIONS ARE FOR SALT WATER AT 59 DEG.F.                          TRIM =  0.00 FT. BY THE STERN
                                                               SHIP MODEL CORRELATION ALLOWANCE 0.00000

    DIMENSIONAL            COEFF. BASED ON LENGTH              COEFF. BASED ON DISPLACEMENT
     V        PE         FN    CTM(59)    CR       CTS         FNVOL   CTVOL    TAU     TAUR
   KNOTS     H.P.              X1000     X1000    X1000                 X100    X100    X100

    9.00     1547.      0.105   4.957    1.161    2.740        0.245   1.698   0.051   0.022
   10.00     2080.      0.116   4.847    1.127    2.686        0.272   1.665   0.062   0.026
   11.00     2732.      0.128   4.762    1.110    2.650        0.299   1.643   0.074   0.031
   12.00     3522.      0.140   4.700    1.108    2.632        0.327   1.631   0.087   0.037
   13.00     4469.      0.151   4.656    1.118    2.627        0.354   1.628   0.102   0.043
   14.00     5595.      0.163   4.627    1.138    2.633        0.381   1.632   0.118   0.051
   15.00     6924.      0.175   4.611    1.167    2.649        0.408   1.642   0.137   0.060
   16.00     8501.      0.186   4.612    1.209    2.680        0.435   1.661   0.157   0.071
   17.00    10383.      0.198   4.634    1.269    2.729        0.463   1.691   0.181   0.084
   18.00    12618.      0.209   4.674    1.344    2.794        0.490   1.732   0.208   0.100
   19.00    15245.      0.221   4.727    1.430    2.870        0.517   1.779   0.238   0.118
   20.00    18390.      0.233   4.804    1.537    2.968        0.544   1.840   0.273   0.141
   21.00    22337.      0.244   4.930    1.691    3.115        0.571   1.930   0.315   0.171
   22.00    27543.      0.256   5.136    1.925    3.340        0.599   2.070   0.371   0.214
   23.00    34677.      0.268   5.458    2.272    3.680        0.626   2.281   0.447   0.276
   24.00    44602.      0.279   5.927    2.765    4.166        0.653   2.582   0.551   0.366
   25.00    58340.      0.291   6.566    3.427    4.821        0.680   2.988   0.692   0.492
   26.00    75903.      0.303   7.306    4.189    5.577        0.708   3.456   0.865   0.650
```

TABLE 5.1 RESULTS OF RESISTANCE EXPERIMENTS DESIGN

```
                              RESULTS OF RESISTANCE EXPERIMENTS
MODEL NO. 299B                     WITH GRILLS (AHEAD)                        TEST DATE  14-JUL-81
L =  656.17 FT.                    T =  46.04 FT.                             TRIM =  0.00 FT. BY THE STE
SHIP PREDICTIONS ARE FOR SALT WATER AT 59 DEG.F.                 SHIP MODEL CORRELATION ALLOWANCE 0.000

     DIMENSIONAL                  COEFF. BASED ON LENGTH                COEFF. BASED ON DISPLACEMENT
     V          PE             FN    CTM(59)     CR        CTS          FNVOL    CTVOL      TAU       TAUR
   KNOTS       H.P.                   X1000     X1000     X1000                   X100      X100      X100

    9.00       5794.          0.105    8.851     5.005     6.584          0.231    5.073     0.136     0.103
   10.00       8042.          0.116    8.871     5.104     6.662          0.257    5.133     0.170     0.130
   11.00      10809.          0.128    8.886     5.187     6.727          0.283    5.183     0.207     0.160
   12.00      14145.          0.139    8.895     5.258     6.781          0.309    5.225     0.249     0.193
   13.00      18103.          0.151    8.900     5.318     6.826          0.334    5.259     0.294     0.229
   14.00      22741.          0.163    8.903     5.371     6.865          0.360    5.290     0.343     0.268
   15.00      28121.          0.174    8.907     5.420     6.902          0.386    5.318     0.396     0.311
   16.00      34312.          0.186    8.914     5.469     6.939          0.411    5.347     0.453     0.357
   17.00      41397.          0.198    8.927     5.520     6.980          0.437    5.378     0.514     0.406
   18.00      49467.          0.209    8.947     5.577     7.026          0.463    5.414     0.580     0.460
   19.00      58639.          0.221    8.979     5.642     7.082          0.489    5.457     0.651     0.519
   20.00      69076.          0.232    9.027     5.721     7.153          0.514    5.511     0.729     0.583
   21.00      80988.          0.244    9.098     5.821     7.244          0.540    5.582     0.814     0.654
   22.00      94642.          0.256    9.197     5.948     7.363          0.566    5.673     0.908     0.733
   23.00     110369.          0.267    9.330     6.107     7.514          0.591    5.790     1.013     0.823
   24.00     128972.          0.279    9.527     6.328     7.729          0.617    5.955     1.134     0.929
   25.00     153381.          0.291    9.914     6.738     8.132          0.643    6.265     1.295     1.073
```

TABLE 5.2 RESULTS OF RESISTANCE EXPERIMENTS WITH GRILLS (AHEAD)

RESULTS OF RESISTANCE EXPERIMENTS
WITH GRILLS (ASTERN)

MODEL NO. 299B
L = 656.17 FT.
T = 46.04 FT.
SHIP PREDICTIONS ARE FOR SALT WATER AT 59 DEG.F.

TEST DATE 14-JUL-81
TRIM = 0.00 FT. BY THE STERN
SHIP MODEL CORRELATION ALLOWANCE 0.00000

DIMENSIONAL		COEFF. BASED ON LENGTH				COEFF. BASED ON DISPLACEMENT			
V KNOTS	PE H.P.	FN	CTM(59) X1000	CR X1000	CTS X1000	FNVOL	CTVOL X100	TAU X100	TAUR X100
9.00	10359.	0.105	14.038	10.192	11.771	0.231	9.069	0.243	0.210
10.00	14178.	0.116	13.954	10.187	11.745	0.257	9.050	0.299	0.260
11.00	18700.	0.128	13.797	10.099	11.639	0.283	8.968	0.359	0.311
12.00	24119.	0.139	13.676	10.039	11.562	0.309	8.909	0.424	0.368
13.00	30842.	0.151	13.703	10.121	11.629	0.334	8.960	0.501	0.436
14.00	39378.	0.163	13.925	10.393	11.888	0.360	9.160	0.594	0.519
15.00	49973.	0.174	14.270	10.784	12.266	0.386	9.451	0.703	0.618
16.00	62668.	0.186	14.648	11.204	12.674	0.411	9.765	0.827	0.731
17.00	77317.	0.198	14.983	11.577	13.036	0.437	10.044	0.960	0.852
18.00	93980.	0.209	15.270	11.899	13.349	0.463	10.285	1.102	0.982
19.00	112984.	0.221	15.543	12.205	13.646	0.489	10.514	1.255	1.123
20.00	134709.	0.232	15.824	12.518	13.949	0.514	10.748	1.422	1.276

TABLE 5.3 RESULTS OF RESISTANCE EXPERIMENTS WITH GRILLS (ASTERN)

```
                          RESULTS OF RESISTANCE EXPERIMENTS
MODEL NO. 299B                 WITHOUT GRILLS (AHEAD)                    TEST DATE  16-JUL-81
L =  656.17 FT.                T =  46.04 FT.                            TRIM =  0.00 FT. BY THE STERN
SHIP PREDICTIONS ARE FOR SALT WATER AT 59 DEG.F.              SHIP MODEL CORRELATION ALLOWANCE 0.00000

    DIMENSIONAL              COEFF. BASED ON LENGTH            COEFF. BASED ON DISPLACEMENT
     V        PE          FN    CTM(59)    CR       CTS         FNVOL    CTVOL    TAU      TAUR
   KNOTS     H.P.                X1000    X1000    X1000                 X100     X100     X100

    9.00     4158.       0.105   7.499    3.654    5.233        0.231    3.641    0.098    0.068
   10.00     5777.       0.116   7.509    3.742    5.300        0.257    3.687    0.122    0.086
   11.00     7783.       0.128   7.523    3.825    5.364        0.283    3.732    0.149    0.106
   12.00    10224.       0.139   7.542    3.905    5.428        0.309    3.776    0.180    0.129
   13.00    13152.       0.151   7.566    3.984    5.492        0.334    3.821    0.214    0.155
   14.00    16621.       0.163   7.595    4.063    5.557        0.360    3.866    0.251    0.183
   15.00    20690.       0.174   7.629    4.142    5.624        0.386    3.913    0.291    0.214
   16.00    25420.       0.186   7.668    4.223    5.693        0.411    3.961    0.335    0.249
   17.00    30877.       0.198   7.712    4.306    5.766        0.437    4.011    0.383    0.286
   18.00    37152.       0.209   7.765    4.395    5.844        0.463    4.066    0.436    0.328
   19.00    44363.       0.221   7.831    4.493    5.934        0.489    4.128    0.493    0.373
   20.00    52658.       0.232   7.913    4.607    6.039        0.514    4.201    0.556    0.424
   21.00    62233.       0.244   8.019    4.742    6.165        0.540    4.289    0.625    0.481
   22.00    73389.       0.256   8.157    4.908    6.323        0.566    4.399    0.704    0.547
   23.00    86552.       0.267   8.342    5.119    6.526        0.591    4.540    0.794    0.623
   24.00   102301.       0.279   8.587    5.389    6.789        0.617    4.723    0.900    0.714
   25.00   122028.       0.291   8.947    5.771    7.165        0.643    4.985    1.030    0.830
```

TABLE 5.4 RESULTS OF RESISTANCE EXPERIMENTS WITHOUT GRILLS (AHEAD)

```
                              RESULTS OF RESISTANCE EXPERIMENTS
MODEL NO. 2998                    WITHOUT GRILLS (ASTERN)
L =  656.17 FT.                   T =  46.04 FT.                        TEST DATE  15-JUL-81
                                                                        TRIM =  0.00 FT. BY THE STERN
SHIP PREDICTIONS ARE FOR SALT WATER AT 59 DEG.F.           SHIP MODEL CORRELATION ALLOWANCE 0.00000

    DIMENSIONAL                COEFF. BASED ON LENGTH             COEFF. BASED ON DISPLACEMENT
     V         PE          FN     CTM(59)    CR       CTS          FNVOL   CTVOL     TAU     TAUR
   KNOTS      H.P.                 X1000    X1000    X1000                  X100     X100    X100

    9.00      7968.       0.105   12.294    8.448   10.027         0.231   6.976    0.187   0.157
   10.00     11197.       0.116   12.481    8.714   10.272         0.257   7.146    0.236   0.200
   11.00     14930.       0.128   12.449    8.751   10.291         0.283   7.160    0.286   0.244
   12.00     19284.       0.139   12.352    8.715   10.238         0.309   7.123    0.339   0.289
   13.00     24777.       0.151   12.420    8.838   10.346         0.334   7.198    0.402   0.344
   14.00     31716.       0.163   12.641    9.109   10.604         0.360   7.377    0.478   0.411
   15.00     40363.       0.174   12.976    9.490   10.972         0.386   7.633    0.568   0.491
   16.00     50806.       0.186   13.354    9.909   11.379         0.411   7.917    0.670   0.584
   17.00     62920.       0.198   13.696   10.290   11.749         0.437   8.174    0.781   0.684
   18.00     76652.       0.209   13.979   10.608   12.058         0.463   8.389    0.899   0.791
   19.00     92302.       0.221   14.243   10.905   12.346         0.489   8.589    1.025   0.906
   20.00    110224.       0.232   14.515   11.209   12.640         0.514   8.794    1.163   1.031
```

TABLE 5.5 RESULTS OF RESISTANCE EXPERIMENTS WITHOUT GRILLS (ASTERN)

```
                          RESULTS OF RESISTANCE EXPERIMENTS
MODEL NO. 299C                      DESIGN                  TEST DATE  16-FEB-82
L =  200.0  m                     T =  14.03 m                                 TRIM =  0.00 m BY THE STERN
SHIP PREDICTIONS ARE FOR SALT WATER AT 15 DEG.C.              SHIP MODEL CORRELATION ALLOWANCE 0.0000

      DIMENSIONAL                COEFF. BASED ON LENGTH              COEFF. BASED ON DISPLACEMENT
      V          PE           FN    CTM(59)    CR       CTS         FNVOL    CTVOL     TAU      TAUR
    KNOTS        KW                  X1000    X1000    X1000                  X100     X100     X100

     5.00       866.        0.058  10.265    5.933    7.636         0.128    5.908    0.049    0.038
     6.00      1409.        0.070   9.695    5.523    7.186         0.154    5.559    0.066    0.051
     7.00      2099.        0.081   9.156    5.113    6.744         0.180    5.217    0.084    0.064
     8.00      3006.        0.093   8.802    4.866    6.469         0.206    5.004    0.106    0.080
     9.00      4214.        0.105   8.637    4.791    6.370         0.231    4.928    0.132    0.099
    10.00      5857.        0.116   8.663    4.896    6.454         0.257    4.993    0.165    0.125
    11.00      7871.        0.128   8.675    4.977    6.517         0.283    5.042    0.201    0.154
    12.00     10287.        0.139   8.674    5.037    6.560         0.308    5.075    0.241    0.185
    13.00     13136.        0.151   8.662    5.080    6.588         0.334    5.097    0.284    0.219
    14.00     16455.        0.163   8.645    5.113    6.608         0.360    5.112    0.331    0.256
    15.00     20279.        0.174   8.626    5.139    6.621         0.385    5.122    0.380    0.295
    16.00     24681.        0.186   8.614    5.169    6.640         0.411    5.137    0.434    0.338
    17.00     29718.        0.198   8.612    5.206    6.665         0.437    5.157    0.492    0.384
    18.00     35501.        0.209   8.628    5.258    6.708         0.462    5.189    0.555    0.435
    19.00     42100.        0.221   8.660    5.323    6.764         0.488    5.233    0.623    0.491
    20.00     49759.        0.232   8.728    5.422    6.854         0.514    5.302    0.700    0.554
    21.00     58954.        0.244   8.868    5.592    7.015         0.540    5.427    0.790    0.630
    22.00     69354.        0.256   9.011    5.762    7.177         0.565    5.553    0.887    0.712
    23.00     80384.        0.267   9.096    5.872    7.280         0.591    5.632    0.983    0.793
    24.00     92067.        0.279   9.137    5.938    7.339         0.617    5.678    1.079    0.873
```

TABLE 5.6 RESULTS OF RESISTANCE EXPERIMENTS DESIGN

RESULTS OF RESISTANCE EXPERIMENTS
BARE HULL

MODEL NO. 299D
L = 656.17 FT.
T = 46.05 FT.
SHIP PREDICTIONS ARE FOR SALT WATER AT 59 DEG.F.

TEST DATE 01-OCT-81
TRIM = 0.00 FT. BY THE STERN
SHIP MODEL CORRELATION ALLOWANCE 0.00000

DIMENSIONAL		COEFF. BASED ON LENGTH				COEFF. BASED ON DISPLACEMENT			
V KNOTS	PE H.P.	FN	CTM(59) X1000	CR X1000	CTS X1000	FNVOL	CTVOL X100	TAU X100	TAUR X100
9.00	2577.	0.105	6.195	2.349	3.928	0.232	2.277	0.061	0.037
10.00	3357.	0.116	5.939	2.172	3.730	0.258	2.162	0.072	0.042
11.00	4245.	0.128	5.703	2.005	3.544	0.284	2.054	0.083	0.047
12.00	5265.	0.139	5.500	1.863	3.386	0.309	1.962	0.094	0.052
13.00	6528.	0.151	5.376	1.794	3.302	0.335	1.914	0.107	0.058
14.00	8119.	0.163	5.326	1.794	3.288	0.361	1.906	0.124	0.068
15.00	10056.	0.174	5.316	1.829	3.311	0.387	1.919	0.143	0.079
16.00	12311.	0.186	5.315	1.870	3.340	0.412	1.936	0.165	0.092
17.00	14896.	0.198	5.316	1.910	3.370	0.438	1.953	0.187	0.106
18.00	17814.	0.209	5.315	1.945	3.395	0.464	1.967	0.212	0.121
19.00	21186.	0.221	5.330	1.993	3.433	0.490	1.990	0.239	0.138
20.00	25389.	0.232	5.402	2.096	3.527	0.516	2.044	0.272	0.161
21.00	30947.	0.244	5.568	2.291	3.714	0.541	2.152	0.315	0.195
22.00	37302.	0.256	5.727	2.478	3.893	0.567	2.256	0.363	0.231
23.00	44236.	0.267	5.856	2.633	4.041	0.593	2.342	0.412	0.268
24.00	54204.	0.279	6.156	2.957	4.358	0.619	2.526	0.483	0.328
25.00	71102.	0.291	6.839	3.664	5.057	0.644	2.931	0.609	0.441
26.00	96709.	0.302	7.881	4.728	6.115	0.670	3.544	0.796	0.615

TABLE 5.7 RESULTS OF RESISTANCE EXPERIMENTS BARE HULL

RESULTS OF RESISTANCE EXPERIMENTS
MODEL NO. 299E 1 TEST DATE 05-MAY-82
L = 200.01 m T = 14.03 m TRIM = 0.00 m BY THE ST
SHIP PREDICTIONS ARE FOR SALT WATER AT 15 DEG.C. SHIP MODEL CORRELATION ALLOWANCE 0.000

DIMENSIONAL		COEFF. BASED ON LENGTH				COEFF. BASED ON DISPLACEMENT			
V KNOTS	PE KW	FN	CTM(59) X1000	CR X1000	CTS X1000	FNVOL	CTVOL X100	TAU X100	TAUR X100
5.00	496.	0.058	7.743	3.411	5.114	0.129	3.398	0.028	0.019
6.00	788.	0.070	7.213	3.041	4.704	0.154	3.125	0.037	0.024
7.00	1166.	0.081	6.794	2.751	4.381	0.180	2.911	0.047	0.030
8.00	1655.	0.093	6.499	2.563	4.166	0.206	2.768	0.059	0.036
9.00	2287.	0.105	6.310	2.464	4.043	0.231	2.686	0.072	0.044
10.00	3102.	0.116	6.206	2.439	3.997	0.257	2.656	0.088	0.054
11.00	4139.	0.128	6.166	2.468	4.008	0.283	2.663	0.107	0.066
12.00	5429.	0.139	6.163	2.526	4.049	0.309	2.690	0.128	0.080
13.00	6996.	0.151	6.177	2.595	4.104	0.334	2.727	0.152	0.096
14.00	8858.	0.163	6.198	2.666	4.160	0.360	2.764	0.179	0.115
15.00	11043.	0.174	6.221	2.735	4.217	0.386	2.802	0.208	0.135
16.00	13586.	0.186	6.249	2.804	4.275	0.412	2.840	0.240	0.158
17.00	16458.	0.198	6.264	2.858	4.317	0.437	2.868	0.274	0.181
18.00	19575.	0.209	6.247	2.876	4.326	0.463	2.874	0.308	0.205
19.00	23214.	0.221	6.259	2.922	4.362	0.489	2.898	0.346	0.232
20.00	28288.	0.232	6.432	3.126	4.557	0.514	3.028	0.401	0.275
21.00	34735.	0.244	6.687	3.411	4.834	0.540	3.212	0.468	0.331
22.00	41043.	0.256	6.802	3.552	4.968	0.566	3.301	0.528	0.378
23.00	46878.	0.267	6.781	3.558	4.965	0.592	3.299	0.577	0.414
24.00	54951.	0.279	6.921	3.722	5.123	0.617	3.404	0.648	0.471

TABLE 5.8 RESULTS OF RESISTANCE EXPERIMENTS 1

ers that the increase in displacement and wetted surface area of the models, compared with Model 299, is almost entirely due to the fitment of the proposed protection arrangement and the subsequent modifications to the lines plans to accommodate the device, rather than due to intended changes in the principle dimensions or the payload, then one can cautiously conduct a general qualitative comparison without impairing the basic principals.

Graphically, Figure 5.1 shows plots of the predicted full scale effective power, PE, over a speed range from 9 to 28 knots for the different models tested.

The following discussion deals with the resistance test results of each model; comparison with earlier test results; suggested modifications and reasons behind them; predicted performance of the modified model; and test results of the modified model. The discussion is presented in chronological order with regard to the time of testing, starting with Model 299, the parent hull form.

5.3.1 Model 299

Figure 5.1 contains a plot of the predicted PE versus speed based on model test results. It can be seen that beyond 20 knots, the ship resistance increases quite rapidly. This is not unexpected for an icebreaker hull which has relatively high wave making resistance, as Figures 2.3(a) and 2.3(b) also suggest.

As indicated earlier, the above plot will be used as the basis for comparing the resistance characteristics of the various models.

5.3.2 Model 299B

This model represents the initial design for incorporating the recommended protection scheme with minimum alteration to the principal dimensions of the parent hull represented by Model 299.

The main features of the developed hull (i.e., Model 299B) compared with Model 299 are:

- squared-off transom;
- wall-sided hull;
- increased displacement by about 23%; and,
- increased wetted surface by about 44%.

A full-detailed discussion of the results obtained with Model 299B is presented herein, to assist in identifying problem areas and, consequently, to suggest a proper course of action for improvements.

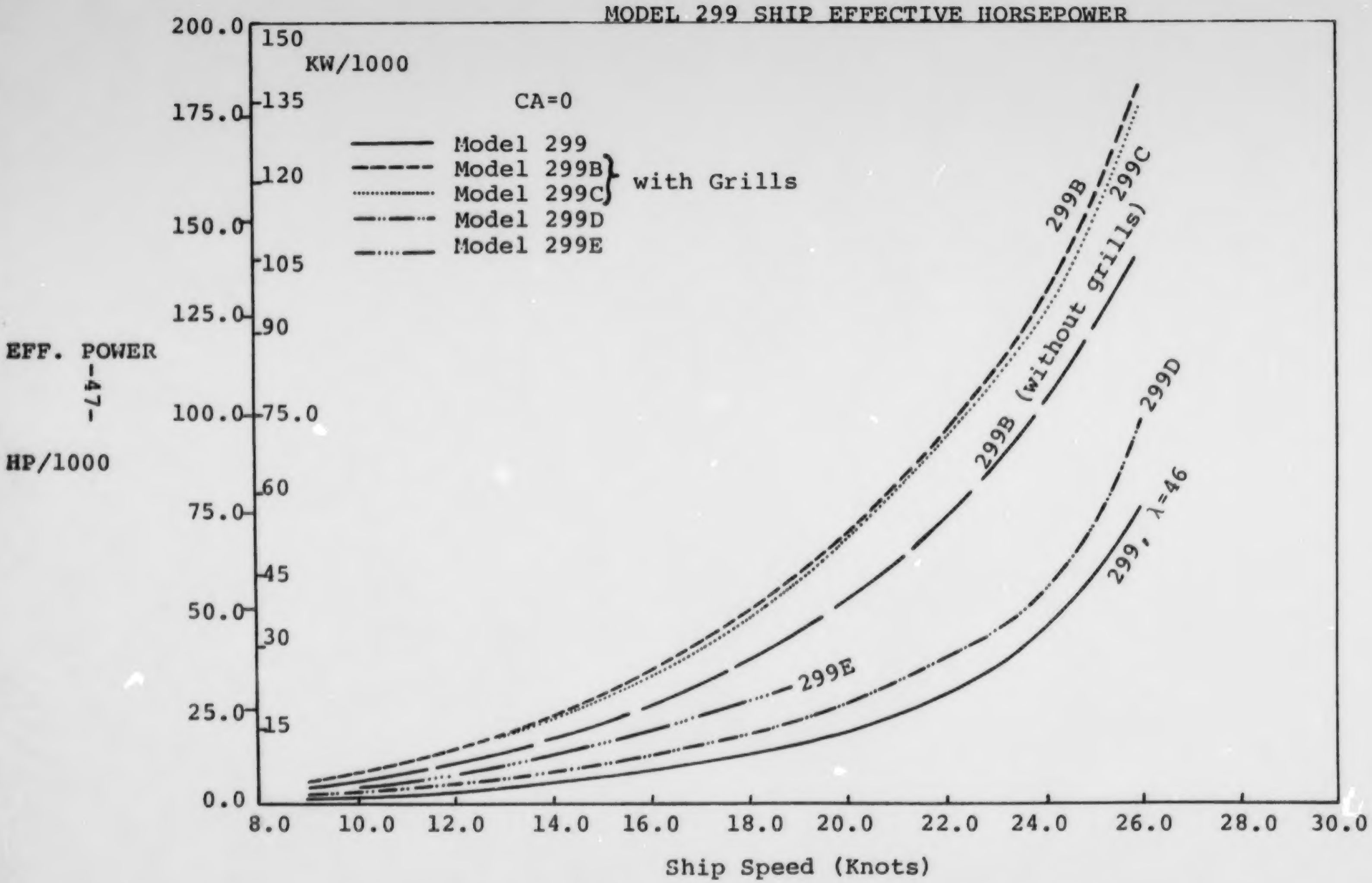

FIGURE 5.1 MODEL 299 SHIP EFFECTIVE HORSEPOWER

Figures 5.2 and 5.3 show model resistance coefficients versus Froude number for Model 299B, with and without grills, in ahead and astern conditions. It is clear from Figure 5.2 that there is no interaction between the bow and stern wave system in ahead condition over a speed range of 9 to 25 knots equivalent full scale. This conclusion is equally true for the model with and without grills where the resistance increases steadily with speed as shown in Figure 5.2.

On the other hand, Figure 5.3 shows the total resistance coefficient versus Froude number in astern conditions. It appears that there is a crest and a trough corresponding to Froude numbers of about 0.122 and 0.142, respectively. In this instance, assuming the distance between the stern and the bow pressure systems is typically 0.9L, the corresponding "N" values for the "bump" and "hollow" are 19 (odd integer) and 14 (even integer), respectively. The resulting wave system at N = 19 due to the coincidence of the crests of the stern and bow wave system is certainly not very alarming for a number of reasons. First, it occurs well below the most pronounced humps; usually at Froude numbers of 0.54 (N = 1, main hump) and 0.31 (N = 3, prismatic hump). Second, the corresponding speed at which this hump occurs is about 10 1/2 knots equivalent full scale which is well above the estimated icebreaking speed of 4 knots; and well below the estimated cruising speed of 16 knots in clear water.

In the preceding discussion with regard to Figures 5.2 and 5.3, two interrelated assumptions were made. First, it was assumed that the total resistance consists of a frictional resistance and a residuary resistance which in turn is mainly a wave-making resistance. The two components of resistance are then added linearly using Froude's principal. Second, as far as the locations of the humps and hollows on the resistance curve are concerned, it makes not difference whether to locate them using the total resistance curve or the wave-making resistance curve; based on the first assumption. Figures 5.4 and 5.5 show the effective power for Model 299B with and without grills in ahead and astern conditions.

These results show the considerable effect of the bottom and stern guards on the open water resistance and consequently on the effective power. For a ship speed of 16 knots, the effective power is reduced by about 29% when the guards (Figures 2.10 and 2.11) are removed. Allowing for the difference in the wetted surface area, the reduction is about 22%. Although both the bottom and stern guards were removed, it is believed that the bottom guards had the greater effect. It is hard, however, to assess quantitatively their separate effects without supporting experimental data.

Figure 5.1 contains a plot of the predicted effective power PE versus speed of the full scale ship (Model 299B, $\lambda = 46$) in the

MODEL 299B

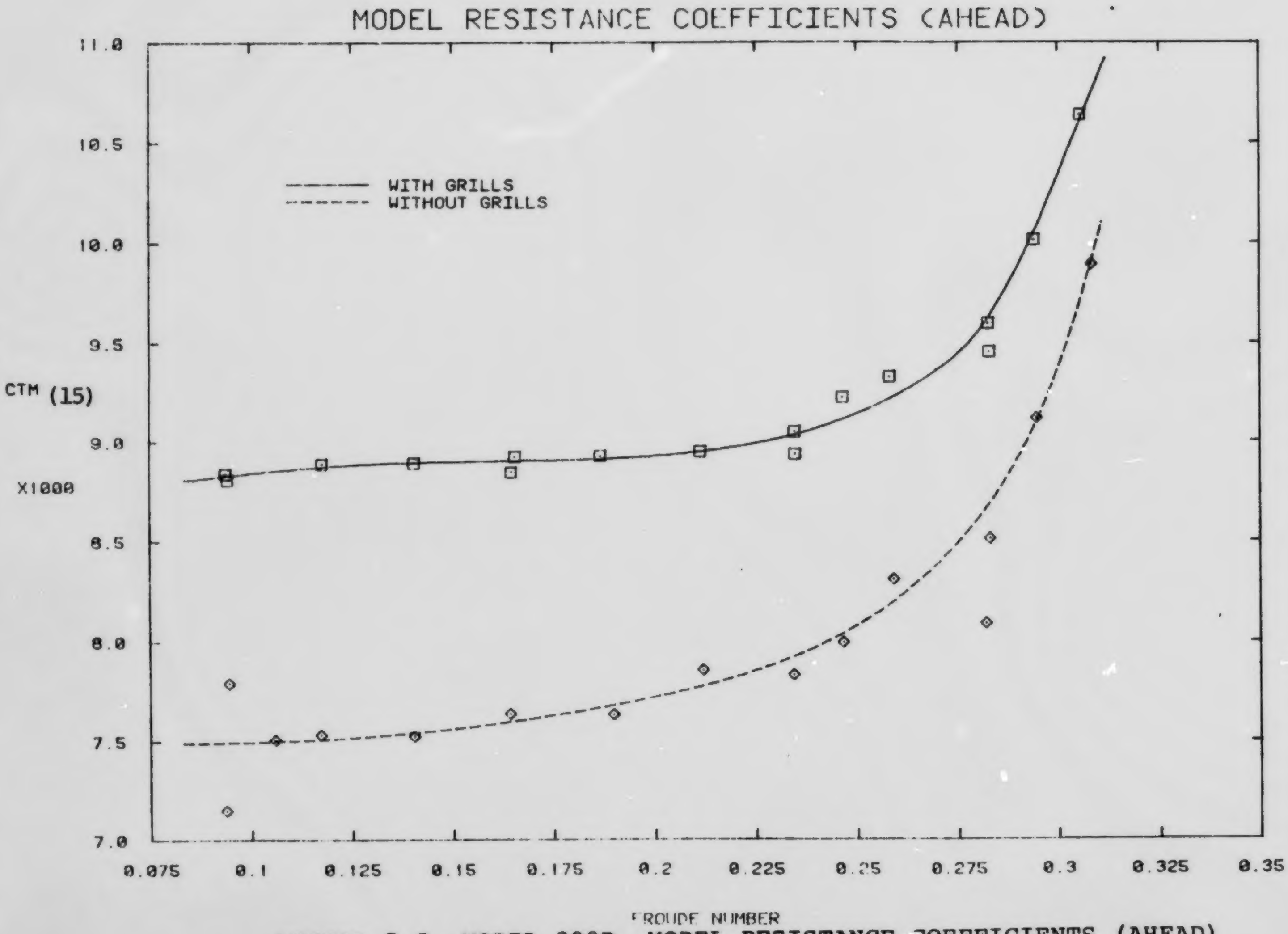

FIGURE 5.2 MODEL 299B MODEL RESISTANCE COEFFICIENTS (AHEAD)

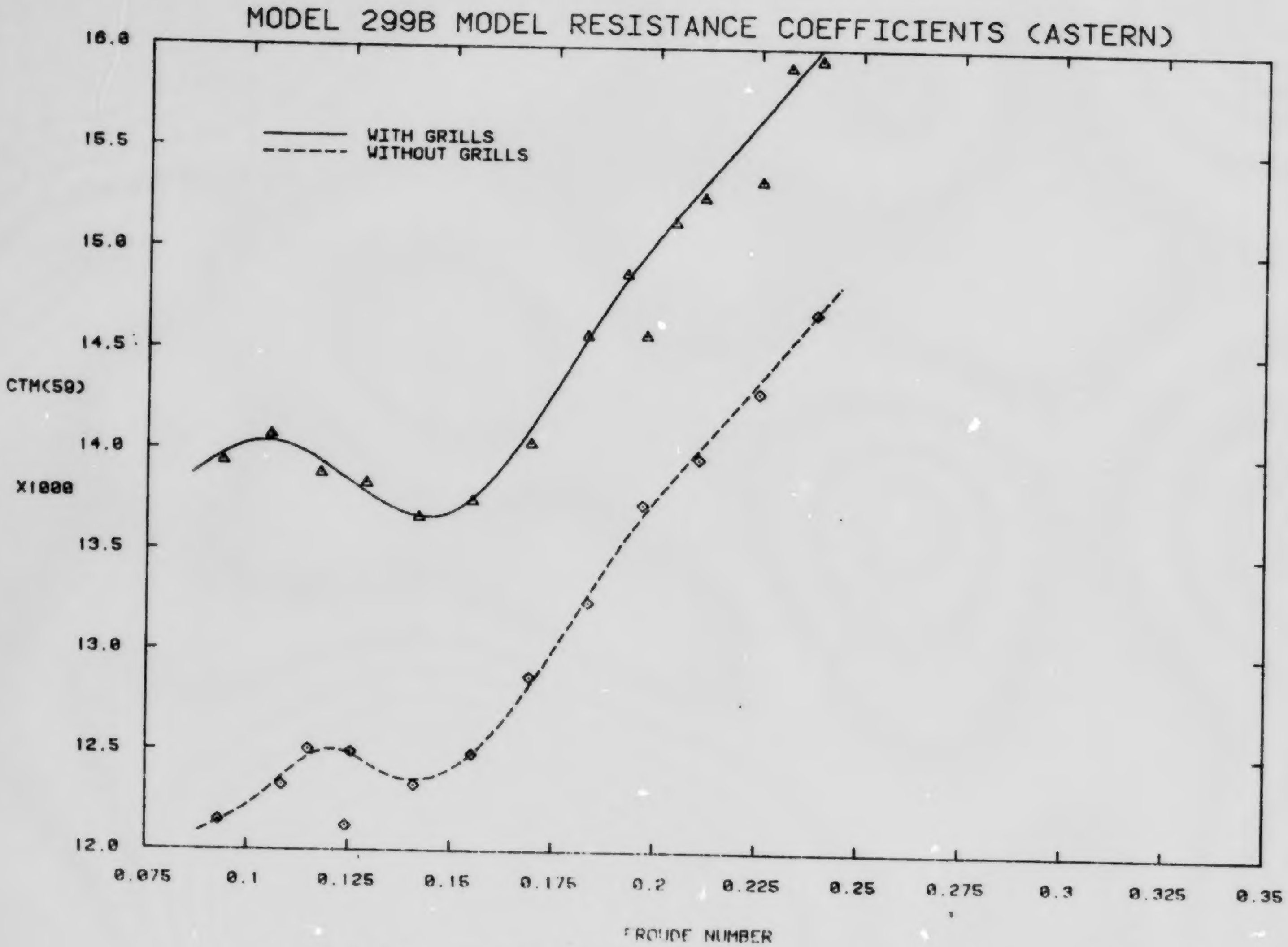

FIGURE 5.3 MODEL 299B MODEL RESISTANCE COEFFICIENTS (ASTERN)

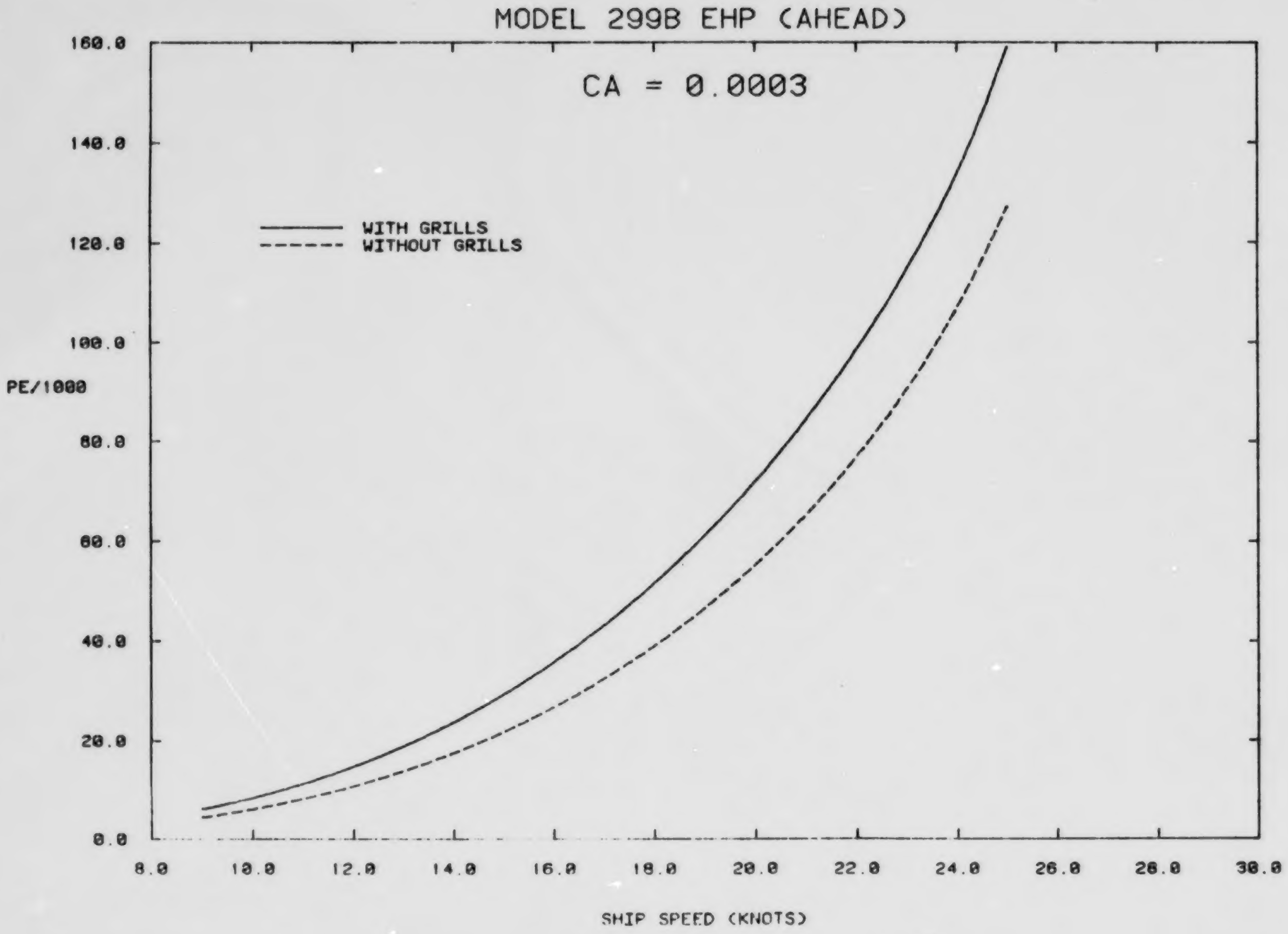

FIGURE 5.4 MODEL 299B EHP (AHEAD)

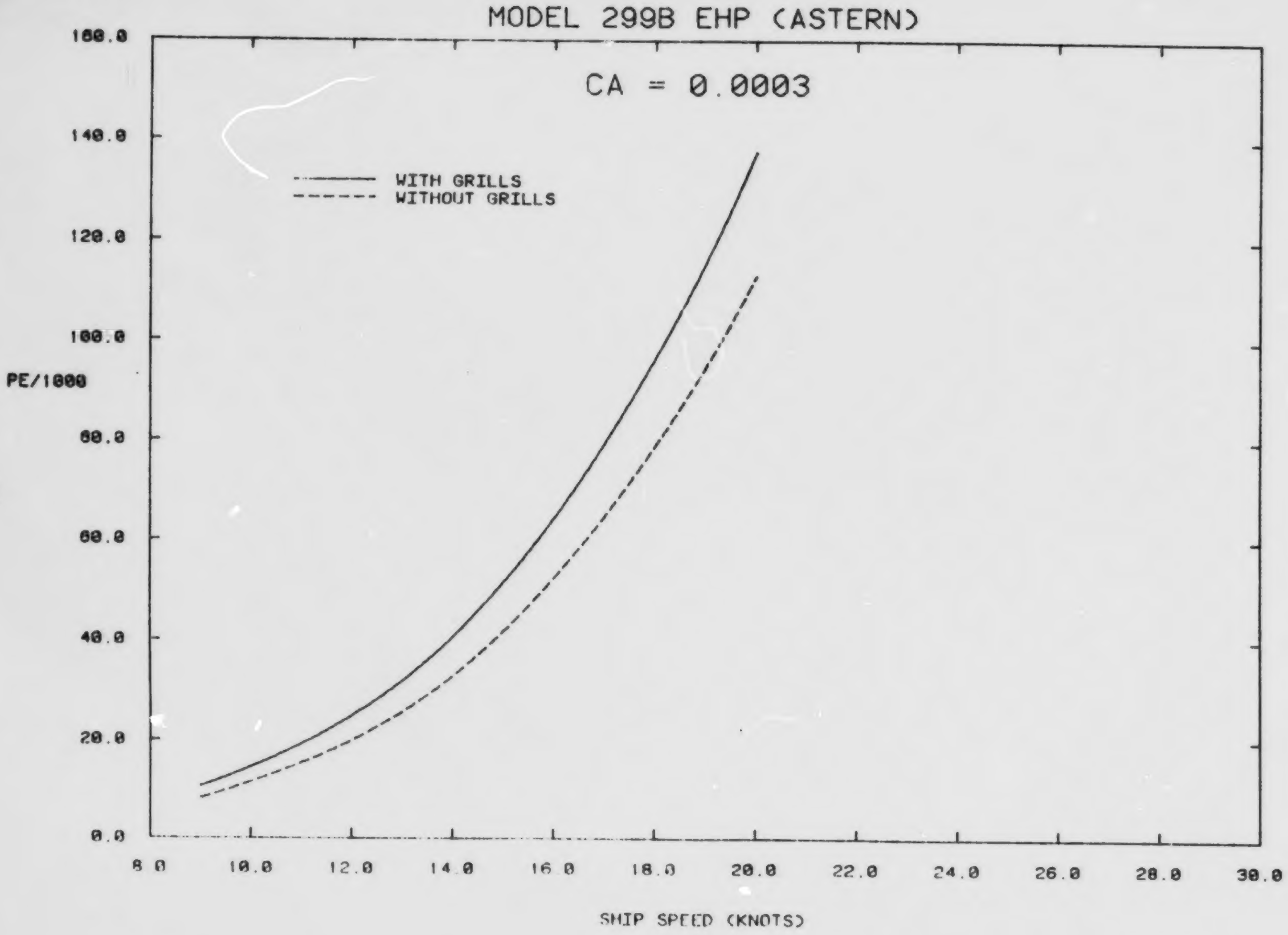

FIGURE 5.5 MODEL 299B EHP (ASTERN)

ahead condition with the full protection arrangement in place. It is clear that there is a substantial increase in PE for the proposed ship POLAR 7A compared with POLAR 7. Bearing in mind, that the wetted surface areas of the two vessels are not the same, (due to the use of skirts, guards, etc.), the ratio of the effective powers is about 3.4 at 16 knots.

It is worth noting that a direct comparison between the absolute values of the resistance coefficients of the two Models 299 and 299B (or the other models in this matter) should not be performed as the models are not geometrically similar. Indeed, if Model A has a greater total resistance than Model B, it does not necessarily mean that in the full scale, ship A would be more resistive than B. However, some important features can be detected from their general tendency if plotted versus the proper nondimensional numbers as explained below.

Figure 5.2 shows the relation between the measured total resistance coefficient of Model 299B versus Froude number. The independence of the total resistance coefficients on F_r for F_r up to about 0.18 suggests that the residuary resistance component of Model 299B is also a function of F_r even at low speeds. The existence of gravitational forces at such low speeds is certainly uncommon in ship's hydrodynamic studies and requires some explanations and hard evidence.

It is reasonable to assume that the wave-making resistance is almost negligible at low Froude numbers and below $F_r \approx 0.18$ in particular. Therefore, there must be some other component(s) of the residuary resistance that affects the resistance at relatively low speeds. This component of resistance is a function of F_r as shown in Figure 5.6 and increases with increasing F_r.

For the normal hull form, Figure 5.7 shows the relationship between the measured total resistance coefficient of Model 299 ($\lambda = 46$) and Froude number. As one would expect, the total resistance decreases with increasing F_r for lower velocities (up to $F_r = 0.18$). The wave-making resistance for $F_r < 0.18$ is insignificant in this case and the other components of the residuary resistance are certainly independent of F_r, as shown in Figure 5.6.

For higher Froude numbers, the resistance due to the formation of bow and stern waves starts to manifest itself as the velocity increases and the total resistance of the model then increases with increasing Froude number, as shown in Figure 5.7.

Another interesting point, the total resistance coefficients are plotted versus Reynolds number for Models 299 and 299B as shown in Figure 5.8. At low Reynolds numbers up to $R_e = 5 \times 10^5$, the residuary resistance of Model 299B is almost independent on R_e, whereas for Model 299B, it is a function of Reynolds number over the same range.

It is quite evident that the tendency of the resistance coefficients for Model 299 are in agreement with normal ship model testing results whereas those for Model 299B are not.

It is concluded from the foregoing discussion that the residuary resistance component for Model 299B, at low speeds, is in fact a function of both Reynolds and Froude numbers.

This may be explained if flow separation has occurred. Flow separation may occur even on a streamlined body depending, among other factors, on the nature of the boundary layer flow, the surface roughness, and pressures and forces associated with the motion. Therefore, flow separation on the ship's hull is by no means a surprise. However, the magnitude of its effect, which manifested itself as a sharp increase in the total resistance of Model 299B is a cause for concern.

If flow separation near the water surface close to the stern has occurred, a separation zone with negative pressure is created right behind the stern which tends to change the pressure drag drastically.

One can consider the pressure drag in this case as a summation of two components: form drag, and induced drag. The first component may be regarded as a result of the change in pressure distribution at the after-body of the model and therefore is a function of the gravitational force, or in other words, a function of Froude number. The second component is a result of formation of eddies by the rolling up of the separated shear layers, and it is reasonable to relate it to the viscosity forces, or in other words, to Reynolds number.

The above theory gives reasonable explanation to the sharp increase in the measured resistance of Model 299B compared with Model 299.

Before we proceed further with the analysis of the problem in hand, namely the sharp increase in the effective horsepower of Model 299B, it is advisable to clarify a number of relevant points in order to avoid any possible confusion.

FIRST, one must always remember that Froude principles for full-scale resistance prediction apply only to normal ship forms. Therefore, the technique used to break the total resistance of the Model 299B to its different components and then the use of the law of comparison to predict the resistance of the full scale POLAR 7A, may contain some error. In our opinion, the only quantitative figures which can be relied upon, as far as Model 299B is concerned - or the subsequent models in that matter - are those of the total resistance.

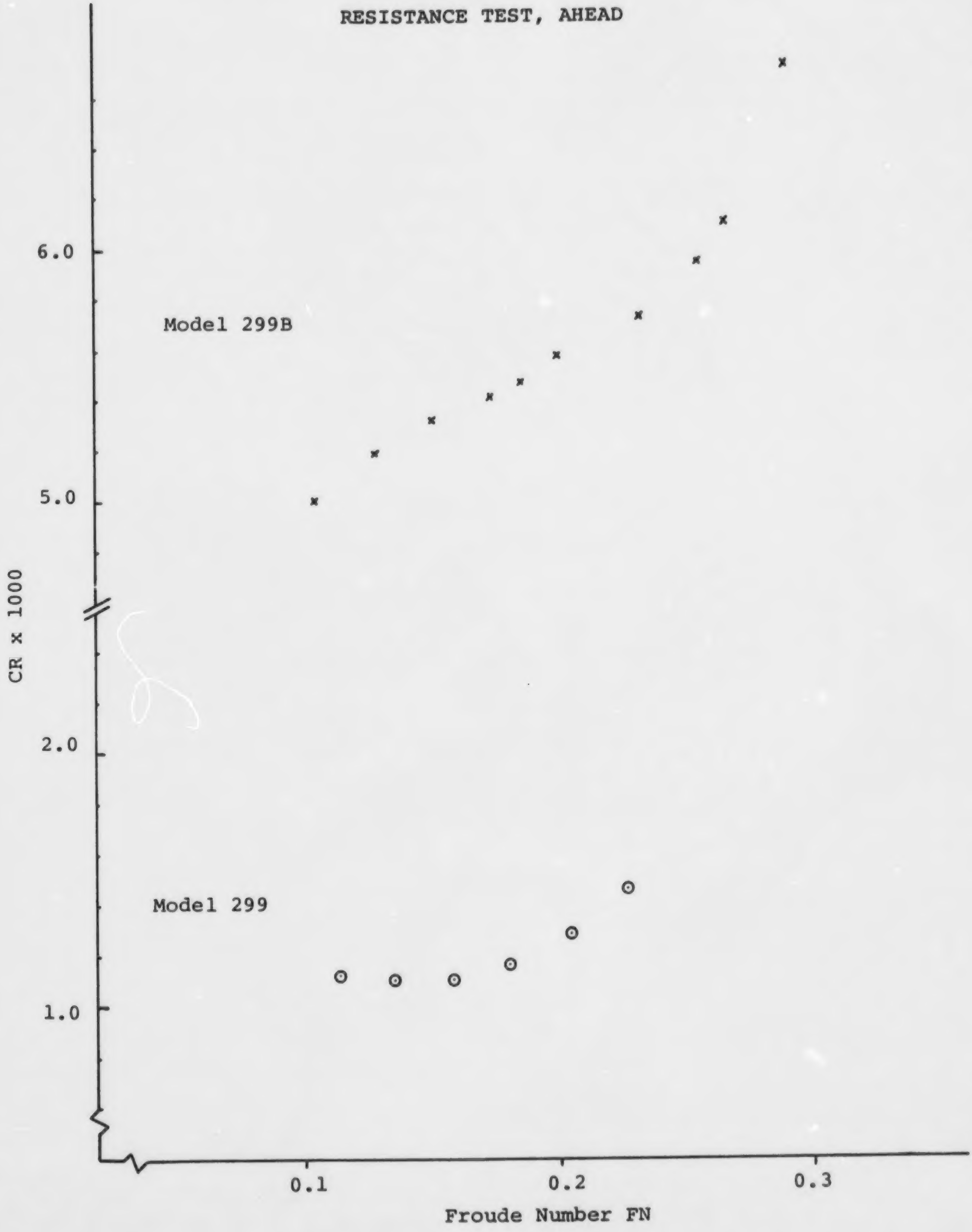

FIGURE 5.6 RESISTANCE TEST, AHEAD

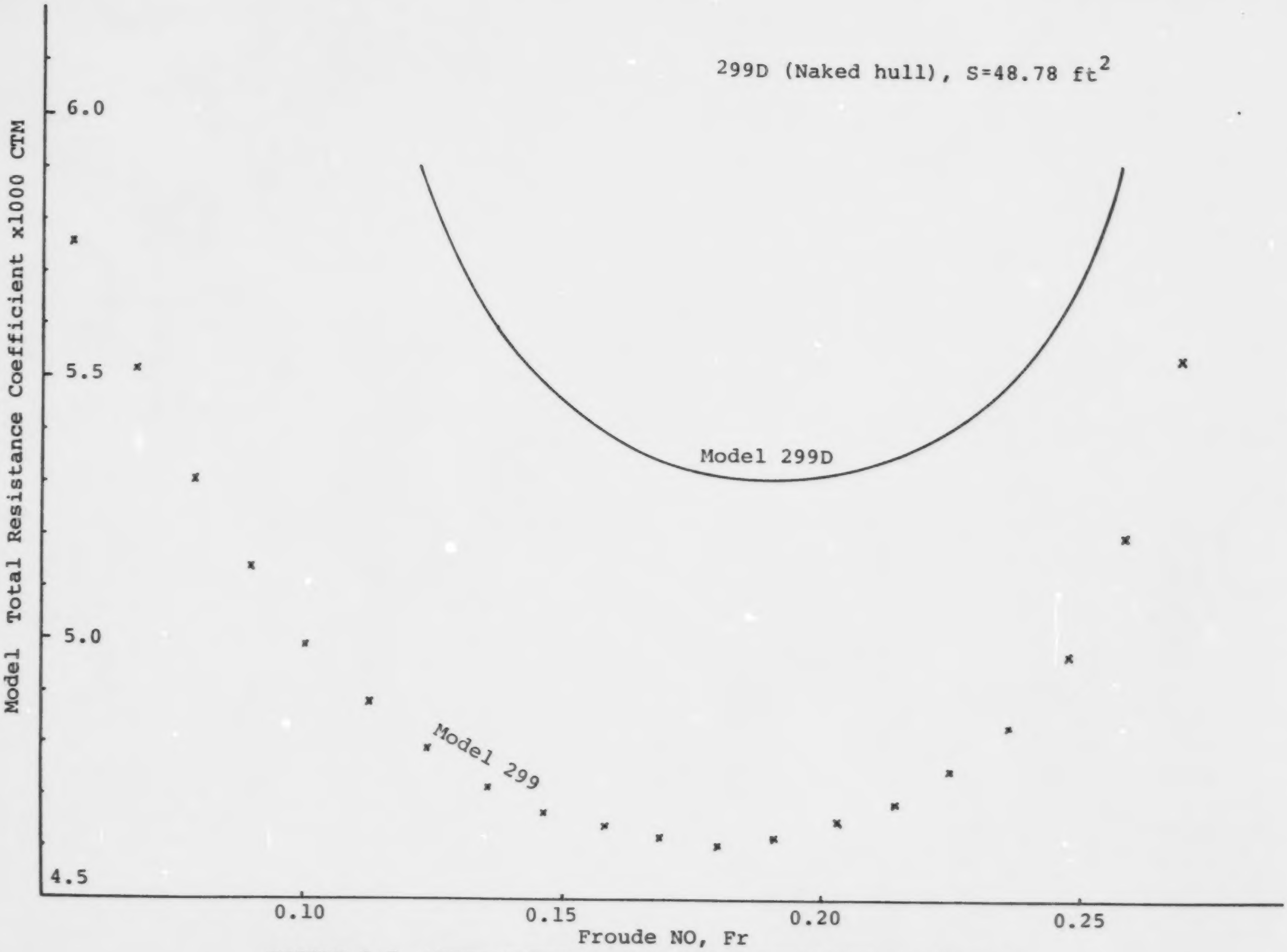

FIGURE 5.7 MODEL TOTAL RESISTANCE COEFFICIENT x 1000 CTM

The above statement can only be substantiated or refuted by producing trial data together with the experimental data of a hull form similar to Model 299B.

SECOND, the predictions for Model 299B with grills have not been corrected for the individual Reynolds number of the grills. In the analysis, the wetted area of the grills has been included in the total wetted area of the hull and is subjected to the same Reynolds number as the hull. A qualitative analysis of the situation suggests that the flow around the grills in the model is laminar and a larger C_F correction for the full scale would be required. Furthermore, separation in the model would be more pronounced, due to the laminar flow, for even small misalignments of the grill member.

For these reasons, the full scale predictions for Model 299B (with grills) must be regarded as being overestimated. By allowing for a proper model/ship correlation for the grills, as proposed for example in Appendix B, the predicted total resistance and consequently the effective power for the full scale is reduced by about 16% (see points marked by asterisk (*) in Figure 5.8).

THIRD, the overall hydrodynamic characteristics of a ship depend strongly on the mutual interaction between the hull and the propulsor, and unless these data are available (from propulsion tests) it is unrealistic to predict the ship's performance based on resistance data only. The problem is complicated still further by the fact that the designed hull has a non-standard form and therefore propulsion coefficients are hard to estimate.

FOURTH, since we are dealing with icebreakers, one might argue that the open water resistance is not critical as long as the icebreaking performance is improved or the propellers are well protected. It is known that open water resistance is insignificant compared with the other components of ice resistance. In addition, icebreakers break ice by virtue of weight and power, and an after-body squared hull form seems to help in that aspect. Finally, the importance of the open water performance of an icebreaker depends on its mission profile.

FIFTH, in order to provide the required protection of the propellers from ice, one has to pay a penalty in terms of increased resistance.

SIXTH, during the design process, the use of the wall-sided after-body was considered as a means of easing the waterline slopes and preventing separation along the sides of the ship. Also, in order to simplify the construction of the unit, a squared-off transom stern was used instead of a rounded stern. Results show that at low speeds the separation behind the transom, with the accompanying separation drag, was minimal.

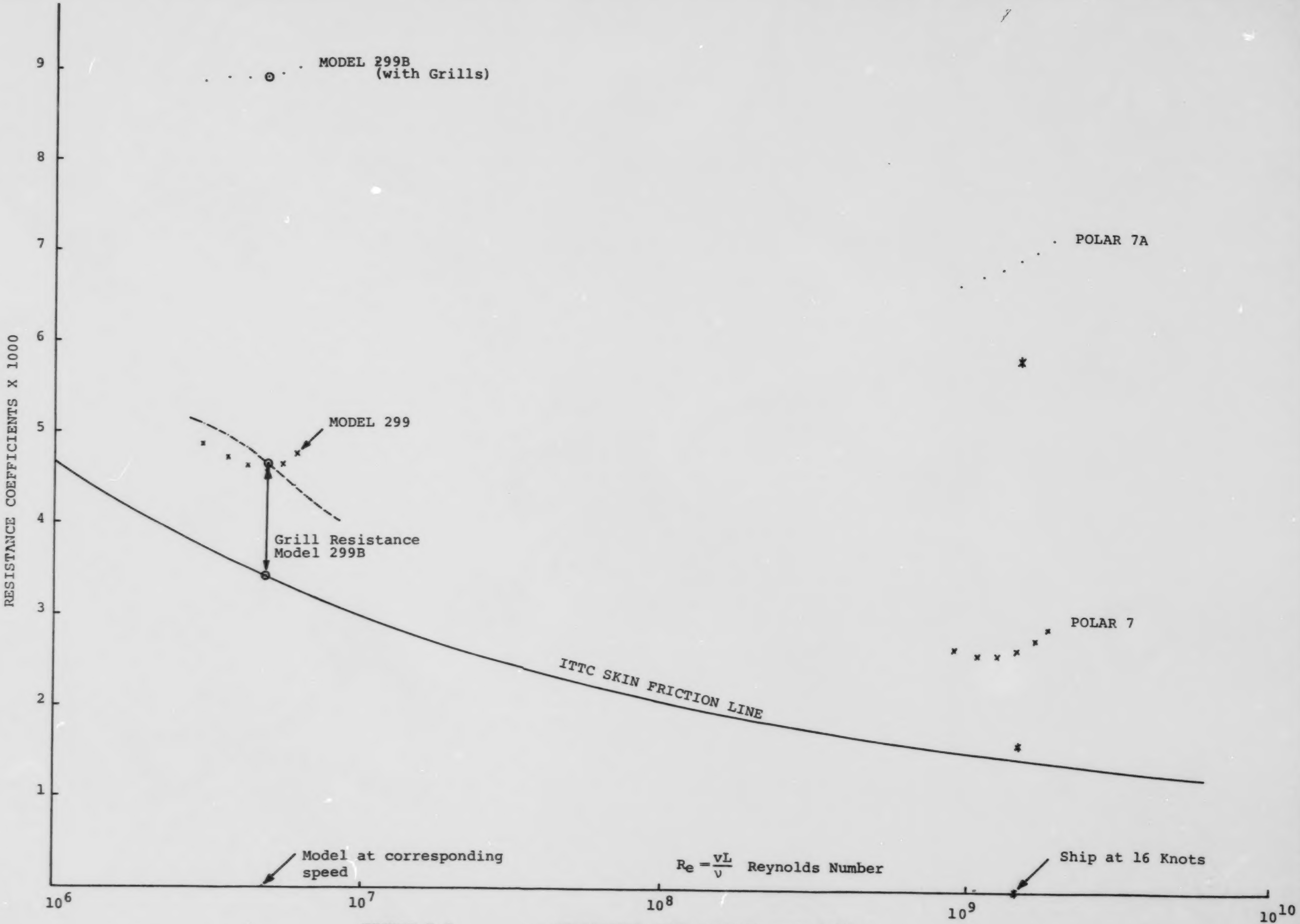

FIGURE 5.8 RESISTANCE COEFFICIENTS x 1000

The shape of the load waterline resulting from the fitment of a squared-off stern for Model 299B is shown in Figure 5.10. The sharp edges do in fact exist not only at the transom but also as knuckles along the outer edges of the tunnel arrangement as shown in Figure 5.9. Looking at Figure 5.10, one can easily conclude that the abrupt change of waterline slope at outer corner E is so great that the liquid cannot possibly follow around them. Consequently, the flow separates from the surface and eddies are formed as a result. The same flow behaviour occurs along any of the sharp edges and corners shown in Figure 5.9. It is known from fluid mechanics studies that separation on oblong surfaces definitely occurs at points where body contours do have abrupt changes of slope (θ) of between 90 and 165 degrees. There are similar criteria with regard to vertical slopes (buttocks) which may be applied as well, with the hydrostatic pressure affecting both the depth of point E_2 and slope ϕ (Figure 5.11). However, adapting criteria in two orthogonal 2-D planes of the same body does not necessarily result in a separation-free zone. The correct slopes, depths, widths, etc., would have to be determined from a 3-D boundary layer analysis over curved surfaces, which by itself is still an unresolved fluid mechanics problem.

The practical approach which was pursued consisted of carrying out minor alterations to the after-body shape. The abrupt change in surface slopes of the transom stern was removed, which then became a rounded (cruiser) stern. This was done by adding a suitably designed unit attached to the original squared-off transom and dealt with the after-body shape from the top trailing edge of the tunnels to the weather deck, thus eliminating the sharp edges and corners near the water surface.

The above modification was considered a simple and logical step to investigate the effect of the transom shape on the resistance of a fuller form ship. The modified model was designated as model 299C.

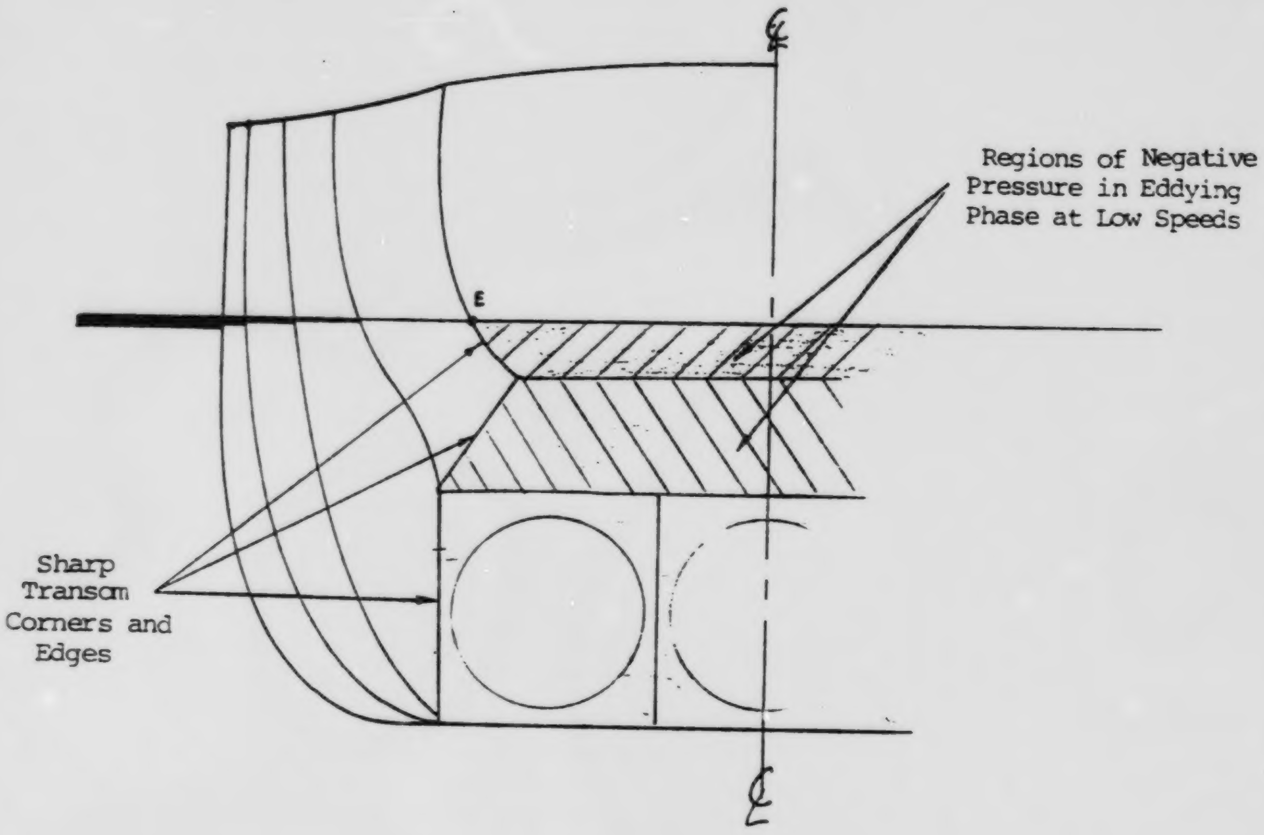
℄
Regions of Negative Pressure in Eddying Phase at Low Speeds
E
Sharp Transom Corners and Edges
℄

FIGURE 5.9 - MODEL 299B BODY PLAN

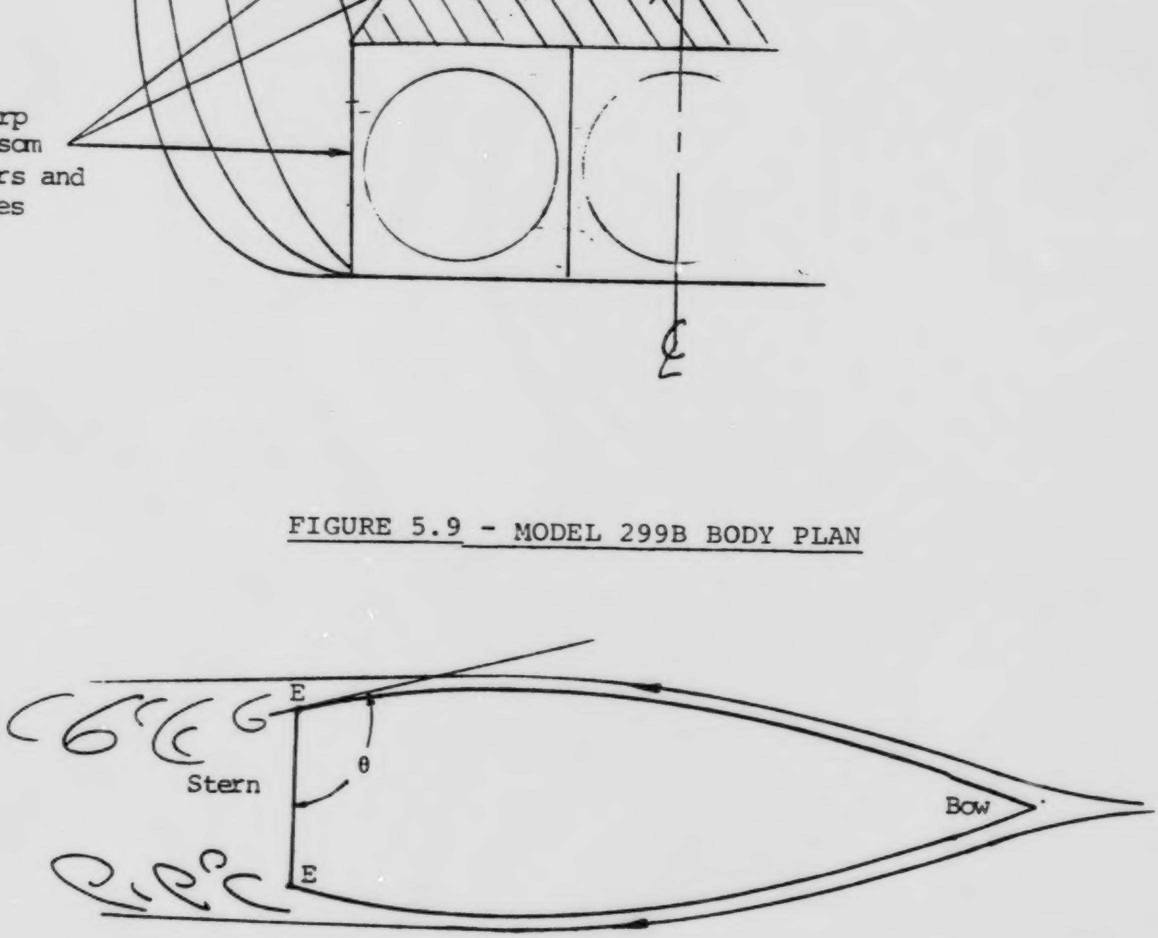
E
θ
Stern
Bow
E

FIGURE 5.10 - MODEL 299B LOAD WATERLINE

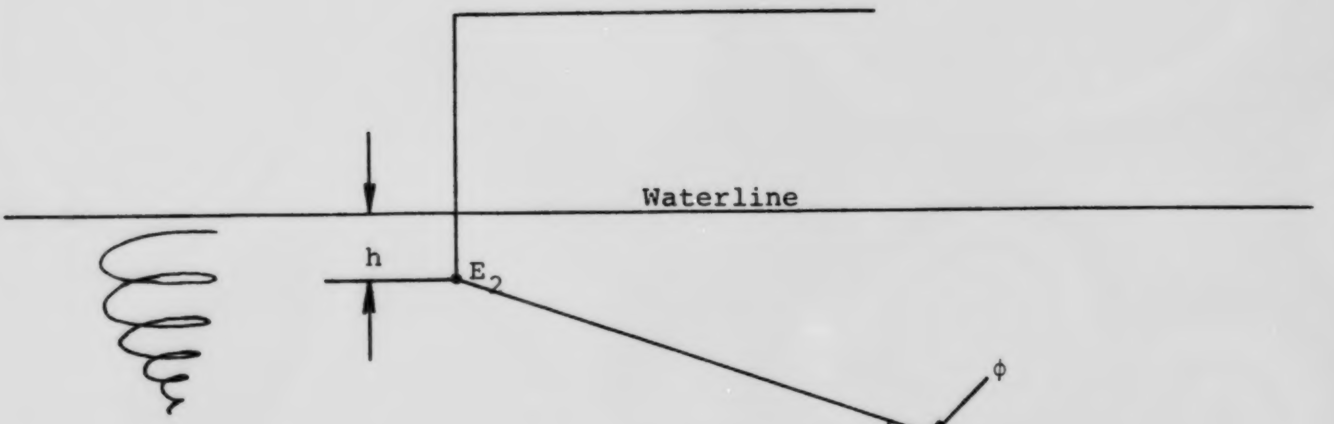
Waterline
h
E_2
ϕ

FIGURE 5.11 - MODEL 299B SHEER VIEW

5.3.3 Model 299C

No quantitative figures could be given to the expected improvement in the open water performance which resulted from the modification to the stern shape. This was due to the complexity of the flow in a highly turbulent, non-uniform, viscous state, which cannot be modelled mathematically. The alternative was to carry out a resistance test on Model 299C.

Figure 5.1 contains a plot of the predicted effective power PE versus speed, based on resistance test results on Model 299C. The predicted improvement in the ship open water performance, measured as a reduction in the effective power, compared with that for Model 299B*, is shown to be about 5% to 6% at 16 knots in the ahead condition with the same grill and skirt arrangement as Model 299B.

Assuming no serious malfunctioning of the test equipment this improvement was certainly much smaller than what had been anticipated.

As the transom shape was not a major contributor to the high resistance, it was decided to pursue the investigation by determining the effect of the hull shape on resistance.

The protection device was taken off Model 299C and then conduct resistance tests conducted on the modified model, which was designated as Model 299D.

5.3.4 Model 299D (Bare Hull)

Resistance tests on Model 299D were carried out and the predicted effective powers over a speed range are shown in Figure 5.1. Again, taking Model 299 as the basis for comparison, Model 299D requires about 45% more effective power at 16 knots equivalent ship speed.

This increase in the effective power (or resistance) may be attributed to the following factors:

- the displacement of Model 299D is about 21% higher than that of Model 299 (Table 2.1);
- the wetted surface area of Model 299D is about 6.2% higher than that of Model 299; and,
- the separation drag associated with Model 299D is undoubtedly much higher than that with Model 299 as a result of removing the side skirts in particular.

---

* For convenience, whenever reference is made to "Model 299B", it means Model 299B in ahead condition and with the full protection arrangement in place; unless specified otherwise.

The axial nominal wake contours, such as those shown in Figure 4.10, can be utilized in two ways in the preliminary propeller design. A circumferential mean wake factor for any radius can be obtained by integrating the wake velocity over the angular position θ for that radius. These factors may then be used to design a wake-adapted propeller. Alternatively, these factors may be averaged over the disk and a "mean wake fraction" is then obtained and used in the propeller design. The latter approach was adopted in the preliminary design of the propellers in the present project. However, since optimum propeller performance at a speed of 4 knots as well as 16 knots (according the suggested mission profile of POLAR 7A; see Volume II, Protection of Propellers in Ice - Detail Design of Protection Schemes) should be achieved, the variation of the mean wake fraction with speed must be considered. A wake survey at a speed of 4 knots equivalent full scale was not carried out since errors associated with low speed measurements are usually large. Therefore, the wake distribution, obtained at a speed of 16 knots equivalent full scale, would have to be the basis for predicting the distribution at different speeds, and in particular at an equivalent speed of 4 knots full scale. One can consider the "wake" as a combination of various kinds of wake flows namely: potential wake, viscous wake, pre-separation wake*, full separation eddying wake, and wave wake, (and propulsion device jet wake in the case of effective wake measurements). Of the above forms of wake, the potential flow itself, neglecting surface waves, does not change pattern with speed since wake and other velocities retain their proportions to the body speed, V, regardless of the magnitude of their velocity. The boundary layer thickness increases as the speed decreases and as a result the viscous wake decreases. The shape and position of separation zones may change with speed. The Velox wave system around the ship changes with speed and therefore corresponding changes occur in the orbital velocity at any given point depending on the positions of the adjacent crests and troughs relative to that point.

When the above wake variations are averaged over the propeller disk, the net result is a wake fraction that can be assumed fairly constant with speed (Ref. 6, pp. 194). Therefore, the wake survey conducted at 16 knots equivalent full scale was considered as a representation of the nominal wake distribution at any speed including the 4 knots.

Obviously, it is by no means sufficient to have information concerning only the axial (fore and aft) nominal wake fraction representing the local speeds of advance. The graphical method,

---

* This is strictly speaking a viscous wake. However, as it is caused by a longitudinal pressure gradient, involving an increase of pressure with distance downstream, rather than directly by friction between the liquid and the solid surface, it is given a special name.

Therefore, one cannot regard the increase in the effective power of Model 299D compared with the parent Model 299, as entirely a result of the adapted full form since, apart from the increased displacement and wetted surface area, the abrupt truncation of the waterlines (which becomes apparent with the removal of the side skirts) would cause the flow to separate vigorously and thus form large-scale vortices which would increase the induced drag sharply.

Also there is no flow similarity at the aft body between Model 299D and that of Model 299B since the nozzle inner flow in the latter model produces a positive pressure on the outer edge of the separated layers of the outer flow, and thus reduces its severity.

The high negative pressure on the tunnel roof indicated by the high flow suction inside the tunnels (wake survey, Model 299B), together with the relatively low resistance of Model 299D, may justify the conclusion that the behaviour of the inner flow is the root of the problem and not the outer flow around the hull.

To this point in the testing program, the results had not produced a clear indication of where in the propeller protection concept, gains in performance could be obtained. As step-by-step changes to the model with subsequent testing were both expensive and time consuming, it was decided to implement a number of major changes simultaneously to determine if a significant improvement to performance could be achieved. The changes to the model were:

(1) Remove bottom grills and stern guards
(2) Remove walls separating the propeller tunnels
(3) Shaping the rectangular section containing the ducts into three circular nozzles
(4) Fairing the nozzle outlets with the hull

Figure 2.10 shows a photograph of the modified model which was designated 299E.

5.3.5 Model 299E

Variations of effective power with speed, based on resistance test results of Model 299E, is shown in Figure 5.1. Again, no additional model-ship correlation allowance was used.

It is clear that there is a considerable improvement in the effective power for Model 299E over Model 299C. At 16 knots, for example, the effective powers for Models 299E and 299C are 13,586 kW and 24,681 kW respectively, indicating about 45% power saving.

Model 299E does not provide complete propeller protection and also, from these tests alone, it is difficult to determine whether the improvement in the open water performance is due to:

- the reduction in the viscous drag and a more favourable flow condition inside the tunnel, that is to say, a more favourable inner flow; or,

- the reduction in the residual resistance by fairing the ducts and the protection appendages, removing the sharp corners and dead areas, and smoothing and rounding off the edges of the protection members.

A summary of the predicted effective powers at three selected speeds for the various models tested is given in Table 5.9.

	EFFECTIVE POWER, PE in HP (kW)		
	9 KNOTS	16 KNOTS	20 KNOTS
Model 299	1,547(1,154)	8,501 (6,339)	18,390(13,713)
Model 299B (with all appendages)	5,794(4,321)	34,312(25,586)	69,076(51,510)
Model 299B (without grills)	4,158(3,101)	25,420(18,956)	52,658(39,267)
Model 299C (with all appendages)	5,651(4,214)	33,098(24,681)	66,728(49,759)
Model 299D (bare hull)	2,577(1,922)	12,311 (9,180)	25,389(18,933)
Model 299E	3,067(2,287)	18,219(13,586)	37,935(28,288)

$\lambda = 46$
Ahead Condition

TABLE 5.9 - COMPARISON OF EFFECTIVE POWER AT THREE SPEEDS

6.0 PROPELLER OPEN WATER TESTS

6.1 General

In order to carry out a complete analysis of the self-propulsion tests it was necessary to perform open water tests with the model propellers. For Model 299, the model propellers were numbers 56 L, R, and C, whereas for Models 299C and 299E, the model propellers were numbers 74 L, R, and C. The R and C propellers were right handed whereas the L propellers are left handed. Full descriptions of the two series (i.e., 56 and 74) are given in Table 2.2. The submersion at the propeller centerline was the same as that of the propeller operating behind the model. To ascertain there was no Reynolds number effect, three different r.p.m. were selected within the self-propulsion range. For each r.p.m. the range for the advance coefficient was covered by varying the speed of the carriage.

For each test, the thrust, torque, and r.p.m. together with the carriage speed was recorded in a way similar to that reported in subsection 5.1.

6.2 Test Results

Results of the open water experiments for the model propellers are given in Tables 6.1 and 6.2 respectively. These show the variations of faired values of non-dimensional thrust and torque coefficients (KT, KQ) and propeller efficiency (ETAO) with advance coefficient (J). There was no noticeable effect either from r.p.m. to r.p.m. or from propeller to propeller within the same series*. The above results are shown graphically in Figures 6.1 and 6.2 for model propellers 56 and 74 respectively. It must be noted that model propellers number 74 were not tested in ducts for the open water experiments. This renders a quantitative analysis of the results less reliable since the propellers were assembled from stock blades having B-series profile with squared-off tips to resemble the Kaplan type screws. The net effect of the propulsion unit is not the additive effects of its components in isolation and therefore the model propeller (number 74) should have been tested inside a duct or a circular cylinder to create a reasonable radial loading on the blade with non-zero value at the tip.

The results, however, are still considered valid for the qualitative study which follows.

---

* Propellers 74 L, R, and C were each tested in open water as well as propellers 56 L, R, and C.

RESULTS OF OPEN WATER TESTS

PROPELLER 56L,R,C   MODEL 299

TEST DATE 27-MAY-80

J	KT	10KQ	ETAO
0.020	0.228	0.220	0.033
0.040	0.223	0.216	0.066
0.060	0.219	0.213	0.098
0.080	0.214	0.210	0.130
0.100	0.209	0.206	0.162
0.120	0.205	0.203	0.193
0.140	0.200	0.199	0.223
0.160	0.194	0.196	0.253
0.180	0.189	0.192	0.282
0.200	0.184	0.188	0.311
0.220	0.178	0.184	0.339
0.240	0.173	0.180	0.367
0.260	0.167	0.175	0.393
0.280	0.161	0.171	0.419
0.300	0.155	0.166	0.445
0.320	0.148	0.161	0.469
0.340	0.142	0.156	0.492
0.360	0.135	0.151	0.515
0.380	0.129	0.145	0.536
0.400	0.122	0.139	0.556
0.420	0.115	0.133	0.575
0.440	0.108	0.127	0.592
0.460	0.100	0.121	0.608
0.480	0.093	0.114	0.621
0.500	0.085	0.107	0.632
0.520	0.077	0.100	0.639
0.540	0.069	0.092	0.643
0.560	0.061	0.085	0.641
0.580	0.053	0.077	0.633
0.600	0.044	0.068	0.614
0.620	0.035	0.060	0.582
0.640	0.026	0.051	0.526
0.660	0.017	0.042	0.433
0.680	0.008	0.033	0.268

TABLE 6.1 RESULTS OF OPEN WATER TESTS PROPELLER 56L, R,C MODEL 299

RESULTS OF OPEN WATER TESTS

PROPELLER 74 L.R.C   MODELS 299C, 299E

TEST DATE 18-FEB-82

J	KT	10KQ	ETAO
0.000	0.343	0.385	0.000
0.025	0.337	0.379	0.035
0.050	0.331	0.374	0.071
0.075	0.325	0.368	0.105
0.100	0.318	0.362	0.140
0.125	0.311	0.356	0.174
0.150	0.303	0.350	0.207
0.175	0.295	0.343	0.239
0.200	0.287	0.337	0.271
0.225	0.278	0.330	0.302
0.250	0.269	0.323	0.332
0.275	0.260	0.315	0.361
0.300	0.251	0.308	0.389
0.325	0.241	0.300	0.416
0.350	0.232	0.292	0.442
0.375	0.222	0.283	0.467
0.400	0.212	0.275	0.491
0.425	0.202	0.266	0.513
0.450	0.191	0.257	0.534
0.475	0.181	0.247	0.554
0.500	0.171	0.237	0.572
0.525	0.160	0.227	0.589
0.550	0.149	0.217	0.603
0.575	0.138	0.206	0.615
0.600	0.127	0.195	0.625
0.625	0.116	0.183	0.631
0.650	0.105	0.171	0.634
0.675	0.093	0.159	0.631
0.700	0.082	0.146	0.622
0.725	0.070	0.133	0.604
0.750	0.057	0.119	0.574
0.775	0.045	0.105	0.526
0.800	0.032	0.091	0.450
0.825	0.019	0.076	0.328
0.850	0.005	0.060	0.121

TABLE 6.2 RESULTS OF OPEN WATER TESTS PROPELLER 74L,R,C MODELS 299C, 299E

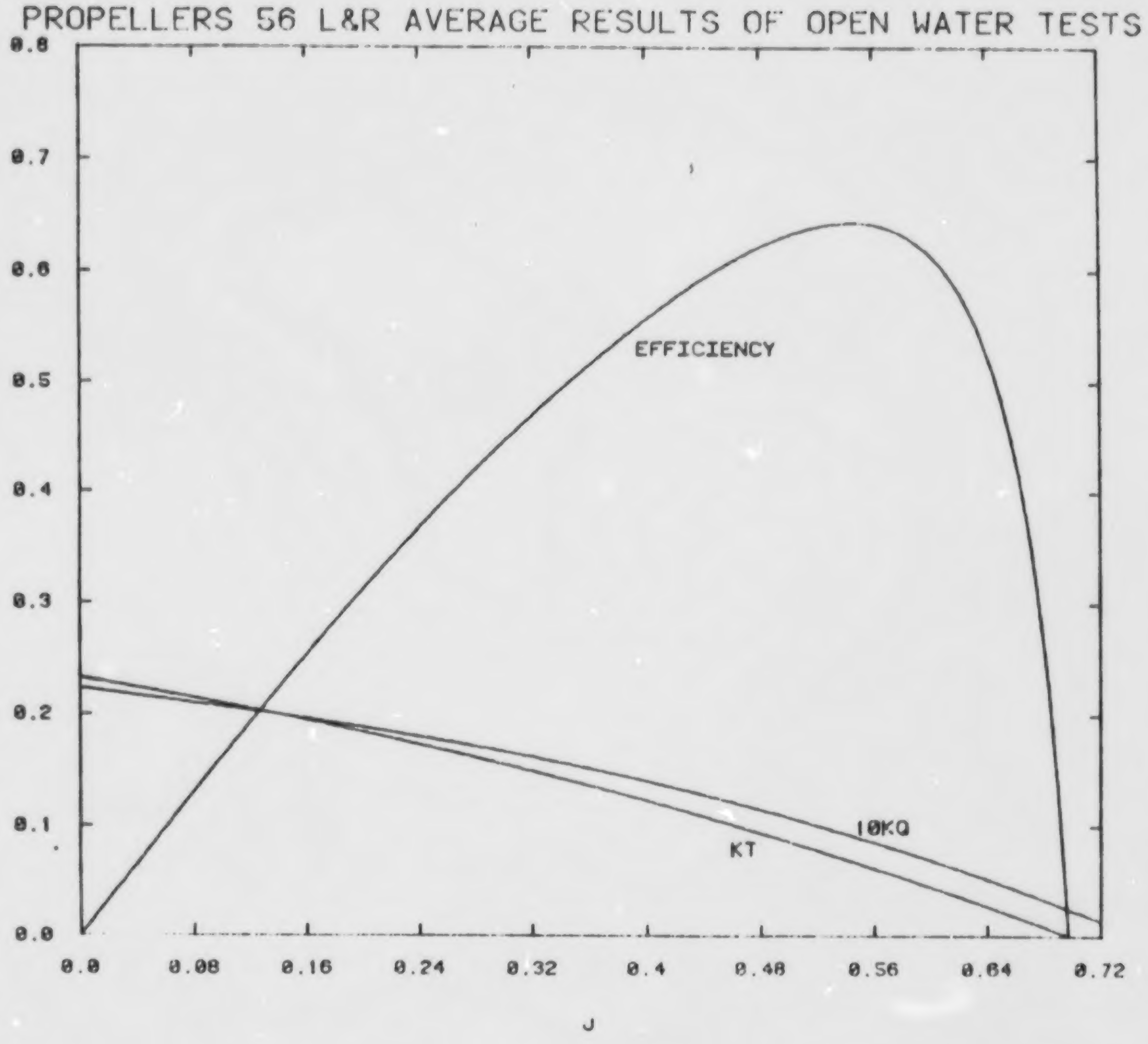

FIGURE 6.1 PROPELLERS 56 & L&R AVERAGE RESULTS OF OPEN WATER TESTS

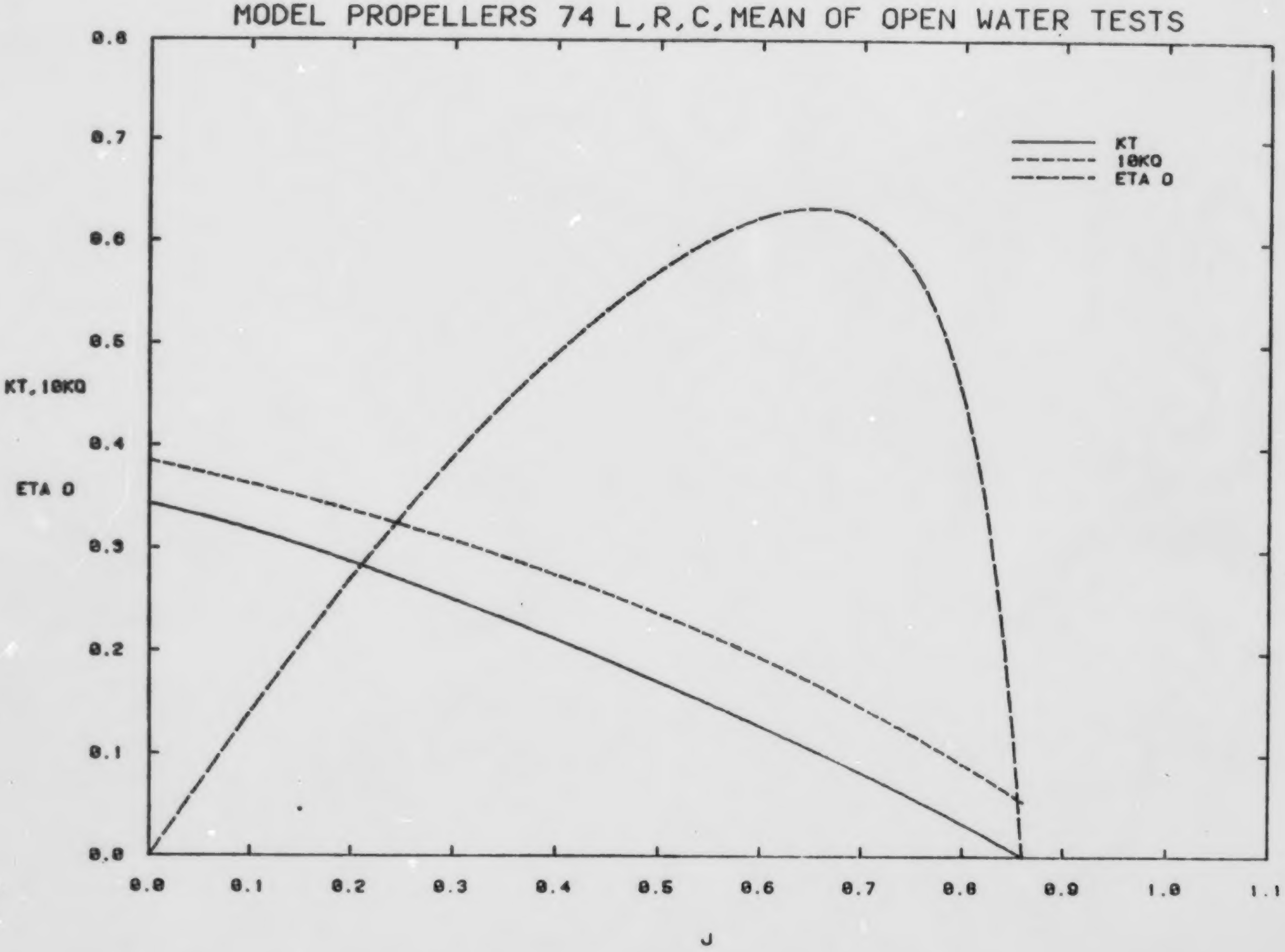

FIGURE 6.2 MODEL PROPELLERS 74 L,R,C, MEAN OF OPEN WATER TESTS

7.0 SELF-PROPULSION AND OVERLOAD EXPERIMENTS

7.1 General

As indicated in the test program Table 3.1, self-propulsion and overload experiments were carried out with Models 299, 299C, and 299E.

For each test, the model guided by the carriage was self-propelled, using variable tow rope forces in the speed range of 8 to 24 knots, while thrust, torque, and r.p.m. for each shaft, together with the carriage speed were recorded.

The power distribution was that of 1-1-1, i.e., 1/3 of the total power per shaft.

In the case of the overload condition, the propeller loading was adjusted to account for the expected additional resistance due to icebreaking. Ice interaction with the propeller, however, is not taken into consideration in this analysis.

7.2 Test Results

Results from the self-propulsion tests on the parent hull form, Model 299, $\lambda = 46$, are presented in Tables 7.1 to 7.5. The results for the overload experiments for a roughness allowance of $C_A = 0$ are presented in Tables 7.6 to 7.9.

For Models 299C, results of the analysis of the self-propulsion experiments together with predictions for the ship performance are given in Tables 7.10 to 7.14. The results of the overload experiments are given in Tables 7.15 to 7.18.

The results of the corresponding analysis for Model 299E are given in Tables 7.19 to 7.22 (self-propulsion) and Tables 7.24 to 7.27 (overload).

No additional model-ship correlation allowance was used in the analysis of the results.

7.3 Discussion

7.3.1 Self-Propulsion

Figure 7.1 shows a comparison of the delivered power and r.p.m. at the ship self-propulsion point for Models 299, 299C, and 299E. It can be seen that at the design power of 150,000 SHP (112,500

```
                          RESULTS OF PROPULSION EXPERIMENTS
MODEL NO. 299                  PROPELLER NO. 56L,R&C                    TEST DATE  06-JUN-80
L =  684.71 FT.                T =   46.05 FT.                          TRIM =   0.00 FT. BY THE STERN
                               DESIGN WL
SHIP PREDICTIONS ARE FOR SALT WATER AT 59 DEG. F        SHIP MODEL CORRELATION ALLOWANCE 0.00000

                 POWERS,SPEEDS AND THRUST PREDICTED FOR MODEL TEST PROPELLER

                                       WING PROPS.              CENTRE PROP.           TOTAL
    V       FN      PE       PD       NS     TH       PD       NS     TH       PD        TH
  KNOTS            H.P.     H.P.     RPM    TONS     H.P.     RPM    TONS     H.P.      TONS

   5.47   0.062     428.     760.    31.0    3.2     424.    31.0     5.4    1184.      8.5
  10.15   0.115    2371.    3616.    53.7   22.6    2211.    53.7    21.2    5828.     43.8
  13.51   0.154    5461.    7285.    70.4   32.8    5241.    70.4    47.3   12526.     80.2
  17.54   0.200   12454.   14452.    90.5   58.5   10763.    90.5    76.2   25215.    134.7
  22.05   0.251   29248.   32068.   116.2  121.2   23112.   116.2   130.1   55180.    251.3
  26.04   0.296   77447.   90049.   151.1  330.0   60077.   151.1   276.1  150126.    606.0
  29.48   0.335  136280.  149420.   175.5  490.9   95791.   175.5   381.4  245211.    872.3
```

TABLE 7.1 RESULTS OF PROPULSION EXPERIMENTS PROPELLER NO. 56L,R&C

```
MODEL NO. 299                  RESULTS OF PROPULSION EXPERIMENTS
L =  684.71 FT.                   PROPELLER NO. 56L,R&C
                                  T =   46.05 FT.                          TEST DATE  06-JUN-80
                                  DESIGN WL                                TRIM =  0.00 FT. BY THE STE
SHIP PREDICTIONS ARE FOR SALT WATER AT 59 DEG. F              SHIP MODEL CORRELATION ALLOWANCE 0.000

                         PROPULSION FACTORS PREDICTED FOR MODEL TEST PROPELLER

                                  WING PROPS.                  CENTRE PROP.               TOTAL
      V        FN        WFTT       ETAO      ETAR      WFTT      ETAO      ETAR      ETAD      THDF
    KNOTS

     5.47    0.062    -0.029     0.349     0.460     0.069     0.604     0.735     0.362    -0.335
    10.15    0.115     0.092     0.541     0.733     0.173     0.634     0.874     0.407     0.225
    13.51    0.154     0.092     0.507     0.751     0.240     0.643     0.991     0.436     0.267
    17.54    0.200     0.107     0.523     0.835     0.242     0.643     1.007     0.494     0.234
    22.05    0.251     0.109     0.567     0.900     0.234     0.643     1.017     0.530     0.233
    26.04    0.296     0.091     0.632     0.943     0.227     0.629     1.012     0.516     0.287
    29.48    0.335     0.087     0.639     0.951     0.215     0.626     1.012     0.556     0.229
```

TABLE 7.2 RESULTS OF PROPULSION EXPERIMENTS PROPELLER NO. 56L,R&C

```
                              RESULTS OF PROPULSION EXPERIMENTS
MODEL NO. 299                     PROPELLER NO. 56L,R&C
L =  684.71 FT.                   T =  46.05 FT.                            TEST DATE  06-JUN-80
                                  DESIGN WL                                 TRIM =  0.00 FT. BY THE STER
SHIP PREDICTIONS ARE FOR SALT WATER AT 59 DEG. F          SHIP MODEL CORRELATION ALLOWANCE 0.0000

                                          PROPELLER COEFFICIENTS

                                             WING PROPELLERS
                             BEHIND MODEL                  TEST PROPELLER              SERIES PROPELLER
      FN   CT-R(60.8)   JP       KTF       KQF      JOM       KTOM      KQOM      JOS       KTOS      KQOS
             X1000                         X10                          X10                           X10

    0.062   -2.501    0.653    0.012     0.079    0.672     0.012     0.037
    0.115   -2.156    0.700    0.028     0.072    0.636     0.028     0.053
    0.154   -2.012    0.711    0.024     0.065    0.645     0.024     0.049
    0.200   -1.893    0.718    0.026     0.061    0.641     0.026     0.051
    0.251   -1.796    0.703    0.033     0.063    0.626     0.033     0.057
    0.296   -1.730    0.639    0.052     0.081    0.580     0.052     0.076
    0.335   -1.687    0.622    0.058     0.086    0.568     0.058     0.082
```

TABLE 7.3 RESULTS OF PROPULSION EXPERIMENTS PROPELLER NO. 56L,R&C

```
MODEL NO. 299                     RESULTS OF PROPULSION EXPERIMENTS
L =  684.71 FT.                      PROPELLER NO. 56L,R&C
                                     T =  46.05 FT.                     TEST DATE  06-JUN-80
                                     DESIGN WL                          TRIM =  0.00 FT. BY THE STER
SHIP PREDICTIONS ARE FOR SALT WATER AT 59 DEG. F           SHIP MODEL CORRELATION ALLOWANCE 0.0000

                                        PROPELLER COEFFICIENTS

                                           CENTRE PROPELLER
                             BEHIND MODEL                 TEST PROPELLER
     FN   CT-R(60.8)  JP       KTP      KQP      JOM      KTOM     KQOM        SERIES PROPELLER
            X1000                       X10                        X10      JOS      KTOS     KQOS
                                                                                              X10
   0.062  -2.501    0.653    0.041    0.088    0.608    0.041    0.065
   0.115  -2.156    0.700    0.053    0.088    0.578    0.053    0.077
   0.154  -2.012    0.711    0.069    0.093    0.540    0.069    0.092
   0.200  -1.893    0.718    0.067    0.090    0.544    0.067    0.091
   0.251  -1.796    0.703    0.070    0.091    0.538    0.070    0.093
   0.296  -1.730    0.639    0.088    0.108    0.493    0.088    0.109
   0.335  -1.687    0.622    0.090    0.110    0.488    0.090    0.111
```

TABLE 7.4 RESULTS OF PROPULSION EXPERIMENTS PROPELLER NO. 56L,R&C

```
                            RESULTS OF PROPULSION EXPERIMENTS
MODEL NO. 299                    PROPELLER NO. 56L,R&C                    TEST DATE  06-JUN-80
L =  684.71 FT.                  T =  46.05 FT.                           TRIM =  0.00 FT. BY THE STER
                                 DESIGN WL
SHIP PREDICTIONS ARE FOR SALT WATER AT 59 DEG. F          SHIP MODEL CORRELATION ALLOWANCE 0.0000

          NON-DIMENSIONAL PROPULSION COEFFICIENTS PREDICTED  FOR MODEL TEST PROPELLER

                    FN        FNVOL       CDVOL       PDVOL       TAUT       PDC/PD
                                           X100       X1000       X1000

                  0.062       0.146       5.292       0.082       0.152       0.358
                  0.115       0.270       4.078       0.402       0.781       0.379
                  0.154       0.359       3.717       0.863       1.428       0.418
                  0.200       0.467       3.420       1.737       2.400       0.427
                  0.251       0.587       3.763       3.802       4.476       0.419
                  0.296       0.693       6.216      10.344      10.795       0.400
                  0.335       0.784       7.003      16.896      15.537       0.391
```

TABLE 7.5 RESULTS OF PROPULSION EXPERIMENTS PROPELLER NO.56L,R&C

MODEL NO. 299
L = 684.71 FT.

RESULTS OF OVERLOAD EXPERIMENTS
PROPELLER NO. 56L,R&C
T = 46.05 FT.
DESIGN WL

TEST DATE 06-JUN-80
TRIM = 0.00 FT. BY THE STE

SHIP PREDICTIONS ARE FOR SALT WATER AT 59 DEG. F

SHIP MODEL CORRELATION ALLOWANCE 0.000

POWERS AND TOW FORCES PREDICTED FOR MODEL TEST PROPELLER

		WING PROPS.			CENTRE PROP.			TOTAL		
V KNOTS	FN	PD H.P.	NS RPM	TH TONS	PD H.P.	NS RPM	TH TONS	PD H.P.	TH TONS	FP TONS
0.00	0.000	12441.	55.0	166.8	5688.	55.0	90.6	18129.	257.4	252.0
0.00	0.000	30663.	75.0	322.0	14636.	75.0	172.4	45299.	494.4	477.6
0.00	0.000	61630.	95.0	529.3	30060.	95.0	281.4	91690.	810.7	763.0
0.00	0.000	109893.	115.0	781.5	53565.	115.0	416.2	163459.	1197.7	1145.5
0.00	0.000	160061.	130.0	996.2	77403.	130.0	533.5	237464.	1529.7	1463.7
0.00	0.000	201111.	140.0	1151.1	96612.	140.0	619.4	297723.	1770.5	1705.1
5.47	0.062	11851.	60.0	127.1	5964.	60.0	79.9	17816.	207.0	175.6
5.47	0.062	30848.	80.0	276.7	15458.	80.0	162.6	46306.	439.2	387.0
5.47	0.062	62825.	100.0	477.2	31596.	100.0	271.4	94421.	748.5	655.7
5.47	0.062	111057.	120.0	728.5	56112.	120.0	406.4	167170.	1134.9	1025.6
5.47	0.062	159385.	135.0	942.3	80685.	135.0	521.6	240070.	1463.9	1347.5
10.15	0.115	6406.	60.0	48.8	4113.	60.0	42.6	10519.	91.4	40.9
10.15	0.115	23270.	80.0	180.4	12919.	80.0	119.2	36189.	299.5	225.5
10.15	0.115	53090.	100.0	355.6	27848.	100.0	222.8	80938.	578.4	479.8
10.15	0.115	99222.	120.0	574.6	50341.	120.0	353.4	149564.	928.0	808.8
10.15	0.115	129454.	130.0	700.5	64876.	130.0	428.8	194331.	1129.2	998.8
10.15	0.115	184939.	145.0	909.7	91295.	145.0	554.5	276234.	1464.3	1321.4
13.51	0.154	15994.	80.0	103.4	9688.	80.0	84.0	25683.	187.4	92.4
13.51	0.154	42942.	100.0	275.4	23844.	100.0	181.2	66786.	456.6	329.1
13.51	0.154	84905.	120.0	490.0	45473.	120.0	302.9	130378.	792.9	624.8
13.51	0.154	112429.	130.0	613.3	59524.	130.0	372.9	171953.	986.2	815.7
13.51	0.154	162919.	145.0	818.2	85136.	145.0	489.3	248055.	1307.5	1122.1
17.54	0.200	27445.	100.0	141.5	17879.	100.0	123.7	45324.	265.2	111.8
17.54	0.200	66561.	120.0	349.5	38664.	120.0	242.3	105225.	591.9	397.4
17.54	0.200	124408.	140.0	603.5	68521.	140.0	386.6	192929.	990.1	737.8
17.54	0.200	182026.	155.0	824.3	97728.	155.0	511.5	279754.	1335.8	1058.0
22.05	0.251	167579.	160.0	709.2	95007.	160.0	458.9	262586.	1168.0	777.2
26.04	0.296	165826.	170.0	616.7	100919.	170.0	440.5	266745.	1057.3	400.5
29.48	0.335	170654.	180.0	564.8	107504.	180.0	424.2	278158.	988.9	93.1

MODEL NO. 299
L = 684.71 FT.

RESULTS OF OVERLOAD EXPERIMENTS
PROPELLER NO. 56L,R&C
T = 46.05 FT.
DESIGN WL

TEST DATE 06-JUN-80
TRIM = 0.00 FT. BY THE STERN

SHIP PREDICTIONS ARE FOR SALT WATER AT 59 DEG. F

SHIP MODEL CORRELATION ALLOWANCE 0.00000

PROPULSION FACTORS PREDICTED FOR MODEL TEST PROPELLER

V	NS	WING PROPS.			CENTRE PROP.				TOTAL	
KNOTS	RPM	WFTT	ETAO	ETAR	WFTT	ETAO	ETAR	ETAD	THDF	FP/PD LB./H.P.
0.00	55.0	0.000	0.000	0.961	0.000	0.000	1.051	0.000	0.021	31.142
0.00	75.0	0.000	0.000	0.989	0.000	0.000	1.036	0.000	0.034	23.618
0.00	95.0	0.000	0.000	1.000	0.000	0.000	1.025	0.000	0.059	18.641
0.00	115.0	0.000	0.000	0.994	0.000	0.000	1.020	0.000	0.044	15.698
0.00	130.0	0.000	0.000	0.986	0.000	0.000	1.020	0.000	0.043	13.807
0.00	140.0	0.000	0.000	0.980	0.000	0.000	1.020	0.000	0.037	12.829
5.47	60.0	-0.135	0.539	0.849	0.169	0.420	0.997	0.395	0.097	22.078
5.47	80.0	-0.163	0.438	0.896	0.209	0.312	1.004	0.324	0.093	18.720
5.47	100.0	-0.185	0.367	0.923	0.246	0.242	1.006	0.266	0.109	15.555
5.47	120.0	-0.202	0.315	0.941	0.279	0.195	1.007	0.233	0.086	13.742
5.47	135.0	-0.254	0.294	0.948	0.267	0.177	1.007	0.213	0.072	12.573
10.15	60.0	0.061	0.627	0.797	0.204	0.631	0.911	0.497	0.181	8.707
10.15	80.0	0.031	0.604	0.868	0.229	0.517	0.960	0.500	0.134	13.957
10.15	100.0	-0.012	0.537	0.882	0.258	0.418	0.991	0.443	0.112	13.280
10.15	120.0	-0.063	0.484	0.887	0.289	0.343	1.016	0.393	0.092	12.114
10.15	130.0	-0.091	0.463	0.889	0.305	0.313	1.026	0.371	0.085	11.513
10.15	145.0	-0.135	0.437	0.891	0.329	0.274	1.040	0.343	0.074	10.715
13.51	80.0	0.095	0.640	0.850	0.242	0.617	0.989	0.547	0.193	8.058
13.51	100.0	0.077	0.609	0.903	0.254	0.529	0.995	0.540	0.150	11.039
13.51	120.0	0.049	0.553	0.922	0.261	0.455	1.006	0.487	0.138	10.734
13.51	130.0	0.032	0.528	0.928	0.262	0.425	1.012	0.473	0.113	10.626
13.51	145.0	0.003	0.497	0.936	0.262	0.386	1.020	0.442	0.097	10.133
17.54	100.0	0.102	0.631	0.885	0.248	0.626	1.002	0.572	0.189	5.526
17.54	120.0	0.090	0.628	0.918	0.260	0.557	1.004	0.574	0.154	8.459
17.54	140.0	0.074	0.584	0.928	0.271	0.490	1.011	0.526	0.151	8.566
17.54	155.0	0.061	0.550	0.933	0.279	0.447	1.018	0.501	0.131	8.472
22.05	160.0	0.099	0.608	0.952	0.261	0.533	1.015	0.560	0.170	6.630
26.04	170.0	0.084	0.639	0.955	0.238	0.586	1.017	0.559	0.212	3.363
29.48	180.0	0.085	0.642	0.955	0.217	0.618	1.013	0.558	0.226	0.749

TABLE 7.7 RESULTS OF OVERLOAD EXPERIMENTS PROPELLER NO. 56L,R&C

```
                              RESULTS OF OVERLOAD EXPERIMENTS
MODEL NO. 299                       PROPELLER NO. 56L,R&C
L =  684.71 FT.                     T =  46.05 FT.                        TEST DATE  06-JUN-80
                                    DESIGN WL                             TRIM =  0.00 FT. BY THE STERN
SHIP PREDICTIONS ARE FOR SALT WATER AT 59 DEG. F          SHIP MODEL CORRELATION ALLOWANCE 0.0000C

                                      PROPELLER COEFFICIENTS

                                         WING PROPELLERS
                         BEHIND MODEL                             TEST PROPELLER
       FN  CT-R(60.8)  JF       KTF      KQF      ZETO       JOM      KTOM     KQOM
               X1000                     X10                                     X10

     0.000    0.000   0.000    0.199    0.232    0.620     0.000    0.232    0.223
     0.000    0.000   0.000    0.207    0.225    0.656     0.000    0.232    0.223
     0.000    0.000   0.000    0.212    0.223    0.677     0.000    0.232    0.223
     0.000    0.000   0.000    0.214    0.224    0.680     0.000    0.232    0.223
     0.000    0.000   0.000    0.213    0.226    0.674     0.000    0.232    0.223
     0.000    0.000   0.000    0.212    0.227    0.669     0.000    0.232    0.223
     0.062   45.120   0.338    0.128    0.170    0.488     0.383    0.128    0.144
     0.062  102.466   0.253    0.156    0.187    0.561     0.295    0.156    0.167
     0.062  175.365   0.203    0.173    0.195    0.602     0.240    0.173    0.180
     0.062  275.715   0.169    0.183    0.199    0.629     0.203    0.183    0.187
     0.062  363.049   0.150    0.187    0.201    0.639     0.188    0.187    0.190
     0.115    1.063   0.627    0.049    0.092    0.282     0.588    0.049    0.073
     0.115   15.612   0.470    0.102    0.141    0.441     0.455    0.102    0.122
     0.115   35.656   0.376    0.129    0.165    0.502     0.380    0.129    0.145
     0.115   61.584   0.313    0.144    0.178    0.535     0.333    0.144    0.158
     0.115   76.557   0.289    0.150    0.183    0.546     0.315    0.150    0.162
     0.115  101.983   0.259    0.157    0.188    0.559     0.294    0.157    0.168
     0.154    2.093   0.626    0.058    0.097    0.325     0.566    0.058    0.082
     0.154   12.624   0.500    0.100    0.133    0.448     0.462    0.100    0.120
     0.154   25.775   0.417    0.123    0.152    0.506     0.397    0.123    0.140
     0.154   34.268   0.385    0.131    0.159    0.525     0.373    0.131    0.147
     0.154   47.901   0.345    0.141    0.166    0.547     0.344    0.141    0.155
     0.200    1.054   0.650    0.051    0.085    0.310     0.583    0.051    0.075
     0.200    8.593   0.541    0.088    0.119    0.425     0.493    0.088    0.110
     0.200   17.580   0.464    0.111    0.141    0.483     0.430    0.111    0.130
     0.200   26.035   0.419    0.124    0.152    0.512     0.394    0.124    0.141
     0.251   11.172   0.511    0.100    0.127    0.465     0.460    0.100    0.121
     0.296    3.059   0.567    0.077    0.105    0.408     0.520    0.077    0.100
     0.335   -0.817   0.607    0.063    0.091    0.366     0.555    0.063    0.087
```

TABLE 7.8 RESULTS OF OVERLOAD EXPERIMENTS PROPELLER NO. 56L, R&C

MODEL NO. 299
L = 684.71 FT.

RESULTS OF OVERLOAD EXPERIMENTS
PROPELLER NO. 56L,R&C
T = 46.05 FT.
DESIGN WL

TEST DATE 06-JUN-80
TRIM =   0.00 FT. BY THE STER

SHIP PREDICTIONS ARE FOR SALT WATER AT 59 DEG. F

SHIP MODEL CORRELATION ALLOWANCE 0.0000

PROPELLER COEFFICIENTS

CENTRE PROPELLER

		BEHIND MODEL				TEST PROPELLER		
FN	CT-R(60.8) X1000	JP	KTP	KQP X10	ZETO	JOM	KTOM	KQOM X10
0.000	0.000	0.000	0.217	0.212	0.715	0.000	0.232	0.223
0.000	0.000	0.000	0.222	0.215	0.724	0.000	0.232	0.223
0.000	0.000	0.000	0.226	0.217	0.732	0.000	0.232	0.223
0.000	0.000	0.000	0.228	0.218	0.736	0.000	0.232	0.223
0.000	0.000	0.000	0.228	0.218	0.738	0.000	0.232	0.223
0.000	0.000	0.000	0.229	0.218	0.739	0.000	0.232	0.223
0.062	45.120	0.338	0.161	0.171	0.611	0.281	0.161	0.171
0.062	102.466	0.253	0.184	0.187	0.658	0.200	0.184	0.188
0.062	175.365	0.203	0.196	0.196	0.682	0.153	0.196	0.197
0.062	275.715	0.169	0.204	0.201	0.697	0.122	0.204	0.203
0.062	363.049	0.150	0.207	0.203	0.702	0.110	0.207	0.205
0.115	1.063	0.627	0.086	0.118	0.417	0.499	0.086	0.108
0.115	15.612	0.470	0.135	0.156	0.544	0.362	0.135	0.150
0.115	35.656	0.376	0.161	0.173	0.609	0.279	0.161	0.171
0.115	61.584	0.313	0.178	0.181	0.651	0.223	0.178	0.183
0.115	76.557	0.289	0.184	0.183	0.667	0.201	0.184	0.188
0.115	101.983	0.259	0.191	0.186	0.687	0.174	0.191	0.193
0.154	2.093	0.626	0.095	0.117	0.465	0.474	0.095	0.116
0.154	12.624	0.500	0.131	0.148	0.550	0.373	0.131	0.147
0.154	25.775	0.417	0.152	0.163	0.598	0.308	0.152	0.164
0.154	34.268	0.385	0.160	0.168	0.615	0.284	0.160	0.170
0.154	47.901	0.345	0.168	0.173	0.636	0.255	0.168	0.177
0.200	1.054	0.650	0.089	0.111	0.455	0.488	0.089	0.111
0.200	8.593	0.541	0.122	0.139	0.533	0.400	0.122	0.139
0.200	17.580	0.464	0.143	0.155	0.580	0.338	0.143	0.157
0.200	26.035	0.419	0.154	0.163	0.606	0.302	0.154	0.166
0.251	11.172	0.511	0.130	0.144	0.554	0.377	0.130	0.146
0.296	3.059	0.567	0.110	0.127	0.511	0.433	0.110	0.130
0.335	-0.817	0.607	0.095	0.114	0.472	0.475	0.095	0.116

TABLE 7.9 RESULTS OF OVERLOAD EXPERIMENTS PROPELLER NO. 56L,R&C

```
MODEL NO. 299C                    RESULTS OF PROPULSION EXPERIMENTS
L =  200.00 m                        PROPELLER NO. 74,L,R,C
                                     T =  14.03 m                            TEST DATE  17-FEB-82
                                         DESIGN                              TRIM =   0.00 m BY THE STERN
SHIP PREDICTIONS ARE FOR SALT WATER AT 15 deg C                  SHIP MODEL CORRELATION ALLOWANCE 0.0000

                          POWERS,SPEEDS AND THRUST PREDICTED FOR MODEL TEST PROPELLER

                                        WING PROPS.                    CENTRE PROP.               TOTAL
      V        FN       PE       PD       NS       TH       PD       NS       TH       PD        TH
    KNOTS               KW       KW       RPM      KN       KW       RPM      KN       KW        KN

     8.65    0.101    3715.    5625.     76.9    905.0    2075.     76.9    474.9    7700.    1379.9
    12.85    0.149   12695.   20758.    111.8   1976.4    9279.    111.8   1071.2   30036.    3047.6
    17.26    0.201   31171.   53919.    149.1   3589.9   25588.    149.1   2004.7   79506.    5594.6
    19.37    0.225   44771.   77050.    167.1   4568.0   37432.    167.1   2561.5  114482.    7129.4
    19.49    0.227   45641.   81333.    168.6   4686.9   38530.    168.6   2605.1  119862.    7292.0
```

TABLE 7.10 RESULTS OF PROPULSION EXPERIMENTS PROPELLER NO. 74, L,R,C

```
                              RESULTS OF PROPULSION EXPERIMENTS
MODEL NO. 299C                  PROPELLER NO. 74,L,R,C                          TEST DATE  17-FEB-82
L =  200.00 m                   T =  14.03 m                                    TRIM =  0.00 m BY THE STERN
                                  DESIGN
SHIP PREDICTIONS ARE FOR SALT WATER AT 15 deg C             SHIP MODEL CORRELATION ALLOWANCE 0.0000

                       PROPULSION FACTORS PREDICTED FOR MODEL TEST PROPELLER

                               WING PROPS.                   CENTRE PROP.               TOTAL
          V       FN       WFTT      ETAO      ETAR      WFTT      ETAO      ETAR      ETAD      THDF
        KNOTS

         8.65    0.101    -0.197    0.627     1.366    -0.170     0.623     1.913     0.482     0.395
        12.85    0.149    -0.151    0.625     1.162    -0.104     0.615     1.372     0.423     0.371
        17.26    0.201    -0.132    0.622     1.076    -0.066     0.607     1.222     0.392     0.373
        19.37    0.225    -0.123    0.621     1.069    -0.053     0.604     1.189     0.391     0.370
        19.49    0.227    -0.123    0.620     1.047    -0.058     0.605     1.187     0.381     0.376
```

TABLE 7.11 RESULTS OF PROPULSION EXPERIMENTS PROPELLER NO. 74,L,R.C

```
                         RESULTS OF PROPULSION EXPERIMENTS
MODEL NO. 299C                   PROPELLER NO. 74,L,R,C
L =  200.00 m                    T =  14.03 m                        TEST DATE  17-FEB-82
                                   DESIGN                            TRIM =   0.00 m BY THE STERN
SHIP PREDICTIONS ARE FOR SALT WATER AT 15 deg C          SHIP MODEL CORRELATION ALLOWANCE 0.0000

                                      PROPELLER COEFFICIENTS

                                         WING PROPELLERS
                        BEHIND MODEL                     TEST PROPELLER            SERIES PROPELLER
        FN  CT-R(60.4)  JP      KTP      KQP      JOM      KTOM      KQOM      JOS      KTOS      KQOS
              X1000                      X10                          X10                          X10

      0.101   -2.273   0.509   0.124    0.140    0.609    0.124     0.191
      0.149   -2.065   0.520   0.128    0.168    0.599    0.128     0.195
      0.201   -1.926   0.524   0.130    0.184    0.593    0.130     0.198
      0.225   -1.876   0.525   0.132    0.187    0.589    0.132     0.200
      0.227   -1.873   0.523   0.133    0.192    0.587    0.133     0.201
```

TABLE 7.12 RESULTS OF PROPULSION EXPERIMENTS PROPELLER NO. 74,L,R,C

```
                                  RESULTS OF PROPULSION EXPERIMENTS
MODEL NO. 299C                        PROPELLER NO. 74,L,R,C
L =  200.00 m                                                                TEST DATE  17-FEB-82
                                      T =   14.03 m                          TRIM =  0.00 m BY THE STERN
                                        DESIGN
SHIP PREDICTIONS ARE FOR SALT WATER AT 15 deg C               SHIP MODEL CORRELATION ALLOWANCE 0.0000

                                            PROPELLER COEFFICIENTS

                                              CENTRE PROPELLER
                          BEHIND MODEL                 TEST PROPELLER             SERIES PROPELLER
      FN  CT-R(60.4)  JP       KTP       KQP      JOM      KTOM      KQOM      JOS       KTOS       KQOS
            X1000                        X10                          X10                            X10

     0.101  -2.273   0.509    0.130    0.103    0.595    0.130    0.197
     0.149  -2.065   0.520    0.139    0.150    0.575    0.139    0.206
     0.201  -1.926   0.524    0.146    0.174    0.558    0.146    0.213
     0.225  -1.876   0.525    0.148    0.181    0.552    0.148    0.216
     0.227  -1.873   0.523    0.148    0.182    0.553    0.148    0.215
```

TABLE 7.13 RESULTS OF PROPULSION EXPERIMENTS PROPELLER NO. 74,L,R,C.

```
MODEL NO. 299C               RESULTS OF PROPULSION EXPERIMENTS
L =   200.00 m                    PROPELLER NO. 74,L,R,C
                                  T =   14.03 m                       TEST DATE   17-FEB-82
                                     DESIGN                           TRIM =   0.00 m BY THE STERN
SHIP PREDICTIONS ARE FOR SALT WATER AT 15 deg C            SHIP MODEL CORRELATION ALLOWANCE 0.000C

          NON-DIMENSIONAL PROPULSION COEFFICIENTS PREDICTED  FOR MODEL TEST PROPELLER

                  FN       FNVOL      CDVOL      PDVOL      TAUT      PDC/PD
                                       X100      X1000      X1000

                0.101      0.222     10.157      0.557      1.999      0.269
                0.149      0.330     12.055      2.171      4.414      0.309
                0.201      0.444     13.172      5.747      8.103      0.322
                0.225      0.498     13.432      8.276     10.326      0.327
                0.227      0.501     13.813      8.665     10.562      0.321
```

TABLE 7.14 RESULTS OF PROPULSION EXPERIMENTS PROPELLER NO. 74,L,R,C,

MODEL NO. 299C
L = 200.00 m

RESULTS OF OVERLOAD EXPERIMENTS
PROPELLER NO. 74,L,R,C
T = 14.03 m

TEST DATE 17-FEB-82
TRIM = 0.00 m BY THE STERN

SHIP PREDICTIONS ARE FOR SALT WATER AT 15 deg C

SHIP MODEL CORRELATION ALLOWANCE 0.00000

POWERS AND TOW FORCES PREDICTED FOR MODEL TEST PROPELLER

		WING PROPS.			CENTRE PROP.			TOTAL		
V KNOTS	FN	PD KW	NS RPM	TH KN	PD KW	NS RPM	TH KN	PD KW	TH KN	FP KN
0.00	0.000	4454.	60.0	938.7	1229.	60.0	481.8	5683.	1420.5	1568.3
0.00	0.000	11440.	80.0	1706.8	4521.	80.0	918.0	15961.	2624.8	2777.4
0.00	0.000	23244.	100.0	2703.5	10144.	100.0	1477.0	33388.	4180.5	4423.9
0.00	0.000	41123.	120.0	3923.5	18856.	120.0	2159.4	59979.	6082.9	6415.2
0.00	0.000	66452.	140.0	5372.6	31673.	140.0	2971.7	98125.	8344.3	8847.2
0.00	0.000	82252.	150.0	6184.8	39832.	150.0	3422.2	122084.	9606.9	10256.2
4.36	0.051	9315.	80.0	1416.8	3909.	80.0	768.1	13224.	2184.9	1624.6
4.36	0.051	20505.	100.0	2351.4	8895.	100.0	1295.7	29400.	3647.0	3017.0
4.36	0.051	38096.	120.0	3518.1	16824.	120.0	1957.4	54919.	5475.5	4789.4
4.36	0.051	63515.	140.0	4917.0	28363.	140.0	2753.3	91878.	7670.3	6812.9
4.36	0.051	79607.	150.0	5703.5	35696.	150.0	3201.6	115303.	8905.1	8083.2
8.65	0.101	6788.	80.0	1025.2	2550.	80.0	536.5	9338.	1561.7	116.5
8.65	0.101	17127.	100.0	1913.7	7473.	100.0	1049.2	24600.	2962.9	1141.5
8.65	0.101	34053.	120.0	3054.9	15784.	120.0	1713.3	49837.	4768.2	2689.8
8.65	0.101	59130.	140.0	4449.1	28322.	140.0	2528.8	87452.	6977.9	4847.6
8.65	0.101	75214.	150.0	5241.0	36437.	150.0	2993.4	111651.	8234.3	6071.1
12.85	0.149	27761.	120.0	2437.1	12607.	120.0	1335.1	40368.	3772.1	550.5
12.85	0.149	37900.	130.0	3044.5	17599.	130.0	1696.2	55499.	4740.7	1263.4
12.85	0.149	50124.	140.0	3714.2	23661.	140.0	2095.7	73785.	5809.9	2025.6
12.85	0.149	64622.	150.0	4446.1	30893.	150.0	2533.7	95515.	6979.8	2959.7
12.85	0.149	81582.	160.0	5240.2	39395.	160.0	3010.1	120978.	8250.3	4077.3
17.26	0.201	55329.	150.0	3665.3	26171.	150.0	2036.7	81499.	5702.0	76.0
17.26	0.201	62766.	155.0	4038.7	30047.	155.0	2250.7	92813.	6289.4	508.0
17.26	0.201	70810.	160.0	4428.2	34258.	160.0	2474.1	105068.	6902.3	950.9
17.26	0.201	79483.	165.0	4834.0	38815.	165.0	2706.9	118299.	7540.9	1389.9

TABLE 7.15 RESULTS OF OVERLOAD EXPERIMENTS PROPELLER NO. 74, L,R,C

MODEL NO. 299C
L = 200.00 m

RESULTS OF OVERLOAD EXPERIMENTS
PROPELLER NO. 74,L,R,C
T = 14.03 m

TEST DATE 17-FEB-82
TRIM = 0.00 m BY THE STERN

SHIP PREDICTIONS ARE FOR SALT WATER AT 15 deg C

SHIP MODEL CORRELATION ALLOWANCE 0.00000

PROPULSION FACTORS PREDICTED FOR MODEL TEST PROPELLER

		WING PROPS.			CENTRE PROP.					
V KNOTS	NS RPM	WFTT	ETAO	ETAR	WFTT	ETAO	ETAR	ETAD	TOTAL THDF	FP/PD N/KW
0.00	60.0	0.000	0.000	1.651	0.000	0.000	2.992	0.000	-0.104	275.965
0.00	80.0	0.000	0.000	1.524	0.000	0.000	1.928	0.000	-0.058	173.996
0.00	100.0	0.000	0.000	1.465	0.000	0.000	1.678	0.000	-0.058	132.492
0.00	120.0	0.000	0.000	1.431	0.000	0.000	1.560	0.000	-0.055	106.953
0.00	140.0	0.000	0.000	1.406	0.000	0.000	1.475	0.000	-0.060	90.159
0.00	150.0	0.000	0.000	1.397	0.000	0.000	1.443	0.000	-0.068	84.005
4.36	80.0	-0.948	0.558	1.192	-0.800	0.529	1.500	0.321	0.135	122.850
4.36	100.0	-1.299	0.537	1.102	-1.057	0.496	1.356	0.251	0.100	102.613
4.36	120.0	-1.648	0.522	1.051	-1.312	0.472	1.279	0.207	0.077	87.203
4.36	140.0	-1.998	0.511	1.020	-1.566	0.454	1.232	0.173	0.077	74.148
4.36	150.0	-2.172	0.506	1.008	-1.692	0.446	1.214	0.163	0.062	70.101
8.65	80.0	-0.218	0.623	1.313	-0.190	0.618	1.803	0.456	0.387	12.480
8.65	100.0	-0.374	0.596	1.147	-0.285	0.574	1.399	0.359	0.331	46.402
8.65	120.0	-0.528	0.571	1.069	-0.374	0.533	1.246	0.315	0.260	53.969
8.65	140.0	-0.680	0.550	1.023	-0.461	0.498	1.165	0.290	0.185	55.429
8.65	150.0	-0.756	0.541	1.007	-0.503	0.483	1.137	0.276	0.161	54.373
12.85	120.0	-0.194	0.617	1.125	-0.132	0.602	1.317	0.405	0.346	13.636
12.85	130.0	-0.249	0.608	1.093	-0.162	0.585	1.266	0.379	0.329	22.763
12.85	140.0	-0.303	0.598	1.068	-0.191	0.569	1.228	0.354	0.321	27.451
12.85	150.0	-0.356	0.589	1.048	-0.220	0.552	1.198	0.338	0.301	30.985
12.85	160.0	-0.410	0.581	1.032	-0.248	0.537	1.174	0.328	0.273	33.702
17.26	150.0	-0.134	0.622	1.074	-0.070	0.607	1.220	0.391	0.372	0.932
17.26	155.0	-0.153	0.618	1.067	-0.082	0.600	1.200	0.384	0.362	5.473
17.26	160.0	-0.172	0.614	1.061	-0.094	0.594	1.182	0.377	0.354	9.050
17.26	165.0	-0.190	0.610	1.055	-0.106	0.588	1.166	0.368	0.351	11.748

TABLE 7.16 RESULTS OF OVERLOAD EXPERIMENTS PROPELLER NO. 74,L,R,C

MODEL NO. 299C
L = 200.00 m

RESULTS OF OVERLOAD EXPERIMENTS
PROPELLER NO. 74,L,R,C
T = 14.03 m

TEST DATE 17-FEB-82
TRIM = 0.00 m BY THE STERN

SHIP PREDICTIONS ARE FOR SALT WATER AT 15 deg C

SHIP MODEL CORRELATION ALLOWANCE 0.00000

PROPELLER COEFFICIENTS

WING PROPELLERS

BEHIND MODEL						TEST PROPELLER		
FN	CT-R(60.4) X1000	JP	KTP	KQP X10	ZETO	JOM	KTOM	KQOM X10
0.000	0.000	0.000	0.211	0.233	0.652	0.000	0.343	0.385
0.000	0.000	0.000	0.215	0.253	0.632	0.000	0.343	0.385
0.000	0.000	0.000	0.218	0.263	0.624	0.000	0.343	0.385
0.000	0.000	0.000	0.220	0.269	0.620	0.000	0.343	0.385
0.000	0.000	0.000	0.221	0.274	0.616	0.000	0.343	0.385
0.000	0.000	0.000	0.222	0.275	0.615	0.000	0.343	0.385
0.051	45.745	0.247	0.179	0.206	0.602	0.480	0.179	0.245
0.051	87.270	0.197	0.190	0.232	0.591	0.454	0.190	0.255
0.051	140.126	0.164	0.197	0.249	0.585	0.435	0.197	0.262
0.051	200.474	0.141	0.203	0.262	0.581	0.422	0.203	0.267
0.051	238.358	0.132	0.205	0.267	0.580	0.417	0.205	0.269
0.101	-1.389	0.489	0.129	0.150	0.538	0.596	0.129	0.197
0.101	6.389	0.391	0.155	0.194	0.542	0.538	0.155	0.222
0.101	18.137	0.326	0.171	0.223	0.547	0.498	0.171	0.238
0.101	34.509	0.279	0.183	0.244	0.552	0.469	0.183	0.249
0.101	43.793	0.261	0.188	0.252	0.553	0.458	0.188	0.254
0.149	-0.175	0.485	0.137	0.182	0.500	0.579	0.137	0.204
0.149	2.272	0.447	0.146	0.195	0.508	0.559	0.146	0.213
0.149	4.888	0.415	0.153	0.206	0.514	0.541	0.153	0.220
0.149	8.095	0.388	0.160	0.216	0.519	0.526	0.160	0.227
0.149	11.931	0.364	0.165	0.225	0.524	0.512	0.165	0.232
0.201	-1.782	0.521	0.132	0.185	0.475	0.591	0.132	0.199
0.201	-0.960	0.504	0.136	0.190	0.481	0.581	0.136	0.203
0.201	-0.117	0.488	0.140	0.195	0.487	0.572	0.140	0.207
0.201	0.719	0.473	0.143	0.200	0.492	0.564	0.143	0.211

TABLE 7.17 RESULTS OF OVERLOAD EXPERIMENTS PROPELLER NO 74, L.R.C

MODEL NO. 299C
L = 200.00 m

RESULTS OF OVERLOAD EXPERIMENTS
PROPELLER NO. 74,L,R,C
T = 14.03 m

TEST DATE 17-FEB-82
TRIM = 0.00 m BY THE STERN

SHIP PREDICTIONS ARE FOR SALT WATER AT 15 deg C

SHIP MODEL CORRELATION ALLOWANCE 0.00000

PROPELLER COEFFICIENTS

CENTRE PROPELLER

FN	CT-R(60.4) X1000	JP	KTP	KQP X10	ZETO	JOM	KTOM	KQOM X10
		BEHIND MODEL				TEST PROPELLER		
0.000	0.000	0.000	0.216	0.129	0.995	0.000	0.343	0.385
0.000	0.000	0.000	0.232	0.200	0.796	0.000	0.343	0.385
0.000	0.000	0.000	0.239	0.229	0.747	0.000	0.343	0.385
0.000	0.000	0.000	0.242	0.247	0.722	0.000	0.343	0.385
0.000	0.000	0.000	0.245	0.261	0.704	0.000	0.343	0.385
0.000	0.000	0.000	0.246	0.267	0.695	0.000	0.343	0.385
0.051	45.745	0.247	0.194	0.173	0.734	0.444	0.194	0.259
0.051	87.270	0.197	0.209	0.201	0.715	0.406	0.209	0.273
0.051	140.126	0.164	0.220	0.220	0.707	0.380	0.220	0.282
0.051	200.474	0.141	0.227	0.234	0.702	0.362	0.227	0.288
0.051	238.358	0.132	0.230	0.239	0.700	0.354	0.230	0.290
0.101	-1.389	0.489	0.135	0.113	0.681	0.582	0.135	0.203
0.101	6.389	0.391	0.170	0.169	0.651	0.503	0.170	0.236
0.101	18.137	0.326	0.192	0.206	0.645	0.448	0.192	0.257
0.101	34.509	0.279	0.208	0.233	0.645	0.408	0.208	0.272
0.101	43.793	0.261	0.215	0.244	0.646	0.392	0.215	0.277
0.149	-0.175	0.485	0.150	0.165	0.584	0.549	0.150	0.217
0.149	2.272	0.447	0.162	0.181	0.594	0.520	0.162	0.229
0.149	4.888	0.415	0.173	0.195	0.603	0.495	0.173	0.239
0.149	8.095	0.388	0.182	0.207	0.610	0.473	0.182	0.248
0.149	11.931	0.364	0.190	0.217	0.616	0.454	0.190	0.255
0.201	-1.782	0.521	0.146	0.175	0.548	0.557	0.146	0.214
0.201	-0.960	0.504	0.151	0.182	0.552	0.545	0.151	0.219
0.201	-0.117	0.488	0.156	0.189	0.556	0.534	0.156	0.223
0.201	0.719	0.473	0.161	0.195	0.560	0.524	0.161	0.228

TABLE 7.18 RESULTS OF OVERLOAD EXPERIMENTS PROPELLER NO. 74,L,R,C

MODEL NO. 299E
L = 200.00 m

RESULTS OF PROPULSION EXPERIMENTS
PROPELLER NO. 74,L,R,C
T = 14.03 m
DESIGN

TEST DATE 06-MAY-82
TRIM = 0.00 m BY THE STERN

SHIP PREDICTIONS ARE FOR SALT WATER AT 15 deg C

SHIP MODEL CORRELATION ALLOWANCE 0.000

POWERS,SPEEDS AND THRUST PREDICTED FOR MODEL TEST PROPELLER

V KNOTS	FN	PE KW	WING PROPS. PD KW	 NS RPM	 TH KN	CENTRE PROP. PD KW	 NS RPM	 TH KN	TOTAL PD KW	 TH KN
8.64	0.100	2043.	3913.	68.4	289.5	1551.	68.4	92.3	5463.	381.8
12.84	0.149	6720.	11758.	101.1	669.0	4783.	101.1	234.6	16542.	903.7
17.23	0.200	17150.	29812.	135.9	1285.9	12026.	135.9	495.4	41837.	1781.2
19.30	0.224	24523.	41987.	152.3	1646.4	17338.	152.3	634.8	59325.	2281.2
20.03	0.233	28491.	48425.	159.2	1827.6	20482.	159.2	706.5	68908.	2534.2
20.45	0.238	31096.	52273.	162.5	1925.9	21818.	162.5	738.2	74091.	2664.1
22.42	0.261	43536.	74274.	181.2	2514.2	31090.	181.2	977.9	105364.	3492.0

TABLE 7.19 RESULTS OF PROPULSION EXPERIMENTS PROPELLER NO. 74,L,R,C

```
                            RESULTS OF PROPULSION EXPERIMENTS
MODEL NO. 299E                    PROPELLER NO. 74,L,R,C
L =  200.00 m                     T =  14.03 m                         TEST DATE  06-MAY-82
                                    DESIGN                             TRIM =  0.00 m BY THE STERN
SHIP PREDICTIONS ARE FOR SALT WATER AT 15 deg C          SHIP MODEL CORRELATION ALLOWANCE 0.0000

                         PROPULSION FACTORS PREDICTED FOR MODEL TEST PROPELLER

                                   WING PROPS.                CENTRE PROP.            TOTAL
          V        FN       WFTT     ETAO     ETAR      WFTT     ETAO     ETAR     ETAD     THDF
        KNOTS

         8.64    0.100   -0.337    0.548    0.803    -0.399    0.449    0.826    0.374   -0.203
        12.84    0.149   -0.322    0.559    0.889    -0.376    0.484    0.922    0.406   -0.125
        17.23    0.200   -0.311    0.571    0.879    -0.356    0.519    0.955    0.410   -0.086
        19.30    0.224   -0.308    0.574    0.888    -0.354    0.523    0.942    0.413   -0.082
        20.03    0.233   -0.314    0.577    0.887    -0.361    0.527    0.919    0.413   -0.090
        20.45    0.238   -0.312    0.579    0.880    -0.361    0.527    0.919    0.420   -0.109
        22.42    0.261   -0.324    0.587    0.881    -0.373    0.541    0.922    0.413   -0.080
```

TABLE 7.20 RESULTS OF PROPULSION EXPERIMENTS PROPELLER NO. 74,L,R,C

```
                               RESULTS OF PROPULSION EXPERIMENTS
MODEL NO. 299E                   PROPELLER NO. 74,L,R,C
L =  200.00 m                    T =  14.03 m                            TEST DATE  06-MAY-82
                                     DESIGN                              TRIM =  0.00 m BY THE STE
SHIP PREDICTIONS ARE FOR SALT WATER AT 15 deg C              SHIP MODEL CORRELATION ALLOWANCE 0.0

          NON-DIMENSIONAL PROPULSION COEFFICIENTS PREDICTED  FOR MODEL TEST PROPELLER

                    FN        FNVOL       CDVOL       PDVOL       TAUT       PDC/PD
                                           X100       X1000       X1000

                  0.100       0.222       7.245       0.398       0.557       0.284
                  0.149       0.330       6.697       1.205       1.318       0.289
                  0.200       0.443       7.007       3.049       2.598       0.287
                  0.224       0.496       7.070       4.323       3.327       0.292
                  0.233       0.515       7.340       5.022       3.696       0.297
                  0.238       0.526       7.424       5.399       3.886       0.294
                  0.261       0.577       8.008       7.678       5.093       0.295
```

TABLE 7.21 RESULTS OF PROPULSION EXPERIMENTS PROPELLER NO. 74, L,R,C,

```
MODEL NO. 299E                  RESULTS OF PROPULSION EXPERIMENTS
L =  200.00 m                       PROPELLER NO. 74,L,R,C
                                       T =  14.03 m                       TEST DATE  06-MAY-82
                                         DESIGN                           TRIM :  0.00 m BY THE STERN
SHIP PREDICTIONS ARE FOR SALT WATER AT 15 deg C         SHIP MODEL CORRELATION ALLOWANCE 0.0006

                                     PROPELLER COEFFICIENTS

                                        WING PROPELLERS
                          BEHIND MODEL              TEST PROPELLER                SERIES PROPELLER
   FN   CT-R(62.1)   JP      KTF      KQF      JOM      KTOM      KQOM      JOS      KTOS      KQOS
          X1000                        X10                          X10                          X10

 0.100   -2.256    0.572   0.050    0.138    0.765    0.050     0.111    1.104    0.104     0.263
 0.149   -2.050    0.574   0.053    0.129    0.759    0.053     0.114    1.089    0.109     0.270
 0.200   -1.913    0.574   0.056    0.134    0.752    0.056     0.118    1.071    0.114     0.278
 0.224   -1.863    0.573   0.057    0.134    0.750    0.057     0.119    1.065    0.116     0.280
 0.233   -1.847    0.569   0.058    C.136    0.748    0.058     0.120    1.060    0.117     0.282
 0.238   -1.839    0.569   0.059    0.138    0.747    0.059     0.121    1.056    0.118     0.284
 0.261   -1.801    0.560   0.062    0.141    0.741    0.062     0.124    1.039    0.122     0.289
```

TABLE 7.22 RESULTS OF PROPULSION EXPERIMENTS PROPELLER NO. 74,L,R,C,

MODEL NO. 299E
L = 200.00 m

RESULTS OF PROPULSION EXPERIMENTS
PROPELLER NO. 74,L,R,C
T = 14.03 m
DESIGN

TEST DATE 04-MAY-82
TRIM = 0.00 m BY THE STERN

SHIP PREDICTIONS ARE FOR SALT WATER AT 15 deg C

SHIP MODEL CORRELATION ALLOWANCE 0.0000

PROPELLER COEFFICIENTS

CENTRE PROPELLER

		BEHIND MODEL			TEST PROPELLER			SERIES PROPELLER		
FN	CT-R(62.1) X1000	JP	KTP	KQP X10	JOM	KTOM	KQOM X10	JOS	KTOS	KQOS X10
0.100	-2.256	0.572	0.032	0.110	0.800	0.032	0.091	1.186	0.070	0.213
0.149	-2.050	0.574	0.037	0.105	0.790	0.037	0.096	1.164	0.080	0.229
0.200	-1.913	0.574	0.043	0.108	0.778	0.043	0.104	1.136	0.092	0.246
0.224	-1.863	0.573	0.044	0.111	0.776	0.044	0.105	1.132	0.094	0.249
0.233	-1.847	0.569	0.045	0.115	0.775	0.045	0.105	1.128	0.095	0.251
0.238	-1.839	0.569	0.045	0.115	0.775	0.045	0.106	1.127	0.096	0.251
0.261	-1.801	0.560	0.048	0.118	0.769	0.048	0.109	1.113	0.101	0.259

TABLE 7.23 RESULTS OF PROPULSION EXPERIMENTS PROPELLER NO.74,L,R,C

MODEL NO. 299E
L = 200.00 m

RESULTS OF OVERLOAD EXPERIMENTS
PROPELLER NO. 74 L,R,C
T = 14.03 m

TEST DATE 06-MAY-82
TRIM = 0.00 m BY THE STERN

SHIP PREDICTIONS ARE FOR SALT WATER AT 15 deg C

SHIP MODEL CORRELATION ALLOWANCE 0.00000

POWERS AND TOW FORCES PREDICTED FOR MODEL TEST PROPELLER

V	FN	WING PROPS.			CENTRE PROP.			TOTAL		
KNOTS		PD KW	NS RPM	TH KN	PD KW	NS RPM	TH KN	PD KW	TH KN	FP KN
0.00	0.000	12411.	90.0	1519.8	7459.	90.0	795.5	19871.	2315.3	3677.8
0.00	0.000	22794.	110.0	2332.3	13693.	110.0	1193.4	36487.	3525.7	5551.4
0.00	0.000	37850.	130.0	3305.0	22751.	130.0	1677.6	60601.	4982.5	7801.3
0.00	0.000	58505.	150.0	4424.5	35360.	150.0	2269.6	93865.	6694.1	10522.6
0.00	0.000	85703.	170.0	5700.3	53016.	170.0	3007.4	138718.	8707.7	13415.1
4.39	0.051	18034.	90.0	1503.5	7675.	90.0	733.5	25710.	2237.0	2862.7
4.39	0.051	34074.	110.0	2422.3	14930.	110.0	1199.1	49004.	3621.4	4719.6
4.39	0.051	57555.	130.0	3545.2	25691.	130.0	1773.9	83246.	5319.1	6865.6
4.39	0.051	89892.	150.0	4873.3	40645.	150.0	2458.3	130537.	7331.7	9669.3
4.39	0.051	109824.	160.0	5614.6	49909.	160.0	2841.7	159733.	8456.3	11068.3
8.64	0.100	11515.	90.0	879.8	4994.	90.0	396.1	16509.	1275.8	1265.4
8.64	0.100	23743.	110.0	1658.9	10648.	110.0	794.5	34391.	2453.4	2612.8
8.64	0.100	42298.	130.0	2614.7	19325.	130.0	1305.8	61624.	3920.5	4574.3
8.64	0.100	68479.	150.0	3727.7	31657.	150.0	1930.0	100136.	5657.7	7165.4
8.64	0.100	103582.	170.0	5002.5	48276.	170.0	2667.1	151858.	7669.7	9538.2
12.84	0.149	17331.	110.0	1022.4	7229.	110.0	398.0	24560.	1420.4	567.1
12.84	0.149	34703.	130.0	1960.0	15070.	130.0	872.3	49773.	2832.3	2317.4
12.84	0.149	59928.	150.0	3105.1	26683.	150.0	1473.0	86611.	4578.1	4769.8
12.84	0.149	94396.	170.0	4444.4	42777.	170.0	2216.1	137173.	6660.5	7458.9
17.23	0.200	46686.	150.0	2059.1	19462.	150.0	870.0	66148.	2929.0	1296.6
17.23	0.200	61431.	160.0	2673.3	25921.	160.0	1171.9	87352.	3845.2	2373.3
17.23	0.200	78734.	170.0	3340.4	33457.	170.0	1504.4	112192.	4844.9	3640.7
19.30	0.224	53166.	160.0	2096.8	22152.	160.0	854.7	75318.	2951.5	726.4
19.30	0.224	61215.	165.0	2412.9	25620.	165.0	1006.2	86835.	3419.1	1262.1
19.30	0.224	69943.	170.0	2749.8	29386.	170.0	1165.3	99329.	3915.1	1867.9
20.03	0.233	49636.	160.0	1877.5	21005.	160.0	729.8	70641.	2607.4	95.7
20.03	0.233	65721.	170.0	2515.7	28080.	170.0	1035.2	93800.	3550.9	1226.2
20.03	0.233	84539.	180.0	3219.2	36376.	180.0	1371.1	120916.	4590.3	2354.5

TABLE 7.24 RESULTS OF OVERLOAD EXPERIMENTS PROPELLER NO. 74 L,R,C

```
MODEL NO. 299E                  RESULTS OF OVERLOAD EXPERIMENTS
L =  200.00 m                       PROPELLER NO. 74 L,R,C
                                    T =   14.03 m                          TEST DATE  06-MAY-82
                                                                           TRIM =   0.00 m BY THE STERN
SHIP PREDICTIONS ARE FOR SALT WATER AT 15 deg C                 SHIP MODEL CORRELATION ALLOWANCE 0.00000

                   PROPULSION FACTORS PREDICTED FOR MODEL TEST PROPELLER

                           WING PROPS.                    CENTRE PROP.
    V        NS       WFTT     ETAO     ETAR      WFTT     ETAO     ETAR      ETAD     TOTAL
  KNOTS     RPM                                                                        THDF     FP/FD
                                                                                                 N/KW

   0.00     90.0     0.000    0.000    2.000     0.000    0.000    1.664     0.000   -0.588   185.081
   0.00    110.0     0.000    0.000    1.988     0.000    0.000    1.655     0.000   -0.575   152.138
   0.00    130.0     0.000    0.000    1.976     0.000    0.000    1.644     0.000   -0.566   128.726
   0.00    150.0     0.000    0.000    1.964     0.000    0.000    1.625     0.000   -0.572   112.098
   0.00    170.0     0.000    0.000    1.952     0.000    0.000    1.578     0.000   -0.541    96.703
   4.39     90.0    -1.487    0.602    0.778    -1.526    0.607    0.898     0.265   -0.349   111.342
   4.39    110.0    -1.888    0.586    0.791    -1.909    0.588    0.896     0.225   -0.346    96.306
   4.39    130.0    -2.293    0.574    0.798    -2.291    0.574    0.894     0.190   -0.320    82.469
   4.39    150.0    -2.701    0.565    0.802    -2.672    0.562    0.892     0.170   -0.340    74.070
   4.39    160.0    -2.905    0.561    0.803    -2.863    0.557    0.891     0.159   -0.327    69.289
   8.64     90.0    -0.581    0.628    0.856    -0.624    0.619    0.926     0.465   -0.352    76.647
   8.64    110.0    -0.792    0.633    0.880    -0.821    0.634    0.954     0.397   -0.252    75.970
   8.64    130.0    -1.013    0.627    0.884    -1.014    0.627    0.966     0.363   -0.284    74.227
   8.64    150.0    -1.246    0.620    0.878    -1.204    0.615    0.972     0.339   -0.348    71.553
   8.64    170.0    -1.485    0.614    0.870    -1.393    0.603    0.975     0.293   -0.303    62.807
  12.84    110.0    -0.379    0.602    0.893    -0.437    0.560    0.933     0.426   -0.115    23.088
  12.84    130.0    -0.509    0.631    0.892    -0.559    0.624    0.955     0.443   -0.177    46.557
  12.84    150.0    -0.641    0.633    0.888    -0.674    0.634    0.964     0.442   -0.264    55.069
  12.84    170.0    -0.777    0.627    0.882    -0.779    0.627    0.971     0.408   -0.273    54.373
  17.23    150.0    -0.378    0.612    0.881    -0.424    0.588    0.959     0.433   -0.103    19.600
  17.23    160.0    -0.425    0.625    0.880    -0.470    0.612    0.963     0.437   -0.120    27.168
  17.23    170.0    -0.472    0.631    0.878    -0.515    0.625    0.967     0.441   -0.151    32.449
  19.30    160.0    -0.342    0.597    0.880    -0.387    0.563    0.945     0.421   -0.082     9.644
  19.30    165.0    -0.363    0.608    0.878    -0.409    0.581    0.946     0.427   -0.091    14.533
  19.30    170.0    -0.383    0.616    0.876    -0.430    0.595    0.947     0.434   -0.108    18.805
  20.03    160.0    -0.317    0.580    0.887    -0.364    0.531    0.920     0.417   -0.096     1.355
  20.03    170.0    -0.357    0.606    0.885    -0.405    0.576    0.928     0.439   -0.123    13.072
  20.03    180.0    -0.396    0.621    0.883    -0.445    0.602    0.933     0.436   -0.115    19.471
```

TABLE 7.25 RESULTS OF OVERLOAD EXPERIMENTS PROPELLER NO. 74, L,R,C,

```
MODEL NO. 299E                RESULTS OF OVERLOAD EXPERIMENTS
L =  200.00 m                     PROPELLER NO. 74 L,R,C
                                   T =  14.03 m                        TEST DATE  06-MAY-82
                                                                       TRIM =   0.00 m BY THE STERN
SHIP PREDICTIONS ARE FOR SALT WATER AT 15 deg C              SHIP MODEL CORRELATION ALLOWANCE 0.00000

                                      PROPELLER COEFFICIENTS

                                          WING PROPELLERS
                            BEHIND MODEL
     FN   CT-R(62.1)   JP       KTP       KQP      ZETO          TEST PROPELLER
             X1000                        X10                  JOM     KTOM     KQOM
                                                                                 X10

   0.000      0.000   0.000    0.152    0.192    0.533       0.000    0.343    0.385
   0.000      0.000   0.000    0.156    0.194    0.546       0.000    0.343    0.385
   0.000      0.000   0.000    0.158    0.195    0.552       0.000    0.343    0.385
   0.000      0.000   0.000    0.159    0.196    0.552       0.000    0.343    0.385
   0.000      0.000   0.000    0.159    0.197    0.552       0.000    0.343    0.385
   0.051     96.038   0.221    0.150    0.280    0.411       0.548    0.150    0.217
   0.051    160.070   0.180    0.162    0.289    0.434       0.521    0.162    0.229
   0.051    234.070   0.153    0.169    0.296    0.447       0.503    0.169    0.236
   0.051    330.753   0.132    0.175    0.301    0.457       0.490    0.175    0.241
   0.051    378.995   0.124    0.177    0.303    0.461       0.484    0.177    0.243
   0.100      8.981   0.435    0.088    0.179    0.325       0.687    0.088    0.153
   0.100     20.946   0.356    0.111    0.202    0.378       0.637    0.111    0.177
   0.100     38.365   0.301    0.125    0.218    0.405       0.605    0.125    0.192
   0.100     61.373   0.261    0.134    0.229    0.419       0.585    0.134    0.201
   0.100     82.444   0.230    0.140    0.238    0.427       0.572    0.140    0.207
   0.149      0.233   0.528    0.068    0.147    0.287       0.728    0.068    0.131
   0.149      7.280   0.447    0.094    0.179    0.347       0.674    0.094    0.159
   0.149     17.154   0.387    0.112    0.201    0.381       0.636    0.112    0.178
   0.149     27.981   0.342    0.124    0.217    0.403       0.607    0.124    0.191
   0.200      0.985   0.520    0.074    0.156    0.299       0.716    0.074    0.138
   0.200      3.392   0.487    0.084    0.170    0.323       0.694    0.084    0.149
   0.200      6.225   0.459    0.093    0.181    0.342       0.675    0.093    0.159
   0.224     -0.569   0.546    0.066    0.147    0.279       0.732    0.066    0.129
   0.224      0.385   0.529    0.072    0.154    0.292       0.721    0.072    0.135
   0.224      1.465   0.514    0.077    0.161    0.305       0.710    0.077    0.141
   0.233     -1.689   0.567    0.059    0.137    0.262       0.746    0.059    0.121
   0.233      0.180   0.533    0.070    0.151    0.291       0.724    0.070    0.134
   0.233      2.045   0.504    0.080    0.164    0.314       0.703    0.080    0.145
```

FIGURE 7.26 RESULTS OF OVERLOAD EXPERIMENTS PROPELLER NO. 74 L.R.C

```
                               RESULTS OF OVERLOAD EXPERIMENTS
MODEL NO. 299E                    PROPELLER NO. 74 L,R,C                    TEST DATE  06-MAY-82
L =  200.00 m                     T =  14.03 m                              TRIM =  0.00 m BY THE STERN

SHIP PREDICTIONS ARE FOR SALT WATER AT 15 deg C          SHIP MODEL CORRELATION ALLOWANCE 0.00000

                                    PROPELLER COEFFICIENTS

                                       CENTRE PROPELLER
                        BEHIND MODEL                               TEST PROPELLER
        FN  CT-R(62.1)  JP      KTP      KQP      ZETO        JOM      KTOM     KQOM
               X1000                      X10                                     X10

      0.000    0.000   0.000   0.159    0.231    0.494       0.000    0.343    0.385
      0.000    0.000   0.000   0.159    0.233    0.494       0.000    0.343    0.385
      0.000    0.000   0.000   0.160    0.234    0.495       0.000    0.343    0.385
      0.000    0.000   0.000   0.163    0.237    0.499       0.000    0.343    0.385
      0.000    0.000   0.000   0.168    0.244    0.505       0.000    0.343    0.385
      0.051   96.038   0.221   0.146    0.238    0.447       0.557    0.146    0.214
      0.051  160.070   0.180   0.160    0.254    0.469       0.525    0.160    0.227
      0.051  234.070   0.153   0.170    0.264    0.483       0.502    0.170    0.236
      0.051  330.753   0.132   0.177    0.272    0.493       0.486    0.177    0.243
      0.051  378.995   0.124   0.179    0.275    0.497       0.479    0.179    0.246
      0.100    8.981   0.435   0.079    0.155    0.321       0.706    0.079    0.143
      0.100   20.946   0.356   0.106    0.181    0.389       0.647    0.106    0.173
      0.100   38.365   0.301   0.125    0.199    0.430       0.606    0.125    0.192
      0.100   61.373   0.261   0.139    0.212    0.457       0.575    0.139    0.206
      0.100   82.444   0.230   0.149    0.222    0.477       0.550    0.149    0.217
      0.149    0.233   0.528   0.053    0.123    0.252       0.759    0.053    0.115
      0.149    7.280   0.447   0.083    0.155    0.339       0.696    0.083    0.148
      0.149   17.154   0.387   0.106    0.179    0.391       0.648    0.106    0.172
      0.149   27.981   0.342   0.124    0.197    0.429       0.608    0.124    0.191
      0.200    0.985   0.520   0.062    0.130    0.285       0.740    0.062    0.125
      0.200    3.392   0.487   0.074    0.143    0.317       0.716    0.074    0.138
      0.200    6.225   0.459   0.084    0.154    0.343       0.695    0.084    0.149
      0.224   -0.569   0.546   0.054    0.122    0.257       0.757    0.054    0.115
      0.224    0.385   0.529   0.060    0.129    0.274       0.745    0.060    0.122
      0.224    1.465   0.514   0.065    0.135    0.290       0.734    0.065    0.128
      0.233   -1.689   0.567   0.046    0.116    0.227       0.773    0.046    0.107
      0.233    0.180   0.533   0.058    0.129    0.266       0.749    0.058    0.120
      0.233    2.045   0.504   0.068    0.141    0.296       0.728    0.068    0.132
```

TABLE 7.27 RESULTS OF OVERLOAD EXPERIMENTS PROPELLER NO. 74, L,R,C

kW) and assuming a transmission efficiency of 0.98, the following ship speeds in clear water are predicted:

Model 299	26.0 knots
Model 299C	19.0 knots
Model 299E	22.6 knots

TABLE 7.28 - Maximum Speed at Full Power in Clear Water

While Model 299C has a speed discrepancy of 7.0 knots when compared with Model 299, this is reduced to 3.4 knots with Model 299E.

It should be noted that for Model 299E, the full power condition was not quite reached in open water due to reaching the maximum revolutions of the model propeller speed control, as can be seen from Figure 7.1.

The powers required at 9, 16, and 20 knots for the different models are as follows:

Transmission Efficiency = 0.98
= 46 Ahead

	9 Knots	16 Knots	20 Knots
Model 299	2,319 kW	13,684 kW	41,230 kW
Model 299C	9,276 kW	64,316 kW	---
Model 299E	6,184 kW	34,388 kW	69,880 kW

TABLE 7.29 - Comparison of Delivered Power at Three Selected Speeds

The above shaft powers (at the engine) are related to the effective powers, given in Table 5.9, by the propulsive coefficient or by the Quasi-Propulsive Coefficient ETAD assuming the transmission efficiency as unity. It can be seen that ETAD values for Model 299C at 9 knots are the highest compared with the other two models.

The variation of ETAD over a range of speeds from 6 to 26 is shown in Figure 7.2. The quasi-propulsive coefficients of the proposed design POLAR 7A, based on Model 299C, are higher than those of the parent ship (POLAR 7, Model 299) for speeds up to 12 1/2 knots. At 16 knots, the ETAD values are 0.462, 0.397, and 0.412 respectively. There is some improvement in the propulsive efficiency of Model 299E over Model 299C at higher speeds, but

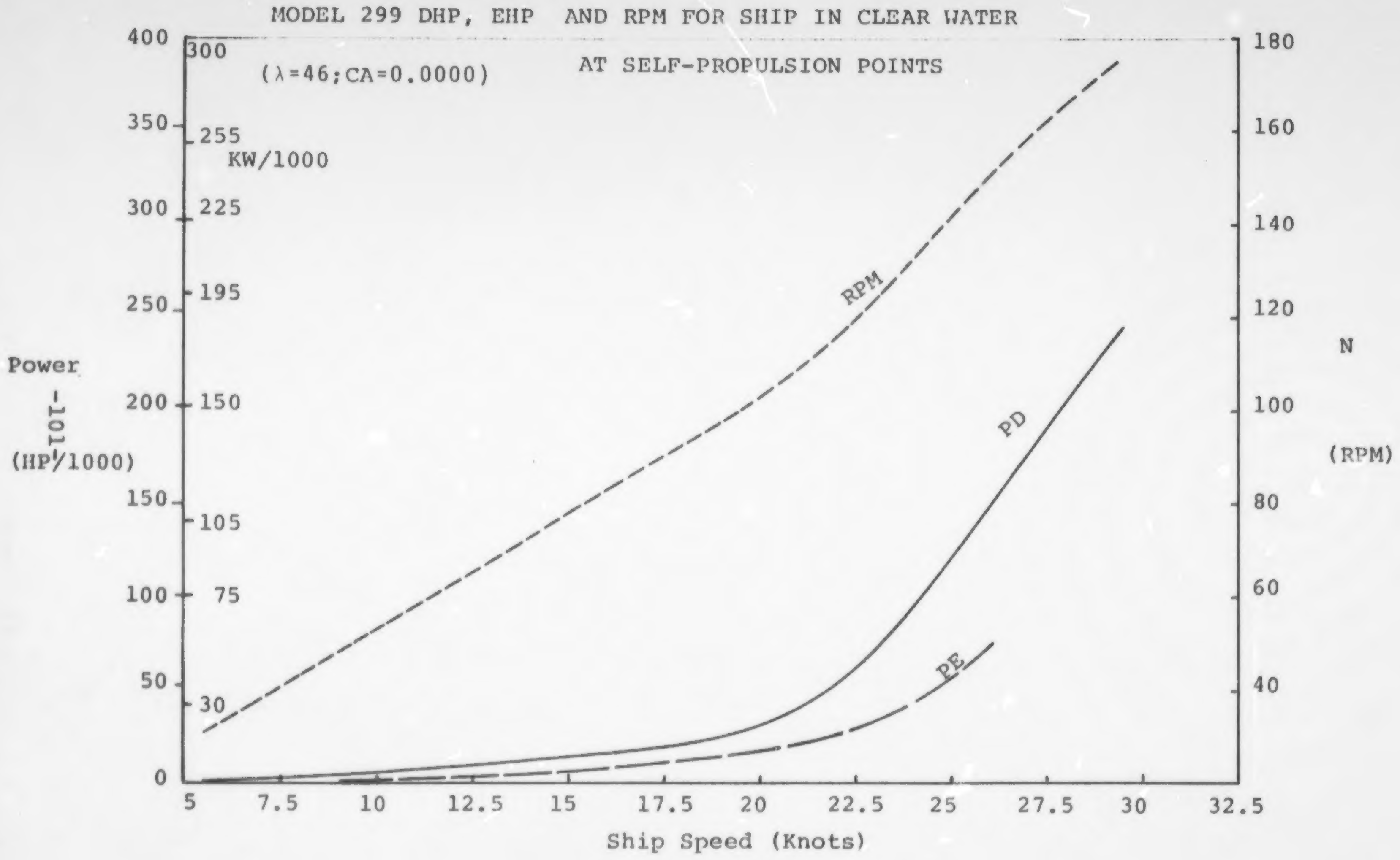

FIGURE 7.1a MODEL 299 DHP, EHP AND RPM FOR SHIP IN CLEAR WATER

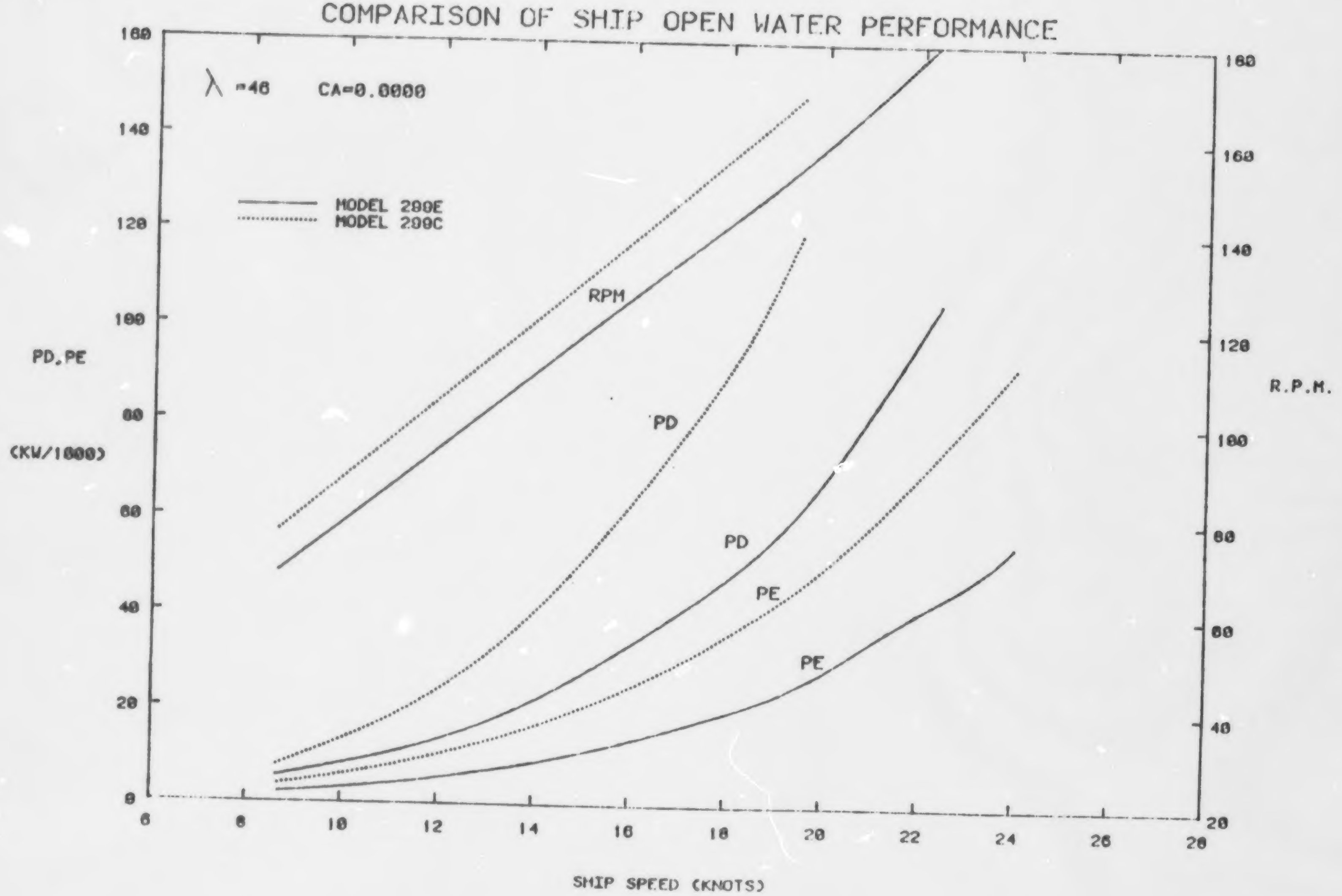

FIGURE 7.1b COMPARISON OF SHIP OPEN WATER PERFORMANCE

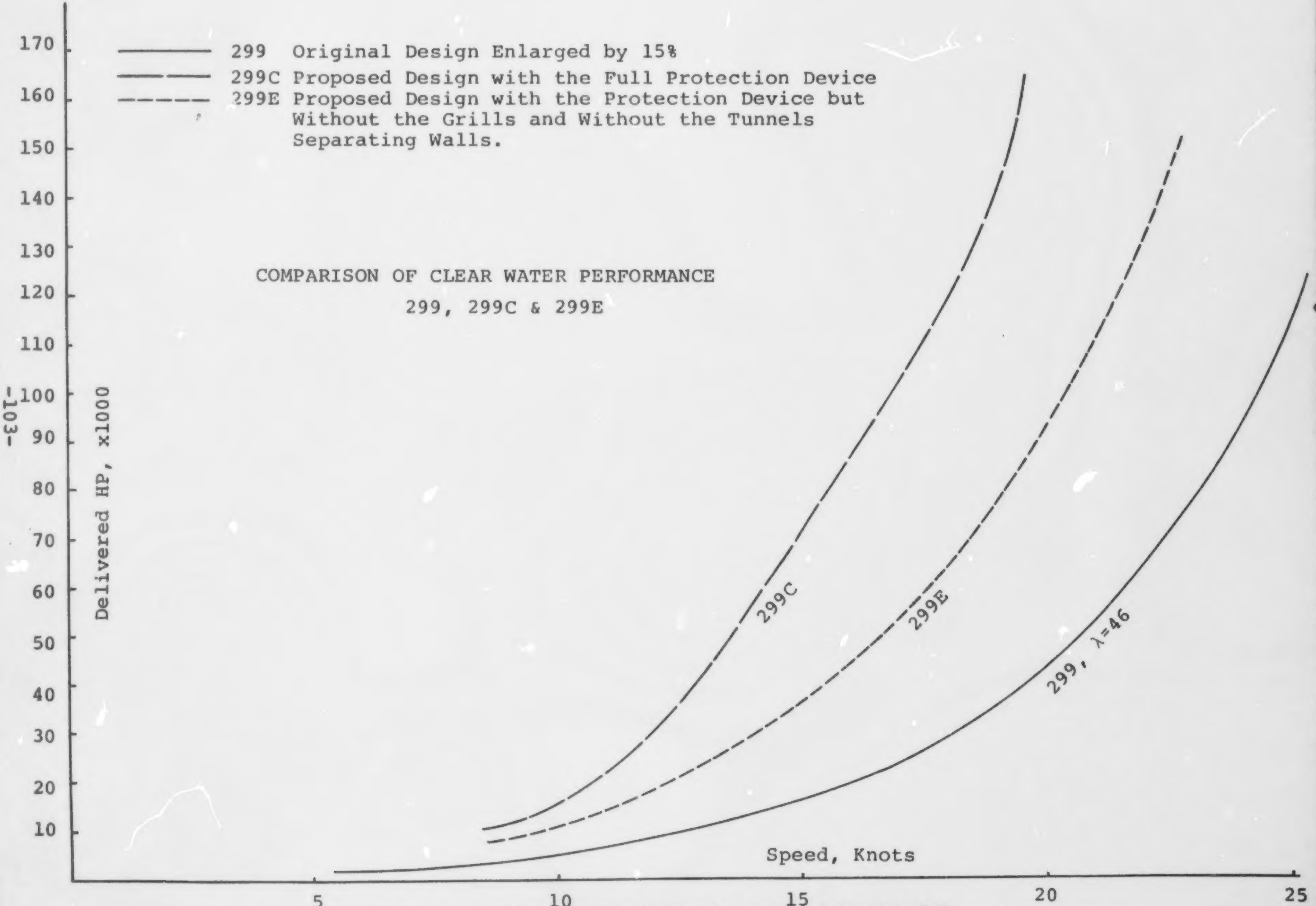

FIGURE 7.1c COMPARISON OF CLEAR WATER PERFORMANCE
299, 299C & 299E

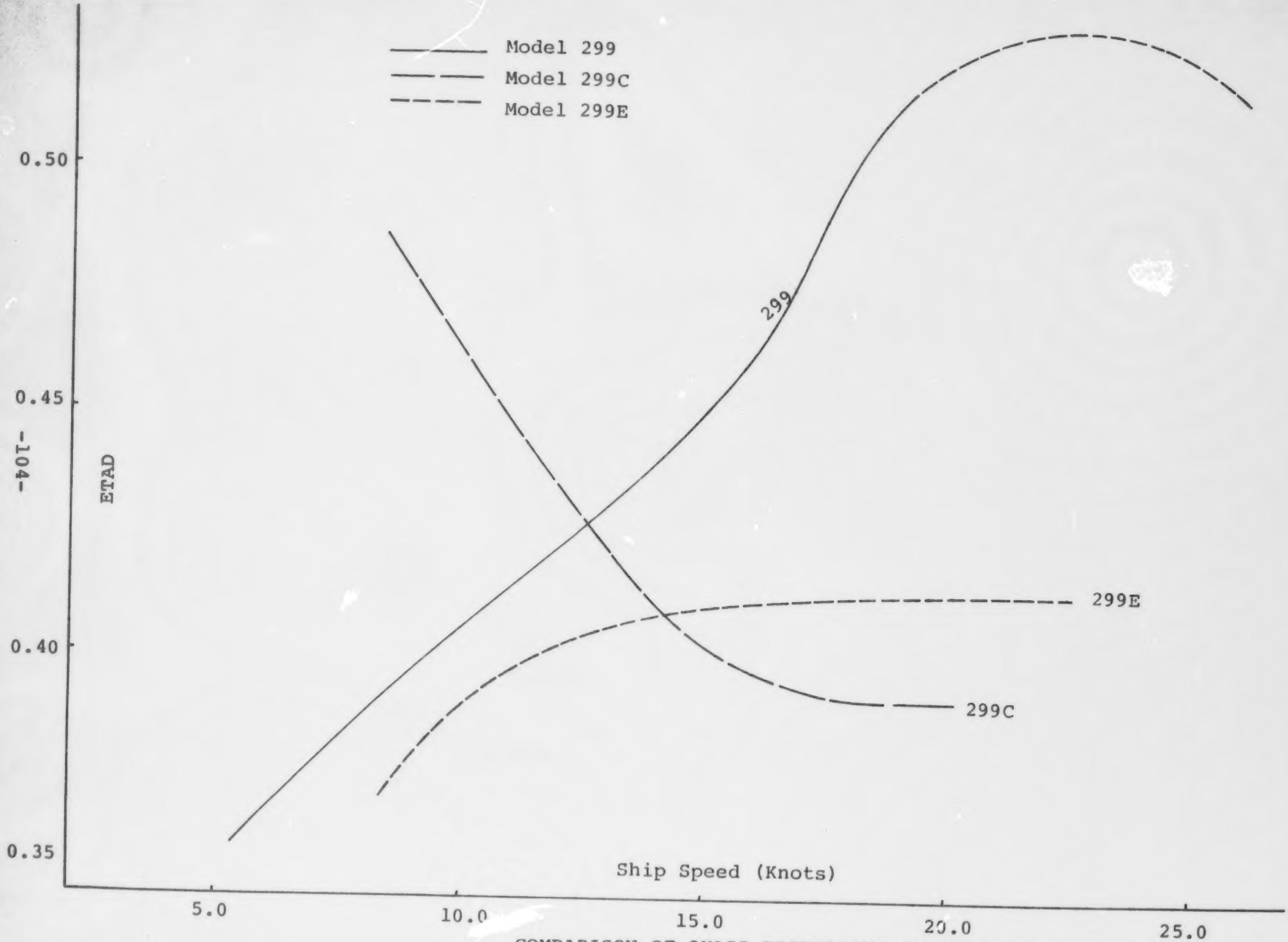

COMPARISON OF QUASI PROPULSIVE COEFFICIENT
FIGURE 7.2

still below that of Model 299, which by itself has relatively lower propulsive coefficients compared with those for normal hull forms. It is clear also from Figure 7.2 that the quasipropulsive coefficient for Model 299C decreases with increasing speed, while for Models 299 and 299E the trend is reversed. In order to explain this behaviour one has to analyse the basic propulsion factors which constitute the overall propulsive efficiency. If we write:

$$\text{Propulsive Coefficient} = \frac{PE}{SHP}$$

$$= \left[\frac{\eta_o \times \eta_r \times \eta_h}{\text{Appendage Coeff}}\right] \times \eta_{\text{Transmission}} \qquad (7.1)$$

$$= [\text{ETAD}] \times \eta_{\text{Transmission}} \qquad (7.2)$$

and since the effective powers were measured for the hull complete with all appendages, then the Appendage Coeff. is 1.0. Therefore:

$$\text{ETAD} = \frac{PE}{PD}$$

$$= \text{ETAO} \times \text{ETAR} \times \text{ETAH} \qquad (7.3)$$

Figure 7.3 shows the propulsion factors read from Tables 7.2, 7.11, and 7.20. As far as the values of the open water efficiency ETAO are concerned, no comparison should be made between Model 299 (POLAR 7) and the other models (POLAR 7A) for two specific reasons: first, different propellers were used in the experiments to suit each design and operating conditions, and secondly, the Kaplan propeller numbers 74 L, R, C, for POLAR 7A were tested with no ducts, and therefore the performance obtained from the experiments (Figure 6.2) does not reflect the true performance in open water.

It must be noted, however, that the above remark does not affect in any way the comparison between the quasi-propulsive coefficients ETAD measured from the experiments (Figure 7.2), which still may be regarded as an effective criteria in assessing the propulsion characteristics of the ship, but certainly not its overall performance.

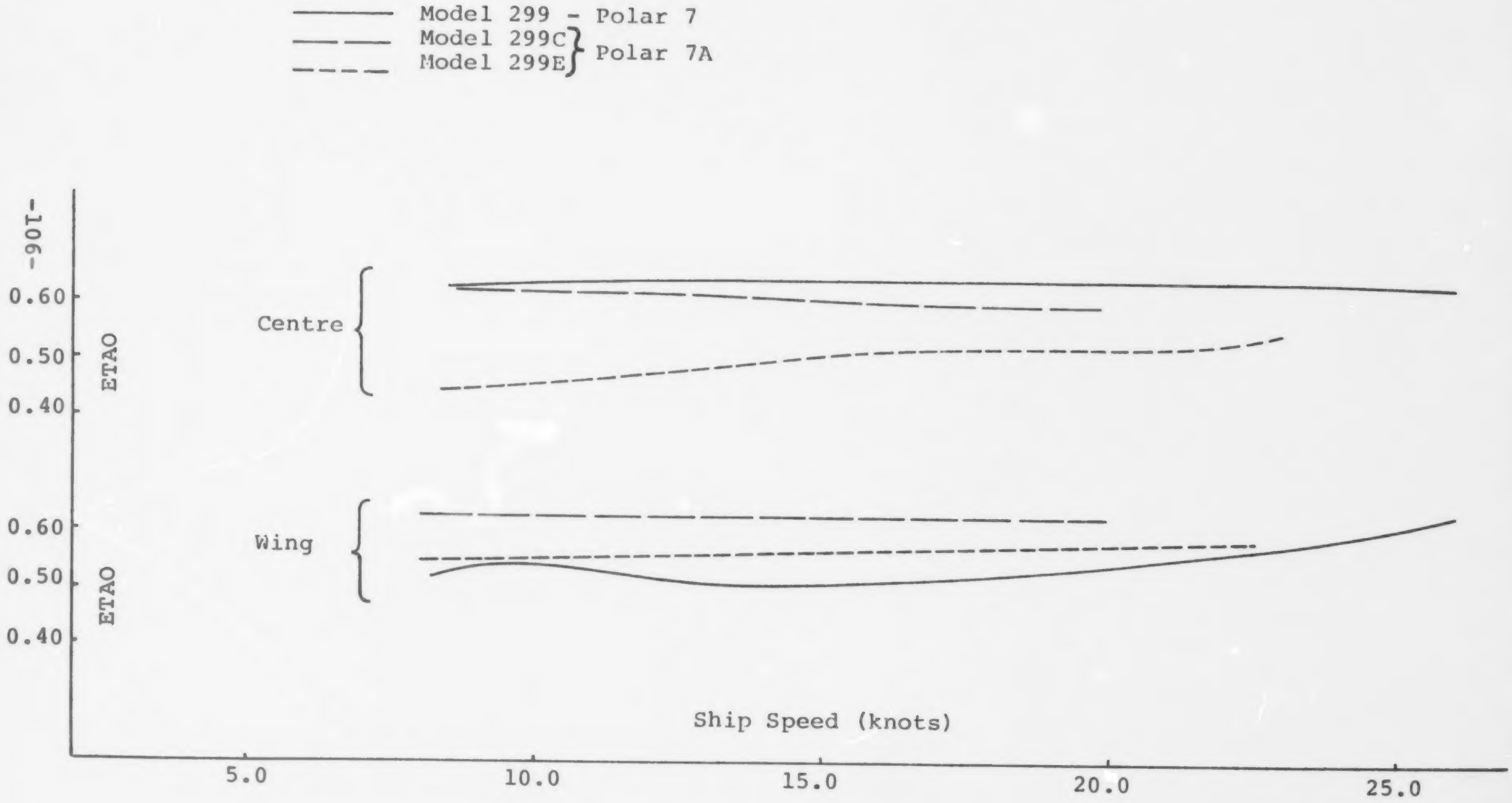

FIGURE 7.3a COMPARISON OF PROPULSION FACTORS

A number of conclusions can be drawn from Figure 7.3. The open water efficiency of the wing propellers for POLAR 7A is less sensitive to the variations in ship speed compared with that for POLAR 7, as one would expect due to the effect of the tunnels and ducts. The values of ETAO for Model 299C (wing and center propellers) are higher than those for Model 299E, a result which can be attributed to the elimination of the slip stream interaction in the former model as a result of using separate tunnels. The relative rotative efficiency ETAR, which is a measure of the propeller efficiency behind the ship to that in open water, is higher for Model 299C over the selected range of speeds. The values of ETAR at 16 knots are as follows:

	ETAR-Wing	ETAR-Center
Model 299	0.80	0.994
Model 299C	1.06	1.255
Model 299E	0.883	0.95

TABLE 7.30 - Comparison of Relative Rotative Efficiency, at 16 Knots

The above figures indicate that the improvement in ETAR for Model 299C, over the original enlarged Model 299, is about 33% for the wing propeller and 26% for the centre propeller. For Model 299E the wing propeller loses some of its efficiency as a result of removing the separating walls, and, the center propeller loses even more due to the slip stream interaction in the unseparated tunnels.

The discussion so far has dealt with the quasi-propulsive coefficient ETADs and the propulsion factors ETAOs and ETARs. The remaining propulsion factor, ETAH, needs special attention since it seems to be the predominant factor affecting the propulsion characteristic of the ship under consideration.

The hull efficiency, ETAH, is the ratio between the effective power, PE, and the thrust power, PT.

Therefore:

$$\text{ETAH} = \frac{R.V}{TH.V_1}$$

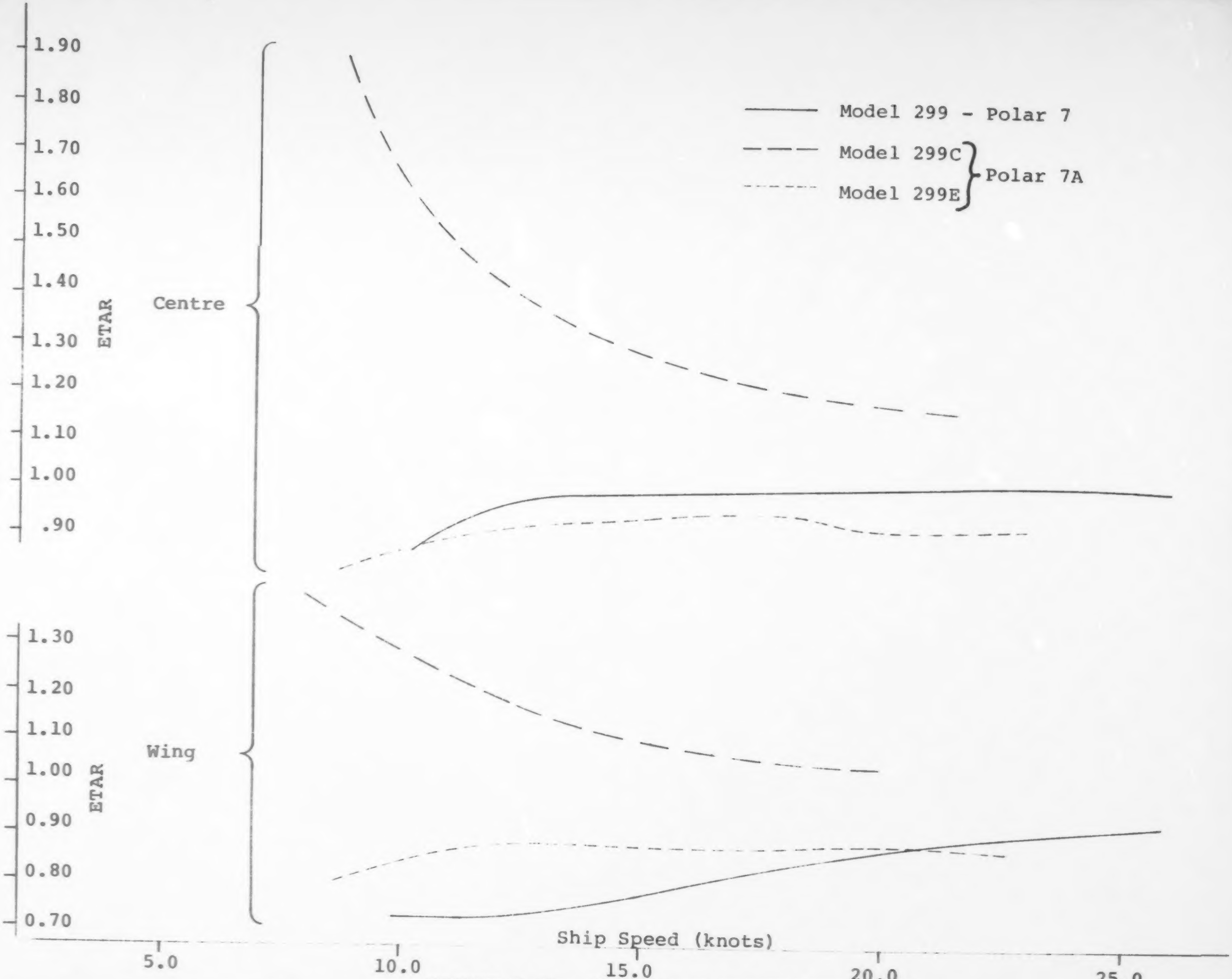

FIGURE 7.3b COMPARISON PROPULSION FACTORS

where

R = ship resistance = TH(1 - THDF)
V = ship speed
TH = thrust
THDF = thrust deduction factor
V_1 = speed of advance = V(1 - WFTT)
WFTT = effective mean wake fraction

Therefore $$ETAH = \frac{1 - THDF}{1 - WFTT} \qquad (7.4)$$

In a multi-screw arrangement, the above expression can be rewritten as:

$$ETAH = \frac{(1 - THDF) \sum_{i=1}^{N} TH_i}{\sum_{i=1}^{N} TH_i (1 - WFTT_i)} \qquad (7.5)$$

$$\text{or} = \frac{PE}{\sum_{i=1}^{N} TH_i (1 - WFTT_i)} \qquad (7.6)$$

where N is number of propellers.

Let us first study the variation of wake fraction and thrust deduction factor versus ship speed. Figure 7.4 shows the mean wake fractions for Models 299, 299C, and 299E (from Tables 7.2, 7.11, 7.20) over a speed range from 8.0 to about 20 knots. The highest wake fractions are those shown for Model 299, i.e., open propeller, and at 16 knots the values are about 0.1 and 0.25 for the wing and center propellers, respectively. These values are in general agreement with those for a normal triple-screw arrangement fitted to a normal hull. The other two Models 299C and 299E show lower WFTT, with the latter providing the lowest values (negative). The negative values of the WFTT for Models 299C and 299E are attributed to the effect of the duct in accelerating the flow into the propeller. This duct effect is more noticeable with Model 299E, especially for the center propeller, compared with the other two models. The more negative WFTT found with Model 299E may be explained by the fact that the separating walls and guards were removed, and in addition, the modified ducts bear more resemblence to the classical accelerating (i.e., Kort) nozzles. At 16 knots the values of the wake fraction are as follows:

	Wing	Center
Model 299	0.10	0.25
Model 299C	-0.135	-0.075
Model 299E	-0.315	-0.036

TABLE 7.31 - Effective Mean Wake Fraction, WFTT, at 16 Knots

The value of the wake fraction has a direct implication in the design of the propeller, a fact that will be explained after the analysis of the thrust deduction factors.

Generally speaking, the propeller causes variation in local pressures in the water and this will react upon the hull, leading to an effective increase in resistance. At the self-propulsion point the difference between the thrust produced by the propeller behind the ship and the resistance of the ship without propeller, can be referred to either as a thrust deduction or a resistance augument.

Figure 7.5 shows the variation of the thrust deduction factors, THDF, over the speed range considered. The parent hull form (299, $\lambda = 46$) has a relatively high thrust deduction factor in comparison with "normal" hull forms. It can be seen also from

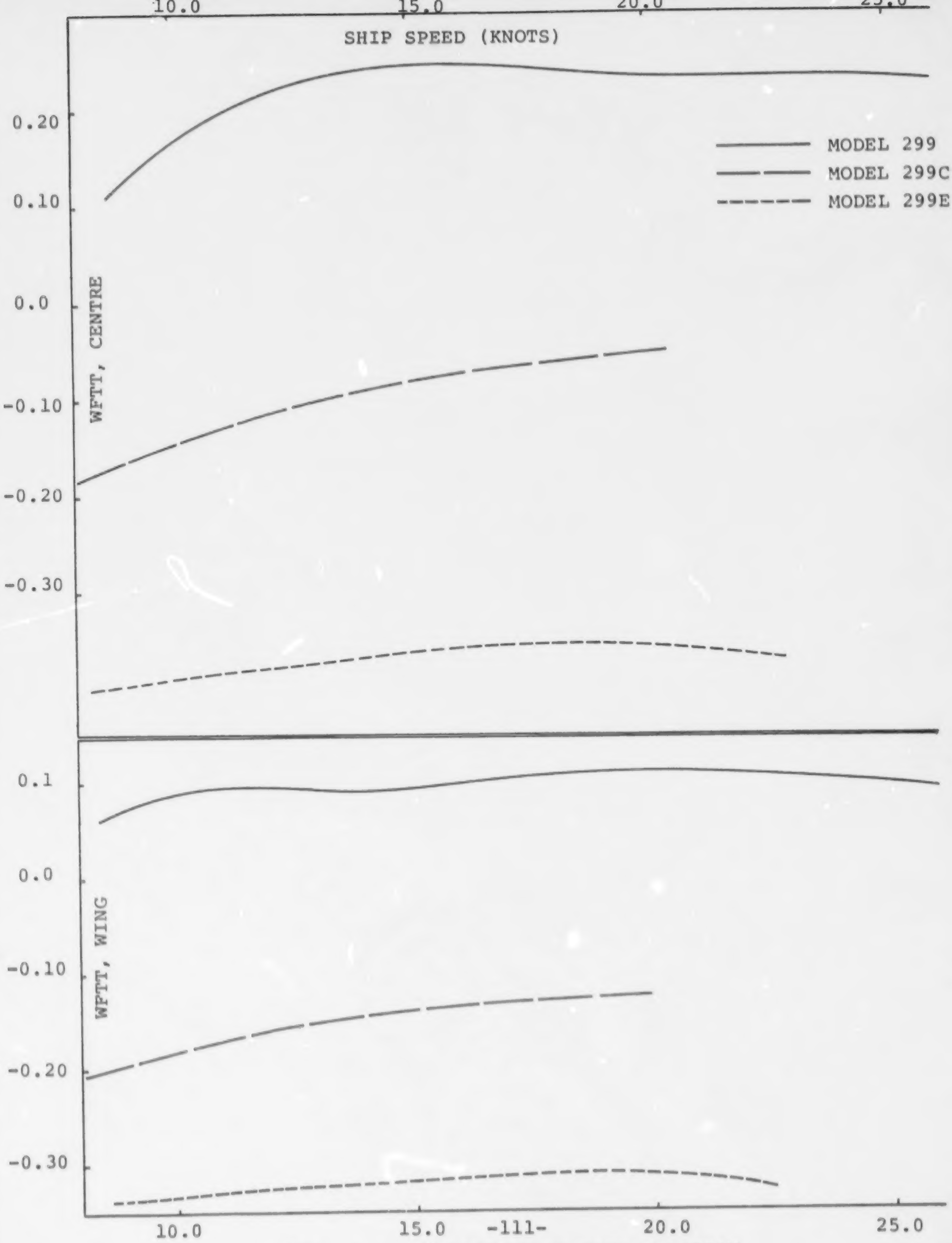

FIG. 7.4 COMPARISON OF WAKE FRACTION

Figure 7.5 that while Model 299C has the highest THDF, Model 299E has the lowest (negative). That means the propellers for Model 299C have to develop much more thrust than the resistance of the ship, whereas for Model 299B, they are not generating all the thrust required to overcome the resistance. It is reasonable to assume that, in the latter case, the remaining thrust is developed by the propeller duct.

At 16 knots, the thrust deduction factors are as follows:

	THDF
Model 299	0.24
Model 299C	0.365
Model 299E	-0.095

TABLE 7.32 - Comparison of Thrust Deduction Factors, THDF, at 16 Knots

The effects of both the thrust deduction factor and the wake fraction are partially included in the expression of the hull efficiency,

$$\text{ETAH} = \frac{\text{Effective Power}}{\text{Thrust Power}}$$

However, it is clear, that the extent of each effect varies considerably. Moreover, a higher or lower ETAH does not necessarily reflect the true picture of a specific design. For example, if ship A has a higher ETAH than ship B, it does not necessarily mean that ship A performs any better than ship B. As ETAH is only one coefficient in the expression of the overall propulsive coefficient.

For a given ETAD value

$$\left(\frac{\text{Effective Power}}{\text{Delivered Power}}\right),$$

a higher or lower ETAH would proportionally affect the remaining propulsion factors to end up with the same ETAD.

The values of ETAH, at 16 knots, can be estimated by expression 7.6 using the following summary table.

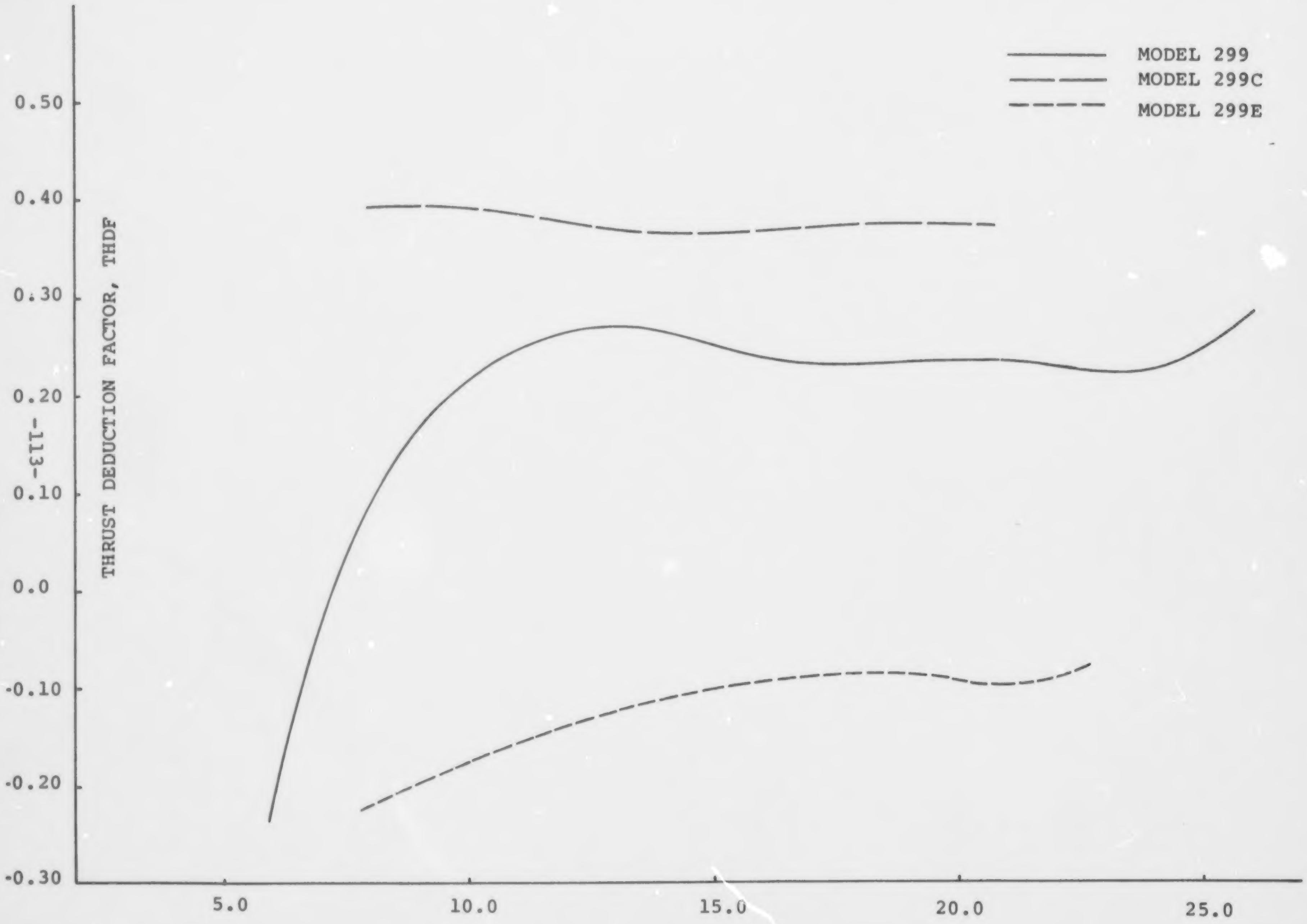

FIG. 7.5 COMPARISON OF THRUST DEDUCTION FACTORS

	THRUST-TONS (Fig. 7.6)		WAKE FRACTION (Table 7.31)		EFFECTIVE POWER (Table 5.9)
	Wing(2)	Center	Wing	Center	HP
Model 299	46.5	64	0.10	0.25	8,501
Model 299C	315	175	-0.135	-0.075	33,098
Model 299E	112	42	-0.315	-0.36	18,219

TABLE 7.33 - SUMMARY TABLE

	ETAH
Model 299	0.958
Model 299C	0.553
Model 299E	0.812

TABLE 7.34 - COMPARISON OF HULL EFFICIENCY AT 16 KNOTS

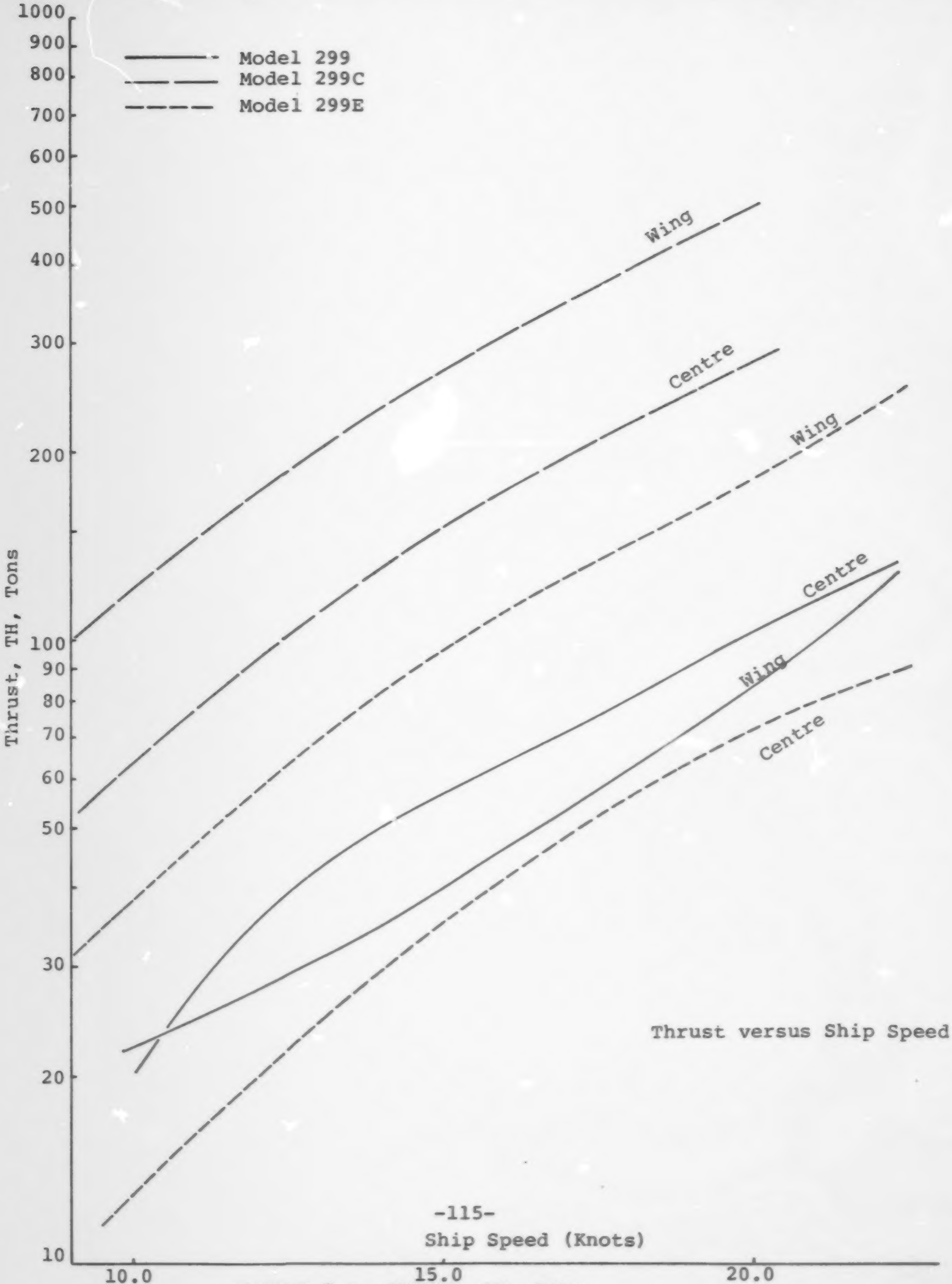

FIGURE 7.6 THRUST, TH, TONS

Let us now summarize the estimated propulsion factors for each model at 16 knots:

	ETAD	ETAO		ETAR		ETAH
		Wing	Center	Wing	Center	
Model 299	0.462	0.513	0.64	0.8	0.994	0.958
Model 299C	0.397	0.62	0.605	1.06	1.255	0.553
Model 299E	0.411	0.57	0.513	0.883	0.95	0.812

TABLE 7.35 - COMPARISON OF PROPULSION FACTORS, AT 16 KNOTS

The above table suggests that the estimated low quasi-propulsive coefficient, ETAD, for Model 299C can be attributed to the low value of ETAH. With the propeller open water efficiency near, but beyond the optimum, and the relative rotative efficiency higher than unity, one can conclude that the high thrust deduction factor for Model 299C is the main reason for the low quasi propulsive coefficient. It should be noticed also from Table 7.35, that by removing the separating walls and roundingoff all sharp edges (i.e., Model 299E), the ETAH is increased, which can be explained as the result of reducing the thrust deduction factor due to the effect of the modified duct. However, by comparison to Model 299C, the ETAR is reduced due to the unfavourable flow into the propeller disk, and ETAO is reduced due to the considerable difference in the mean wake fraction obtained with the two models (Table 7.31)*.

Finally, it seems unlikely that any improvement in the propeller design to suit the new wake field for Model 299C will result in a noticeable improvement in the propulsion characteristics of the proposed design. This statement can be substantiated by the fact that the propellers for Model 299C are already working near their optimum point. Furthermore, redesigning the propellers according to the wake field at 16 knots (clear water) will not necessarily provide the required thrust at near-bollard pull conditions; a condition that is equally important in the design of propellers for icebreakers.

---

* It must be noted that the same propellers were used in Models 299C and 299E and therefore a change in the speed of advance will result in lower advance coefficient and thus lower open water efficiency.

Modifications to Model 299C that will result in a lower thrust deduction factor without impairing the other propulsion factors will result in a higher propulsive efficiency. This may be accomplished by pursuing the separate tunnel concept as in Model 299C (where propeller open water and relative rotative efficiencies are high), and at the same time reducing the thrust deduction factor by increasing the net forward thrust produced by the duct as in Model 299E. A considerable improvement in the resistance and propulsion characteristics of the proposed design can be expected by eliminating flow separation that occurred on the tunnels (Section 8.0). By reshaping the tunnels, a favourable pressure gradient along the roof can be achieved which would have a direct effect in reducing the open water resistance, improving the flow into the propellers and increasing the net forward thrust produced by the ducts. In other words, further attempts should be made to reduce the effective power and increase the propulsive efficiency as a results of reducing propeller/hull interaction.

7.3.2 Overload

Tabulated results of the overload experiments were given earlier in Tables 7.6 to 7.27 for Models 299, 299C, and 299E, respectively.

Figures 7.7, 7.8, and 7.9 show the available tow force for variation in delivered power. This presentation was chosen because of the noticeable differences in the relationship between delivered power and revolutions for Models 299C and 299E. A comparison of Figures 7.8 and 7.9 shows that for a given speed Model 299E has more available tow force at a given power than Model 299C. At full power (110,325 kW), the excess is approximately 2,100 kN at the bollard case and approximately 2,400 kN at 17.23 knots. The variation of THDF with delivered power is shown in Figures 7.10, 7.11, and 7.12 for the various speeds analysed for overload conditions. The general trend is for an increase in THDF with an increase in speed. The value of THDF for Model 299C is negative at the bollard pull case, but becomes positive as the speed increases. The negative THDF would imply that some forward thrust is produced by the protection device.

A similar trend occurs for Model 299E, but the value of THDF starts with a substantial negative value and remains negative over the speed range shown. Again, this can be interpreted to be the effect of the ducts producing some forward thrust for Model 299E, and continuing to be effective at forward speeds.

Figure 7.13 shows a comparison of tow force against delivered power for the bollard (zero speed) case for Models 299, 299C, and 299E.

This shows that for a given delivered power Model 299E produces the most tow force at the bollard condition. The tow force is larger than that developed by Model 299. Model 299C produces the lowest tow force for a given power of the three models compared. At the design power of 110,325 kW, assuming a transmission efficiency of 0.98, the following values of bollard pull were predicted:

Model 299	10,700 kN
Model 299C	9,500 kN
Model 299E	11,600 kN

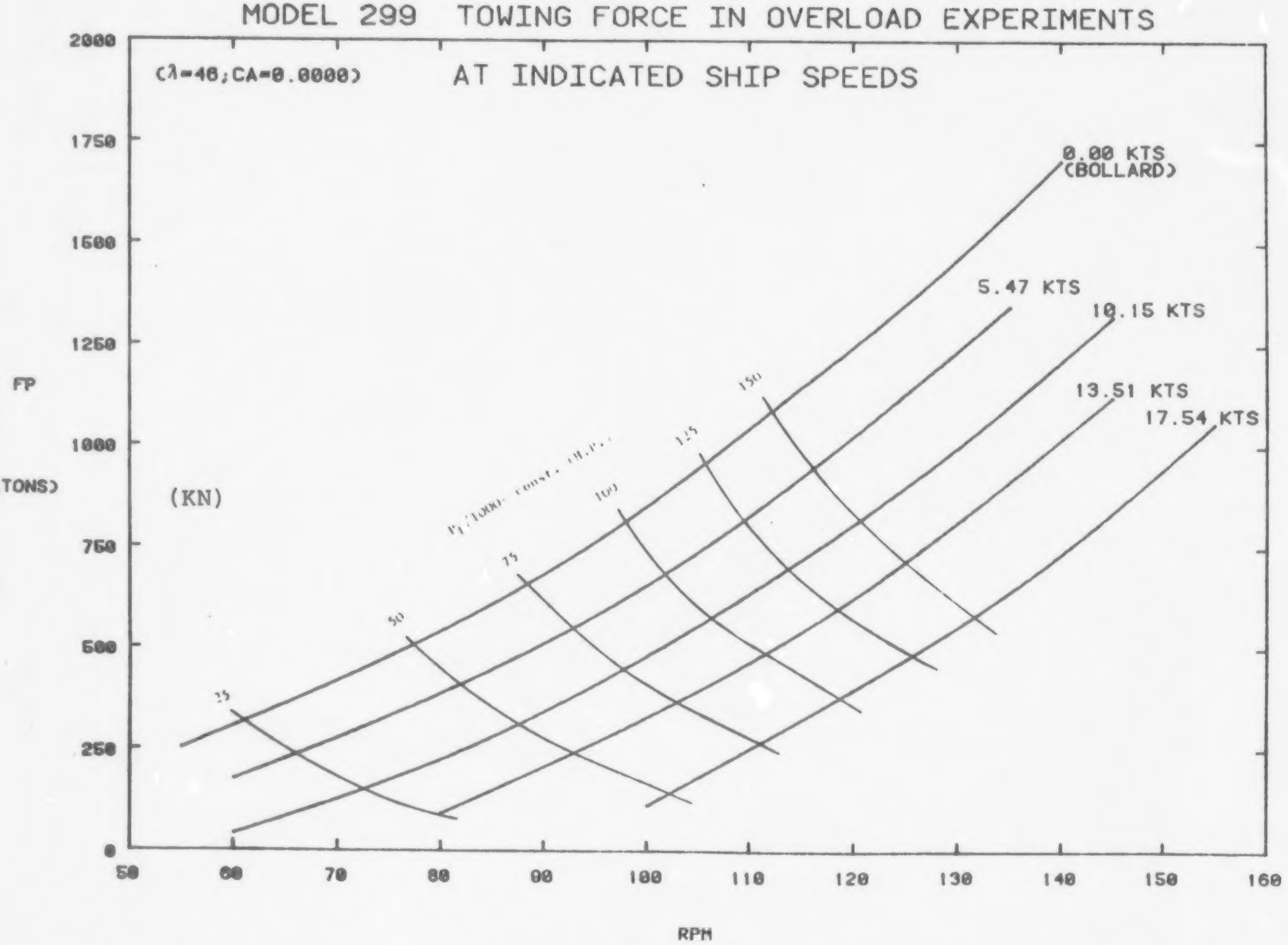

FIGURE 7.7 MODEL 299 TOWING FORCE IN OVERLOAD EXPERIMENTS

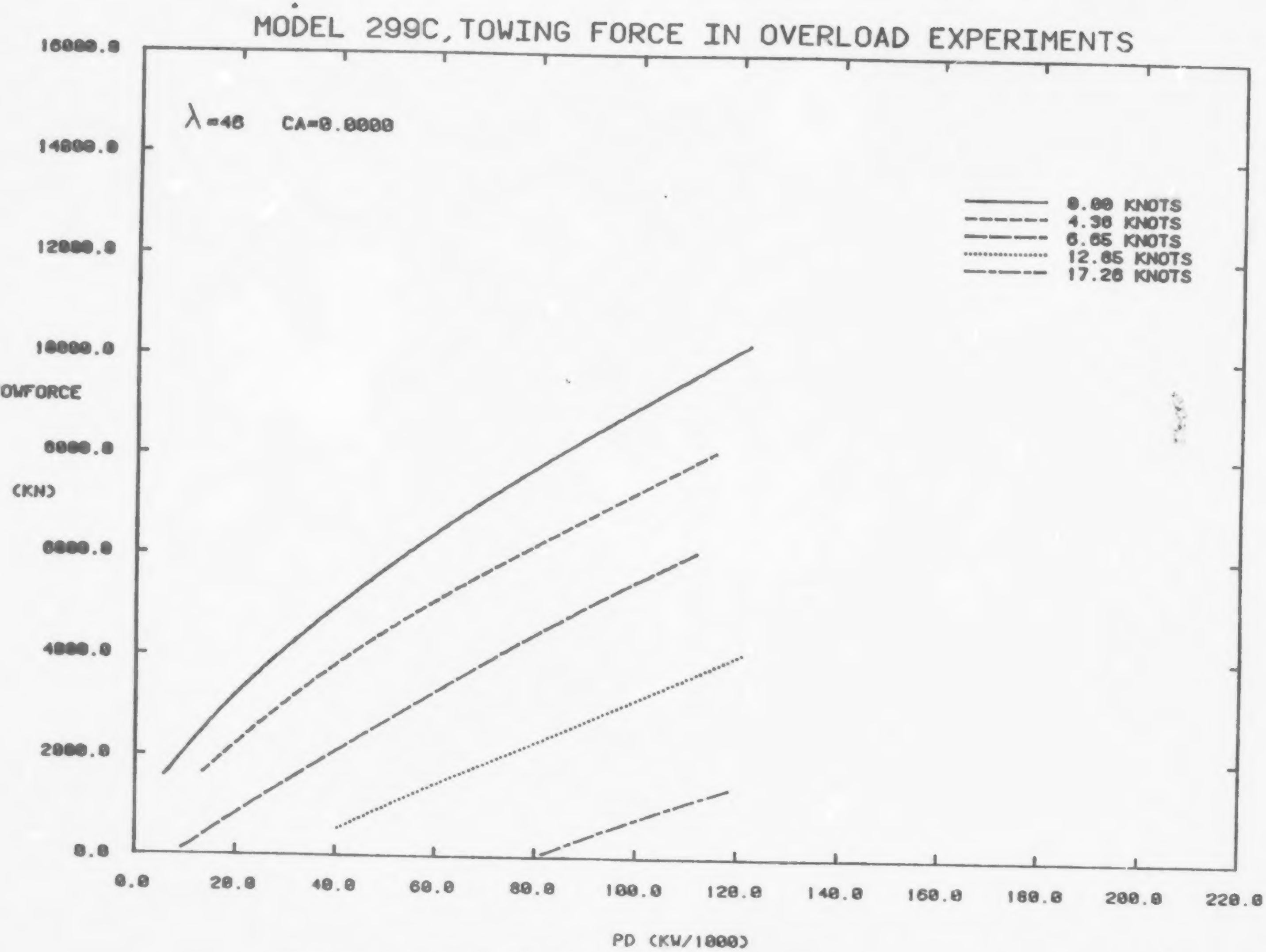

FIGURE 7.8 MODEL 299C TOWING FORCE IN OVERLOAD EXPERIMENTS

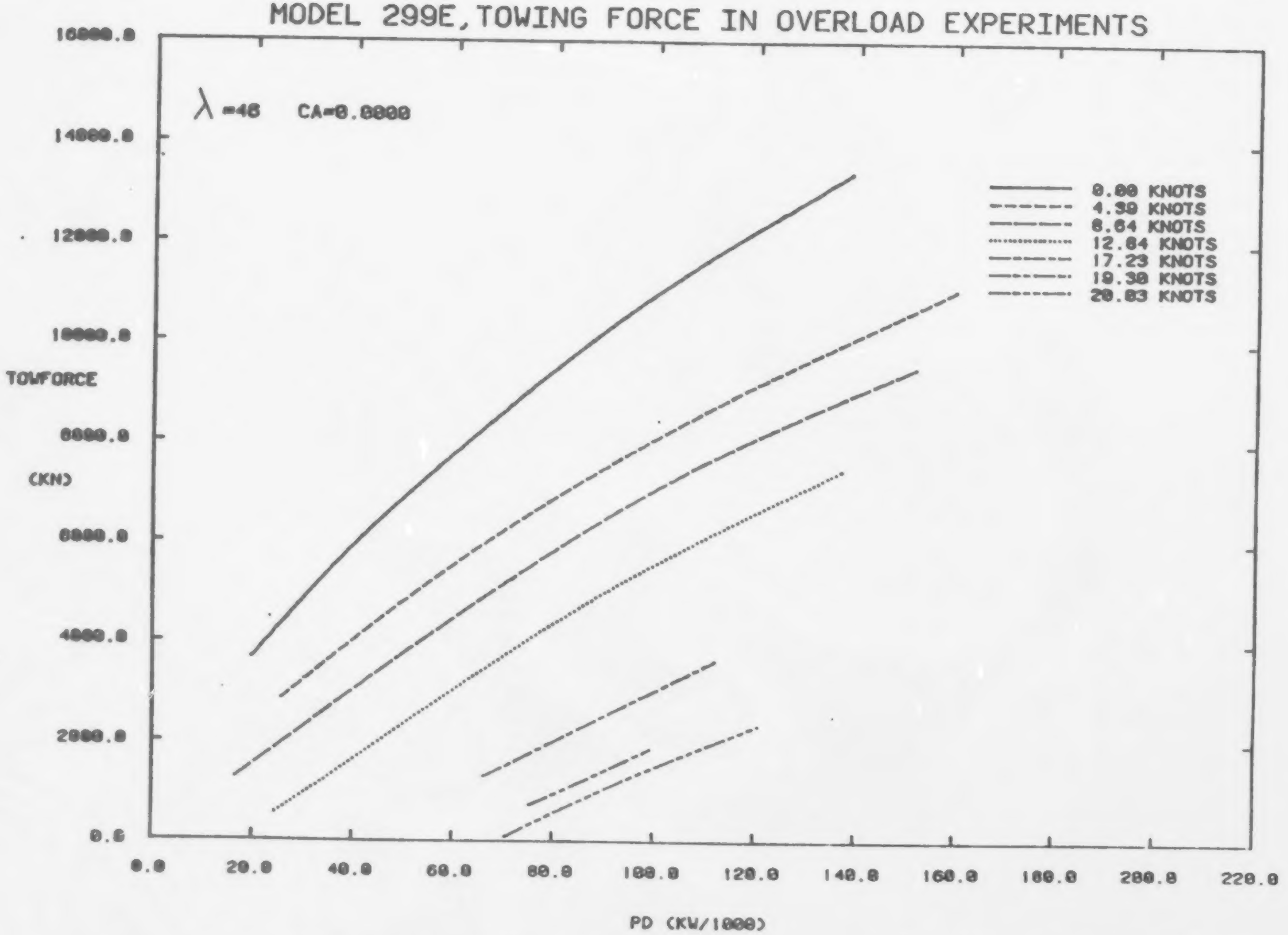

FIGURE 7.9 MODEL 299E TOWING FORCE IN OVERLOAD EXPERIMENTS

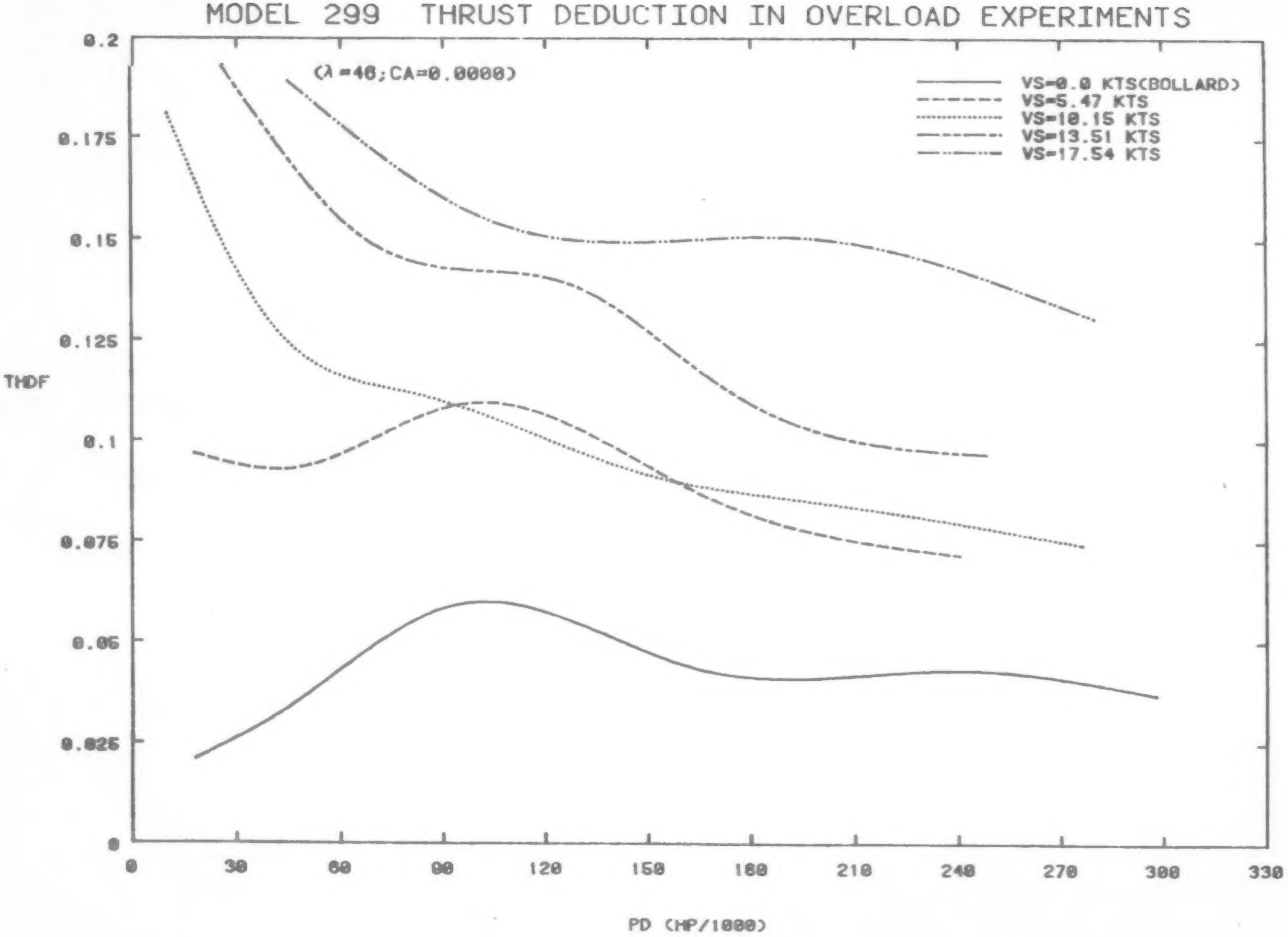

FIGURE 7.10 MODEL 299 THRUST DEDUCTION IN OVERLOAD EXPERIMENTS

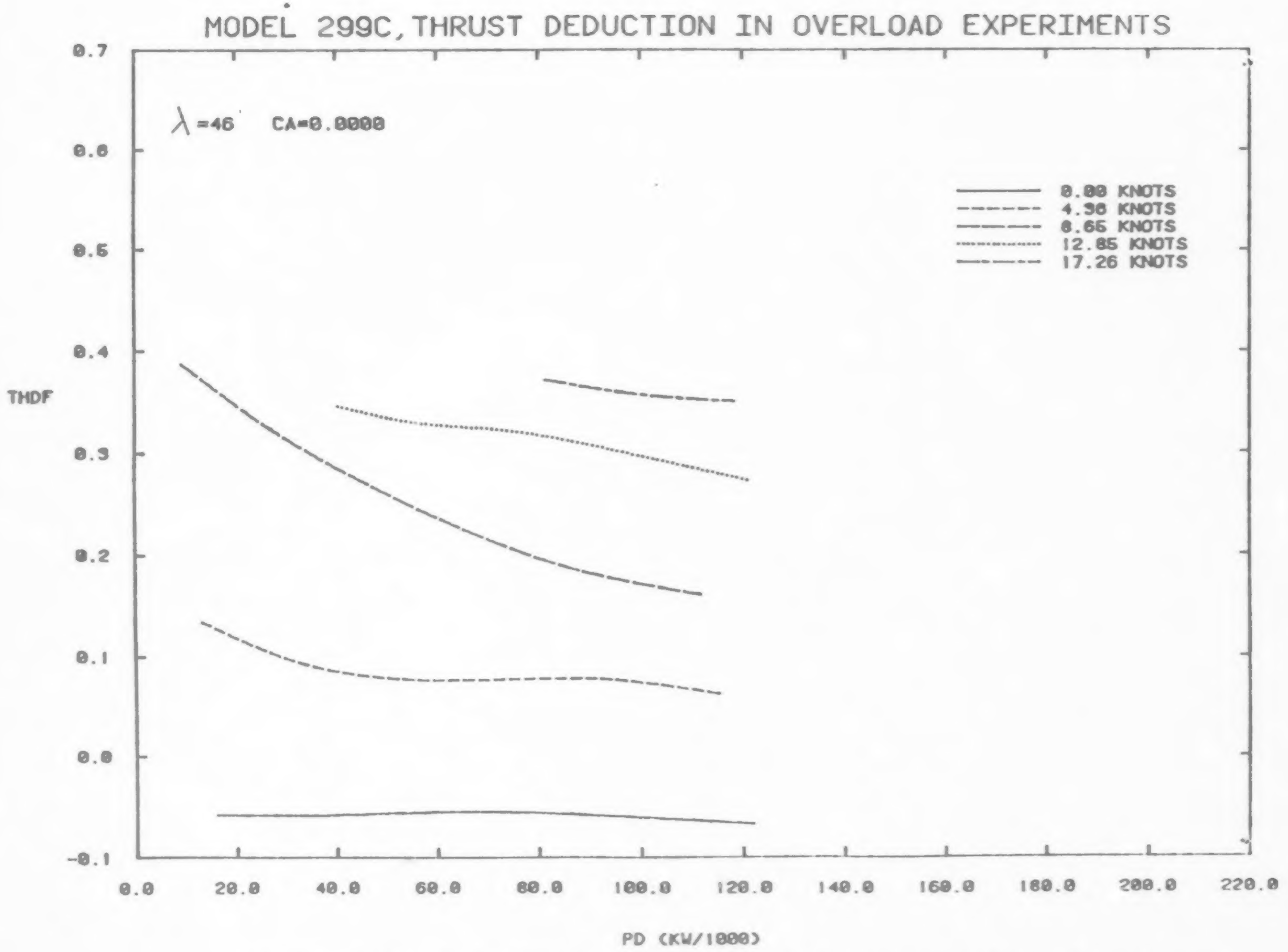

FIGURE 7.11 MODEL 299C, THRUST DEDUCTION IN OVERLOAD EXPERIMENTS

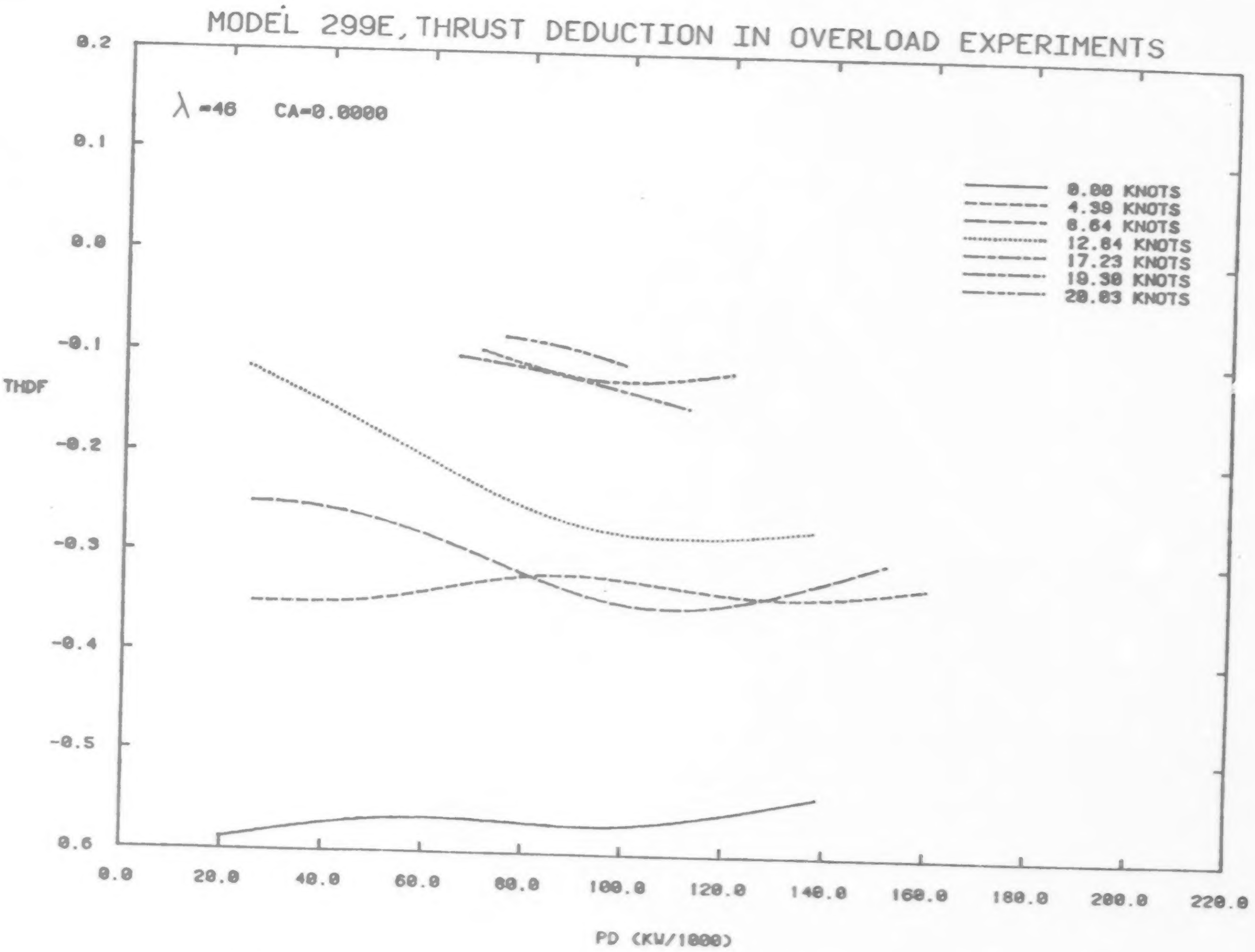

FIGURE 7.12 MODEL 299E THRUST DEDUCTION IN OVERLOAD EXPERIMENTS

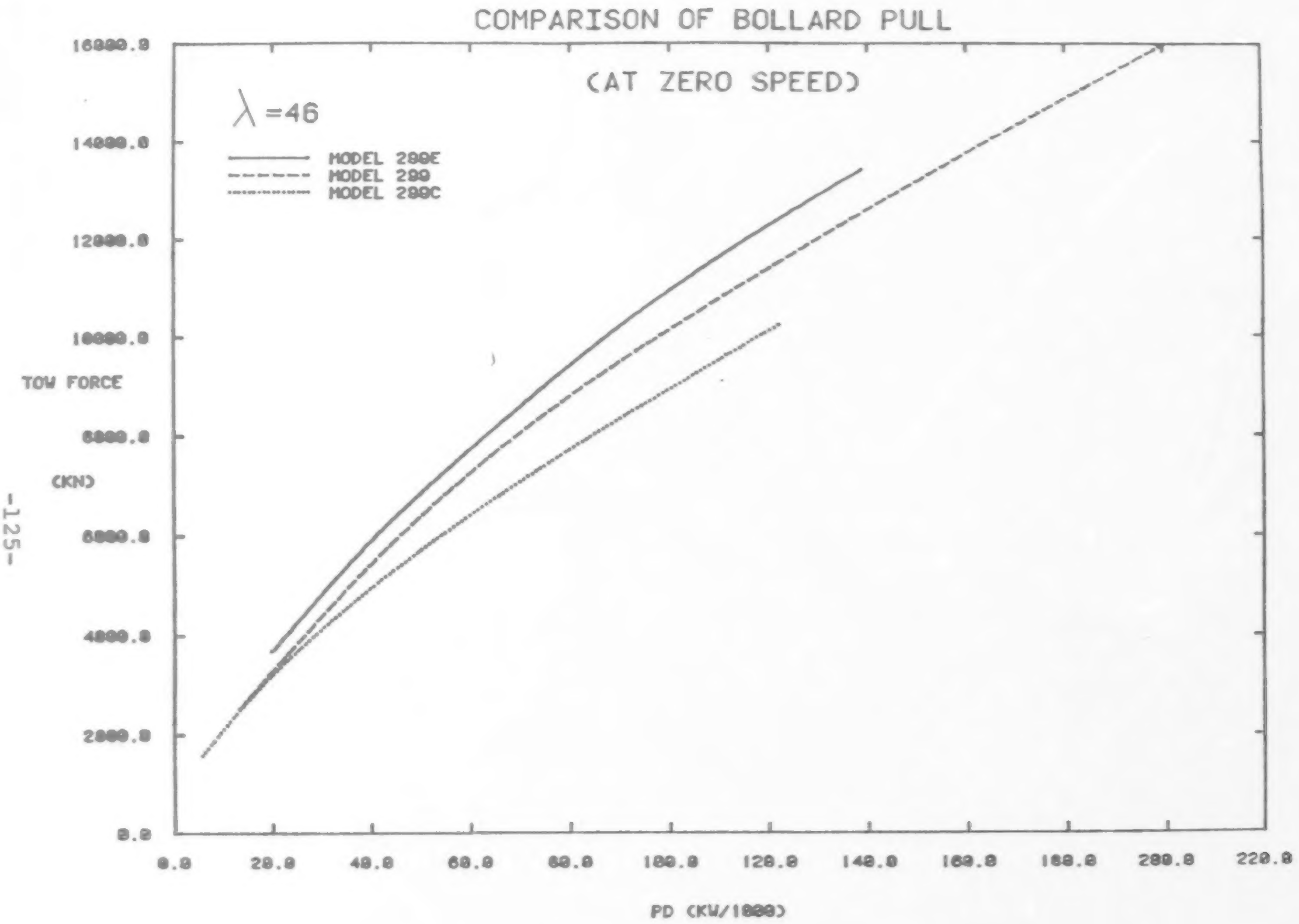

FIGURE 7.13 COMPARISON OF BOLLARD PULL

8.0 FLOW TESTS ON MODEL 299E

To determine the flow around the stern of Model 299E, paint was applied to the inside and outside of the tunnel and around the propeller duct.

The model was ballasted to the displacement given in Table 2.1 and towed at a speed corresponding to 16 knots for the full scale ship. No propellers were fitted during the test. The resulting flow pattern is shown in Figures 8.1 to 8.4.

Figure 8.1 shows the flow pattern on the outside of the skegs. This shows strong flow in an even pattern.

Figure 8.2 shows the flow on the inside of the skegs. This indicates that there was a strong downward flow out of the tunnel. This is confirmed in Figure 8.3, by the fact that the paint has not streaked on the tunnel roof, which indicates a separated flow just above the bossings.

There was also a strong flow into the duct as indicated in Figures 8.2 and 8.3.

The flow indicated is a nominal flow without the propellers operating. It is likely that the weak flow in the region of the tunnel roof may be improved with the propeller rotating. On the other hand, with flow separation taking place inside the tunnels, the pressure drag increases sharply and the flow into the propeller disk becomes highly turbulent. The net result is an increase in resistance and a lower propulsive efficiency for the ship.

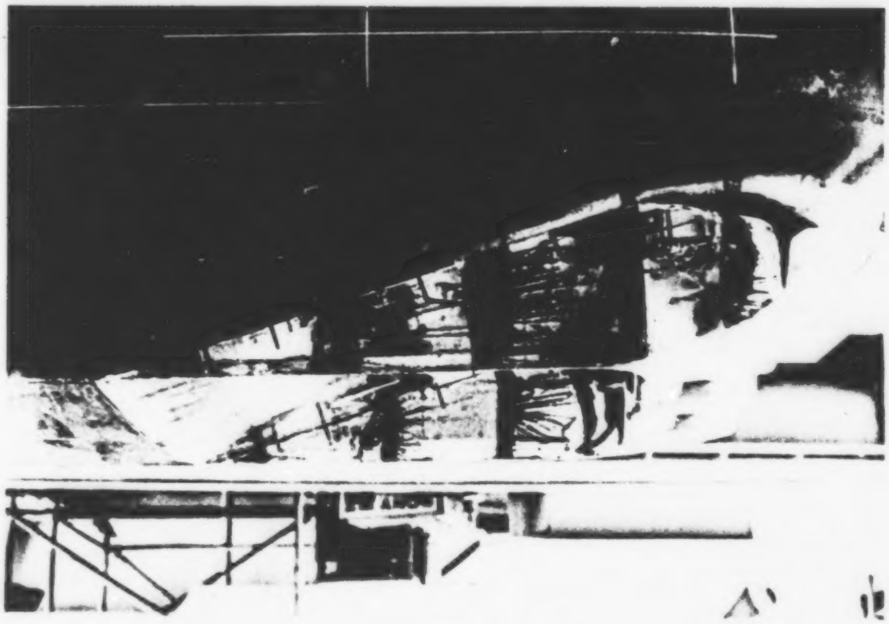

FIGURE 8.1 MODEL 299E, STREAMFLOWS ON OUTSIDE OF SKEGS

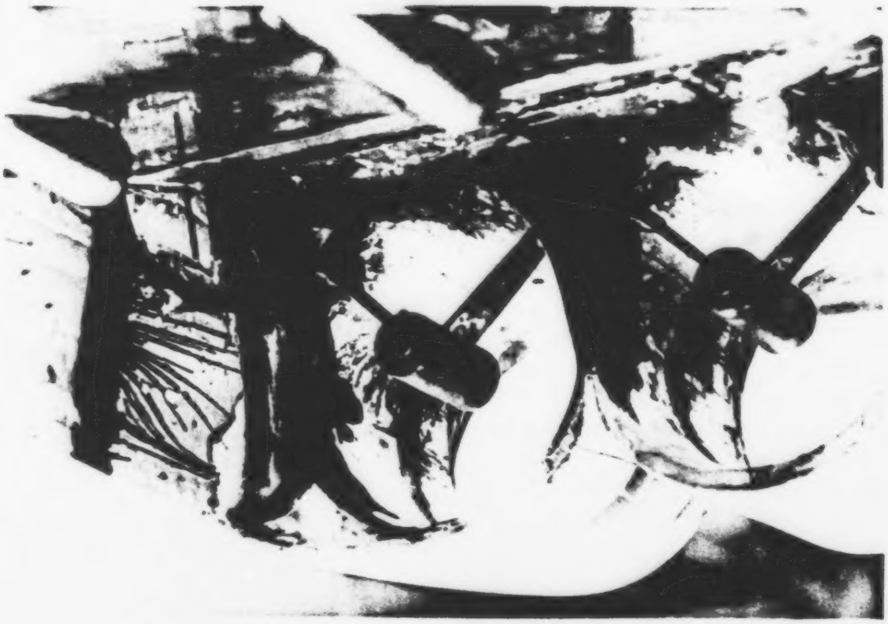

FIGURE 8.2 MODEL 299E, STREAMFLOWS ON INSIDE OF SKEGS AND NOZZLES

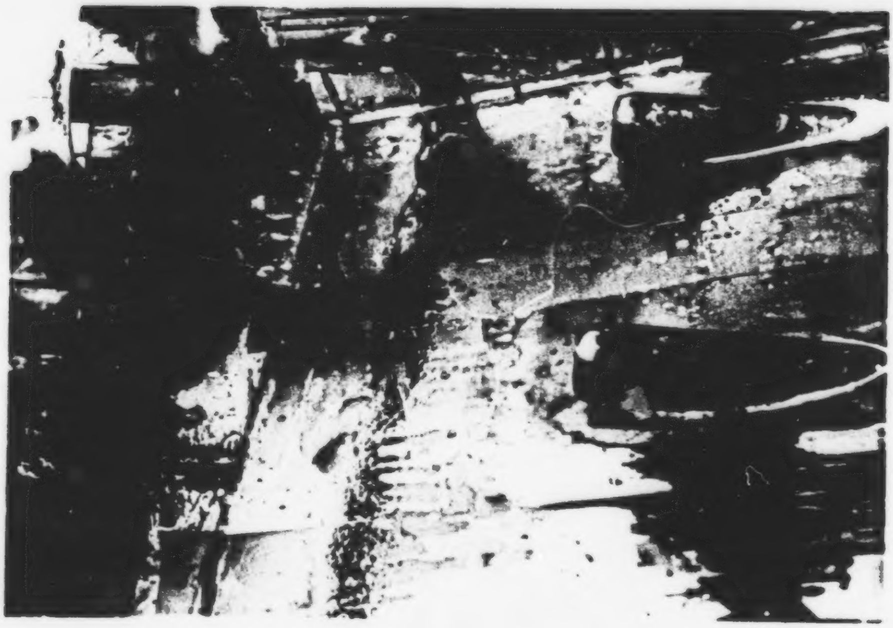

FIGURE 8.3 MODEL 299E,
STREAMFLOWS ON
TUNNEL ROOF AND
TOP NOZZLES

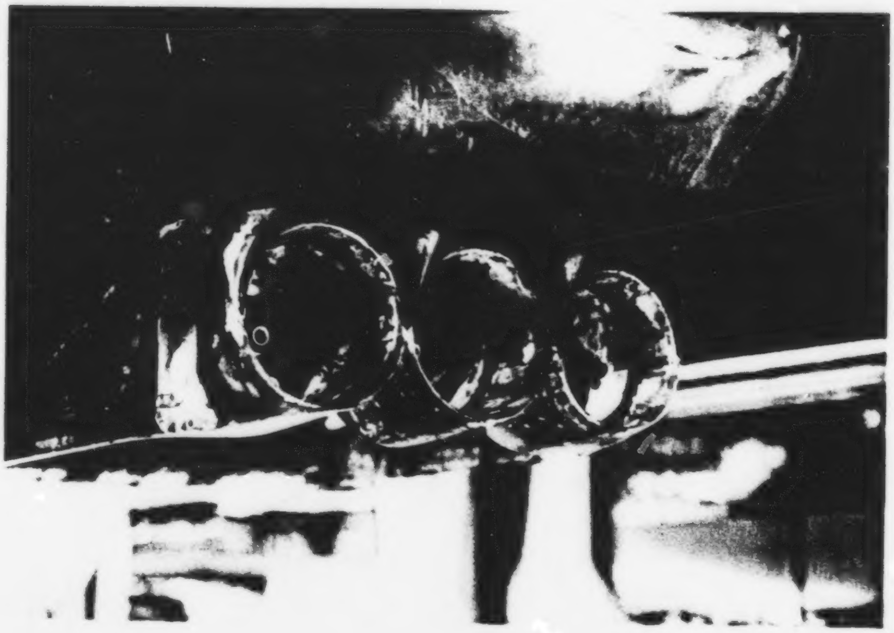

FIGURE 8.4 MODEL 299E,
STREAMFLOWS ON
THE AFT BODY

9.0 CONCLUSIONS

The intention of the tests carried out was to determine the effect on performance of fitting complete propeller protection on a ship developed from the lines of the POLAR 7 Class icebreaker.

The effective power and delivered power for Model 299C were both higher than Model 299, the unmodified form. The result was such that there was a speed loss of about 7.0 knots at the design power of 150,000 HP (110,325 kW) for Model 299C compared with Model 299. The bollard pull for Model 299C was also lower than Model 299 for a given power. This would affect its ability to operate in ice.

In an attempt to improve the performance, Model 299C was modified to Model 299E by removing the tunnel separating walls, removing the grills, and fairing the ducts. This reduced the speed loss to about 3.4 knots when compared with Model 299. The bollard pull for Model 299E was better than Model 299 for a given power. From a hydrodynamic viewpoint, Model 299E represents a considerable improvement over Model 299C.

In light of this improvement, it was decided to conduct a further model test with the separating walls refitted to Model 299E. This decision was made for three basic reasons. First, to assess the affect of the separating walls on the performance. Second, to achieve higher propeller open water efficiency and higher relative rotative efficiency (see Table 7.35). Third, to provide the means for supporting the bottom grills to fully protect the propeller from ice and grounding.

The modified model was designated as Model 299F. Figure 9.1 shows the comparison between the measured total resistance of Models 299E and 299F. One can see from the figure that the results are almost identical for the two models. This indicates that removing the separating walls had not contributed to the better performance obtained with Model 299E. The self-propulsion tests were not completed at the time of writing this report. It is anticipated, however, that the quasi-propulsive coefficient, ETAD, for Model 299F will be comparable to, if not higher than, that of Model 299. Test results, analysis, and discussion on Model 299F are presented in Appendix C.

As a summary the conclusions drawn so far suggest the following modifications for further improvement in the performance of the proposed design with the full protection device in place.

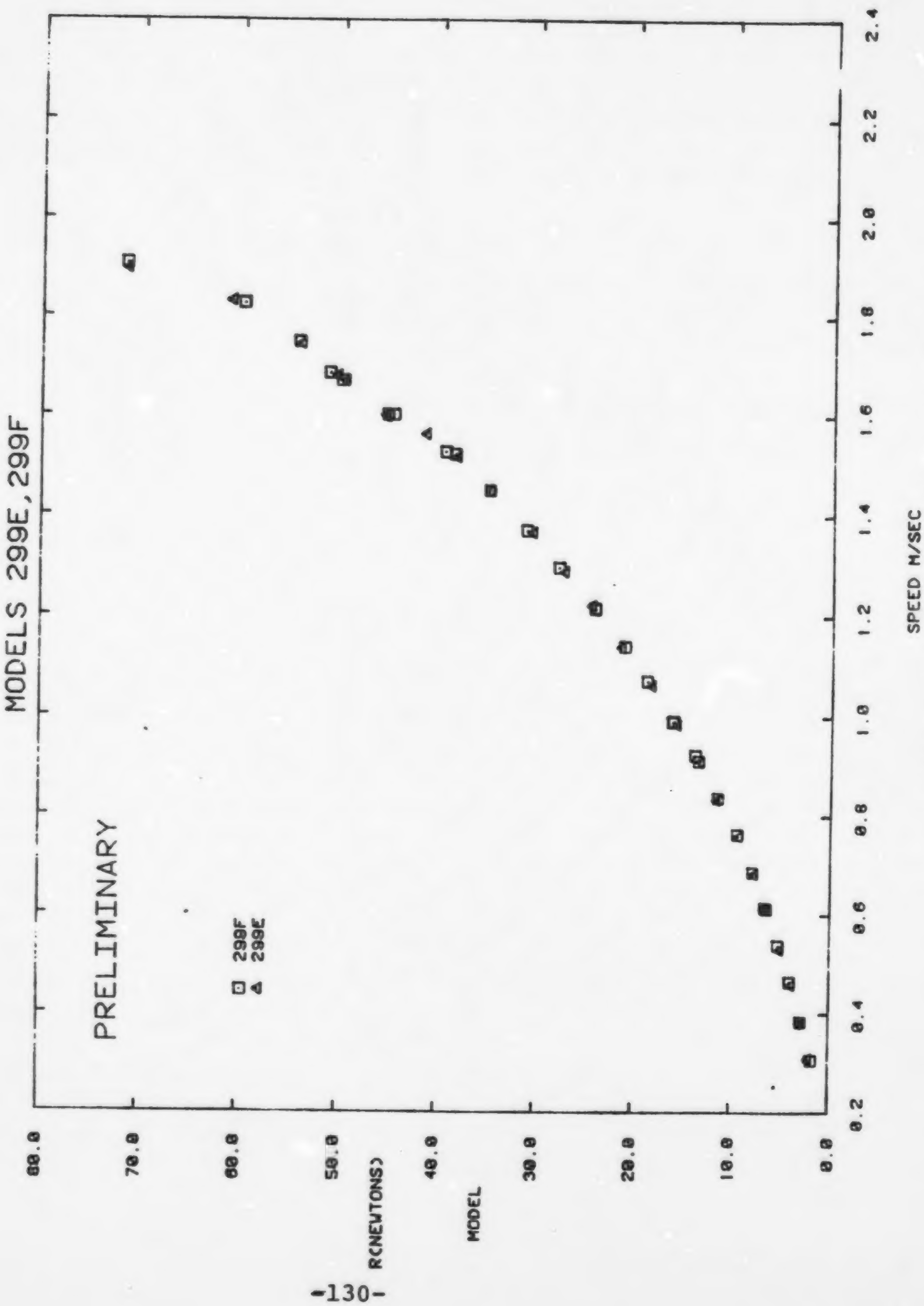

FIGURE 9.1 MODELS 299E, 299F

1. Action: eliminate flow separation within the tunnels by redesigning both the tunnel roof and the tunnel entrance.

   Predictions: lower effective power, lower thrust deduction factor, higher ETAD.

2. Action: fair the entrance and exit to each duct.

   Predictions: lower thrust deduction factor (negative), higher ETAD, higher developed thrust at near-bollard pull condition (icebreaking).

3. Action: use concept of three separate tunnels.

   Predictions: higher relative rotative efficiency, three identical propellers, strong rigid structure against grounding.

4. Action: redesign propellers to suit the wake field.

   Predictions: better propeller open water performance.

5. Action: redesign bottom guards with increased flow inlet areas; redesign retractable stern guards

   Predictions: lower effective power in clear water.

It seems appropriate to conclude this report with a positive observation. In comparing the effective powers for Models 299C (with full protection device in place) and 299 (parent model), it was found that the ratio is about 3.9 at 16 knots (Table 5.9). From Table 2.1, Model 299C has about 44% larger wetted surface area and 31% larger displacment compared with the parent model (299, $\lambda = 46$). If one assumes a hypothetical situation where the protection device can be implemented in a ship with the same principal dimensions, same displacement, (different prismatic coefficient), and same wetted surface area as 299, then the ratio of the effective power would be:

$$3.9 \times \frac{1}{1.44} \times 0.8 = 2.17$$

Now, with proper scaling laws of the grills, the estimated reduction in PE for Model 299C at 16 knots is about 16%. Thus, the hypothetical ratio of the effective power at 16 knots is:

$$2.17 \times 0.84 = 1.82$$

That is to say, at 16 knots in clear water, the resistance of POLAR 7A is only 82% higher than the parent POLAR 7 providing that the two ships have the same displacement and same wetted surface area. With the elimination of flow separation and redesigning wake adapted propellers, one can expect a further reduction in the effective power and a higher propulsive efficiency.

REFERENCES

1. Resistance and Propulsion Experiments with Model 299 and Propellers 56 L, R, C
   Resistance Test with Models 299 B, C, and D
   NRC, LTR-SH-313, October 1981.

2. Resistance and Propulsion Experiments with Models 299C and 299E, and Propellers 74 L, R, C
   NRC, LTR-SH-329, May 1982.

3. "Protection of Propellers in Ice" - Volume I - "Assessment of Protection Schemes"
   Report TP 2704 by Davis Engineering Limited, Ottawa
   August 1980.

4. "Protection of Propellers in Ice" - Volume II - "Detail Design of Protection Schemes"
   by Davis Engineering Limited (under review by TDC)
   June 1981

5. "Resistance, Self-Propulsion and Wake Survey Experiments with a Model of a Triple-Screw Arctic Class '7' Icebreaker - Model 299"
   NRC, LTR-SH-196, September 1976.

6. Hydrodynamics in Ship Design - Volume I,
   H. E. Saunders, 1957.

7. Brief Discussion on the Resistance Tests of Model 299B,
   Interim Report I, Davis Engineering Limited, Ottawa
   August 1981.

APPENDIX A

Harmonic Analysis of the Wake Components

APPENDIX A

Harmonic Analysis of the Wake Components

$$\frac{V(\theta)}{V} = C_o + \sum_{k=1}^{N} C_k \operatorname{Sin}(k\theta + \phi_k)$$

HARMONIC ANALYSIS OF THE WAKE COMPONENTS

M-299B

Centre Propeller

R/R_{max} = 0.311

K	Axial Component: V_x/V		Tangential Component: V_T/V		Radial Component: V_R/V	
	$C(K)_x$	$\phi(K)_x$(deg)	$C(K)_T$	$\phi(K)_T$(deg)	$C(K)_R$	$\phi(K)_R$(deg)
0	1.01023		0.00000		0.07716	
1	-0.09325	90.00	0.16382	0.00	-0.02397	90.00
2	0.01515	90.00	-0.03344	0.00	0.04265	90.00
3	-0.01408	90.00	-0.01738	0.00	0.03655	90.00
4	0.01945	90.00	0.00096	0.00	0.00821	90.00
5	0.02088	90.00	-0.00308	0.00	0.01493	90.00
6	0.01916	90.00	0.00202	0.00	-0.00212	90.00
7	0.00959	90.00	0.00080	0.00	0.00379	90.00
8	-0.00506	90.00	-0.00040	0.00	-0.00074	90.00
9	-0.01374	90.00	0.00037	0.00	0.00055	90.00
10	-0.01752	90.00	-0.00028	0.00	-0.00020	90.00
11	-0.01294	90.00	-0.00004	0.00	0.00004	90.00
12	-0.00510	90.00	0.00006	0.00	-0.00031	90.00
13	0.00266	90.00	-0.00008	0.00	0.00021	90.00
14	0.00666	90.00	0.00004	0.00	-0.00007	90.00
15	0.00635	90.00	-0.00002	0.00	0.00024	90.00
16	0.00294	90.00	0.00001	0.00	-0.00005	90.00
17	-0.00092	90.00	0.00003	0.00	0.00011	90.00
18	-0.00336	90.00	0.00000	0.00	-0.00002	90.00
19	-0.00353	90.00	0.00000	0.00	0.00000	90.00
20	-0.00203	90.00	-0.00001	0.00	0.00002	90.00

TABLE A.1 HARMONIC ANALYSIS OF THE WAKE COMPONENTS

Centre Propeller

HARMONIC ANALYSIS OF THE WAKE COMPONENTS

M-299B Centre Propeller R/R_{max} = 0.492

	Axial Component: V_x/V		Tangential Component: V_T/V		Radial Component: V_R/V	
K	$C(K)_x$	$\phi(K)_x$(deg)	$C(K)_T$	$\phi(K)_T$(deg)	$C(K)_R$	$\phi(K)_R$(deg)
0	1.06368		0.00000		0.09794	
1	-0.10494	90.00	0.14442	0.00	-0.06746	90.00
2	0.02557	90.00	-0.04177	0.00	0.06643	90.00
3	-0.00627	90.00	-0.03488	0.00	0.05338	90.00
4	0.00872	90.00	-0.00235	0.00	0.01764	90.00
5	0.01225	90.00	-0.01287	0.00	0.01528	90.00
6	-0.00252	90.00	-0.00362	0.00	0.00006	90.00
7	-0.00867	90.00	-0.00154	0.00	0.00550	90.00
8	-0.01531	90.00	-0.00179	0.00	-0.00115	90.00
9	-0.01175	90.00	0.00034	0.00	0.00436	90.00
10	-0.00506	90.00	-0.00028	0.00	-0.00162	90.00
11	0.00312	90.00	0.00004	0.00	0.00060	90.00
12	0.00862	90.00	0.00020	0.00	-0.00222	90.00
13	0.00871	90.00	-0.00007	0.00	-0.00090	90.00
14	0.00525	90.00	0.00007	0.00	-0.00157	90.00
15	0.00020	90.00	0.00002	0.00	-0.00080	90.00
16	-0.00341	90.00	0.00003	0.00	-0.00076	90.00
17	-0.00401	90.00	0.00006	0.00	-0.00050	90.00
18	-0.00236	90.00	0.00005	0.00	-0.00025	90.00
19	0.00027	90.00	0.00004	0.00	-0.00016	90.00
20	0.00187	90.00	0.00002	0.00	-0.00002	90.00

TABLE A.2 HARMONIC ANALYSIS OF THE WAKE COMPONENTS

Centre Propeller

HARMONIC ANALYSIS OF THE WAKE COMPONENTS

M-299B Centre Propeller $R/R_{max} = 0.674$

	Axial Component: V_x/V		Tangential Component: V_T/V		Radial Component: V_R/V	
K	$C(K)_x$	$\phi(K)_x$(deg)	$C(K)_T$	$\phi(K)_T$(deg)	$C(K)_R$	$\phi(K)_R$(deg)
0	1.02082		0.00000		-0.01604	
1	-0.09340	90.00	0.08523	0.00	-0.07181	90.00
2	0.01768	90.00	-0.00910	0.00	0.05935	90.00
3	-0.06016	90.00	-0.00315	0.00	0.05441	90.00
4	-0.02777	90.00	-0.00104	0.00	0.01039	90.00
5	0.02277	90.00	-0.00020	0.00	0.01052	90.00
6	-0.00081	90.00	0.00014	0.00	-0.00913	90.00
7	0.01061	90.00	0.00006	0.00	0.00812	90.00
8	0.00097	90.00	0.00000	0.00	0.00082	90.00
9	0.00986	90.00	0.00002	0.00	0.01020	90.00
10	-0.00196	90.00	0.00002	0.00	0.00449	90.00
11	0.00343	90.00	0.00001	0.00	0.00493	90.00
12	-0.00042	90.00	0.00000	0.00	-0.00188	90.00
13	0.00185	90.00	-0.00001	0.00	-0.00225	90.00
14	0.00003	90.00	-0.00001	0.00	-0.00470	90.00
15	0.00092	90.00	0.00000	0.00	-0.00246	90.00
16	-0.00004	90.00	0.00000	0.00	-0.00134	90.00
17	0.00027	90.00	0.00000	0.00	0.00067	90.00
18	-0.00002	90.00	0.00000	0.00	0.00116	90.00
19	0.00018	90.00	0.00000	0.00	0.00094	90.00
20	0.00003	90.00	0.00000	0.00	0.00026	90.00

TABLE A.3 HARMONIC ANALYSIS OF THE WAKE COMPONENTS

Centre Propeller

HARMONIC ANALYSIS OF THE WAKE COMPONENTS

M-299B   Centre Propeller $R/R_{max} = 0.855$

	Axial Component: V_x/V		Tangential Component: V_T/V		Radial Component: V_R/V	
K	$C(K)_x$	$\phi(K)_x$(deg)	$C(K)_T$	$\phi(K)_T$(deg)	$C(K)_R$	$\phi(K)_R$(deg)
0	0.97578		0.00000		0.01808	
1	-0.13366	90.00	-0.01031	0.00	-0.06217	90.00
2	0.07931	90.00	0.02847	0.00	0.03506	90.00
3	-0.06568	90.00	0.05104	0.00	0.04795	90.00
4	-0.00053	90.00	-0.01315	0.00	-0.00344	90.00
5	0.00630	90.00	0.01281	0.00	0.00339	90.00
6	0.00687	90.00	-0.00252	0.00	-0.01435	90.00
7	0.02552	90.00	0.00116	0.00	0.00441	90.00
8	-0.00643	90.00	-0.00200	0.00	0.00240	90.00
9	0.00201	90.00	0.00025	0.00	0.01420	90.00
10	-0.01609	90.00	-0.00041	0.00	0.00713	90.00
11	-0.00499	90.00	0.00005	0.00	0.00598	90.00
12	-0.00761	90.00	0.00022	0.00	-0.00304	90.00
13	0.00305	90.00	-0.00016	0.00	-0.00427	90.00
14	0.00293	90.00	0.00011	0.00	-0.00531	90.00
15	0.00512	90.00	-0.00004	0.00	-0.00130	90.00
16	0.00211	90.00	0.00009	0.00	0.00156	90.00
17	0.00053	90.00	-0.00004	0.00	0.00359	90.00
18	-0.00161	90.00	0.00005	0.00	0.00283	90.00
19	-0.00207	90.00	-0.00002	0.00	0.00073	90.00
20	-0.00194	90.00	0.00000	0.00	-0.00139	90.00

TABLE A.4 HARMONIC ANALYSIS OF THE WAKE COMPONENTS

Centre Propeller

HARMONIC ANALYSIS OF THE WAKE COMPONENTS

M-299B

Wing Propeller

$R/R_{max} = 0.311$

	Axial Component: V_x/V		Tangential Component: V_T/V		Radial Component: V_R/V	
K	$C(K)_x$	$\phi(K)_x$(deg)	$C(K)_T$	$\phi(K)_T$(deg)	$C(K)_R$	$\phi(K)_R$(deg)
0	1.04745		0.06607		0.05784	
1	0.09819	-87.02	0.16706	-1.12	0.02678	-135.27
2	0.03957	96.50	0.04133	-172.84	0.05772	98.67
3	0.01707	-119.88	0.02630	136.13	0.04037	57.72
4	0.03136	113.44	0.01457	171.88	0.02130	110.94
5	0.01451	76.28	0.01204	161.66	0.00621	64.47
6	0.01260	-132.38	0.00387	128.97	0.00287	112.31
7	0.02001	-12.38	0.00272	79.38	0.00545	-117.38
8	0.02287	-69.52	0.00303	36.35	0.00166	-46.20
9	0.01732	-27.16	0.00266	42.80	0.00213	-122.86
10	0.00602	-32.77	0.00235	39.90	0.00019	148.16
11	0.00991	152.39	0.00135	52.88	0.00009	-32.97
12	0.01001	145.74	0.00083	69.19	0.00027	95.82
13	0.01416	161.33	0.00030	80.42	0.00015	-77.02
14	0.00441	172.59	0.00024	55.72	0.00038	-61.37
15	0.00321	-74.62	0.00044	3.29	0.00022	-107.34
16	0.00724	-23.97	0.00051	-4.78	0.00021	-47.27
17	0.00858	-20.96	0.00054	-5.88	0.00009	106.19
18	0.00483	6.07	0.00048	-17.02	0.00006	83.00
19	0.00179	65.80	0.00035	-36.50	0.00006	31.60
20	0.00493	149.87	0.00027	-59.25	0.00003	-92.05

TABLE A.5 HARMONIC ANALYSIS OF THE WAKE COMPONENTS
Wing Propeller

HARMONIC ANALYSIS OF THE WAKE COMPONENTS

M-299B Wing Propeller $R/R_{max} = 0.492$

	Axial Component: V_x/V		Tangential Component: V_T/V		Radial Component: V_R/V	
K	$C(K)_x$	$\phi(K)_x$(deg)	$C(K)_T$	$\phi(K)_T$(deg)	$C(K)_R$	$\phi(K)_R$(deg)
0	1.05379		−0.03274		0.08890	
1	0.11055	-92.27	0.13991	-8.70	0.06447	-96.27
2	0.00958	-5.14	0.05145	-162.46	0.07361	93.70
3	0.03744	-70.29	0.01084	117.90	0.05680	61.81
4	0.01816	151.64	0.00459	-112.37	0.00594	102.89
5	0.02908	107.04	0.00762	148.72	0.00891	55.14
6	0.01858	93.79	0.00671	29.49	0.01567	-115.20
7	0.01784	106.23	0.00637	-10.63	0.00474	-72.85
8	0.00896	118.15	0.00423	-27.18	0.00700	-165.13
9	0.00709	173.67	0.00263	-32.34	0.00097	140.37
10	0.00747	-159.50	0.00091	-19.83	0.00437	153.63
11	0.00813	-141.23	0.00030	80.95	0.00153	8.19
12	0.00742	-137.58	0.00058	90.31	0.00051	76.98
13	0.00520	-132.07	0.00058	100.54	0.00140	-12.48
14	0.00316	-117.80	0.00045	86.74	0.00077	-69.33
15	0.00174	-77.34	0.00013	65.32	0.00061	-99.17
16	0.00208	-33.35	0.00016	-176.67	0.00062	-103.27
17	0.00256	-23.76	0.00020	176.85	0.00048	178.42
18	0.00262	-20.95	0.00022	169.82	0.00006	74.70
19	0.00233	-21.22	0.00018	155.78	0.00024	111.28
20	0.00182	-16.84	0.00009	161.15	0.00031	8.55

TABLE A.6 HARMONIC ANALYSIS OF THE WAKE COMPONENTS
Wing Propeller

HARMONIC ANALYSIS OF THE WAKE COMPONENTS

M-299B

Wing Propeller

R/R_{max} = 0.674

	Axial Component: V_x/V		Tangential Component: V_T/V		Radial Component: V_R/V	
K	$C(K)_x$	$\phi(K)_x$(deg)	$C(K)_T$	$\phi(K)_T$(deg)	$C(K)_R$	$\phi(K)_R$(deg)
0	0.99333		−0.00444		−0.00462	
1	0.11568	-113.37	0.08645	-4.51	0.06693	-105.45
2	0.04431	-15.38	0.01534	-113.17	0.06934	96.32
3	0.08200	-125.56	0.01367	-119.88	0.04782	56.96
4	0.01786	145.63	0.01170	-135.80	0.01626	101.31
5	0.01035	-94.45	0.00646	-151.15	0.01775	65.91
6	0.01755	145.56	0.00446	-168.37	0.01041	-72.84
7	0.00709	40.42	0.00291	174.18	0.00725	-172.12
8	0.00507	-174.93	0.00182	149.96	0.00273	-52.89
9	0.00441	34.81	0.00124	137.02	0.00695	-152.77
10	0.00434	-103.80	0.00090	116.05	0.00328	107.79
11	0.00269	122.98	0.00065	95.63	0.00156	-82.81
12	0.00088	-57.94	0.00046	80.09	0.00129	136.87
13	0.00215	135.35	0.00037	65.58	0.00179	-7.19
14	0.00176	31.44	0.00025	47.86	0.00105	-104.77
15	0.00021	-74.59	0.00017	36.28	0.00029	54.23
16	0.00092	19.25	0.00013	26.09	0.00059	-68.72
17	0.00100	-76.00	0.00008	13.29	0.00044	178.58
18	0.00035	-154.33	0.00004	14.00	0.00030	49.51
19	0.00037	-109.39	0.00002	31.85	0.00021	-84.44
20	0.00055	166.25	0.00001	100.46	0.00017	140.14

TABLE A.7 HARMONIC ANALYSIS OF THE WAKE COMPONENTS

Wing Propeller

HARMONIC ANALYSIS OF THE WAKE COMPONENTS

M-299B Wing Propeller R/R_{max} = 0.855

	Axial Component: V_x/V		Tangential Component: V_T/V		Radial Component: V_R/V	
K	$C(K)_x$	$\phi(K)_x$(deg)	$C(K)_T$	$\phi(K)_T$(deg)	$C(K)_R$	$\phi(K)_R$(deg)
0	0.96474		-0.09707		0.02342	
1	0.17303	-108.46	0.04360	70.97	0.05544	-101.03
2	0.06736	-3.34	0.06690	14.20	0.05766	89.13
3	0.05358	-111.66	0.04071	-75.02	0.04743	59.38
4	0.01398	51.95	0.00675	68.57	0.01359	80.90
5	0.03617	-112.88	0.02051	-49.28	0.01473	72.24
6	0.03029	153.77	0.00797	-117.80	0.00711	-131.31
7	0.00717	-37.85	0.00523	-56.84	0.00634	145.77
8	0.01366	-123.82	0.00584	-94.19	0.00247	-77.45
9	0.01178	-50.50	0.00428	-101.28	0.00310	-158.87
10	0.00933	-74.25	0.00376	-130.64	0.00126	52.39
11	0.00935	23.94	0.00160	-108.79	0.00129	-96.93
12	0.00559	0.08	0.00326	-123.78	0.00110	140.40
13	0.00547	105.17	0.00199	-172.33	0.00055	-33.76
14	0.00196	68.82	0.00097	-117.94	0.00098	-155.53
15	0.00290	-148.47	0.00194	-149.50	0.00044	43.11
16	0.00079	-44.14	0.00109	164.50	0.00068	-82.95
17	0.00265	-50.21	0.00069	-138.74	0.00035	115.13
18	0.00193	32.17	0.00117	-175.16	0.00046	-10.07
19	0.00284	23.44	0.00061	150.06	0.00031	-173.03
20	0.00161	86.13	0.00052	-175.32	0.00028	69.06

TABLE A.8 HARMONIC ANALYSIS OF THE WAKE COMPONENTS

Wing Propeller

APPENDIX B

Thoughts on Resistance Prediction of Full-Scale Grills

APPENDIX B

Thoughts on Resistance Prediction of Full-Scale Grills

The grill has its own typical characteristic length, and is running at its own Reynolds' number. Therefore, it has a resistance which would scale differently to full size if run at model size, although obeying the same scaling laws.

To include an appendage such as the grills in a normal resistance model would therefore upset the scaling of the hull resistance which would be overestimated for the full-scale.

It is for this reason that it is preferable to run the model without grills and then modify the resulting total ship resistance by adding in an estimate of the resistance due to the full-scale grill.

Generally, the resistance of the appendages may be estimated from one of the following approaches:

(a) use of formulae based on previous experience; or,

(b) running model both with and without appendages and scaling the difference to full-scale using different laws from those used for the hull proper.

Usually, resistances due to appendages such as rudders, shaft brackets or bossings, stabilizers and bilge keels are small (of the order of 10% of that of the hull) so that errors in their assessment are not likely to be critical.

With an appendage such as the grills, approach (a) mentioned above is not applicable since no previous experience exists with such an arrangement. Approach (b), therefore, is the only alternative to estimate the resistance of the grills.

The problem here is how to break the total resistance of the model with the grills to its basic components including that due to the grills, and then scale each component properly to predict the full-scale total resistance.

This can be carried out as follows:

- run model tests both with and without the grills;
- estimate the frictional drag of the model using the ITTC standard formula F_{FM};

- assuming no effect of the grills on the residuary resistance of the hull, then plot the friction line, the model total resistance line (with the grills), and the difference between the total model resistance both with and without the grills on the top of the friction line R_{gM};
- subtract the model total friction resistance from the model total resistance to obtain the model residuary resistance; R_w
- calculate the ship friction resistance at the corresponding speed (ITTC standard formula) R_{FS};
- estimate the resistance of the full-size grills (R_{gS}) at the corresponding Reynolds' number R_{gS} would be much lower than R_{gM}; and,
- add R_w to estimate the total resistance of the ship.

This proposed procedure is shown schematically in Figure B.1 where:

$R_{total} = R_w + R_{FM} + R_{gM}$ ......Model

and

$R_{total} = R_w + R_{FS} + R_{gS}$ ......Ship

As already indicated in the text, the creation of a separation zone just behind the squared-off transom may largely be responsible for the sharp increase in the total resistance.

However, the resistance data of Model 299B are used herein to give some idea about the suggested procedure.

The dependence of the grills' resistance on the Reynolds' number is very noticeable as shown in Figure B.2. With the Reynolds' number for the full scale in the order of 10^9, one would expect according to Figure B.2 that the contribution of the grill resistance to the total hull resistance of the ship would be minimal.

To be on the conservative side, if C_{RgS} at 16 knots is 10% of C_{RgM} at the corresponding speed, the hull resistance (and effective power) of POLAR 7A (based on Model 299B) would be in fact 16% lower than that predicted from model/ship direct scaling given in Table 5.2 or shown in Figure 5.1. The corrected values are marked by an asterisk (*) in Figure 5.8. A more accurate model/full scale grill correlation may be obtained by carrying out proper wind tunnel tests.

G GRAPHIC CONTROLS CANADA LTD.
MADE IN CANADA

SQUARE 10 X 10 TO 1/2 CM
SPECIFY TRACING OR DRAWING PAPER

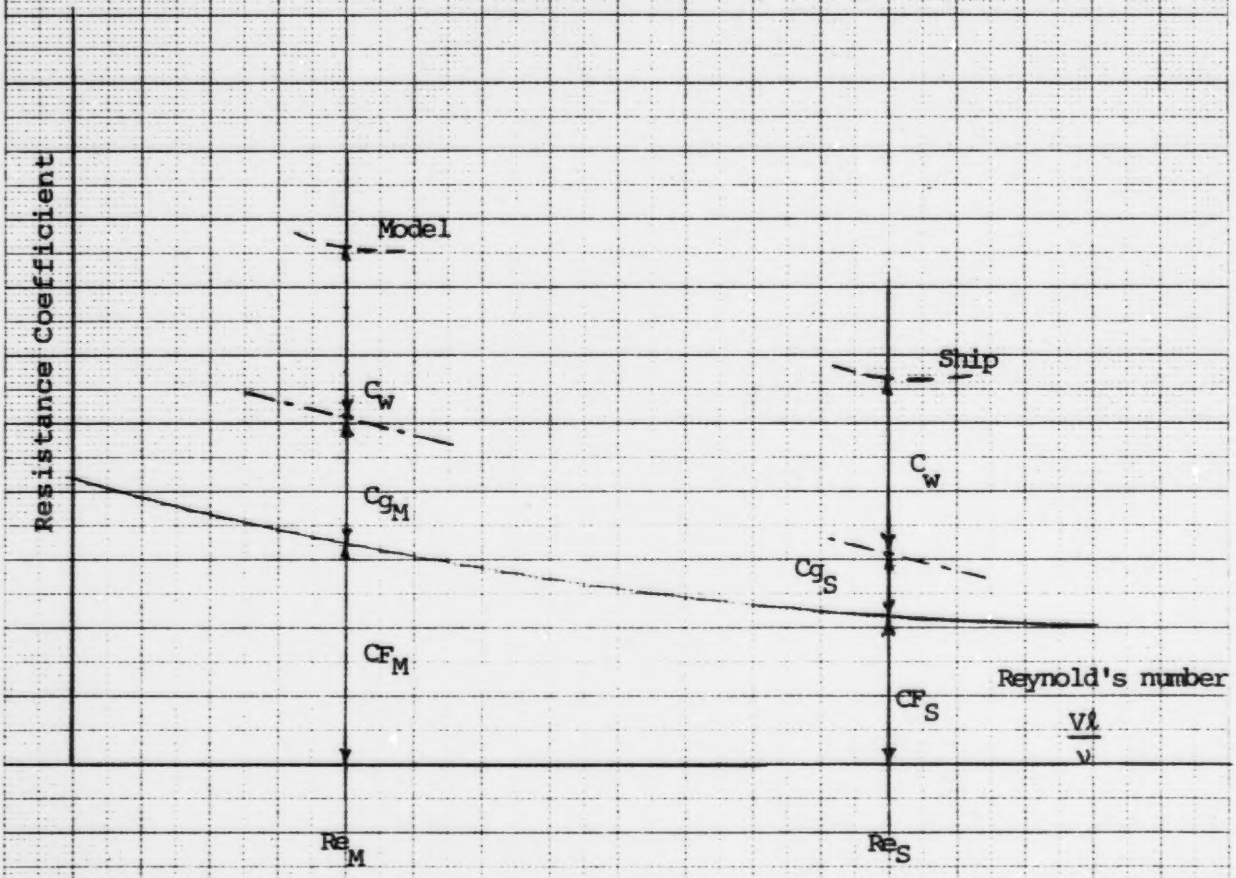

FIGURE B-1: RESISTANCE PREDICTION OF FULL SCALE GRILLS

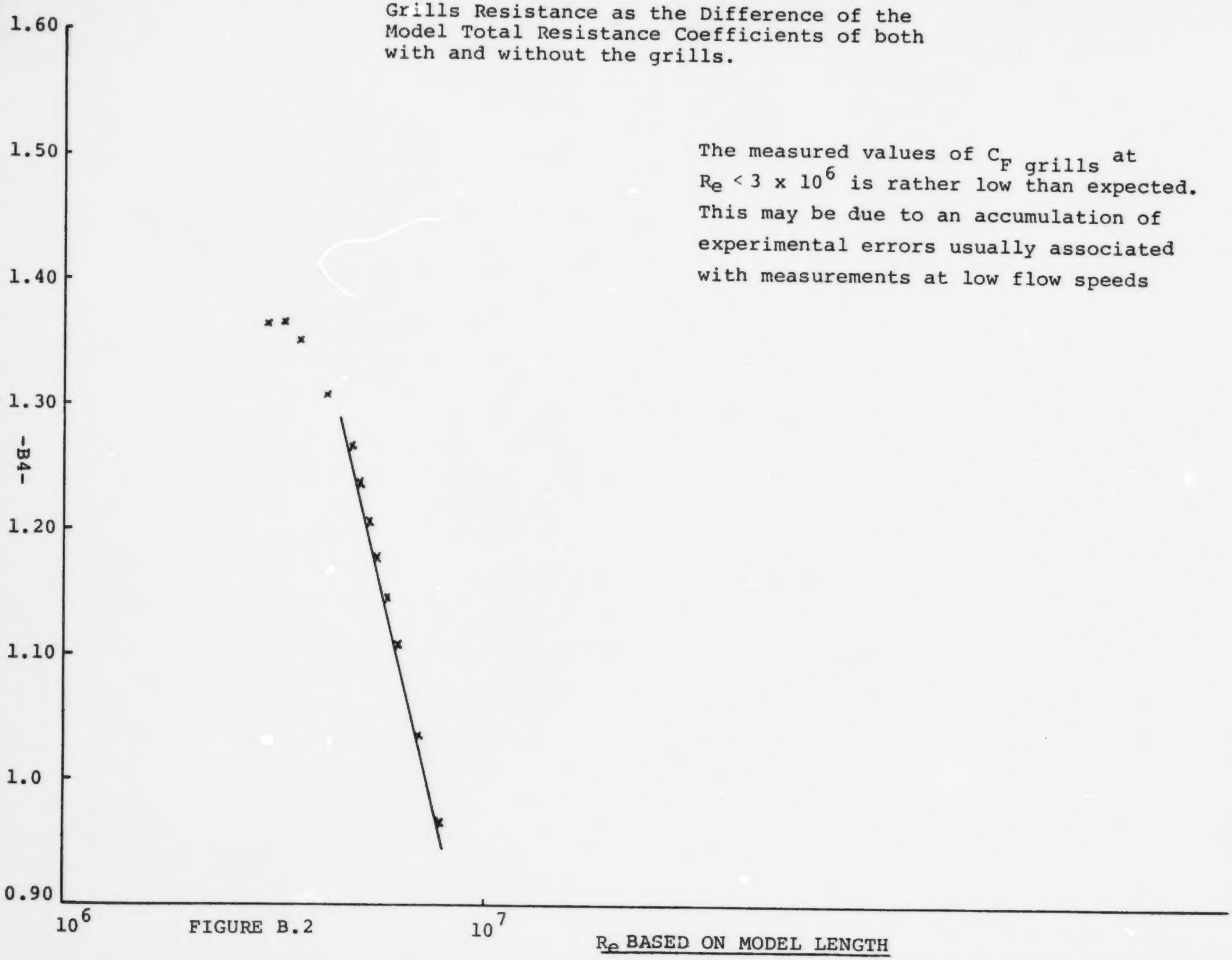

Grills Resistance as the Difference of the Model Total Resistance Coefficients of both with and without the grills.

The measured values of C_F grills at $R_e < 3 \times 10^6$ is rather low than expected. This may be due to an accumulation of experimental errors usually associated with measurements at low flow speeds

FIGURE B.2

V_S Knots	V_m m/sec	With Grills CT_M *1000	Without Grills CT_M *1000	CF_{grills} *1000	Re_M
9	0.68	8.851	7.499	1.342	2.74×10^6
10	0.758	8.871	7.509	1.362	3.04×10^6
11	0.834	8.886	7.523	1.363	3.34
12	0.910	8.895	7.542	1.353	3.64
13	0.986	8.900	7.566	1.334	3.95
14	1.062	8.903	7.595	1.308	4.26
15	1.138	8.907	7.629	1.278	4.56
16	1.214	8.914	7.668	1.246	4.87
17	1.289	8.927	7.712	1.215	5.17
18	1.365	8.947	7.765	1.182	5.47
19	1.441	8.979	7.831	1.148	5.78
20	1.517	9.027	7.913	1.114	6.07×10^6
22	1.669	9.197	8.157	1.04	6.68
25	1.896	9.914	8.947	0.967	7.60×10^6

TABLE B-1: RESISTANCE PREDICTION OF FULL SCALE GRILLS

APPENDIX C

Model Test Results of Configuration 299F

APPENDIX C

Model Test Results of Configuration 299F

C.1 Summary

This appendix describes resistance and propulsion tests carried out with Model 299F, a modification of Model 299E, which consisted of refitting the tunnel separating walls. The results were analysed to give predictions for ship self-propulsion and overload conditions.

A comparison with Model 299E shows that the modifications produced a very small increase in effective power, but a reasonable reduction in delivered power.

C.2 Model Description

Model 299F was identical to Model 299E described in Section 2.0. Full particulars of the model are given in Table C.1. For the self-propulsion tests the model was fitted with the same propellers used earlier with Models 299B to 299E. The particulars of these propellers are given in Table C.2.

C.3 Model Experiments

C.3.1 Resistance Experiments

The model was fitted with dummy propeller hubs for the resistance tests. Rudders were not fitted during the resistance tests.

Resistance measurements were taken over a range of speeds corresponding to 5 to 24 knots for the full scale ship.

C.3.2 Propeller Open Water Tests

The procedure for carrying out these tests is described in Section 6.0. It was not repeated for this series of tests.

C.3.3 Propulsion and Overload Experiments

Model 299F was ballasted as described in Table C.1 and propelled at the speed of the carriage to cover a range of propeller overloads from ship self-propulsion point to full delivered power.

HYDROSTATICS FOR FULL SCALE SHIP

SCALE : 46

MODEL 299F

LENGTH BETWEEN PERPENDICULARS (L_{BP})	(M)	200.00
LENGTH ON WATERLINE (L_{WL})	(M)	216.43
WATERLINE BEAM AT MIDSHIPS (B)	(M)	35.16
DRAFT AT MIDSHIPS (T)	(M)	14.032
TRIM' POSITIVE STERN DOWN	(M)	0
VOLUME OF DISPLACEMENT	(M^3)	68855
DISPLACEMENT (S.W.)	(TONNES)	70044
WETTED SURFACE AREA (ACTUAL)	(M^2)	11549
WETTED SURFACE AREA (ANALYSED)	(M^2)	11090
AREA OF MAXIMUM SECTION	(M^2)	435.7
BLOCK COEFFICIENT, C_B		0.693

TABLE C-1 HYDROSTATICS FOR FULL SCALE SHIP

PROPELLER DESCRIPTION

MODEL PROPELLER 74 L, R, C

Run on Model 299C	17 February 1982
Run on Model 299E	6 May 1982
Run on Model 299F	20 August 1982

Scale = 46.00

Diameter	6826 mm
Pitch at 0.7 R	5710 mm
P/D	0.836
B.A.R.	0.412
Number of Blades	4
Design	Wageningen B-Screw with Squared-off Tips

TABLE C-2 PROPELLER DESCRIPTION
MODEL PROPELLER 74 L, R, C

```
                              RESULTS OF RESISTANCE EXPERIMENTS
MODEL NO. 2991                        I                   TEST DATE   09 AUG 82
L =  200.0  m                         T =  14.03 m                                  TRIM =  0.00 m BY THE STERN
SHIP PREDICTIONS ARE FOR SALT WATER AT 15 DEG.C.                   SHIP MODEL CORRELATION ALLOWANCE 0.00000

    DIMENSIONAL                  COEFF. BASED ON LENGTH               COEFF. BASED ON DISPLACEMENT
     V          PE            FN     CTM(59)    CR       CTS          FNVOL     CTVOL     TAU      TAUR
   KNOTS        KW                    X1000    X1000    X1000                  X100     X100      X100

    5.00        476.          0.058   7.538    3.206    4.909          0.129    3.254    0.027    0.018
    6.00        782.          0.070   7.173    3.001    4.664          0.154    3.092    0.037    0.024
    7.00       1242.          0.081   7.081    3.038    4.668          0.180    3.095    0.050    0.033
    8.00       1761.          0.093   6.766    2.830    4.433          0.206    2.939    0.062    0.040
    9.00       2401.          0.105   6.511    2.666    4.245          0.231    2.814    0.075    0.047
   10.00       3230.          0.116   6.372    2.605    4.163          0.257    2.760    0.091    0.057
   11.00       4265.          0.128   6.288    2.590    4.130          0.283    2.738    0.109    0.069
   12.00       5556.          0.139   6.257    2.620    4.144          0.308    2.747    0.131    0.083
   13.00       7201.          0.151   6.297    2.716    4.224          0.334    2.800    0.156    0.101
   14.00       9103.          0.163   6.313    2.781    4.275          0.360    2.834    0.184    0.119
   15.00      11243.          0.174   6.298    2.811    4.293          0.386    2.846    0.212    0.139
   16.00      13789.          0.186   6.313    2.868    4.338          0.411    2.876    0.243    0.161
   17.00      16903.          0.198   6.380    2.974    4.434          0.437    2.939    0.281    0.188
   18.00      20212.          0.209   6.387    3.017    4.466          0.463    2.961    0.317    0.214
   19.00      23893.          0.221   6.386    3.049    4.489          0.488    2.976    0.355    0.241
   20.00      28652.          0.232   6.490    3.184    4.616          0.514    3.060    0.404    0.279
   21.00      35209.          0.244   6.753    3.477    4.900          0.540    3.248    0.473    0.336
   22.00      42094.          0.256   6.929    3.680    5.095          0.566    3.378    0.540    0.390
   23.00      47648.          0.267   6.863    3.639    5.047          0.591    3.346    0.585    0.422
   24.00      55333.          0.279   6.957    3.758    5.159          0.617    3.420    0.651    0.474
```

TABLE C-3 RESULTS OF RESISTANCE EXPERIMENTS

```
                         RESULTS OF PROPULSION EXPERIMENTS
MODEL NO. 299F               PROPELLER NO. 74 L,R,C                  TEST DATE  20-AUG-82
L =  200.0  m                T =  14.03 m                            TRIM =  0.00 m BY THE STERN
                               14.0M TMLD L.K.
SHIP PREDICTIONS ARE FOR SALT WATER AT 15 deg C          SHIP MODEL CORRELATION ALLOWANCE 0.00000

                   POWERS,SPEEDS AND THRUST PREDICTED FOR MODEL TEST PROPELLER

                                     WING PROPS.             CENTRE PROP.          TOTAL
      V       FN       PE       PD      NS      TH      PD      NS      TH      PD      TH
    KNOTS              KW       KW      RPM     KN      KW      RPM     KN      KW      KN

     8.63   0.100    2146.    3891.    66.5   283.2    999.    66.5    87.4   4890.   370.6
    12.83   0.149    6906.   12255.    98.6   661.8   3561.    98.6   208.3  15816.   870.1
    17.21   0.200   17592.   28302.   131.4  1239.1   9632.   131.4   393.1  37934.  1632.3
    19.28   0.224   25088.   39507.   148.9  1662.5  15287.   148.9   551.2  54794.  2213.8
    21.49   0.250   38687.   60471.   170.5  2320.5  25329.   170.5   843.2  85800.  3163.7
```

TABLE C-4 RESULTS OF PROPULSION EXPERIMENTS
PROPELLER NO. 74, L,R,C

```
MODEL NO. 299F                    RESULTS OF PROPULSION EXPERIMENTS
L = 200.6 m                            PROPELLER NO. 74 L,R,C
                                          D = 14.03 m                           TEST DATE  20-AUG-82
                                         14.0M TMLD L.K.                        TRIM =  0.00 m BY THE STERN
SHIP PREDICTIONS ARE FOR SALT WATER AT 15 deg C                 SHIP MODEL CORRELATION ALLOWANCE 0.00000

                              PROPULSION FACTORS PREDICTED FOR MODEL TEST PROPELLER

                                    WING PROPS.                    CENTRE PROP.                  TOTAL
        V        FN       WETT      ETAO      ETAR      WETT      ETAO      ETAR      ETAD      THDF
      KNOTS

       8.63    0.100    -0.297    0.555     0.756    -0.363     0.449     1.180     0.439    -0.303
      12.84    0.149    -0.282    0.566     0.807    -0.350     0.468     1.115     0.437    -0.201
      17.21    0.200    -0.263    0.576     0.851    -0.334     0.482     1.001     0.464    -0.216
      19.28    0.224    -0.269    0.583     0.909    -0.338     0.502     0.955     0.458    -0.142
      21.49    0.250    -0.290    0.593     0.923    -0.352     0.535     0.931     0.451    -0.105
```

TABLE C-5 RESULTS OF PROPULSION EXPERIMENTS
PROPELLER NO. 74, L,R,C

```
                         RESULTS OF PROPULSION EXPERIMENTS
MODEL NO. 299F              PROPELLER NO. 74 L,R,C                        TEST DATE  20-AUG-82
L =  200.0  m                 T =  14.03 m                                TRIM =  0.00 m BY THE STERN
                               14.0M TMLD L.K.
SHIP PREDICTIONS ARE FOR SALT WATER AT 15 deg C          SHIP MODEL CORRELATION ALLOWANCE 0.00000

                                  PROPELLER COEFFICIENTS

                                     WING PROPELLERS
                        BEHIND MODEL               TEST PROPELLER            SERIES PROPELLER
      FN  CT-R(67.3)  JP       KTP       KQP      JOM      KTOM      KQOM      JOS       KTOS      KQOS
           X1000                         X10                         X10                           X10

    0.100  -2.202    0.587    0.052    0.149    0.762    0.052    0.113
    0.149  -2.002    0.589    0.055    0.145    0.755    0.055    0.117
    0.200  -1.869    0.593    0.058    0.141    0.749    0.058    0.120
    0.224  -1.821    0.586    0.061    0.135    0.744    0.061    0.123
    0.250  -1.776    0.570    0.065    0.138    0.736    0.065    0.127
```

TABLE C-6 RESULTS OF PROPULSION EXPERIMENTS
PROPELLER NO. 74, L,R,C

```
                                 RESULTS OF PROPULSION EXPERIMENTS
MODEL NO. 299F                       PROPELLER NO. 74 L,R,C                       TEST DATE  20-AUG-82
L =  200.0  m                        T =  14.03 m                                 TRIM =  0.00 m BY THE STERN
                                        14.0M TMLD L.K.
SHIP PREDICTIONS ARE FOR SALT WATER AT 15 deg C           SHIP MODEL CORRELATION ALLOWANCE 0.00000

                                      PROPELLER COEFFICIENTS

                                         CENTRE PROPELLER
                         BEHIND MODEL                TEST PROPELLER              SERIES PROPELLER
     FN   CT-R(67.4)  JP      KTP      KQP      JOM      KTOM     KQOM      JOS      KTOS     KQOS
             X1000                     X10                         X10                         X10

)  0.100  -2.202   0.587    0.032    0.077    0.800    0.032    0.091
   0.149  -2.002   0.589    0.035    0.084    0.795    0.035    0.094
   0.200   1.869   0.593    0.037    0.096    0.791    0.037    0.096
   0.224  -1.821   0.586    0.040    0.105    0.784    0.040    0.100
   0.250  -1.776   0.570    0.047    0.116    0.771    0.047    0.108
```

TABLE C-7 RESULTS OF PROPULSION EXPERIMENTS
PROPELLER NO. 74, L,R,C

```
                            RESULTS OF PROPULSION EXPERIMENTS
MODEL NO. 299F                   PROPELLER NO. 74 L,R,C                TEST DATE  20-AUG-82
L =  200.0  m                    T =  14.03 m                          TRIM =  0.00 m BY THE STERN
                                   14.0M TMLD L.K.
SHIP PREDICTIONS ARE FOR SALT WATER AT 15 deg C            SHIP MODEL CORRELATION ALLOWANCE 0.000

          NON-DIMENSIONAL PROPULSION COEFFICIENTS PREDICTED  FOR MODEL TEST PROPELLER

                      FN         FNVOL       CDVOL      PDVOL      TAUT      PDC/PD
                                              X100      X1000      X1000

                    0.100        0.222       6.490      0.355      0.539      0.204
                    0.149        0.330       6.391      1.148      1.264      0.225
                    0.200        0.442       6.357      2.753      2.372      0.254
                    0.224        0.496       6.530      3.976      3.217      0.279
                    0.250        0.552       7.387      6.226      4.597      0.295
```

TABLE C-8 RESULTS OF PROPULSION EXPERIMENTS
PROPELLER NO. 74, L,R,C

RESULTS OF OVERLOAD EXPERIMENTS

MODEL NO. 299F
L = 200.0 m

PROPELLER NO. 74 L,R,C
T = 14.03 m

TEST DATE 20-AUG-82
TRIM = 0.00 m BY THE STERN

SHIP PREDICTIONS ARE FOR SALT WATER AT 15 deg C

SHIP MODEL CORRELATION ALLOWANCE 0.00000

POWERS AND TOW FORCES PREDICTED FOR MODEL TEST PROPELLER

		WING PROPS.			CENTRE PROP.			TOTAL		
V KNOTS	FN	PD KW	NS RPM	TH KN	PD KW	NS RPM	TH KN	PD KW	TH KN	FP KN
0.00	0.000	16537.	90.0	1698.4	7211.	90.0	744.1	23748.	2442.6	3803.6
0.00	0.000	30554.	110.0	2618.2	13719.	110.0	1163.4	44272.	3781.6	5689.9
0.00	0.000	49788.	130.0	3698.3	23268.	130.0	1677.3	73057.	5375.7	7889.3
0.00	0.000	75440.	150.0	4892.4	36473.	150.0	2259.8	111912.	7152.2	10529.1
0.00	0.000	109115.	170.0	6201.0	54302.	170.0	2889.3	163417.	9090.3	13501.8
4.42	0.051	15293.	90.0	1454.3	6975.	90.0	511.9	22269.	1966.2	2534.5
4.42	0.051	28446.	110.0	2287.0	13158.	110.0	870.0	41604.	3157.0	4248.6
4.42	0.051	47521.	130.0	3288.2	22203.	130.0	1317.0	69724.	4605.2	6286.1
4.42	0.051	73628.	150.0	4462.6	34652.	150.0	1852.8	108280.	6315.4	8739.9
4.42	0.051	107697.	170.0	5812.9	51048.	170.0	2476.9	158745.	8289.8	11449.9
8.63	0.100	12940.	90.0	1102.5	4899.	90.0	335.7	17838.	1438.2	1257.7
8.63	0.100	25535.	110.0	1955.5	10921.	110.0	649.0	36455.	2604.5	2805.6
8.63	0.100	43618.	130.0	2959.2	19952.	130.0	1049.6	63570.	4008.8	4726.1
8.63	0.100	68359.	150.0	4120.9	32675.	150.0	1537.5	101033.	5658.4	7006.8
8.63	0.100	100943.	170.0	5461.9	49771.	170.0	2112.4	150714.	7574.3	9308.0
12.83	0.149	20073.	110.0	1241.0	6090.	110.0	368.4	26163.	1609.4	798.6
12.83	0.149	37462.	130.0	2242.2	13912.	130.0	807.0	51374.	3049.2	2407.1
12.83	0.149	61647.	150.0	3465.1	26313.	150.0	1334.5	87960.	4799.7	4647.0
12.83	0.149	94030.	170.0	4858.9	44244.	170.0	1957.6	138274.	6816.5	7431.0
17.21	0.200	49534.	150.0	2438.2	19162.	150.0	779.6	68697.	3217.7	1678.5
17.21	0.200	62809.	160.0	3078.3	26598.	160.0	1041.8	89407.	4120.1	2790.0
17.21	0.200	78026.	170.0	3770.9	35439.	170.0	1315.1	113465.	5086.0	4022.4
19.28	0.224	56070.	160.0	2499.5	21561.	160.0	820.9	77631.	3320.4	1189.1
19.28	0.224	63746.	165.0	2842.7	25339.	165.0	964.9	89084.	3807.7	1762.0
19.28	0.224	72007.	170.0	3200.8	29500.	170.0	1101.2	101506.	4302.0	2324.6

TABLE C-9 RESULTS OF OVERLOAD EXPERIMENTS
PROPELLER NO. 74 L,R,C

MODEL NO. 2996
L = 200.0 m

RESULTS OF OVERLOAD EXPERIMENTS
PROPELLER NO. 74 L.R.C
T = 14.03 m

TEST DATE 20-AUG-82
TRIM = 0.00 m BY THE STERN

SHIP PREDICTIONS ARE FOR SALT WATER AT 15 deg C

SHIP MODEL CORRELATION ALLOWANCE 0.00000

PROPULSION FACTORS PREDICTED FOR MODEL TEST PROPELLER

V KNOTS	NS RPM	WING PROPS. WFTT	ETAO	ETAR	CENTRE PROP. WFTT	ETAO	ETAR	ETAD	TOTAL THDF	FP/PD N/KW
0.00	90.0	0.000	0.000	1.501	0.000	0.000	1.721	0.000	-0.557	160.155
0.00	110.0	0.000	0.000	1.484	0.000	0.000	1.652	0.000	-0.505	128.516
0.00	130.0	0.000	0.000	1.503	0.000	0.000	1.608	0.000	-0.468	107.983
0.00	150.0	0.000	0.000	1.524	0.000	0.000	1.576	0.000	-0.472	94.079
0.00	170.0	0.000	0.000	1.533	0.000	0.000	1.541	0.000	-0.485	82.618
4.42	90.0	-1.517	0.608	0.896	-1.950	0.634	0.778	0.275	-0.369	113.809
4.42	110.0	-1.979	0.599	0.911	-2.435	0.631	0.820	0.241	-0.396	102.116
4.42	130.0	-2.453	0.593	0.918	-2.919	0.626	0.846	0.211	-0.399	90.152
4.42	150.0	-2.930	0.588	0.922	-3.400	0.620	0.864	0.187	-0.409	80.712
4.42	170.0	-3.409	0.585	0.927	-3.882	0.615	0.877	0.167	-0.400	72.124
8.63	90.0	-0.472	0.633	0.880	-0.683	0.599	0.856	0.434	-0.210	70.501
8.63	110.0	-0.670	0.622	0.913	-0.941	0.627	0.818	0.401	-0.263	76.955
8.63	130.0	-0.890	0.612	0.931	-1.196	0.633	0.811	0.364	-0.299	74.342
8.63	150.0	-1.124	0.605	0.941	-1.450	0.633	0.809	0.330	-0.324	69.348
8.63	170.0	-1.359	0.599	0.948	-1.702	0.630	0.809	0.289	-0.293	61.756
12.83	110.0	-0.321	0.623	0.866	-0.452	0.545	1.065	0.466	-0.146	30.521
12.83	130.0	-0.444	0.634	0.901	-0.588	0.617	0.987	0.444	-0.132	46.852
12.83	150.0	-0.568	0.627	0.929	-0.730	0.632	0.917	0.428	-0.186	52.827
12.83	170.0	-0.701	0.618	0.940	-0.874	0.633	0.865	0.405	-0.243	53.738
17.21	150.0	-0.324	0.628	0.920	-0.451	0.570	0.918	0.473	-0.139	24.432
17.21	160.0	-0.370	0.633	0.941	-0.506	0.596	0.877	0.473	-0.159	31.204
17.21	170.0	-0.417	0.634	0.957	-0.565	0.611	0.842	0.469	-0.181	35.449
19.28	160.0	-0.295	0.619	0.926	-0.396	0.555	0.951	0.475	-0.119	15.316
19.28	165.0	-0.313	0.625	0.930	-0.419	0.574	0.935	0.478	-0.127	19.778
19.28	170.0	-0.332	0.629	0.934	-0.445	0.586	0.914	0.474	-0.128	22.900

TABLE C-10 RESULTS OF OVERLOAD EXPERIMENTS
PROPELLER NO. 74 L,R,C

MODEL NO. 299F
L = 200.0 m

RESULTS OF OVERLOAD EXPERIMENTS
PROPELLER NO. 74 L,R,C
T = 14.03 m

TEST DATE 20-AUG-82
TRIM = 0.00 m BY THE STERN

SHIP PREDICTIONS ARE FOR SALT WATER AT 15 deg C

SHIP MODEL CORRELATION ALLOWANCE 0.00000

PROPELLER COEFFICIENTS

WING PROPELLERS

		BEHIND MODEL				TEST PROPELLER		
FN	CT-R(67.3) X1000	JP	KTP	KQP X10	ZETO	JOM	KTOM	KQOM X10
0.000	0.000	0.000	0.169	0.256	0.492	0.000	0.343	0.385
0.000	0.000	0.000	0.175	0.259	0.504	0.000	0.343	0.385
0.000	0.000	0.000	0.177	0.256	0.514	0.000	0.343	0.385
0.000	0.000	0.000	0.176	0.253	0.516	0.000	0.343	0.385
0.000	0.000	0.000	0.173	0.251	0.511	0.000	0.343	0.385
0.051	83.270	0.222	0.145	0.237	0.444	0.560	0.145	0.213
0.051	141.351	0.182	0.153	0.242	0.462	0.542	0.153	0.220
0.051	210.385	0.154	0.157	0.244	0.471	0.532	0.157	0.224
0.051	293.530	0.133	0.160	0.247	0.478	0.525	0.160	0.227
0.051	385.351	0.118	0.162	0.248	0.483	0.519	0.162	0.230
0.100	8.989	0.434	0.110	0.201	0.376	0.639	0.110	0.177
0.100	22.762	0.355	0.131	0.217	0.424	0.593	0.131	0.198
0.100	39.852	0.301	0.141	0.224	0.449	0.568	0.141	0.209
0.100	60.146	0.260	0.148	0.229	0.464	0.553	0.148	0.215
0.100	80.622	0.230	0.153	0.232	0.474	0.542	0.153	0.220
0.149	1.215	0.528	0.083	0.170	0.316	0.697	0.083	0.148
0.149	7.693	0.447	0.107	0.193	0.377	0.645	0.107	0.174
0.149	16.714	0.387	0.124	0.206	0.418	0.607	0.124	0.192
0.149	27.926	0.342	0.136	0.216	0.442	0.581	0.136	0.203
0.200	1.891	0.519	0.088	0.166	0.340	0.688	0.088	0.153
0.200	4.380	0.487	0.097	0.173	0.366	0.667	0.097	0.163
0.200	7.140	0.458	0.105	0.179	0.389	0.649	0.105	0.172
0.224	0.301	0.545	0.079	0.155	0.321	0.706	0.079	0.143
0.224	1.323	0.529	0.084	0.160	0.335	0.694	0.084	0.149
0.224	2.327	0.513	0.089	0.166	0.348	0.683	0.089	0.155

TABLE C-11 RESULTS OF OVERLOAD EXPERIMENTS
PROPELLER NO. 74 L,R,C

```
                              RESULTS OF OVERLOAD EXPERIMENTS
MODEL NO. 299F                   PROPELLER NO. 74 L,R,C                    TEST DATE  20-AUG-82
L =  200.0  m                    T =  14.03 m                              TRIM =  0.00 m BY THE STERN

SHIP PREDICTIONS ARE FOR SALT WATER AT 15 deg C             SHIP MODEL CORRELATION ALLOWANCE 0.00000

                                        PROPELLER COEFFICIENTS

                                          CENTRE PROPELLER
                         BEHIND MODEL                                  TEST PROPELLER
     FN  CT-R(67.3)  JP         KTP        KQP        ZETO         JOM       KTOM       KQOM
           X1000                           X10                                          X10

   0.000    0.000    0.000     0.148      0.224      0.473       0.000     0.343     0.385
   0.000    0.000    0.000     0.155      0.233      0.481       0.000     0.343     0.385
   0.000    0.000    0.000     0.160      0.239      0.488       0.000     0.343     0.385
   0.000    0.000    0.000     0.162      0.244      0.487       0.000     0.343     0.385
   0.000    0.000    0.000     0.162      0.250      0.478       0.000     0.343     0.385
   0.051   83.270    0.222     0.102      0.216      0.332       0.656     0.102     0.168
   0.051  141.351    0.182     0.116      0.223      0.370       0.625     0.116     0.183
   0.051  210.385    0.154     0.126      0.228      0.395       0.603     0.126     0.193
   0.051  293.530    0.133     0.133      0.232      0.413       0.587     0.133     0.200
   0.051  385.351    0.118     0.138      0.235      0.427       0.575     0.138     0.206
   0.100    8.989    0.434     0.067      0.152      0.276       0.731     0.067     0.130
   0.100   22.762    0.355     0.087      0.185      0.312       0.689     0.087     0.152
   0.100   39.852    0.301     0.100      0.205      0.338       0.660     0.100     0.166
   0.100   60.146    0.260     0.110      0.219      0.357       0.638     0.110     0.177
   0.100   80.622    0.230     0.118      0.229      0.370       0.621     0.118     0.185
   0.149    1.215    0.528     0.049      0.103      0.262       0.767     0.049     0.110
   0.149    7.693    0.447     0.077      0.143      0.331       0.709     0.077     0.141
   0.149   16.714    0.387     0.096      0.176      0.358       0.670     0.096     0.162
   0.149   27.926    0.342     0.109      0.204      0.371       0.640     0.109     0.176
   0.200    1.891    0.519     0.056      0.128      0.258       0.753     0.056     0.118
   0.200    4.380    0.487     0.066      0.147      0.277       0.733     0.066     0.129
   0.200    7.140    0.458     0.074      0.163      0.289       0.717     0.074     0.137
   0.224    0.301    0.545     0.052      0.119      0.251       0.761     0.052     0.113
   0.224    1.323    0.529     0.057      0.127      0.265       0.750     0.057     0.119
   0.224    2.327    0.513     0.062      0.136      0.273       0.742     0.062     0.124
```

TABLE C-12 RESULTS OF OVERLOAD EXPERIMENTS
PROPELLER NO. 74,L,R,C

COMPARISON OF SPEED AT DESIGN POWER

SCALE : 46.0
CA : 0.0000
P_D : 110325 KW, ETAT = 0.98

MODEL NUMBER	KNOTS
299	26.0
299C	19.0
299E	22.6
299F	22.9

All results are predictions for stock propellers 74 L, R, C.

TABLE C-13 COMPARISON OF SPEED AT DESIGN POWER

C.4 Results

C.4.1 Resistance Experiments

The results of resistance tests on Model 299F are given in Table C.3. The table presents variation of faired resistance coefficient, CTM, corrected to 15°C with Froude number. Also given are CTS predictions for the full scale ship, assuming a frictional resistance correction recommended by the 8th ITTC in 1957, based on the wetted surface area including all appendages, except the internal separating walls. From these values a prediction for effective power (in KW) has been derived. Variation of effective power with speed is shown for Model 299F in Figure C.1. No additional model-ship correlation allowance was used.

C.4.2 Propeller Open Water Experiments

Results of the propeller open water experiments are given in Table 6.2. This shows the variation of faired values of KT, KQ, and ETAO with J. The results are shown, plotted in Figure 6.2.

C.4.3 Self-Propulsion and Overload Experiments

Measured values of KT, KQ, and CT-R for Model 299F were faired against J for each speed tested. The resulting curves were then interpolated at a propeller loading equivalent to the ship propulsion point, based on the frictional resistance coefficient recommended by ITTC with no additional correlation allowance.

Results of the analysis of the self-propulsion experiments, together with predictions of ship performance for Model 299F are given in Tables C.4 to C.8. Variation of delivered power (KW) with ship speed (knots) and revolutions (r.p.m.) are shown in Figure C.1. Variation of THDF and WFT with ship speed are shown in Figure C.2 and variation of ETAR, ETAO, and ETAD with ship speed are shown in Figure C.3.

The propulsion experiments were also analysed to obtain variation of available towforce with delivered power for a given speed. These results are presented for Model 299F in Tables C.9 to C.12. Figure C.4 shows the variation of available towforce (KN) with delivered power (KW) over a range of speeds from 0 to 19.28 knots for Model 299F. Figure C.5 shows variation of THDF with delivered power (KW) for Model 299F. The analysis does not include any effects of ice interaction with the hull and/or propeller.

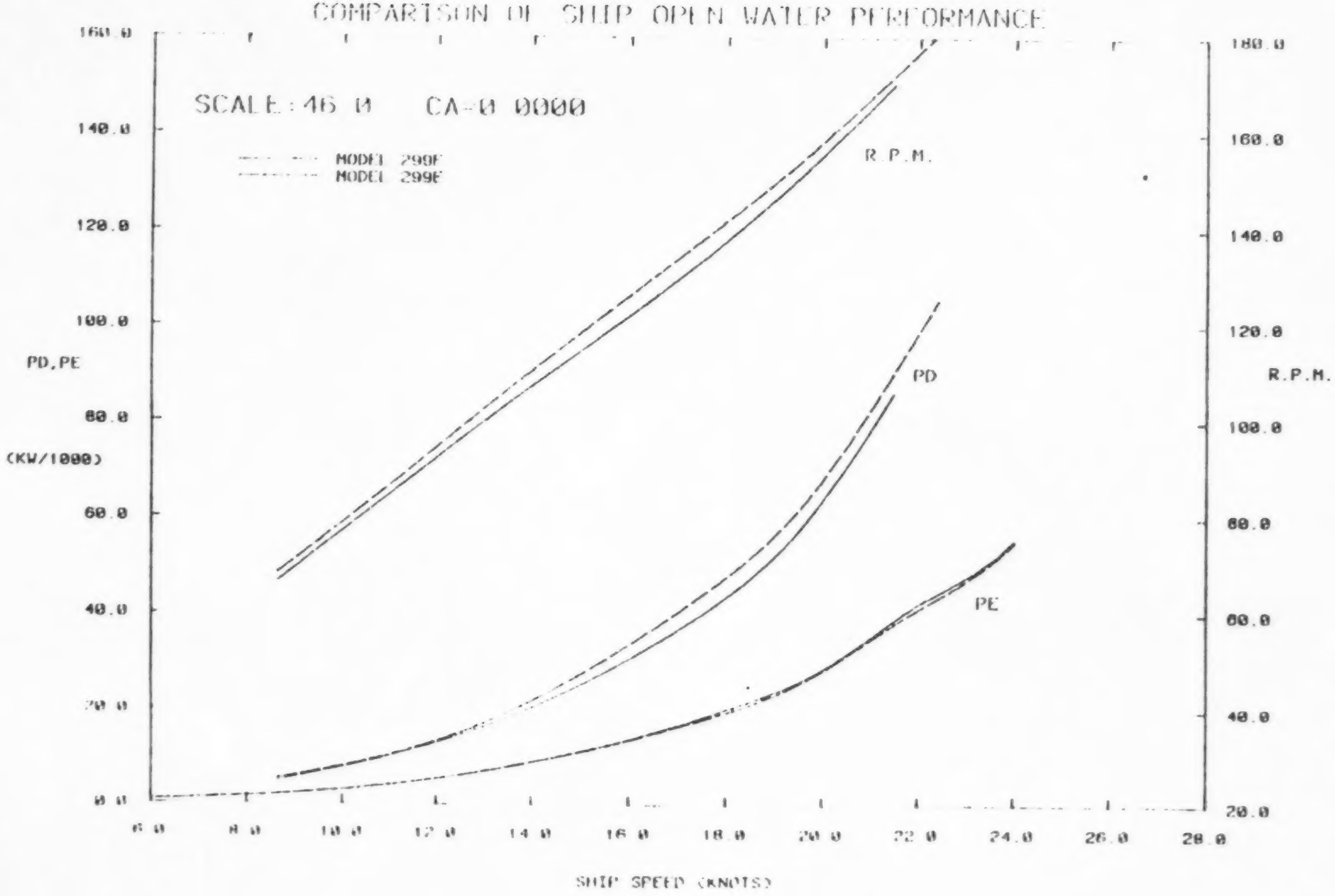

FIGURE C-1 COMPARISON OF SHIP OPEN WATER PERFORMANCE

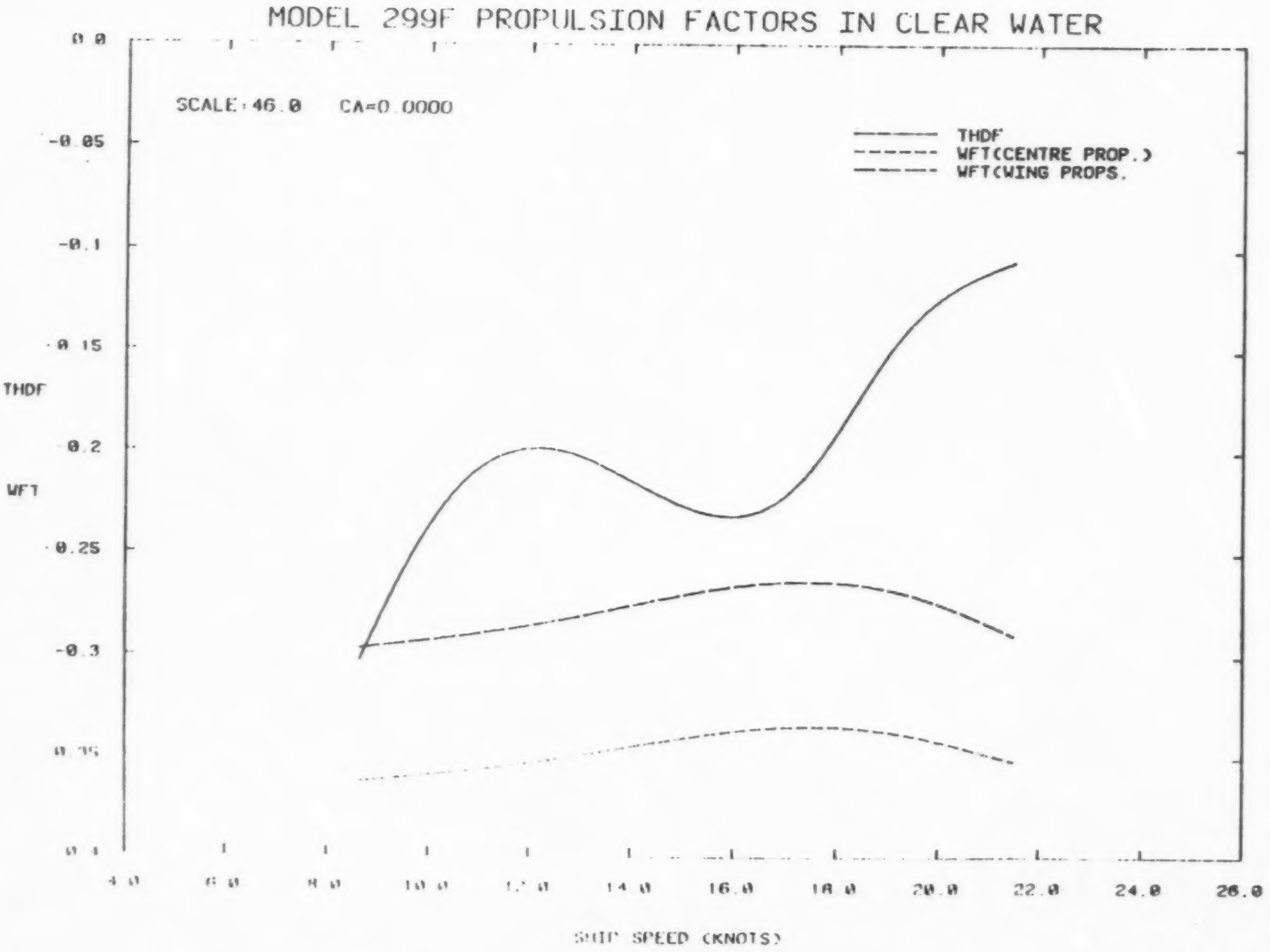

FIGURE C-2 MODEL 299F PROPULSION FACTORS IN CLEAR WATER

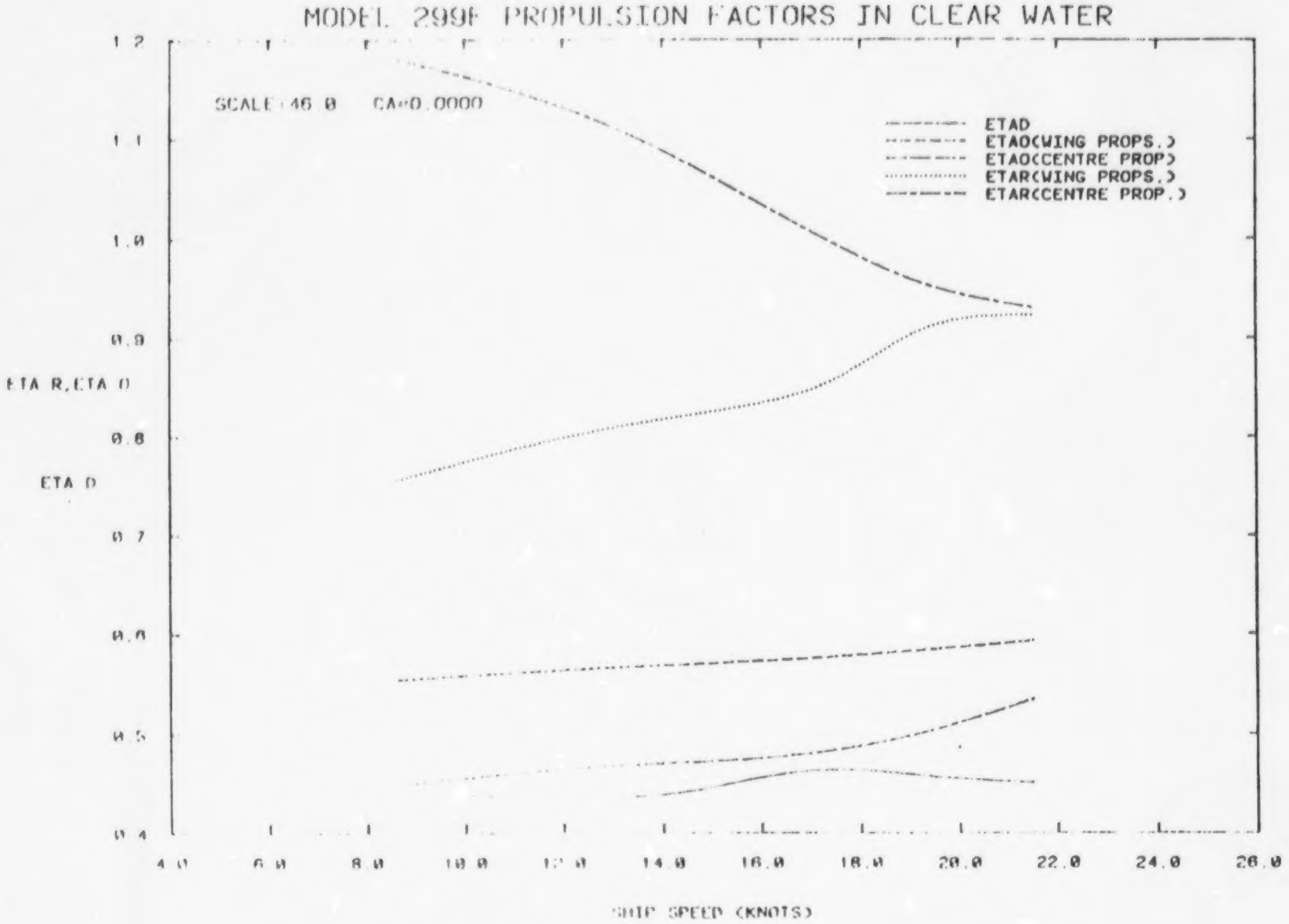

FIGURE C-3 MODEL 299F PROPULSION FACTORS IN CLEAR WATER

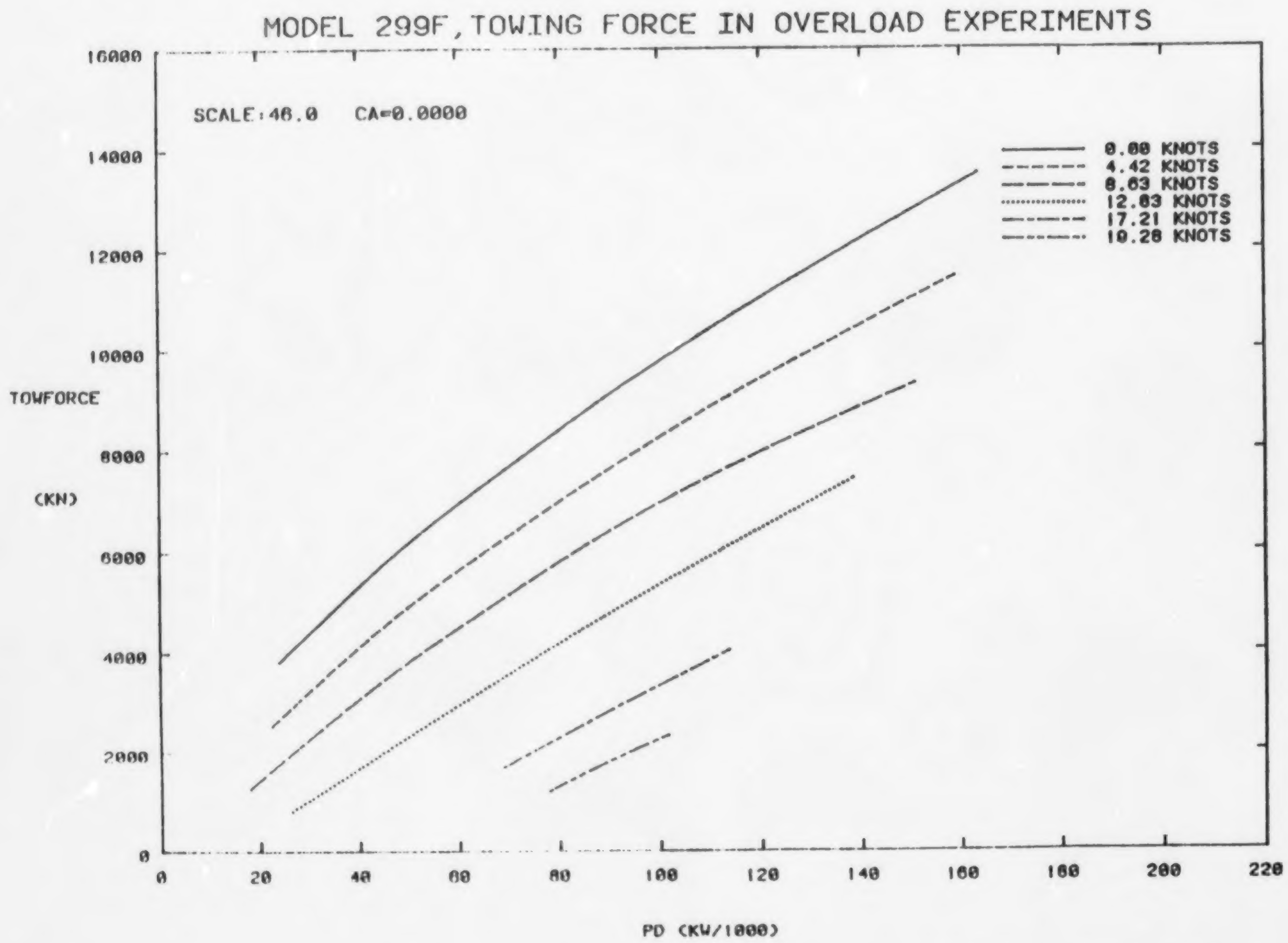

FIGURE C-4 MODEL 299F, TOWING FORCE IN OVERLOAD EXPERIMENTS

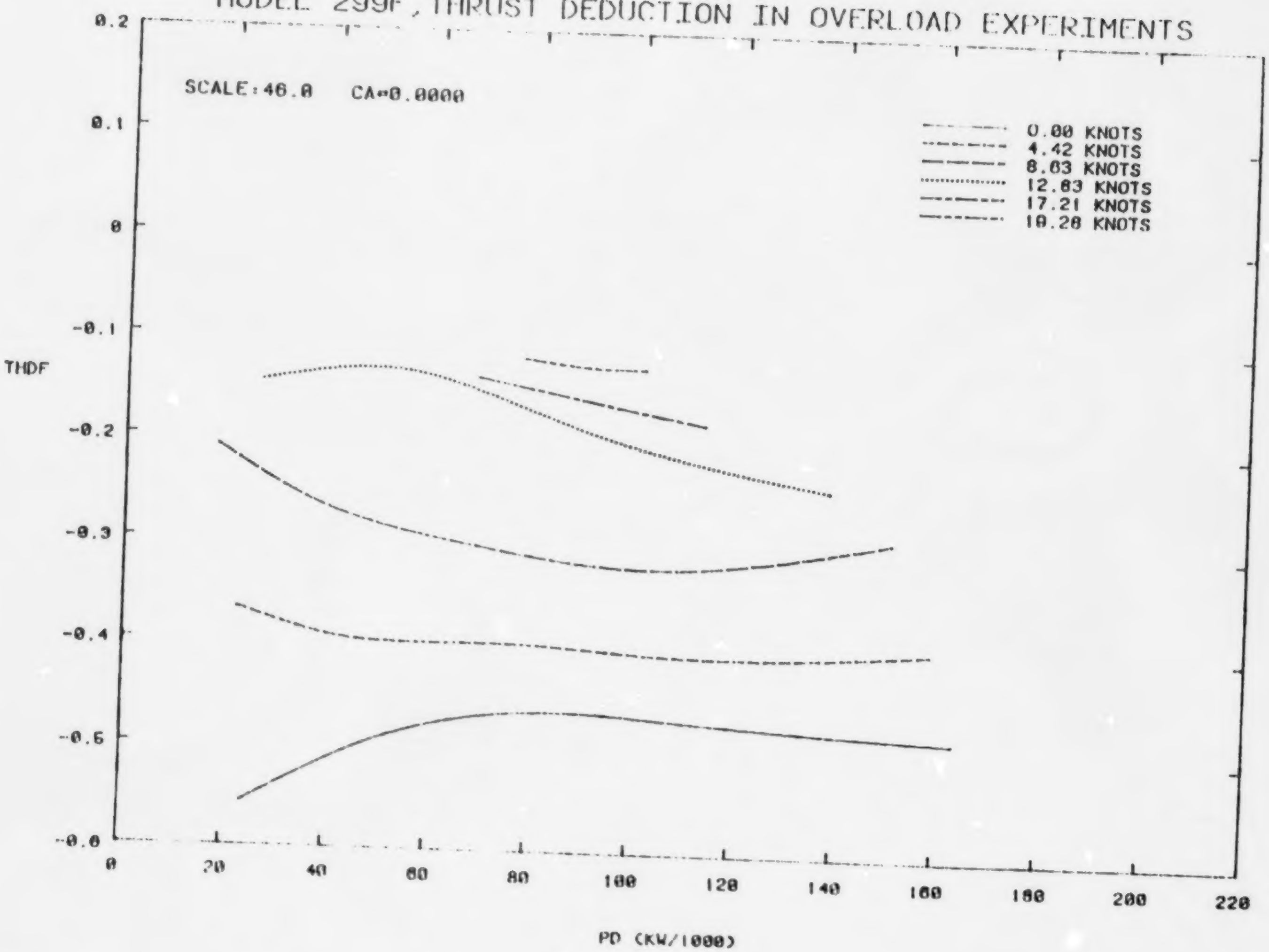

FIGURE C-5 MODEL 299F, THRUST DEDUCTION IN OVERLOAD EXPERIMENTS

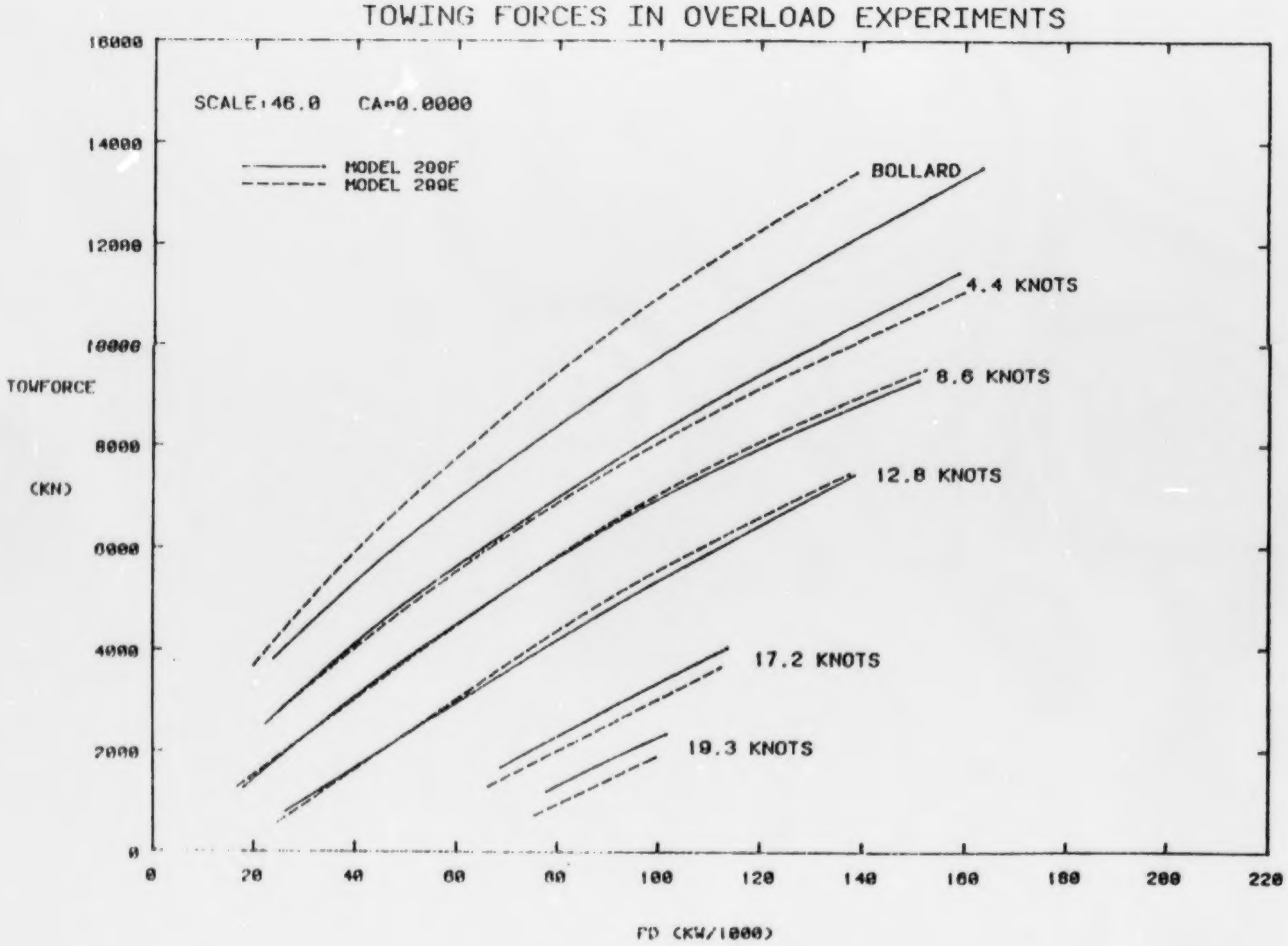

FIGURE C-6 TOWING FORCES IN OVERLOAD EXPERIMENTS

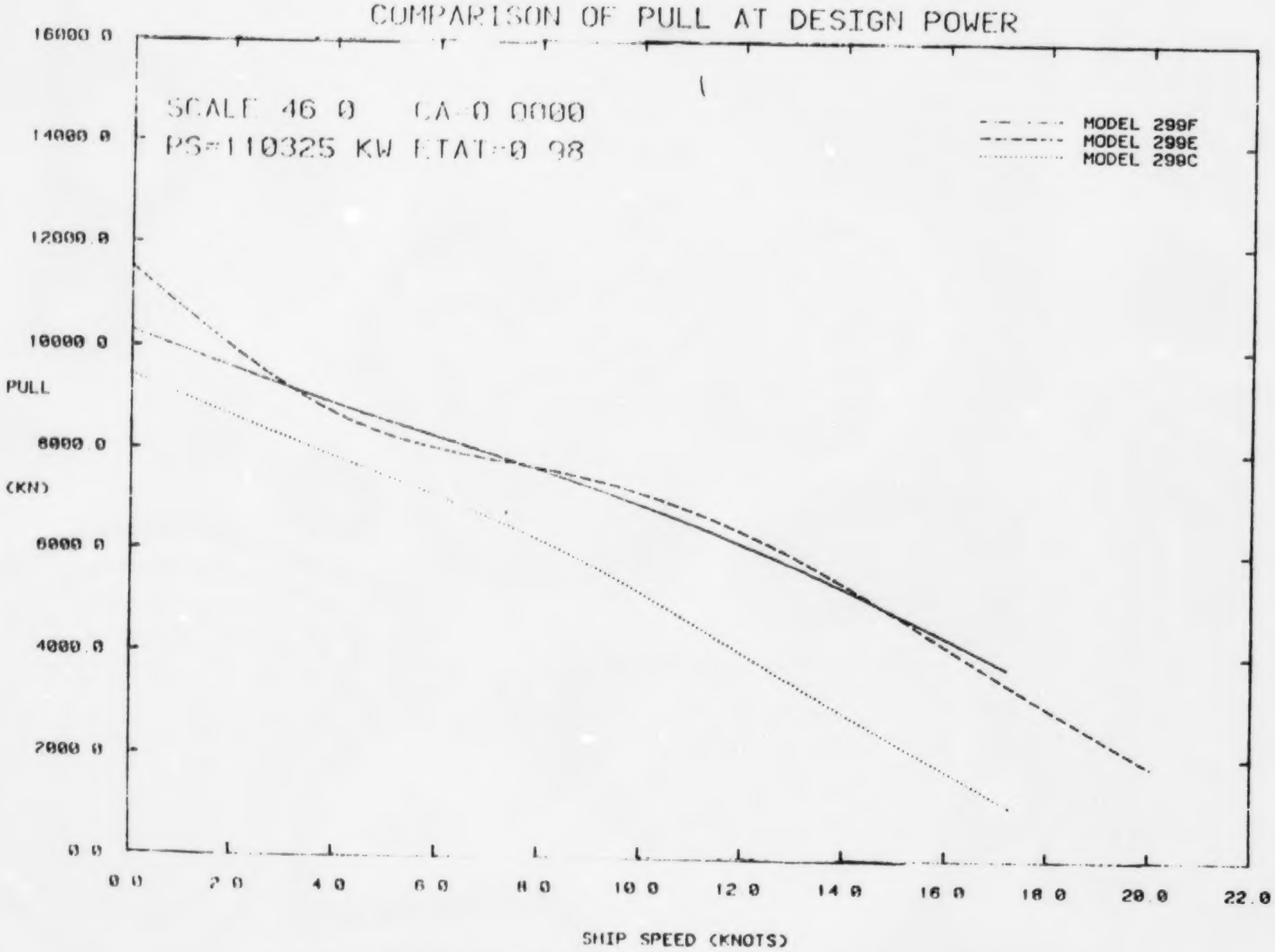

FIGURE C-7 COMPARISON OF PULL AT DESIGN POWER

C.5 Discussion

A full discussion of the relative values of effective and delivered powers for Model 299, 299B, 299C, 299D, and 299E is given in Sections 5.0 and 7.0. However, for comparison purposes, values of PE, PD, and RPM are also given in Figure C.1 for Model 299E.

Some discussion is necessary on the analysis of the effective power. When the results of resistance tests, on Model 299F were analysed using the actual wetted area, the final ship prediction showed a reduction in effective power over 299E at some speeds. However, the model results showed a consistent, but very slight increase in resistance for 299F over 299E. To avoid this inconsistency the analysis was therefore based on a nominal wetted area as given by Model 299E.

This was thought to be reasonable as evidence of the flow test in Section showed there to be weak flow in the region of the tunnel roof. The skin friction correction used (ITTC) does not really apply in this case as it assumes a Reynold's number based on ship speed. As the flow in this region is clearly not close to the ship speed, the additional resistance is better accounted for as a component of the residuary resistance.

It can be seen in Figure C.1, the increase in resistance of Model 299F over 299E is very small. This difference is of the same order as the repeatability of the experiments. One may therefore conclude, that whichever analysis method is chosen, there is no significant difference in the effective powers of the two models.

The delivered power also produces some interesting discussion. For reasons explained in Section 7.3.1, it was not possible to obtain the maximum power requirement of 110,325 KW. However, over the range tested, Model 299F requires a lower delivered power for a given speed than Model 299E.

The increase in propulsive efficiency of Model 299F has not been produced by one single factor. The largest influence was the increase in hull efficiency caused by a more negative thrust deduction factor. The wake fraction for Model 299F is less negative than Model 299E, which would be consistent with the flow into the propellers being slowed down by the drag of the additional sidewalls. Also, whilst the open water efficiency of the wing propellers for Model 299F has increased over Model 299E, that of the centre propeller is reduced. The final effect is an increase in propulsive efficiency of between 8 to 17 per cent.

A comparison of speeds at the design power of 110,325 KW (ETAT = 0.98) is given in Table C.13 for the ship with a correlation

CA1
DTC 801
80
P661
v. 3,
c. 1.

allowance of 0.0000.

Results of the overload tests for Models 299F and 299E may be compared, since the speeds are practically equivalent. This shows the bollard pull of Model 299F to be lower than Model 299E for a given delivered power. For other speeds, up to 12.8 knots, the difference is very slight. Above 12.8 knots, Model 299F has superior towforce capability. This is shown plotted in Figure C.6.

A comparison of the towforce available at the design power of 110,325 KW, (ETAT = 0.98), is shown in Figure C.7 for Models 299C, 299E, and 299F.

C.6 Conclusions

The addition of the separating sidewalls to produce Model 299F has had a beneficial effect on the propulsive efficiency of the design proposal.

The speed predicted at a design power of 110,325 KW is estimated to be 0.3 knots faster than Model 299E.

The bollard pull, however, has been reduced for a given delivered power.

One may conclude that the flow in the area of the propeller tunnels has separated from the hull to such an extent that the addition of the sidewalls had no effect on the resistance. This has combined with an improvement in propulsive efficiency to produce the increase in speed at the design power.

References:

1. "Resistance and Propulsion Experiments with Model 299F, and Propellers 74 L, R, C",
   NRC Report LTR-SH-339, September 1982.

Library and Information Centre /
Centre de Documentation (GSLA)
RECEIVED - REÇU LE
APR AVR 7 1983
Transport Canada / Transports Canada